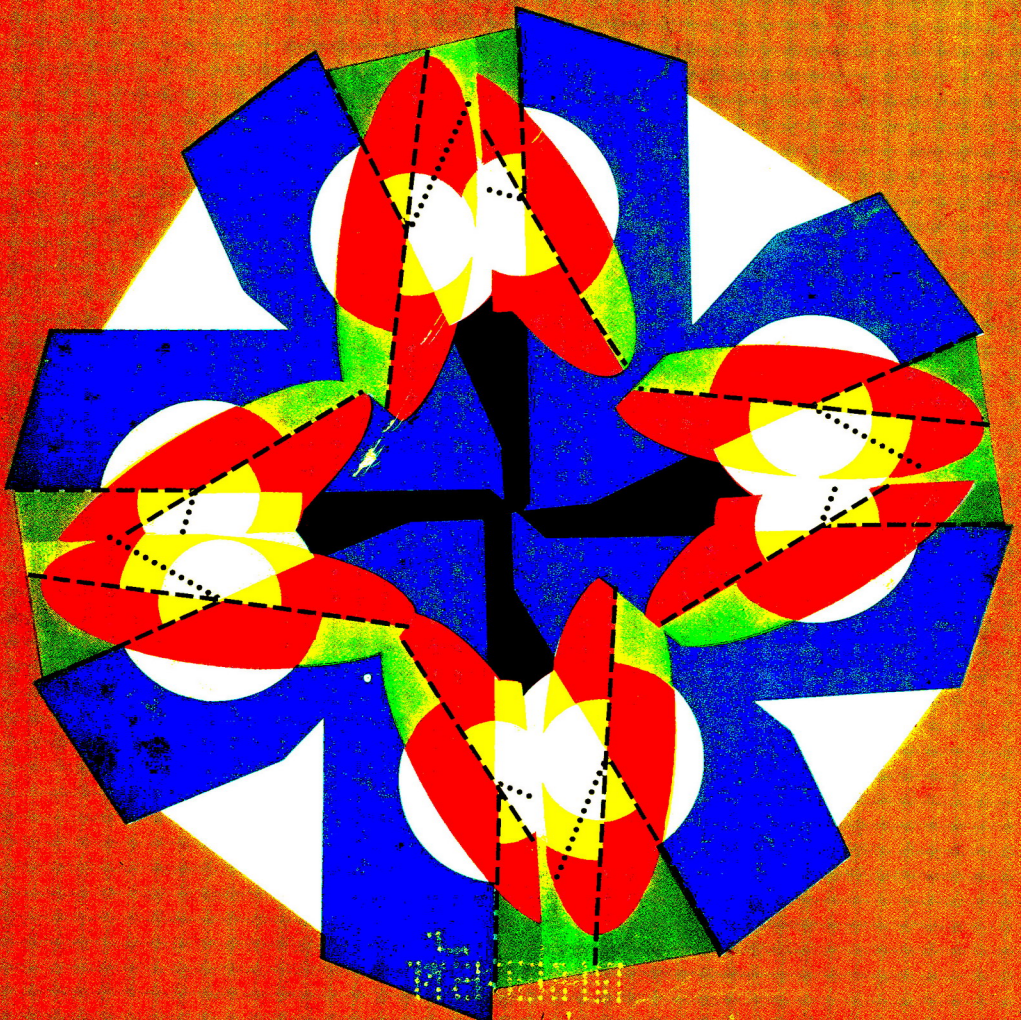
JUNE 1966

ANALYTICAL CHEMISTRY

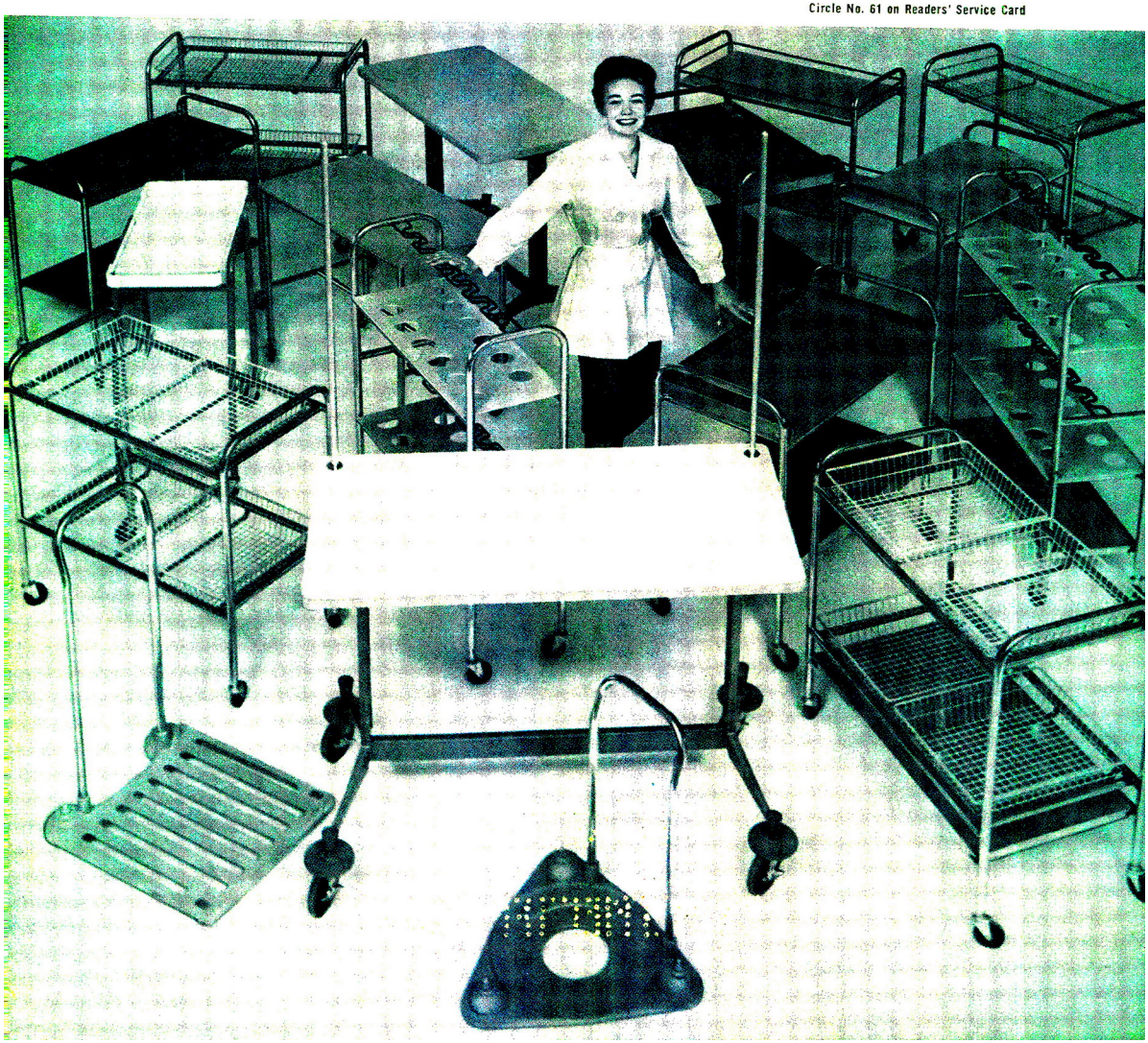


CIRCULAR DICHROISM—THEORY AND INSTRUMENTATION 29A

Only Labconco makes 17 different laboratory carts

This is the most complete line of laboratory carts in the industry. And it's the only line of carts designed exclusively for use in the laboratory. Labconco carts aren't just "warmed over" restaurant or shopping carts. They are specifically engineered and manufactured with the needs of the laboratory in mind. ■ For instance, Labconco carts are all of heavy steel, welded for extra strength. There are no rivets or bolts to work loose. To assure lasting beauty, all steel parts are chrome plated. ■ Typical of the material used in the construction of Labconco carts are fiberglass, compressed asbestos, and poly vinyl. These materials are chemically inert, rugged, and easy to maintain. Labconco carts provide many years of trouble-free service. ■ Labconco carts start as low as $35 (F.O.B. Kansas City). For a FREE COPY of our 32-page, fully-illustrated brochure, write Labconco, 8815 Prospect Ave., Kansas City, Mo. LAB CON CO

Circle No. 61 on Readers' Service Card





There are a lot of pH meters for sale...

but only the Zeromatic® II keeps on selling you after you buy it

The Zeromatic II is more than just the pH meter with the large, 8.2-inch, easy-to-read scale—the convenient push-button controls—the high accuracy (±0.05 pH) and repeatability (±0.015 pH)—the rugged, chemical-resistant case.

When you buy a Zeromatic II pH Meter—or for that matter, any Beckman pH meter—you buy: Sales Engineers to assist you on instrument operation and the selection of accessories and electrodes... Application Engineers to advise you on difficult or unusual applications... Service Engineers to provide you with periodic maintenance or on-the-spot repair... plus, 30 years of experience behind every Beckman pH meter.

Why not call your local Beckman Sales Office and ask for a demonstration of the Zeromatic II? Or request Data File LpH-466.

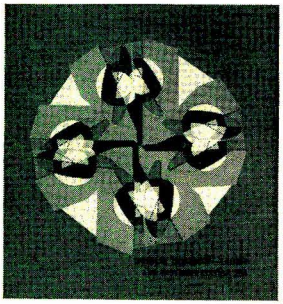
The Zeromatic II offers more—because it *is* more instrument—with more to back it up. Let it sell you.

Beckman® INSTRUMENTS, INC.
SCIENTIFIC AND PROCESS INSTRUMENTS DIVISION
FULLERTON, CALIFORNIA • 92634

INTERNATIONAL SUBSIDIARIES: GENEVA; MUNICH; GLENROTHES, SCOTLAND; TOKYO; PARIS; CAPETOWN; LONDON

Circle No. 30 on Readers' Service Card

VOLUME 38, NO. 7 JUNE 1966



This Month's Cover is an artist's conceptualization of the color effects produced by a multiple reflection of a basic design element conceived from Figure 2 of the Report for Analytical Chemists on circular dichroism. See page 29 A.

© Copyright 1966
by the American Chemical Society
Issued May 23, 1966

MANUSCRIPT REQUIREMENTS published in December 1965 issue, page 1815, outlines scope and copy requirements to be observed in preparing manuscripts for consideration. Manuscript (3 copies) should be submitted to ANALYTICAL CHEMISTRY, 1155 Sixteenth St., N.W., Washington, D. C. 20036.

The American Chemical Society assumes no responsibility for the statements and opinions advanced by contributors to its publications. Views expressed in the editorials are those of the editors and do not necessarily represent the official position of the American Chemical Society.

1966 Subscription Rates

	1 yr.	2 yr.	3 yr.
Members, domestic and foreign	$ 4.00	$ 7.00	$10.00
Nonmembers, domestic and Canada	5.00	9.00	12.00
Nonmembers, foreign except Canada	15.00	27.50	40.00

Postage: Canada and Pan-American Union, $2.50; foreign, $3.50. Single copies: current, $1.50. Postage: Canada and Pan-American Union $0.15; foreign, $0.20. Rates for back issues and volumes are available from Special Issues Sales Dept., 1155 Sixteenth St., N.W., Washington, D. C. 20036. Claims for missing numbers will not be allowed if received more than 60 days from date of mailing plus time normally required for postal delivery of journal and claim. No claims allowed because of failure to notify the Subscription Service Department of a change of address, or because copy is "missing from files."

Published monthly with review issue added in April by the American Chemical Society, from 20th and Northampton Sts., Easton, Pa. 18042; Executive offices, Editorial Headquarters, and Subscription Service Department, 1155 Sixteenth St., N.W., Washington, D. C. 20036; Advertising Office, 430 Park Ave., New York, N. Y. 10022; News Bureaus: 733 Third Ave., New York, N. Y. 10017; Philadelphia National Bank Bldg., Broad & Chestnut Sts., Philadelphia, Pa. 10103; 530 William Penn Place, Pittsburgh, Pa. 15230; 36 South Wabash Ave., Chicago, Ill. 60603; 1367 East Sixth St., Cleveland, Ohio 44114; 57 Post St., San Francisco, Calif. 94104; 422 South Western Ave., Los Angeles, Calif. 90005; 1121 Walker St., Houston, Tex. 77002; 1155 Sixteenth St., N.W., Washington, D. C. 20036; Grosse Bockenheimerstrasse 32, Frankfort/Main, West Germany; Apt. 306, 47 Dai-machi, Akasaka, Minato-ku, Tokyo, Japan, 27 John Adam St., London W.C. 2, England.

Second class postage paid at Easton, Pa.

CHANGE OF ADDRESS: Notify Subscription Service Department, American Chemical Society, 1155 Sixteenth St., N.W., Washington, D. C. 20036. Such notification should include both old and new addresses, with ZIP code numbers, and be accompanied by mailing label from a recent issue. Allow four weeks for change to become effective.

ANALYTICAL CHEMISTRY

CONTENTS

REPORT FOR ANALYTICAL CHEMISTS

A resurgence of interest in the phenomenon of circular dichroism is discussed in this month's Report. Fundamental background information and the present state of the art are given.....**29 A**

NEWS SECTION

Two winners of the Analytical Division Summer Fellowship Awards are announced. Meetings and training courses are scheduled.**65 A**

EDITORS' COLUMN

Recent developments in a new chemical information system and the present demand for engineers and scientists are discussed
..... **85 A**

LABORATORY OF THE MONTH

Chemical process research at the M. W. Kellogg Co. makes great demands on many technologies and requires a versatile analytical chemical approach.....**95 A**

INSTRUMENTATION

Dr. Müller discusses several new devices and comments on two books which deal with Michael Faraday.....**109 A**

AUTHOR INDEX...4 A
BOOK REVIEWS AND NEW BOOKS...77 A
BRIEFS...9 A
CALENDAR OF EVENTS...68 A
NEW CHEMICALS...133 A
EDITORIAL...809
FUTURE ARTICLES...148 A
MANUFACTURERS' LITERATURE...135 A
NEW PRODUCTS...119 A
READERS' INFORMATION SERVICE...116 B

Scientific Communication

Liquid-Liquid Extraction of Anionic Americium and Europium Complexes of Hydroxyethylethylenediaminetriacetic Acid and Diethylenetriaminepentaacetic acid. F. L. Moore 905

Determination of Calcium-48 in Natural Calcium by Neutron Activation Analysis. J. T. Corless 810

Application of Lithium-Drifted Germanium Gamma-Ray Detectors to Neutron Activation Analysis. Nondestructive Analysis of a Sulfide Ore. J. F. Lamb, S. G. Prussin, J. A. Harris, and J. M. Hollander 813

Reactor Neutron Activation Analysis. Instrumental Sensitivities in Six Matrix Materials. H. P. Yule . . . 818

Determination of Trace Amounts of Carbon, Oxygen, and Nitrogen in Metals by Spark Source Mass Spectrometry. W. L. Harrington, R. K. Skogerboe, and G. H. Morrison 821

Quantitative Separation of Mercury–Thallium Mixtures. R. G. Dosch 826

Automatic Continuous Determination of Small Quantities of Gaseous Ammonia. N. S. Segal and Robin Wodley-Smith 828

Determination of Diphenhydramine and Certain Related Compounds by Ultraviolet Spectrophotometry. J. E. Wallace, J. D. Biggs, and E. V. Dahl 831

Ultra Sensitive, Specific Method for Cyanide Using *p*-Nitrobenzaldehyde and o-Dinitrobenzene. G. G. Guilbault and D. N. Kramer 834

Apparatus and Procedures for Rapid Extraction and Identification of Pesticides by Single and Multiple Distribution in Binary Solvent Systems. Morton Beroza and M. C. Bowman 837

Characterization of Position Isomers of Secondary Straight-Chain Alcohols and Their 3,5-Dinitrobenzoate Derivatives by Nuclear Magnetic Resonance. C. E. Godsey 842

Kinetics of Bromination of Certain Substituted 8-Quinolinols. George O'Dom and Quintus Fernando . . . 844

Intermolecular Energy Transfer as a Means of Chemical Analysis. Sensitization of Rare Earth Emission in Dilute Solution by Aromatic Carbonyl Compounds. W. J. McCarthy and J. D. Winefordner. 848

Rapid Determination of Primary Hydroxyl Content of Poly(Oxyalkylene) Glycols and Poly(Oxyalkylene) Sorbitols by Pseudo First-Order Differential Reaction Kinetics. Friso Willeboordse and R. L. Meeker 854

Synthesis of Tetranitrobenzylpolystyrene Resin for Chromatographic Stationary Phase. J. T. Ayres and C. K. Mann 859

Column Chromatography with Tetranitrobenzylpolystyrene Resin Stationary Phase. J. T. Ayres and C. K. Mann. 861

Electrolysis with Constant Potential. Diffusion Currents for the Formation of an Amalgam at a Hanging Mercury Drop Electrode. W. G. Stevens and Irving Shain 865

The Depletion Effect in Pulse Polarography with Stationary Electrodes. K. B. Oldham and E. P. Parry . . 867

Polarographic Study of the Iodine-Iodide Couple at the Rotating Platinum Electrode. E. C. Toren, Jr., and C. P. Driscoll 872

Coulometric Generation of Hydrogen Ions in Water and Methanol Using Hydrogen-Permeable Membrane Electrodes. T. R. Blackburn and R. B. Greenberg . . 877

Reversible Charge Transfer at the Tubular Platinum Electrode. W. J. Blaedel and L. N. Klatt. 879

Twin-Electrode Thin-Layer Electrochemistry. Determination of Chemical Reaction Rates by Decay of Steady-State Current. Bruce McDuffie, L. B. Anderson, and C. N. Reilley 883

Comprehensive Computer Program for Electron Probe Microanalysis. J. D. Brown. 890

Optical and Electron Microscope Studies of Thin Fuel Cell Electrode Structures. W. R. Lasko and G. P. McCarthy 894

Photochemical Determination of Oxalate. W. M. Riggs and C. E. Bricker 897

Determination of Dissolved Polonium-210 in Water by Coprecipitation with Tellurium by Stannous Chloride. D. E. Rushing 900

Correspondence

Spectrophotometric Determination of Tertiary Aromatic Amines in the Presence of Primary and Secondary Amines by Complexation with Tetracyanoethylene. G. H. Schenk, Peter Warner, and William Bazzelle 907

Mercuric Determination of Organic Disulfides Using Reaction with Butyllithium. Stig Veibel and Mieczyslaw Wronski 910

Spectrophotometric Determination of Copper in Lead, Tin, Aluminum, Zinc, and Their Alloys with Biscyclohexanone Oxalyldihydrazone. R. K. Rohde 911

Determination of Sulfur in Inorganic Sulfides Using Oxygen Flask Combustion. A. R. Johnson, Jr., and G. B. McVicker. 913

Spectrophotometric Determination of Cobalt in Iron and Steel with 2-Nitroso-1-Naphthol. Manuel Needleman 915

Spectrophotometric Determination of Cyclohexanone Oxime in Sulfuric Acid Solution of Epsilon-Caprolactam. Yoshinari Kobayashi 917

CONTRIBUTED ARTICLES

Gravimetric Determination of Palladium with Di-2-Thienylketoxime. **W. J. Holland and Jesse Gerard** . . 919

Note on the Determination of Lead in Gasolines by Atomic Absorption Spectrometry. **H. W. Wilson** . . 920

Analysis of α-Olefin-Derived Sodium Sulfonates by Ion Exchange and Potentiometric Titrimetry. **E. H. Griffin, Jr., and E. W. Albaugh** 921

A Simple and Accurate Calibration Model for Hydrogen-Content, Beta-Particle Transmission Gauges. **R. P. Gardner and K. F. Roberts** 923

Extraction of Metal Pyridine Azides. Spectrophotometric Determination of Copper, Nickel, and Palladium. **R. G. Clem and E. H. Huffman** 926

Use of an Alkali Additive for Gas Chromatographic Analysis of Organic Bases on Open Tubular Columns. **E. W. Cieplinski** 928

Polarographic Behavior in the Oxidation of Sodium Formaldehyde Sulfoxylate. **Remigio Fernandez-Martin, R. G. Rinker, and W. H. Corcoran** 930

Chelometric Titration for Zinc in Municipal and Industrial Water Supplies. **J. J. Hickey and C. J. Overbeck** 932

Quantitative Determination of Impurities in Salicylic Acid. **N. E. Skelly** 934

Stability Constants of Some Dihydrazide Complexes of Cadmium. **A. F. Krivis, G. R. Supp, and R. L. Doerr.** 936

Trace Impurity Analysis of Plutonium–Uranium–Zirconium Alloys by Anion Exchange–Partition Chromatography. **E. A. Huff and S. J. Kulpa** 939

Aids for Analytical Chemists

A Semiautomatic Device for Measuring and Drawing Mass Spectra. **R. N. Stillwell** 940

Stainless Steel Capsule with Iron "Window" for Determining Hydrogen in Alkali Metal by Vacuum Extraction. **J. W. Glass, C. M. Larsen, and J. M. Scarborough** 942

Improvements in Carbon-14 Assay of Organic Compounds by Dry Combustion. **Masayuki Hamada and Eiko Kawano** 943

Indium Capsules for Microdetermination of Carbon and Hydrogen. **G. E. Secor and L. M. White** 945

Computerized Procedure for Editing Data from a Mass Spectrometer Digitizer. **H. E. Howard** 946

High Sensitivity Oxygen Analysis of Metallic Samples with Fast Neutrons. **R. W. Benjamin, K. R. Blake, and I. L. Morgan** 947

Pulseless High Pressure Pump for Liquid Chromatography. **R. E. Jentoft and T. H. Gouw** 949

The Purity, Properties, and Analytical Determination of 4-sec-Butyl-2-(α-Methylbenzyl)Phenol. **B. Z. Egan and W. D. Arnold** 950

AUTHOR INDEX

Albaugh, E. W., 921
Anderson, L. B., 883
Arnold, W. D., 950
Ayres, J. T., 859, 861

Bazzelle, W., 907
Benjamin, R. W., 947
Beroza, M., 837
Biggs, J. D., 831
Blackburn, T. R., 877
Blaedel, W. J., 879
Blake, K. R., 947
Bowman, M. C., 837
Bricker, C. E., 897
Brown, J. D., 890

Cieplinski, E. W., 928
Clem, R. G., 926
Corcoran, W. H., 930
Corless, J. T., 810
Couw, T. H., 949

Dahl, E. V., 831
Doerr, R. L., 936
Dosch, R. G., 826
Driscoll, C. P., 872

Egan, B. Z., 950

Fernandez-Martin, R., 930
Fernando, Q., 844

Gardner, R. P., 923
Gerard, J., 919
Glass, J. W., 942
Godsey, C. E., 842
Gouw, T. H., 949
Greenberg, R. B., 877
Griffin, E. H., Jr., 921
Guilbault, G. G., 834

Hamada, M., 943
Harrington, W. L., 821
Harris, J. A., 813
Hickey, J. J., 932
Holland, W. J., 919
Hollander, J. M., 813
Howard, H. E., 946
Huff, E. A., 939
Huffman, E. H., 926

Jentoft, R. E., 949
Johnson, A. R., Jr., 913

Kawano, E., 943
Klatt, L. N., 879
Kobayashi, Y., 917
Kramer, D. N., 834
Krivis, A. F., 936
Kulpa, S. J., 939

Lamb, J. F., 813
Larsen, C. M., 942
Lasko, W. R., 894

Mann, C. K., 859, 861
McCarthy, G. P., 894
McCarthy, W. J., 848
McDuffie, B., 883
McVicker, G. B., 913
Meeker, R. L., 854
Moore, F. L., 905
Morgan, I. L., 947
Morrison, G. H., 821

Needleman, M., 915

O'Dom, G., 844
Oldham, K. B., 867
Overbeck, C. J., 932

Parry, E. P., 867
Prussin, S. G., 813

Reilley, C. N., 883
Riggs, W. M., 897
Rinker, R. G., 930
Roberts, K. F., 923
Rohde, R. K., 911
Rushing, D. E., 900

Scarborough, J. M., 942
Schenk, G. H., 907
Secor, G. E., 945
Segal, N. S., 828
Shain, I., 865
Skelly, N. E., 934
Skogerboe, R. K., 821
Stevens, W. G., 865
Stillwell, R. N., 940
Supp, G. R., 936

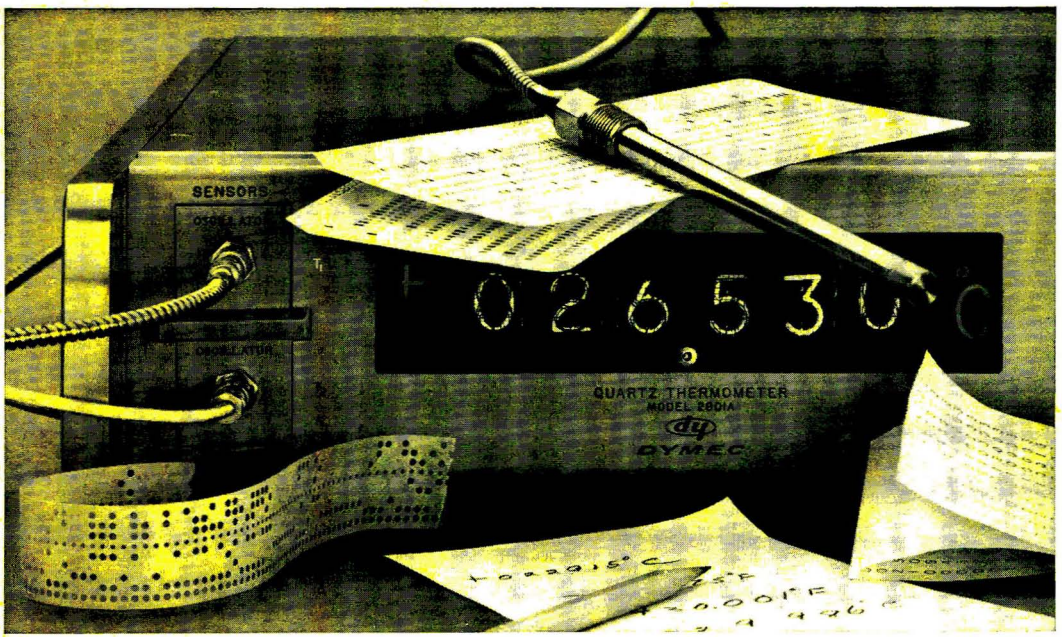
Toren, E. C., Jr., 872

Veibel, S., 910

Wallace, J. E., 831
Warner, P., 907
White, L. M., 945
Willeboordse, F., 854
Wilson, H. W., 920
Winefordner, J. D., 848
Wodley-Smith, R., 828
Wronski, M., 910

Yule, H. P., 818

measure temperature!



for lab research... or automatic monitoring:

TEMPERATURE MEASUREMENTS −80 TO +250°C WITH THE 2801A QUARTZ THERMOMETER

Direct digital readout with up to 0.0001°resolution C or F

High-accuracy absolute or difference measurements

Automatic scanning of up to 60 temperature points... at up to a mile from thermometer

Outputs for recording on digital recorder, punched tape, cards, magnetic tape or strip-chart

Whether you need high-accuracy, high-resolution laboratory-type temperature measurements or need to monitor a series of temperatures, the Hewlett-Packard Quartz Thermometer is the answer. You get direct-reading measurements in degrees C or F without bridge balancing, conversion charts, temperature references or computer processing.

The unique 2801A Thermometer measures frequency of a temperature-sensitive quartz oscillator, rather than voltage or resistance as associated with thermocouples or platinum-resistance devices. This technique gives you the most convenient high-accuracy, high-resolution instrument available . . . plus automatic monitoring capability.

Multi-point temperature measurement can be automatic, unattended—with a recorded output in a variety of useful forms. Use the DY-2918A Thermometer Scanner to cover up to 60 measurement points with a single 2801A Quartz Thermometer. Measurements can be manually stepped or automatic with single scan, continuous scan and single-channel monitoring. Or, the DY-2840A Sensor Selector permits manual scanning of 10 sensors, with a slave capability to permit measurement at up to 100 points.

Thermometers provide digital output signals for recording on strip printer, card or tape punch, magnetic tape recorder or strip-chart recorder. Scanners provide channel identification.

The thermometer is equipped with probes useful to 1000 feet from the instrument without loss in accuracy or resolution. Further, DY-2831A booster amplifiers are available for measurements to greater than 5000 feet away without loss in thermometer specifications.

A variety of probes are available for various measuring requirements, including operation in ocean depths in excess of 36,000 feet, an assortment of lengths for special applications, probes with electronics for measurements at great distances from the thermometer. All possess rigid environmental characteristics. Special probe configurations and materials are available for unusual requirements.

Discuss your specific temperature-measuring problem with your Hewlett-Packard field engineer or write for complete specifications to Dymec Division, Hewlett-Packard, 395 Page Mill Road, Palo Alto, California 94306. Phone (415) 326-1755, TWX 910-373-1296; Europe: 54 Route des Acacias, Geneva.

PRICES:

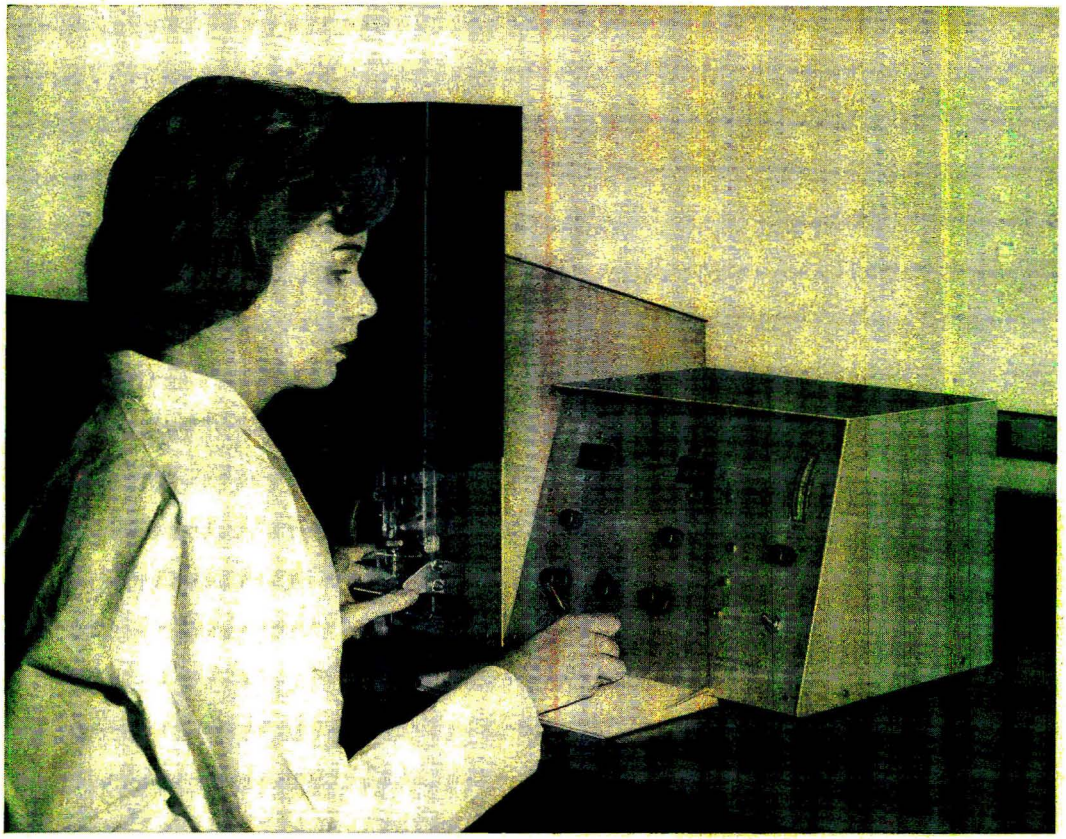
DY-2801A 0.0001° resolution, two-probe Thermometer, $3250
DY-2800A 0.1° resolution, one-probe Thermometer, $2250
DY-2918A Thermometer Scanner, $3750
DY-2840A Sensor Selector, $650
DY-2831A Oscillator Amplifier, $100

Data subject to change without notice. Prices f.o.b. factory.

988

HEWLETT PACKARD hp DYMEC DIVISION

Circle No. 134 on Readers' Service Card



ANALYZE 30 SAMPLES FOR Na+ AND K+ IN TWO MINUTES

The answers are presented simultaneously as large, legible numbers on the new IL Flame Photometer. It is a completely solid state unit. It provides fast response, extreme wide range and a degree of reproducibility unobtainable by even the most expert and painstaking application of conventional flame photometers.

The Model 143 is a new concept in flame photometry. It is well suited for the clinical, research or industrial laboratory. The data collection system is an analog computer and results can be indicated in whatever unit of concentration you select.

One dilution (1:200) covers the entire range of concentrations seen in biological samples, thus providing great convenience when widely ranging samples such as serum and urine are being run together.

For further information call or write your nearest IL authorized dealer and let him show you how fast, accurate and reliable flame photometry has become. Or write for Instrument Data 143 and a list of users in your area.

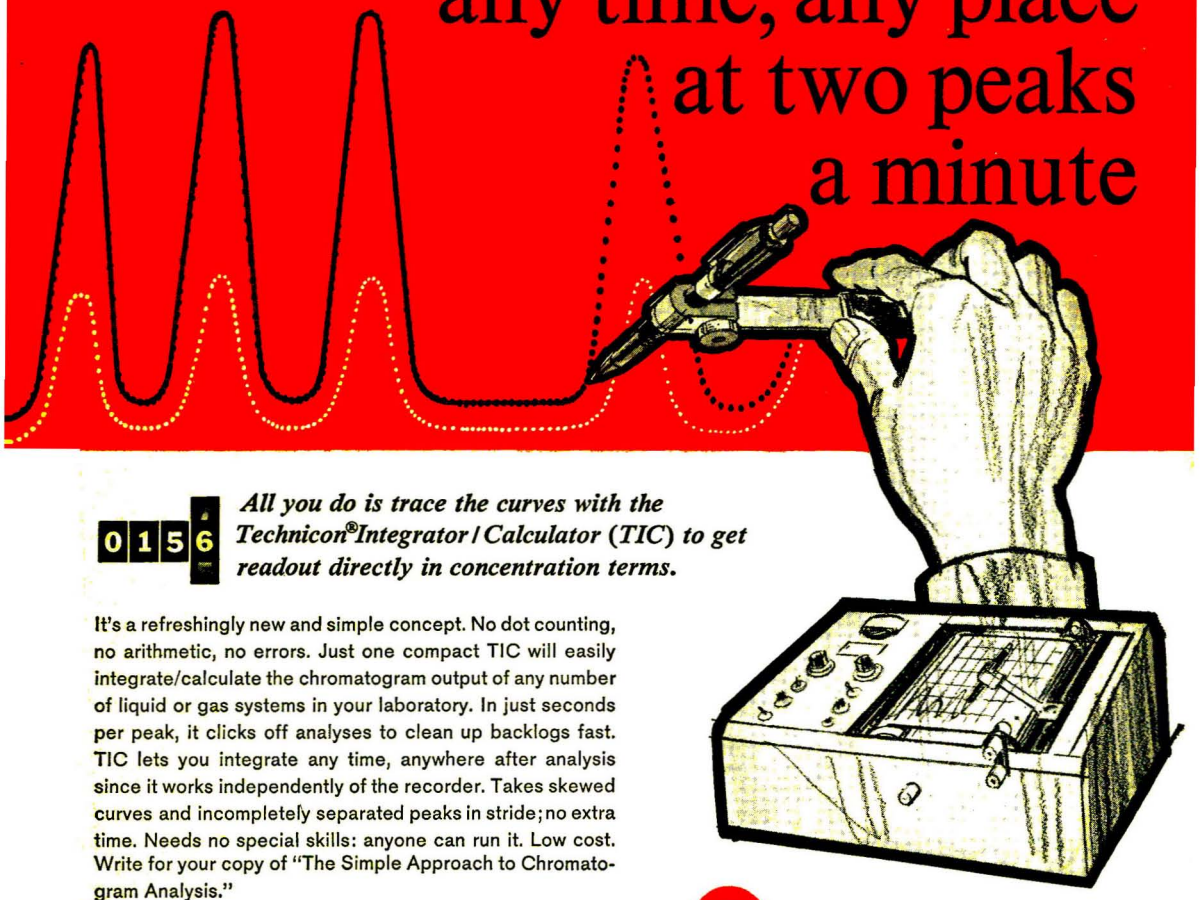
INSTRUMENTATION LABORATORY INC.

9 GALEN STREET • WATERTOWN, MASS. 02172 • TELEPHONE (617) 926-1700

DISTRIBUTED IN THE U. S. BY ALOE SCIENTIFIC, DIV. OF BRUNSWICK; AND SCIENTIFIC PRODUCTS, DIV. OF AMERICAN HOSPITAL SUPPLY CORP.

See Buyers' Guide for all products/sales offices.
Circle No. 52 on Readers' Service Card

Integrate & calculate any chromatogram— liquid or gas— any time, any place at two peaks a minute



0156

All you do is trace the curves with the Technicon® Integrator / Calculator (TIC) to get readout directly in concentration terms.

It's a refreshingly new and simple concept. No dot counting, no arithmetic, no errors. Just one compact TIC will easily integrate/calculate the chromatogram output of any number of liquid or gas systems in your laboratory. In just seconds per peak, it clicks off analyses to clean up backlogs fast. TIC lets you integrate any time, anywhere after analysis since it works independently of the recorder. Takes skewed curves and incompletely separated peaks in stride; no extra time. Needs no special skills: anyone can run it. Low cost. Write for your copy of "The Simple Approach to Chromatogram Analysis."

Appropriate Adjectives: fast, economical, versatile, flexible.

Appropriate Conclusion: TIC belongs in your laboratory.

TECHNICON
CHROMATOGRAPHY CORP.
Research Park • Chauncey, N.Y.

Technicon International of Canada, Ltd., Montreal • Technicon Instruments Company, Ltd., London • Compagnie Technicon, Paris • Technicon GmbH, Frankfurt/M. • Technicon AB, Stockholm • Techpicon, Basle • Technicon Italiana S.r.L., Rome • Technicon Equipment Pty., Ltd., Sydney • Compagnie Belge Technicon, Brussels • Conitech A/S, Copenhagen

Circle No. 162 on Readers' Service Card



AT CLEMSON UNIVERSITY...

Mettler top-loading balances keep chemistry calculations out of the dorm

Clemson's general chemistry program is solidly based on experimentation. Students must carry out their work, gather data, make calculations and draw their conclusions... all in a three-hour laboratory period.

Dr. F. I. Brownley, head of the Department of Chemistry and Geology, says, "If a student has to go back to his dormitory room to work out the calculations, he loses most of the impact of the experiment. He may even put off his calculations until the last minute and end up figuring them by proportion from another person's work.

"By finishing the complete experiment in a single period, he gains a sense of accomplishment and a full awareness of the problem." Student weighings, usually a time-consuming congested activity, are improved radically by the use of the Mettler P120 top-loading balance.

Clemson has sixteen P120's in a single weighing room. These meet all the weighing needs of the 140 students in a single laboratory section – without crowding, waiting lines, or undue haste.

According to Dr. Brownley, who fondly regards Clemson students as the most destructive in the country, "The P120 is just about student-proof. Our students know that we provide them with good equipment; they take care and pride in their experimental work and this is reflected in the quality of their results."

Choosing the P120 over slower conventional instruments has enabled Clemson to meet the severe demands of 1400 students in beginning chemistry. This progressive thinking helps set the stage for the next five years, when Clemson will more than double its enrollment.

Find what the half-milligram precision and 7-second speed of the Mettler P120 can do for your weighing operations. Write for a copy of the brochure describing its use in general chemistry. Mettler Instrument Corporation, 20 Nassau St., Princeton, N. J. 08540.

Mettler®

Circle No. 66 on Readers' Service Card

AC BRIEFS

HIGHLIGHTS OF THE SCIENTIFIC AND TECHNICAL ARTICLES IN THIS ISSUE

Determination of Calcium-48 in Natural Calcium by Neutron Activation Analysis

The method for determining the ratio of calcium-48 to total calcium in natural materials relative to that of a reference standard employs precision neutron activation analysis and an EDTA weight titration of separated and purified calcium.

JAMES T. CORLESS, Graduate School of Oceanography, University of Rhode Island, Kingston, R. I.

Anal. Chem. 38, 810 (1966)

Application of Lithium-Drifted Germanium Gamma-Ray Detectors to Neutron Activation Analysis. Nondestructive Analysis of a Sulfide Ore

The results of the application of lithium-drifted germanium detectors to the nondestructive determination of minor and trace constituents in a sample of a sulfide ore are reported. The concentrations of ten elements were determined in the range 1.8×10^5 p.p.m. (iron) to 2.0 p.p.m. (gold).

J. F. LAMB, S. G. PRUSSIN, J. A. HARRIS, and J. M. HOLLANDER, Lawrence Radiation Laboratory, University of California, Berkeley, Calif.

Anal. Chem. 38, 813 (1966)

Reactor Neutron Activation Analysis. Instrumental Sensitivities in Six Matrix Materials

This paper presents experimentally determined matrix sensitivities of over 65 elements in six matrix materials: whole blood, urine, milk, tap water, "pure" water, and polyethylene.

HERBERT P. YULE, General Atomic Division/General Dynamics Corp., San Diego, Calif.

Anal. Chem. 38, 818 (1966)

Determination of Trace Amounts of Carbon, Oxygen, and Nitrogen in Metals by Spark Source Mass Spectrometry

The method, which utilizes cryosorption pumping in the source chamber, allows the simultaneous determination of C, O, and N (and other impurities) in metal samples with a limit of detection better than 0.5 p.p.m. A sample scanning technique is suggested which gives an estimate of bulk concentrations and an indication of sample homogeneity.

W. L. HARRINGTON, R. K. SKOGERBOE, and G. H. MORRISON, Department of Chemistry, Cornell University, Ithaca, N. Y.

Anal. Chem. 38, 821 (1966)

Quantitative Separation of Mercury–Thallium Mixtures

A cation exchange method and a reduction procedure were applied to mixtures ranging from Hg(II)–Tl(I) ratios of 20:1 to Tl(I)–Hg(II) ratios of 5:1

R. G. DOSCH, Sandia Laboratory, Albuquerque. N. M.

Anal. Chem. 38, 826 (1966)

Continuous Electrolytic Determination of Small Quantities of Gaseous Ammonia

The ammonia is absorbed in an aqueous solution and the resulting solution is titrated with electrolytically-generated hydrogen ions. The apparatus has been used in analyzing flow rates of ammonia from 10^{-6} to 10^{-3} mg. per second.

NEIL S. SEGAL and ROBIN WODLEY-SMITH, Department of Chemistry, University of the Witwatersrand, Jan Smuts Ave., Johannesburg, South Africa

Anal. Chem. 38, 828 (1966)

Determination of Diphenhydramine and Certain Related Compounds by Ultraviolet Spectrophotometry

In this rapid method, specific for diphenhydramine and those related compounds which extract as bases and which have a diphenylmethyl ether functional group, preliminary separation from other alkaline drugs is unnecessary. It is sufficiently sensitive to determine concentrations of the drugs in urine after therapeutic doses.

JACK E. WALLACE, JOHN D. BIGGS, and ELMER V. DAHL, Forensic Toxicology Branch, USAF Epidemiological Laboratory, Lackland Air Force Base, Texas

Anal. Chem. 38, 831 (1966)

Ultra Sensitive, Specific Method for Cyanide Using p-Nitrobenzaldehyde and o-Dinitrobenzene

Only cyanide, as little as 1.3×10^{-9} gram per ml. of total solution, of more than 35 anions tested is detectable by this procedure.

GEORGE G. GUILBAULT and DAVID N. KRAMER, Defensive Research Division, U. S. Army Edgewood Arsenal, Md.

Anal. Chem. 38, 834 (1966)

Apparatus and Procedures for Rapid Extraction and Identification of Pesticides by Single and Multiple Distribution in Binary Solvent Systems

An apparatus for the extraction of one liquid phase with another immiscible one, especially in small volumes, was applied to the analysis of pesticides. Equilibration of a solute between the phases is usually complete after 2 seconds of mechanical agitation. Many samples can be extracted simultaneously.

MORTON BEROZA, Entomology Research Division, Agricultural Research Service, U. S. Department of Agriculture, Beltsville, Md., MALCOLM C. BOWMAN, Agricultural Research Service, Tipton, Ga.

Anal. Chem. 38, 837 (1966)

Characterization of Position Isomers of Secondary Straight-Chain Alcohols and Their 3,5-Dinitrobenzoate Derivatives by Nuclear Magnetic Resonance

Proton chemical shifts of methyl groups for all position isomers of secondary straight-chain octanols, decanols, and dodecanols, and their 3,5-dinitrobenzoate derivatives are correlated empirically with the number of C-C bonds between the carbon of the methyl group and the carbon adjacent to the functional group.

CHARLES E. GODSEY, Research and Development Department, Continental Oil Co., Ponca City, Okla.

Anal. Chem. 38, 842 (1966)

THIS FLOW CELL INSTANTLY ADAPTS TRI-CARB® SPECTROMETERS TO THE CONTINUOUS RADIOASSAY OF CHROMATOGRAPHY EFFLUENTS





It takes less than a minute to position the cell in the instrument's counting chamber, and then the Tri-Carb Spectrometer becomes a Tri-Carb Flow Monitor. With it you can do both quantitative and qualitative analysis of radioactivity in liquid and gas chromatography effluents, freeing you from the need for collecting and analyzing individual fractions. Of course, the flow cell can be removed at any time to resume normal sample counting. ▪ Flow Cells are also available (in suitably shielded detectors) as part of complete Tri-Carb Flow Monitor Systems. There are sixteen different systems with choice of one or two channels of analysis, analog or digital readout, floor or bench models. Call your Packard Sales Engineer for complete information or request Bulletin 1075 from Packard Instrument Company, Inc., 2200 Warrenville Road, Downers Grove, Illinois 60515.

Packard

Kinetics of Bromination of Certain Substituted 8-Quinolinols

A constant current generator and an amperometric indicator system were used to measure the rates of bromination of 8-quinolinol and its 4-methyl, 5-bromo, 5-chloro, and 5-fluoro derivatives in acid solutions in the presence of bromide ions. The bromide molecule was the active brominating agent when bromination occurred in the 5-position. For bromination in the 7-position, the tribromide ion as well as the molecular bromine was used.

GEORGE O'DOM and QUINTUS FERNANDO, Department of Chemistry, University of Arizona, Tucson, Ariz.

Anal. Chem. 38, 844 (1966)

Intermolecular Energy Transfer as a Means of Chemical Analysis. Sensitization of Rare Earth Emission in Dilute Solution by Aromatic Carbonyl Compounds

An empirical equation was developed to facilitate prediction of sensitization by a specific aromatic carbonyl compound for a specific rare earth. The system was excited by monochromatic light at the wavelength of maximum absorption for the phosphorescence transition of the carbonyl compound, and emission was measured at the wavelenth corresponding to the rare earth ion emission line. Analytical possibilities are discussed.

W. J. McCARTHY and J. D. WINEFORDNER, Department of Chemistry, University of Florida, Gainesville, Fla.

Anal. Chem. 38, 848 (1966)

Rapid Determination of Primary Hydroxyl Content of Poly(Oxyalkylene) Glycols and Poly(Oxyalkylene) Sorbitols by Pseudo First-Order Differential Reaction Kinetics

A differential pseudo first-order reaction rate approach is described which requires only a fraction of the analysis time of the conventional extrapolation method and does not need a calculation procedure.

FRISO WILLEBOORDSE and R. L. MEEKER, Chemicals Division, Union Carbide Corp., Technical Center, South Charleston, W. Va.

Anal. Chem. 38, 854 (1966)

Synthesis of Tetranitrobenzylpolystyrene Resin for Chromatographic Stationary Phase

The synthesis consists of Friedel-Crafts benzylation of crosslinked divinylbenzene–polystyrene copolymer, followed by nitration. The resin is stable to heat to at least 160° C., not affected by prolonged exposure to the atmosphere, and exhibits the chemical properties of 2,4-dinitrophenyls.

JAMES T. AYRES and CHARLES K. MANN, Department of Chemistry, Florida State University, Tallahassee, Fla. 32306

Anal. Chem. 38, 859 (1966)

Column Chromatography with Tetranitrobenzylpolystyrene Resin Stationary Phase

The curve for acetone elution of a mixture of tetraphenylethylene, *m*-terphenyl, and phenanthrene, a study of solvent effects with acetone and acetone–hexane eluents, and chromatographic R values to describe elution characteristics of 26 compounds are presented.

JAMES T. AYRES and CHARLES K. MANN, Department of Chemistry, Florida State University, Tallahassee, Fla. 32306

Anal. Chem. 38, 861 (1966)

←See Buyers' Guide for all products/sales offices.
←Circle No. 73 on Readers' Service Card

Electrolysis with Constant Potential. Diffusion Currents for the Formation of an Amalgam at a Hanging Mercury Drop Electrode

The potentiostatic reduction of Cd(II) near the formal $E°$ of the system Cd(II)/Cd(Hg) was studied to verify the theory.

WILLIAM G. STEVENS and IRVING SHAIN, Chemistry Department, University of Wisconsin, Madison, Wis.

Anal. Chem. 38, 865 (1966)

The Depletion Effect in Pulse Polarography with Stationary Electrodes

The depletion effect is described from both theoretical and experimental approaches. Both stirring and proper choice of resting potential can eliminate this effect in applications of normal pulse polarography.

K. B. OLDHAM and E. P. PARRY, North American Aviation Science Center, Thousand Oaks, Calif. 91360

Anal. Chem. 38, 867 (1966)

Polarographic Study of the Iodine–Iodide Couple at the Rotating Platinum Electrode

Results of a voltammetric investigation of the oxidation of iodide in 0.1M $HClO_4$ indicate that the formation of triiodide must be considered in the polarographic equation. The investigation elucidates anomalous anodic and cathodic peak behavior at the electrode.

E. CLIFFORD TOREN, Jr., and CHARLES P. DRISCOLL, Department of Chemistry, Duke University, Durham, N. C.

Anal. Chem. 38, 872 (1966)

Coulometric Generation of Hydrogen Ions in Water and Methanol Using Hydrogen-Permeable Membrane Electrodes

As an illustration of the analytical potentialities of the easily-fabricated membrane electrode described, 2-amino, 2-(hydroxymethyl)-1,3-propanediol was titrated in water and in methanol.

THOMAS R. BLACKBURN and ROSALIND B. GREENBERG, Department of Chemistry, Wellesley College, Wellesley, Mass. 02181

Anal. Chem. 38, 877 (1966)

Reversible Charge Transfer at the Tubular Platinum Electrode

Current–potential equations for the reversible charge transfer at the tubular platinum electrode have been theoretically derived and experimentally verified with the ferricyanide–ferrocyanide system.

W. L. BLAEDEL and L. N. KLATT, Department of Chemistry, University of Wisconsin, Madison, Wis.

Anal. Chem. 38, 879 (1966)

WHY YOU SHOULD INVESTIGATE SADTLER RESEARCH . . .

"Sadtler is a research laboratory that speeds the growth of other companies"

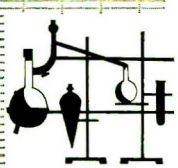
The above quotation is how one of Sadtler's many satisfied customers recently described the company's unique experience and facilities.

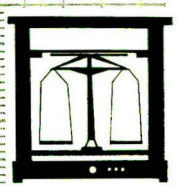
The Sadtler record is impressive. It has made important contributions to the sciences, helped spur the growth of many industrial giants, and materially furthered innumerable Government and university research projects.

The basic phenomenon of pH was introduced to industry by Sadtler. Its studies of air pollution was instrumental in establishing industrial pollution controls. Industry and the peoples throughout the world have benefited from its work on tobacco, cigarette filters, petroleum refining, asphalt, minerals, ores, paper making, food, chemicals and other processes.

The modern and highly sophisticated research and chemical analysis facilities of Sadtler Research offer you laboratory equipment and an experienced research group that is difficult to match anywhere.

Following are some of the many Sadtler services:





SADTLER STANDARD SPECTRA — A comprehensive collection of 29,000 reference infrared prism spectrograms of pure organic materials. Additions are made annually to keep up with new compounds of both research and industry.

SADTLER STANDARD ULTRAVIOLET SPECTRA — Those chemical compounds, included in the infrared collection, that absorb in the ultraviolet region have been selected for this useful compendium of 16,000 ultraviolet spectra. Indices and the unique Locator are part of the collection.

COMMERCIAL INFRARED SPECTRA — A collection of 12,000 infrared spectra of commercially available compounds — agricultural chemicals; polyols; surface active agents; natural resins and gums; monomers and polymers; pyrolyzates; plasticizers; perfumes and flavors; fats, waxes and derivatives; lubricants; rubber chemicals; fibers; solvents; intermediates; petroleum chemicals; textiles chemicals; dyes, pigments and stains.

NMR — Spectra determined on a Varian A-60A instrument are included in this collection with integration of the curves and spectral assignments. All compound information is found with the spectra and locating them is made easy by use of complete Indices, by name, molecular formula, chemical class and chemical shift.

DTA — Thermograms of both commercially available and research materials are included with interpretation of the graphs. Materials such as monomers, polymers, agricultural chemicals and pharmaceuticals are present.

INORGANICS — Grating spectra covering the region of 2.5 to 40 microns of classical inorganics and coordination compounds make up this collection.

PHARMACEUTICALS—Infrared and ultra violet spectra, when applicable, of commercially available pharmaceutical products listed in the leading drug books comprise this group. Additions are made.

BIOCHEMICALS — Infrared and ultraviolet spectra of compounds of interest to the biochemist are included in this group of 2,000 infrared and over 650 ultra violet spectra.

STEROIDS — A publication containing 250 prism spectra from 2 to 15 microns and 250 grating spectra from 2.5 to 40 microns of steroids. Additions are made to this group employing the grating instrument.

MULTIPLE INDEXING:

Alphabetical—Chemical Abstracts nomenclature classified by parent compounds and substituent derivatives.

Molecular Formula—Compounds listed by increasing order of carbon, hydrogen and other atoms.

Chemical Classes — Location of any single spectrum or group of spectra by functional group.

Numerical — Quickly identifies spectra where Sadtler Serial Number is known but name is not.

Spec Finder—A Sadtler technical reference book method for Standard IR and Commercial IR.

UV Locator—A Sadtler technical reference book method for identification of unknown Ultra Violet Spectra.

LABORATORY SERVICES — Thermoanalysis • Infrared Spectroscopy • N.M.R. Spectroscopy • Food & Drug Analysis • Gas Chromatography • Organic Analysis • Analytical Testing • Polymer Research • Ultra Violet Analysis • Analysis of Commercial Products • Consultation.

IR COMPUTER SERVICE — Unknown samples searched and results reported within 72 hours.

TAPE RENTAL SERVICE—For searching IR and UV spectra. Available to laboratories equipped with or having access to computer installations.

SADTLER COURSES — Unique five-day courses to qualified personnel in the latest techniques in laboratory instrumentation.

Write for brochures including sample spectras

3330 Spring Garden Street PHILADELPHIA, PA. 19104

Agents in principal countries of the world

SADTLER RESEARCH LABORATORIES, INC.

Circle No. 83 on Readers' Service Card

Twin-Electrode Thin-Layer Electrochemistry. Determination of Chemical Reaction Rates by Decay of Steady-State Current

A continuous monitor of reactant concentration with time, provided by the steady-state current attainable with a twin-electrode thin-layer cell, was applied to the study of the rate of the benzidine rearrangement under varying conditions of acidity and ethanol concentration. The method appears to be generally applicable in the study of rates of first- or higher-order chemical reactions.

BRUCE McDUFFIE, LARRY B. ANDERSON, and CHARLES N. REILLEY, Department of Chemistry, University of North Carolina, Chapel Hill, N. C.

Anal. Chem. 38, 883 (1966)

Comprehensive Computer Program for Electron Probe Microanalysis

A program for calculating composition from x-ray data can be used with several calculation procedures including absorption, fluorescence, and atomic number corrections. The comparison of calculation procedures and the evaluation of errors associated in parameter uncertainties are facilitated.

JAMES D. BROWN, Bureau of Mines, College Park Metallurgy Research Center, U. S. Department of the Interior, College Park, Md.

Anal. Chem. 38, 890 (1966)

Optical and Electron Microscope Studies of Thin Fuel Cell Electrode Structures

The physical structure of platinum–Teflon catalyzed grid-typed electrodes was characterized. Examinations showed that the platinum part of the electrode consisted of loosely packed flocculates intermixed with fibrils of Teflon and spherical-shaped particles of Teflon.

WILLIAM R. LASKO and GERALD P. McCARTHY, United Aircraft Research Laboratories, East Hartford, Conn.

Anal. Chem. 38, 894 (1966)

Photochemical Determination of Oxalate

The two indirect methods described are based on the photochemical decomposition of ferric oxalate complexes in aqueous acidic solution. One which is applicable for 10 to 100 mg. of sodium oxalate has a detection limit of 5 μg. The other method is useful in the milligram range.

WILLIAM M. RIGGS and CLARK E. BRICKER, Department of Chemistry, University of Kansas, Lawrence, Kan.

Anal. Chem. 38, 897 (1966)

Determination of Dissolved Polonium-210 in Water by Coprecipitation with Tellurium by Stannous Chloride

The doubly precipitated tellurium–polonium-210 precipitates are alpha counted on 0.22-micron membrane filters. A single-precipitation method is also presented. Both methods have sufficient sensitivity to permit their use in the determination of lead-210 in water by polonium-210 ingrowth.

D. E. RUSHING, Colorado River Basin Water Quality Control Project, U. S. Department of Health, Education, and Welfare, 1750 South Redwood Road, Salt Lake City, Utah 84104

Anal. Chem. 38, 900 (1966)

Scientific Communication

Liquid–Liquid Extraction of Anionic Americium and Europium Complexes of Hydroxyethylethylenediaminetriacetic Acid and Diethylenetriaminepentaacetic Acid

FLETCHER L. MOORE, Oak Ridge National Laboratory, Oak Ridge, Tenn.

Anal. Chem. 38, 905 (1966)

Correspondence

Spectrophotometric Determination of Tertiary Aromatic Amines in the Presence of Primary and Secondary Amines by Complexation with Tetracyanoethylene

GEORGE H. SCHENK, PETER WARNER, and WILLIAM BAZZELLE, Department of Chemistry, Wayne State University, Detroit, Mich. 48202

Anal. Chem. 38, 907 (1966)

Mercurimetric Determination of Organic Disulfides Using Reaction with Butyllithium

STIG VEIBEL and MIECZYSLAW WRONSKI, Department of Organic Chemistry, Technical University, Copenhagen, Denmark

Anal. Chem. 38, 910 (1966)

Spectrophotometric Determination of Copper in Lead, Tin. Aluminum, Zinc, and Their Alloys with Biscyclohexanone Oxalyldihydrazone

R. K. ROHDE, Non-Ferrous Metals Division, Brooklyn Works, Laboratory, W. Brown & Sons (Vic.) Pty., Ltd., Melbourne, Australia

Anal. Chem. 38, 911 (1966)

Determination of Sulfur in Inorganic Sulfides Using Oxygen Flask Combustion

ARNOLD R. JOHNSON, Jr., and GARY B. McVICKER, Department of Chemistry, University of Wyoming, Laramie, Wyo.

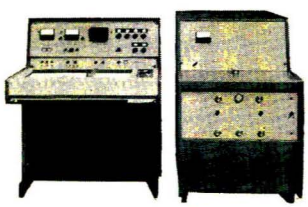
Anal. Chem. 38, 913 (1966)

Spectrophotometric Determination of Cobalt in Iron and Steel with 2-Nitroso-1-Naphthol

MANUEL NEEDLEMAN, Department of Supply, Defence Standards Laboratories, Australian Defence Scientific Service, Maribyrnong, Victoria, Australia

Anal. Chem. 38, 915 (1966)

does a mass spectrometer have to be massive?



no!

Our new M-66 cycloidal mass spectrometer is pretty compact, as these instruments go. It has a price to match, too—about $45,000.

In previous ads, we've told you that it can go to mass 2000, and has resolution $\geqslant$ 2000. But are you aware that this is a double-focusing instrument with precise mass measurement capabilities? Or that it has direct sample introduction? A total ion current monitor?

If any of that's news to you, there may be other points about this exciting new analytical instrument you'd like to know. Just drop us a card at 611 Hansen Way, Palo Alto, California 94303, or contact your nearest Varian field sales office. We'll be glad to fill you in.

varian
analytical instrument division

Circle No. 21 on Readers' Service Card

Spectrophotometric Determination of Cyclohexanone Oxime in Sulfuric Acid Solution of Epsilon-Caprolactam

YOSHINARI KOBAYASHI, Nagoya Research Laboratory, Toyo Rayon Co., Nagoya, Japan

Anal. Chem. 38, 917 (1966)

Gravimetric Determination of Palladium with Di-2-Thienylketoxime

WILLIAM J. HOLLAND and JESSE GERARD, Department of Chemistry, University of Windsor, Windsor, Ontario, Canada

Anal. Chem. 38, 919 (1966)

Note on the Determination of Lead in Gasolines by Atomic Absorption Spectrometry

H. W. WILSON, British American Research and Development Co., Sheridan Park, Ontario, Canada

Anal. Chem. 38, 920 (1966)

Analysis of α-Olefin-Derived Sodium Sulfonates by Ion Exchange and Potentiometric Titrimetry

EDWIN H. GRIFFIN, Jr. and EDGAR W. ALBAUGH, Gulf Research & Development Co., Pittsburgh, Pa.

Anal. Chem. 38, 921 (1966)

A Simple and Accurate Calibration Model for Hydrogen-Content, Beta-Particle Transmission Gauges

ROBIN P. GARDNER and KENNETH F. ROBERTS, Measurement and Controls Laboratory, Research Triangle Institute, P. O. Box 490, Durham, N. C. 27702

Anal. Chem. 38, 923 (1966)

Extraction of Metal Pyridine Azides. Spectrophotometric Determination of Copper, Nickel, and Palladium

RAY G. CLEM and E. H. HUFFMAN, Lawrence Radiation Laboratory, University of California, Berkeley, Calif.

Anal. Chem. 38, 926 (1966)

Use of an Alkali Additive for Gas Chromatographic Analysis of Organic Bases on Open Tubular Columns

E. W. CIEPLINSKI, Perkin-Elmer Corp., Norwalk, Conn.

Anal. Chem. 38, 928 (1966)

Polarographic Behavior in the Oxidation of Sodium Formaldehyde Sulfoxylate

REMIGIO FERNANDEZ-MARTIN, R. G. RINKER, and W. H. CORCORAN, Chemical Engineering Laboratory, California Institute of Technology, Pasadena, Calif.

Anal. Chem. 38, 930 (1966)

Chelometric Titration for Zinc in Municipal and Industrial Water Supplies

JAMES J. HICKEY and CHARLES J. OVERBECK, Analytical Laboratory, Nalco Chemical Co., 6216 W. 66th Pl., Chicago, Ill. 60638

Anal. Chem. 38, 932 (1966)

Quantitative Determination of Impurities in Salicylic Acid

NORMAN E. SKELLY, Special Services Laboratory, The Dow Chemical Co., Midland, Mich.

Anal. Chem. 38, 934 (1966)

Stability Constants of Some Dihydrazide Complexes of Cadmium

ALAN F. KRIVIS, GEORGE R. SUPP, and RICHARD L. DOERR, Chemicals Division Research, Olin Mathieson Chemical Corp., New Haven, Conn.

Anal. Chem. 38, 936 (1966)

Trace Impurity Analysis of Plutonium–Uranium–Zirconium Alloys by Anion Exchange–Partition Chromatography

EDMUND A. HUFF and STANLEY J. KULPA, Argonne National Laboratory, Argonne, Ill.

Anal. Chem. 38, 939 (1966)

When you buy our Multipoint... be prepared for surprises



10 at least*

X's indicate standard features at no extra cost	Esterline Angus	Brands (Names available on request) A	B	C	D
List price $1450 or lower	X			X	
Solid state amplifier	X		X		
50,000 ohm off balance input impedance or better	X				
Stray rejection: longitudinal 60 cycles AC, 1,000 times span or 120 volts	X		X		
Accuracy ±¼% span or ±3½ microvolts or better	X		X		
Manual point advance. Dial in any point without disturbing synchronization	X				
Permanently sealed slidewire requires no cleaning	X				
5 chart speeds	X				
Choice of 8 print frequencies from 1½ to 60 seconds per point	X				
Tilt out writing platen and chart tear-off bar	X				

Discover additional surprises, such as optional electrical programmed printing which permits point skipping as fast as ¼ second. Write for Series "E" Catalog.

Esterline Angus Instrument Company, Inc.
Box 24000AC • Indianapolis, Indiana 46224

Excellence in instrumentation for over 60 years

ESTERLINE ANGUS

Circle No. 39 on Readers' Service Card

AC BRIEFS

Aids for Analytical Chemists

A Semiautomatic Device for Measuring and Drawing Mass Spectra

RICHARD N. STILLWELL, Department of Biochemistry, Baylor University, College of Medicine, Houston, Texas

Anal. Chem. 38, 940 (1966)

Stainless Steel Capsule with Iron "Window" for Determining Hydrogen in Alkali Metal by Vacuum Extraction

JOSEPH W. GLASS, CHRIS M. LARSEN, and JAMES M. SCARBOROUGH, Atomics International, A Division of North American Aviation, Inc., P. O. Box 309, Canoga Park, Calif.

Anal. Chem. 38, 942 (1966)

Improvements in Carbon-14 Assay of Organic Compounds by Dry Combustion

MASAYUKI HAMADA and EIKO KAWANO, Radiation Center of Osaka Prefecture, Sakai, Osaka, Japan

Anal. Chem. 38, 943 (1966)

Indium Capsules for Microdetermination of Carbon and Hydrogen

G. E. SECOR and L. M. WHITE, Western Utilization Research and Development Division, Agricultural Research Service, U. S. Department of Agriculture, Albany, Calif. 94710

Anal. Chem. 38, 945 (1966)

Computerized Procedure for Editing Data from a Mass Spectrometer Digitizer

H. EVERT HOWARD, Union Oil Co. of California, Union Research Center, P. O. Box 76, Brea, Calif. 92621

Anal. Chem. 38, 946 (1966)

High Sensitivity Oxygen Analysis of Metallic Samples with Fast Neutrons

RICHARD W. BENJAMIN, KENNETH R. BLAKE, and IRA L. MORGAN, Texas Nuclear Corp., Austin, Texas

Anal. Chem. 38, 947 (1966)

Pulseless High-Pressure Pump for Liquid Chromatography

R. E. JENTOFT and T. H. GOUW, Chevron Research Co., Richmond, Calif.

Anal. Chem. 38, 949 (1966)

The Purity, Properties, and Analytical Determination of 4-sec-Butyl-2-(α-Methylbenzyl) Phenol

B. Z. EGAN and W. D. ARNOLD, Oak Ridge National Laboratory, Oak Ridge, Tenn.

Anal. Chem. 38, 950 (1966)

florisil®

Description . . . Highly selective, synthetic chromatographic adsorbent. An extremely white, hard, granular or powdered magnesia-silica gel frequently referred to as magnesium silicate.

Uses . . . In preparative and analytical chromatography and in production for the separation and isolation of a variety of compounds.

Available Grades . . . Standard mesh sizes of 16/30, 30/60, 60/100, 100/200 and -100 mesh. Packaged in 1, 5, 10, 25 and 50-pound containers.

Chemical Composition

MgO	15.5 ± 0.5%
SiO_2	84.0 ± 0.5%
Na_2SO_4	0.5% avg (1.0% max)

Physical Properties

Color	White
pH	8.5
Surface Area, M^2/g (BET method)	298
Specific Gravity	2.51
Surface Acidity, pKa	1.5 approx.
Voids, %	26

Produced by Floridin Company and also distributed by Fisher Scientific Company.

Floridin

FULLER'S EARTH • ATTAPULGITE CLAY • ACTIVATED BAUXITE

Plant: Quincy, Florida. Sales Offices: 375 Park Ave., New York • 2 Gateway Center, Pittsburgh 3390 Peachtree Road, Atlanta • 8000 Bonhomme Ave., St. Louis • 5645 Milton Street, Dallas

TWO CUT-OUTS WORTH CUTTING OUT

FLORIDIN COMPANY, Two Gateway Center, Pittsburgh, Pa. 15222

( ) Please send complete FLORISIL information.

( ) Please send a test sample of FLORISIL.

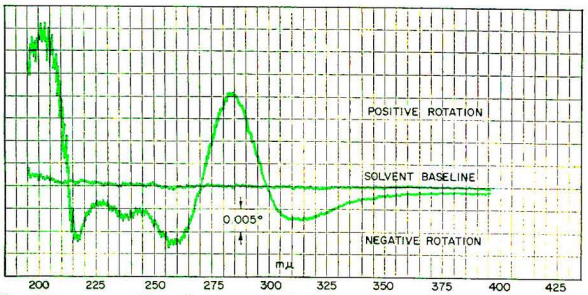
Name & Title_____

Company_____

Address_____

City & State_____

Circle No. 44 on Readers' Service Card



Ultraviolet rotatory dispersion curve obtained from 10 μg of iso-chlorotetracycline.

ON GETTING TO KNOW YOUR OPTICALLY ACTIVE SAMPLE

Optical rotatory dispersion (ORD) and *circular dichroism* (CD), when used as complementary tools for exploring the structure of optically active molecules, have become indispensable techniques in the laboratory. The recent availability of reliable, well-performing ORD and CD instruments, transforming a once difficult measurement into a laboratory routine, has encouraged widespread use of these techniques.

This new class of ORD and CD instruments has been used in studies of such optically active substances as steroids, alkaloids, proteins, polypeptides, nucleic acids, triterpenes, synthetic polymers, and many others. A partial list of the types of information that may be derived from the use of ORD-CD would include:

- conformation and configuration of molecules
- stereochemical characteristics
- kinetic properties
- concentrations of optically active components in mixtures
- secondary structure of high molecular weight substances

Maximum capability for conducting these studies is available in the Durrum-Jasco[1] Recording Spectropolarimeter, which combines in a single instrument the complementary techniques of ORD and CD. This dual capability, offered at a price lower than some instruments having ORD or CD only, puts the acquisition of both valuable techniques well within the budgetary reach of many laboratories. Among the instrument's basic features are numbered:

- modes for measuring ORD, CD, absorbance, and per cent transmittance in one instrument
- wavelength range from 185 to 700 mμ
- circular dichroism sensitivity of 2×10^{-5} O.D.
- angular rotation sensitivity of 0.001°
- simultaneous recording of slit width and photomultiplier voltage along with spectra
- $32,000 for ORD and CD; $22,950 for ORD only (price includes installation, training of operators, two preventive maintenance calls, and one year's warranty)

A 16-page reprint entitled "Applications of Optical Rotatory Dispersion and Circular Dichroism in Stereochemistry" is now available. For a free copy, plus the new brochure describing the Durrum-Jasco instrument, write to:

(1) Japan Spectroscopic Company, Ltd.

DURRUM

Durrum Instrument Corp., 925 E. Meadow Drive, Palo Alto, California 94303
Telephone (415) 321-6302

Circle No. 103 on Readers' Service Card

explosion safe chemical refrigerators

Why rework a cabinet to make it explosion safe when you can buy one especially engineered and ready to plug in?

Be completely safe with a Puffer-Hubbard refrigerator.

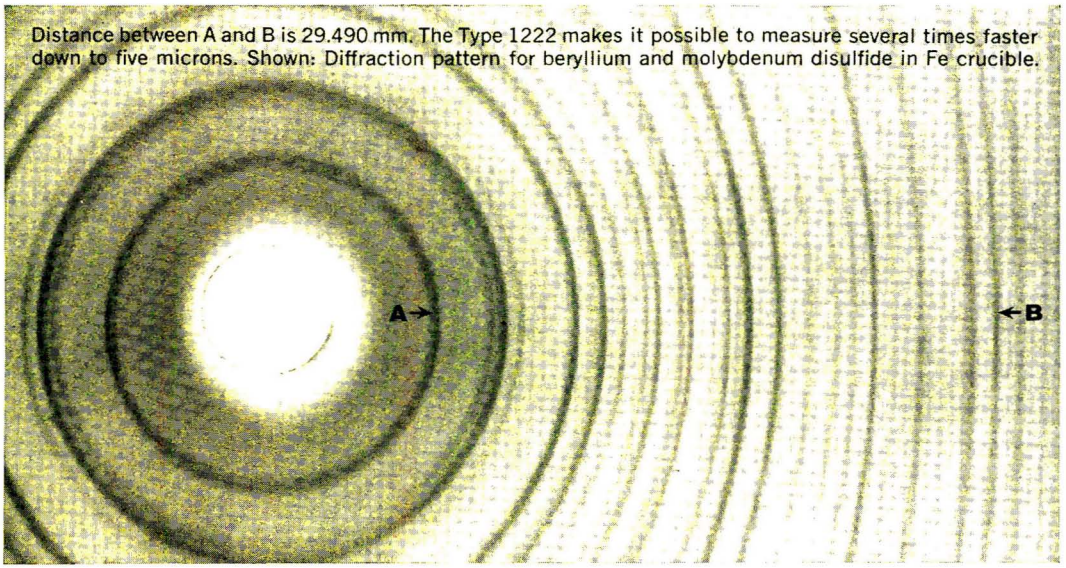


- Adjustable Temperature Control Outside Cabinet.
- Adjustable Stainless Steel Roll-Out Drawers or Shelves.
- Special Pressure Relief Hardware. Magnetic Gasketing . . . Magnetic Latch.
- All Porcelain Construction — Inside and Out . . . Available in a Wide Range of Sizes from 4 Cu. Ft. to 69 Cu. Ft.

Name of your local representative available upon request.

PUFFER-HUBBARD
REFRIGERATOR DIVISION
Challenge Stamping & Porcelain Co.
GRAND HAVEN, MICHIGAN
TELEPHONE 616 842-2080

See Buyers' Guide for all products/sales offices.
Circle No. 82 on Readers' Service Card

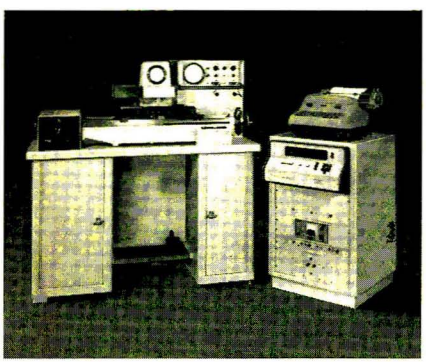


Distance between A and B is 29.490 mm. The Type 1222 makes it possible to measure several times faster down to five microns. Shown: Diffraction pattern for beryllium and molybdenum disulfide in Fe crucible.

Now measure X-ray diffraction spectra with 20 times greater accuracy.

With the Mann Type 1222 Photoelectric Line Setting Instrument you can measure diffraction line positions more precisely and quickly than ever before—without introducing visual errors. You can also determine film densities with higher accuracy.

The Type 1222 is a complete data reduction and recording instrument. It has a film-measuring precision comparator...a photoelectric setting device for accurately positioning the line of interest on the reference axis ...a digital readout for recording the information by typewriter, card punch or tape punch.



Line center is found by using the oscilloscope. The density profile of the line is presented on the scope face as the line is scanned first from one side, then the other. The profile traces are therefore mirror images, and center is where the peaks coincide. Photoelectric setting is far more accurate and reproducible than visual methods. Faint lines, previously unusable, can now be measured.

Density readings taken from the oscilloscope are manually entered into the memory of the digitizer. The operator presses a foot switch to record density and position on an output writer or other recorder. If desired, the density reading can be recorded during a continuous power scan.

The X-coordinate allows you 380 mm of travel and the Y-coordinate provides 50 mm of cross-motion. There is also a pivot table that permits motion for precise alignment in X. Maximum error is ± 0.005 mm or .003% of stage travel, giving an accuracy 20 times greater than usual methods of measuring X-ray diffraction films.

With modifications, the Mann Type 1222 Photoelectric Line Setting Instrument may be used in optical mass spectrography and electron diffraction analysis. For more details on the construction, operation and capabilities of this advanced instrument and recording system, write today for our new Mann Type 1222 brochure.

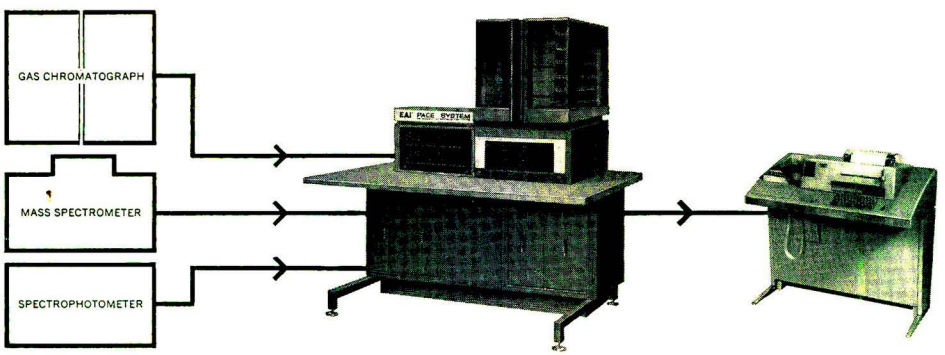
DAVID W. MANN COMPANY
182 Middlesex Tpke., Burlington, Mass. 01804, Tel: 617-272-5600

DIVISION OF GCA CORPORATION

Circle No. 11 on Readers' Service Card

Put in the sample. Push the "go" button.

Out come the finished reports.



That's modern analysis with the EAI® PACE System

For the first time you can get truly automatic analytical data processing.

The EAI PACE (Precision Analytical Computing Equipment) System is a real-time, digital-computer-based system which processes automatically the electrical signals generated by analytical instruments.

All the lab technician does is introduce the sample and signal the PACE System. There's no need to manually attenuate or monitor the signal. The System will do it. There's no need for strip chart recorders or analysis of graphs. When the run is completed, a printed report of the analysis is ready for distribution.

Results are more accurate, consistent and reliable. Speed is limited only by instrument speed. Economies can be tremendous, particularly for larger laboratories. One technician can now run up to 10 gas chromatographs at a time.

PACE will simultaneously process—by time-sharing—chromatographs, mass spectrometers, spectrophotometers, NMR spectrometers, physical testing machines—in fact, virtually any analytical instruments.

Potential? An expanded PACE System can process signals from 40 or more gas chromatographs plus a complement of other instruments . . . simultaneously.

And the PACE System is more than just hardware—it is a fully-operating system. You get—1. Equipment 2. Complete Software 3. Pre-installation planning and training 4. Start-up assistance and maintenance. And, EAI tailors this system to your individual needs.

Read our 20-page booklet "Breakthrough for Analytical Chemistry". It describes the System, its operation and advantages. Send for it today.

EAI® ELECTRONIC ASSOCIATES, INC., *West Long Branch, New Jersey*

Circle No. 76 on Readers' Service Card

Circle No. 171 on Readers' Service Card ⟶

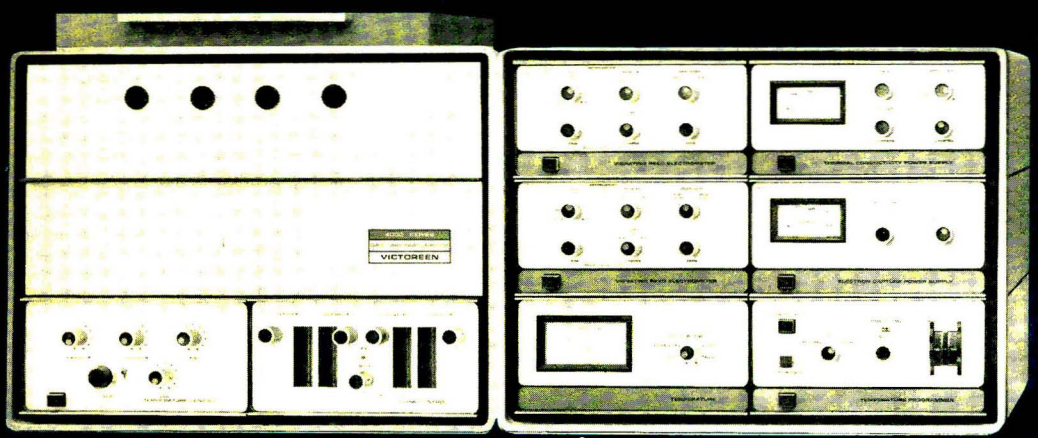
UNIMODULAR 4000 SERIES GAS CHROMATOGRAPHS FOR CHEMICAL, BIOMEDICAL, PESTICIDE ANALYSIS

EXCLUSIVE FEATURES – All Standard

Most advanced 4-column oven – allows unparalleled column-detector combinations. All-glass or metal columns. ■ **4 universal injection ports.** For use with 1/16 to 3/4" columns. ■ **Up to 4 detector ovens,** each individually temperature controlled on standby for immediate operation. ■ **Vibrating reed electrometer.** All solid-state design. Drift less than 1% per month. Sensitivity 3×10^{-13} amps. ■ **Digital Log Electrometer.** 1000-fold range increase. No switching or attenuation. For use with standard recorder. ■ **Priced from $2095.** Nowhere else can you obtain the combination of desirable features – plus exclusive Victoreen features – found in GC4000 Series instruments. For versatility... accuracy... stability... economy Victoreen Gas Chromatographs lead the entire field.

6960-A

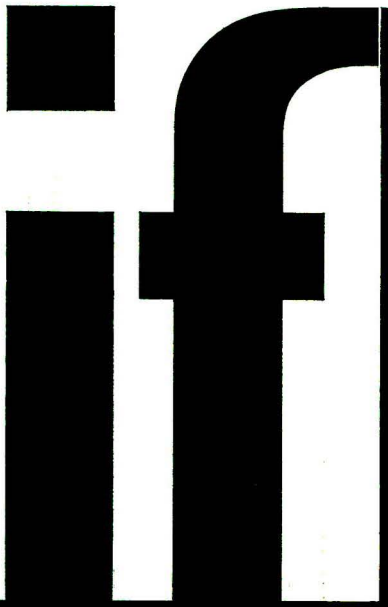
VICTOREEN



Research 4000 Series Instrument System

Analytical Instrumentation Division
THE VICTOREEN INSTRUMENT COMPANY
10101 WOODLAND AVENUE • CLEVELAND, OHIO 44104
EUROPEAN SALES OFFICE: GROVE HOUSE, LONDON RD., ISLEWORTH, MIDDLESEX, ENGLAND

VICTOREEN



YOU WANT

to add another mode to your counting system...

to increase your counting capacity...

to automate your manual counting system...

you can save up to 35% with Tracerlab System Modules

That's right. In nuclear counting systems, the Tracerlab Systems Module Concept can give you exceptional flexibility and versatility by making the most of your present equipment.

Tracerlab System Modules enable you to buy just one additional instrument for major gains in capability — instead of starting all over again.

Result: You can switch from one type of analysis to another, from single to multiple counting modes, from manual to fully automatic operation — simply by buying an additional unit each time.

Or buy one type of system and add on any type of sample changer at a future date — and you get total system versatility at lowest cost.

All Tracerlab nuclear counting System Modules are based on the Systems Module Concept, and are fully compatible with each other as well as other makes of instruments now in use.

So: Take one instrument, add another, plug them together — and you've got a system. Add another instrument—and you've got still another system.

Call your Tracerlab sales representatives for a complete preview on all the permutations possible (8758 so far!) with Tracerlab System Modules. He'll help you pick the one you need — and soon you'll be counting your money as well as your samples!

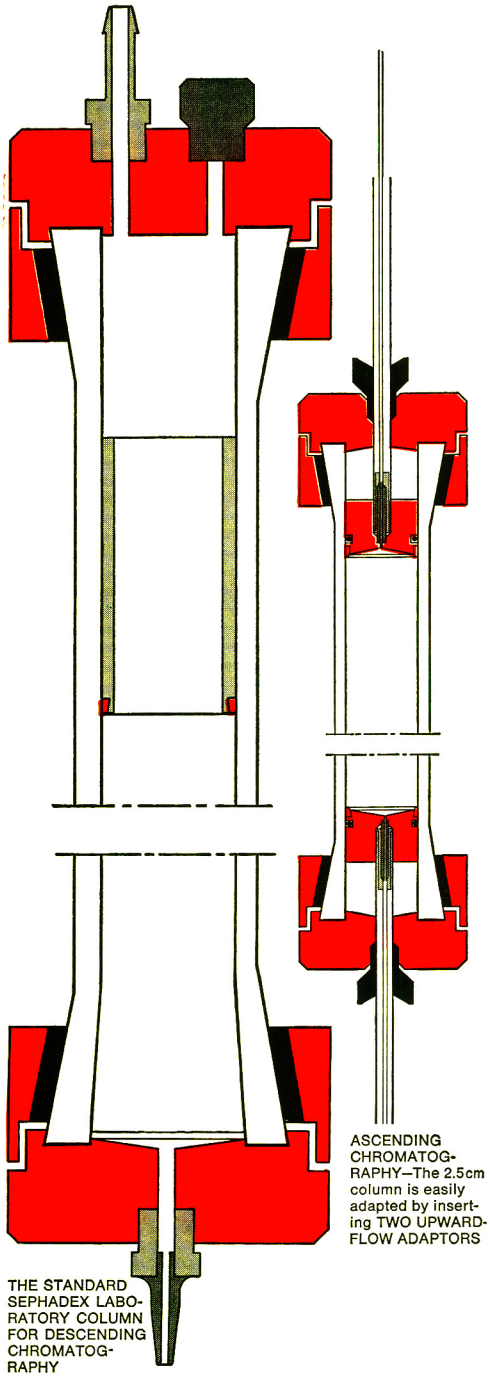
LFE | TRACERLAB

A Division of Laboratory For Electronics, Inc.
WALTHAM, MASSACHUSETTS 02154

Richmond, California • Malines, Belgium • Sales Offices in Principal Cities

Film Badge Service • Health Physics • Bioassays • Sources • Nuclear Instrumentation • Radiochemicals
Radioactive Waste Disposal • Radiation Monitoring Instrumentation • Isotope Applications

Circle No. 121 on Readers' Service Card



THE STANDARD SEPHADEX LABORATORY COLUMN FOR DESCENDING CHROMATOGRAPHY

ASCENDING CHROMATOGRAPHY—The 2.5cm column is easily adapted by inserting TWO UPWARD-FLOW ADAPTORS

Especially designed for Gel Filtration Chromatography Ion Exchange Chromatography

Sephadex®

Laboratory Columns

A product of over six years' research know-how brings you these "exclusive" column features:

1. SPECIAL DESIGN BED SUPPORT—eliminates troublesome sintered glass disc
2. MIXING CHAMBER—of less than 1/10% of bed volume minimizes sample dilution to insure optimal zone sharpness for critical separations
3. INERT NYLON NETTING—on both the sample applicator and bottom endpiece eliminates adsorption of biologic material
4. DESCENDING TO ASCENDING SYSTEM—easily converted by replacing both endpieces with upward-flow adaptors
5. SAMPLE APPLICATOR—distributes the sample evenly over the bed surface to insure sharp zones for critical separations and protects as well as stabilizes the bed
6. SELECTED CONSTRUCTION MATERIALS—to avoid destruction of sensitive biologic materials

AVAILABLE SEPHADEX COLUMNS AND ACCESSORIES

Type	Size cm	ACCESSORIES Cooling Jacket	Sample Applicator	Upward-Flow Adaptors
K 15/30	1.5x30	–	–	–
K 15/90	1.5x90	–	–	–
K 25/45	2.5x45	–	S	O
K 25/45 "Jacketed"	2.5x45	S	S	O
K 25/100	2.5x100	–	S	O
K 25/100 "Jacketed"	2.5x100	S	S	O
K 50/100 "Jacketed"	5.0x100	S	–	S
SEPHADEX COLUMN "SR" RESISTANT TO ORGANIC SOLVENT				
SR 25/45	2.5x45	–	–	S

S = Standard Accessories O = Optional Accessories

UPWARD-FLOW ADAPTORS	
Upward-Flow Adaptors	To fit all K 25 Sephadex Lab. Columns

Information Service A comprehensive reference list, abstract cards, and other information on Sephadex products are available. Direct inquiries on your letterhead to the local Pharmacia representative or to:

PHARMACIA FINE CHEMICALS INC.
800 Centennial Avenue, Piscataway, N.J. 08854
Pharmacia (Canada) Ltd., 110 Place Crémazie, Suite 412, Montreal 11, P.Q.
(Inquiries outside U.S.A. or Canada should be directed to PHARMACIA FINE CHEMICALS, Uppsala, Sweden.)

See Buyers' Guide for all products/sales offices.
Circle No. 75 on Readers' Service Card

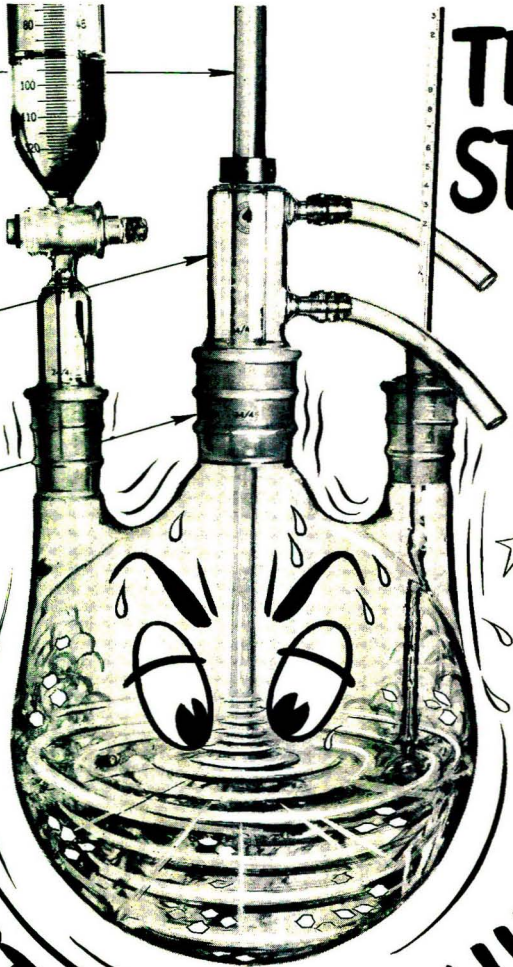
TRUBORE® STIRRERS

Stir Best!

Rods are plateau ground for smoothness, lubricant retention.

Bearings and rod guaranteed interchangeable. Smooth transparent surfaces reduce leak path. Every rod and bearing is individually inspected and air gauged (clearance must be less than 0.001").

Joints available ground or Teflon Clad.



Frustrating problem? Get rid of your frustrations—order Trubore Stirrer and

STIR MADLY !!!



STIR-LUBE Lubricant 3X capacity of comparable petroleum oils.

Performance assured by individual gauging has made the Ace Trubore Stirrer the most widely used precision glass stirrer in research today. To get an idea of how versatile Ace stirrers are, send for the Ace Trubore Brochure: There are 8 types of interchangeable bearings, 10 types of rod (glass or fluorocarbon), with a choice of paddles. There is a complete line of Trubore accessories, connectors, stirring motors. Ace Trubore Stirrers feature everything you need for unequalled performance in stirring, including StirLube lubricant, the only lubricant especially made for glass bearings. Send for your copy of Ace Trubore Brochure!

Send for FREE Trubore Brochure!

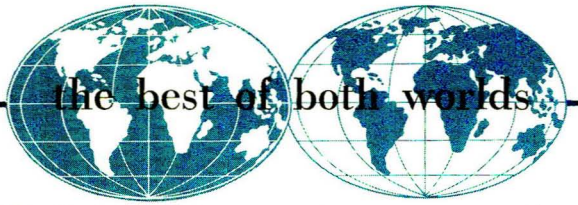
®Trubore is a Reg. TM Ace Glass Inc.

ACE GLASS INCORPORATED

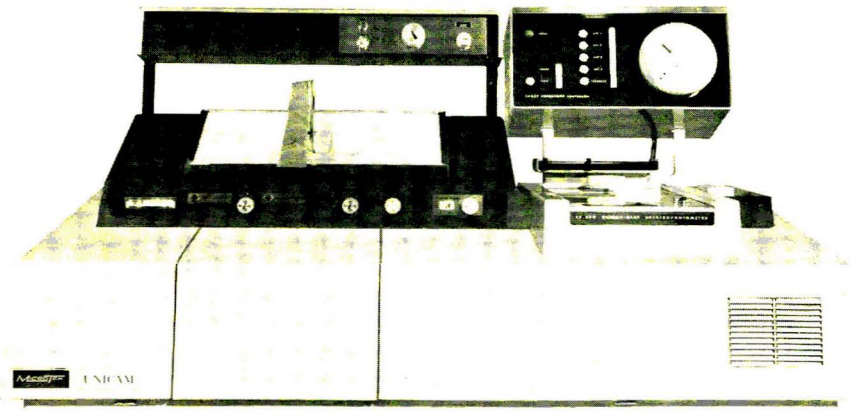
Vineland, New Jersey

LOUISVILLE, Ky. SPRINGFIELD, MASS.

Circle No. 102 on Readers' Service Card



PRESENTS SP800 Double Beam Automation In Enzyme Analysis

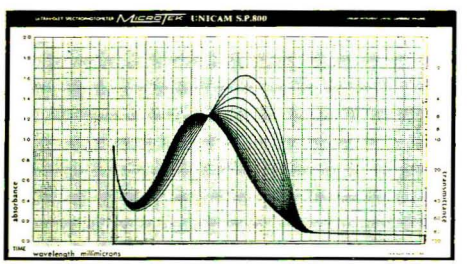


At last you can realize the full potential of a double beam recording spectrophotometer *plus* automatic multi-sampling at fixed wavelengths or recycling over any wavelength range.

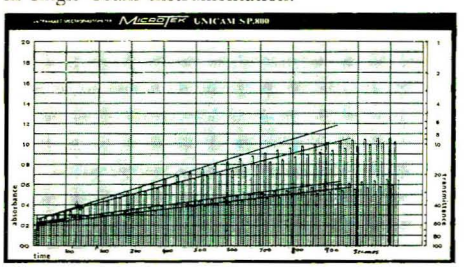
A recent marketing agreement between Micro Tek and Unicam makes it so easy.

Why settle for less than the fully automatic double beam compensation of the SP800?

The maximum capacity with automatic selection of 4 sample and 4 reference cells permits sophisticated experiments in enzymology without the tedious calculations often involved in single beam instrumentation.



Progress of a hydrolysis showing classic isosbestic point. Automatic recording single sample 500-270 mu.



Each of 4 sample cells and reference pairs is examined for 5 seconds in turn and repeated indefinitely.

The SP800 Spectrophotometer is ideal for routine recording of all standard spectra in the ultraviolet and visible. It is robust and simple to operate but presents many advanced design features including a unique capability with turbid solutions.

Zero drift in this null balancing system is simply specified; there is none. The SP800 has a maximum linear wavelength scale of 190-850 mu. For more details simply call your area, Micro Tek Sales Engineer or write to the Home Office.

HOME OFFICE
P. O. Box 15409
Baton Rouge, Louisiana

MICROTEK UNICAM

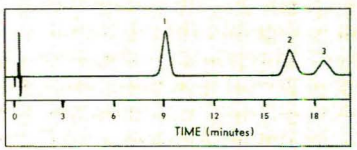
ASSOCIATED IN SERVICE AND TECHNOLOGY

Circle No. 145 on Readers' Service Card



...must have been something he ate!

. . . the problem now is: What was it? Up until recently, pesticide analysis has been a long, drawn-out, tedious affair. With commercial supports, a D.C. 200 column has generally required 3 to 4 weeks of conditioning at 250° C, or 96 hours of conditioning at 250° C, then pretreatment with milligram quantities of pesticides, and finally several hundred analyses before an endrin peak equivalent to that below is obtained.



Pesticide mix (3 ng. each) of (1) aldrin, (2) dieldrin and (3) endrin on 10 wt. % D.C. 200 silicone (12,500 cstks.) on 100/120 GAS-CHROM Q. Radium detector. Carrier gas rate: 120 ml/min.

The chromatograph shown is an analysis by GC of a standard mixture of high purity aldrin, dieldrin, and endrin at Applied Science. The column packing was D.C. 200 silicone on GAS-CHROM Q. The results look quite good, but are not unique or new — EXCEPT FOR ONE THING! The sample was the FIRST INJECTION made after the column was CONDITIONED FOR ONLY 24 HOURS at 250° C and 20 psig. and then for 20 HOURS at 200° C and 30 psig.

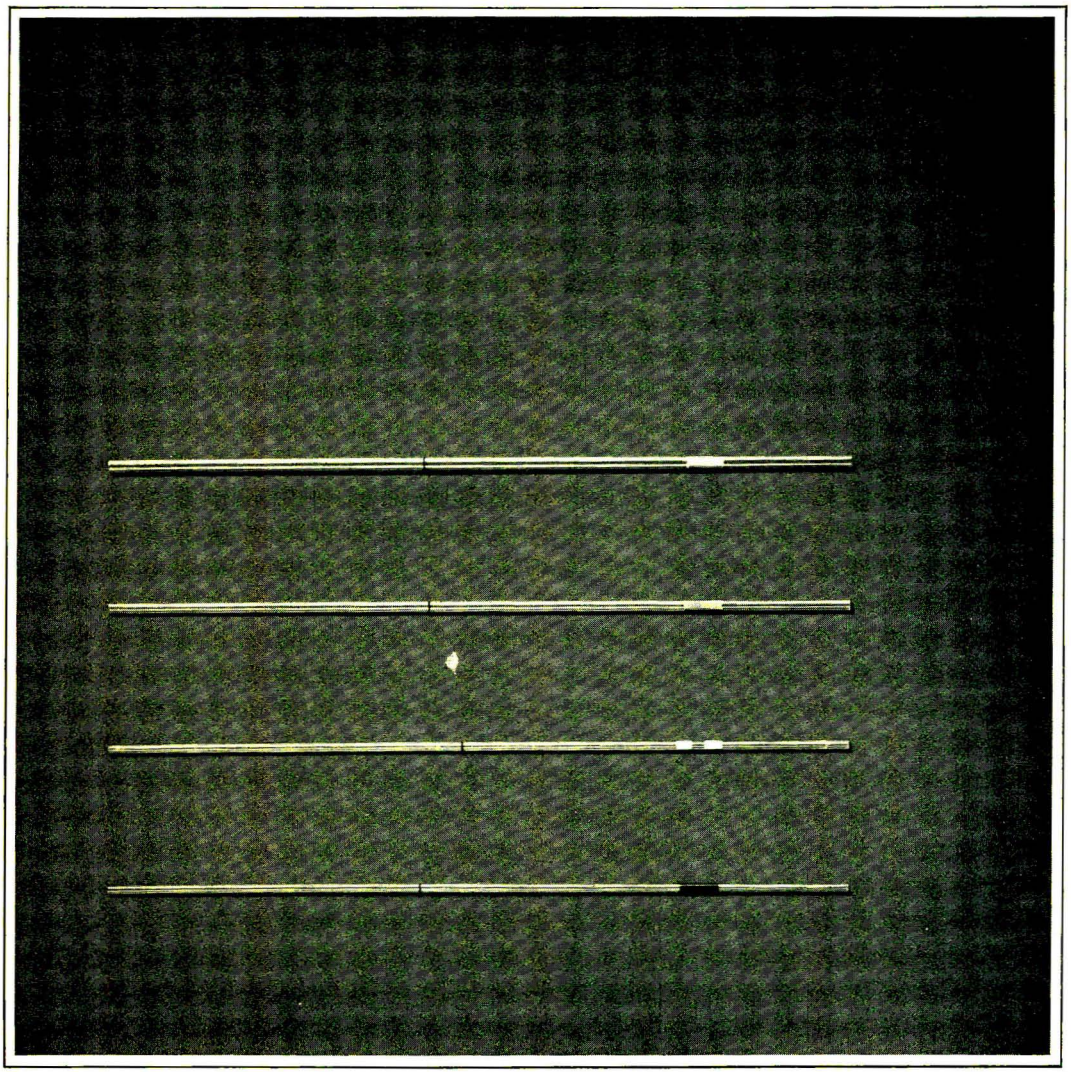
Much, much easier to use GAS-CHROM Q.

For more extensive results and discussion, send for our GAS-CHROM Newsletter, Vol. 6, No. 2 (April, 1965). One more thing — the packing used for that analysis above — we have it in stock — pretested packing . . . $25/25g; $40/50g; $60/100g.

APPLIED SCIENCE LABORATORIES, INC.
Post Office Box 440 • State College, Penna. 16801
Telephone (Area 814) 238-2406

West Coast Office: Unit M • 5140 W. 106th St. • Inglewood, Calif.

Circle No. 5 on Readers' Service Card



To duplicate the accuracy of a YANKEE® DISPOSABLE MICROPET™ Lambda Pipette ...use another one



Use lots of them. They're guaranteed accurate to ±1%. And they're used only once—no cross-contamination between samples or reagents.

Available in the four most frequently used sizes—20, 25, 50 and 100 lambda—YANKEE DISPOSABLE MICROPET pipettes are color-coded at the top.* The cardboard vials they're packed in are also color-coded to correspond to the pipettes.

Take the top off the vial and you've got 200 pipettes at your fingertips. The specially designed vial holds the pipettes upright so that they do not fan out and the vial may be recapped easily. In each vial there's an 18" rubber suction tube designed to fit all four pipette sizes—without an adapter.

Measure accurately—and economically—with YANKEE DISPOSABLE MICROPET lambda pipettes.

Clay-Adams
New York, N.Y. 10010

*According to the draft recommendations of Technical Committee No. 48 of the International Organization for Standardization (ISO).

Circle No. 149 on Readers' Service Card

Your neutron generator requirements are stringent?

Good.

Now match them against our specifications.

Picker Nuclear set out to develop a neutron generator that would incorporate the important recent advances most meaningful to users. The successful result of this effort is available as Accelerator I.

Accelerator I is distinguishable from other neutron generators by these attributes (and more): truly stable beam current and beam location, extremely fine focus control, high beam currents that are continuously maintainable, five minute target change, and operation with a pump-down of only two to three minutes. The traditional stability and focus problems have become virtually obsolete.

More precisely now, our exacting performance specifications—which this instrument actually meets—include:

Fast neutron yields: up to 2.5 x 10^{11} neutrons/second from the T (d,n) reaction.

Thermal neutron fluxes: up to 5 x 10^{8} neutrons/cm^2-sec.

Beam current: greater than 2.5 mA of deuterons (90% atomic beam).

Beam energy: continuously variable from 0 to 150 keV (intermittent operation at 175 keV).

Gamma yield: 10^{6} gammas/sec (11 MeV) from the B^{11} (p, gamma) reaction.

It is also worth observing that the engineering decisions for Accelerator I have inevitably leaned toward the conservative. Accordingly, one finds things like an extra large vacuum pump. Or a conservative rating on all power supplies permitting continuous operation exceeding all ratings. Typical.

But if, despite our vaunted conservative engineering, the need for service should nevertheless arise, you're still in good hands. Picker Nuclear, which sells and services an exceptionally broad line of nuclear instruments (small sample: liquid scintillation counters, automatic counting systems for gamma-emitting samples, counting systems for alpha and beta samples, a variety of instrument systems designed for the study of organ function), will do the same for Accelerator I. This is comforting.

Summary and conclusion: Picker Nuclear provides a pretty distinctive pedigree for a neutron generator. And the offspring shows it. Write for details; ask for bulletin A1AC6.

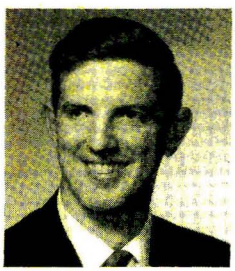
PICKER nuclear 1275 Mamaroneck Avenue, White Plains, N.Y. 10605

Circle No. 78 on Readers' Service Card

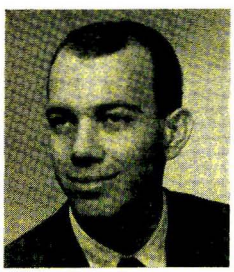
CIRCULAR DICHROISM — THEORY AND INSTRUMENTATION

A. ABU-SHUMAYS and JACK J. DUFFIELD
Applied Physics Corporation, Monrovia, Calif.

IN THIS REPORT THE GENERAL RELATIONS BETWEEN CIRCULAR DICHROISM, OPTICAL ROTATION, ORDINARY ABSORPTION AND DISPERSION ARE DISCUSSED. CLASSICAL AND MODERN THEORIES, AND APPROACHES TO THE MEASUREMENT OF CIRCULAR DICHROISM ARE REVIEWED. THE NATURE OF CIRCULARLY POLARIZED LIGHT AND MEANS OF PRODUCING IT IN THE VISIBLE AND ULTRAVIOLET REGIONS ARE ANALYZED, AND SPECIAL EMPHASIS IS GIVEN TO INTERNAL REFLECTION RETARDERS AND ELECTRO-OPTIC MODULATORS. FINALLY, THE MAJOR PARAMETERS INVOLVED IN A CIRCULAR DICHROISM MEASURING SYSTEM ARE DESCRIBED AND THEIR PERFORMANCE IS ANALYZED AND EVALUATED.



Jack J. Duffield is currently a Senior Engineer at Applied Physics Corporation. Dr. Duffield received his B.A. in Chemistry in 1955 from Pomona College. In 1960 he received a Ph.D. in Analytical Chemistry from M.I.T., where his thesis work was in gas chromatography. Dr. Duffield is a member of the Analytical Division of the ACS and the Society of the Sigma Xi.



A. Abu-Shumays received his B.Sc. and M.Sc. degrees from California Institute of Technology in 1962 and 1963. He is currently a Research Engineer at Applied Physics Corporation, where he is engaged in activities related to the field of polarized light instrumentation. Mr. Abu-Shumays is a member of ASME and the Society of the Sigma Xi.

THE INTERACTION of electromagnetic radiation with matter results in a number of changes that take place in both the radiation and the matter: the speed of the radiation may change, this change being dependent on the wavelength, or frequency, of the radiation (DISPERSION); the intensity of the radiation may be reduced resulting in energy dissipation into the matter (ABSORPTION). In addition, if the incident radiation is linearly polarized, a change in azimuth angle may occur (OPTICAL ROTATION) and the radiation may become elliptically polarized (CIRCULAR DICHROISM.) Theoretical and experimental studies of these changes and their underlying causes constitute the subject matter for an important segment of chemical analysis. The use of light, or electromagnetic radiation, as a tool to probe the properties of matter, is one of the oldest and most specialized means of scientific investigations. An enormous amount of work by outstanding scientists, both theoretical and experimental, has been and continues to be devoted to this field and the wealth of results in terms of theories and applications is overwhelming.

General Relations

Ordinary Absorption and Dispersion

The origin of the absorption phenomenon in the visible and ultraviolet regions is generally attributed to electronic transitions involving some redistribution of the electronic structure of the absorbing molecule or atom. The quantum mechanical theory assigns a number of natural energy levels and sublevels to every molecule (*18*); absorption of electromagnetic radiation is most pronounced when the frequency, ν, of the radiation corresponds to the energy between two such molecular levels in accordance with Planck's formula

$$\Delta E = h\nu \qquad (1)$$

Return of the excited molecule to lower energy levels is accompanied with reemission of electromagnetic radiation of the corresponding frequency. Charge redistributions associated with the phenomena of absorption and reemission result in producing a scattered wave of electromagnetic radiation which is superimposed on the incident wave leading to the observed dispersion characteristics of the medium.

Contributions of a single transition to absorption and dispersion properties are shown in Figure 1. Several features may be noted: outside the absorption band, the value of the refractive index, n, increases with decreasing wavelength (normal dispersion); in the absorption region, however, the value of the refractive index decreases with decreasing wavelength (anomalous dispersion), and at approximately the wavelength of maximum absorption the contribution of the transition to the refractive index becomes zero. The relationship between absorption and dispersion may be expressed in terms of integral transforms known as the Kronig-Kramers relations (*37*):

$$n_K(\lambda) = \frac{1}{2\pi^2} \int_0^\infty k_K(\lambda') \times \frac{\lambda^2}{\lambda^2 - \lambda'^2} d\lambda' \qquad (2)$$

$$k_K(\lambda) = -8 \int_0^\infty n_K(\lambda') \times \frac{1}{\lambda^2 - \lambda'^2} d\lambda' \qquad (3)$$

where n_K and k_K are the refractive index and absorption coefficient associated with the Kth transition. It is sometimes more convenient, particularly for theoretical considerations, to express Equations 2 and 3 in terms of angular frequencies instead of wavelengths. The two quantities are related by the expression:

$$\omega = \frac{2\pi c}{\lambda} \qquad (4)$$

where c is the speed of electromagnetic radiation. Contributions of the type shown in Figure 1 come from every transition and the overall absorption and dispersion curves are thus a superposition of curves associated with individual transitions. According to Equations 2 and 3, a knowledge of the refractive index for all wavelengths may be used to deduce the absorption coefficient at any wavelength and conversely, a knowledge of the absorption coefficient for all wavelengths may be used to determine the refractive index at any wavelength. In principle, therefore, the information contained in either set of curves, dispersion or absorption, may be deduced from the other set. For most applications, determination of molecular structure for example, the two phenomena reveal equivalent information. Experimental determination of the absorption coefficient, however, is more desirable and the ready availability of commercial spectrophotometers makes the measurement more convenient. Spectroscopists deduce structural information from absorp-

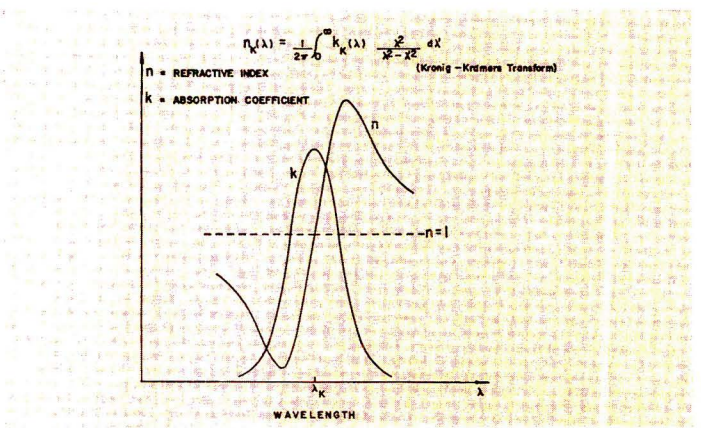


Figure 1. Refractive index and absorption coefficient in the vicinity of an isolated band

tion spectra in terms of three parameters associated with each transition or absorption band: the wavelength corresponding to maximum absorption, λ_K, the half-width of the band, Δ_K, and the dipole strength for the transition, D_K. The last parameter is proportional to the area under the absorption band and may be defined for the Kth transition by the expression (*34*):

$$D_K = \frac{3hc}{8\pi^3 N_1} \int_0^\infty \frac{k_K(\lambda)}{\lambda} d\lambda \quad (5)$$

where h is Planck's constant, c is the speed of light, N_1 is the number of absorbing molecules per cubic centimeter of solution, and k_K is the partial absorption coefficient for the Kth transition. If the absorption band is approximated by a Gaussian curve, its dipole strength, D_K, may be shown to be directly proportional to the product $k\ (\lambda_K) \cdot \Delta_K$, where $k(\lambda_K)$ is the peak absorption coefficient and Δ_K is now defined as the half width of the absorption band at $1/e$ of its maximum value.

Circular Dichroism and Optical Rotatory Dispersion

The phenomena of circular dichroism and optical rotation are closely related to the phenomena of ordinary absorption and dispersion described above. The difference in absorption coefficients of an optically active medium for left and right circularly polarized light is termed circular dichroism, while the difference in the refractive indices of the medium for the two circular polarizations, circular birefringence, is a measure of optical rotation. Variations, as a function of wavelength, of circular dichroism (CD) and optical rotation (optical rotatory dispersion, ORD) give even more structural information on dissymmetric molecules than ordinary absorption or dispersion. The influence of an optically active absorbing sample on a linearly polarized wave of electromagnetic radiation is illustrated in Figure 2: the incident linearly polarized wave may be resolved into two circular components, in phase, with equal amplitudes but opposite sense; the two components traverse the medium with unequal speeds due to the circular birefringence, $n_L - n_R$, of the medium; further, the two circular components suffer unequal absorption due to the circular dichroism, $k_L - k_R$, of the medium. The transmitted components exhibit unequal amplitudes and are no longer in phase. These components combine to produce a resultant wave which is elliptically polarized: the major axis of elliptical vibrations is rotated relative to the direction of the incident linear polarization by an angle α called the optical rotation, and the arctangent of the ratio of minor to major axes of elliptical vibration, θ, is referred to as the angle of ellipticity. Measured

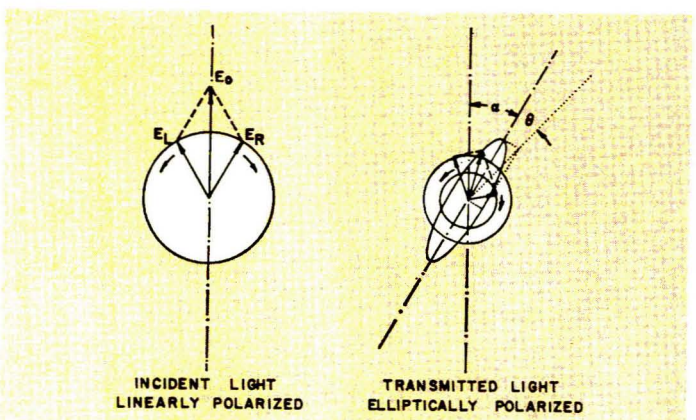
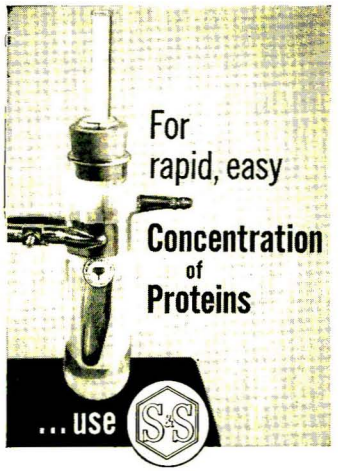


Figure 2. Influence of an optically active absorbing sample on linearly polarized light



COLLODION BAGS

Concentration and enrichment of protein solutions is a preliminary step to electrophoretic differentiation. A simple, time saving method is by use of S&S Collodion Bags, an exclusive specialty marketed only by S&S.

Properties of S&S Collodion Bags

Collodion bags retain proteins of a molecular weight of approximately 70,000 to 100,000. Each bag is about 8 cm in height with a maximum open end width of 1.5 cm. Capacity is 8 ml. The bag tapers to the closed end where albumen is concentrated.

Filtration rate is 6-9 ml of distilled water per hour. Bags may be reused as many as 5 times, if carefully cleaned and kept in moist condition.

Apparatus is simple, inexpensive

S&S Collodion Bags require a special glass holder, which is shown on the illustration above. The apparatus is inexpensive, simple in construction, and easy to operate.

Ask your laboratory supply house for S&S Collodion Bags—an important advancement in preparatory techniques for albumen determination that saves time, effort, and contributes to increased accuracy of measurement.

For free data sheet and prices, mail coupon below. Information will be sent with no obligation.

MAIL COUPON FOR FREE DATA

S&S Carl Schleicher & Schuell Co.
Keene, New Hampshire, Dept. AC-66

Please send free data sheet and prices on S&S Collodion Bags.

Name_____

Company_____

Address_____

City_____ Zone____ State____

Circle No. 85 on Readers' Service Card

RESEARCH QUALITY RADIOCHEMICALS
CURRENT LIST

CARBON-14 LABELLED CARBOHYDRATES

COMPOUND	SPECIFIC ACTIVITY (mc/mM)
D-Arabinose-1-C14	1-4
D-Arabinose-C14 (U)	1-4
Erythritol-C14 (U)	2-4
D-Fructose-C14 (U)	2-4
D-Fructose-C14 (U) [High S.A.]	50-100
D-Galactosamine-1-C14 hydrochloride	2-4
D-Galactose-1-C14	2-4
D-Galactose-1-C14 [High S.A.]	20-30
D-Glucosamine-1-C14 hydrochloride	2-4
D-Glucose-C14 (U)	2-4
D-Glucose-C14 (U) [Aqueous solution, sterilized, pyrogen tested]	1-5
D-Glucose-C14 (U) [High S.A.]	50-150
D-Glucose-C14 (U) [High S.A., aqueous solution, 3% ethanol, sterilized]	50-100
D-Glucose-1-C14	2-4
D-Glucose-1-C14 [High S.A.]	20-35
D-Glucose-1-C14 [High S.A., aqueous solution, 3% ethanol, sterilized]	20-35
L-Glucose-1-C14	2-4
D-Glucose-2-C14	1-4
D-Glucose-2-C14 [High S.A.]	20-35
D-Glucose-2-C14 [High S.A., aqueous solution, 3% ethanol, sterilized]	20-35
D-Glucose-6-C14	2-4
D-Glucose-6-C14 [High S.A.]	20-35
D-Glucose-6-C14 [High S.A., aqueous solution, 3% ethanol, sterilized]	20-35
D-Glucose-C14 (U)-6-phosphate	2-4
D-Glucose-C14 (U)-6-phosphate [High specific activity]	50-150
D-Glucose-1-C14-6-phosphate	2-4
myo-Inositol-C14 (U)	30-200
Lactose-1-C14	4-12
Maltose-C14 (U)	4-10
Maltotriose-C14 (U)	100-250
D-Mannitol-1-C14	10-30
D-Mannose-C14 (U)	2-5
D-Mannose-1-C14	1-4
D-Mannose-1-C14 [High S.A.]	20-30
D-Mannose-2-C14	1-3
Methyl-(α-D-gluco-C14 (U)) pyranoside	2-5
Potassium D-glucuronate-C14 (U)	2-4
Potassium D-glucuronate-6-C14	2-4
D-Ribose-C14 (U)	2-4
D-Ribose-C14 (U) [High S.A.]	15-30
D-Ribose-1-C14	2-4
D-Ribose-1-C14 [High S.A.]	15-30
Sodium D-gluconate-C14 (U)	2-6
Sodium D-gluconate-1-C14	2-5
Sodium D-gluconate-6-C14	1-4
Sorbitol-C14 (U)	5-10
Sorbitol-1-C14	2-5
L-Sorbose-C14 (U)	2-4
Starch-C14 (U) [Tobacco leaf; amorphous]	2-50 μc/mg
Sucrose-C14 (U)	5-15
Sucrose-C14 (U) [High S.A.]	150-200
D-Xylose-C14 (U)	1-4

Data sheets available on request for every compound. Please write for current schedules containing complete radiochemical listings and information. Or call 312 827-4456 collect. NUC:9-8-215

NUCLEAR-CHICAGO
A DIVISION OF NUCLEAR-CHICAGO CORPORATION
351 Howard Avenue, Des Plaines, Illinois 60018
Circle No. 18 on Readers' Service Card

angles of rotation and ellipticity, α and θ, may be expressed in terms of the refractive indices and absorption coefficients of the medium for left and right circularly polarized light, thus:

$$\alpha = \frac{\pi}{\lambda}(n_L - n_R) \qquad (6)$$

and

$$\theta = \frac{1}{4}(k_L - k_R) \qquad (7)$$

In Equations 6 and 7, α and θ have the dimensions of radians per centimeter. The difference between the refractive indices for left and right circularly polarized light is typically in the seventh or eighth decimal place while the difference in absorption of the two circularly polarized waves does not amount to more than a few hundredths of the average absorption. For comparison purposes, molecular rotation [ ] and molecular ellipticity $[\theta]$ are commonly reported (*9*); these quantities are defined by the expressions:

$$[\varphi] = \frac{\alpha}{\pi}\frac{18}{}\frac{M}{C'} \qquad (8)$$

and

$$[\theta] = \frac{\theta}{\pi}\frac{18}{}\frac{M}{C'} \qquad (9)$$

where M is the molecular weight of the optically active material and C' is its concentration in grams per cubic centimeter. $[\varphi]$ and $[\theta]$ have the dimensions of degrees — cm.^{2} per decimole. The molecular ellipticity $[\theta]$ is related to the decadic molar circular dichroism, $[\epsilon_L - \epsilon_R]$, by the approximate expression:

$$[\theta] \approx 3305\,[\epsilon_L - \epsilon_R] \qquad (10)$$

where $[\epsilon_L - \epsilon_R]$ has the units of liter per mole-cm.

The combined phenomena of circular dichroism and optical rotatory dispersion in the vicinity of an optically active absorption band are commonly known as the Cotton effect. Contributions of a single optically active transition to the molecular ellipticity $[\theta]$ and molecular rotation $[\varphi]$ are illustrated in Figure 3 for both positive and negative Cotton effects. The close analogy of the relationships between CD and ORD to those between ordinary absorption and dispersion may be noted. Like the ordinary dispersion curve, ORD exhibits normal and anomalous characteristics; the contribution of the transition to optical rotations extends beyond the immediate vicinity of the dichroism band, and at approximately the wavelength of maximum dichroism the optical rotation due to the transition becomes zero.

Unlike absorption curves, however, circular dichroism and optical rotation curves may assume positive or negative signs. Circular dichroism bands are commonly described in terms of three parameters analogous to those used in conjunction with absorption bands; these

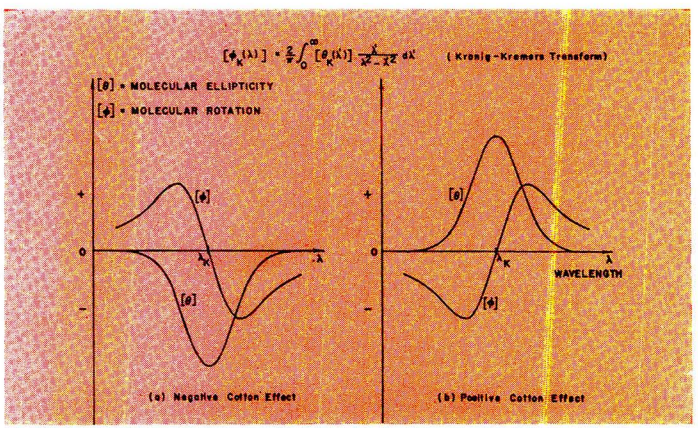


Figure 3. Idealized Cotton effect of an isolated absorption band

parameters are the wavelength of maximum circular dichroism, λ'_K, the half-width of the band Δ'_K, and the rotational strength R_K of the transition defined by an expression analogous to Equation 5.

$$R_K = \frac{3hc}{8\pi^3 N_1} \int_0^\infty \frac{\theta_K}{\lambda}(\lambda) d\lambda \quad (11)$$

In general, the wavelengths λ_K and λ'_K, corresponding to maximum absorption and maximum CD, respectively, are not exactly equal; the same holds true for Δ_K and Δ'_K. As in the case of absorption, for a Gaussian CD band, the associated rotational strength, R_K, is proportional to the product $\theta(\lambda'_K) \cdot \Delta'_K$ where $\theta(\lambda'_K)$ is the peak ellipticity and Δ'_K is now defined as the half-width of the circular dichroism band at $1/e$ of its maximum value.

Whereas λ'_K and Δ'_K offer no more information than the corresponding parameters of absorption bands, the rotational strength R_K represents additional useful information about the intensity of optical activity associated with the Kth transition (*32*). As in the case of absorption and dispersion, circular dichroism and optical rotatory dispersion are related at Kronig-Kramers integral transforms; thus, for the Kth transition:

$$[\varphi_K(\lambda)] = \frac{2}{\pi} \int_0^\infty [\theta_K(\lambda')] \times \frac{\lambda'}{\lambda^2 - \lambda'^2} d\lambda' \quad (12)$$

and

$$[\theta_K(\lambda)] = -\frac{2}{\pi\lambda} \int_0^\infty [\varphi_K(\lambda') \frac{\lambda'^2}{\lambda^2 - \lambda'^2} d\lambda' \quad (13)$$

In principle, information contained in either set of curves, ORD or CD, may also be deduced from the other set. Recent comparative studies (*10, 27*) of CD and ORD demonstrate the equivalence of the two techniques in terms of their usefulness in most structural and stereochemical applications. However, for a number of specialized applications it is sometimes found advantageous to determine one or the other. Background effects typical of ORD curves often represent a useful feature not available in



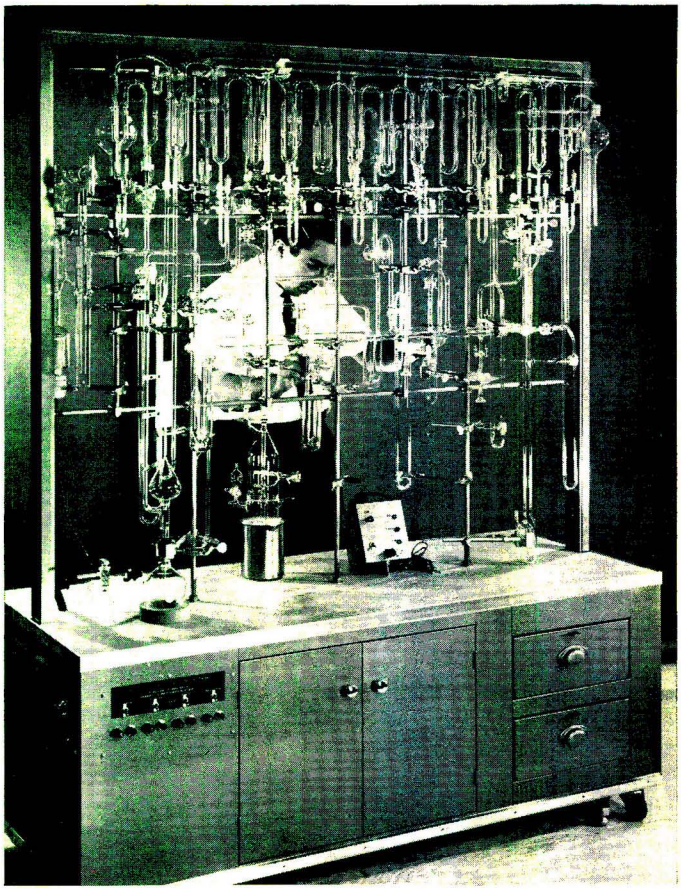
YOU'D ALMOST THINK IT RAINED INSIDE THE REXYN™ BOTTLE, TOO It's wet in there. That's because Fisher's Rexyn ion exchange resins are packaged wet, ready to use. Dry ion exchangers must be slurried in distilled or deionized water for proper conditioning prior to use. The beads may fracture, reducing their effectiveness . . . but not with Rexyn! We do the slurrying by a carefully controlled procedure, and make sure of uniform particle size by direct inspection with microscopes and calibrated verniers, rather than by the less precise sieve method. And the purity of Rexyn resins is certified, with low metallic content assured by atomic absorption analyses. Three grades are available. **Research Grade** gives you highest purity and regeneration efficiency in ultrasensitive analytical and research techniques. **Chromatographic Grade** provides excellent resolution and sharp, clear chromatographic separations. **Analytical Grade** is Fisher's economical ion exchanger for routine analytical use. Most Rexyn exchangers come in all three grades. *For a handy chart* with complete specifications, write Fisher Scientific Company, 100 Fisher Building, Pittsburgh, Pa. 15219. J-539

FISHER SCIENTIFIC CO.

Instruments, Apparatus, Furniture and Chemicals for Laboratories

Complete stocks in all these locations: Atlanta • Boston • Chicago • Cleveland • Houston • New York Philadelphia • Pittsburgh • St. Louis • Union, N. J. • Washington • Edmonton • Montreal • Toronto • Vancouver

Circle No. 42 on Readers' Service Card



Portable glass high vacuum system is complete and ready to use

Supplied complete and ready to operate, this unit brings high vacuum techniques within the scope of any laboratory. Designated the Delmar-Urry Portable Glass High Vacuum System, it is ideal for research ranging from studies of air- and moisture-sensitive substances to preparation of samples for isotope geology.

Classical design, adaptable—the classical design of the basic system is easily modified for special applications.

Compact, movable—unit rolls through standard doorways, easily positions under ducts or near utility outlets.

Grease-free—O-ring connectors end need for greased fittings and joints.

Money-saving—unit totally eliminates these expenses:

- purchases of individual components
- fabrication of individual racks
- specialized glassblowing talent
- supervision of glassblowers by research workers
- space taken up by permanent system

Wide range—10^{-6} mm Hg provides working range for broad spectrum of volatile substances.

Quick delivery—complete system is shipped by special carrier; it will arrive at your laboratory within one month from your order.

Write for High Vacuum Catalog A60-D-4.

Delmar SCIENTIFIC LABORATORIES

317 MADISON ST., MAYWOOD, ILL. • A SUBSIDIARY OF COLEMAN INSTRUMENTS, INC.

Circle No. 148 on Readers' Service Card

CD curves, while the discreteness of CD curves is particularly useful in identifying overlapping or hidden optically active transitions. CD measurements are also to be preferred where studies of rotational strengths of individual transitions are of importance. When expressed in terms of ellipticity, the magnitude of peak CD due to a single optically active transition is approximately equal to the peak to trough magnitude of the corresponding ORD curve and, in principle at least, the ultimate sensitivities of systems measuring CD or ORD are very nearly the same.

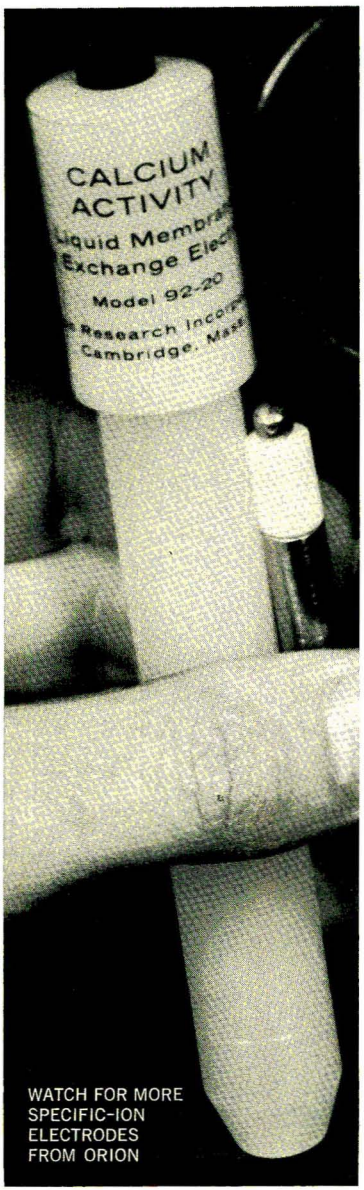
Theories of Optical Activity

In 1848 Pasteur (*24*) presented the first molecular theory of optical activity; he proposed that molecules, like geometrical figures, may be divided into two classes: those with superposable mirror images and those with nonsuperposable images. Pasteur postulated that molecules belonging to the second class exhibit optical rotatory power. The term "molecular dissymmetry" was introduced to characterize this class. Further, Pasteur speculated that molecular dissymmetry may be attributed to some form of dissymmetric grouping of atoms in a helical or tetrahedral configuration. In 1874, Le Bel adopted the tetrahedral model of the carbon atom and associated optical activity with centers of asymmetry in the active compound (*24*). Van't Hoff, in 1874, distinguished between two types of optically active compounds and attributed optical activity to either of two properties: the presence of an asymmetric center in the molecule or an overall dissymmetric structure containing no asymmetric centers. In 1893, Werner used available data on optical rotation of metal complexes to establish octahedral structural models exhibiting dissymmetric configurations (*24*).

Drude formulated, in 1896, a physical theory of optical activity based on the assumption that in a dissymmetric structure, charged particles are constrained to move along helical paths (*18*). The time dependent electric and magnetic fields associated with an incident wave of electromagnetic radiation induce electronic motions which in

FIRST IN ORION'S NEW SERIES OF CHEMICAL SENSING ELECTRODES

now—measure calcium ion activity directly with any expanded scale pH meter



Number One in a series of specific ion electrodes, the Calcium Activity electrode from Orion Research Incorporated is the first major advance in potentiometric electrochemistry since the glass electrode.

This electrode makes possible, for the first time, direct rapid continuous measurement of calcium ion activity in aqueous solutions.

In applications where concentration measurement is required the electrode makes an ideal endpoint detector for EDTA.

SELECTIVITY

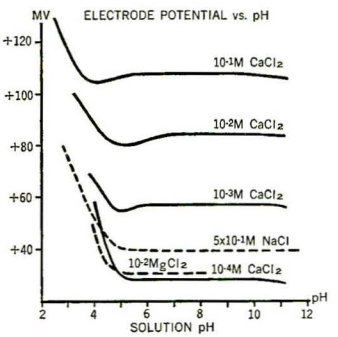
The electrode is extremely selective for calcium ion. Measurement of a millimolar calcium solution can be made with negligible error due to the presence of a 100-fold excess of sodium or potassium. The electrode is at least 50 times more sensitive to calcium than magnesium.

INSTRUMENTATION

Required instrumentation: any modern expanded scale pH meter or millivolt electrometer and a conventional saturated KCl reference electrode. Technique is similar to that of simple pH measurement.

AVAILABILITY

The Orion Calcium Activity electrode is priced at $145.00 and is available from major laboratory supply dealers. It is supplied as a kit with complete instructions, ion exchange and reference solutions, porous membranes, and all necessary handling equipment.



CONDENSED SPECIFICATIONS

Concentration range: from saturated calcium solutions to 10^{-5} m/1.

pH range: 5.5 to 11 pH

Temperature range: 0 to 50° C.

Electrical resistance: 25 megohms at 25° C.

Use this coupon to request complete product literature or an electrode for evaluation.

☐ Please send a copy of the Calcium Activity Electrode bulletin.

☐ Please arrange a demonstration through my laboratory supply dealer.

Name _____

Organization _____

Street _____

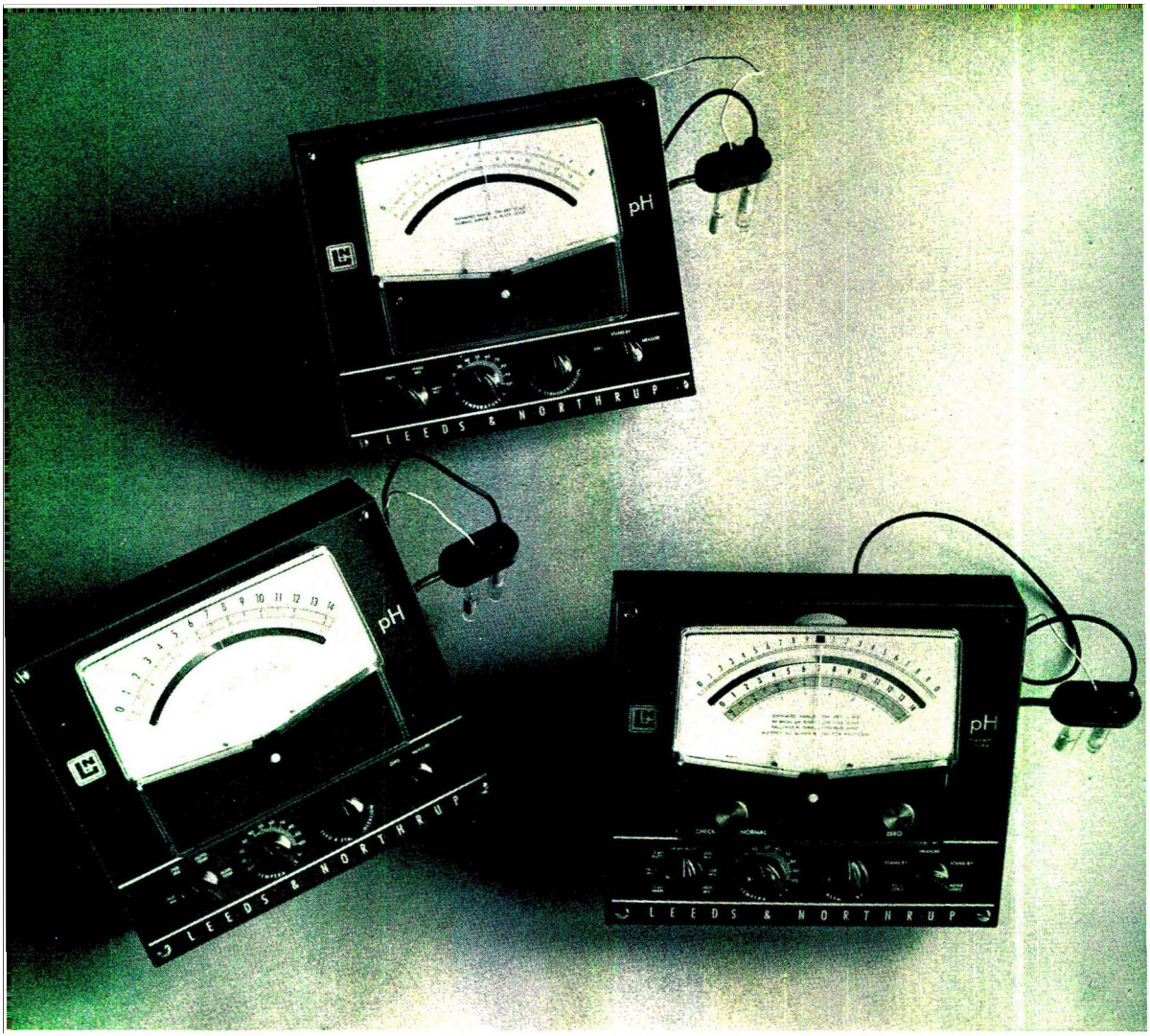
City _____ State _____ ZIP _____

Laboratory Supply Dealer _____

ORION RESEARCH INCORPORATED

11 Blackstone St., Cambridge, Massachusetts 02139/(617) UN 4-5400

Circle No. 71 on Readers' Service Card



± 1/20, ± 1/100, ± 1/200 of a pH.
If the first isn't accurate enough, pick one of the other two.

We've designed a whole new family of pH meters—the A2 Series. They give you a choice of relative accuracies: ± 0.05, ± 0.01 and ± 0.005 pH.

But that's not all by a long shot. We've modernized and perfected the meters in every significant detail.

For instance, we've changed to photoconductive choppers which are inherently more stable and trouble-free. They avoid the self-generated stray signals of mechanical converters.

We've adopted the glass-electrode connections now popular in U. S. practice.

We've given the meters a new look. Increased their stability, reliability, reproducibility.

But we still rely on our feedback-stabilized amplifier whose basic concept has been so widely imitated.

And hand wiring.

And a highly responsive meter with the practical scale length of 7″. (Not for us the unstable zero of oversized meters!)

And taut-band suspension. Eliminating the dead band you get with pivot systems.

And a rugged housing. Epoxy-coated case. Melamine-coated front panel.

And our own pH electrodes manufactured to perfectionist standards.

All the new meters are line-operated. All have a 10 microamp polarizing current for measurements by the Karl Fischer method and output terminals for recorder display.

Choose the one you need. General Purpose – good for routine measurements in lab and plant. Expanded Scale –for the more exacting requirements of research or quality control. Precision – for highest practical accuracy in research, medicine or industry.

You'll get a great deal that's new... at the same old price.

For details on each and for the name of the L&N laboratory pH dealer nearest you, write to: Leeds & Northrup, 4906 Stenton Ave., Philadelphia, Pa. 19144.

LEEDS & NORTHRUP
Philadelphia 44 • Pioneers in Precision

Circle No. 119 on Readers' Service Card

turn give rise to electric and magnetic dipole moments in the molecule. These moments are parallel for a right-handed helical pattern and antiparallel for a left-handed one. Interactions between fields produced by the electronic helical motions and the original electromagnetic wave result in the observed physical phenomena of optical activity. The sign and magnitude of the observed optical rotations are determined by the sense and physical parameters of the helical model.

In 1916, Gray developed a theory attempting to combine ideas of geometrical molecular configurations set forth by Pasteur, LeBel, and Van't Hoff with the physical arguments of Drude's theory (*24*). Gray used a tetrahedral model consisting of a central atom surrounded by four different atoms; an electromagnetic wave induces electric moments in each of the atoms which interact with each other and with the incident wave to modify its polarization characteristics. Similar multiparticle molecular models were considered by De Mallemann, Boys, and others, while elaborate electronic theories of optical activity based on the coupled oscillators and polarizabilities were formulated by Born and Oseen (*24*). The basic hypothesis of these later theories assume a molecule to consist of a number of discrete charged units of particles geometrically fixed relative to one another. An incident wave of electromagnetic radiation induces time-dependent polarizations and vibrations into the various units of the molecule, the resultant polarization of each unit being determined not only by the field of the radiation but also by fields produced by other units of the molecule (coupling). Born analyzed several multiparticle models and deduced that a model of only three coupled oscillators does not exhibit optical rotatory power whereas a model of four non-planar coupled oscillators may exhibit optical activity. While Born's analysis confirmed the general relations between optical activity and molecular dissymmetry, his mathematical formulas involved a large number of molecular parameters, thus limiting their direct applications to chemical problems.

Kuhn (*22*) developed, in 1930, a special simplified case of Born's theory and formulated a model consisting of only two anisotropic charged oscillators (the minimum number required to give rise to optical activity) satisfying two conditions: they possess no plane or center of symmetry and they are coupled by interaction forces. Kuhn's detailed theory is, in a sense, a semi-empirical one; it was based on an extensive review of available experimental data on optical activity and was directed towards deriving practical formulas applicable to problems of establishing configurations of optically active dissymmetric molecules.

The electronic and molecular

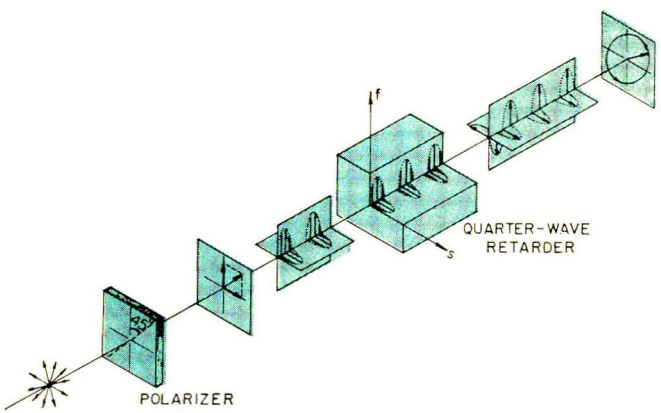
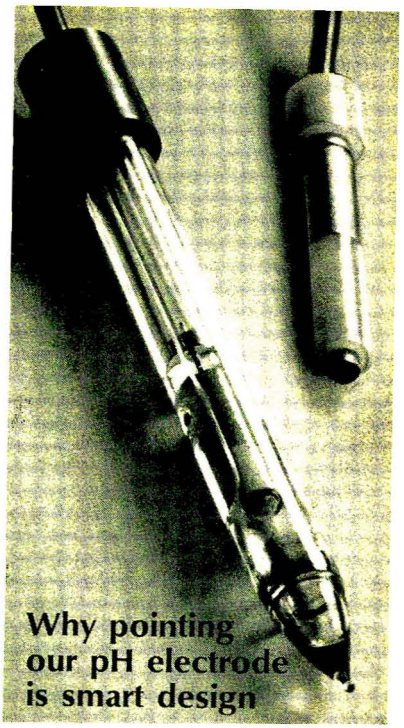


Figure 4. Production of circularly polarized light



This new L&N glass electrode has been dropped on its tip 25,000 times—just as it might if you let it fall into a beaker. It still works with full accuracy and sensitivity. No breakage. We've strengthened it at a critical point, where most electrodes are fragile.

Rugged electrode design is what you'd expect from a company that's been making pH-sensitive glass electrodes for 30 years—longer than anyone now in business.

We're continually improving pH glass formulations and technology. Our electrodes have excellent linearity in the presence of Na and K ions. Their generously packed internal elements allow exceptional stability and long life over a wide range of solution temperatures. They're equipped with the glass-electrode connectors now popular in the lab pH field.

Both measuring and reference electrodes have exactly the same internal element construction, so that they develop identical half-cell potentials no matter how the temperature changes. This balanced configuration prevents drift and uncertainty.

To avoid uncertainty, specify L&N electrodes. Talk to your lab supply dealer about them and their use with other pH meters. Or let us send you the details and the name of the L&N laboratory pH dealer nearest you. Write: Leeds & Northrup, 4906 Stenton Ave., Philadelphia, Pa. 19144.

LEEDS & NORTHRUP
Philadelphia 44 • Pioneers in Precision
Circle No. 120 on Readers' Service Card

MAKE YOUR ESR/NMR COMPLETE

with the jeol RA-1

SPECTRUM ACCUMULATOR PLUS!



A 4096 channel, program-stored, digital device — compatible with your present ESR/NMR system — providing signal-to-noise enhancement at high resolution . . . PLUS

- Integration
- Smoothing
- Theoretical calculation of NMR spectra
- Theoretical calculation of ESR spectra
- Calculation of 2nd order moment
- Differentiation
- Addition
- Subtraction
- Fourier transformations
- Correlation functions

ALL for the cost of an ordinary 1024 accumulator!

jeol

JEOLCO (U.S.A.), INC. • 461 Riverside Ave., Medford, Massachusetts 02155 – (617) 396-8620 • 828 Mahler Road, Burlingame, California 94010 – (415) 697-9220

Circle No. 137 on Readers' Service Card

theories outlined above, although successful in explaining phenomena of optical activity and in deriving a useful set of empirical relations, suffer from two serious limitations: first, the classical theory of electromagnetic radiation on which the above theories are based does not account for the quantum nature of radiation; and second, the basic structural models employed by these theories are purely hypothetical in nature and do not correspond to the physical structure of atoms and molecules.

The quantum mechanical theory attributes optical activity to electronic transitions resulting in parallel or antiparallel electric and magnetic moments (*18*, *32*, *36*). The basic conclusions of this theory are, in many respects, similar to those obtained by classical theories, although a significant difference in assumptions and interpretations exists. For most practical applications a mixed theory combining the classical theory of electromagnetic radiation and optics with the quantum mechanical concepts of atomic and molecular structure is found useful and consistent (*18*).

Circularly Polarized Light

Polarized electromagnetic radiation is the basic tool for experimental determination of the two parameters of optical activity. According to the classical theory, electromagnetic radiation is said to be polarized if the vibrations of the electric, or magnetic, field vector representing the radiation at a fixed point in its path exhibit a long term preference to direction or sense of vibration. Thus the electric field vector representing linearly polarized radiation vibrates parallel to a fixed direction.

Electromagnetic radiation is said to be circularly polarized if the tip of the electric field vector, at a fixed point in the path of the radiation, generates a circular pattern in time. A circularly polarized wave is mathematically equivalent to two orthogonal linearly polarized waves of equal amplitudes but differing in phase by a quarter wave. The sense of circular polarization, right or left, is determined by the sense of the circular pattern, clock-

wise or counterclockwise, or by the sign of the phase difference between the two linear components, positive or negative. Figure 4 illustrates the conventional way of producing circularly polarized light: linearly polarized light from the polarizer is resolved into two components, of equal amplitude and phase, polarized parallel to the fast and slow axes of the quarter-wave retarder. The two waves emerging from the retarder exhibit a quarter-wave phase difference and recombine to produce a circularly polarized wave. If the amplitudes of the two linear components were not equal, or if the relative phase retardation was different from quarter-wave, elliptically polarized light will be produced.

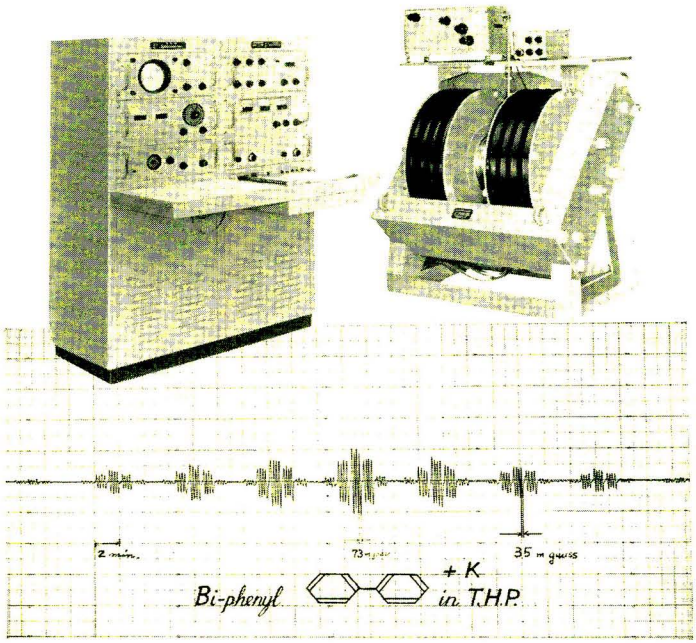
Linear Polarizers for Visible and Ultraviolet Radiation

Several types of linear polarizers have been used in the visible and ultraviolet spectral regions: they include reflection polarizers, dichroic polarizers, and birefringence polarizers. Light reflected externally from a dielectric surface is partially polarized; when the angle of incidence is equal to Brewster's polarizing angle ($\varphi = \tan^{-1} n$; n = index of refraction), the polarization of the reflected beam becomes complete. Practical applications of reflection polarizers are limited due to a number of drawbacks; the polarizing angle varies with the wavelength of the incident beam; the deviation of the incident beam is often inconvenient; furthermore, only a small fraction (few percent) of the incident light flux is reflected. The transmitted, or refracted, beam is only partially polarized but the degree of polarization may be substantially improved by a number of successive refractions at the polarizing angle. Several refined designs (*3*, *35*) employing a pile-of-plates have received wide applications as infrared polarizers but their usefulness for visible and ultraviolet radiation remains limited. Recently, a polarizer consisting of a pile of LiF plates has been described for use in the vacuum ultraviolet (*41*).

The most widely used linear polarizers for visible radiation are dichroic polarizers commonly known

POSITIVELY NO OTHER ESR

. . . gives you guaranteed sensitivity of 1×10^{11} ΔH



. . . and unmatched resolution!

- The JEOL 3BS-X features a high-Q sample cavity which gives sensitivities presently unattainable in any other EPR equipment.
- The JEOL 3BS-X features magnet homogeneity of within 15 milligauss in a 1"ϕ x 1/2" air gap volume and within 7.5 milligauss over the sample area. It is capable of producing the finest spectral splittings.
- The JEOL 3BS-X has a *Linear Field Sweep System* associated with its low-impedance magnet and power supply. This system provides regulated linear sweep from low to high fields and accurate digital readout of magnetic field intensity.

jeol

JEOLCO (U.S.A.), INC. • 461 Riverside Ave., Medford, Massachusetts 02155 – (617) 396-8620 • 828 Mahler Road, Burlingame, California 94010 – (415) 697-9220

Circle No. 138 on Readers' Service Card

as polaroid. These polarizers exhibit linear dichroism: they absorb the component of light polarized perpendicular to their "axes" more strongly than the parallel component. One process of manufacturing polaroid sheets (*23*) consists of subjecting a sheet of polyvinyl alcohol to large tensile strains which result in orienting the molecules and making the sheet doubly refracting. The sheet is then stained with iodine to make it dichroic. Optical and polarizing properties of polyvinyl alcohol-iodine polarizers are described in the literature (*23*); an extensive survey is included in Shurcliff's book (*38*). The use of polaroids for ultraviolet radiation is limited by their high absorbance and weak dichroism in this region. Recently, some investigators have studied ultraviolet properties of dichroic films that may be used as ultraviolet polarizers: a modification of conventional sheet polaroid extends its usefulness to 2600 A. (*25*), while specially prepared films of azo dyes exhibit useful dichroic properties at wavelengths as short as 2150 A. (*26*).

Birefringence polarizers are, by far, the most suited for ultraviolet applications and have been extensively employed despite their high cost. These polarizers are constructed from doubly refracting uniaxial crystals and operate by resolving the incident beam into two separate beams, ordinary and extraordinary, which are linearly and orthogonally polarized. Calcite, a uniaxial crystal with relatively large birefringence, is most commonly used for making such polarizers; however, due to its high absorption below 2200 A., materials such as crystal quartz and magnesium fluoride, having much smaller birefringence, are employed in far ultraviolet polarizers. Polarizers using uniaxial crystals of the dihydrogen phosphate type have also been used (*7*) to wavelengths as short as 1850 A. Figure 5 shows several designs of birefringence polarizers of common use; the name associated with each polarizer refers to its inventor and the four digit figure to the year of invention. Dots and arrows represent directions of the optic axis normal to and in the plane of the paper, respectively.

The most widely used birefringence polarizer today belongs to the Rochon type; this polarizer is composed of two prisms cut from a uniaxial crystal with the optic axis as shown. The prisms are placed together either in optical contact or separated by a thin film of transparent contacting fluid whose refractive index nearly matches the ordinary index of refraction of the birefringent crystal used. A light beam enters the first prism normal to the surface and travels parallel to the optic axis. The beam is doubly refracted at the diagonal of the second prism, the two beams produced are separated by a small

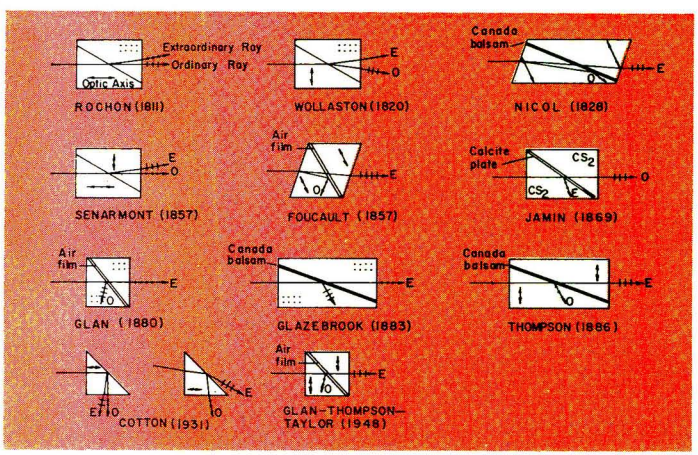


Figure 5. Birefringence polarizers



Lavoisier would have *(if he could have)* **used ACCULUTE®**

FOR RAPID PREPARATION OF STANDARDIZED VOLUMETRIC SOLUTIONS.

You'll be surprised to see how much time, money and errors "Acculute" can save you. There's a complete range of concentrates in stock for immediate delivery at leading laboratory supply houses across the U.S.A. and Canada. Write for a free sample today to:

ANACHEMIA CHEMICALS LTD.
CHAMPLAIN, N.Y.

Please send me a **FREE SAMPLE** of one of the items checked off below:

☐ Acid Hydrochloric ..... I N $2.25 value
☐ Iodine ..... N/10 $2.25 value
☐ Sodium Hydroxide ..... N/10 $2.00 value

Name .....
Company .....
Address .....

Circle No. 8 on Readers' Service Card

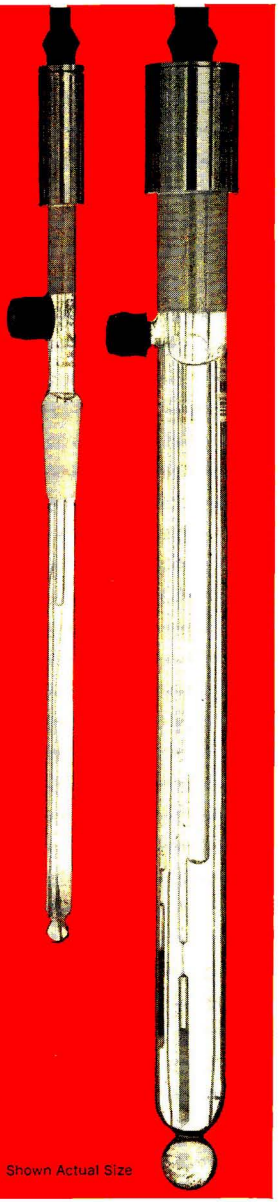
angle whose magnitude depends on the angles of the prisms and the birefringence of their crystalline material. The ordinary beam travels undeviated and is linearly polarized while the extraordinary beam suffers an angular deviation and is linearly polarized in an orthogonal direction. Rochon polarizers fabricated from optically contacted crystal quartz prisms are of particular interest in the far ultraviolet region down to 1750 A. because of their relatively high transmission. Other types of double beam polarizers include the Wollaston and Senarmont polarizers illustrated in the figure. In the Wollaston polarizer, both beams suffer angular deviations of approximately the same magnitude.

Historically, the Nicol polarizer is perhaps the most known birefringence polarizer. This polarizer consists of two prisms cut from a calcite crystal, and cemented together with Canada balsam. The ordinary beam undergoes total internal reflection at the diagonal surface while the extraordinary beam is transmitted. Light enters and leaves the polarizer at oblique incidence and suffers a lateral displacement. This inconvenience in addition to the relatively small acceptance angle and high absorbance of ultraviolet radiation by the Canada balsam limits the practical utility of Nicol polarizers.

The Foucault polarizer was designed in order to overcome the various limitations of the Nicol polarizer. It consists of two prisms of calcite, cut from the natural crystal, separated by an air film. The polarizer is more conservative in use of material; the lateral displacement of the beam is considerably smaller but the useful angular field is even more limited than that of the Nicol polarizer.

A polarizer consisting of a thin plate of calcite cut parallel to the optic axis and immersed in a rectangular cell filled with carbon bisulfide was used by Jamin. The transmitted ordinary beam suffers no appreciable displacement; further the polarizer has a relatively high transmission and a wide angular field. Later designs sandwiched a thin plate of calcite or sodium nitrate between two prisms

SARGENT
pH
combination
electrodes



include both glass and reference in a single probe for the entire range 0 to 14 pH, from 0 to 80°C. All-glass construction has no rubber or plastic to contaminate the sample, and no crevices or pockets to trap solution for carry-over from one sample to the next. In both standard and miniature sizes for as little as 1 ml and ½ ml of sample.

Range, 0 to 14 pH with linear response even in highly acid solutions. Alkali ion response is insignificant below pH 12.5; it is low and — more important — stable in higher pH solutions.

Shock-resistant construction derived from inherent strength of the glass and careful fabrication.

Fast response, both in sensitivity of the glass and in symmetrical internal and external references—for rapid temperature equilibrium.

High efficiency, with a millivolt/pH response close to the Nernst coefficient.

Shown Actual Size

S-30070-10 COMBINATION ELECTRODE — 0 to 14 pH, Miniature, Sargent/Jena. pH range, 0-14; temperature, 0-80°C; total length, 6 inches; stem diameter, 5mm; immersion depth, 10 to 78 mm; cap length, ⅞ inch; cap diameter, 8 mm.
Complete with 20-inch connecting cable and plugs directly fitting Sargent, Corning, Coleman and Beckman pH meters **38.00**

S-30072-15 COMBINATION ELECTRODE — 0 to 14 pH, Sargent/Jena. pH range, 0-14; temperature, 0-80°C; internal buffer, pH 7; total length, 8 inches; body diameter, 12 mm; cap diameter, 41/64 inch; cap length, 1 inch.
Complete with 30-inch connecting lead and plugs directly fitting Sargent, Corning, Coleman and Beckman pH meters **35.00**

SARGENT®
SCIENTIFIC LABORATORY INSTRUMENTS • APPARATUS • CHEMICALS

E. H. SARGENT & CO.
4647 West Foster Avenue
Chicago, Illinois 60630

Chicago • Anaheim, Calif. • Birmingham • Cincinnati • Dallas
Denver • Detroit • Springfield, N.J. • Toronto, Canada

Circle No. 159 on Readers' Service Card

mini-pet ™

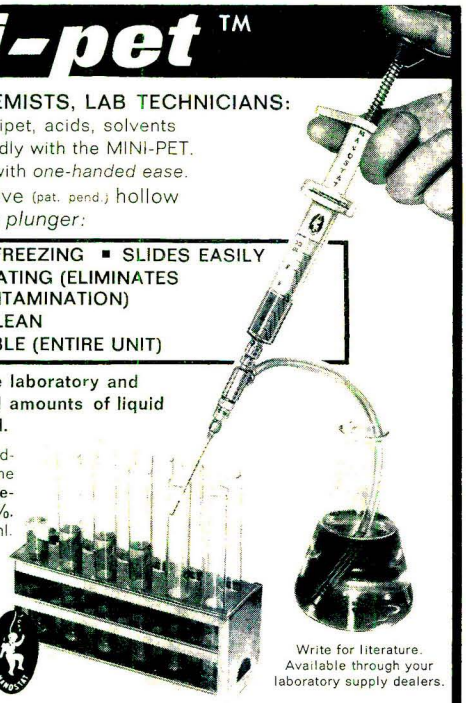
BIOLOGISTS, CHEMISTS, LAB TECHNICIANS:
Dispense, dilute or pipet, acids, solvents or chemicals repeatedly with the MINI-PET. Quick, simple, safe, with *one-handed ease.*
MINI-PET'S exclusive (pat. pend.) hollow *NON-STICK Teflon plunger:*

- ELIMINATES FREEZING
- SLIDES EASILY
- SELF-LUBRICATING (ELIMINATES GREASE CONTAMINATION)
- SIMPLE TO CLEAN
- AUTOCLAVABLE (ENTIRE UNIT)

Unlimited uses in the laboratory and industry where equal amounts of liquid have to be dispensed.

MINI-PETS are easily adjustable to any volume within their capacity. **Repetitive accuracy ± 0.5%.** Sizes 1 ml, 2 ml and 10 ml.

Prices from $21.50 complete.



MANOSTAT *Corporation*

Write for literature. Available through your laboratory supply dealers.

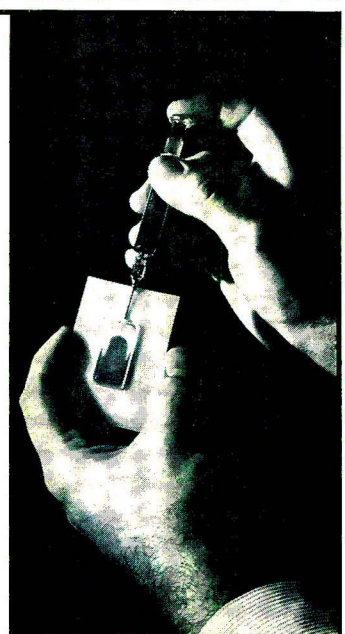
20-22 N. Moore St., Dept. 521, N.Y.C. 10013

Circle No. 50 on Readers' Service Card

FROM STOCK DELIVERY

EXTENDED WAVELENGTH LIQUID CELLS AT $1.55

For all standard extended-range spectrophotometers. Fabricated of high-linearity polyethylene. These brand new cells produce excellent spectra beyond 650cm-1 at a tiny fraction of the cost of KBr, CsBr or CsI. No interference fringes. Virtually no absorption bands. Complete range of pathlengths from 0.1mm to 10.0mm. Only $16.74/dozen. See the new Barnes catalog for complete details.



BARNES ENGINEERING COMPANY
INSTRUMENT DIVISION/30 Commerce Rd./Stamford, Conn./Telephone 203 348-5381

Circle No. 141 on Readers' Service Card

made out of a glass whose refractive index matches that of the ordinary index of the plate.

In 1880 Glan fabricated a polarizer consisting of two right-angle prisms of calcite separated by an air gap. The optic axis in each prism of this polarizer is perpendicular to the light path as shown in the figure. A beam of light travels normal to the end faces, thus suffering no lateral displacement. The ordinary beam undergoes total internal reflection at the calcite-air interface in the first prism. The angle of the prism between the diagonal and the entrance face is about 38° and the acceptance angle of the polarizer is limited to about 7°. As in the case of the Foucault polarizer, the transmitted extraordinary ray suffers additional losses at the calcite-air interfaces. Glazebrook used a polarizer of the Glan type replacing the air gap with a brook's polarizer has a narrower angular field, approximately half that of a Glan polarizer and its useful spectral range is limited by the absorption of the Canada balsam film. Modified polarizers of the Glan and Glazebrook type in which the optic axis is rotated by 90° were used by Thompson and others. Taylor (*1*) used a modified Glan-Thompson polarizer and demonstrated its superior performance in terms of transmission and polarizing characteristics. Single prisms of the type shown in Figure 5 were used by Cotton and others to produce two beams of linearly polarized light. Recent designs employ specially cut prisms of crystal quartz in which the dispersing as well as polarizing characteristics are used. Several designs of polarizing monochromators using such prisms have been reported (*13, 15*).

Quarter-Wave Phase Retarders

Several types of quarter-wave retarders are currently in use. Specially cut thin plates of uniaxial or biaxial crystals may be used as quarter-wave plates for monochromatic radiation; relatively large changes of retardation with respect to wavelength make it necessary to employ several plates to cover a wide spectral region. Adjustable

phase retarders, such as the Babinet-Soliel compensator, are sometimes used for the production and analysis of circularly and elliptically polarized light. These compensators, in general, have narrow angular fields and the tolerances required in their construction are extremely critical. Recently, a tunable retarder based on the photoelastic effect induced by lateral compression of a rectangular plate of fused silica was proposed for use with visible and ultraviolet radiation (*12*). Phase retarders based on total internal reflection and the electro-optic Pockel effect are of particular interest because of their wide applications in circular dichroism measurements. The principle of operation and performance characteristics of these retarders are discussed in some detail below.

Total Internal Reflection

Snell's law of refraction at the boundary of two isotropic media, of refractive indices n and n', relates the angles of incidence and refraction, φ and φ', by the following equation:

$$n \sin \varphi = n' \sin \varphi' \qquad (14)$$

If the incident beam is in the optically denser medium ($n > n'$), the angle of refraction, φ' will be larger than the angle of incidence, φ. The value of φ for which φ' is 90° is known as the critical angle and may be derived from Equation 14.

$$\sin \varphi_c = n'/n. \qquad (15)$$

When the angle of incidence exceeds φ_c, the corresponding angle of refraction is not real, ($\sin \varphi' > 1$), and the incident beam is totally reflected in the denser medium according to the laws of reflection. This phenomenon, called total internal reflection, is represented in Figure 6. The phase of the totally reflected beam may be calculated from Fresnel's laws of reflection and the properties of the incident beam (*11*). The phase difference δ of waves polarized in and perpendicular to the plane of incidence is given by the expression:

$$\tan \frac{\delta}{2} = \frac{\cos \varphi}{\sin^2 \varphi} \sqrt{\sin^2 \varphi - \frac{1}{n^2}} \qquad (16)$$

Figure 7 shows plots of $\delta = \delta(\varphi)$ for internal reflection in fused silica. It may be noted that when the angle of incidence φ is close to that for which the retardation δ is maxi-

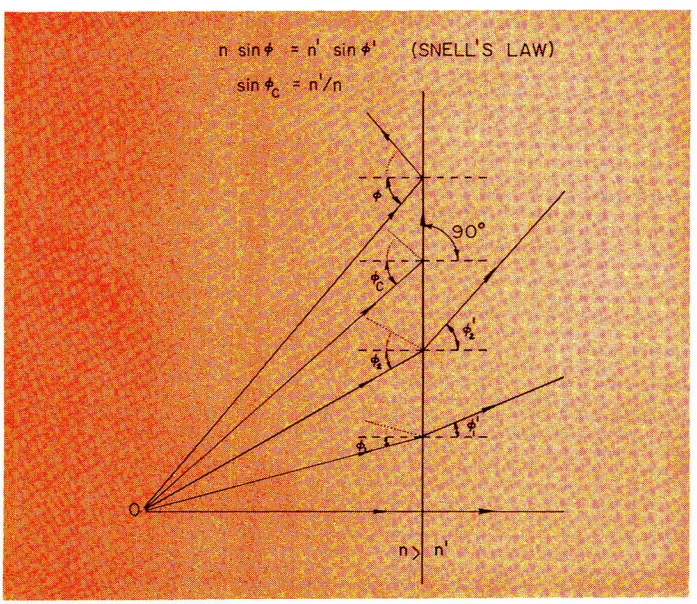
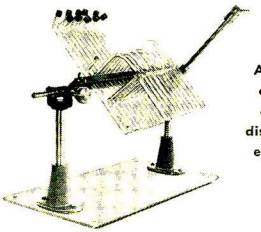


Figure 6. Total internal reflection

OPEN UP NEW AVENUES OF RESEARCH with these versatile analytical tools from POPE SCIENTIFIC

POLY-STAGE FRACTIONATOR

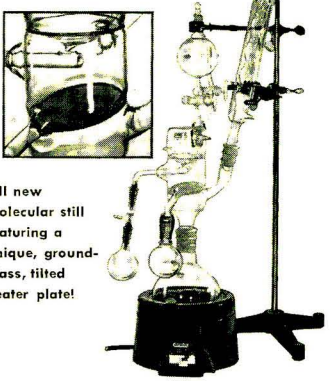


All-glass countercurrent distribution extractor

Add countercurrent distribution apparatus to your laboratory at a price you can afford. The complete unit illustrated sells for just $225.00. The POLY-STAGE FRACTIONATOR gives you... ■ sturdy, heavy-duty rack to help prevent accidents ■ easy access to each cell, provided by Teflon®-lined screw caps ■ simultaneous runs, if desired ■ provision for adding more cells to same rack later on.

TILTA-PLATE STILL

(patent applied for)



All new molecular still featuring a unique, ground-glass, tilted heater plate!

Only the Pope TILTA-PLATE STILL gives you all these features... ■ the ground-glass, tilted plate which presents many times the evaporating surface of a smooth plate ■ adequate capacity for almost all laboratory analytical applications ■ no mechanical parts to wear out ■ all borosilicate glass construction ■ quick removal of non-volatile residue ■ available with two heating arrangements: electric ring-type heater, or refluxing vapors.
Prices start at just $108.00, ready to operate!

Write today for literature and prices.

Are you receiving Pope PACERS*? If not, we will be happy to add your name to our mailing list.

*Our own periodical, featuring lab tips and new apparatus.

pope SCIENTIFIC INC

13604 WEST REICHERT AVENUE
MENOMONEE FALLS, WIS. 53052
PHONE 781-4920 AREA CODE 414

Circle No. 183 on Readers' Service Card

mum, the variation of δ with respect to φ is quite small; therefore, a relatively wide angular field may be used without introducing large errors in the retardation value. Furthermore, for the same choice of φ, variations in δ over a wide range of wavelengths are relatively small; hence, total internal reflection results in near achromatic (wavelength independent) phase retardations.

The principle of the well known Fresnel rhomb is based on adding phase changes due to two successive internal reflections. Curves for retardation as a function of wavelength are shown in Figure 8 for Fresnel rhombs of several angles. The choice of rhomb angle is in general dictated by the wavelength range of interest, the value of phase retardations and the degree of achromaticity desired. It may be noted from Figures 7 and 8 that two internal reflections in silica are not sufficient to introduce quarter-wave retardation in the visible region. Such retardations may be attained, however, by using optical glasses of refractive indices higher than that of silica. Multiple-reflections devices have been used as near achromatic retarders in the visible and near-infrared spectral regions (*20*).

Figure 9 shows the light path inside four internal reflections devices. The Mooney rhomb is a modification of the Fresnel rhomb (*33*); it deviates the incident beam instead of displacing it. Retardation errors due to oblique incidence, in the plane of the diagram, are much smaller in a Mooney rhomb than in a Fresnel rhomb because errors introduced at the two reflecting surfaces compensate each other in the former case and add in the latter case. Devices with more than two reflections may be designed to have better achromaticity and wider angular fields than the Fresnel rhomb (*19*). In general, such devices have the advantage of maintaining the light direction but the disadvantages of size and cost. The material from which internal reflection devices are fabricated should be free of strain or birefringence effects. Fused silica blanks of good quality are now commercially available for this purpose, covering the wavelength range from 1750 A. to 2.5μ. It is important to emphasize that surfaces at which internal reflection takes place should, in principle, be free of optical imperfections and the silica-to-air, or glass-to-air, interfaces should be clearly defined.

Electro-Optic Polarization Modulator (Pockel's Effect)

A complete theoretical analysis of the linear electro-optic effect in uniaxial crystals of the dihydrogen phosphate type was developed by Billings (*2*). These crystals belong to the tetragonal system; they are normally uniaxial and exhibit piezoelectric properties. When an electric field is applied to a crystal of this type, the crystal becomes biaxial. If the applied field is in the direction of the natural optic axis of the crystal, Z-direction, the plane of the induced optic axes will be inclined at $\pm 45°$ to the X- and Y-crystallographic axes, this inclination being independent of the magnitude of the applied field. Figure 10 shows an ammonium dihydrogen phosphate crystal and the orientation of a Z-cut plate in the crystal. The orientation of the crystallographic axes (X, Y) and the electro-optically induced axes (X′, Y′) are also indicated. The induced birefringence for light polarized along the induced axes, X′ and Y′, is given by the expression:

$$(n_{x'} - n_{y'}) = n_o^3 r_{63} \frac{V_z}{d} \qquad (17)$$

where n_o is the ordinary refractive index of the non-excited crystal, r_{63} is the electro-optic coefficient (related to the Pockel's constant), V_z is the applied voltage, and d is the plate thickness. The induced retardation for rays parallel to the applied field may be written as:

$$\delta_0 = (n_{x'} - n_{y'}) \cdot \frac{2\pi d}{\lambda} = \left(\frac{2\pi}{\lambda} n_o^3 r_{63}\right) V_z \qquad (18)$$

Thus for a fixed wavelength, the induced retardation δ_0 is directly proportional to the applied voltage but independent of the thickness of the crystal plate used. Published data for the ordinary refractive index (*42*), n_o, and the electro-optic

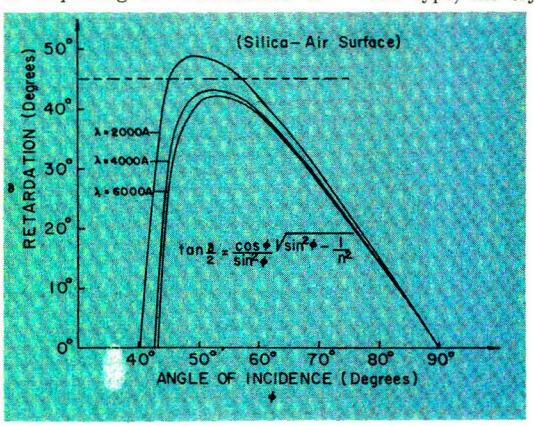


Figure 7. Total internal reflection relative phase retardation

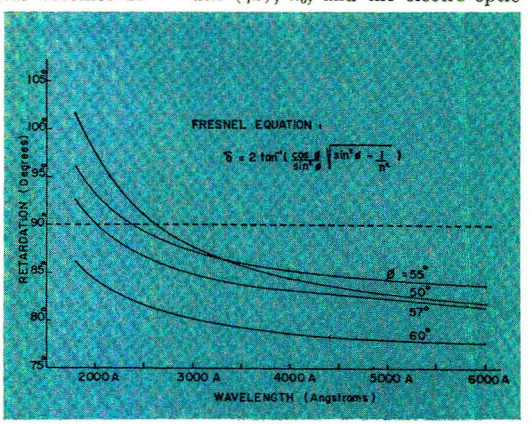


Figure 8. Relative phase retardation due to two total internal reflections in silica at $\phi°$ incidence angle

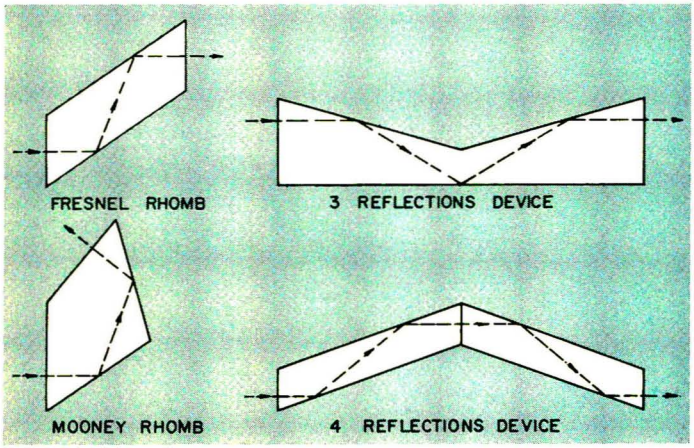


Figure 9. Quarter-wave internal reflection retarders

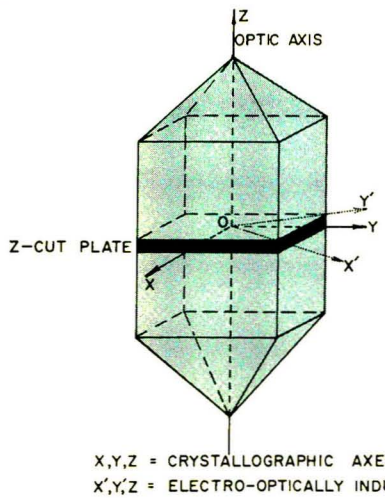
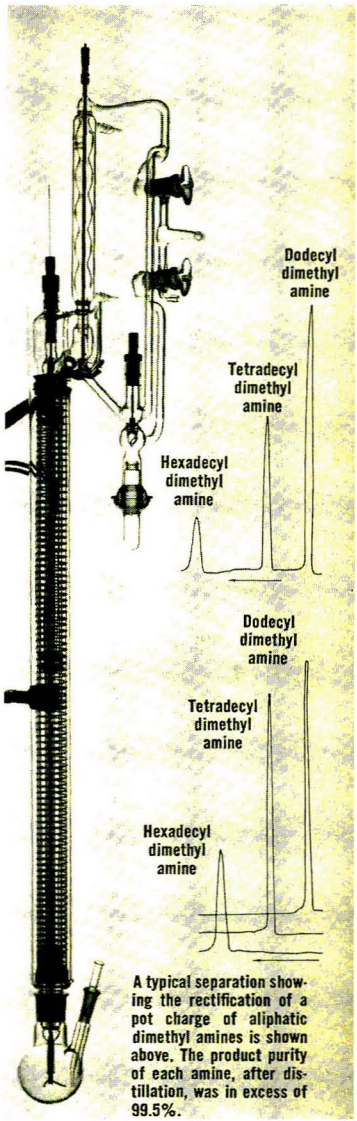


Figure 10. Ammonium dihydrogen phosphate crystal

coefficient (*6*), r_{63} are used in conjunction with Equation 18 to calculate the voltages required for quarter-wave retardation in $NH_4H_2PO_4$, KH_2PO_4, and KD_2PO_4 crystal plates. Figure 11 shows plots of voltage *vs.* wavelength for the three crystals (the ordinary refractive index for KD_2PO_4 (*39*) is assumed to be equal to that for KH_2PO_4). These plots are applicable to normally incident rays on freely supported plates where a uniform electric field is established. Practical voltages may be higher than indicated. It is important to note the almost linear relation of voltage *vs.* wavelength.

Several types of electrodes are used for applying electric voltages across modulator plates. One type consists of metallic laminations, grids or rings, which are evaporated or mounted on the crystal surfaces. The useful aperture of modulators with this type of electrode is necessarily reduced to the clear spacings on the surface. The electric field through the clear spacings, caused by fringing of the field between the electrodes, results in nonuniform retardations across the aperture. Further, high voltages required for operation at long wavelengths result in corona discharge, thus limiting the useful life of the modulator.



A typical separation showing the rectification of a pot charge of aliphatic dimethyl amines is shown above. The product purity of each amine, after distillation, was in excess of 99.5%.

Annular Spinning Band Distillation Column* for High Purity Separations

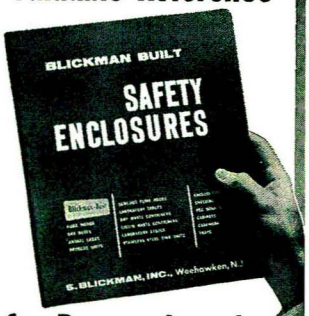
Nester/Faust's new Annular Still employs a **Teflon** band in annular configuration for high plate efficiency (in excess of 125 plates), low holdup (0.3 ml) and low pressure drop (3 mmHg at 50 cc boil-up) to produce **previously unattainable rectification.** Complete price is under $900. Specifications and application data are contained in Distillation Brochure PIB-65630.

Nester/Faust Glass Products Division, 2401 Ogletown Road, Newark, Delaware.
*U.S. and foreign patents pending.

Circle No. 70 on Readers' Service Card →

NESTER/FAUST

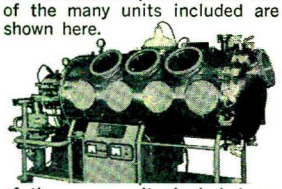
Valuable Reference



for Research and Production Men Working with

- TOXIC CHEMICALS
- RADIOACTIVE MATERIALS
- CONTAMINANTS
- MIRACLE METALS

This book illustrates a wide variety of safety enclosures and controlled-atmosphere boxes. Two of the many units included are shown here.



of the many units included are

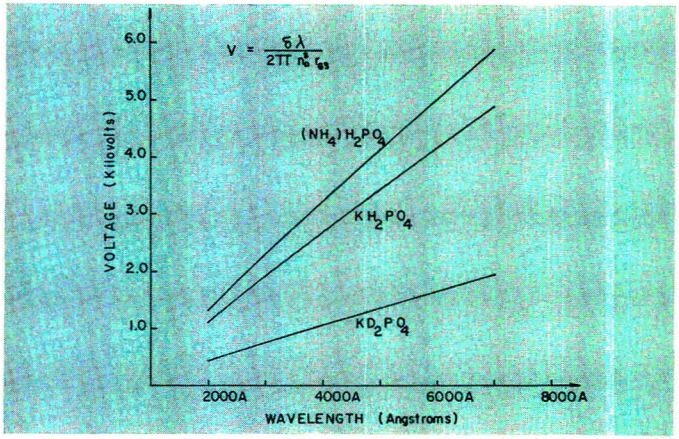


Figure 11. Electro-optic light modulator voltage *vs.* wavelength for $\pi/2$ retardation

Transparent electrodes consisting of glass or silica plates with a thin conducting layer or electrolytic film result in uniform field, and hence uniform retardation across the crystal, but they subject the crystal to undesirable stresses and their usefulness is ultimately limited by problems of electrolysis.

Another important limitation in the use of electro-optic modulators for quantitative measurements is optical in nature. Substantial er-

cut normal to the bisector of the optic axes. The expression for phase retardation due to such a plate is given, to a good approximation by the following equation (*11*):

$$\delta = \frac{2\pi}{\lambda} \frac{d}{\cos r} (n_e - n_o) \sin \theta_1 \sin \theta_2 \qquad (19)$$

where n_o, n_e are the ordinary and extraordinary refractive indices; r is the angle of refraction of either of the wave normals inside the

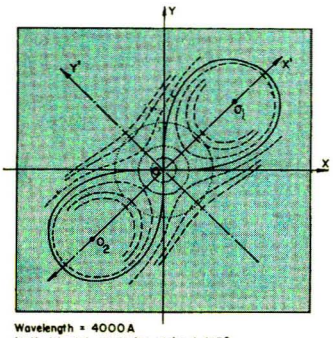


Figure 13. Electro-optic modulator equal retardation contours, 1.0 mm. Z-cut plate (ADP)

Equation 19 gives for normal incidence ($\theta = \theta_2 = \Omega$, $\cos r = 1$):

$$\delta_0 = \frac{2\pi d}{\lambda}(n_e - n_o)\sin^2 \Omega \qquad (20)$$

Equations 18 and 20 may be used to derive an expression for the half biaxial angle:

$$\sin^2 \Omega = \frac{n_o^3 r_{63}}{(n_e - n_o)} \frac{V_z}{d} \qquad (21)$$

Thus for a given wavelength, the sine of the half-biaxial angle, sin Ω, is proportional to the square root of the applied electric field. Figure 12 shows the variation of Ω with wavelength for 1.0-mm. thick plates subjected to quarter-wave voltages. Combining Equations 19 and 20, the expression for retardation may now be written as:

$$\delta = \delta_o \frac{\sin \theta_1 \sin \theta_2}{\cos r \sin^2 \Omega} \qquad (22)$$

which, for small angles of incidence, may be simplified to:

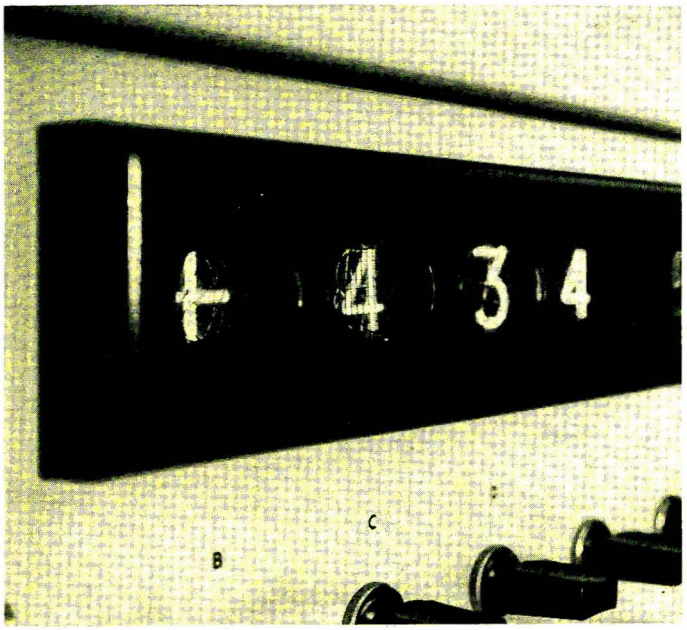
$$\delta = \delta_o \frac{\theta_1 \theta_2}{\Omega^2} \qquad (23)$$

or, in terms of the corresponding angles outside the crystal:

$$\delta = \delta_o \frac{\theta_1' \theta_2'}{\Omega'^2} \qquad (24)$$

Equation 24 is used to calculate retardations for obliquely incident rays on a modulator plate. Figure 13 is a bipolar representation of equi-retardation contours. A gen-

ELIMINATE COSTLY DATA REDUCTION!



READ TEMPERATURE DIRECTLY.....

WITH REC'S NEW MODEL 414 LINEAR BRIDGE

Now you can read temperature directly and accurately to 0.03 per cent, in a range of −100° to +500°F! Simply combine REC's Model 414 Bridge with platinum resistance temperature sensor* and any digital voltmeter.

REC's Model 414 linear bridge provides 1 millivolt per °C or °F suitable for direct presentation on digital voltmeters, printers, etc. Or use it as an input for recorders, computers and control systems. No further signal conditioning is required. Ideal for differential measurements (2 units required).

The cost? Approximately $155.00 complete for bridge and integral power supply. Write today for full details.

*REC also manufactures a complete line of Surface and Immersion Temperature Sensors, Air Data Sensors, Pressure Calibration equipment, Mass Flow and Pressure Sensors and related accessory equipment.

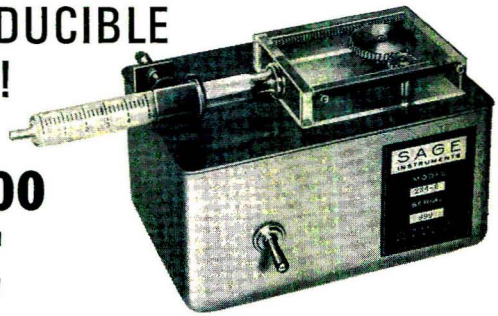
we invite inquiries regarding your particular requirements...

REC ETI DIVISION ROSEMOUNT ENGINEERING COMPANY

4900 WEST 78th STREET • MINNEAPOLIS, MINNESOTA 55435

Circle No. 185 on Readers' Service Card

LOW COST INFUSION PUMP ...REPRODUCIBLE TO ±0.1%!



$145.00 *complete*

Sage Series 234 Constant Speed Syringe Pumps accept all types of syringes, including convenient disposables. Several models are available, each offering a large number of discrete flow rates—obtained by varying syringe sizes (up to 10cc) and "quick-change" gears. Flow rates range from 0.112 μl/day to 16.8 ml/min—depending on specific model chosen.

Large constant speed pumps (up to 100cc capacity) and continuously variable speed models are also available. Variable speed pumps feature a linear flow control dial and a five million to one flow rate range. Optional accessories for both types include a double syringe holder for 2 channel pumping. Infusion-withdrawal models also available.

Whatever your application, there's a Sage Syringe Pump to provide uniform, accurate, and reproducible infusion at the right rate. Ask your lab-ware dealer for a demonstration, or send *today* for complete data.

SAGE INSTRUMENTS, INC.

2 Spring Street, White Plains, N. Y. 10601 • 914 WH 9-4121

Circle No. 158 on Readers' Service Card

RUGGED

YET *FAST-ACTING*—THE NEW PHOTOVOLT ELECTRODES

Always ready for immediate use. Adaptable for all makes and models of pH meters. Manufactured in Photovolt's own U.S.A. plant. Choose from more than 20 different types.



Ask your Laboratory Supply Dealer, or write to:

PHOTOVOLT

1115 Broadway, New York, N.Y. 10010

Circle No. 153 on Readers' Service Card

eral ray is represented by a point whose distance from the pole O is a measure of the angle of incidence of the ray, and whose polar angle relative to OX′ is a measure of the angle between the plane of incidence and the plane of the optic axes of the plate. O_1' and O_2' represent rays parallel to the optic axes; such rays experience no retardation. The lemniscate represents the locus of rays whose retardation is equal to the retardation for normal incidence, δ_0. Rays represented by points inside the lemniscate have lower retardation than δ_0, while rays represented by exterior points have higher retardations. A conical pencil of light is represented in Figure 13 by a circle whose radius is equal to the half-angle of the cone. The dashed contours shown correspond to retardations of 90 ± 8.1, 18.2, and 25.7 degrees; deviations of the retardation from 90 degrees by these increments correspond to an equivalent error of 1, 5, and 10%, respectively, in the circular dichroism value measured by a system employing the above phase retardations. The variations of retardation for rays along a conical pencil is shown in Figure 14 for three pencils of 1°, 2°, and 3° half-angles. Curves shown illustrate the importance of using beams of only small divergence angles when an electro-optic phase retarder is employed.

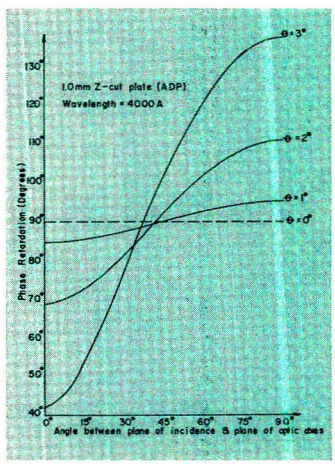


Figure 14. Electro-optic modulator retardation for oblique rays

Measurement of Circular Dichroism

Classical Methods

The circular dichroism of an optically active substance may be measured by one of two equivalent methods. The first involves a direct determination of the difference between the absorption coefficients of the substance in right and left circularly polarized light; the second method measures the ellipticity, defined as the arctangent of the ratio of minor to major axes, introduced to a linearly polarized light beam traversing the optically active substance. The difference between the absorption coefficients, $(k_L\text{-}k_R)$, is related to the ellipticity per unit length, θ, according to Equation 7.

In a classical paper on optical activity published in 1896, Cotton (*8*) describes two apparatus which he designed and used to measure the circular dichroism of optically active tartrates. Cotton's first apparatus is represented in Figure 15. Light from source P_1 is collimated by lens L_1 and linearly polarized by Nicol N_1. Part of the beam from N_1 traverses the Fresnel rhomb F_1 oriented to give a 45° angle between the plane of polarization and the plane of incidence at the total internal reflection surfaces. The circularly polarized beam from F_1 passes through the sample S of pathlength c into a second Fresnel rhomb F_2 which changes the polarization state of the beam back to linear but orthogonally oriented with respect to the initial polarization. The portion of the beam which is attenuated due to sample absorption is now compared with the portion which did not pass through the sample. The comparison is carried out by viewing both portions through a second Nicol N_2 and orienting N_2 such that the two portions are of equal intensity. If the two beams are represented by their electric vectors a and b, it may be noted from Figure 15 that there are two angular positions of N_2 for which the intensities of the transmitted beams will be equal. The absorption coefficient of the sample, for the circularly polarized light used, may be deduced from Beer's law and the measured angle, 2α, between the two positions of N_2. Beer's law expresses the intensity of the attenuated beam in terms of the incident intensity and the absorption coefficient of the sample; for right circularly polarized light:

$$T_R = T_0 e^{-k_R c} \qquad (25)$$

The ratio of the two electric vectors a and b is equal to the tangent of the half-angle between the two positions of N_2; for right circularly polarized light

$$\tan \alpha_R = (a/b)_R. \qquad (26)$$

Since the electric vector is proportional to the square root of the in-

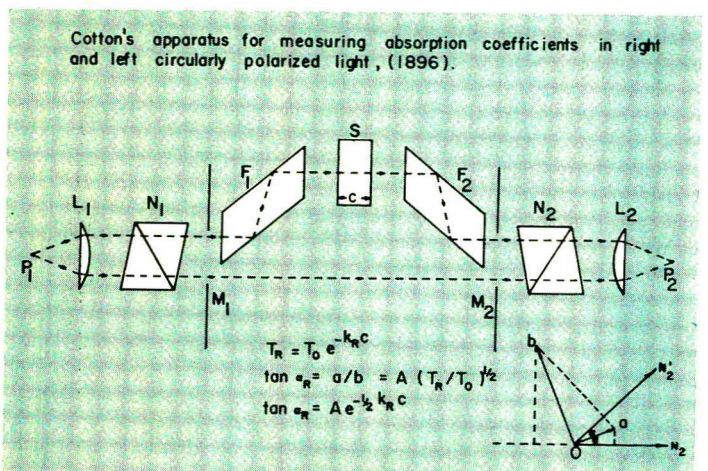
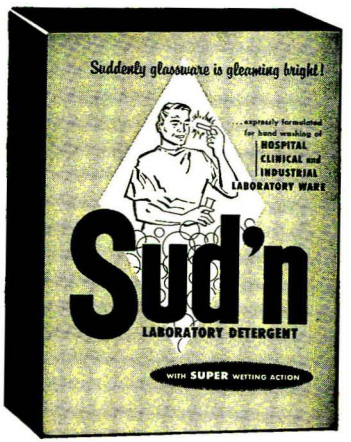


Figure 15. Measurement of circular dichroism

TODAY ITS

BIODEGRADABLE

Sud'n



for BRUSH and ULTRA-SONIC Washing of all laboratory glassware, missile and outer space components. . .used wherever the ULTIMATE in cleaning is ESSENTIAL —where any thing less would be too EXPENSIVE!

CLEANS completely—
RINSES freely—

MONARCH QUALITY PRODUCTS

without film or residue even in **COLD WATER!**

SPECIFY SUD'N

See your laboratory supplier or mail coupon for sample.

SEP-KO CHEMICALS, INC.
3900 Jackson St., N.E.
Minneapolis, Minnesota

OK send free test package of
☐ SUD'N for hand washing
☐ LAB-GLO Mechanical cleaning

Name

Address

City State

Circle No. 86 on Readers' Service Card

NEW... FREE...



VITREOSIL®

PURE FUSED QUARTZ

CATALOG

From Thermal American Fused Quartz Company . . . A comprehensive 48 page catalog describing the latest in **VITREOSIL** pure fused quartz laboratory ware, industrial ware, tubing, fabrication and special quartz products.

Also included are informative sections giving technical and application data.

Price information is included with each catalog — see separate price list.

Ask for your copy today. 46

THERMAL AMERICAN
FUSED QUARTZ CO.
RT. 202 & CHANGE BRIDGE RD.
MONTVILLE, NEW JERSEY
ZIP CODE 07045

Circle No. 90 on Readers' Service Card

tensity, Equations 25 and 26 may be used to derive the following relation:

$$\tan \alpha_R = A(T_R/T_0)^{1/2} = Ae^{-(1/2)k_R c} \quad (27)$$

where A is a constant representing intensity attenuation due to factors other than sample absorption. A and k_R may be determined from Equation 27 and the experimental values of two half-angles, α_R corresponding to two pathlengths of the same sample solution. The absorption coefficient for left circularly polarized light, k_L, is determined in a similar manner, N_1 being oriented to result in left circular polarization on the sample.

Cotton's second apparatus measures circular dichroism in terms of ellipticities. The same apparatus may also be used to measure optical rotation and therefore represents the first "universal" polarimeter. Cotton's original apparatus is shown in Figure 16. Linearly polarized light from the Nicol P traverses a Fresnel rhomb F oriented so that the plane of polarization is parallel to the plane of incidence at the total internal reflection surfaces. A Bravais double-plate B is placed between the rhomb and a Nicol analyzer A set to extinction. A Bravais double-plate consists of two quartz plates of the same thickness, cut parallel to the optic axis and cemented so that the optic axes of the two halves are perpendicular to each other and make ±45° with the cemented edge. An achromatic lens C images the Bravais plate on the slit of a spectroscope. Two spectra, corresponding to the two halves of the Bravais plate, are seen with coincident dark bands at wavelengths for which the two halves of the Bravais plate give phase retardations of $+n\lambda$ and $-n\lambda$, respectively; for adjacent wavelengths, the Bravais plate imparts elliptical polarization which is partially transmitted through the analyzer. The presence of a circularly dichroic sample in position C_3 results in separating the dark bands in the two spectra: the bands will shift to wavelengths for which ellipticities due to the Bravais plate cancel those produced by the sample. The polarizer is then rotated until the ellipticity of the light from the rhomb compensates that due to the sample and the alignment of the dark bands in the image of the Bravais plate is restored. The angle through which the polarizer is rotated will then be equal to the ellipticity of the dichroic sample. Optical rotation is measured in the same manner with the sample placed in position C_2. It is interesting to note that Cotton estimated the accuracy of this apparatus to be of the order of 0.2°.

Measurements of circular dichroism after the pioneering work of Cotton were generally confined to "ellipticity" methods. Bruhat

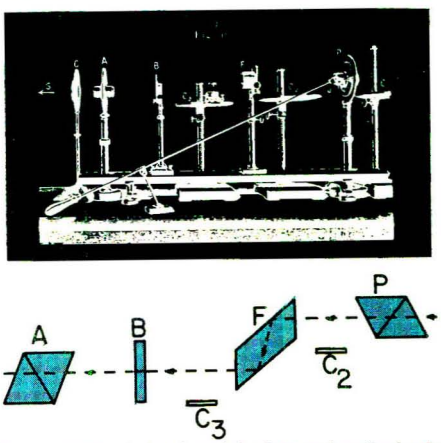


Figure 16. Measurement of circular dichroism and optical rotation—Cotton's universal polarimeter (1896)

(4), in 1915, described an apparatus designed to measure ellipticity and rotation; later, a simplified version of this apparatus (5) was used to measure the ellipticities of weakly dichroic samples. The latter device is represented in Figure 17 and operates as follows: in the absence of an active sample, the quarter-wave plate Q is removed and the polarizer P and analyzer A are first set to extinction. A is a Lippich-double-field analyzer whose angular setting is precisely defined at extinction by a condition of equal illumination in the two halves of its field. Q is then inserted and rotated until its axis is parallel to the transmission axis of the polarizer and extinction is restored. Q is mechanically mounted in such a manner as to allow its removal and reinsertion without disturbing its relative orientation. The optically active sample S is now added, Q is removed and P rotated to compensate for optical rotation due to the sample and restore extinction with A. Q is then reinserted and A rotated to restore extinction again; the angle of rotation of A is then equal to the ellipticity produced by the sample, provided Q is exactly a quarter-wave plate at the wavelength used for the measurement. If δ is the phase retardation due to Q, it may be shown that the measured and true ellipticities, θ' and θ, are related by the following expression:

$$\theta' = \theta \sin \delta \qquad (28)$$

In practice, it may be necessary to use a number of quarter-wave plates to cover a wide range of wavelengths.

Kuhn and Braun (22) described in 1930 an apparatus employing photographic methods for measuring circular dichroism in the visible and ultraviolet spectral regions; this apparatus is represented in Figure 18: light from an arc source illuminates slit S_1; lens L_1 images S_1 on S_2; P is a split polarizer consisting of two Rochon polarizers wedged and cemented with a small angle, 2 θ, between their transmission axes. The two ordinary beams from P are linearly polarized at $+\theta$ and $-\theta$ relative to the plane of incidence at total internal reflection in a specially designed Fresnel water-rhomb F; the beams exiting F exhibit equal elliptical polarizations of opposite sense and of ellipticities $\pm\theta$. In the absence of a dichroic sample, the analyzer

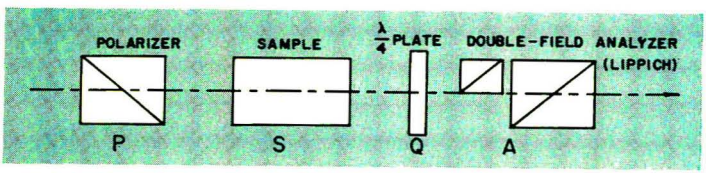


Figure 17. Measurement of circular dichroism and optical rotation—Bruhat's apparatus (1930)

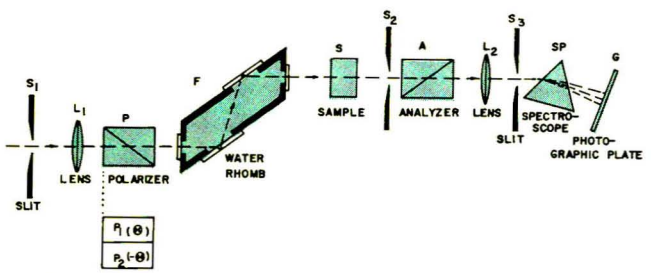
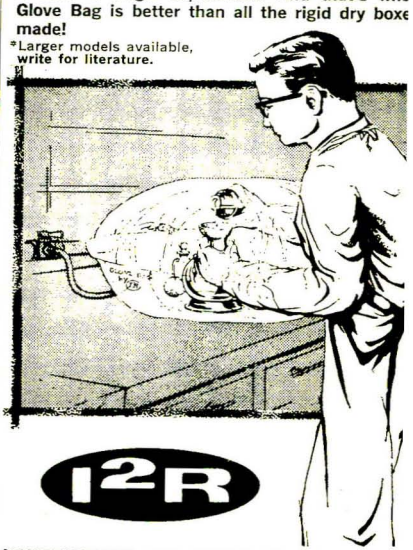


Figure 18. Measurement of circular dichroism in the visible and ultraviolet—Kuhn and Braun's apparatus (1930)



Both Glove Bag and dry box are made to do a equal job: provide a dry, inert or clean atmosphere. But I²R's polyethylene Glove Bag is faste to purge because it starts out flat . . . savir time and gas! It's also transparent, light an portable. Folded, Glove Bag slips easily into you coat pocket . . . expanded you have up to tw cu. ft.* of clear work space! Most importan you may use it over and over again or discar it after a single experiment! **And that's whe Glove Bag is better than all the rigid dry boxe made!**

*Larger models available, write for literature.

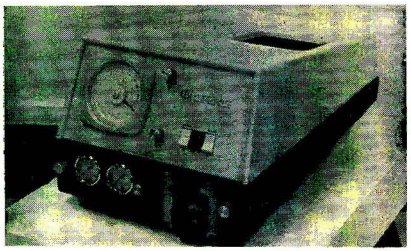


I²R

INSTRUMENTS FOR RESEARCH & INDUSTRY
106 Franklin Ave. Cheltenham, Pa.

Circle No. 53 on Readers' Service Card →

EEL



EEL 140 Atomic Absorption Spectrophotometer

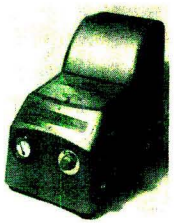
Atlanta, Georgia—0.1 ppm Cu for 1% absorption
Pittsburgh, Pa.—0.03 ppm Ca for 1% absorption
Philadelphia, Pa.—Better than 2Å resolution for difficult to separate lines (iron and nickel)

The above are actual practical results as the EEL 140 proves itself in the field.

* * * * * *

The EEL Flame Photometer uses no acetylene, no oxygen—just natural gas and air.

From a university in Long Island, N. Y.—2.5 ppm Na full scale (.025 ppm 1 scale division)
—5.0 ppm K full scale (.05 ppm 1 scale division)
—40 ppm Ca full scale (.4 ppm 1 scale division)



EEL Flame Photometer

For more information on these and other EEL instruments, contact your nearest

FISHER SCIENTIFIC CO. or

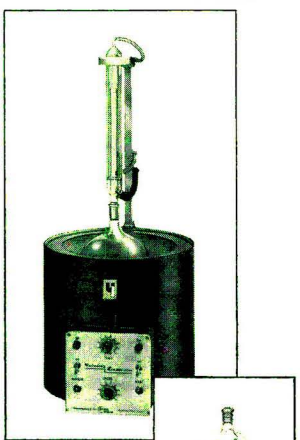
VAN WATERS & ROGERS, INC.

sales offices

INTERNATIONAL SALES ASSOCIATES

115 EAST MAPLE AVE., LANGHORNE, PA. (215) SK7-9874

See Buyers' Guide for all products/sales offices.
Circle No. 54 on Readers' Service Card



evaporate

from one flask . . . 4 flasks . . . 50 test tubes* . . . any way you need . . . with the**

NUTATING EVAPORATOR SYSTEM

ZYMEL CORPORATION

Versatility is only half the story. Look at the efficiency of the unique vertical design and 'nutating' agitation—

- you can fill flasks to 80% of capacity — up to 4000 ml. in one flask
- you can forget about contamination and leaking—all liquid and vapor handling components are glass, with no rotating joints
- you get maximum evaporation rates — unchanged throughout the run
- you get minimum reflux—vapor doesn't condense until it leaves the vacuum jacketed transfer tube
- you get true continuous feed **and** continuous removal of the condensate

*these are our **standard** manifolds
**custom manifolds can be designed for just about any application

YORK INSTRUMENT CORP.

55 W. 42nd St. / New York, N. Y. 10036

Circle No. 178 on Readers' Service Card

A is set with its transmission axis parallel to the minor axes of the elliptical polarizations establishing equal illuminations of the two fields. S_2 serves as a mask to block the extraordinary beams from P. An achromatic lens L_2 images S_2 on the entrance slit S_3 of a spectroscope. The two spectra corresponding to the split polarizer are observed visually or photographically and exhibit equal brightness. The presence of a circularly dichroic sample results in increasing the ellipticity of one of the beams and decreasing that of the other by an amount equal to the ellipticity due to dichroism; this changes the relative illumination of the two spectra. The angle through which the polarizer must be rotated in order to restore equal brightness of the two spectra at a given wavelength is equal to the ellipticity due to the sample at that same wavelength. A series of observations or photographic plates are made for several settings of the polarizer and the spectra are analyzed to locate wavelengths for which the ellipticity due to sample dichroism is equal to the polarizer setting. It is important to note that results obtained in this manner should be corrected for errors due to sample rotation and to deviation of phase retardations of the rhomb from quarter-wave. Measured and true ellipticities, θ' and θ, are related by the expression:

$$\theta' = \theta \sin \delta + \alpha \cos \delta \qquad (29)$$

where α represents optical rotation due to the sample and δ the phase retardation due to the rhomb.

Modern Methods

No significant developments in the field of circular dichroism instrumentation took place for nearly two decades after the publication of Kuhn and Braun. Mitchell and Cormack (*30*) adapted, in 1932, a modification of Bruhat's method using photographic techniques of measurement. However, the apparatus described by Kuhn and Braun remained the only useful apparatus for circular dichroism measurement in the ultraviolet region. With the advent of photoelectric techniques several experi-

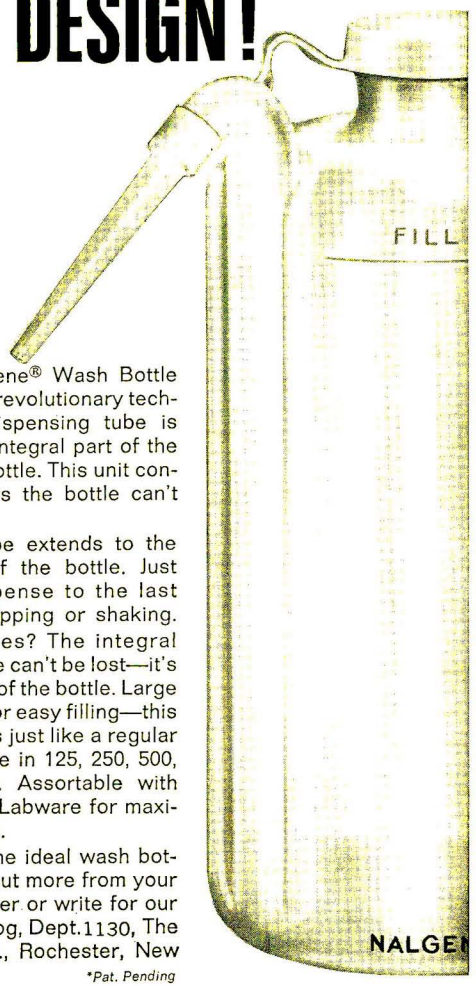
menters devised methods for the measurement of circular dichroism either by ellipsometry or by the direct measurement of the difference in absorption coefficients for left and right circularly polarized light. Mitchell (*29*) (*31*) described, in the early 1950's, an accessory which enables the measurement of circular dichroism with a single-beam photoelectric spectrophotometer. An improved version of this accessory appeared in 1957 (*28*). It consists of optical components that may be inserted in the cell space of the spectrophotometer; a Glazebrook polarizer is followed by a quarter-wave plate, suitable for the wavelength range being studied, which may be rotated between two stops corresponding to $\pm 45°$ angle between the axes of the plate and the transmission axis of the polarizer. Measurements are made at the selected wavelength by placing the sample cell after the quarter-wave plate; the plate is set to give right circularly polarized light and the spectrophotometer's controls are adjusted for 100 per cent transmission, (zero density); the quarter-wave plate is then rotated through 90° resulting in left circularly polarized light at the sample, the corresponding reading on the density scale is the difference in absorption of the sample for the two circularly polarized beams. Mitchell's equipment used a quarter-wave plate made of mica and covered the spectral region from 3500 to 10000 A. The sensitivity of this method of measurement is, in principle, limited to the sensitivity and stability of the spectrophotometer; in practice, however, other sources of uncertainties constitute the limitation: such sources may include beam displacement, as a result of rotating the quarter-wave plate, as well as unequal reflection and absorption losses in the system for the two positions of the quarter-wave plate. Errors due to deviation of retardation in the wave plate from 90° and to angular misalignment of the plate relative to the polarizer may be accounted for by the approximate expression:

$$\Delta A_{\text{measured}} = \Delta A_{\text{true}} \cdot \sin \delta \cdot \cos 2\xi \qquad (30)$$

A REVOLUTIONARY WASH BOTTLE!

NEW CONCEPT!

NEW DESIGN!



The new Nalgene® Wash Bottle incorporates a revolutionary technique.* The dispensing tube is molded as an integral part of the polyethylene bottle. This unit construction means the bottle can't leak!

And, the tube extends to the very bottom of the bottle. Just squeeze. Dispense to the last drop without tipping or shaking.

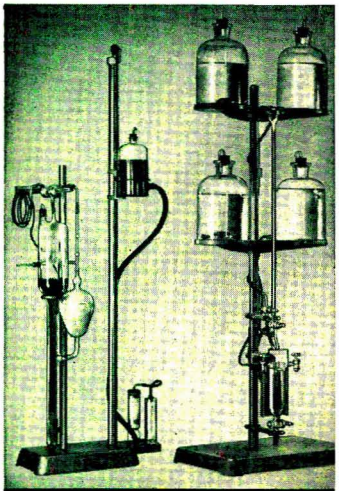
More features? The integral snap-on closure can't be lost—it's molded as part of the bottle. Large neck opening for easy filling—this wash bottle fills just like a regular bottle. Available in 125, 250, 500, 1000 ml sizes. Assortable with other Nalgene Labware for maximum discounts.

Sound like the ideal wash bottle? It is. Find out more from your lab supply dealer or write for our new 1966 catalog, Dept. 1130, The Nalge Co., Inc., Rochester, New York 14602. *Pat. Pending

NALGENE LABWARE
Leader in quality plastic labware since 1949

Another new product of Nalge Research

Circle No. 69 on Readers' Service Card



(Left) Carbon Determinator, (Right) Sulfur Determinator

CARBON & SULFUR DETERMINATORS

BY

DIETERT-DETROIT

ARE THE

MOST DEPENDABLE
EASIEST TO OPERATE
LEAST EXPENSIVE
MOST VERSATILE

Hot tube combustion is still the simple, fail-safe way to make carbon and sulfur tests in a hurry.

If you are interested in the analysis of–

IRON AND STEEL
PETROLEUM CATALYST
STAINLESS ALLOYS
ORGANICS
FOUNDRY SANDS

. . . let us send you detailed information on the Dietert-Detroit Two Minute Carbon Determinator and Three Minute Sulfur Determinator.

HARRY W. DIETERT CO.
9330 Roselawn • Detroit 4, Mich.
Area Code 313 • Phone: WEbster 3-9790

Send me free 16-page Sulfur-Carbon Bulletin

Name_____

Company_____

Address_____

City_____ State_____

Circle No. 36 on Readers' Service Card

where ΔA is the difference in absorption of the sample for left and right circularly polarized light, δ is the phase retardation due to the quarter-wave plate and ξ is the error angle in setting the quarter-wave plate relative to the polarizer.

A novel approach to circular dichroism measurements based on the use of an electro-optic retardation modulator, (Pockel cell), was described by Grosjean and Legrand (*14*) in 1960 for use in the spectral region 2200 to 6000 A. A diagram of their apparatus is shown in Figure 19: a high intensity light source illuminates a single-prism monochromator; the monochromatic beam is collimated by the exit lens of the monochromator and is linearly polarized by a quartz Rochon polarizer. Both beams from the polarizer, ordinary and extraordinary, pass through an electro-optic modulator consisting of a Z-cut plate of ammonium dihydrogen phosphate sandwiched between two transparent electrodes subjected to an alternating voltage. The plate is oriented so that the electro-optically induced axes make an angle of 45° with the direction of the incident linear polarization. The state of polarization following the plate is modulated, at the same frequency as the driving voltage, alternating between left and right circular polarization. The extraordinary beam from the polarizer is masked at the entrance to the sample space while the ordinary beam traverses a sample cell and is then focussed on a phototube. If the sample is circularly dichroic, the output voltage of the phototube will contain an alternating component superimposed on an average component; the alternating voltage is related to the difference in transmission of the sample for left and right circularly polarized light, while the average voltage is related to the average transmission of the sample. The ratio of these two voltages is very nearly proportional to the difference in absorption of the sample for left and right circularly polarized light. This ratio is measured in the following manner: the output voltage of the phototube is separated into its two components, V_{ac} and V_{dc}, by means of a separating amplifier of unit gain. The average component, V_{dc}, is inverted in an amplifier of gain -1 and voltages of $+V_{dc}$ and $-V_{dc}$ are applied across a slidewire. The alternating component, V_{ac}, is amplified by a linear AC feedback amplifier whose output is then rectified, filtered, and compared to the voltage at the sliding contact of the slidewire by means of a servo-amplifier. A servo-motor drives the sliding contact to reduce to zero the difference between the two compared voltages. A pen, mechanically coupled to the sliding contact, records the circular dichroism of the sample. Grosjean and Legrand estimated this system of measurement to be sensitive to absorption differences of approximately 10^{-4} optical density unit. A modified

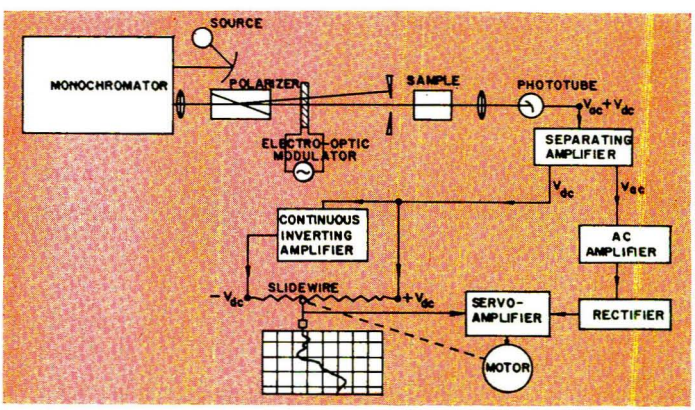


Figure 19. Measurement of circular dichroism—Grosjean-Legrand method

version based on the same principle of measurement but using a polarizing double-prism monochromator and higher efficiency optical system was recently described (*15*). The latter system is claimed to make possible circular dichroism measurements to wavelengths as short as 1850 A. with about three times greater precision than the earlier system. A number of instrument manufacturers are currently producing commercial instruments and accessories for the measurement of circular dichroism, employing electro-optic modulators in a manner analogous to that described above.

A simple optical device for the measurement of circular dichroism between 2500 and 1850 A. with a double beam ultraviolet spectrophotometer was recently described by Holzwarth (*16*, *17*). A quartz Rochon polarizer and a quartz multiwave retardation plate, with optic axis at 45° with respect to the transmission axis of the polarizer, are inserted in the sample beam of the spectrophotometer. The thickness of the retardation plate is chosen to give a phase retardation of about 30 waves in the wavelength region being studied. As the wavelength is scanned, the corresponding phase retardation of the quartz plate varies through several waves. As a result, the polarization state of the sample beam is continually changing (plane, elliptical, circular, elliptical, plane, etc.) as a scan is being made. At successive discrete wavelengths (those for which the plate has odd $\lambda/4$ retardations), the state of polarization in the sample beam becomes left and right circularly polarized. Two matched cells filled with the same solution are placed in the sample and reference beams of the spectrophotometer. The reference compartment is also equipped with a neutral density beam attenuator to compensate for intensity losses due to reflection, polarization, and absorption in the optical elements of the sample beam. A pseudo-depolarizer consisting of a thick slab of crystal quartz, cut parallel to the optic axis, is placed in the sample area immediately before the beam enters the phototube compartment, and serves to minimize artifacts due to the polarization sensitivity of the phototube. Two positions are provided for the sample cell: in the first position, between the polarizer and the quartz plate, the instrument records a baseline exhibiting the difference in absorbance, or transmittance, of the elements in the sample and reference beams, respectively. When the sample cell is placed in the second position, after the retardation plate, an optically active absorption band causes sinusoidal oscillations in the spectrum; the envelope and phase of these oscillations are directly related to the magnitude and sign of the circular dichroism of the sample. Figure 20 illustrates the type of curves obtained with this method of measurement: curves shown for a 1.0-cm. pathlength cell filled with a 2.9 mg. per cc. solution of *d*-camphor in cyclohexane were recorded on a Cary Model 14 spectrophotometer equipped with optical components similar to those described above.

Holzwarth cites three useful characteristics of this type of circular dichroism measurement: first, the sinusoidal nature of oscillations facilitates visual separation of the signal from the noise; second, the high transmittance of the optical elements used makes this method useful for measurements in the low ultraviolet region; and finally, the method of measurement is an absolute one requiring no calibration. Disadvantages of this method of measurement include the fact that circular dichroism values are obtained only at a finite number of wavelengths, and that the spectral bandwidths used are severely restricted since not only the circular dichroism but also the oscillatory character of the curve must be fully resolved. Furthermore, measurements can not in general be carried

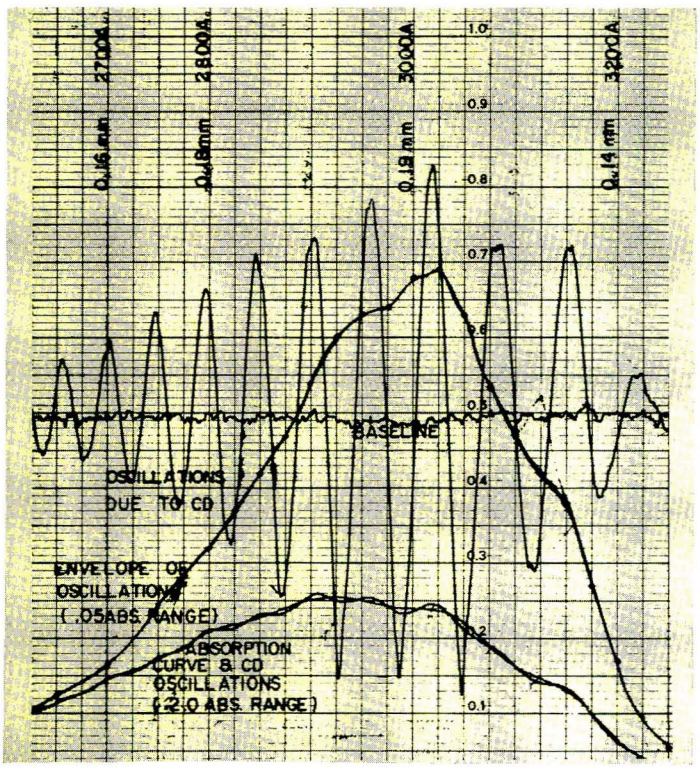


Figure 20. Measurement of circular dichroism in a spectrophotometer—Holzwarth method



Two top-flight, low-cost lines of laboratory equipment that combine compact design with outstanding performance: high-efficiency midget pumps — **both** centrifugal and positive displacement . . . a wide selection of stirrers in variable speeds — both Eastern lines are easily adaptable where minimum space and portability are absolute requisites . . . where mass production prices are essential.

Pump motors powered from 1/30 to 1/3 h.p. offer a range of performance characteristics up to 20 G.P.M. at 15 P.S.I. . . . many of them practically custom-geared to do your job.

Screw-clamp or ringstand mounted, non-sparking stirrers from 1/1000 to 1/15 h.p. perform versatile mixing operations . . . from small quantities of light liquids to 10 gallons of thick, viscous material. Also portable, fixed mounts, and turbine mixers.

These are just two of the Eastern species . . . but there's a whole flock to choose from in the free folder that lists scores of pumping and stirring units for hundreds of applications.

Send for literature Series "L"

LFE | *EASTERN INDUSTRIES*

A DIVISION OF LABORATORY FOR ELECTRONICS, INC.
100 SKIFF STREET • HAMDEN 14, CONNECTICUT

BRANCH OFFICES: Nashua, N.H., Lyndhurst, N.J., Wilmington, Del., Chicago, Ill. Los Altos, Calif., Torrance, Calif. **IN CANADA:** ENTERPRISE AGENCIES., INC., Montreal, Quebec

Circle No. 123 on Readers' Service Card

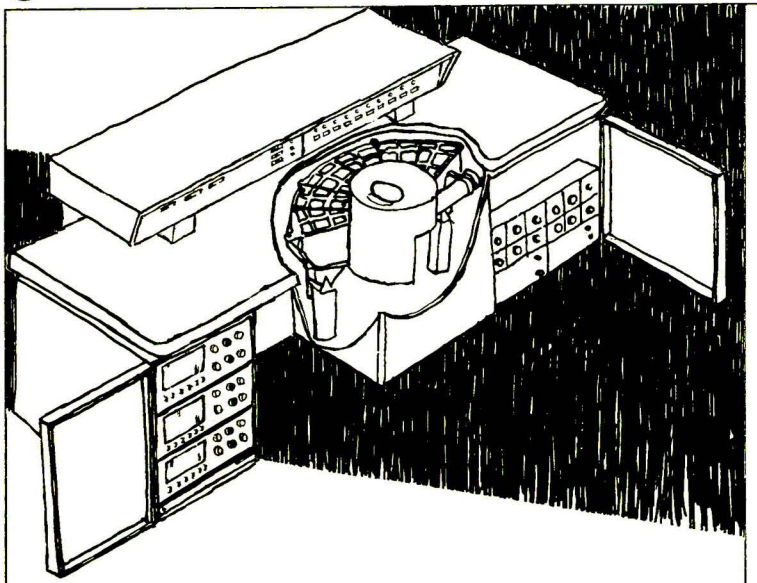
out at a fixed wavelength setting of the monochromator.

Performance Parameters and Error Analysis

A typical system for the measurement of circular dichroism will now be considered. The principle of this system is based on the production of two circularly polarized beams of opposite sense separated in space and/or time. For purposes of mathematical analysis, the system may be characterized by a single polarizer in series with a retarder to produce left and right circularly polarized light, followed by a sample and a detector, respectively. The expression for the CD measured by such a system, (ΔA), is given by the decadic logarithm of the ratio of the two intensities reaching the detector. An expression for these intensities in terms of parameters of the optical elements used and the properties of the sample may be readily obtained by making use of Mueller calculus.

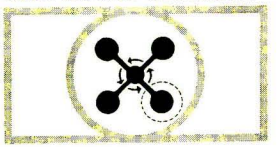
The polarizer employed is assumed to be linear, homogeneous, and scattering; the scattered component produced by the polarizer is considered to be completely depolarized. The performance of the polarizer is represented by the ratio, R, of light intensities transmitted parallel and perpendicular to the axis of the polarizer. A linear phase retarder of retardation δ is oriented so that its axes make an angle of $\pm 45°$, nominally, with the axis of the polarizer. A small angle ξ represents an error in the angular setting of the retarder relative to the polarizer. The sample is considered to be optically active and is characterized by the following parameters: α represents optical rotation; T_L and T_R represent transmittances for left and right circularly polarized light, respectively; furthermore, the sample is assumed to be scattering and the parameter S represents the fraction of radiation reaching the detector which has been completely depolarized as a result of sample scattering.

The expression for CD measured by means of the system described above may be derived as:



A NEW INSTRUMENT FOR ON-THE-SPOT CHEMICAL ANALYSIS OF SOLIDS, LIQUIDS, OR POWDERS!!

MODEL 1050 X-RAY SPECTROMETER



Baird-Atomic's Model 1050 is a *new* X-Ray Spectrometer designed specifically for production control applications.

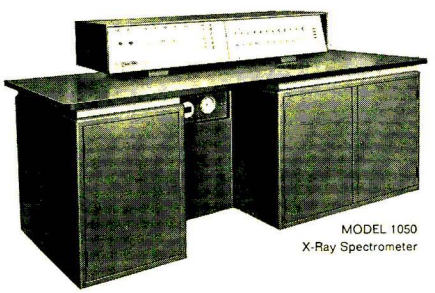
Consistent with Baird-Atomic's outstanding reputation as pioneer-developers of effective emission optical spectroscopy, the Model 1050 represents *another* Baird-Atomic improvement in new chemical analysis techniques.

The Model 1050 will perform multi-element analysis of *solids, liquids,* or *powders simultaneously* in a non-laboratory environment. For efficient, on-the-spot production control, the Model 1050 uses a combination of *sequential* and *simultaneous* channels for maximum analytical speed and minimum cost.

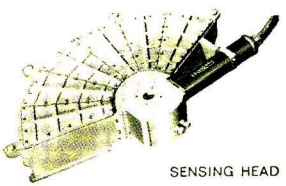
Featuring a teletypewriter as the standard readout, the Model 1050 can be coupled with nearly *any* data handling system. A *spinning sample holder* is standard equipment and *a vacuum system* and *automatic calibration* are available if desired. Moreover, the Model 1050's modular construction provides for the future addition of analytical channels as they become necessary, and its simple rugged construction permits easy maintenance and minimum technical knowledge for operation.

Call or write today for *Brochure No. SC-52* containing complete Model 1050 information.

SCIENTISTS: Investigate challenging opportunities at Baird-Atomic — an equal opportunity employer.



MODEL 1050
X-Ray Spectrometer



SENSING HEAD

Heart of the Model 1050 is its *Sensing Head* which will accept *any* X-Ray tube. The casting is simple yet rugged enough to accomplish production control analysis under the most severe environmental conditions!

BAIRD-ATOMIC

SPECTROCHEMICAL EQUIPMENT DIVISION

33 UNIVERSITY ROAD, CAMBRIDGE, MASSACHUSETTS 02138, Telephone: 617 864-7420

OFFICES: ATLANTA BOSTON CHICAGO DALLAS DETROIT LOS ANGELES NEW YORK PHILADELPHIA PITTSBURGH SAN FRANCISCO WASHINGTON, D.C.
EUROPE: BAIRD-ATOMIC (EUROPE) N.V., 26-27 VEENKADE, THE HAGUE, HOLLAND

Circle No. 107 on Readers' Service Card

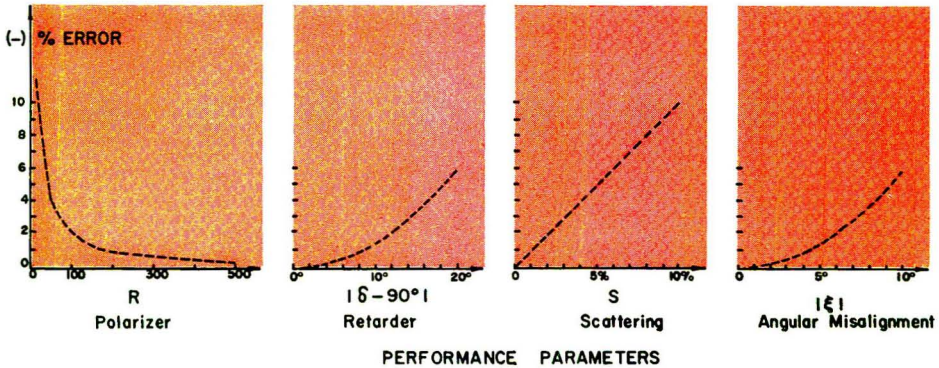


Figure 21. Error analysis of CD measuring system (Differential Absorption Method)

$$(\Delta A)_{\text{measured}} = \log_{10} \frac{T_R F_1 + T_L F_2}{T_L F_1 + T_R F_2} \quad (31)$$

where $$F_1 = 1 + \left(\frac{R-1}{R+1}\right) \times (1 - S) \sin \delta \cos 2\xi \quad (32)$$

and $$F_2 = 1 - \left(\frac{R-1}{R+1}\right) \times (1 - S) \sin \delta \cos 2\xi \quad (33)$$

As the various parameters tend to their "perfect" values, ($R \to \infty$ $S \to 0$; $\delta \to 90°$ and $\xi \to 0$), Equation 31 reduces to:

$$(\Delta A)_{\text{true}} = \log \frac{T_R}{T_L} \quad (34)$$

It is to be noted that Equation 31 does not include the angle of optical rotation α, that is the above measurement is independent of α. Figure 21 illustrates the per cent errors between Equations 31 and 34 as a result of partial variations of the parameters involved. It is important to note that all errors contribute to make the measured magnitude of circular dichroism lower than its true one.

Conclusions

Circular dichroism is currently recognized as one of the most fundamental and useful physical methods of modern stereochemistry. Interest in its measurements and applications is now in the process of undergoing an extensive revival parallel to that given to the field of optical rotatory dispersion during the past decade. Numerous new applications of circular dichroism have appeared in the past few years, notably in the fields of organic chemistry and biological sciences. Circular dichroism studies have also been employed in elucidating the structure of metal ligand complexes. Circular dichroism measurements continue to be used in conjunction with optical rotatory dispersion and ordinary absorption studies in establishing and verifying configurations and properties of matter.

Literature Cited

(1) Archard, J. F., Taylor, A. M., *J. Sci. Instr.* **25**, 407 (1948).
(2) Billings, B. H., *J. Opt. Soc. Am.* **39**, 797 (1949).
(3) Bird, G. R., Shurcliff, W. A., *J. Opt. Soc. Am.* **49**, 239 (1959).
(4) Bruhat, G., *Ann. Phys. (Paris), Sec. 9*, **3**, 232 (1915).
(5) Bruhat, G., *Bull. Soc. Chim. France, Sec. 4*, **47**, 251 (1930).
(6) Carpenter, R., *J. Opt. Soc. Am.* **40**, 225 (1950).
(7) Cary, H. H., *et al., Appl. Opt.* **3**, 329 (1964).
(8) Cotton, A. M., *Ann. Chim., Phys., Sec. 8*, **8**, 347 (1896).
(9) Djerassi, C., "Optical Rotatory Dispersion", McGraw-Hill, New York, 1960.
(10) Djerassi, C., *et al., J. Am. Chem. Soc.* **84**, 4552 (1962).
(11) Drude, P., "Theory of Optics", p. 350, Dover, 1959.
(12) Ennos, A. E., *Opt. Acta* **10**, 105 (1963).
(13) Gates, J. W., King, R. J., *Opt. Acta* **9**, 13 (1961).
(14) Grosjean, M., Legrand, M., *Compt. Rend. Acad. Sci. (Paris)* **251**, 2150 (1960).
(15) Grosjean, M., Tari, M., *ibid.*, **258**, 2034 (1964).
(16) Holzwarth, G. M., Ph.D. Thesis, Harvard Univ. (1964).
(17) Holzwarth, G. M., *Rev. Sci. Instr.* **36**, 59 (1965).
(18) Kauzmann, W., "Quantum Chemistry", Academic Press, New York, 1957.
(19) Kizel, V. A., *et al., Opt. Spectr. (USSR)* (English Transl.) **17**, 248 (1964).
(20) *Ibid.*, **18**, 62 (1965).
(21) Kuhn, W., *Trans. Faraday Soc.* **46**, 293 (1930).
(22) Kuhn, W., Braun, E., *Z. Physik Chem.* **B. 8**, 445 (1930).
(23) Land, E. H., *J. Opt. Soc. Am.* **41**, 957 (1951).
(24) Lowry, T. M., "Optical Rotatory Power", Dover, New York, 1964.
(25) Makas, A. S., *J. Opt. Soc. Am.* **52**, 43 (1962).
(26) McDermott, M. N., Novick, R., *J. Opt. Soc. Am.* **51**, 1008 (1961).
(27) Mislow, K., *et al., J. Am. Chem. Soc.* **85**, 1342 (1963).
(28) Mitchell, S., *J. Sci. Instr.* **34**, 89 (1957).
(29) Mitchell, S., *Nature (London)* **166**, 434 (1950).
(30) Mitchell, S., Cormack, S., *J. Chem. Soc. (London)*, 415 (1932).
(31) Mitchell, S., Veitch, J., *Nature (London)* **168**, 662 (1951).
(32) Moffitt, W., Moscowitz, A., *J. Chem. Phys.* **30**, 648 (1959).
(33) Mooney, F., *J. Opt. Soc. Am.* **42**, 181 (1952).
(34) Mulliken, R. S., *J. Chem. Phys.* **7**, 14 (1939).
(35) Newman, R., Halford, R. S., *Rev. Sci. Instr.* **19**, 270 (1948).
(36) Rosenfeld, L., *Z. Physik* **52**, 161 (1928).
(37) Screaton, G. R., "Dispersion Relations", Interscience, New York, 1960.
(38) Shurcliff, W. A., "Polarized Light", Harvard U. Press., Cambridge, 1962.
(39) Sliker, T. R., Burlage, S. R., *J. App. Phys.* **34**, 1837 (1963).
(40) Velluz, L., Legrand, M., Grosjean, M., "Optical Circular Dichroism", Academic Press, New York, 1965.
(41) Walker, W. C., *Appl. Opt.* **3**, 1457 (1964).
(42) Zernike, F., *J. Opt. Soc. Am.* **54**, 1215 (1964).

Even the "miscellaneous" took us 24 pages.



Get the full details on our radiation counting instruments and accessories (as well as our complete counting systems) for life-science research.

Ask for our new 96-page catalog.

It has 24 pages on our liquid scintillation counting systems, 16 on planchet counting systems, 12 on gamma counting systems, 12 on radiochromatography systems, and, as the picture shows, 24 pages on "miscellaneous." The remaining 8 pages tell you about radiochemicals, the Data Retrieval Computer System, and other items of interest.

Within these 96 pages, you're sure to find the instrument or system that you're looking for. To get a copy of Catalog LSR-100, call your local Nuclear-Chicago sales engineer or write to us.

NUC:8-8-235

NUCLEAR-CHICAGO CORPORATION

351 East Howard Avenue, Des Plaines, Illinois 60018, U.S.A. / Donker Curtiusstraat 7, Amsterdam W, The Netherlands.

Circle No. 157 on Readers' Service Card

Every Bausch & Lomb constant



bandpass SPECTROPHOTOMETER is best in its class!





The SPECTRONIC 600...for SPEED, SENSITIVITY, SIMPLICITY

. . . double-beam, double-grating, ratio-indicating. UV-visible range, 200mμ-650mμ. Best for concentrating on a few selected wave lengths. Best for high stability and reliability requirements. Best for getting many determinations in a short time.

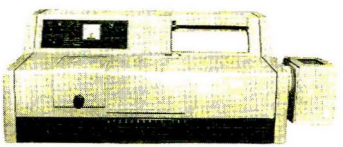
EXTRA SPEED. 3 scanning speeds—10, 50, 250 mμ/minute. 2 slewing speeds—forward and reverse. Automatic zero adjustment. Quick-set 100% line. All operating controls are grouped, readily accessible.

EXTRA SENSITIVITY. Two 1200 groove/mm Certified-Precision gratings in series—assure top performance. Wavelength accuracy and bandpass are constant—5A over the entire range.

EXTRA CONVENIENCE AND EASE OF OPERATION. Two built-in light sources. Large, 103mm long, sample compartment—takes all sizes and shapes of adsorption cells and 10mm square cuvettes. Emission or transmittance measurements with a flick of a switch. Built-in utility receptacle, V.O.M. Recorder jack and wavelength marker. Large, 3 square feet, working surface. Modular, circuit-board design for rapid, simple servicing.

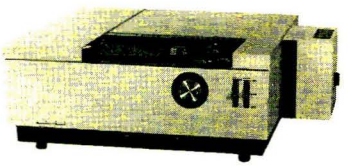
SPECTRONIC 505

. . . double-beam, double-grating, ratio-recording. UV-visible range, 200mμ-650mμ. 6 built-in scanning speeds, combination light source; built-in wavelength calibration. Wavelength accuracy—.5A. Narrow, constant bandpass—5A and 50A standard.



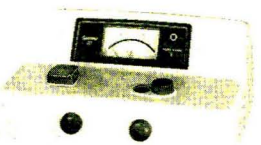
PRECISION SPECTROPHOTOMETER

. . . single-beam, double-grating. UV-visible range, 190mμ-700mμ. Large sample compartment (6" x 6" x 8 1/16"). Choice of collimating or focusing optics. Wavelength accuracy—.5A. Wavelength graduations—.2mμ. Combination light source. Constant bandpass—2A, 5A and 20A.



SPECTRONIC 20

. . . extended range from 340mμ-950mμ. Low stray light, high sensitivity at all wavelengths. Direct scale readings, fast warmup, remarkable stability, easy interchangeability of parts. A Spectrophotometer as well as a Colorimeter.



AND TO GIVE YOU TOTAL FLEXIBILITY . . . THESE BEST OF CLASS ACCESSORIES:

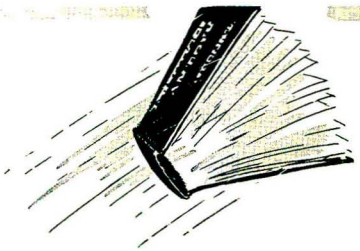
- UV Reflectance Attachment
- Fluorescence Accessory
- Flame Attachment
- End-on Photomultiplier Housing
- Flow-thru Cell
- Constant Temperature Cell Holder
- V.O.M. Strip Chart Recorders
- Microcell Cuvettes
- Time Rate Accessory
- Trichromatic Chart Paper
- Transmittance Chart Paper
- Absorbance Chart Paper
- Tri-Stimulus Integrator
- DT-20 Digital Readout
- AT-20 Digital Readout
- Automatic 100% Adjust
- Specular Reflectance Attachment
- Thermoelectric Heater-Cooler
- Thermindicator
- Gear-Shifter Accessory
- Scale and Pointer Accessory
- Wavelength Reversing Gear Accessory
- Temperature Coefficient Meter

For complete information on all 4 instruments write for Brochure 33-2184, Bausch & Lomb, 60930 Bausch St., Rochester, N.Y. 14602. Or let us arrange a demonstration at your convenience.

BAUSCH & LOMB

See Buyers' Guide for all products/sales offices.
Circle No. 27 on Readers' Service Card

GO AHEAD, THROW AWAY THE TEXT!



The analyst who has been looking for a way to simplify derivative spectrometry need look no further.

The **Block** **Engineering, Inc. Model 200 Interferometer Spectrometer** does just that — simplify! The standard 200 gives you all the IR instrumentation you need for the most complicated analyses — but without tedious mathematical calculations. The 200 has many advantages over conventional dispersion-type spectrometers because it combines the high optical efficiency of interference spectroscopy with the signal enhancing capabilities of modern computer techniques. One can do quantitative micro-analyses, analyze monolayers, or investigate surface interactions with ease. And the 200 brings an entirely new approach to IR work with coatings on opaque substrates, pigmented polymers, sub-toxic concentrations of pesticides and insecticides, air pollution, inorganic and organic crystals, and other samplings heretofore beyond the capabilities of standard IR instruments.



We will be more than happy to send you informative literature; just call or write:

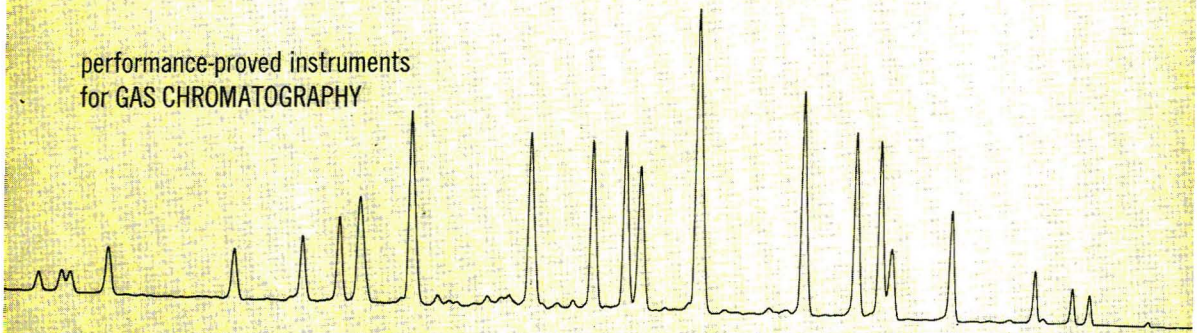
AZTEC INSTRUMENTS, INC.

2 Silverbrook Road • Westport, Connecticut 06880 • (203) 227-1722

See Buyers' Guide for all products/sales offices.
Circle No. 106 on Readers' Service Card

Circle No. 108 on Readers' Service Card ⟶

performance-proved instruments
for GAS CHROMATOGRAPHY



Analysis of Linear Alkyl Benzenes C_9-C_{14}.

NEW MODEL 880: THE FINEST GAS CHROMATOGRAPH BUILT— AND WE'RE READY TO PROVE IT!

Here's the new gas chromatograph that stands as the sum of Perkin-Elmer's twelve years of development and manufacture in gas chromatography: the Model 880.

The Model 880 most closely meets the research and routine requirements of the user; it's the instrument shaped by *your* needs, *your* comments, *your* criticisms. Add up these benefits:

BUILT-IN RELIABILITY:

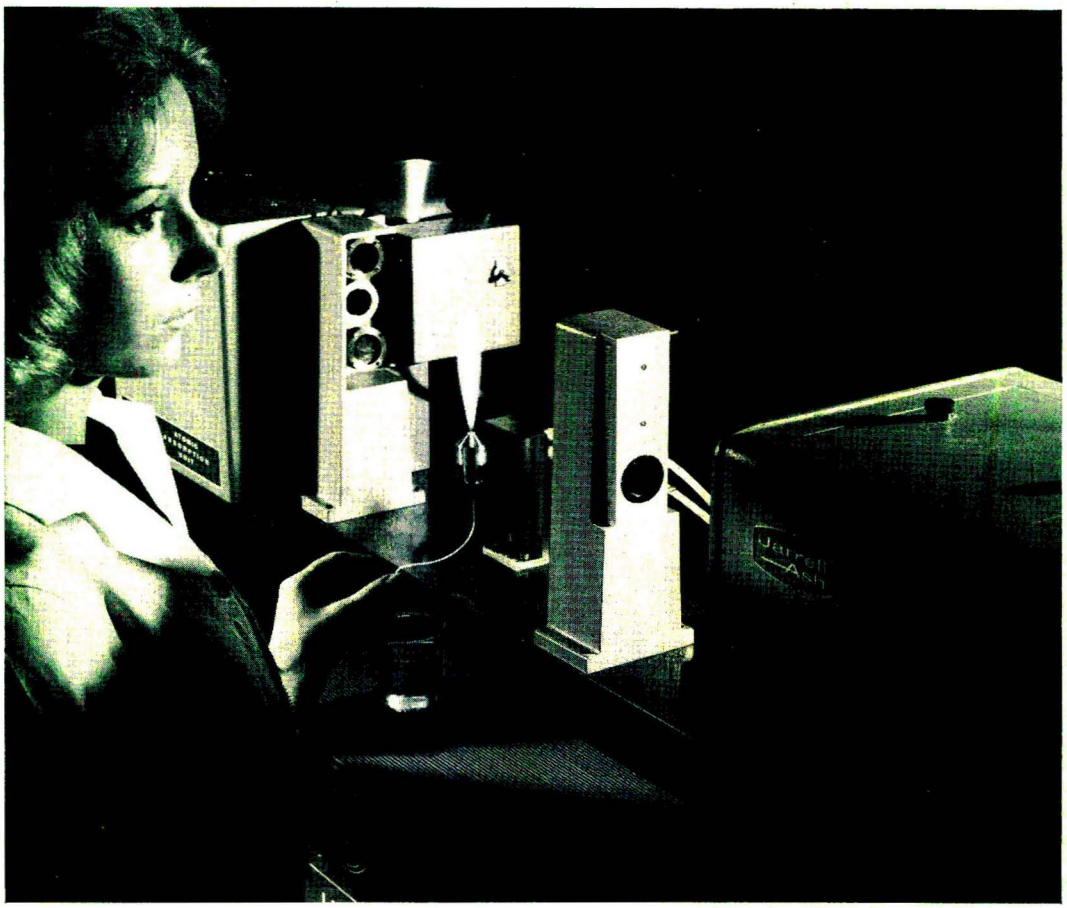
- Easy service—all parts accessible, and readily removable. New dual flame and hot-wire thermal conductivity detectors... and a new electron capture detector, ruggedly built to the exacting standards you asked for.
- A modern, solid-state, electrometer-amplifier—providing reliable unattended operation, particularly when coupled with today's electronic digital data and integration systems.

ANALYTICAL VERSATILITY

- Initial isothermal period control, with a new multi-purpose dial-controlled timer.
- Controls for both hydrogen and helium flows, hydrogen individually controlled to each side of the dual flame ionization detector. For capillary column operation, there's a switch-operated helium flow control bypass.
- Improved gas sampling valve: extremely low dead volume, with one valve serving either column.

Add the already-proven features of Perkin-Elmer gas chromatographs: dual columns, packed or capillary—dual differential detection—linear temperature programming to 400°C—thermally stable, high-velocity circulating air Dynathermal oven—fully-proportional oven temperature control—and you have an instrument that can't be overlooked when you're shopping for GC hardware. If you require on-column injection and glass columns, with all the features of the Model 880, specify Perkin-Elmer Model 881. For complete details, write Instrument Division, Perkin-Elmer Corporation, 702 Main Avenue, Norwalk, Connecticut.





For atomic absorption *(everyday or esoteric)* see Jarrell-Ash

Jarrell-Ash offers three distinct systems, each combining both atomic absorption and flame emission spectrometry. One of them will prove ideal for your needs.

For routine analysis, there's the budget-priced 82-700. It is capable of performing up to 120 analyses per hour and designed for use where dependability, simplicity, space and price are prime considerations.

For maximum versatility, no other atomic absorption spectrometer can compare with the 82-500. Based on the famous Model 82-000 Ebert Spectrometer, it contains a unique multi-pass optical system, plus facilities for altering system components and adding new developments. The 82-500 provides the lowest known limits of detection.

For multi-element analysis, the Model 82-600 gives you the first direct-reading polychromator in the atomic absorption field. Precise and speedy, it analyzes very low concentrations of metallic elements in agricultural, biomedical or industrial samples . . . can determine up to 12 elements simultaneously, perform up to 600 analyses an hour.

We'd like to send you complete technical information on the instrument or instruments that interest you. Also available are copies of a new 16mm color sound movie "Atomic Absorption Spectrometry". Write: Jarrell-Ash, Film Library, 510 Lincoln Street, Waltham, Mass. 02154. Tel. (617) 899-4300. Jarrell-Ash (Europe) S.A., rue de la Jaluse 6, Le Locle, Switzerland.



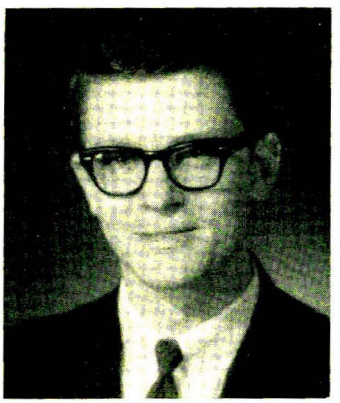
Jarrell Ash

ANALYTICAL INSTRUMENTATION
SPECTROSCOPY · X-RAY DIFFRACTION

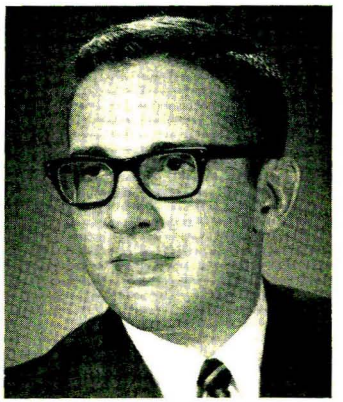
Circle No. 56 on Readers' Service Card

Analytical Division Announces Two Summer Fellowship Winners

THE ANALYTICAL DIVISION of the American Chemical Society has announced two winners of the Division Summer Fellowships. Each award carries a stipend of $800 plus tuition and fees. The winners are Allen G. Hiebert of the University of Illinois and James R. Birk of Purdue University. Brief biographical sketches and descriptions of the winners' major fields of interest and proposed areas of study are given below.



Allen G. Hiebert



James R. Birk

Allen G. Hiebert was born in Hillsboro, Kansas. He received his A.B. degree summa cum laude in 1963 from Tabor College. Since that time he has been at the University of Illinois where he earned his M.S. degree in 1965. He has been awarded a University of Illinois Fellowship in chemistry (1965–66) and a Socony Mobil Oil Company Fellowship in chemistry (1966–67). Mr. Hiebert's general area of research concerns the uses and characteristics of mercury film electrodes. Specifically, he is interested in the formation and behavior of intermetallic compounds. The effects of these compounds have been observed in anodic stripping from a hanging mercury drop. Because of the larger mole fraction of deposited metal in mercury film electrodes the effects of intermetallic compounds may be greater. Mr. Hiebert plans to study these effects in detail.

James R. Birk graduated with distinction from Iowa State University in 1963. Since that time he has been at Purdue University studying under Dr. S. P. Perone. Mr. Birk's major field of interest is electroanalytical chemistry and he has published a paper with Dr. Perone [ANAL. CHEM. 37, 9 (1965)] on the application of derivative techniques to anodic stripping voltammetry. Mr. Birk has been awarded a SOhio Fellowship for 1965–66. His research involves the application of electroanalytical techniques for the identification and determination of transient photo-products produced by flash irradiation. Objectives of the research are: kinetic and mechanistic studies and electrochemical studies of excited states. Having shown that potentiostatic analysis and delayed-time potentiostatic analysis are useful for studying the kinetics and mechanism of a moderately fast photochemical reduction (paper submitted to journal), Mr. Birk plans to investigate increasing the response time for the study of very short-lived photochemical transients.

Conference on Small-Angle Scattering of Electrons and X-Rays

The Institute of Physics and The Physical Society announces that its Electron Microscopy and X-Ray Analysis Groups are arranging a joint conference on Small-Angle Scattering of Electrons and X-Rays to be held at the Institution of Electrical Engineers, Savoy Place, London, W.C. 2., Nov. 17 to 18, 1966. The purpose of the meeting is to stimulate interest in the use of these techniques especially for the study of metals, ceramics, glasses, polymers, and biological materials. Both theoretical and experimental aspects of the subject will be covered. Offers of short contributions of about 20 minutes presentation time are invited. Titles and abstracts, of not more than 300 words, should be sent before July 29 to either Dr. D. E. Henn, Division of Molecular Science, National Physical Laboratory, Teddington, Middlesex (x-ray analysis group) or to Mr. A. E. B. Presland, Department of Chemical Engineering and Chemical Technology, Imperial College, London, S.W. 7. (electron microscopy and analysis group). Further details and applications forms are available by writing to the Meetings Officer, The Institute of Physics and The Physical Society, 47 Belgrave Square, London, S.W.1.

16th NIH Instrument Symposium and Research Equipment Exhibit

The National Institutes of Health, Bethesda, Md., will host the 16th Annual Instrument Symposium and Re-

(Continued on page 67 A)

THE WARNER & SWASEY CO.
CONTROL INSTRUMENT DIVISION

NEW
RAPID
SCANNING
SPECTROMETER

1 Millisecond to scan a broad wavelength region

MODEL 501



Designed to Study:

1. Transient biological phenomena, such as oxidation of blood; changes in visual pigments; changes in enzymes; etc.
2. Chemical kinetics of combustion of solid or liquid propellants.
3. Chemical history of ablation of materials subject to high temperatures and pressures.
4. Transient spectroscopic phenomena in hypersonic wind tunnels, shock tubes and plasmajets.
5. Chemical kinetic reactions, such as stopped flow, relaxation, fluorescence, phosphorescence.
6. The separated fractions from a gas chromatograph.
7. Emission and/or absorption spectra from any transient phenomenon.

Features:

1. Wavelength region from 3000A to 9μ. Width of scan determined by grating chosen.
2. Seven scanning speeds from 1 msec to 100 msec. 30A/μsec. max.
3. Continuous scanning with only 20% off time between scans.
4. Wavelength scale is linear.
5. Adjustable time delay between scans and before 1st scan is initiated.
6. Internal secondary standard for absolute radiance measurements.
7. Cassegrainian collector (f/5.5) focusable from 11″ to infinity.
8. For emission or absorption spectroscopy.
9. Offset multiple scan data presentation.
10. Wide choice of detectors and gratings, easily interchangeable.

WRITE FOR DETAILS AND SPECIFICATION SHEETS

THE WARNER & SWASEY CO.
CONTROL INSTRUMENT DIVISION
32-16 Downing Street • Flushing, New York

Circle No. 173 on Readers' Service Card

Scheduled Courses in Analytical Techniques

June 6 to 10—Activation Analysis Course. San Diego, Calif. *Contact:* Robert M. Watkins, General Atomic Div., General Dynamics Corp., P. O. Box 608, San Diego, Calif. 92112.

June 7 to 8—Workshop on Internal Reflection Spectroscopy. South Norwalk, Conn. *Contact:* Wilks Scientific Corp., 140 Water St., South Norwalk, Conn. Page 66 A, Mar.

June 8 to 10—Fundamental Principles of Nuclear Magnetic Resonance Spectroscopy. University of California, Riverside. *Contact:* University of California Extension, University of California, Riverside, Calif. 92502.

June 11 to 13—ACS Short Course on Spectrometric Identification of Organic Compounds. California State College, Fullerton, Calif. Page 62 A, Apr.

June 13 to 17—Thermoanalysis Institute. Principles and Applications of Thermoanalysis. Fairleigh Dickinson University. *Contact:* Dr. Saul Gordon, Director Thermoanalysis Institute, Fairleigh Dickinson University, Madison, N. J. 07940.

June 13 to 17—Infrared Course. Philadelphia, Pa. *Contact:* Sadtler Research Laboratories, Inc., 3314 Spring Garden St., Philadelphia, Pa. 19104.

June 13 to 17—Gas Chromatography Course. Philadelphia, Pa. *Contact:* Sadtler Research Laboratories, Inc., 3314 Spring Garden St., Philadelphia, Pa. 19104.

June 13 to 18—Biochemical Applications of Gas Chromatography. Curry College, Milton, Mass. *Contact:* Dr. Herbert H. Wotiz, Dept. of Biochemistry, Boston University School of Medicine, 15 Stoughton St., Boston, Mass. 02118.

June 13 to 22—Course in Statistical Techniques in Quality Control. Rochester Institute of Technology. *Contact:* James Swanton, Rochester Institute of Technology, 65 Plymouth Ave. So., Rochester, N. Y. 14608.

June 18 to 20—ACS Short Course on Spectrometric Identification of Organic Compounds. University of Chicago Center for Continuing Education. Page 62 A, Apr.

June 20 to 22—Thermoanalysis Institute. Recent Advances in Thermoanalysis. Fairleigh Dickinson University. *Contact:* Dr. Saul Gordon, Director Thermoanalysis Institute, Fairleigh Dickinson University, Madison, N. J. 07940.

June 20 to 24 and June 27 to July 1—Color Measurement and Specification. Rensselaer Polytechnic Institute. *Contact:* Dr. Fred W. Billmeyer, Jr., Rensselaer Polytechnic Institute, Troy, N. Y. 12181.

June 20 to 24—Nuclear Magnetic Resonance Course. Philadelphia, Pa. *Contact:* Sadtler Research Laboratories, Inc., 3314 Spring Garden St., Philadelphia, Pa. 19104.

June 20 to July 15—Uses of Radioisotopes in Research. Oak Ridge, Tenn. *Contact:* Special Training Division, Oak Ridge Institute of Nuclear Studies, Oak Ridge, Tenn. 37831. Page 57 A, Mar.

June 21 to 25—Nuclear Magnetic Spectroscopy Institute. Canisius College. *Contact:* Dr. Herman A. Szymanski, Canisius College, 2001 Main St., Buffalo, N. Y. 14208.

June 22 to 24—ACS Short Course on Spectrometric Identification of Organic Compounds. Hoboken-Newark-New Brunswick area. Page 62 A, Apr.

June 22 to 30—Course in Design of Experiments. Rochester Institute of Technology. *Contact:* James Swanton, Rochester Institute of Technology, 65 Plymouth Ave. So., Rochester, N. Y. 14608.

June 23 to 24—Basic Gas Chromatography Course, Chicago, Ill. *Contact:* Varian Aerograph, Chicago, Ill.

June 25 to July 16—Electronics for Scientists. University of Illinois. *Contact:* Dr. H. V. Malmstadt, Department of Chemistry and Chemical Engineering, University of Illinois, Urbana, Ill. 61803. Page 63, Jan.

June 26 to 28—ACS Short Course on Spectrometric Identification of Organic Compounds. State University of New York, Binghamton, N. Y. Page 62 A, Apr.

June 27 to 29—Three-Day Laboratory Course on Basic Techniques in Infrared Spectroscopy. Philadelphia, Pa. *Contact:* Sadtler Research Laboratories, Inc., 3314 Spring Garden St., Philadelphia, Pa. 19104.

June 27 to July 1—Second Annual Spectroscopy and Molecular Structure Workshop. Fairleigh Dickinson University. *Contact:* Dr. Raymond Baylouny, Fairleigh Dickinson University, Madison, N. J. 07940.

June 27 to July 8—Modern Industrial Spectroscopy. Boston College. *Contact:* Rev. James J. Devlin, S. J. Director, Department of Physics, Boston College, Chestnut Hill, Mass. 02167.

June 29 to July 1—ACS Short Course on Spectrometric Identification of Organic Compounds. Beacon, N. Y. *Contact:* Dr. Moses Passer, Educational Secretary, ACS, 1155 16th St., N. W., Washington, D. C. 20036.

July 8 to 22 and 25 to 29—Laboratory Techniques—Part I, Methods of Separation; Part II, Instrumental Methods of Identification. Philadelphia, Pa. *Contact:* Sadtler Research Laboratories, Inc., 3314 Spring Garden St., Philadelphia, Pa. 19104.

July 10 to 30—Introduction to Chemical Instrumentation. Purdue University. *Contact:* Prof. H. L. Pardue, Department of Chemistry, Purdue University, Lafayette, Ind. 47907. Page 66 A, Jan.

July 11 to 15—Fine-Particle Properties Workshop (Involves particle size, shape, surface area, and porosity). Fairleigh Dickinson University. *Contact:* Dr. Saul Gordon, Fairleigh Dickinson University, Madison, N. J. 07940.

July 11 to 15—Infrared Course. Philadelphia, Pa. *Contact:* Sadtler Research Laboratories, Inc., 3314 Spring Garden St., Philadelphia, Pa. 19104.

July 11 to 15—Gas Chromatography Course. Philadelphia, Pa. *Contact:* Sadtler Research Laboratories, Inc., 3314 Spring Garden St., Philadelphia, Pa. 19104.

July 11 to 16—Symposium in Modern Instrumental Analytical Chemistry. Lehigh University, Bethlehem, Pa. *Contact:* Robert S. Sprague, Department of Chemistry, Lehigh University, Bethlehem, Pa.

July 12 to 22—Infrared Spectroscopy. University of Minnesota. Two courses: Techniques, July 12 to 16; Chemical Interpretation of Infrared Spectra, July 18 to 22. *Contact:* Center for Continuation Study, University of Minnesota, Minneapolis, Minn. 55455.

July 17 to Aug. 6—Electronics for Scientists. Oregon State University. (Sponsored

by NSF). *Contact:* Harry Freund, Oregon State University, Corvallis, Ore. 97331.

July 18 to 29—The Electron Microanalyzer and Its Applications. Massachusetts Institute of Technology. *Contact:* Director of the Summer Session, Room E-19-356, Massachusetts Institute of Technology, Cambridge, Mass. 02139.

July 18 to Aug. 12—Radioisotope Techniques Institute. State University of New York at Buffalo. *Contact:* Radioisotope Techniques Institute, Western New York Nuclear Research Center, Inc., Power Drive, Buffalo, N. Y. 14214.

July 25 to 27 and July 28 to 29—Introductory NMR/EPR Workshop. Western Reserve University. *Contact:* Dr. Chris Cupas, Dept. of Chemistry, Western Reserve University, Cleveland, Ohio 44106.

July 25 to 29—Polymer Characterization Workshop. Fairleigh Dickinson University. *Contact:* Dr. Norbert Bikales, Fairleigh Dickinson University, Madison, N. J. 07940.

Aug. 1 to 5—Infrared and Ultraviolet Absorption Spectroscopy. Arizona State University. *Contact:* Jacob Fuchs, Department of Chemistry, Arizona State University, Tempe, Ariz.

Aug. 1 to 5—Jarrell-Ash Training School Course on Photographic Emission Spectroscopy. Waltham, Mass. *Contact:* Director, Jarrell-Ash Training Institute, 590 Lincoln St., Waltham, Mass. 02154.

Aug. 1 to 5 and 8 to 12—Jarrell-Ash Training School Course on Direct Reading Spectroscopy. Waltham, Mass. *Contact:* Director, Jarrell-Ash Training Institute, 590 Lincoln St., Waltham, Mass. 02154.

Aug. 8 to 12—Technique of Infrared Spectroscopy. MIT. *Contact:* Dr. J. M. Austin, Director of the Summer Session, Room E19-356, Massachusetts Institute of Technology, Cambridge, Mass. 02139.

Aug. 8 to 12—Short Course on Gas Chromatography for Practicing Chromatographers. Colorado Woman's College, Denver, Colo. *Contact:* Dr. C. E. Borchers, ISA Gas Chromatography Short Course Coordinator, Instrument Society of America, 530 William Penn Place, Pittsburgh, Pa. 15219.

Aug. 15 to 18—Jarrell-Ash Training School Course on Atomic Absorption Spectrometry. Waltham, Mass. *Contact:* Director, Jarrell-Ash Training Institute, 590 Lincoln St., Waltham, Mass. 02154.

Aug. 15 to 19—Applications of Infrared Spectroscopy. MIT. *Contact:* Dr. J. M. Austin, Director of the Summer Session, Room E19-356, Massachusetts Institute of Technology, Cambridge, Mass. 02139.

Aug. 15 to 26—Modern Industrial Spectroscopy. Arizona State University. *Contact:* Jacob Fuchs, Department of Chemistry, Arizona State University, Tempe, Ariz.

Aug. 22 to 26—Infrared Course. Philadelphia, Pa. *Contact:* Sadtler Research Laboratories, Inc., 3314 Spring Garden St., Philadelphia, Pa. 19104.

Aug. 22 to 26—Gas Chromatography Course. Philadelphia, Pa. *Contact:* Sadtler Research Laboratories, Inc., 3314 Spring Garden St., Philadelphia, Pa. 19104.

Aug. 23 to 27—First Infrared Spectroscopy Session of the 17th Annual Fisk University Schedule. *Contact:* Director, Fisk Infrared Institute, Box 8, Fisk University, Nashville, Tenn. 37203.

Aug. 23 to 27—Gas Chromatography Session of the 17th Annual Fisk University Schedule. *Contact:* Director, Fisk Infrared Institute, Box 8, Fisk University, Nashville, Tenn. 37203.

Aug. 27 to 28—ACS Short Course on Computer Programs in Chemical Research. University of Maryland Computer Science Center, College Park, Md. *Contact:* Dr. Moses Passer, 1155 Sixteenth St., N. W., Washington, D. C. 20036.

Aug. 29 to Sept. 2—Second Infrared Spectroscopy Session of the 17th Annual Fisk University Schedule. *Contact:* Director, Fisk Infrared Institute, Box 8, Fisk University, Nashville, Tenn. 37203.

Aug. 29 to Sept. 2—Infrared Spectroscopy. Canisius College. Four simultaneous 5-day sessions. *Contact:* Dr. Herman A. Szymanski, Canisius College, 2001 Main St., Buffalo, N. Y. 14208.

Sept. 4 to 10—Summer School in Spectroscopy: Organic (Infrared and NMR) and Inorganic (Emphasis on Infrared). School of Pharmacy, Brunswick Square, London, W.C.1. and Royal Free Hospital Medical School. *Contact:* Royal Institute of Chemistry, Summer School 1966, 30, Russell Square, London, W.C. 1, England.

Sept. 12 to 16—Activation Analysis Course. San Diego, Calif. *Contact:* Robert M. Watkins, General Atomic Div., General Dynamics Corp., P. O. Box 608, San Diego, Calif. 92112.

Sept. 12 to Oct. 7—Uses of Radioisotopes in Research. Oak Ridge, Tenn. *Contact:* Special Training Division, Oak Ridge Institute of Nuclear Studies, Oak Ridge, Tenn. 37831. Page 57 A, Mar.

(*Continued from page 65 A*)

search Equipment Exhibit, Oct. 3 to 6. The instrument symposium will cover recent developments in research methods and instrumentation. Primary discussion topics include: chemical genetics; analog simulation of biological systems; optical methods of macromolecular structure; physical methods for the determination of the structure of small molecules; trace metal analysis; advances in gas-liquid chromatography; objective methods in psychology; and telemetry. Chairman of the instrument symposium is Dr. Gerald Vurek, NIH; chairman of the research equipment exhibit is Louis Heiss, American Instrument Co., Inc., 8030 Georgia Ave., Silver Spring, Md. Exhibit Manager and symposium executive secretary is James B. Davis, NIH. Inquiries on the symposium and exhibit should be directed to Mr. Davis, National Institutes of Health, Bethesda, Md. 20014.

If the heating system you want hasn't been built yet... build it!

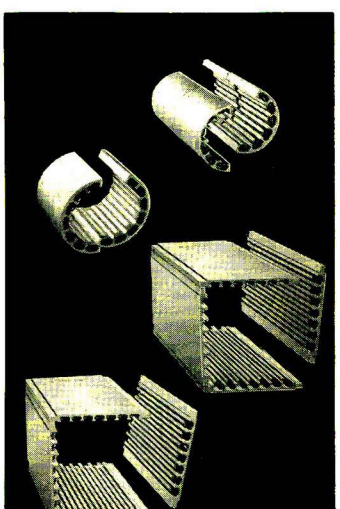
It's simple—with Lindberg Hevi-Duty building blocks of heat. These flexible, low-cost elements can be assembled in countless ways.

They're perfect to heat piping systems where liquids must be kept at constant temperature. Or for special lab requirements that don't justify a furnace. Or where there isn't a furnace to do the job.

They have excellent capacity. High watt density. 1000° or 1200° C. Control them manually, or automatically.

They're available from leading lab dealers in sizes, shapes, and lengths to fit your projects.

Write for bulletin 50910, Lindberg Hevi-Duty, Watertown, Wis. 53094.

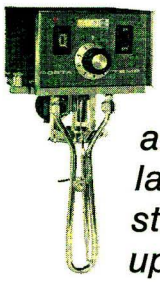


LINDBERG HEVI-DUTY SB

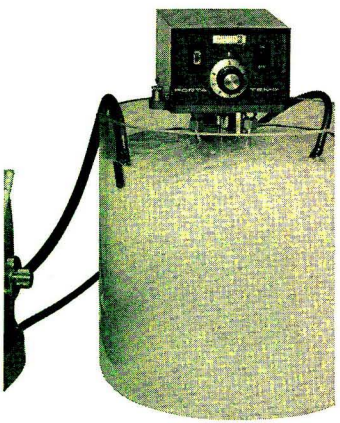
DIVISION OF SOLA BASIC INDUSTRIES

Circle No. 63 on Readers' Service Card

this little character likes to hang around labs and stir things up... and that's not all!



PORTA-TEMP is a constant temperature bath heater, a controller and a circulator, as well as being a born agitator. These abilities are all packed into an 8 pound unit that measures only 6¼" x 7¼" x 13" high.



Clamps to the side of the container —up to ¾" wall—just plug it in for a constant temperature bath, add two pieces of tubing for a circulating system. Maintains bath at any temperature up to 90°C with a ±0.25°C uniformity and ±125°C sensitivity. Pumps up to 180 liters an hour at 0" head, maximum height 48".

Porta-Temp likes variety, hard work, long hours, and has the stamina to stay at it for years. For complete resume of job qualifications, ask your Precision Scientific Distributor or write to us.

Since 1920 • The Finest in Quality Laboratory Apparatus

PRECISION SCIENTIFIC CO.

SUBSIDIARY OF GCA CORPORATION

3737 W. Cortland Street, Chicago, Illinois 60647
Local Offices in New York • Chicago • Los Angeles

Circle No. 80 on Readers' Service Card

CALENDAR OF EVENTS

June 1 to 3	**20th Annual Technical Conference of American Society for Quality Control.** Statler Hilton Hotel, New York City. *Contact:* L. R. Dorsky, Remington Office Systems, 122 E. 42nd St., New York, N. Y.
June 6 to 7	**Research Conference on Progress in Chemical Applications of Nuclear Magnetic Resonance.** University of California, Riverside. *Contact:* University of California Extension, University of California, Riverside, Calif. 92502.
June 6 to 8	**49th Annual Chemical Conference of The Chemical Institute of Canada.** Saskatoon, Canada. Includes papers of interest to analytical chemists. *Contact:* The Chemical Institute of Canada, 48 Rideau St., Ottawa 2, Ontario, Canada.
June 8 to 10	**11th Annual Symposium on the Art of Glassblowing.** Sponsor: American Scientific Glassblowers Society. Statler-Hilton, Boston, Mass. *Contact:* Anthony J. Velluto, Ryan, Velluto, and Anderson, 103 First St., Cambridge, Mass.
June 13 to 17	**Fifth National Meeting of Society for Applied Spectroscopy.** Sheraton-Chicago Hotel, Chicago, Ill. *Contact:* Dr. E. Lanterman, Borg-Warner Corp., Des Plaines, Ill. 60018. Page 55 A, May.
June 16 to 17	**First Great Lakes Regional Meeting, ACS.** Lake Towers Motel, Chicago, Ill. *Contact:* Great Lakes Regional Meeting, 86 East Randolph St., Chicago, Ill. 60601. Page 45 A, Dec.
June 16 to 17	**21st Annual Northwest ACS Regional Meeting.** University of British Columbia, Vancouver, Canada. Includes Analytical Division Sessions. *Contact:* G. B. Porter, Dept. of Chemistry, University of British Columbia, Vancouver 8, B. C.
June 22 to 24	**Nineteenth Analytical Division Summer Symposium.** Sponsor: Analytical Division, ACS, and ANALYTICAL CHEMISTRY. University of Alberta, Edmonton, Alberta, Canada. Subject: Separation Techniques. *Contact:* Dr. W. E. Harris, Dept. of Chemistry, University of Alberta, Canada, Page 47 A, Apr.
June 26 to July 1	**ASTM 69th Annual Meeting and 17th Materials Testing Exhibit.** Chalfonte-Haddon Hall, Atlantic City, N. J. *Contact:* American Society for Testing and Materials, 1916 Race St., Philadelphia, Pa. 19103.
June 26 to July 2	**International Symposium on the Chemistry of Natural Products.** Stockholm, Sweden. *Contact:* Division of Chemistry and Chemical Technology, National Research Council, 2101 Constitution Ave., Washington, D. C. 20418. Page 45 A, Dec.

Coming Events

July 7 to 8—Conference on Spectroscopy and Automation. University of Bristol. *Contact:* Meetings Officer, The Institute of Physics and The Physical Society, 47 Belgrave Square, London, S. W. 1., England. Page 70 A, Mar.

July 7 to 8—Chemically Grown Surface Films. University of Stratchclyde. *Contact:* Meetings Officer, The Institute of Physics and The Physical Society, 47 Belgrave Square, London, S. W. 1., England. Page 73 A, May.

July 11 to 15—Gordon Research Conference on Resonance Phenomena in Metals. Crystal Inn, Crystal Mountain, Enumclaw, Wash. *Contact:* W. George Parks, Department of Chemistry, University of Rhode Island, Kingston, R. I. 02881.

July 12 to 19—Seventh General Assembly and International Congress of the International Union of Crystallography. Moscow, Russia. *Contact:* Dr. D. W. Smits, Rekencentrum der Rijksuniversiteit, Grote Appelstraat 11, Groningen, The Netherlands. Page 46 A, Oct.

July 20 to 21—Symposium on Crystal Growth. Moscow, Russia. *Contact:* See Above, July 12 to 19. Page 46 A, Oct.

July 26 to 30—International Congress and Exhibition on Clinical Chemistry. Munich, Germany. *Contact:* Münchener Mess- und Ausstellungsgesellschaft mbH, München 12, Theresienhöhe 13., Germany. Page 70 A, Mar.

Aug. 8 to 9—Eighth Annual Rocky Mountain Spectroscopy Conference. Albany Hotel, Denver, Colo. *Contact:* R. C. Reinke, Dow Chemical Co., Rocky Flats Division, P. O. Box 888, Golden, Colo. 80402. Page 49 A, Apr.

Aug. 8 to 12—Gordon Research Conference on Separation and Purification. Colby Junior College, New London, N. H. *Contact:* W. George Parks, Department of Chemistry, University of Rhode Island, Kingston, R. I. 02881.

Aug. 10 to 12—Fifteenth Annual Conference on Applications of X-Ray Analysis. Albany Hotel, Denver, Colo. *Contact:* Dept. of Metallurgy, University of Denver, Denver Research Institute, Denver, Colo. 80210. Page 70 A, Mar.

Aug. 15 to 19—International Symposium on Microscopy. Chicago, Ill. *Contact:* Walter C. McCrone, FRMS, The McCrone Research Institute, 451 East 31st St., Chicago, Ill. 60616. Page 70 A, Mar.

Aug. 15 to 19—18th National Meeting American Association of Clinical Chemists. Americana Hotel, Bal Harbour (Miami Beach), Fla. *Contact:* George T. Lewis, P. O. Box 359, S. Miami, Fla. 33143.

Aug. 22 to 26—Gordon Research Conference on Analytical Chemistry. New Hampton

School, New Hampton, N. H. *Contact:* W. George Parks, Department of Chemistry, University of Rhode Island, Kingston, R. I. 02881.

Aug. 22 to 26—Gordon Research Conference on Infrared Spectroscopy. Kimball Union Academy, Meriden, N. H. *Contact:* W. George Parks, Department of Chemistry, University of Rhode Island, Kingston, R. I. 02881.

Aug. 28 to Sept. 4—Sixth International Congress of Electron Microscopy. Kyoto, Japan. *Contact:* Prof. E. Snito, Secretary General, Institute of Chemical Research, Kyoto University, Kyoto, Japan.

Sept. 5 to 7—Rare Earth Conference. University of Durham, England. *Contact:* Meetings Officer, The Institute of Physics and The Physical Society, 47 Belgrave Square, London S. W. 1., England.

Sept. 5 to 9—IX International Conference on Coordination Chemistry. St. Moritz-Bad, Switzerland. Sponsors: Swiss Chemical Society, Swiss Society of Chemical Industries, and IUPAC. *Contact:* Dr. R. Gut, IX I.C.C.C., Anorg. Chemie Eth, Universitaetstr. 6, 8006 Zurich, Switzerland.

Sept. 6 to 10—20th Annual Molecular Spectroscopy Symposium. Columbus, Ohio. *Contact:* Prof. Harald H. Nielsen, Ohio State University, Dept. of Physics, 174 West 18th Ave., Columbus, Ohio. 43210. Page 72 A, May.

Sept. 11 to 16—National American Chemical Society Meeting. New York City. Includes Analytical Division Sessions. *Contact:* Charles V. Banks, Department of Chemistry, Iowa State University, Ames, Iowa. 50012.

Sept. 12 to 16—Conference on the Measurement of Nuclear Radiation. Berkeley, Gloucestershire, England. *Contact:* Meetings Officer, The Institute of Physics and The Physical Society, 47 Belgrave Square, London S. W. 1., England. Page 68 A, Mar.

Sept. 15 to 16—Symposium on Pyrolysis–Gas Chromatography. Ecole Polytechnique, Paris, France. *Contact:* Dr. G. Guiochon, Ecole Polytechnique, 17, rue Descartes, F 75, Paris, 5, France. Page 67 A, Mar.

Sept. 19 to 21—Conference on Instrumental Optics and Optical Design. Chelsea College of Science and Technology. *Contact:* Meetings Officer, The Institute of Physics and The Physical Society, 47 Belgrave Square, London, S. W. 1., England. Page 50 A, Apr.

Sept. 20 to 23—Sixth International Symposium on Gas Chromatography. Catholic University, Rome, Italy. Sponsor: Gas Chromatography Group of the Institute of Petroleum. *Contact:* Dr. A. B. Littlewood, School of Chemistry, The University, Newcastle upon Tyne 1, England. Page 68 A, Sept.

Sept. 24—Symposium on Gel Filtration. Istituto Superiore di Sanita, Rome, Italy. *Contact:* Dr. F. Dentice, Istituto Superiore di Sanita, viale Regina Elena, 299, Roma, Italy.

Sept. 27 to 29—Tenth Conference on Analytical Chemistry in Nuclear Technology. Mountain View Hotel, Gatlinburg, Tenn. *Contact:* Mr. L. J. Brady, Oak Ridge National Laboratory, P. O. Box X, Oak Ridge, Tenn. 37831. Page 70 A, June.

Oct. 3 to 6—National Institutes of Health Annual Research Equipment Exhibit and Instrument Symposium. National Institutes of Health, Bethesda, Md. *Contact:* Mr. James B. Davis, National Institutes of Health, Bethesda, Md. 20014. Page 65 A, June.

Oct. 3 to 7—Conference on Trace Characterization, Chemical and Physical. Washington, D. C. *Contact:* Dr. W. W. Meinke, Analytical Chemistry Division, National Bureau of Standards, Washington, D. C. 20234. Page 95 A, Mar.

Oct. 8 to 16—Second International Chemical Exhibition and the Seventeenth International Congress "Chemistry Days." Milan, Italy. Includes instruments and apparatus. *Contact:* General Secretary, Piazzale Rodolfo Morandi 2, Milano, Italy.

Oct. 10 to 13—Association of Official Analytical Chemists 80th Annual Meeting. Marriott Motor Hotel, Twin Bridges, Washington, D. C. *Contact:* Luther G. Ensminger, Association of Official Analytical Chemists, Box 540, Benjamin Franklin Station, Washington, D. C. 20044.

Oct. 11 to 13—Fourteenth Detroit Anachem Conference. McGregor Memorial Conference Center, Detroit, Mich. *Contact:* Roger E. Marce, Allied Research Products, 400 Midland Ave., Detroit, Mich. Page 73 A, May.

Oct. 11 to 14—Conference on Progress in Raman Spectroscopy. Weimar, Germany. *Contact:* Dr. H. Kriegsmann, Deutsche Akademie der Wissenschaften Zu Berlin, 1199 Berlin-Adlershof, den Rudower Chausskee 5, Berlin, Germany.

Oct. 12 to 14—IMEKO Symposium on Microwave Measurement. Budapest, Hungary. *Contact:* Organizing Committee of the IMEKO Symposium on Microwave Measurements, Budapest 5, P.O.B. 457, Hungary.

Oct. 13 to 14—Eleventh Annual Symposium on Advances in Tracer Methodology. Sheraton Plaza Hotel, Boston, Mass. *Contact:* New England Nuclear Corp., 575 Albany St., Boston, Mass. 02118. Page 70 A, Mar.

Oct. 16 to 19—ACS Western Regional Meeting. Jack Tar Hotel, San Francisco, Calif. *Contact:* R. L. LeTourneau, Chevron Research Co., P. O. Box 1627, Richmond, Calif. 94802. Page 57 A, Mar.

Oct. 17 to 19—1966 Technicon International Symposium on Automation in Analytical Chemistry. Statler-Hilton Hotel, New York City. *Contact:* Technicon Instruments Corp., Chauncey, N. Y. 10502.

Oct. 17 to 22—3rd Exhibition and Congress of Laboratory, Measurement, and Automation Techniques in Chemistry. Basle, Switzerland. *Contact:* Exhibition and Congress Secretariat, CH-4000 Basel 21, Switzerland.

Oct. 18 to 19—Symposium on Liquid Scintillation Counting. National Physical Laboratory, Teddington, Middlesex, England. *Contact:* Meetings Officer, The Institute of Physics and The Physical Society, 47 Belgrave Square, London, S. W. 1., England.

Oct. 19 to 21—Nuclear Science Symposium. Statler-Hilton Hotel, Boston, Mass. *Contact:* Dr. J. A. Coleman, Electron Devices Section, National Bureau of Standards, Washington, D. C. 20234. Page 65 A, May.

Oct. 24 to 26—1966 Canadian Symposium on Applied Spectroscopy. Holiday Inn Hotel, Montreal, Quebec. *Contact:* Dr. S. Barabas, Noranda Research Centre, 240 Hymus Blvd., Pointe Claire, Quebec, Canada. Page 49 A, Apr.

TO MICRO-ANALYSIS ADD ASSURANCE

BDH MICRO-ANALYTICAL REAGENTS 'M.A.R.'

Specially prepared to meet the exacting requirements of the Society for Analytical Chemistry, London.

Anhydrone 14-22 mesh 'M.A.R.
Asbestos 'M.A.R.'
Camphor 'M.A.R.'
Cupric oxide 'powder' 'M.A.R.'
Cupric oxide wire form 'M.A.R.'
Cupric sulphate 'M.A.R.'.
p-Cymene 'M.A.R.'
Dekalin (deca-hydronaphthalene) 'M.A.R.'
Diethyl ether 'M.A.R.'
D(+) Glucose 'M.A.R.'
Hydriodic acid 'M.A.R.'
Hydrochloric acid 'M.A.R.'
Hydrogen peroxide 100 volumes 'M.A.R.
Lead chromate 14-22 mesh 'M.A.R.'
Manganese dioxide 10-20 mesh 'M.A.R.'
Mercuric sulphate 'M.A.R.'
Nitric acid 'M.A.R.'
Potassium nitrate 'M.A.R.'
Potassium sulphate 'M.A.R.'
Selenium 'M.A.R.'
Silver (metal) gauze 60 mesh 'M.A.R.'
Silver (metal) wool 'M.A.R.'
Soda asbestos 14-22 mesh 'M.A.R.'
Sodium carbonate anhydrous 'M.A.R.'
Sodium hydrogen sulphite solution 35% w/v 'M.A.R.'
Sodium peroxide 'M.A.R.'
Sodium sulphide 'M.A.R.'
Sodium thiosulphate 'M.A.R.'
Sulphate-molybdate reagent 'M.A.R.'
Sulphuric acid 98% 'M.A.R.'
Toluene-p-sulphonic acid 'M.A.R.'

Name_____

Organization _____

Dept. _____

Address_____

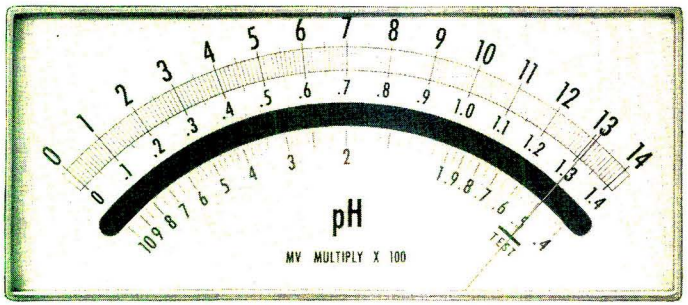
AC666

For prices & specifications plus a complete B.D.H. catalogue fill in the above coupon and mail to:

GALLARD-SCHLESINGER CHEMICAL MFG. CORP.
Carle Place, N.Y. 11514
Phone: (516) 333-5600
EXCLUSIVE DISTRIBUTORS OF BDH CHEMICALS IN THE UNITED STATES

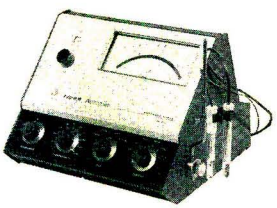
Circle No. 128 on Readers' Service Card

See how precisely you can read this expanded pH scale. To ±0.002 pH unit.



⅔ actual size

It's on Fisher's new Accumet® 310 pH Meter.



When you measure pH, you need an *instrument* that can measure accurately to however many places you require. You also need a *scale* that shows the value as precisely as it's measured. You have both in Fisher's new Accumet 310 pH Meter. Its expanded mode stretches 1.4 pH or 140 mv over 7 inches, giving readings accurate to ±0.005 pH or ±0.5 mv. The 1.4-pH ranges begin at any integral value, overlap so most readings can be made to ±0.002 pH or ±2 mv near midscale. As you see, the Accumet 310 has the usual 0-14 pH, 0 to ±1400 mv scale (±0.05-pH or ±5-mv accuracy), and a logarithmic scale showing relative ion concentrations. You'll use the Accumet 310 for both routine measurements and research, and for electrometric titrations (including Karl Fischer). Scales are mirror-backed to eliminate parallax; response is fast, circuits drift-free; use of recorders is easy; accessory adapts for microsamples. And the unique Accumet test circuit shows whether errors are external or internal when readings are questioned. All for just $595, with guaranteed Fisher electrodes. **For our product bulletin,** write Fisher Scientific Company, 100 Fisher Building, Pittsburgh, Pa. 15219. J-524

FISHER SCIENTIFIC CO.

Instruments, Apparatus, Furniture and Chemicals for Laboratories

Complete stocks in all these locations: Atlanta • Boston • Chicago • Cleveland • Houston • New York Philadelphia • Pittsburgh • St. Louis • Union, N. J. • Washington • Edmonton • Montreal • Toronto • Vancouver

See Buyers' Guide for all products/sales offices.
Circle No. 43 on Readers' Service Card

Tenth Conference on Analytical Chemistry in Nuclear Technology

The Tenth Conference on Analytical Chemistry in Nuclear Technology will be held in Gatlinburg, Tenn., Sept. 27 to 29. This conference is sponsored by the Analytical Chemistry Division of the Oak Ridge National Laboratory with close cooperation and assistance of staff members from Phillips Petroleum Co., Idaho Falls, Idaho; E. I. du Pont de Nemours and Co., Savannah River Plant, Aiken, S. C.; and the Brookhaven National Laboratory, Upton, L. I., N. Y. All sessions of the meeting will be held in the Mountain View Hotel.

Sessions are planned to cover the latest developments in remote analysis of radioactive materials in hot cells; analysis of alkali metal in nuclear technology; and general papers on analytical chemistry in nuclear technology. A limited number of papers up to 25 minutes in length are being solicited. Papers should be directed toward the conference subjects. Authors are requested to submit a letter of intent by June 15, giving the title, authors, and a time estimate for presentation. An abstract of 200–500 words should be sent no later than July 15. Abstracts and inquiries should be directed to L. J. Brady, Oak Ridge National Laboratory, P. O. Box X, Oak Ridge, Tenn. 37830. Reservations for lodging should be made by direct communication with The Mountain View Hotel, Gatlinburg, Tenn. 37738.

International Symposium on Physical Separation Methods in Chemical Analysis

An International Symposium on Physical Separation Methods in Chemical Analysis is being organized by the Analytical Chemistry Section of the Koninklijke Nederlandse Chemische Vereniging to be held in the Congrescentrum, RAI, Amsterdam, April 10 to 14, 1967.

The scientific program will consist of invited and submitted papers. The subjects of the invited papers and the authors are:

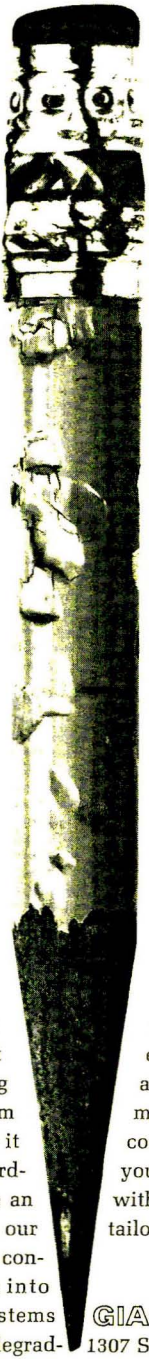
Chromatography. G. W. A. Rijnders, Koninklijke Shell-Laboratorium, Amsterdam.

Ion Exchange Chromatography. O. Samuelson, Technical University, Göteborg.

Zone Melting. H. Schildknecht, University of Heidelberg.

Ultracentrifugation of Synthetic Polymers. H. Benoit, Centre de Recherches sur les Macromolécules, Strasbourg.

This is a data recording system.



(Very expensive)

It keeps high priced researchers occupied with hand tabulations. It keeps expensive computers waiting for data to process. It keeps you from getting the answers you need. Trade it in on a Datex Automatic Digital Recording System. (For instance, if you are an astronomer or a spectroscopist, get our CDS-1 system which automatically converts optical spectrum plate data into digital computer format.) Datex systems will triple your throughput without degrading your data. They can be pre-programmed to run experiments on their own, freeing researchers for creative work. They can be added to your present equipment (virtually any investigation instrument) or become part of a new data recording system. Tell us about your data recording environment. We'll respond quickly with technical descriptions and the cost of a system tailored to suit your needs. *Drop us a line. (Pencil will do.)*

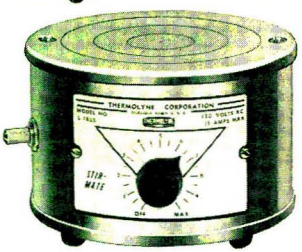
DATEX
GIANNINI CONTROLS CORPORATION
1307 S. MYRTLE AVE., MONROVIA, CALIFORNIA 91017

Circle No. 118 on Readers' Service Card

THERMOLYNE®

Laboratory Apparatus for:
☐ HEAT
☐ LIGHT
☑ MOTION

Compact
Magnetic Stirrer



Stir-Mate type 7800

SMALL (4¼" dia. x 3" h) and LIGHT (1½ lbs.) Type 7800 is best for confined lab setups, stirring hard-to-reach vessels with extra power and positive stepless control.

UNUSUAL STIRRER — Stir-Mate is an excellent Slow Speed Stirrer — stays locked in phase. No "jitterbugging" of stirring bar. Also stirs Conway dishes, Through heating mantles, and on the Side of vessels by its hanger.

Sturdy, attractive, stainless steel case has aluminum concentric ring top. Dovetail bracket with support rod fits standard clamps. Rugged, long-life construction, continuous duty motor.

Price with 2 stirring bars.....$32.50

NEW! 40-Page complete line catalog of heat/light/motion items: furnaces, controllers, hot plates, magnetic stirrers, Stir-Plates, constant temp. apparatus, Dri-Baths, culture incubators, PBI Apparatus, lab lights, meters.



Write now for F R E E copy of Catalog 65

THERMOLYNE CORPORATION
2555 KERPER BLVD.
DUBUQUE, IOWA· 52003 U.S.A.

Contact Dept. 478F for name of nearest dealer.
Circle No. 91 on Readers' Service Card

NEWS

Macromolecular Interactions in Gel Permeation, Electrophoresis, and Ultracentrifugation. G. A. Gilbert, University of Birmingham.

Electrophoresis. H. Bloemendal, University of Nijmegen.

Those wishing to submit papers should send an abstract of about 300 words to the secretary, C. L. de Ligny, c/o Analytisch Chemical Laboratorium, State University, Utrecht, Netherlands, not later than August 1, 1966. The complete texts of accepted papers will be required by October 1. Papers should be original and can be in French, German, or (preferably) English and should have an English summary. Thirty minutes is reserved for each paper, including discussion time.

In addition to the technical program there will be excursions to the research laboratories of some of the large industries and trips to places of interest to tourists. An attractive social program has also been planned.

Intending participants can obtain further information and application forms from the Congres Bureau, St. Agnietenstraat 4, Amsterdam, Netherlands. The final date for registration is Dec. 31, 1966.

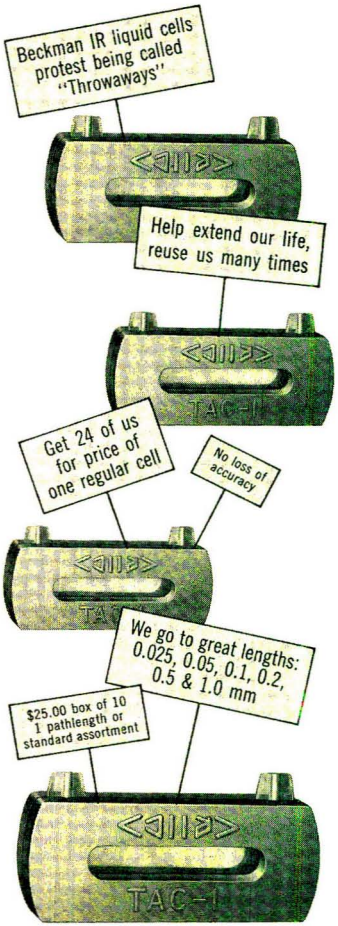
Industry Items

Beckman Instruments, Inc., has announced the formation of a new subsidiary company, **Beckman Instruments de Mexico, S.A. de C.V.**, in Mexico City. The Mexican firm will expand Beckman dealer and customer support programs through the establishment of new service and technical facilities and assembly operations. Beckman is represented in Mexico by two dealer organizations: **Curtin de Mexico, S.A. de C.V.**, and **Hoffmann-Pinther and Bosworth, S.A.**, both headquartered in Mexico City.

A company for the fabrication of analytical instruments in Latin America, **Perkin-Elmer de Mexico S.A.**, has opened a plant at Naucalpan de Juarez, Estado de Mexico. The Mexican company is a subsidiary of the **Perkin-Elmer Corp.**

Ultrapure, 14514 Barkwood Dr., Rockville, Md., has announced the availability of a chemical purifing service.

Wilks Scientific Corp., 140 Water St., South Norwalk, Conn. 06856, has established analytical service for customers interested in gas chromatography–infrared analysis; internal reflection spectroscopy; and general infrared studies.



Let us demonstrate all the advantages and abilities of our so-called "Throwaways": These AgCl cells are usable for aqueous and most non-aqueous samples in IR analysis up to 22 micron wavelength. Wider selection of pathlengths for less money. Reusable *many* times. And if cells get too dirty to clean easily, you can afford to throw them away at only $2.50 a throw. (Special holders adapt them to all IR spectrophotometers.) Write for Data File LIR-466-14* on cells and accessories — the finest, most complete line in the field.

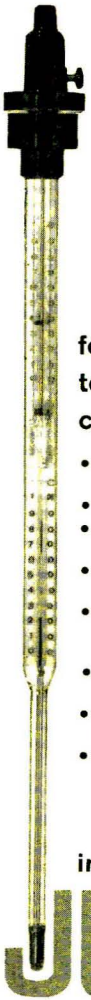
**Includes products manufactured by the Research and Industrial Instrument Company of London, England; formerly marketed by the Limit Research Corporation. Both RIIC and Limit are now a part of Beckman Instruments, Inc.*

Price is stated in U. S. funds and is subject to change without notice.

Beckman® INSTRUMENTS, INC.
SCIENTIFIC AND PROCESS INSTRUMENTS DIVISION
FULLERTON, CALIFORNIA • 92634

INTERNATIONAL SUBSIDIARIES: GENEVA; MUNICH; GLENROTHES, SCOTLAND; TOKYO; PARIS; CAPETOWN; LONDON; MEXICO CITY

Circle No. 25 on Readers' Service Card



for accurate temperature control . . .

- Instant Magnetic Temperature Setting
- Sensitivity ± 0.005° C
- Sealed and Evacuated to avoid Corrosion
- No Arcing at Contact Points
- Available in Ranges from 0-50° to 0-300° C, 1° graduations
- 150 or 300 mm Immersion
- Visible Temperature and Setting Scales
- Maximum Permissible Load: 30 milli-amps at 220 volts

insist on the

JUMO

THERMOMETER-THERMOREGULATOR

Designed to provide accurate temperature control, through a relay, over extended periods of service without failure. To set desired temperature, merely rotate magnet at top. Available in 6 ranges, priced from $32.

BRONWILL SCIENTIFIC

A DIVISION OF WILL SCIENTIFIC, INC.

277 N. Goodman St., Rochester, N.Y. 14601

See Buyers' Guide for all products/sales offices.

Circle No. 7 on Readers' Service Card



Sample cell, slightly enlarged, showing end of 0.5 mm I.D. tube in which sample is irradiated with laser beam. Inset: Kenyon P. George, Development Engineer, checks Raman Spectra on CARY Model 81 Spectrophotometer made by Applied Physics Corporation, Monrovia, California.

Laser sheds new light on molecular structure

When you want to learn about the architecture of a complex molecule, you can tune in on its vibrations and help determine its structure if you irradiate it with monochromatic light and observe the Raman effect – a form of molecular light-scattering which results in a unique spectral signature for any given molecule.

But many molecules have been difficult to study because of a problem in getting strong Raman signals from small-volume samples. With a new Raman Spectrophotometer[1], however, using a Spectra-Physics Model 125 CW gas laser, you can apply the technique much more broadly – for example, to obtain vibrational spectra of biological samples in less than ten microliters of aqueous solution or a few milligrams of solid material.



Raman spectra from a 2x4 mm crystal of β-alanine. Left, conventional mercury arc light source; right, gas laser. Fluorescence caused by blue light of mercury arc obscures Raman bands, when laser-excited, bands are easily seen.

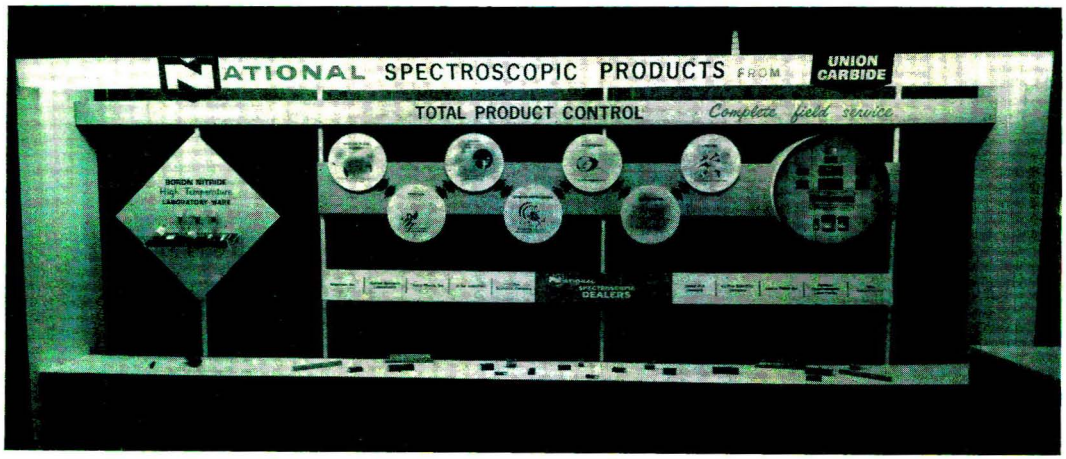
You'll find Spectra-Physics CW gas lasers used as an integral part of an increasingly wide range of precision analytical, recording, and measuring instruments, wherever a stable, high-intensity source of monochromatic, spatially coherent light is required. Is your application optical data processing, plasma diagnostics, distance determination? We'll help keep you up-to-date on laser application by means of our Laser Technical Bulletins if you'll write us at 1255 Terra Bella Avenue, Mountain View, Calif. 94040. In Europe, Spectra-Physics, S.A., Chemin de Somais 14, Pully, Switzerland.

Spectra-Physics

[1] LASER EXCITATION OF RAMAN SPECTRA IN THE CARY MODEL 81 RAMAN SPECTROPHOTOMETER, PRESENTED BY R.C. HAWES AT THE NATIONAL S.A.S. CONFERENCE, DENVER, COLORADO, SEPTEMBER 2, 1965

Circle No. 129 on Readers' Service Card

If you missed the PITTSBURGH EXPOSITION



—you missed the opportunity to see Union Carbide's graphic presentation of

'Total Product Control'

- **Selection of raw materials**
- **Blending**
- **Extrusion**
- **Baking**
- **Graphitization**
- **Grinding**
- **Machining**
- **Purification**
- **Purity Control**
- **Packaging**

Union Carbide's Carbon Products Division is the only manufacturer providing:

- **1 ppm total ash content**
- **2 ppm maximum spot impurity per element**
- **6 ppm maximum total spot impurities**
- **plus the finest structure**

—through complete start-to-finish technology and manufacturing facilities for the production of spectroscopic electrodes.

Call your dealer today for all these benefits—available only in 'National' Spectroscopic Products

"National" is a registered trade-mark of

UNION CARBIDE

UNION CARBIDE CORPORATION
CARBON PRODUCTS DIVISION
270 Park Avenue • New York, N. Y. 10017
In Canada: Union Carbide Canada Limited, Toronto

Circle No. 55 on Readers' Service Card

Circle No. 72 on Readers' Service Card →

Look at it this way... and you'll buy Kimax

This cross-sectional view shows why KIMAX® beakers are a cut above the ordinary. Walls that are uniform and heavier . . . rugged rims built to withstand long hard use . . . an improved pour-out design. And note the printed volume scale — another thoughtful improvement you now get at no extra cost. Altogether, quite a change from the beakers on the market just a few years ago.

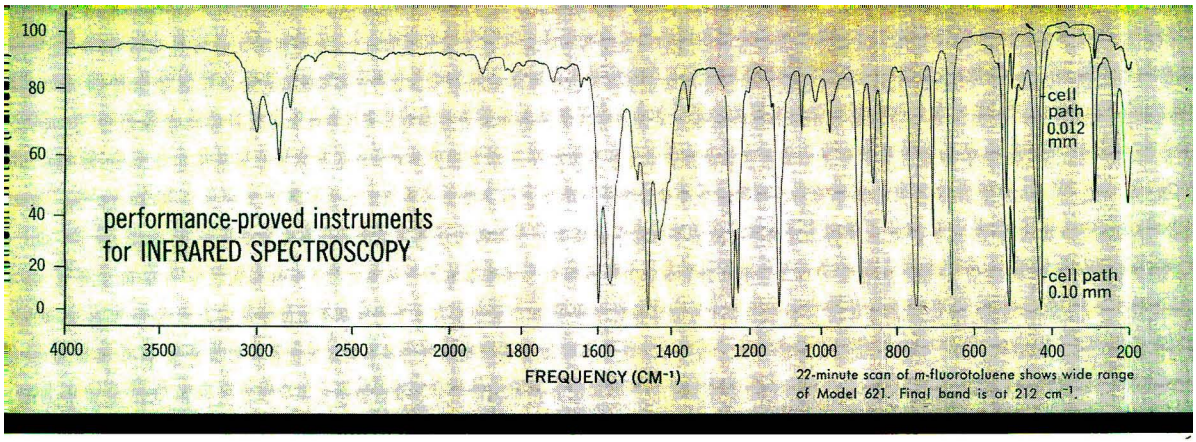
Kimble now is offering beakers and Erlenmeyer flasks *in lower case quantities*, for convenience and economy.

Shouldn't you look at it this way, for the best value in scientific glassware?

OWENS-ILLINOIS

Maker of Kimble Products
Toledo, Ohio 43601





22-minute scan of m-fluorotoluene shows wide range of Model 621. Final band is at 212 cm^{-1}.

NEW MODEL 621 IR SPECTROPHOTOMETER PROVIDES OPTIMUM ENERGY TRANSFER OVER ENTIRE 4000-200 CM^{-1} RANGE

In the Model 621 Filter-Grating* Infrared Spectrophotometer, Perkin-Elmer — world leader in infrared — has achieved a new level of performance over the instrument's total operating range: from 4000 to 200 cm^{-1}. Fundamental to this additional performance is greater utilization of available energy, even where low energy is classically a problem. To do this, Perkin-Elmer has

- widened the slit opening capability to optimize performance under low energy conditions;
- enlarged the size of the Nernst glower source for greater total energy;
- utilized aspheric (toroidal, paraboloidal) optics for most efficient transfer of energy, and precise imagery—a Perkin-Elmer exclusive feature;
- redesigned the thermocouple detector target for greater sensitivity over the total range;
- maintained Perkin-Elmer's unique, fast f/4.5 optical system, with short paths for efficient and rapid purging.

These features provide an energy bonus and increase the optical precision of the Model 621's system. Thus, they enhance a traditional Perkin-Elmer advantage: the unique capacity to perform microanalysis to an unequalled degree of sensitivity. No matter whether the sample is limited, or the component of quantitative interest is present only as the fractional part of a microgram, Perkin-Elmer's total system is geared to provide a quick, easy and precise determination. For more information, including sample spectra, write to Perkin-Elmer Corporation, 702 Main Avenue, Norwalk, Connecticut.

*U. S. Pat. No. 3,144,498

Circle No. 111 on Readers' Service Card



Dynamics of Chromatography: in Three Parts. Part I: Principles and Theory. *J. Calvin Giddings. xii + 323 pages. Marcel Dekker, Inc., 95 Madison Ave., New York, N. Y. 10016. 1965. $11.50.*

Reviewed by W. J. A. Vanden Heuvel, Merck Sharpe & Dohme Research Laboratories, Rahway, N. J. 07065.

In the past decade the field of chromatography has experienced phenomenal growth in its application to a great variety of disciplines. Overshadowed, but also of significance, has been an increase in understanding of the fundamental processes involved in this separation method. In "Dynamics of Chromatography, Part I, Principles and Theory," J. Calvin Giddings draws successfully on his extensive background (as well as the work of others) to rectify this situation. It should be emphasized that this is not, nor is it intended to be, a monograph on chromatographic methodology; rather, it is a mathematical description of chromatographic processes, and it is not unfair to state that a working knowledge of calculus would be a definite asset for the comprehension of much of the subject matter. (The more highly mathematical sections are set off from the rest of the text, and ". . . may be omitted without loss of continuity.") Many of the molecular phenomena are well illustrated by the drawings.

The author has wisely chosen to address himself primarily to those areas of chromatography in which he is eminently qualified, and in this way avoids the mediocrity which inevitably results from dilution. While the subject matter covered may be considered by some to be narrow in scope, Dr. Giddings makes clear the existence of relationships between the theoretical and practical aspects of chromatography.

Following a brief introductory chapter on zone migration, Dr. Giddings presents, in Chapter Two, a discussion of the dynamics of zone spreading, which includes an analysis of various diffusion and kinetic phenomena. The next chapter "Non-equilibrium and the Simple Mass Transfer Terms" prepares the reader for a rigorous examination of the "Generalized Nonequilibrium Theory" in Chapter Four, which is, by the author's admission, the most difficult in the book. Laminar and turbulent flow are covered in Chapter Five, and Chapter Six includes discussions of diffusion rates and adsorption kinetics. The final chapter, "The Achievement of Separation," presents Dr. Gidding's views on the optimization of conditions for separation, and concludes with a brief comparison of gas and liquid chromatography, which will be treated separately in Parts II and III, respectively. Part I has set the stage well for his next efforts.

Computer Programming for Chemists. *E. B. Wiberg. viii + 269 pages. W. A. Benjamin, Inc., One Park Ave., New York, N. Y. 10016. 1965. $12.50, domestic; $13.75, foreign.*

Reviewed by Donald Secrest, Chemistry Department, University of Illinois, Urbana, Ill.

A good introductory textbook on programming for physical scientists has finally appeared. While the examples are directed toward advanced undergraduate and graduate students in chemistry and mature chemists, the material on programming in the book could be understood by anyone in the physical sciences who wishes to gain a familiarity with digital computers. No mathematics beyond calculus is presumed.

Most scientific problems can be solved by the use of a simple algebraic compiler language; however, it is sometimes necessary to use machine language, and it is always desirable for a person using a computer to have some understanding of machine language even though he writes all of his programs in compiler language. So many introductory books discuss only compiler languages. This text discusses both compilers and machine language. The algebraic compiler used is FORTRAN, which is probably the most widely accepted compiler. The machine language used in the text is that common to the IBM 7094, 7090, 709 and 704 computers.

An excellent way to learn programming is to read programs written by an expert. This book contains many examples of long, complex, useful programs which are of current applicability in the solution of chemical problems. Most, but not all, of the examples are well written. The author analyzes the examples pointing out various useful techniques employed. Dr. Wiberg discusses in complete detail such problems as: the solution of a complex chemical kinetics problem using the Runge-Kutta method to solve the differential equations with a program to plot the concentrations as a function of time, computing and plotting an NMR spectrum, giving the chemical shifts and coupling constants, a program to compute the energy levels of complex aromatic molecules in the Hückel approximation, and others.

This book is ideally suited as a textbook for a short course in computer programming for chemists. It would be of great assistance to a person learning programming on his own, though it is by no means a self study text. Every computer center has its own peculiarities and many statements made in this book will be incorrect at any particular center, but this must be true of any book on computing.

My chief objection to this book is its length. It is far too short. It is introductory in scope giving only the fundamentals of FORTRAN programming and it verges on being inadequate in its discussion of machine language. It is shorter than the page count indicates, since it discusses two FORTRAN compilers and two machine language assemblers and repeats much of the material in the duplicate discussions. The idea is that one need read only that part of the book applicable to his own computer installation. The most that any one person would read is 236 pages.

Though most of the examples are good and reasonably well written, one or two examples are sloppy and the matrix inversion technique discussed is poor.

For the most part "Computer Programming for Chemists" is good and any chemist interested in learning about computers would do well to obtain a copy.

Modern Computing Methods. *2nd ed. Staff, Mathematics Division, National Physical Laboratories. Teddington, Middlesex. vi + 170 pages. Philosophical Library, Inc., 15 East 40th St., New York 16, N. Y. Published 1961. Reprinted 1965. $6.00.*

Reviewed by Glenn L. Booman, Atomic Energy Division, Phillips Petroleum Co., Idaho Falls, Idaho, 83401.

The basic material required for a working knowledge of numerical methods as applied to scientific problems is contained in this concise monograph from the National Physical Laboratories series of "Notes on Applied Science." No attempt is made to give mathematical proofs or even to give support for the particular methods presented. By means of these restrictions, the Authors have been able to present the preferred

approaches in a very readable form. The areas of application and limitations are clearly outlined in such a manner that the scientist without a strong background in numerical analysis can easily obtain an understanding of what can be accomplished by use of digital computer techniques. Worked-out examples are used, clearly explaining the procedures.

Linear equations are discussed in the first third of the book, covering iterative methods and an especially practical approach to error analysis. The compactness and economy obtained in the use of Chebyshev series approximations is well presented. Condensation of the material produces a rather restricted discussion of ordinary differential equations and a decidedly restricted discussion of partial differential equations. Again in the chapter on Evaluation of Integrals, the material must be considered introductory, and not comprehensive, even in outline.

The task of condensing a field of this size into 15 short chapters averaging 9 pages in length has been accomplished perhaps better than would be expected. Because of the abbreviated form, use of this book would require recourse to more detailed works. A very useful bibliography (22 pages) is included with a description of the cited material. It may be regretted that the references were not brought up to date at the 1965 reprinting; however, the literature coverage through 1960 appears adequate. The reader would be well advised to consult the literature before beginning an involved program of computation. Applicable journals and review sources are listed in the bibliography.

The use of this book can be recommended as a working manual for persons engaged in numerical computation. As a basis for courses in numerical analysis, the usefulness would be restricted to a lecture series of short duration or to outlining the subject material in a course of normal length.

Methods of Forensic Science. Vol. IV. *A. S. Curry, editor. xii + 369 pages. Interscience Publishers, 605 Third Ave., New York, N. Y. 10016. 1965. $15.50.*

Reviewed by P. L. Kirk, School of Criminology, University of California, Berkeley, Calif.

This is the latest volume of a series without which any forensic science laboratory is handicapped. Like its predecessors in the series, and to a greater extent, its contents are quite variable in subject, in quality, and in editorial standards. This may be explained partly by the fact that nine authors from eight different countries have contributed its eight subjects.

The first, "Methods for Determining Alcohol," by H. Ward Smith, is extensive, thorough, and critical. It is "must" reading for anyone concerned with this problem. Some of the more recent developments, such as gas chromatographic analysis are deficient in coverage, and the final recommended methods are based on the old work of Nicloux and Widmark, but soundly so. Excellent discussions of breath alcohol, and of the fate of alcohol in the body are included, as is an incomplete but very extensive bibliography of 257 references.

"Examination of Glass Fragments," by Donald F. Nelson, probably is the most thorough treatment of this generally neglected subject that is currently available. All present approaches are explored in some depth, and the article will be highly valuable in dealing with glass evidence. Some of the more recent developments in glass technology, especially in the United States, have not been given the consideration they possibly deserve.

"Coloured Fibers in Criminal Investigation with Special Reference to Natural Fibers," by Max Frei-Sulzer, is difficult to evaluate. In places it is excessively detailed, and throughout the article, the reader gets the impression that fiber evidence is new to all other investigators. Only two references are listed. On the other hand, the meticulous techniques described are unquestionably highly reliable, and the author is certainly both soundly informed and skilled in utilizing fiber evidence.

"Searching for Drug Metabolites in Viscera," by L. K. Turner, presents a competent and extensive review of this important aspect of toxicology which has been frequently underestimated or neglected. Listed references total 162. "Thin-Layer Chromatography in Forensic Science," by G. Machata, is largely concerned with toxicological applications, and could well have been somewhat more inclusive. It offers considerable advice on sound working conditions. The somewhat unusual subject, "Detection of Soap Abortions," by Wolfgang Schwerd, unquestionably provides useful information to the legal medical practitioner. It would be improved by eliminating some of the only partially relevant detail. "Infrared Absorption Spectroscopy in Forensic Toxicological Practice," by A. Alha and V. Tamminen, is a useful discussion for the inexperienced, but gives little that is not well-known to anyone using this technique.

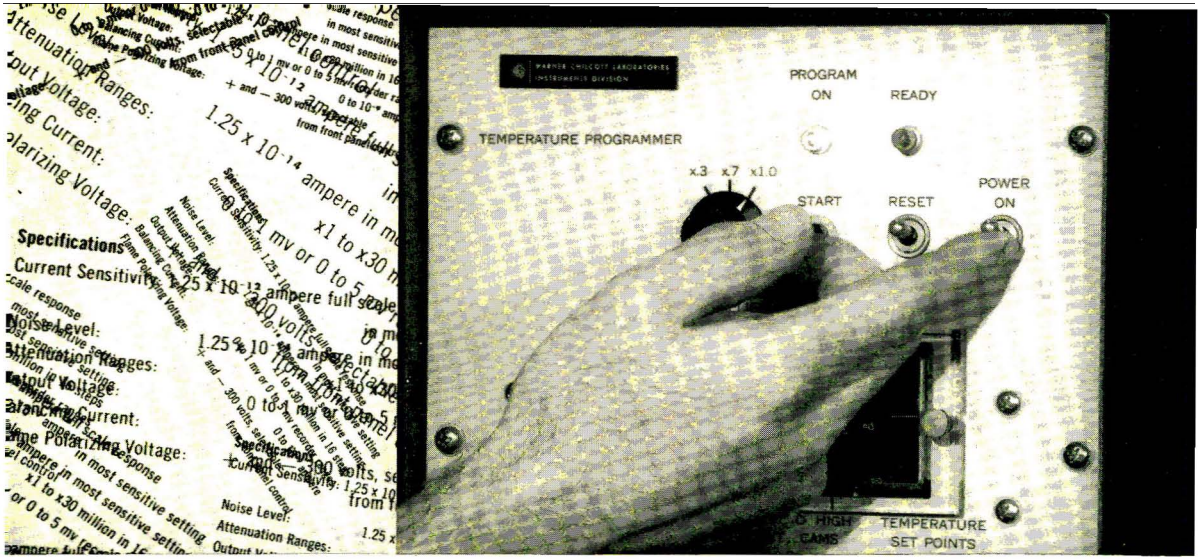
The last subject but not the least in importance, "Recent Advances in the Grouping of Dried Blood and Secretion Stains," by R. A. Cutteridge, is the most complete review of recent work available, and will be appreciated by forensic scientists for its thorough and careful coverage. Although this volume is not an improvement over earlier ones of the series, it is still a welcome addition to the forensic literature.

Testing of Polymers. Vol. 1. *J. V. Schmitz, editor. xiv + 479 pages. Interscience Publishers, 605 Third Ave., New York, N. Y. 10016. 1965. $19.50.*

Reviewed by Bernhard Wunderlich, Department of Chemistry, Rensselaer Polytechnic Institute, Troy, N. Y.

"Testing of Polymers" is in the words of the editor to assist scientists and engineers in the pratice and application of test methods for polymers by providing a forum for authoritative discussions of all aspects of the testing of polymers. It is also stated in the preface that the original conception was a multivolume organized treatise with a large number of contributors. The switch from one to the other can clearly be felt on reading the book.

The most treatise-like section is a block of 5 chapters (146 pages) on electrical property tests by A. H. Sharbaugh (Introduction), A. H. Scott (DC Conductance and Conductivity), R. W. Tucker (Dielectric Constant and Loss) R. W. Warfield (Characterization by Resistivity) and T. W. Dakin (High Voltage). For each test one would expect a short definition of the problem, a description of the theory of the principles involved in the tests, a display of the detailed test methods possibly with a catalogue of the important commercially available equipment, and finally a brief description of the application to polymers with actual data and if possible with present limiting values for typical polymers. Even for the electrical property testing section this is not complete. Only for resistivity tests is there an applications chapter. Dielectric constant and loss test equipment is well-described, but very little about theory and nothing about application is mentioned. Other remnants of the treatise are a well-written and lucid display of mechanical relationships in testing for mechanical properties (J. Marin), and an excellent chapter by M. G. Sharma on the theories of phenomenological viscoelasticity underlying mechanical testing. Both chapters are not followed up in this volume by either test descriptions or polymer application sections. Chapter One, by W. E. Brown, F. C. Frost, and P. E. Willard describes in a much too



An open question to biomedical GAS CHROMATOGRAPHERS:

DO YOU WANT EQUIPMENT SPECIFICATIONS —OR GUARANTEED RESULTS ?

With Warner-Chilcott Gas Chromatography, you get equipment that is *guaranteed* to give the results you need for your specific application. You needn't labor through pages of complex specifications—and then wonder if you've purchased the right system.

We have devised a unique new kind of customer insurance called Operation GRASP. It stands for GAS REVIEW and APPLICATIONS STUDY PROGRAM, and it's a new concept to guarantee that your Warner-Chilcott Gas Chromatograph suits *your* individual needs.

Operation GRASP consists of three major elements:

1. **A Warner-Chilcott Gas Chromatography System**—a versatile, modular system with up to 20 basic building blocks that fit into dozens of configurations depending on your biomedical applications. These include respiratory, anesthetic, and blood gases; blood and tissue volatiles; lipids; fatty acids; glycerides; phospholipids; sterols; steroids; biological toxins and narcotics; barbiturates; tranquilizers; pesticides; and carbohydrates. You get our technical recommendations on how much system capability you need—and what you don't need.

2. **The Warner-Chilcott Training Seminar.** Free to every purchaser of a Warner-Chilcott Gas Chromatography System. In one week, you learn to operate this equipment for your specific application—and you learn in our modern, well-equipped training laboratory at Morris Plains. You learn how simple Warner-Chilcott plumbing and electrical connections are—because you set up the system yourself, step-by-step, using our foolproof set-up method. You even get a certificate of achievement.

3. **You.** You are the reason why Warner-Chilcott has developed the other two elements of Operation GRASP. They're designed to make you a satisfied customer and user, and to give you a good grasp of gas chromatography principles, especially in the practical techniques you need. When you complete the seminar, your equipment will be as familiar to you as your right arm—and just as useful.

A new proficiency for applied chemical analysis by gas chromatography is the result of this combination: the Warner-Chilcott System, and Training Seminar, and You. Send in the handy coupon now and learn more about how Operation GRASP can benefit you.

WARNER-CHILCOTT LABORATORIES
INSTRUMENTS DIVISION
Richmond, Calif. • Morris Plains, N.J.

Warner-Chilcott Laboratories Instruments Division
200 South Garrard B'lvd., Richmond, Calif. 94808

Please tell me more about Operation GRASP.

Name _____ Title/Dept. _____

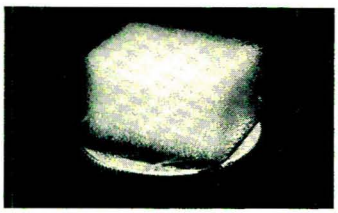
Company/Institution _____

Address _____ Phone _____

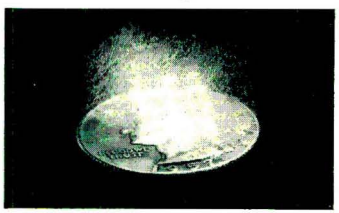
City _____ State _____ Zip _____

Circle No. 98 on Readers' Service Card

cold plasma ashing preserves what you want



before ashing—urethane foam

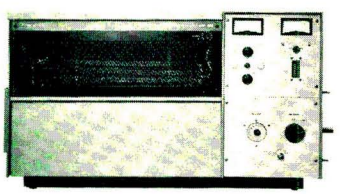


after ashing the delicate inorganic structure remains unaltered for precise quantitative analysis.

Tracerlab's new LTA-600 oxidizes samples with a cold plasma of atomic oxygen to leave inorganic constituents unaltered.

Permits more accurate quantitative elemental and structural analyses of plant and animal tissues, bones, coal, oil well cores, polymers, and radioactive materials. Prepares pure samples for atomic absorption spectrophotometry, mass spectrometry, emission spectroscopy, X-ray diffraction, and electron microscopy.

send for literature on equipment, techniques and services.



LFE | TRACERLAB
A Division of Laboratory for Electronics
2030 WRIGHT AVENUE, RICHMOND, CALIFORNIA
Circle No. 182 on Readers' Service Card

subdivided chapter sources for standard procedures, materials specifications, and methods for classifying polymers. The last chapter presents a list of periodicals, texts, abstracts etc.

Mixed with the portion of treatise-like chapters are chapters on temperature and humidity conditioning for polymer testing (F. M. Gavan and F. A. Joy), erosion of polymers caused by the collapse of cavities formed in liquids under high turbulence or vibration (J. H. Brunton), odor and taste transfer property tests (L. B. Sjöström and F. Sullivan), indentation and compression testing of floor coverings (F. M. Gavan and J. T. Wein, Jr.), and the gas and vapor permeation and diffusion (V. Stannett and H. Yasuda). From the titles alone it can be seen that these tests range from the end use testing to determination of rather fundamental properties of diffusion of small molecules in polymers and accordingly the contents vary from a mere recitation of recipes and description of equipment to the well-rounded chapter by Stannett and Yasuda which includes introduction, theory, measurements, and a sufficient list of references.

The value of the series can only be judged after the next few volumes have appeared. The first volume is a somewhat unsatisfactory mixture of treatise-like chapters and discussions, in particular since the treatise-like portions are incomplete and the danger exists that they will not be completed later on. Its proper place is most likely in the industrial laboratory library. It is hard to see sufficient use for a single researcher for the investment. The overall quality of the book is satisfactory, although the quality of the presentations varies somewhat. Annoying is the fact that of ten German words printed in chapter 5, six contained errors in spelling. A grouping of the articles in the future into volumes describing tests of common fields would make it a useful book to have on the lab bench and not only in the library.

NEW BOOKS

Advances in Mass Spectrometry. Vol. 3. *W. L. Mead, editor. xvii + 1064 pages. American Elsevier Publishing Co., Inc., 52 Vanderbilt Ave., New York, N. Y. 10017. 1966. $27.*

The proceedings of the Mass Spectrometry Conference sponsored by the American Society for Testing Materials, the Groupement pour l'Avancement des Methodes Spectrographiques, and the Hydrocarbon Research Group of the Institute of Petroleum, held in Paris, September 1964, are recorded in this volume.

Theory, instrumentation, relation of molecular structure to analysis, ionization phenomena, ion-molecule reactions, isotopic abundance measurement, and application to the analysis of solids, and free radicals, are among the topics covered.

A bibliography covering the period from January 1961 to December 1962 is included together with an author index.

Hawk's Physiological Chemistry. *14th ed. Bernard L. Oser, editor. xvi + 1472 pages. McGraw-Hill Book Co., 330 W. 42nd St., New York, N. Y. 10036. 1965. $19.50.*

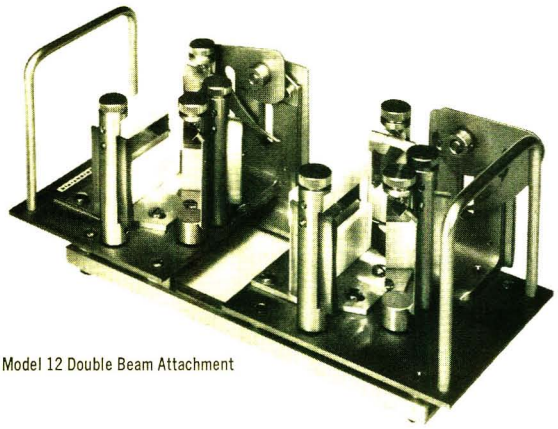
This comprehensive text of physiological chemistry includes modern theory as well as detailed experimental procedures. Among the subjects which have received special emphasis are the composition, configuration and role of nucleic acids and related compounds, enzymes and cofactors and their functions, estimation of steroid hormones in blood and urine, the use of radioisotopes for the study of metabolic processes, and current concepts pertaining to muscular contraction, blood coagulations, and detoxification. Numerous new analytical procedures and instrumental techniques are presented.

Spectrochemical Abstracts. Vol. X. 1963 to 1964. *Ernest H. S. van Someren, F. Lachman, and F. T. Birks. 109 pages. Hilger & Watts, Ltd., 98 St. Pancras Way, London, N. W. 1, England. 1965. £3. 3s. 0d.*

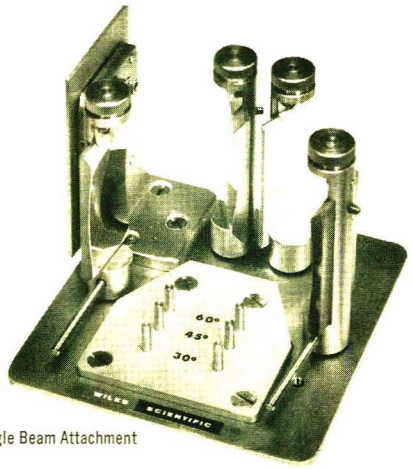
Almost 500 abstracts of papers describing apparatus, methodology, theory, and applications are included in this publication. Abstracts of review articles, tables, and books are also presented together with indices of elements and authors.

Microchemical Techniques. *184 pages. I. U. P. A. C. Butterworth Inc., 7300 Pearl St., Washington, D. C. 20014. 1965. $8.*

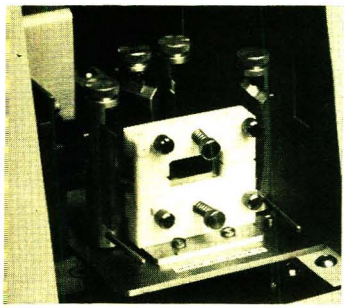
This monograph contains the Plenary Lectures presented at the International Symposium on Microchemical Techniques—1965. A brief discussion of the history, development, and goals of microchemistry is presented along with separate papers describing methods used in forensic chemistry, chemical microscopy, clinical chemistry, and in the identification of functional groups. Photometric titrations, organic microsynthesis, and the status of organic microanalysis in Japan are also included.



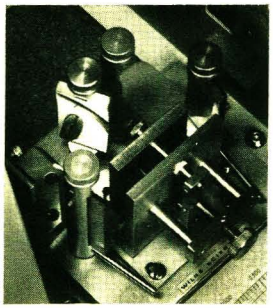
Model 12 Double Beam Attachment



Model 9 Single Beam Attachment



GC Fraction Trap



Multiple Specular Reflectance



Heated Sample Cell



Flow-through Cell

From the experts comes . . .

The Best in Internal Reflection (ATR) Equipment

If you are planning to add an internal reflection (ATR) attachment to your infrared spectrophotometer, why not consult the experts in the field — you will find the best in equipment and at the lowest prices, too.

Wilks Scientific attachments mount directly on nearly all infrared spectrophotometers, may be adjusted in minutes and provide the most all around versatility. With up to 50 or more internal reflections, three different angles of incidence, and a variety of internal reflection plate material, you can vary the sensitivity and depth of penetration to meet the requirements of different analytical problems. In addition, special sample holders such as heated cells, micro-cells, GC fraction traps, and reaction vessels provide still further versatility. Only Wilks Scientific equipment provides this range of operating variables and accessories.

And if you are considering the purchase of a new infrared spectrophotometer, be sure to look at the Wilks Scientific Model 8. It combines the best in internal reflection performance with unimpaired transmission characteristics.

Write for your copy of our 40 page manual on Internal Reflection Spectroscopy.

WILKS SCIENTIFIC CORPORATION

SOUTH NORWALK • CONNECTICUT

Circle No. 100 on Readers' Service Card

Vacuum Science and Engineering. *C. M. Van Atta. xiv + 459 pages. McGraw-Hill Book Co., 330 West 42nd St., New York, N. Y. 10036. $15.*

The nature of gas behavior, and principles of operation and design of vacuum systems are discussed. Circuit diagrams, photographs, data charts, and references are included with each chapter. Appendices containing molecular weights, constants and conversion factors are included.

The Glass Electrode. *G. Eisenman, R. Bates, G. Mattock, and S. M. Friedman. 325 pages. Interscience Publishers, 605 Third Ave., New York, N. Y. 10016. 1966. $7.*

Four chapters on the glass electrode which were published previously in four separate volumes have been combined in this book. The topics covered are: "The Electrochemistry of Cation-Sensitive Glass Electrodes," The Glass Electrode in the Determination of pH," "Laboratory pH Measurements," and the "Measurement of Sodium and Potassium by Glass Electrodes."

L. Ubbelohde, Zur Viskosimetrie. *G. H. Göttner and W. Weber. 7. Auflage. xii + 75 pages. S. Hirzel Verlag, Stuttgart N, Birkenwaldstrasse 185A, Schliessfach 347, Germany. 1965. DM 18.60.*

The foundations, development, and applications of viscometry are described in this edition. Basic concepts, units of measurement, apparatus, and various methods of analysis are presented together with conversion and calculation tables.

Encyclopedia of Industrial Chemical Analysis. Vol. I. *Foster Dee Snell, editor-in-chief. xv + 763 pages. Interscience Publishers, 605 Third Ave., New York, N. Y. 10016. 1966. Subscription, $35, single copy, $45.*

In order to aid the analytical chemist in the development, control, and testing laboratory to select the most suitable procedure for the solution of problems encountered, this encyclopedia was developed.

"Volume I, General Techniques A-E" contains articles which describe in detail how the procedures work, rather than the theoretical basis for the procedures. Among the thirty-two methods presented are activation analysis, air pollution and atmospheric analysis, calorimetry, countercurrent distribution, differential reaction rate analysis, electron microscopy, and complexation in aqueous media.

Dynamic Mass Spectrometers. *Erich W. Blauth. x + 185 pages. American Elsevier Publishing Co., Inc. 52 Vanderbilt Ave., New York, N. Y. 10017. 1966. $13.50.*

This volume is an English translation of "Dynamische Massenspektrometer" listed in the March 1966, issue of ANALYTICAL CHEMISTRY.

U.S. Government Publications

The following can be obtained from the Superintendent of Documents, U. S. Government Printing Office, Washington, D. C. 20402.

Methods for the Chemical Analysis of NBS Copper-Base Spectrochemical Standards. *NBS Miscellaneous Publication 260-7. Rosemond K. Bell. 99 pages. October 1965. 60 cents.*

This publication contains detailed procedures for the determination of constituents in the seven NBS copper-base standard alloys. Electrolytic, photometric, gravimetric, and titration methods are presented. The methods are applied to traces of phosphorus, manganese, arsenic, silicon, and antimony as well as the more abundant elements of copper alloys.

A Peak AC-DC Voltage Comparator for Use in a Standards Laboratory. *NBS Technical Note 280. L. A. Marzetta. 29 pages. January 1966. 25 cents.*

A description of the components of the voltage comparator and its performance in tests is presented, together with the history of electrical measurement relating to a.c. and d.c. voltage. Peak voltage detecting circuits are analyzed and compared to this device.

The following publications are available from the Clearinghouse for Federal Scientific and Technical Information. U. S. Department of Commerce, Springfield, Va. 22151.

Apparatus for Automatic Preparative Gas Chromatography. *21 pages. Lawrence Radiation Laboratory, University of California, Livermore. December 1965. Order UCRL-14359. $1.*

A valveless chromatograph with a pneumatically operated injection system is described for use at high operating temperatures. Operational data is included.

Radiochemical Purification Procedures for the Elements. *99 pages, Lawrence Radiation Laboratory, University of California, Livermore, for the AEC. July 1965. Order UCRL-14258. $4.*

The most recent methods used at the Lawrence Radiation Laboratory for the radiochemical separations of 48 elements are described in this compilation.

Electrodeposition of Actinides and Lanthanides. *20 pages. Oak Ridge Institute of Nuclear Studies, Oak Ridge, Tenn., for the AEC. December 1965. Order ORINS-48. $1. (microfiche, 50 cents).*

A study of the quantitative electrodeposition of thorium, protactinium, and uranium for the preparation of thin film samples to be used in the field of nuclear spectral analysis is presented. The electrodeposition method uses 95 per cent ethanol as an electroplating solution with electrodeposition on platinum metal. Yields of nearly 100 per cent with a reproducibility of 2 per cent were realized.

Evaluation of the Methods in TID-7029, Selected Measurement Methods for Plutonium and Uranium in the Nuclear Fuel Cycle *Atomic Energy Commission, Oak Ridge, Tenn. 37831. 1966. $4.*

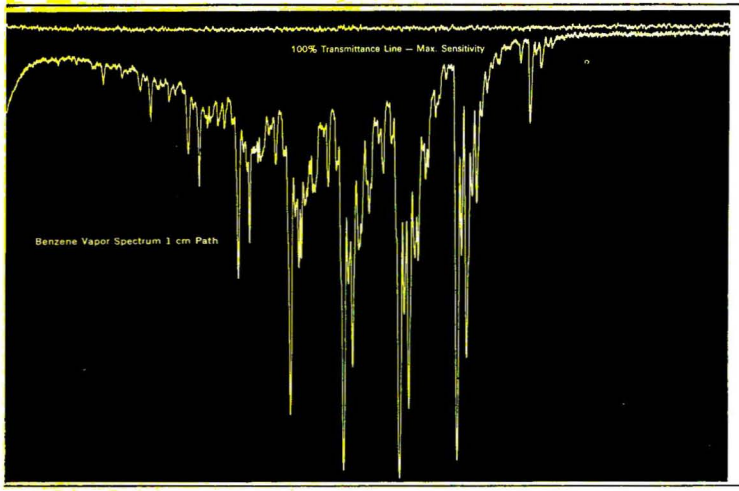
Statistical evaluations of methods for measuring the chemical concentration and isotopic composition of uranium and plutonium in various forms and materials is presented.

Radiochemistry of Selenium. *49 pages. Union Carbide's Mining and Metals Division, Tuxedo, N. Y., for NAS. 1965. Order NAS-NS-3030. $1.*

General references on the inorganic, analytical, and radiochemistry of selenium are provided. Chemical reactions, properties, and isolation procedures are also covered.

Nondestructive Testing of Irradiated Materials in the United States. *15 pages. Union Carbide Corp. for the AEC. April 1965. Order ORNL-P-1109. $1.*

Neutron and X-radiography, gamma-ray attenuation, televised X-ray images, and ultrasonics used for the detection of sodium nonbonding, coolant channel spacing, and internal observation are described.



Is Coleman the best spectrophotometer for your requirements?

Call Matheson Scientific today (collect) and you'll be able to decide within 48 hours.

If you're shopping for a spectrophotometer, we suggest your first move be a collect phone call to your nearest Matheson Scientific branch. Call us and we'll:

a. arrange a demonstration within 48 hours, OR

b. send a MS representative with complete information, OR

c. send literature

Look at Coleman first

There are several good spectrophotometer lines, but we've found it makes sense to look at Coleman first. The Coleman line is unusually versatile, and is more likely than any other to include the instrument that will satisfy everyone in your department. For example, 95% of all analytical spectrophotometry is done within the range of the Coleman 101. Coleman (as a Perkin Elmer subsidiary) provides the most advanced engineering in spectrophotometry. They've been able to combine true simplicity of operation with sophisticated performance. Reliability?—ask the MS Tech Department—"fewer service problems, less down time."

Be sure to call Matheson Scientific.

Others may sell Coleman spectrophotometers, but nobody will demonstrate them more promptly, deliver them faster or provide more reliable service than MS. We're Coleman Spectrophotometer Specialists. We stock all models. We service all models—within 48 hours—wherever you are. Call the Spectro Specialist at your nearest Matheson Scientific branch, today. Call collect, even if you only want literature.

Division of The Matheson Company, Inc.

MATHESON SCIENTIFIC

Call The Spectro Specialist
Collect At The Nearest
Matheson Scientific Branch.

ELK GROVE VILLAGE, ILL.
(Chicago) 60007
1850 Greenleaf Ave.
Phone (312) 439-5880

BELTSVILLE, MD. 20705
10727 Tucker Street
Phone (301) 345-9550

CINCINNATI 45237
6265 Wiehe Road
Phone (513) 731-9100

CLEVELAND 44125
4540 Willow Parkway
Phone (216) 883-2424

DETROIT
1600 Howard Street
Phone (313) 965-6422

HAYWARD, CALIF. 94545
24800 Industrial Blvd.
Phone (415) 783-2500

HOUSTON 77011
6622 Supply Row
Phone (713) 923-1627

KANSAS CITY, MO. 64111
3160 Terrace Street
Phone (816) 561-8780

LOS ANGELES 90022
5922 Triumph Street
Phone (213) 685-8060

PHILADELPHIA 19148
Jackson & Swanson Sts.
Phone (215) 462-4700

EXPORT DEPARTMENT
Our Elk Grove address

Circle No. 144 on Readers' Service Card

To use an A-60 for classroom NMR, you have to teach at a great big huge enormous school.

Like Bowdoin.

Or Union.

Time was, NMR was another piece of esoterica that was fine in Bell Labs or MIT, but just not right for the chemistry department of General Beadle State or a college in Collegevilie.

That time is past. NMR has become one of the tools that will attract and hold the kind of students you like to graduate. And the kind of professors you pride yourself on having.

With the tremendous upsurge in organic chemistry research, it is becoming essential for the men who will go on to graduate work in this field to be acquainted with not only the theory but the actual feel of these wonderful analytical instruments.



The A-60 at Bowdoin College was purchased with the help of gifts from alumni and a grant from the National Science Foundation. Union College bought its A-60 with a gift from the Schenectady Chemical Company.

Bowdoin College thought so. Union College, New York, thought so. They each invested in future excellence by installing one of our A-60 NMR Spectrometers.

What do **you** think?

varian
analytical
instrument
division
611 hansen way / palo alto / california

Circle No. 169 on Readers' Service Card

THE EDITORS' COLUMN

THE NATIONAL SCIENCE FOUNDATION has awarded a contract to Information Management, Inc., of Burlington, Mass., for a plan for development of a national chemical information system. A future need has been envisioned for more effective and high-speed dissemination of the results of chemical research. Since the chemical literature of the world is expected to double in the next eight years, the present plan is to exploit, on a nationwide scale, the modern information handling methods and equipment.

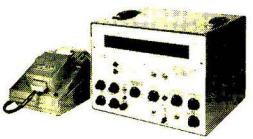
Some of the new methods are still under development. Funds for these projects have been provided by the National Science Foundation, the National Institutes of Health, and the Department of Defense, working under the Office of Science and Technology in the executive office of the President. Related development projects are being carried out by the American Chemical Society and the Goodyear Aerospace Corp.

Under the contract that has been let to Information Management, Inc., an initial conceptualization of the national system will be provided. A development plan containing estimates of costs, time, and personnel required to create the system, and a description of what the system will be required to do and its necessary performance characteristics will be the result of this phase of the project.

Demand for Engineers and Scientists Increases

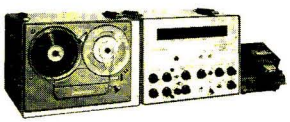
According to the Deutsch and Shea Engineer/Scientist Demand Index, the requirement of industry for technical people has set new records for 1966. Data for this index come from advertising in 42

INFOTRONICS DIGITIZES ANALYTICAL DATA



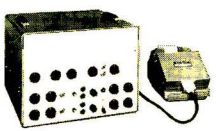
ELECTRONIC INTEGRATOR FOR CHROMATOGRAPHIC ANALYSIS

CRS-11HSB systems provide fully-automatic, accurate digital integration of chromatograms and other analytical records plus digital printing of peak times and peak areas. This all-transistorized instrument accepts any analyzer output of 1 millivolt full-scale or greater.



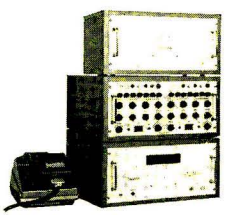
MAGNETIC TAPE PROCESSOR FOR CHROMATOGRAPHIC ANALYSIS

CRS-40 systems collect data from multi-chromatographs in diverse locations on the -40R. Tapes are processed on the -40P play-back console which reproduces analyzer signals, integrates peaks, presenting peak areas and retention times in printed digital form. Computer-compatible outputs are optional.



DUAL CHANNEL INTEGRATOR FOR AMINO ACID ANALYSIS

CRS-12AB systems provide simultaneous automatic detection and digital integration of both the 440 and 570 millimicron signals for amino acid analysis. Built-in baseline correction is included plus an automatic feature to insure integration of the same peaks on both channels. Output is a digital printer.



AUTOMATIC DIGITAL SYSTEM FOR COLORIMETRIC ANALYSIS

CRS-70 systems automatically calibrate their response, detect, digitize and print concentrations from up to 12 simultaneously operating analyzers. Data outputs include digital printer, computer-compatible tape perforator, electric typewriter, many more.

PLUS: CRS-30 systems for automatic peak height measurement; CRS-50 system for data reduction; CRS-11HSB extended-range digital integrator.

CRS DIGITAL SYSTEMS

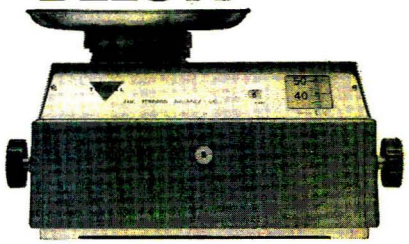
INFOTRONICS CORP.

7800 Westglen Drive • Houston, Texas 77042

250

Circle No. 184 on Readers' Service Card

WEIGH THE SIX FACTS LISTED BELOW



You'll find more advantages with TORBAL balances

1. From 14 kg. balances to 0.1 mg. analyticals, Torbal is the only complete balance line with friction-free pivots and bearings.

2. Only Torsion balances retain accuracy so long. With no knife-edges or friction points to be affected by dusty or abrasive atmospheres, adjustment and high sensitivity of Torsion balances last for 20 years and more!

3. Only Torsion balances are so rugged yet sensitive. The Torsion construction with no knife-edges gives greater protection against damage from objects accidentally dropped on the pans.

4. Only Torsion balances do not get sluggish with time. With no bearings to accumulate dust or foreign material, Torbals do not lose their original speed even after long, tough use.

5. The Torbal EA-1 analytical balance is the only analytical offering the advantages of a null-type read-out. This construction eliminates any effect from variations in sensitivity. Sample weighing is much easier.

6. When you use Torsion balances you don't need a service contract. Torbals are so rugged and dependable that adjustment or repairs are rarely needed.

Write today for a complete catalog of Torsion balances.



TORBAL®

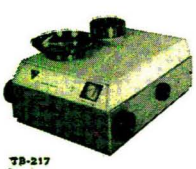
THE TORSION BALANCE COMPANY

Main Office and Factory: Clifton, New Jersey, Sales Offices: Chicago, Ill., Richardson, Texas, San Mateo, Cal., Santa Ana, Cal., Pittsburgh, Pa., Lynnfield, Mass. • Plants and Offices in Montreal, Quebec and London, England

CLIP, ATTACH TO YOUR LETTERHEAD AND WE'LL SEND INFO ON ANY YOU CHECK

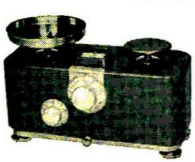
☐ **Fast, accurate direct read out to ±0.01 grams.** Capacity 800 grams. Also available in 1000g. capacity (PL-1) with direct read out to 0.1 gram, and 2000 gram capacity (PL-2) with direct read out to 1.0g. (0.1g. by estimation).

Model PL-800



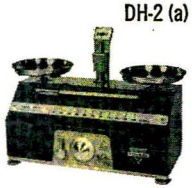
☐ **200 gram capacity.** Weight control dial and fine weighing dial with vernier makes possible direct readings from 100 grams to 0.01 grams. 500 gram capacity model also available (DWL-5).

Model DWL-3V



☐ **2000 gram capacity** and with 10g. x 0.1g. and notched beam 100g. x 10g. increments. Available with tare beam instead of notched beam. (DH-2(b)). 4500 gram capacity models (DH-4(a) and DH-4(b)) also available.

Model DH-2 (a)



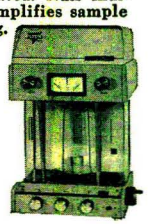
☐ **120 gram capacity.** Dials permit direct readings from 10 grams to 0.01 grams (can also be read to 0.003 grams by estimation).

Model DWL-2



☐ **Analytical balance, direct digital readout to tenth mg., 160g. capacity.** Has exclusive solid-state electronic null indicator. Unaffected by variations in sensitivity. Ease of reading, accuracy and reproducibility greatly enhanced. Null indicator simplifies sample weighing.

Model EA-1



TB-217

Circle No. 165 on Readers' Service Card

publications, including newspapers in 20 major market areas, and technical journals in a variety of industrial and technical fields. The index for January of this year was up 100.1 points above January 1965, and it was 36.8 points above the previous record of 175.9 that was set in November of 1965.

Engineer/Scientist Demand Index

(1961 = 100.0)

January 1966	212.7
January 1965	112.6
January 1964	77.0
January 1963	123.5
January 1962	153.7
January 1961	97.6

Deutsch and Shea predicts that, barring major unforeseen actions on the international scene, the demand for engineers and scientists will remain at a high level throughout 1966. By March of this year, the index registered 211.6, which was 93 points above March 1965. There are indications that the steady growth in demand may be reaching its peak with prospects of levelling off on a new high plateau.

In the sub-index related to technical journal recruitment advertising, there was a new high of 157.4, compared to 123.0 for February 1966 and 120.1 for January 1966. The March high was led by activity in the general science field (which more than doubled) and the electronics field (which was up better than 50%). Demands in the mechanical engineering, metallurgy, physics, and nuclear fields also rose significantly, and demands in the aerospace, civil engineering, and chemical fields rose slightly. The most sobering aspect of the large increase in demand for engineers and scientists is that the rise in the chemical field was very slight, compared to the others.

AgBr

HARSHAW'S

New IR Material

Silver bromide is a new far infrared material that transmits to 35 microns. Large far IR windows are now feasible.

CRYSTAL-SOLID STATE DIVISION

HARSHAW

The Harshaw Chemical Co.

1945 East 97th St. • Cleveland, Ohio 44106 • Phone 216 721-8300

Utrecht, Netherlands—Harshaw-Van Der Hoorn N.V.

Frankfurt, W. Germany—Harshaw Chemie GmbH

Circle No. 49 on Readers' Service Card

The Finest Oils, Greases, Waxes...

for High Vacuum Work—also Lubricant for High Vacuum Equipment, Masking of Circuit Boards and Other Scientific Applications

Vacuum pressures of these excellent oils are as low as 10^{-7} torr. Greases as low as 10^{-11} torr at room temperature. Scientists, who try Apiezon oils, prefer them for equipment used in nuclear physics, cyclotrons, electrical equipment, vacuum tubes, etc.; the greases for general laboratory work and gas-liquid chromatography; wax W with suitable solvent as a masking media.



As exclusive distributor in the United States, we offer immediate shipment from stock on the complete range of Apiezon products.

For applications, working characteristics, and list prices, write for new Bulletin 43-AC.

BIDDLE INSTRUMENTS

JAMES G. BIDDLE CO. 614

Electrical and Speed Measuring Instruments

PLYMOUTH MEETING, PENNSYLVANIA 19462

Phone 215/646-9200

Circle No. 31 on Readers' Service Card

The Radiometer pHM28

pHM28 offers high quality, stability and adaptability for future expansion of applications at low cost. With 0.02 pH reproducibility on a large mirrored and folded scale (0-10, 6-14 pH), it can be used for pH measurement, titration or control applications such as redox and dead stop end point titrations (Karl Fischer). Provision is made for connecting external recorders.

A matching control unit (Model TTT11) converts pHM28 to an automatic titrator or pH controller, and electrodes are available for many applications to match the convenient and integral electrode stand.

There are many other features—ask for literature today.

PRICE $350.00



Model pHM28

pHM28/TTT11

THE LONDON COMPANY

811 SHARON DRIVE, WESTLAKE, OHIO

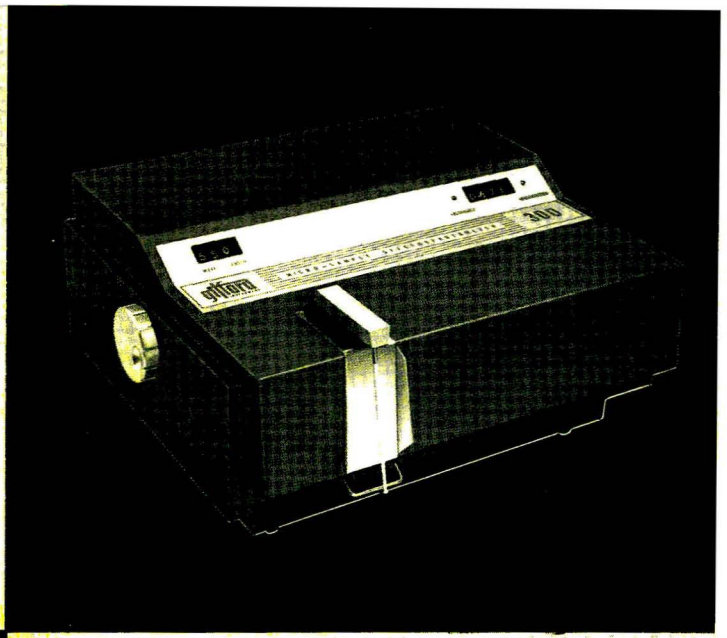
RADIOMETER COPENHAGEN

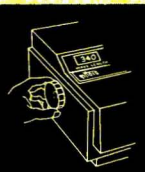
In Canada: Bach-Simpson Limited, Box 2484, London

Circle No. 20 on Readers' Service Card

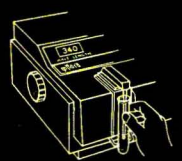
0.001 RESOLUTION

throughout 0.000 to 2.000 ABSORBANCE RANGE





WAVELENGTH RANGE 340 to 700 mu



SIMPLIFIED SAMPLING



DIRECT READOUT IN ABSORBANCE OR CONCENTRATION

...with the Gilford Model 300 MICRO-SAMPLE SPECTROPHOTOMETER

This instrument maintains a usable resolution of 0.001 absorbance unit over its entire measurement span of 0.000 to 2.000 A units. Its long term stability is better than 0.005 A per hour, requiring only occasional zero setting on a reference. And it combines this uncommon performance with explicitly simple operation.

The automatic time-impulse sampling system draws in less than 0.5 ml per sample with no handling of cuvettes or pouring of fluids. Touch a bar, and in a few seconds you flush out the previous sample, then introduce the next. The absorbance value appears immediately on the four-digit numerical indicator. Or, after a single calibration setting, you get direct readings of concentration in any convenient units.

Technicians find the compact Model 300 especially easy to use and maintain. Yet, here is a true spectrophotometer with research accuracy and flexibility, filling a realistic need in busy laboratories.

The remarkable sensitivity and stability of the Model 300 is a product of a unique electronic circuit, sophisticated optical and mechanical design and close tolerance manufacturing.

For special applications there are accessories for continuous flow arrangements, use of standard cuvettes and chart recording of absorbance data.

As vital diagnostic and research techniques improve, measurements often require new orders of sensitivity, precision and speed. The Gilford Model 300 is clearly ahead of this trend.

Gilford Instrument Laboratories Incorporated • Oberlin, Ohio 44074

SALES AND SERVICE OFFICES IN PRINCIPAL CITIES THROUGHOUT THE U.S.A.

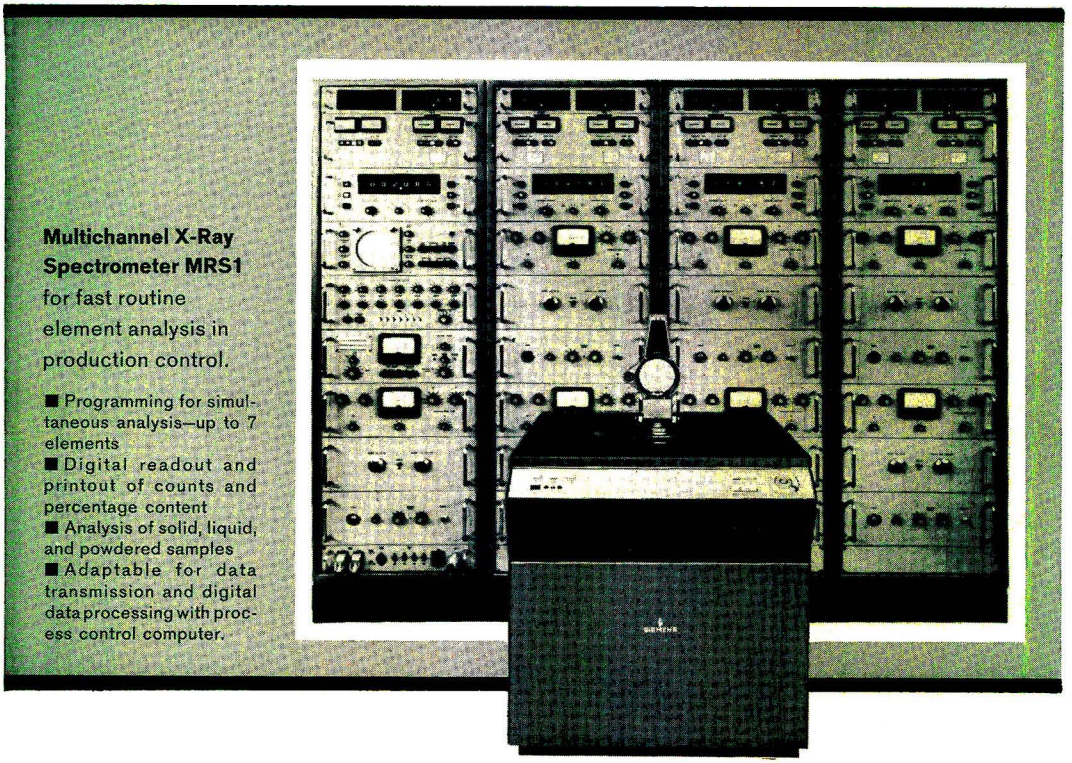
gilford INSTRUMENT®

INSTRUMENTATION FOR BIOLOGY AND MEDICINE

Circle No. 47 on Readers' Service Card

SIEMENS

X-Ray Spectrometry



Multichannel X-Ray Spectrometer MRS1 for fast routine element analysis in production control.

- Programming for simultaneous analysis—up to 7 elements
- Digital readout and printout of counts and percentage content
- Analysis of solid, liquid, and powdered samples
- Adaptable for data transmission and digital data processing with process control computer.

The Siemens Program Includes:

Kristalloflex IV—Simultaneous and sequential air/helium/vacuum spectrometers as goniometer attachments or table models for manual or semi-automatic operation. Can be expanded to provide automatic programming.

Microanalysis attachment for electron microscope ELMISKOP I.

X-Ray Pulse Spectroscope for non-dispersive analysis and easy setting and monitoring of pulse-height analysis.

Complete line of detectors, radiation counting and recording equipment.

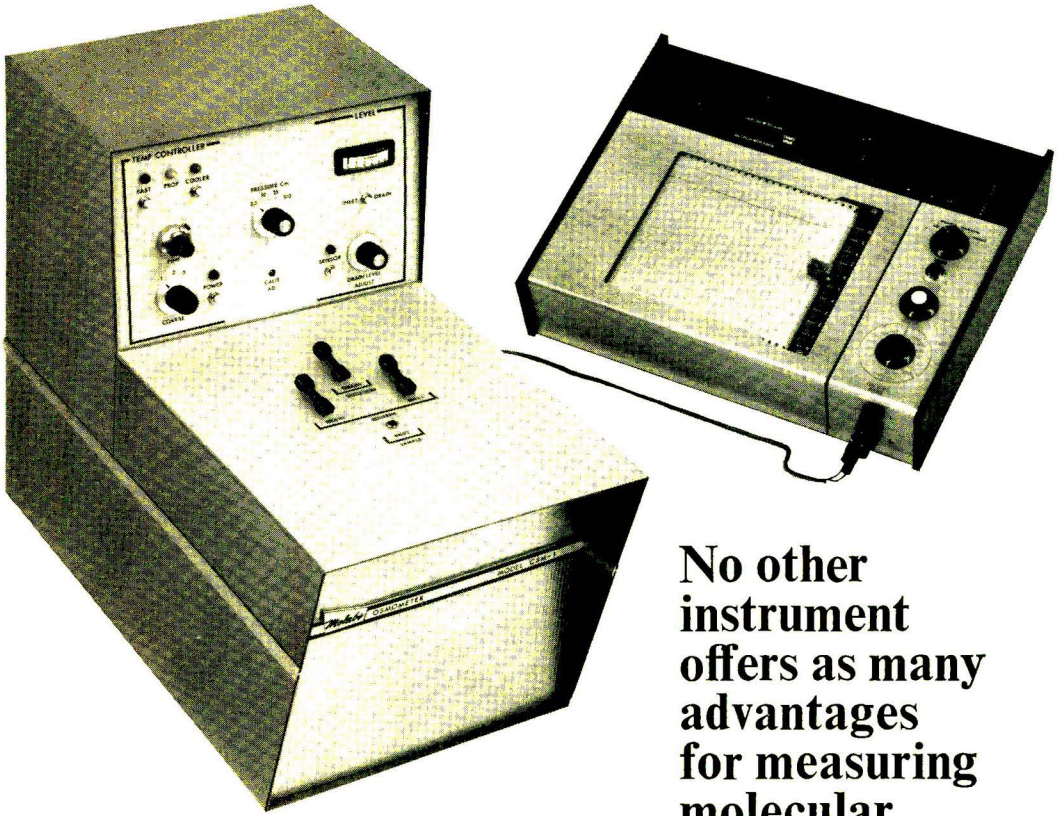
Manual or automatic diffractometers, and X-Ray cameras.

SIEMENS AMERICA INCORPORATED
350 Fifth Avenue, New York, N.Y. 10001

A Corporation of THE SIEMENS GROUP IN GERMANY
Berlin • Munich • Erlangen

In Canada:
SIEMENS CANADA LIMITED
407 McGill Street, Montreal 1, P.Q.

Circle No. 10 on Readers' Service Card



the new Melabs membrane osmometer

No other instrument offers as many advantages for measuring molecular weights of macromolecules: from proteins to polymers.

The new Melabs membrane osmometer is the most versatile, simple and convenient instrument ever designed for measuring osmotic pressures of solutions of large molecules (20,000 to 1,000,000 number average). No other membrane osmometer offers these advantages for biomedical and polymer applications:

☐ Simplified design for easy operation and maintenance. Melabs uses a direct-reading strain gauge detection system—eliminates servo systems and air bubbles. More compact, less complex and less trouble.

☐ Wide temperature ranges. 5° C to well over 100° C in Model CSM-2, 30° C to well over 100° C in Model CSM-1. Built-in *variable temperature control* over entire range in both instruments.

☐ Wide pressure ranges. Four selectable ranges, 0-2.5 cm water, 0-10 cm water, 0-25 cm water, 0-100 cm water.

☐ Performs equally well using *water* or *organic* solvents. Only stainless steel and the membrane contact sample.

☐ Competitively priced. In most instances, Melabs osmometers will be lower-priced than comparable instrumentation.

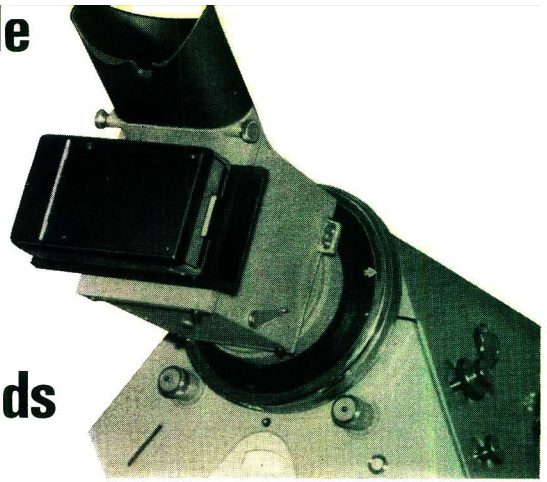
Additional details: sample size, 0.5 ml. Response speed, 5-30 minutes. Accuracy, ±0.5% full scale, any range. Recorder output, 0-1 mv dc.

For complete information, please write to Melabs, Scientific Instruments Department, 3300 Hillview Road, Palo Alto, California.

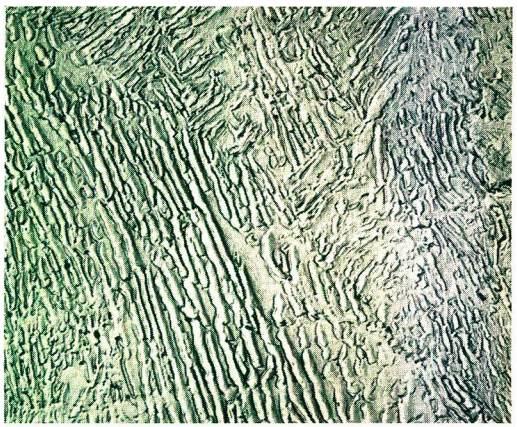
Melabs®

See Buyers' Guide for all products/sales offices.
Circle No. 65 on Readers' Service Card

Unbelievable Savings! Electron Micrographs In Ten Seconds

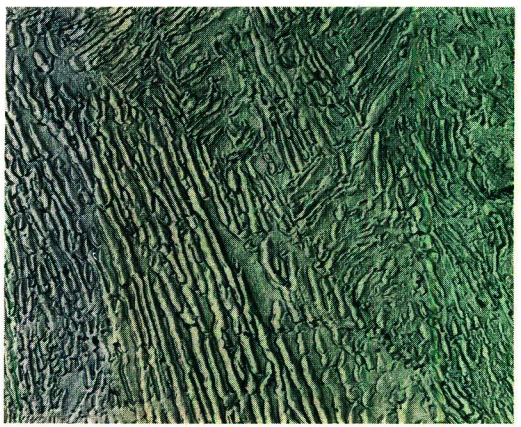


Sample 1



A ☐ Standard electron micrograph with wet film techniques
B ☐ Polaroid electron micrograph with Norelco-Polaroid attachment

Sample 2



A ☐ Standard electron micrograph with wet film techniques
B ☐ Polaroid electron micrograph with Norelco-Polaroid attachment

It is now possible to increase laboratory production by 180%! The cost savings and time reduction of this technique is hard to believe — but true.

Only Philips can offer this time saving innovation. With a front mounted Polaroid camera on the electron microscope, Model EM 100, it is possible to go from sample focus to finished print in less than 1 minute. Standard wet film techniques require at least 3 hours.

You can be the judge! Check the correct box below each high quality comparative micrograph. Can you tell the difference? The correct answers are given below. Same sample area is used in both micrographs. Two stage carbon replica, chromium shadowed at 45°. Both micrographs show 10,000 magnification of Pearlitic Steel.

This new technique is invaluable for applications in:

- Failure analysis
- Fractrography
- Particle size determination
- Routine electron metallography

World's Highest Standards in Quality Instrumentation

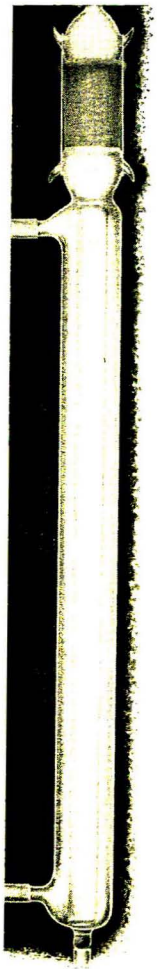
Norelco® PHILIPS ELECTRONIC INSTRUMENTS

Division of Philips Electronics and Pharmaceutical Industries Corp.
750 South Fulton Avenue, Mount Vernon, New York 10550

See Buyers' Guide for all products/sales offices.
Circle No. 152 on Readers' Service Card

Sample 1 A
Sample 2 B

EM-36



Column Chromatography in Three Easy Lessons*

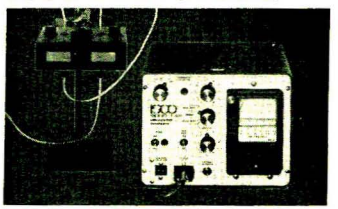
* Three Easy Prices Too!
For Complete Information
Send For Brochure CC11F

Lesson No.1



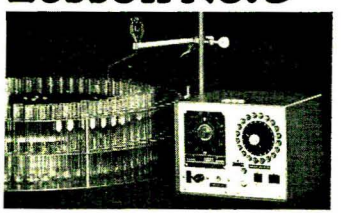
Begin by pumping your solvent into the column in a smooth concentration or pH gradient. ISCO's new programmed gradient pump, the DIALAGRAD, will handle this perfectly. In fact any simple or complex gradient formed by combining two liquids can be dialed directly into the DIALAGRAD. Program duration and pumping rates are easily adjustable over very broad ranges. No more mixing numerous solutions to guessed-at concentrations.

Lesson No.2



Now to identify your fractions. Use an ISCO UA-2 or 222 Ultraviolet Analyzer to get quantitative results with no need for further assay. Select linear absorbance, single or dual-beam monitoring at either 254 or 280 mμ or both. Absorbance recording minimizes need for base-line compensation and allows direct integration of chart record. As each UV absorbing fraction is recorded it is also automatically deposited in a separate collecting tube.

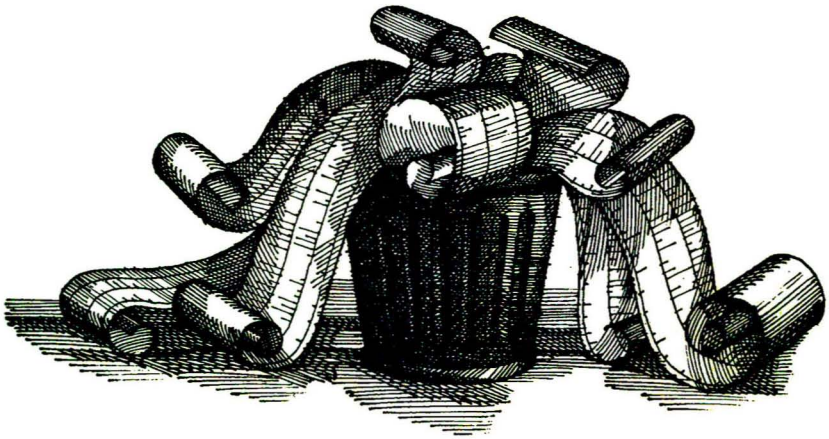
Lesson No.3



Collecting the effluent is then a simple task when ISCO fraction collectors are used. Choose from any of four basic models offering timed or volumetric control. Some have lift-off reels that can be changed as often as they fill, and when not collecting can be used as convenient storage racks. Extras such as drop counters and volumetric dispensers make things even easier. No after-school sessions necessary when you use ISCO equipment.

ISCO INSTRUMENTATION SPECIALTIES COMPANY, INC.
5624 SEWARD AVE. • LINCOLN, NEBRASKA 68507, U.S.A. • PHONE (402) 434-8265 • CABLE ADDRESS: ISCOLAB LINCOLN

Circle No. 135 on Readers' Service Card



High-Resolution Mass Spectrometry and The chart paper flood

(A poignant tale with a pleasing end)

High-resolution mass spectrometry generates an overwhelming amount of invaluable data. Accordingly, it was bound to be useful for many applications. Take gas chromatography. Its marriage with mass spectrometry was a natural and was accordingly aided, abetted, and applauded by organic chemists, biochemists, and their friends. And this happy union is regularly blessed with issue: reams of chart paper requiring manual and mental baby-sitting. Very tiresome. Also quite unnecessary. Reason: the development of the new MS-9 data-handling system. This is a fast-scanning, high-resolution mass spectrometer which can monitor even microgram samples in effluents of gas chromatographs and yield spectra *in a form which can be computer-analyzed automatically* without inundating you in a veritable sea of chart paper.

From your standpoint (and ours) this is a major breakthrough and therefore is now worthy of at least some elaboration: this MS-9 mass spectrometer can eliminate your data-handling problem by enabling you to record spectra on magnetic tape either for instant playback through a recorder or for feeding directly to a computer for automatic analysis. In other words, the MS-9 doesn't abandon the user in the middle of the game by just spewing out data in difficult-to-use form and then quitting on you.

A few words about the MS-9's other specifications. This is a double-focusing instrument that is actually as simple to operate as a single-focusing mass spectrometer. And, although its over-all capabilities will intrigue the most advanced mass spectroscopist, even users who are not specialists in mass spectrometry will find the MS-9 easy to use with comfort and confidence. Its resolving power is uniquely high and guaranteed to be at least 33,000; switching from high to low resolving power can be done automatically by flicking a switch. It scans rapidly; it will, for example, scan a spectrum in 10 seconds at a resolution of 10,000. The sensitivity is high: microgram quantities can be studied at the highest resolving power. The data can be processed by your computer and the masses measured with such accuracy that the elemental composition of every ion can be calculated.

Obviously, this has been a grossly incomplete recitation of the many talents of the MS-9. Additional compelling information will be forthcoming at your request. Or consider this possibility: outline your specific problems and we'll tell you which of our line of mass spectrometers (the most comprehensive line around) is appropriate to your needs.

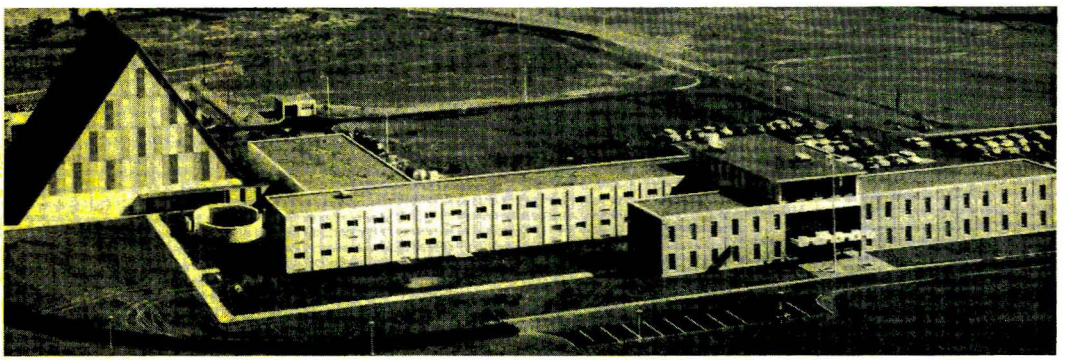
For further information on the MS-9, request bulletin number M9AC6

PICKER NUCLEAR: 1275 Mamaroneck Avenue, White Plains, New York 10605

PICKER AEI

Circle No. 79 on Readers' Service Card

Kellogg's Chemical Process Research Makes Broad Demands on Analytical Section



Research and Development Laboratory of M. W. Kellogg Co., Division of Pullman, Inc., was moved less than two years ago to the new Research and Development Center in Piscataway Township, N. J. The Center has nearly two acres of floor space housing a staff of 180 chemists, engineers, and service people working in chemical process research. The building is an assembly of five interconnected units: the administration and office wing in the front, the connecting unit which houses the auditorium, conference rooms and library, the laboratory wing in the rear, the service unit containing machine shop and storeroom, and the unique A-frame pilot plant building capable of holding as many as 35 pilot plants from 20 to 80 feet high

RESOURCEFUL and imaginative research is basic to the world-wide operations of The M. W. Kellogg Co. This research is responsible for many of Kellogg's contributions to process engineering and plant construction. As a vital partner of the oil industry in the thirties, Kellogg research played a key role in creating and developing many of the basic processes: fluid catalytic cracking, catalytic reforming, alkylation, polymerization. These processes, adopted by the industry on a world-wide basis, are presently responsible for the majority of the world's refined petroleum capacity. More recently, the development of processes for the production of ammonia and ethylene and the extraction of helium from hydrocarbon feedstocks has established new standards of efficiency and yield.

The majority of Kellogg research is chemical process research, involving great depth and breadth. Unlike product research, where investigation is intense but the corridor is narrow, Kellogg research, to be productive, must range the technologies. To support this type of research, there is a constant need for developing a great variety of analytical methods to meet the particular accuracy and man-hour requirements faced by the three phases of exploratory, process, and pilot plant research.

The analytical requirements of Kellogg research effort are met by a centralized Analytical Section with a regular staff of 15, occupying 3800 square feet of laboratory space. Because of the strong dependence on instrumentation, the laboratory space per analytical person is nearly twice that for other technical personnel. The Section includes four groups: Chemical Analysis, Gas Chromatography, Instrumental Analysis, and Chemical and Physical Testing.

The Analytical Section works very closely with the chemist or engineer right from the beginning of a research project. Sampling points and sampling technique are discussed; appropriate analytical methods are tailored to the special needs, keeping both accuracy and man-hour requirements in mind. An example of this cooperation occurred during a recent study of vacuum tower stripping of carbon dioxide from sea water, financed by the Office of Saline Water of the U. S. Department of Interior. A special arrangement was worked out for sampling liquid under vacuum without loss of carbon dioxide through flashing. An ASTM method was adopted to determine carbon dioxide in low p.p.m. range. To monitor the absolute amount of air leak into the tower, a measured quantity of helium was admitted and the ratio of helium to air was determined by mass spectrometry.

The Chemical Analysis Group handles nonroutine organic and inorganic chemical analysis with the use of small instruments such as flame photometer, electroanalyzer, and pH meter. An appreciable amount of time is directed toward analytical research and development. For instance, a rapid method has been developed for the determination of silica in phosphate rock. Aside from handling analytical problems arising out of research endeavor, this group works out reliable, simple tests, and trains operators to analyze pilot

plant streams on 24-hour operation.

The Gas Chromatography Laboratory is equipped with both isothermal and temperature-programmed gas chromatographs with thermal conductivity and flame ionization detectors. There are about 20 gas chromatographs located in various research laboratories. Frequent assistance is given to chemists and engineers to solve the problems encountered in the performance of on-the-spot analysis in gas chromatography. To serve pilot plant operations, this group is responsible for setting up and calibrating stream analyzers such as process chromatograph, modified laboratory chromatograph, density instrument, etc.

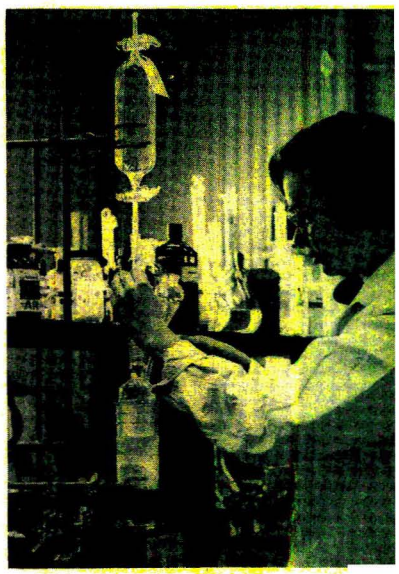
The Instrumental Analysis Group has installed a new analytical mass spectrometer to replace one purchased more than 20 years ago. The new instrument is provided with gas and liquid sample entries at ambient temperature and a 350° C. inlet system for the introduction of high-boiling liquids and solids. It has a mass range of 2 to 700, encompassing the range of petroleum and petrochemical samples encountered in our research efforts. Coupled with the use of a computer located in Kellogg's office in New York, the mass spectrometer is a powerful tool, not only in yielding accurate analysis of complicated mixtures but also in structure elucidation. The laboratory is equipped with a recording spectrophotometer covering the ultraviolet, visible, and near infrared ranges, and both double- and single-beam infrared spectrophotometers. These are used by research chemists for the study of mechanisms of heterogeneous catalysis, and for structure work and functional group analysis by analytical personnel. X-ray diffraction together with differential thermal analysis is employed to study the change in phases and crystallite sizes of catalysts. These bring to light the factors which affect the catalyst performance under various conditions. The x-ray emission spectrometer is equipped with a pulse height analyzer which discriminates the background noise from the radiation of interest. A method has been developed for the direct determination of metals in petroleum products down to the low p.p.m. range by this instrument.

The Chemical and Physical Testing Group carries out all the necessary testing of petroleum products and their related materials, iron ores, fertilizers, etc. It handles the control work generated from a large variety of pilot plant operations and routine analysis from research laboratories. Because of widely fluctuating analytical requirements, the equipment in this laboratory far exceeds the manpower available. All analysts permanently assigned are experienced in manipulating all the equipment and running a wide variety of tests. Heavy work load and shift work demands are met by temporary transfer of technicians from other divisions. Cracking catalyst is evaluated for activity and selectivity in bench scale fluidized catalytic cracking unit. Iron ore reduction is monitored by reducible oxygen measurement and Dings-Davis magnetic separation. Particle size distribution of fluidizable powders is determined by Roller analyzer, micro-mesh sieve, Micromerograph, or sedimentation. Atmospheric and vacuum distillation units equipped with up to 100 theoretical plate fractionation columns handle the fractionation of feeds and products. Two knock test engines are used for octane number measurement. Apparatus is available for measuring such physical properties as viscosity, flash point, pour

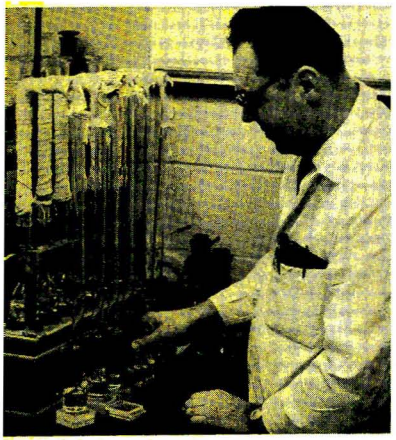


For a laboratory engaging essentially in petroleum and petrochemical research, a mass spectrometer is essential for multicomponent quantitative analysis and frequently for qualitative analysis. This instrument has a usable mass range up to 700 and is equipped with specially designed gas sampling system, 150° C. liquid entry, and 350° C. inlet for high-boiling liquids and solids

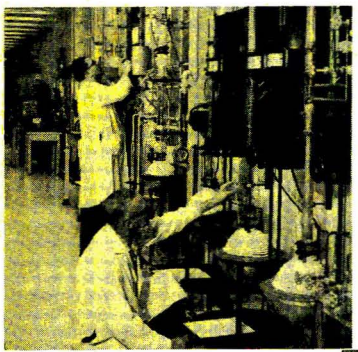
LABORATORY OF THE MONTH



Special analytical methods are developed to handle unusual samples. The components of a calibration gas mixture are accurately determined by wet chemical procedures after reaction in this absorption apparatus



Evaluation of the results of a pilot plant program required numerous trace nitrogen determinations. A modified Devarda's method is carried out using this laboratory-built apparatus with which 12 samples may be handled simultaneously



Various types and sizes of distillation apparatus occupy the entire right wall, 96 feet, of the Chemical and Physical Testing Laboratory. These units are used in preparing feedstocks for pilot plant studies, topping and fractionating products for testing, and carrying out ASTM distillation tests



Pilot plant operator shown is being trained to use a laboratory gas chromatograph. The instrument is set up to measure accurately the main product present in concentrations of less than 1% of the product stream. Because of the large number of inexperienced operators involved and the unstable instrument conditions, internal standard techniques are usually employed for such purposes

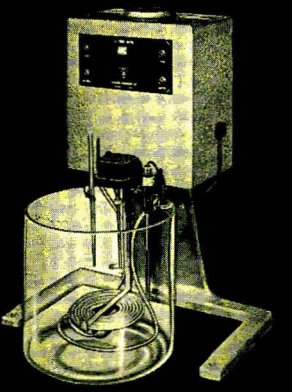
point, surface tension, and color. Chemical analyses include bromine number by electrometric titration, carbon and sulfur by combustion, Orsat analysis, etc.

Kellogg's engineering departments frequently call on the Analytical Section to carry out special assignments in connection with problems arising in the design or operation of Kellogg-built plants. Analytical methods are supplied in connection with setting of product specification guarantees. Corrosion samples and fouling deposits are analyzed and the analyses are interpreted. Special sampling devices have been constructed for sampling multiphase plant streams. The Analytical Section may send an experienced technician, for example, to a refinery to sample the product streams from a catalytic cracker.

WACO LO-TEMP BATH

COOLS HEATS

ONLY...$440.



SEVEN WAYS BETTER

1 Heats and Cools—almost double the range of the average visibility bath.

2 Accuracy — constant temperature at any level from −10°C to +65°C ±.01°C — ideal where precise temperature control is required.

3 Large Capacity — coils fit snug against the bottom, the entire volume of the jar is usable. Glass jar permits fast observation.

4 Compact — only 20½" wide 27½" high. Saves space. Fits on any lab table or desk.

5 Self-contained — heating controls, cooling compressor, all parts are housed in this compact unit.

6 Low Maintenance — Waco Lo-Temp has been proved trouble-free by laboratories from coast to coast.

7 Low Price — $440.00.

Specify: No. 882 Waco Lo-Temp Refrigerated Bath, complete with Pyrex jar 12" in diameter, for 115 volt 50/60 cycle AC

Other sizes and accessories available to fit your needs. Write for Waco Bath Bulletin for complete information.

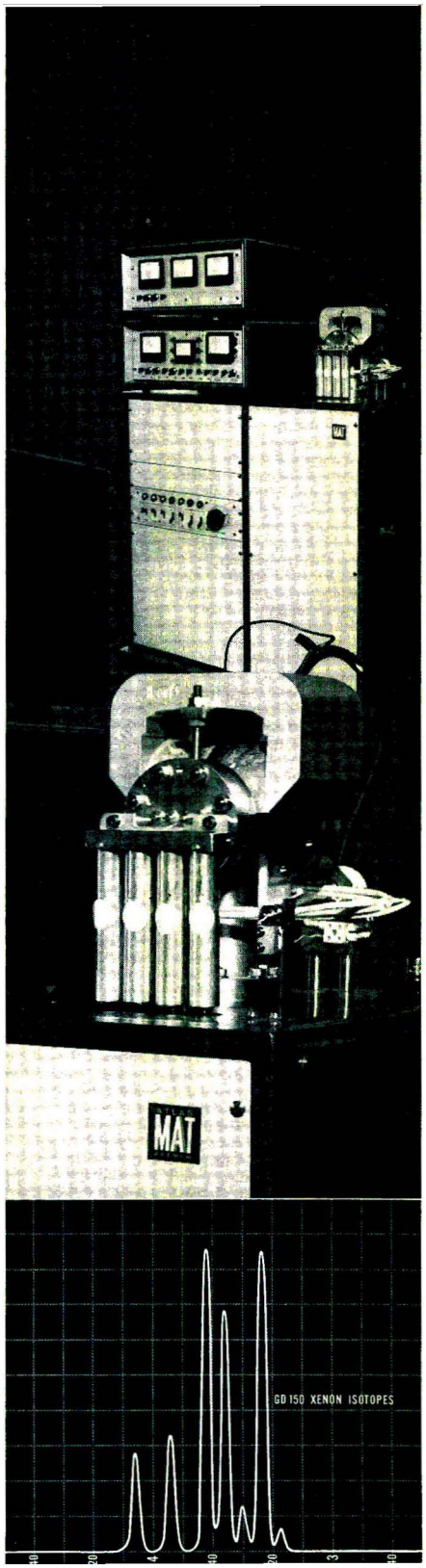
LABORATORY SUPPLIES AND EQUIPMENT

WILKENS-ANDERSON CO.

4525 W. DIVISION ST. CHICAGO 51, ILL.

Circle No. 99 on Readers' Service Card

measure four chemical components simultaneously



WITH THE NEW ATLAS-MAT GD 150 MASS SPECTROMETER.

The MAT GD 150 features a unique four-collector analyzer that now makes possible simultaneous measurement of almost any four peaks. Each collector can be moved individually for fast, convenient peak selection—even during operation.

The new GD 150 studies a broader range of samples than other comparable instruments. It analyzes any gas and accepts solid samples. And it measures samples as small as 1×10^{-5} cc STP—10,000 times smaller than similar mass spectrometers.

Truly the GD 150 is invaluable to the research chemist. It measures total pressure and mass spectra simultaneously. No other instrument can offer higher resolution (120—10% valley), over a wider mass range (2—300), at a lower cost. ($1500 less than equivalent instruments).

If you're interested in versatility, the GD 150 adapts for: vacuum fusion analysis • process monitoring • mixture analysis • chromatograph effluent identification • trace impurity detection • geological age dating • isotope ratio measurement • residual gas analysis • blood alcohol measurement.

Investigate the advantages of the new GD 150 now. Write for Data File A605-66.

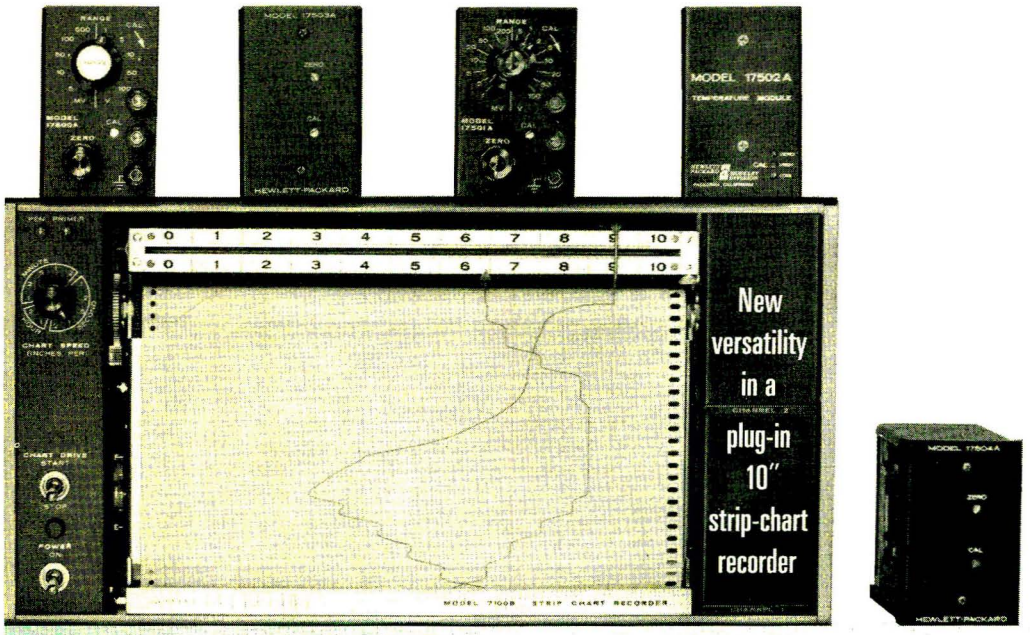
CARY® INSTRUMENTS

APPLIED PHYSICS CORPORATION
2724 S. PECK RD., MONROVIA, CALIF.

Atlas-MAT instruments sold and serviced in North America by Applied Physics Corporation
UV/VIS/IR/Raman Recording Spectrophotometers
Manual Spectrophotometers • Spectropolarimeters
Vibrating Reed Electrometers & Amplifiers

Circle No. 177 on Readers' Service Card

PLUG-IN



- **Input modules provide special purpose capabilities**
- **Mainframe available with one or two pen flexibility**
- **12 instantly selected chart speeds, 1 in/hr-2 in/sec**
- **Half-second response time**
- **Chart tilts in three positions for easy viewing and notation**
- **Easy chart loading, tear off or storage, paper supply indicator**
- **All solid-state circuitry**
- **Rack-mount, metric models available**

The basic mainframe of the 7100B (two pens) and 7101B (one pen) provides 10" strip-chart recording capabilities. Each channel accepts any of the wide variety of input modules which determine the electrical span or special-purpose recording capability.

Features offered, in addition to those above, include event markers, electric pen-lift and chart drive start-stop—all remotely controlled. Retransmitting potentiometers, adjustable high-low limit switches on both channels and remote 10-1 speed changers are also available.

Standard input modules (more to come) offer multiple span ranges, high input resistance (1 meg at null), high cmr and floating inputs to 500 v above ground. Model 17500A has 10 calibrated spans 5 mv-100 v full scale; Model 17501A has 16 calibrated spans 1 mv-100 v full scale. Variable span and full scale zero controls are provided. Model 17502A, a temperature input module with automatically compensated reference junction, linearizes recorder presentation with standard paper. Additional low-cost single range input modules (Model 17503A, 1 mv input with filter; Model 17504A, 5 mv-100 v with plug-in range cards) are also available:

Model 7100B 2-pen Recorder, $1300
Model 7101B 1-pen Recorder, $1000

Model 17500A Input Module, $250
Model 17501A Input Module, $350
Model 17502A Input Module, $250
Model 17503A Input Module, $250
Model 17504A Input Module, $200

Ask your Hewlett-Packard field engineer for a demonstration or write for complete information to Hewlett-Packard, Palo Alto, Calif. 94304, Tel. (415) 326-7000; Europe: 54 Route des Acacias, Geneva.

Data subject to change without notice.
Prices f.o.b. factory.

HEWLETT PACKARD hp MOSELEY DIVISION

1304

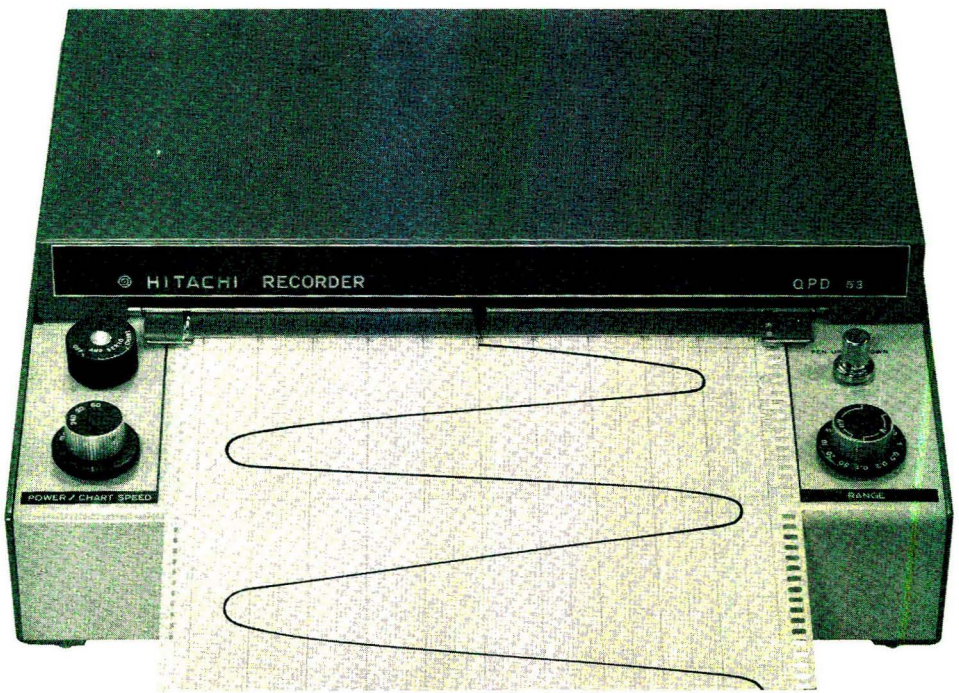
Circle No. 51 on Readers' Service Card

HITACHI MULTI-PURPOSE RECORDER QPD 53

The Hitachi QPD 53 electronic self-balancing multi-range flatbed recorder has many applications in the field of research and experimentation.
Its small size (412×150×352mm) and light weight (11kgs) allow the recorder to be operated almost anyplace.
Hitachi QPD 53 recorder's main features are: High sensitivity responds to any change up to 0.1% of the full scale. High balancing speed enables the pen to travel across the full scale in less than one second. Horizontal chart feed makes it extremely easy to inscribe check marks on the chart. Other features are: Wide input range of 1mV to 10V is available through the eleven-step selector switch. Six chart driving speeds ranging from 240mm/min to 20mm/h are convenient to use. Zero adjuster facilitates shifting the zero point to any position on the scale.

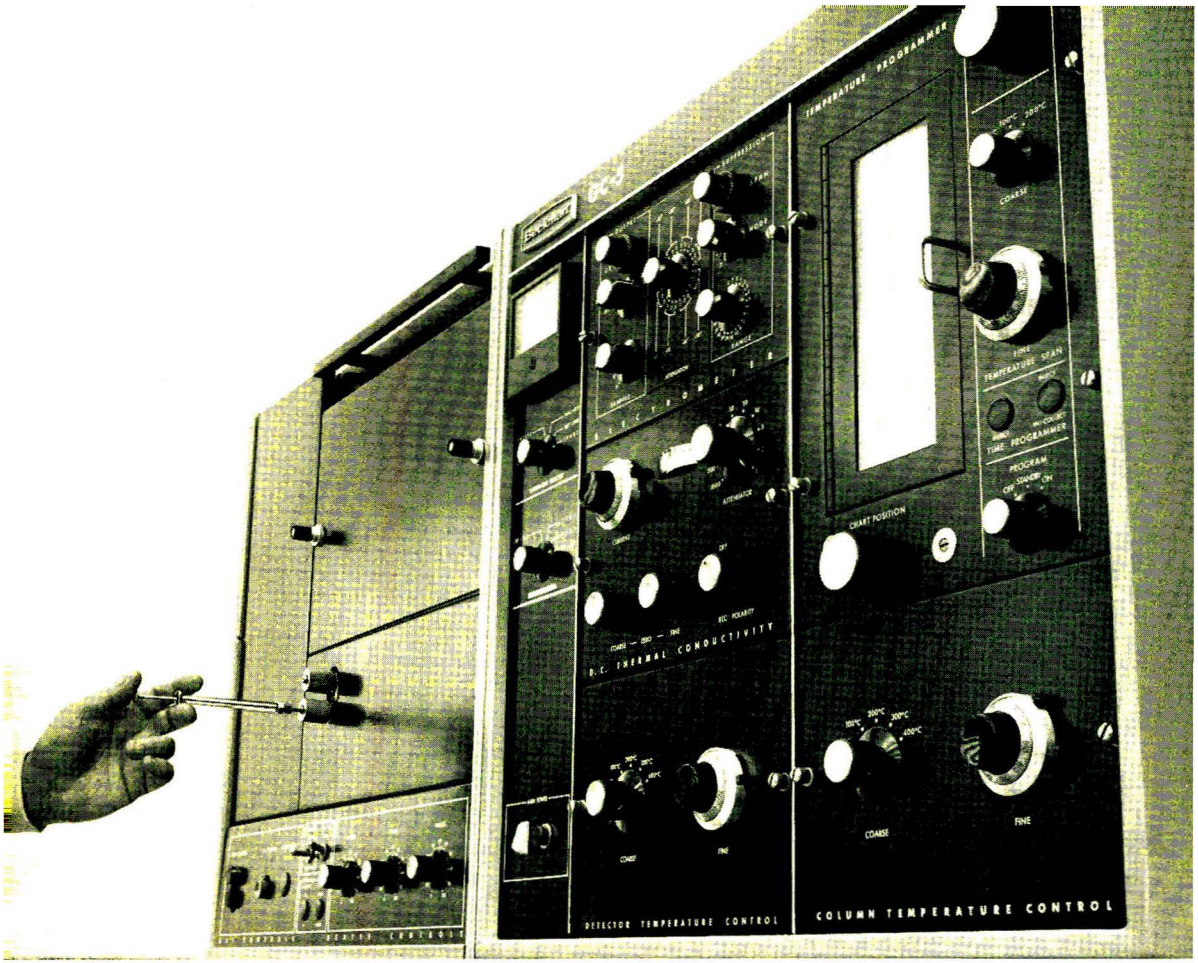
HITACHI
Hitachi, Ltd. Tokyo Japan

For technical information please write to Hitachi, Ltd., Measuring Instrument Department, International Sales Division, Nippon Bldg., Ohtemachi, Chiyoda-ku, Tokyo, Japan



Circle No. 23 on Readers' Service Card

Circle No. 24 on Readers' Service Card →



The second-best gas chromatograph in the world...the new Beckman GC-5*

The new GC-5 is a modular, bench-top instrument offering high performance and reliability at a moderate cost... as low as $2,189.00. It utilizes the performance-proven modules of the GC-4, and permits the selection of a system which specifically matches your application requirements... and your budget. The GC-5 also allows the easy addition of components to extend performance and keep your unit up-to-date.

The GC-5 will accept two inlets, two columns and two detectors simultaneously. A choice of three detectors and four inlets expands the capability of the GC-5 in every area of gas chromatography. Stable power supplies, precise temperature controllers and a sensitive electrometer enhance accuracy and repeatability. Providing isothermal or programmed operation, the large oven permits easy column change and accepts glass or metal columns.

A lot for a second-best chromatograph? Yes, but just what you'd expect from the developer of the best... the GC-4 Research Chromatograph. For more information on either the new GC-5 or the GC-4, see your Beckman Sales Engineer or write for Data File LGC-2-16.

Beckman® INSTRUMENTS, INC.
SCIENTIFIC AND PROCESS INSTRUMENTS DIVISION
FULLERTON, CALIFORNIA • 92634

INTERNATIONAL SUBSIDIARIES: GENEVA; MUNICH; GLENROTHES, SCOTLAND; TOKYO; PARIS; CAPETOWN; LONDON; MEXICO CITY

*In case you're wondering... the best is the Beckman GC-4 Gas Chromatograph

ADVERTISEMENT

Not long after this is published, a great many persons who work professionally with laboratory organics will receive in the mail their copies of the 44th edition of the EASTMAN Organic Chemicals catalog.

Now please turn to August 1, 1966 on your desk calendar.* There please write, "Check if Eastman List 44 arrived." If you have no copy of List 44 by that day, then either 1) it is not known that you need it or 2) something has gone wrong. At that time notify **Distillation Products Industries, Rochester, N. Y. 14603** (Division of Eastman Kodak Company).

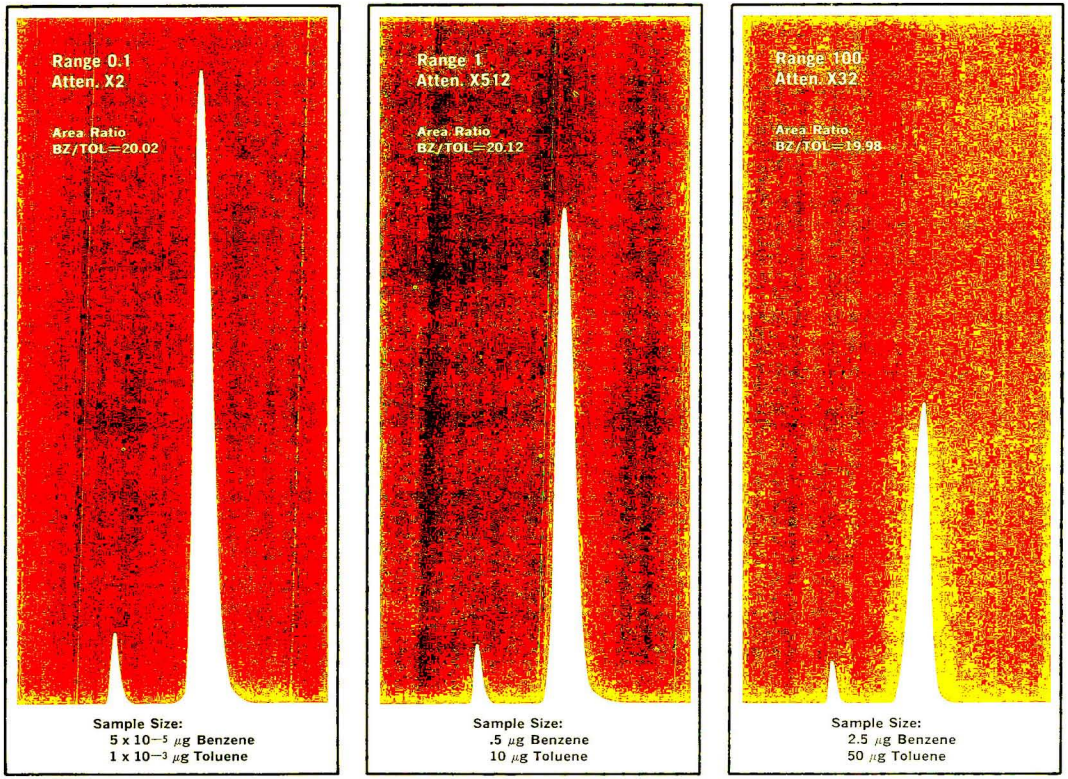
For nearly half a century the Eastman catalog has had a very special role in the working or teaching laboratory. It is in effect the index of compounds that a chemist is freed from preparing himself, except for exercise. The list has had the expected growth, the number of "see" references has tripled to cope with the nomenclature problem, and there is an empirical index that seems by far the simplest way to translate a desired structure into a reliable bottle on the bench.

Nobody has to get along without this tool, particularly since there is no charge for it.

EXCEPT TO NOTIFY OF ADDRESS CHANGE, WAIT UNTIL AUGUST 1, 1966.

* If you expect to be away that day, turn to the *third* working day after your scheduled return. The first two days back are always too busy to take care of the important things.

RELIABLE



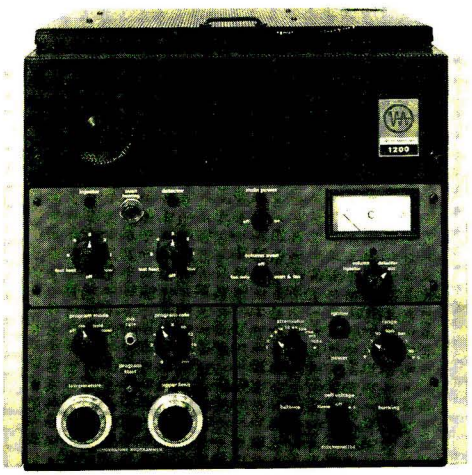
HY-FI III / GAS CHROMATOGRAPH

We feel that the Hy-FI III offers the latest design, maximum versatility and the highest value of any gas chromatograph available today.

Specifically, the new flame ionization detector and solid state electrometer offer a linear dynamic range of one-million fold. Each of four ranges allows attenuation to 1024 without electrometer saturation. This means ***reliable*** quantitative analysis from ppm's to major components.

Shown above is a linear dynamic range of 1,000,000 from the smallest benzene peak to the largest toluene peak. Areas were measured with the Aerograph 471 Automatic Digital Integrator; one of several useful accessories.

Write for detailed report on the above study, or call the closest Varian Aerograph office.



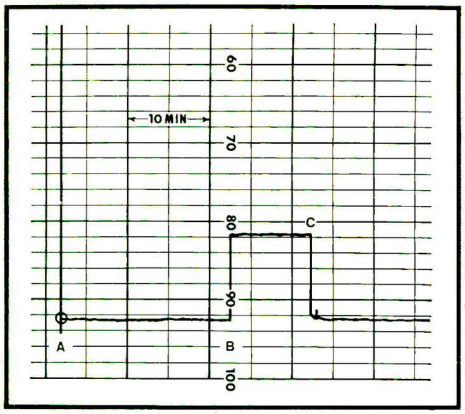
Specialists in Gas Chromatography

varian aerograph

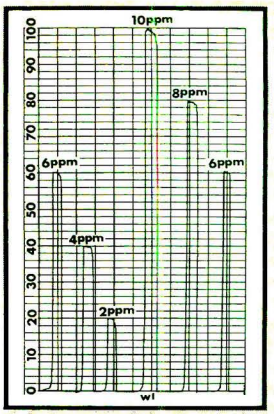
formerly Wilkens Instrument & Research

WALNUT CREEK, CALIFORNIA • REXDALE, ONTARIO, CANADA • BASEL, SWITZERLAND

Circle No. 96 on Readers' Service Card



Model 303 double-beam system eliminates the effects of drift in lamp, detector, and electronics. Here, Ca is run from a cold start. Burner is lighted at A, 1 ppm Ca inserted at B, withdrawn at C. Quiet, stable baseline commonly produces 5X improvement in detection limit and precision.



Model 290 readout in concentration requires no tedious calculations. Here, direct readings on an accessory linear recorder are obtained for 2, 4, 6, 8, and 10 ppm Calcium.

performance-proved instruments for ATOMIC ABSORPTION ANALYSIS

WHY YOU SHOULD USE PERKIN-ELMER ATOMIC ABSORPTION

Atomic absorption for the determination of metallic elements is today's fastest-growing analytical technique. Perkin-Elmer, a leader from the beginning, has the kind of competence that produced its Analytical Methods Book, which gives detailed guidance for 64 elements and over 300 analyses. Perkin-Elmer also publishes the Atomic Absorption Newsletter, the only technical journal devoted to the new technique.

Clearly, such deep analytical experience can result in first-class atomic absorption equipment. Indeed, Perkin-Elmer's two instruments are designed expressly for the special needs of atomic absorption: they are not compromises, accessories, or adaptations of equipment originally developed for other needs.

The Model 303 double-beam system offers speed, precision and sensitivity: With built-in 10X scale expansion, it is possible to detect very small deviations from the stable baseline shown above, left. The ability to measure tiny signals produces the best possible detection limits.

With the DCR-1 accessory, the Model 303 reads out directly in concentration in any desired units on a four-digit illuminated display. A determination can be completed in four seconds. The DCR-1 will also automatically take and present the average of 4, 8, or 16 readings of the same sample.

The Model 290 Reads Directly in Concentration: The most time-consuming portion of conventional atomic absorption analysis is the conversion of linear transmittance readings to their logarithms, followed by curve plotting. With the 290, all this is eliminated. The 5-inch readout scale is linear in concentration.

The Model 290 is a big instrument in a small container. A 50-inch optical path has been folded into a neat 25-inch package; detection limits are therefore equal to or better than those of much larger single-beam instruments. And the price for the complete instrument is only $2900.

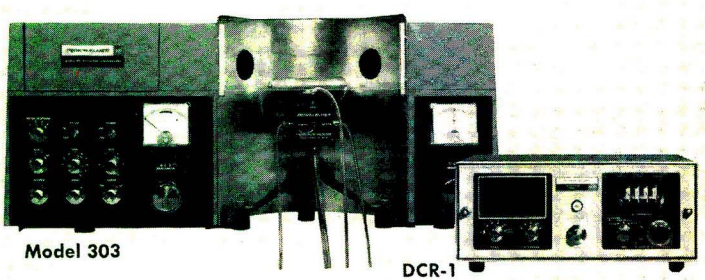
Both instruments can determine over 60 elements with Perkin-Elmer-built single and multi-element hollow-cathode lamps and the versatile premix burner. The nitrous oxide burner head enables analysis for Al, Ti, V, Si, the rare earths and other refractory elements. The new three-slot Boling head, for air-acetylene, does not clog with solutions containing 40% sugar, 20% lead, or undiluted serum. Yet another head provides a short optical path to reduce sensitivity and avoid dilutions.

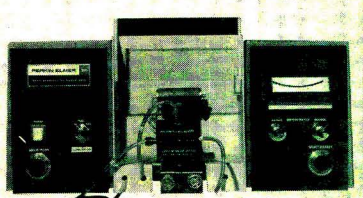
Free training and literature: Subscriptions to the Atomic Absorption Newsletter, a bi-monthly technical journal, are available free on request. A summary of applications reprints can be obtained by writing for AA322. Instrument users receive free training courses in Chicago, Houston, Los Angeles, San Francisco, or Norwalk, Connecticut.

For details, including information on specific applications, write to the Instrument Division, Perkin-Elmer Corporation, 702 Main Avenue, Norwalk, Connecticut.

PERKIN-ELMER

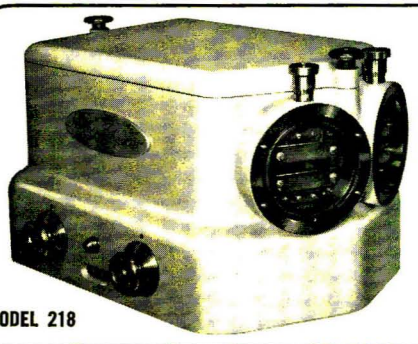
Circle No. 109 on Readers' Service Card





McPherson's complete laboratory for ABSORPTION SPECTROSCOPY in the vacuum UV...

. . . using the 0.3 meter plane grating scanning monochromator, a completely new concept with corrected optics **snap-in** type gratings (pat pend) to operate in the vacuum UV — visible — vacuum IR.

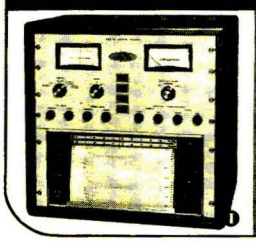


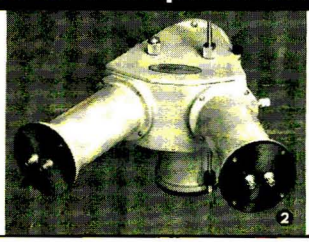
MODEL 218

FEATURES:

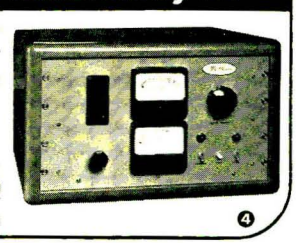
- Wavelength coverage 1050A to 16 microns.
- High Speed, f/5.3.
- Special aspheric mirrors to obtain maximum resolution, 1st order resolution guaranteed better than 0.3A.
- Snap-in type gratings — over 30 different selections designed for your particular job function (no holders needed — instantly focused ready to operate).
- Unique optical system provides exceptional work space between slits without extra reflections.

accessories to complete the absorption laboratory . . .









RATIO RECORDER ❶ — The Model 781 dual-pen recorder charts simultaneously: absorption coefficient and reference beam, or percent transmission and reference beam, or reference beam and sample beam . . . DOUBLE BEAM SAMPLE CHAMBER WITH DETECTORS ❷ — Model 665 has a light transmission efficiency of 90 percent at 1050A using grazing incidence mirrors. New LiF windows in sample cells will transmit over 50 percent per window (25% net) at 1216A . . . LIGHT SOURCE ❸ — Model 630 is a high energy, Hinteregger type gas discharge lamp for vacuum UV spectroscopy . . . POWER SUPPLY ❹ — The Model 720 is a high voltage dual-mode AC power supply which allows the spectroscopist the utmost latitude in his choice of excitation characteristics. Unit may be operated as a Michigan-type, air gap controlled high voltage spark or as an AC arc.

For complete information on this new addition to the wide range of McPherson vacuum instrumentation, or special instruments custom built to your specifications, write or call:

McPherson

McPHERSON INSTRUMENT CORPORATION

530 MAIN STREET, ACTON, MASSACHUSETTS 01720 • TEL: 617 263-7733

Technical Sales and Service Offices in La Canada, California; Cleveland, Ohio; Acton, Massachusetts; London; Germany-Switzerland-Austria; Melbourne; Paris; Tel Aviv; Tokyo.

Circle No. 136 on Readers' Service Card

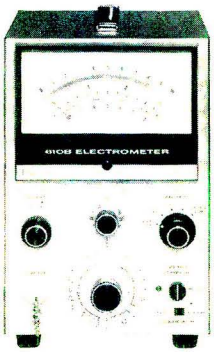
AC AMPLIFIERS PICOAMMETERS ELECTROMETERS
HIGH VOLTAGE SUPPLIES MICROVOLTMETERS NANO
VOLTMETERS MEGOHMMETERS CURRENT SOURCES
NANOVOLT SOURCES AC VOLTMETERS AC/DC AND
DC DIFFERENTIAL VOLTMETERS DC VOLTMETERS

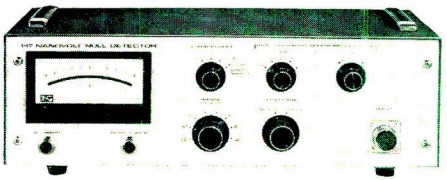
KEITHLEY MEANS INSTRUMENTS

TERS HIGH VOLTAGE SUPPLIES MICROVOLTMETERS
NANOVOLT SOURCES AC VOLTMETERS AC/DC AND

ELECTROMETERS AND PICOAMMETERS

If you're thinking about multi-function flexibility for measuring voltage, current, resistance and charge, you're talking electrometers. We know the language and talk it up with the line operated 610B and battery-powered 601, among others. If you've thought about simplifying the search for low level currents, our versatile picoammeter line has the instrument for you! Different models offer choices of fast response speed, remote ranging, long-term stability, calibrated zero suppression, low cost.



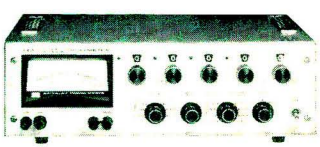


NANOVOLTMETERS, MICROVOLTMETERS AND NULL DETECTORS

Holding nanovolt and microvolt level signals is easier when you count on Keithley's line of low noise, highly stable instruments. Most have built-in zero suppression, too! The Models 148 Nanovoltmeter and 147 Nanovolt Null Detector operate by line or battery power. Sensitivities range from the 148's 10 nv or 147's 30 nv, to 100 mv. The low cost 153 measures from .2 μv to 1000 volts, with high ac rejection. For lower cost and proven performance, with sub-microvolt resolution, you can count on both our 150A and 149.

ac/dc and dc DIFFERENTIAL VOLTMETERS

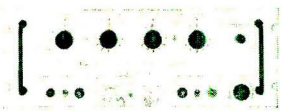
Compare with Keithley! Dc accuracies are .01 and .02%. All dc models provide temperature-compensated zener references, full input guarding and null sensitivities of 100 μv fs. Included are the .01% accurate 662, with 6-dial readout and the .02% accurate 660A, with 5-dial readout. Plus the .01% accurate 630 featuring a vibrating reed electrometer null detector allowing rated performance with source resistances to 10^{10} ohms. The ac/dc 661 highlights .01% dc accuracy; .05% ac accuracy over a 10 cps to 80 kc bandwidth. Every model carries a full year guarantee on accuracy.





ac AMPLIFIERS

If you're amplifying wideband signals, here are 8 dependable ways, spanning 15 cps to 180 mc. Each is an amplifier tuned for either wideband or pulse operation. They feature midband flatness of better than .05%; rise times under 3 nanoseconds and; overload recoveries within 50 nsec. Models 104 and 105 provide one unity-gain and two x10 amplifiers. The 106 and 107 have three x10 amplifiers. Single decade amplifiers are the 108 and 109. For single unity-gain amplifiers, look for the 110 and 111.



dc VOLTAGE SUPPLIES

For long-term studies, you can rely on Keithley ultra-stable high voltage supplies. Calibrated, in-line dials make output selection quick, easy. Choose ranges up to 5 kv, with either floating or grounded operation.

CALIBRATION DEVICES

Keithley devices are excellent secondary standards. Our 261 Current Source calibrates and verifies picoammeter accuracy with ranges from 10^{-5} to 10^{-14} amperes. Use its voltage twin, the 260, for accurate voltages from 10^{-10} volt to 1.11 volts. Both devices have 3-dial readout. Both function as sources for zero suppression, and both are economically priced, line powered units.

Write for technical literature on these and other products

KEITHLEY INSTRUMENTS

12415 Euclid Ave. • Cleveland, Ohio 44106 / EUROPE: 14 Ave. Villardin, 1009 Pully, Suisse

Circle No. 58 on Readers' Service Card

Circle No. 155 on Readers' Service Card →

RCA EMU-4

THE "NEW LOOK" IN ELECTRON MICROSCOPES



Objective aperture shown several times actual size.

Objective-Aperture Contamination Gone... Image Contrast Increased

The reason? . . . controlled heat, applied to the objective aperture so that contaminants refuse to gather on the aperture—at all beam intensities. With such contamination eliminated, the diameter of the hole can be reduced to realize an *increase in image contrast*. In addition, the aperture can be moved in or out of a fully-saturated beam, repeatedly, without contamination.

The *permanent* objective aperture is standard equipment on the RCA Type EMU-4 Microscope and is but one of the many innovations that are "standard" for the *new look in electron microscopes:* transistorized, modularized electronics; an exclusive selected-area diffraction facility; provision for instrument revision and expansion; high-capacity, minimum-backstreaming diffusion pump and many others.

For more information, write RCA Scientific Instruments, Building 15-5, Camden, N. J. 08102. In Canada: RCA-Victor Co. Ltd., Montreal.

Nationwide service available through
RCA Service Company. Offices in major cities.

RCA® **The Most Trusted Name in Electronics**

For better instrumentation for materials analysis...

Choose the supplier offering service innovations like the unique x-ray periodic chart.

X-RAY INSTRUMENTATION from General Electric includes the extra services you need to get top productivity. Both before and after you buy, G-E people and ideas are on call to help solve your application problems. Typical of the G-E product and service innovations is the exclusive x-ray periodic chart.

Designed for use in lab or office, this wall chart condenses computations into easy-to-use tables. It eliminates time-consuming data searching. The spectroscopist can select the appropriate x-ray tube target, analyzing crystal, counter tube and 2θ angle for the element of interest.

As another contribution to x-ray, this chart is typical of G.E.'s history of innovation. The single crystal orienter, the first 100 ma power supply, ultra-stable stabilizer, a dual target x-ray tube, and a four crystal changer/holder were first developed by General Electric.

Call your G-E X-Ray Sales Representative and discuss your x-ray applications. While you're at it, ask him how you can get your own wall chart. For descriptive information on x-ray equipment, write to General Electric, Section 4611, 4855 Electric Ave., Milwaukee, Wisconsin.

GENERAL ELECTRIC

Another example of General Electric's innovations, the X-Ray Periodic Chart, is in use at the U.S. Geological Survey, Washington, D. C.



INSTRUMENTATION



BY RALPH H. MÜLLER

New Devices Measure High Temperature, Low Velocities, Pressure

THERE is a continuing need for new and more precise means for measuring very high temperatures. An interesting development has been described by P. English and M. G. W. Dingle, *J. Sci. Instr.* **43**, 121 (1966) entitled "Rapid Scanning Monochromator for Use with Line Reversal Temperature Measurement." Their instrument is suitable for measuring temperatures of high intensity combustion systems. Light from the flame is mixed with that from a tungsten filament, the temperature of which can be controlled manually or automatically and is passed through a grating monochromator. The exit slit of the monochromator is moved laterally by a solenoid operated from the 50 cycle mains producing an optical frequency modulation of 100 cycles per second. The amplitude of slit motion is chosen to be some 5–10 A. U. If the monochromator is set at one of the *D* lines of sodium, say 5890 A., and has an excursion of a little over 6 A., a photomultiplier receiver can present the doublet 5890, 5896 A. on the screen of an oscilloscope. If the gas temperature is lower than source temperature, the *D* lines appear in absorption. If both temperatures are equal, no peaks appear and if the gas is at a higher temperature, the peaks are in the opposite direction—i.e., emission. The authors have also used a tuned amplifier system for detection. The output is essentially sine wave which exhibits phase change at the reversal point. For flames of emissivity greater than 0.3, a precision of 1% can be obtained—i.e., ±25° in 2500° K.

We are still curious about the fate of a self-balancing pyrometer of the disappearing filament type, which was advertised a few years ago by a prominent manufacturer. As we recall it, a phototube scanned the field, producing a flicker signal depending upon the relative brightness of filament and background. A servo system adjusted the filament brightness until the flicker disappeared. The filament current, or a potential drop derived from it, was continuously recorded.

PHOTOELECTRIC TRANSDUCERS

A short but interesting discussion on a class of photoelectric transducers is given by Russell Johnston of the Transdeveo Division of Kinemotive Corp. in *Instruments and Control Systems* **39**, No. 3, 111 (1966). The description is limited to a diaphragm-type pressure gauge, although other applications to the measurement of small displacements are mentioned. The diaphragm moves a twin shutter surrounding a small lamp in such a manner that it decreases the light intensity falling on one photosensor and increases that on an identical photosensor. This optical "push—pull" effect produces a signal as high as 5 volts without amplification. A feedback circuit minimizes the effects of variations in supply voltage, lamp intensity and photosensor sensitivity. No provision, so far, has been made to correct for the overall effect of ambient temperature variation. A photograph of a commercial version of the device, presumably a pressure transducer, shows a rugged and compact assembly with coupling fittings and connectors for quick installation in a system.

GALVANOMETER MOVEMENTS

From time to time, we have reported new applications of the use of d'Arsonval meter or galvanometer movements as force or torque measuring elements. The general principle is now being rediscovered. Thus, Vogel and Chapman in *Rev. Sci. Instr.* **37**, No. 4, 520 (1966) describe the procedure anew with reference to but one of the most recent applications, that of Head and Surrey in England, who used it in an anemometer to measure very low velocities and which we reviewed in this column some six months ago. Perhaps Lee Cahn, if he can spare the time, should write a brief but definitive review of the subject, sending reprints to editors of domestic and foreign journals. No one has done more to refine and greatly improve this technique and extend it to many more things than weighing. We believe he would agree that further useful applications are almost unlimited.

MICHAEL FARADAY

A book reviewer in *J. Opt. Soc. Am.* **56**, No. 3, 412 (1966) gives a tantalizing report on the appearance of two books. They tempt one to reach immediately for his check book and fill out an order blank. Both publications deal with Michael Faraday. We quote freely and wish to add some of our own observations. A definite and lively biography, "Michael Faraday" by L. Pierce Williams, Basic Books, N. Y., 1965; pp. xvi + 531; price $12.50, makes clear the extent of Faraday's monumental contributions to modern physics. As the reviewer points out—"correcting the misconception that Faraday was an empiricist to whom theory was anathema, Professor Williams recreates each of Faraday's major experiments in step-by-step detail, carefully reconstructing the theoretical links among the discoveries. Illustrated with 118 halftones and drawings, Professor Williams' readable and engaging contribution affords fresh insights into the scientific world of the 19th century and the contributions of one of its foremost figures."

We are pleased to note also that Dover Publications has once more performed a valuable public service in making Faraday's three-volume "Experimental Researches in Electricity" available in a reasonably priced two

simplifies job of cleaning all types of labware . . .

IN 30 SECONDS prepare a super-efficient chromic-sulphuric acid solution safely, easily

CHROMERGE®

1 Add a 25 ml. bottle of Chromerge to a standard 9 lb. container of concentrated sulphuric acid.

2 Cover container, and shake well, for about 30 seconds.

3 Chromic-sulphuric acid solution is mixed and ready for use.

H_2SO_4

CHROMERGE® CLEANS LAB WARE

Chromerge makes old, cumbersome methods of cleaning labware obsolete . . . eliminates danger and time-wasting of previous methods of preparation . . . long, unsatisfactory job of boiling sulphuric acid with potassium dichromate.

Chromerge does a *better* cleaning job, because its more powerful cleaning solution removes stubborn deposits which resist other cleaners, yet it protects glass surfaces, is chemically and bacteriologically clean . . . preserves the capacity of volumetric wear, gives a perfect miniscus for precise volumetric work!

GREINER SCIENTIFIC CORPORATION Dept. 521
20-22 N. Moore St. N.Y., N.Y. 10013

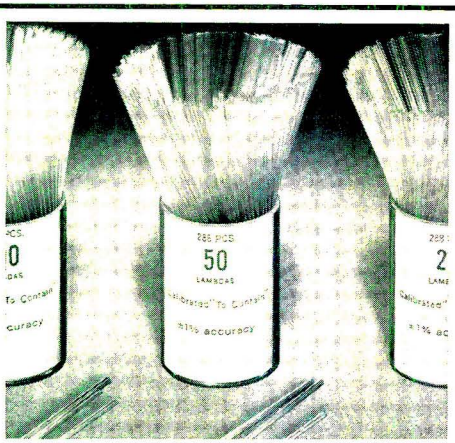
Circle No. 130 on Readers' Service Card

When little things mean a lot

S/P

scientific products

GENERAL OFFICES:
1210 LEON PLACE
EVANSTON, ILLINOIS



Because they mean a lot to you, they mean a lot to us. That's why S/P maintains 16 distribution centers, offers more than 30,000 items. For example — disposable, color-coded diSPo Pipets for micro sampling—calibrated to contain to ±1%. We guarantee you'll enjoy using them. They can mean a lot in your laboratory.

No. P4518X—diSPo® Micro Pipets

Capacity, ml.	Package of 288	6 pkgs., pkg.
0.02 (20λ) 0.025 (25λ) 0.05 (50λ) 0.1 (100λ)	$14.40 (5¢ each)	$12.30 (4.3¢ each)

Send for your free copy of the S/P 1965 Glassware Catalog.

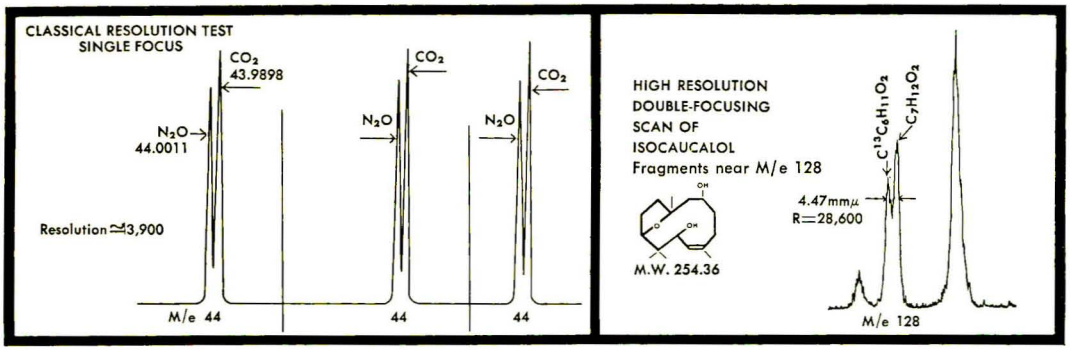
See Buyers' Guide for all products/sales offices.
Circle No. 160 on Readers' Service Card

INSTRUMENTATION

volume format (Volume I, pp. xx + 906; Volume II, pp. viii + 592 for $15.00 or $7.50 per volume). Over the years, we have derived great pleasure and stimulation from these writings. We note also that J. J. Thomson frequently emphasized the point made in Professor Williams' book—i.e., that the great theoretician, James Clark Maxwell was actually appointed to a Professorship in Experimental Physics at Cambridge in 1871 and that his first paper on electricity was on Faraday's "Lines of Force" and was mainly a translation of Faraday's views into mathematical language. Thomson said ("Reflections and Recollection," Macmillan, New York, 1937) that no one appreciated more than Maxwell the advantages gained in concentration of thought, and in the suggestion of new ideas, by considering a concrete case like a model, instead of relying upon algebraical symbols. He says: "For the sake of persons of different types of mind, scientific truth should be presented in different forms, and should be regarded as equally scientific, whether it appears in the robust form and colouring of a physical illustration, or in the tenuity and paleness of a symbolic expression."

We are one of the last of the Victorians (the grand old lady died a few years before we attained the marble-shooting stage) but these affections for Faraday's research accounts are not nostalgic reminiscences of by-gone days. One had the privilege, so to speak, of looking over his shoulder while he discovered benzene, established the electrochemical law bearing his name, probed the anatomy of a candle flame, laid the foundation for electrical industry by his elucidation of electromagnetic induction, and discovered magneto optic rotation. Of the latter, we have little more than a vast, largely undigested, array of Verdet constants and little instrumentation or automation of the technique worthy of present day capabilities.

Like many of his time, Faraday wrote in the first person singular, something which is anathema to present day editors. It is considered vain or too personal to use the "I" in describing one's work. This, of course, ignores the fact that every free man has the inalienable right to make a fool of himself on occasion and leave no doubt about the origin of the mistake. Thinking out loud, as he did, leads the reader to share in the excitement of the investigation. When we are ordered to say, "it was found that," our readers are led to believe that a person or persons unidentified have inadvertently overturned a damp stone and found treasure there quite unexpectedly.



PLANNING A MASS SPECTROMETER?

The new Hitachi Perkin-Elmer RMU-6E is an instrument that gives you exceptional performance and versatility at moderate cost. It is easy to operate, compact and reliable. Its building-block design allows you to add all the analytical capability you need as your mass spectrometer program grows. For example: you can attach the electrostatic sector to allow high resolution (M/△M 10,000 routine, 30,000 attainable) and precision mass measurement (better than 1 in 200,000.) For computer-aided spectral interpretation, our new DDA-1 Digital Data Acquisition System records 12,000 twelve-bit data points per second on magnetic tape with compatible format.

• **The RMU-6E Analyzer** incorporates a 90° 8 inch-radius magnetic sector with rigid, open construction. Its high resolution results from a refined ion optical design. Aberrations are corrected to the second order, and field fringing is minimized. Its wide pole pieces give a homogeneous field across the tube. Externally adjustable slits allow translation, tilting, and width adjustments. The magnet is fully adjustable in all coordinates, and need not be re-aligned when returned to position after bakeout. The solid state electronics are designed for high resolution stability. Masses can be scanned to more than M/e 2000. Positive or negative ion scanning is standard. The all stainless steel vacuum system provides low background while allowing unattended operation without need for cold traps. Once set up, the RMU-6E analyzer requires little attention.

• **All-Glass Heated Sample Inlets** accommodate gases, liquids and solids. Sample introduction is convenient; throughput is high.

• **Dual Direct Sample Introduction into the Ion Source** produces intense spectra even at the low temperatures required with unstable samples. The amino acid spectrum below illustrates this.

• **Gas Chromatograph Connection System** heatable to 350°C with efficient all-glass helium separator allows on-the-fly identification (M/e 12-450 in 2 secs) of as little as 3 nanograms of component injected into the G.C.

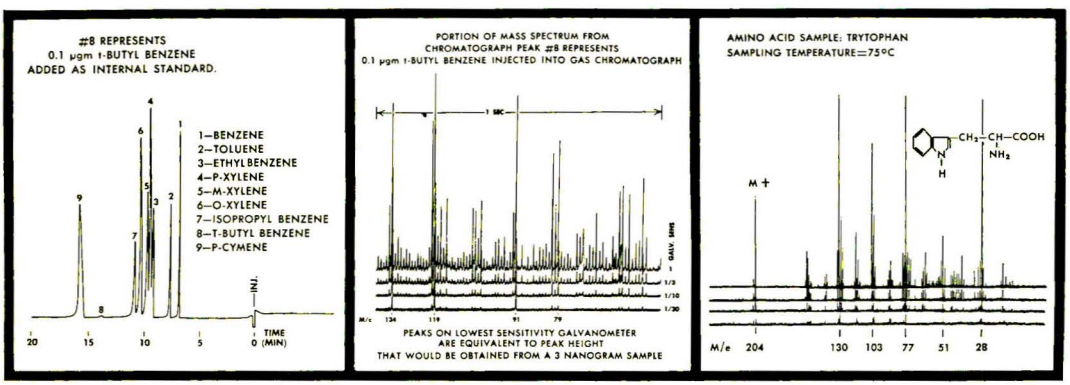
• **Electron Multiplier Detector** is required for highest sensitivity and speed of analysis. It offers a gain of more than 50,000X the Faraday cup detector.

• **Precision Mass Marker** directly indicates the mass number and marks the chart for faster data interpretation.

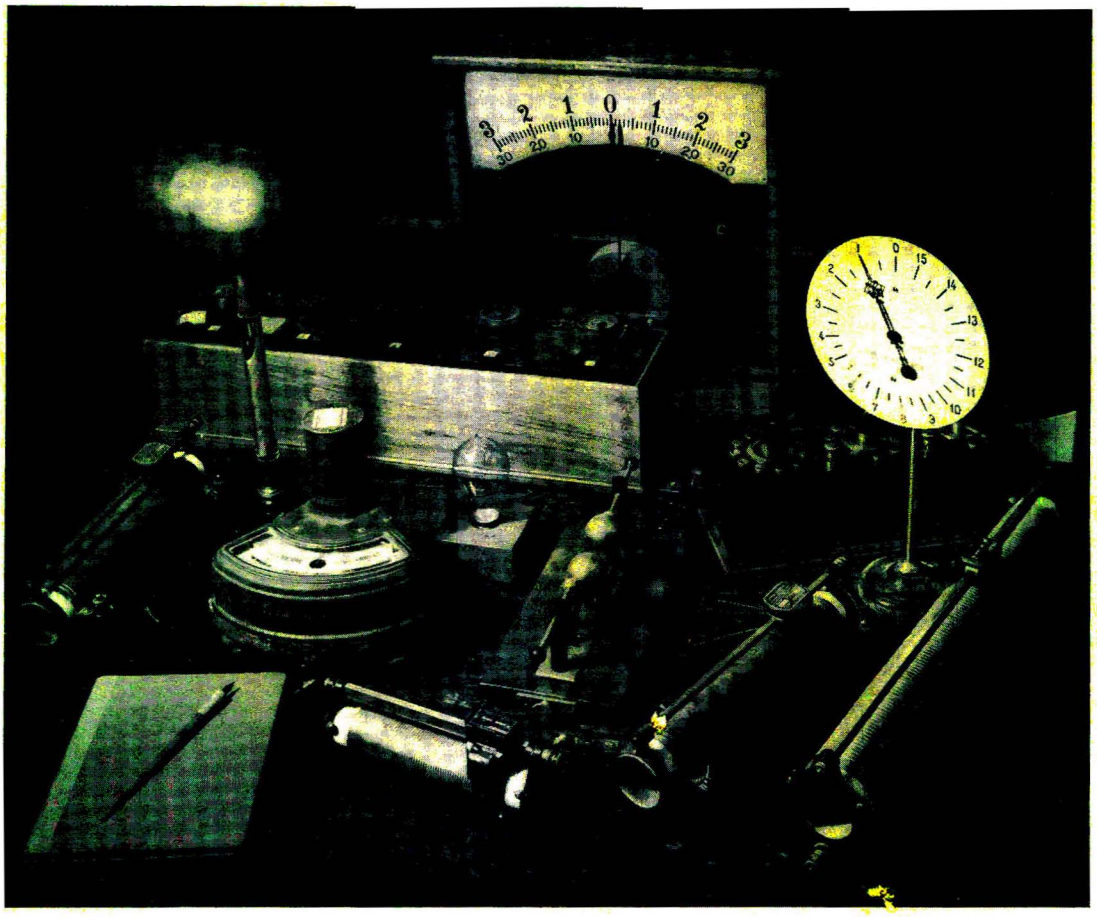
• **Accessories** include Fox-type ion source, Knudsen cell, double collector for isotope ratio work.

The cost of a typical RMU-6E from sample inlet to electron multiplier and high speed recorder is less than $35,000. A high-resolution double-focusing instrument costs less than $60,000. Where diverse requirements exist within a single department, we have been able to install two complete high performance systems within a tight budget originally established for one mass spectrometer. For more information, or to arrange a visit to our Mass Spectrometer Demonstration Laboratory, contact Perkin-Elmer, Distributor Products Department, 702 Main Ave., Norwalk, Conn. 06852.

PERKIN-ELMER

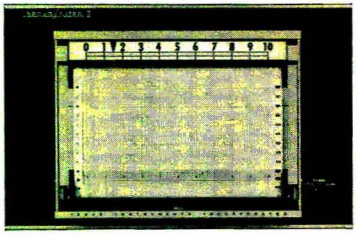


Circle No. 112 on Readers' Service Card



the physics lab has a new potentiometer...

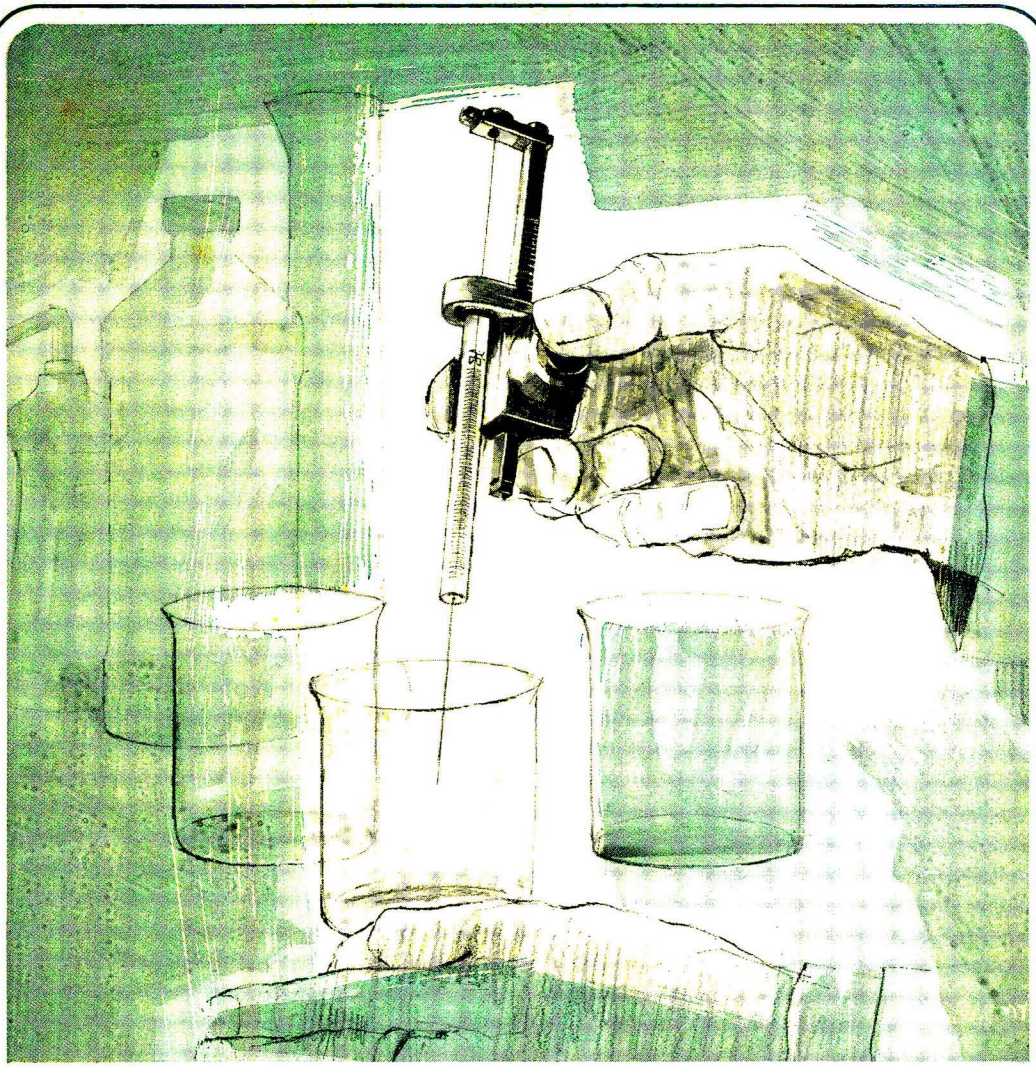
. . . and so does the engineering lab, the gyro test stand, the gas chromatograph and all applications requiring reliable, precise millivolt measurement and recording. That's the reason that more and more *servo/riter® II* recorders are being put into use! Do you require high performance strip chart recorders at a competitive price? The *servo/riter II* recorders have no detectable deadband and have flat frequency response to five cycles (at 10% of full scale). Let us tell you more about them!



TEXAS INSTRUMENTS
INCORPORATED
APPARATUS DIVISION
P. O. BOX 66027 HOUSTON, TEXAS 77006
118 RUE du RHONE GENEVA, SWITZERLAND

776

Circle No. 164 on Readers' Service Card



Uniform quantities at the push of a button

Here is the ideal device for thin layer chromatography, droplet placement, preparation of standard reagents, and uniform injections...Hamilton's PB600. It fits most Hamilton syringes and discharges 1/50th of the capacity at each push of the button. Now you can discharge a series of uniform quantities by simply pushing a button. Try it once and you'll wonder how you ever got along without it. ***Write today for catalog and prices.***

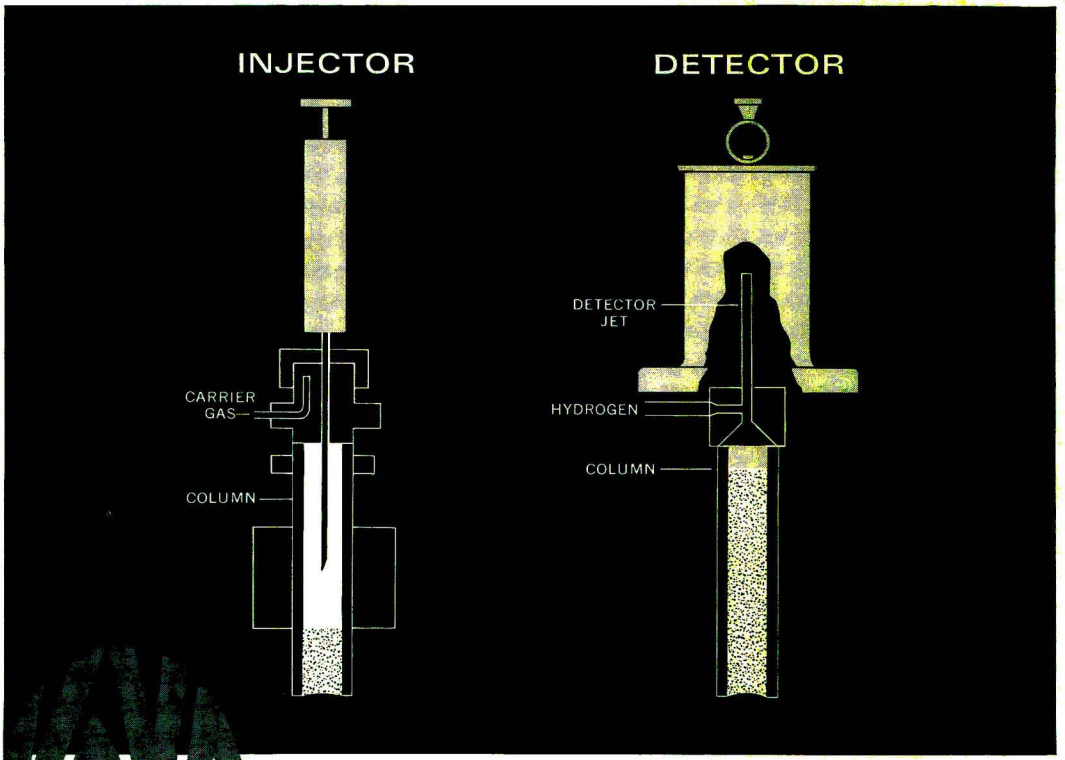
HAMILTON

For a copy of our catalog, simply clip the coupon, attach to company letterhead, and mail.

To: HAMILTON COMPANY · P.O. Box 307-B · Whittier, Calif.
Exclusive European Agent: Micromesure N.V., P.O. Box 205, The Hague

Name_____ Title_____

Circle No. 48 on Readers' Service Card



KEYS TO HIGH-EFFICIENCY GAS CHROMATOGRAPHY

Chromatographing thermally sensitive and polar materials involves serious problems that are only too well known to the chromatographer: component loss, low efficiency, peak tailing. Far from being an immutable phenomenon of the materials themselves, these problems have their origin, to a large extent, in the instrument hardware . . . and these instrumental limits can be completely eliminated through careful attention to the design characteristics of the injection and detector ends of the gc system. The F & M Series 402 High-Efficiency Gas Chromatograph is a case in point.

Injection Port Design. Rather than the standard T-shape injection port, the 402 has a straight-through design which reduces injection volume to a minimum, eliminates dead space, and sweeps the entire volume with high-velocity carrier gas. This unique design prevents thermal downgradients, sample flashback and hold-up. It also accomplishes true on-column injection thus preventing sample contact with metal in the hot injection zone.

Detector Design. Most standard gc's have considerable 'plumbing' in the detector proper and where the column joins the detector, thus creating dead volume and sample contact with metal . . . the two deadliest enemies of high-efficiency gas chromatography of thermally sensitive polar compounds. In the 402 this problem is diminished to its irreducible minimum by attaching the column directly to the detector, and by designing a straight-through flow path for the detectors.

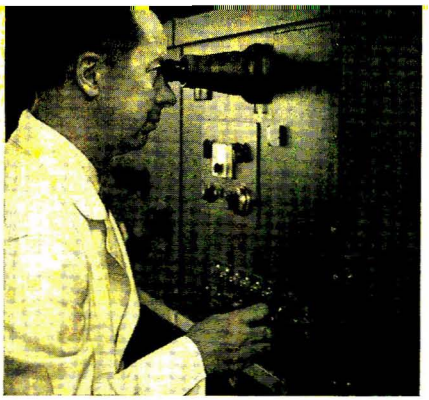
It's these two key design features, above all, that give the 402 its superior performance capability in the analysis of sensitive and polar materials. No matter what kind of difficult-to-chromatograph material you want to analyze, the 402 will respect its chemical integrity and produce a chromatogram that is unsurpassed qualitatively and quantitatively.

For more information, write for Bulletin 4020 or call the Chemical Instrumentation Sales Representative at one of the 41 Hewlett-Packard sales offices in the U.S. Price for the F & M Model 402 with dual flame ionization detector and recorder is $4800.00 (f.o.b. Avondale, Pa.)

Hewlett-Packard, F & M Scientific Division, Route 41 and Starr Road, Avondale, Pennsylvania 19311. In Europe: F & M Scientific Europa N.V., Basisweg (Sloterdijk), Amsterdam, The Netherlands.

HEWLETT PACKARD hp F&M SCIENTIFIC DIVISION

Circle No. 127 on Readers' Service Card

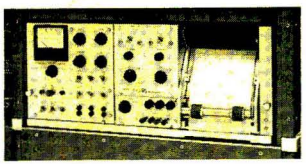


Smaller samples...
stronger forces...
direct scanning...
in the

ANALYTICAL ULTRACENTRIFUGE

As investigations delve ever more deeply into molecular structure and function, the need for and development of advanced accessories for the Model E is inevitable. Several such accessories are briefly described here.

The Photoelectric Scanner

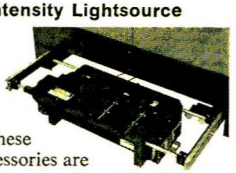


The Scanner looks at the analytical cell through the absorption optical system during centrifugation and, almost instantaneously, translates measures of optical density into chart-recorded curves. Integral and derivative curves are recorded simultaneously, and calibration steps are traced out before each scan. Thus the investigator is freed from the camera, and the developing and handling of film—and has the advantage of seeing what is happening in the cell as it happens.

Since the Scanner utilizes the split-beam photometry principle, double as well as single sector cells can be used with precise results, and the Scanner can also automatically subtract solvent reading in one sector from sample-solvent reading in the other sector to obviate baseline runs. Wavelengths are selectable from 440 mμ to 236 mμ and may be changed during a run.

Several applications of direct scanning were reported last year; in one, an association-dissociation study by Gerhart and Schachman (*Biochemistry 4*, 1054), the authors were able to distinguish the catalytic and regulatory protein subunits of aspartate transcarbamylase. Direct scanning was used to follow the binding of 5-bromocytidine triphosphate to separated subunits of the enzyme and the reconstituted enzyme of the same sample.

The Monochromator and High Intensity Lightsource



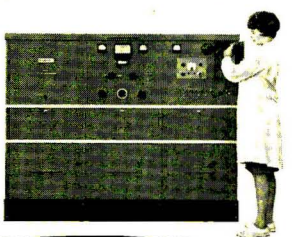
While these two accessories are essential to operation of the Scanner, they can also be utilized independently to add to the versatility of the highly discriminating absorption optical system. The Monochromator provides a selection of wavelengths from 440 mμ to 265 mμ and permits changes in wavelength during a run. It is therefore possible to use lower concentrations, through choice of an appropriate wavelength, and to detect components in the sample whose absorption peaks are at different wavelengths. In itself the Monochromator is primarily for sedimentation equilibrium work. The High Intensity Lightsource provides much more intense monochromatic light to reduce exposure times and facilitate sedimentation velocity studies. It also extends the range of usable wavelengths down to 236 mμ.

The Titanium Rotor



The titanium An-H rotor is identical in configuration to the aluminum An-D, but because of the greater strength-to-weight ratio of the titanium, it can be taken to 68,000 rpm to generate 372,000 *g* at the bottom of the cell, 336,000 *g* at the cell center. Using the stronger forces, Nelson (*J. Biol. Chem. 239*, 3737, 1964) found that multiple peaks too diffused to be recognized with any certainty at previously available speeds became clearly apparent when run at the titanium rotor's maximum speed, and the presence of a third component in the sample could be detected—suggesting another area of usefulness for the rotor.

For additional information on any of these new accessories or on the Model E, itself, please write to Spinco Division of Beckman Instruments, Inc., at the address shown below.



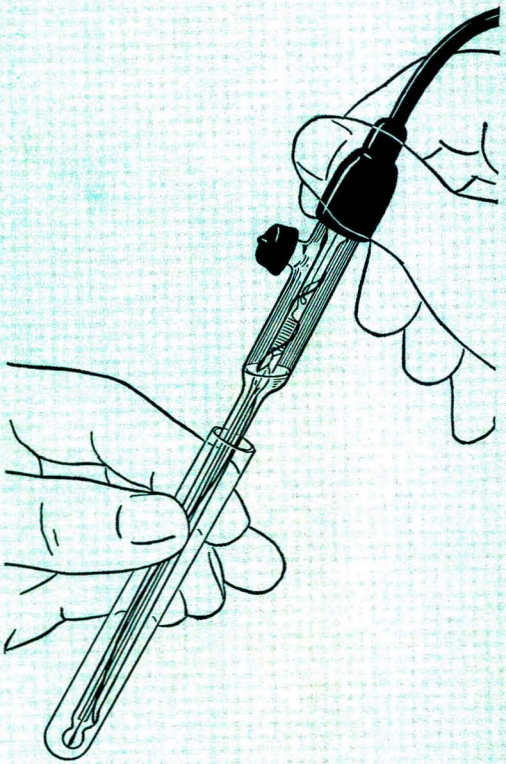
Beckman® INSTRUMENTS, INC.
SPINCO DIVISION
PALO ALTO, CALIFORNIA • 94304

INTERNATIONAL SUBSIDIARIES: GENEVA; MUNICH; GLENROTHES, SCOTLAND; TOKYO; PARIS; CAPETOWN; LONDON

Circle No. 19 on Readers' Service Card

Thomas ***fast response, low resistance . . .***

COMBINATION pH ELECTRODES



- **For samples from 0.2 ml to a tankful**
- **Stem 1/4-inch diameter**
- **Ideal for titrations*— fast response—compact size**

COMBINATION ELECTRODES, Thomas. Consisting of a glass electrode and a silver-silver chloride reference electrode sealed into a single body. Bulb wall thickness and strength provide a sturdier electrode than heretofore available.

The single ¼-inch stem can be used with samples of small volume as well as with larger quantities, and is more convenient for transfer by hand from sample to sample than bringing the sample to electrodes in a fixed position.

The glass electrode inner element is shielded from electrostatic effects and stray electrical fields by the KCl solution of the reference electrode. Port is provided for KCl refill. Liquid junction is made by a sintered oxide plug sealed into the side of the lower stem ⅜-inch above tip.

The stable, fast response of this low resistance glass electrode and the short fixed distance between it and the reference electrode junction make the Thomas Combination Electrode particularly valuable in avoiding endpoint overshooting in electrometric titrations.* The compactness of the design permits use of small vessels and leaves more room for stirrers and buret tips.

Electrodes are each 6 inches long. Upper section is ½-inch diameter for use in standard electrode holders. Stem is ¼-inch diameter over the lower 4-inch length. Can be used with samples as small as 0.2 ml in narrow tubes.

Connector plug of the glass electrode fits into the jacks of most existing pH Meters, either directly or through available adapters.

4858-L15. Combination Electrode, Thomas, as above, 6 inches long, range pH 0 to 11, temperature range 0 to 70°C, with 30-inch shielded lead..... **29.50**

4858-L60. Ditto, range pH 0 to 14..... **38.00**

*See H. V. Malmstadt and E. H. Piepmeier, *Analytical Chemistry, Vol. 37, No. 1 (January, 1965), p. 34*

Detailed descriptive bulletin, consisting of pp 464-468 of our 1965 catalog, sent upon request

Thomas **ARTHUR H. THOMAS COMPANY**

Scientific Apparatus and Reagents

VINE STREET AT 3RD • P. O. BOX 779 • PHILADELPHIA 5, PA., U. S. A.

Circle No. 92 on Readers' Service Card

ANALYTICAL CHEMISTRY

June 1966, Vol. 38, No. 7

Editor: HERBERT A. LAITINEN

EDITORIAL HEADQUARTERS

Washington, D. C. 20036
1155 Sixteenth St., N.W.
Phone: 202-737-3337 Teletype WA 23

Associate Editor: John K. Crum

Assistant Editors: Josephine Pechan, Virginia E. Stewart

Editorial Assistants: Mary Ann Wingard, Martha B. Wood

Contributing Editor: R. H. Müller

Production Staff—Washington:

Art Director: Joseph Jacobs

Art and Layout: Perry Donovan, Herbert Kuttner

Production Staff—Easton, Pa.

Associate Editor: Charlotte C. Sayre

Assistant Editor: Elizabeth R. Rufe

Advisory Board: O. U. Anders, F. C. Anson, C. V. Banks, R. G. Bates, W. J. Blaedel, S. Bruckenstein, H. W. Habgood, G. A. Harlow, D. M. Hercules, F. W. McLafferty, M. W. Mallett, G. H. Morrison, R. E. Thiers, J. C. White, D. H. Wilkins

AMERICAN CHEMICAL SOCIETY PUBLICATIONS

Director of Publications, Richard L. Kenyon

Assistant Director of Publications and Director of Research Journals, Richard H. Belknap

Director of Business Operations, Joseph H. Kuney

Executive Assistant to the Director of Publications, Rodney N. Hader

Assistant to the Director of Publications, William Q. Hull

REGIONAL EDITORIAL BUREAUS

NEW YORK, N. Y. 10017
733 Third Ave.

PHILADELPHIA, Pa. 19107
Philadelphia National Bank Building
Broad & Chestnut Streets

PITTSBURGH, Pa. 15230
530 William Penn Place

CHICAGO, Ill. 60603
36 South Wabash Ave.

CLEVELAND, Ohio 44114
1367 East Sixth St.

SAN FRANCISCO, Calif. 94104
57 Post St.

LOS ANGELES, Calif. 90005
422 South Western Ave.

HOUSTON, Texas 77002
1121 Walker St.

FRANKFURT/MAIN, West Germany
32 Grosse Bockenheimerstrasse

LONDON, W. C. 2, England
27 John Adam St.

TOKYO, Japan
Apt. 306, 47 Dai-machi, Akasaka, Minato-ku

WASHINGTON, D. C. 20036
1155 Sixteenth St., N. W.

Advertising Management

REINHOLD PUBLISHING CORP.
(for Branch Offices, see page 147 A)

For submission of manuscripts, see page 2A.

1966 ACS Analytical Division Summer Fellowships

THE FIRST two awards of summer fellowships by the ACS Division of Analytical Chemistry are announced on page 65A of this issue. The winners, Mr. Allen G. Hiebert and Mr. James R. Birk and their research advisers, Dr. A. M. Hartley of the University of Illinois and Dr. S. P. Perone of Purdue University, receive our warm congratulations.

It is appropriate to point out that support for these fellowships is derived from private and organizational contributions to a special fund administered by the ACS Division of Analytical Chemistry. Divisional members are invited to make contributions at the same time that they renew their divisional memberships. But since the subscription list of ANALYTICAL CHEMISTRY is much larger than the membership roster of the Division, two thoughts are brought to mind. First, any of our subscribers who would like to make a special contribution for this purpose are invited to make their checks payable to the Division of Analytical Chemistry Fellowship Fund and send them to Professor Charles V. Banks, Department of Chemistry, Iowa State University, Ames, Iowa, 50010.

Second, the Division welcomes additional members whether or not they are members of the American Chemical Society. A leaflet describing divisional activities is available from Dr. Frank A. Guthrie, Chairman, Membership Committee, ACS Division of Analytical Chemistry, Rose Polytechnic Institute, 5500 Wabash Ave., Terre Haute, Ind. 47803.

It is to be hoped that substantial numbers of our readers will avail themselves of one or both of these opportunities to support the science of analytical chemistry.



Determination of Calcium-48 in Natural Calcium by Neutron Activation Analysis

JAMES T. CORLESS

Graduate School of Oceanography, University of Rhode Island, Kingston, R. I.

▷An analytical method for determining the ratio of calcium-48 to total calcium in natural materials relative to that of a reference standard employs precision neutron activation analysis and an EDTA weight titration of separated and purified calcium. Data illustrate the applicability of the method to the detection of variations in the relative isotopic abundance of calcium-48.

THE use of neutron activation analysis for the determination of relative isotopic abundances has received comparatively little attention, in the main because of the availability of the high precision techniques of mass spectrometry. It has been suggested that activation analysis may be employed to good advantage for the measurement of isotopic ratios, particularly with elements of low abundance in geologic materials, where it may be undesirable to process a large amount of material (*15*). Measurements of this type have been reported by Reed (*18*), who determined the Hg^{202}/Hg^{196}, Pb^{208}/Pb^{204}, and Ba^{135}/Ba^{131} ratios in meteorites and terrestrial materials; by Rona (*21*), who measured the Th^{232}/Th^{230} ratio; and by Wyttenback *et al.* (*26*), who determined the Br^{81}/Br^{79} ratio in similar materials. A recent series of measurements of the Zn^{68}/Zn^{64} ratio was made by Filby (*10*), who reported attaining a precision within 0.3 to 1%. He has also discussed the requirements of a neutron activation method for measuring an isotope ratio. Aumann and Born (*2*) and Hunt and Miller (*13*) have reported on a technique for the measurement of O^{18} abundances through a recoil proton reaction, for which the latter authors achieved a precision of 3%.

In this investigation a procedure employing neutron activation analysis has been developed which is sufficiently sensitive and precise to be used in the search for variations in the abundances of the stable isotopes of calcium. Calcium possesses six stable isotopes ranging in mass from 40 to 48. This 20% mass difference between the heaviest and lightest isotopes is the largest exhibited by any element, except hydrogen and helium, and suggests the possibility of fractionation during natural processes (*14, 17*). In addition, the isotopes of calcium are of geochronologic interest due to the decay of K^{40} to Ca^{40} (*3, 17*). Several workers have studied the isotopic composition of calcium by solid source mass spectrometry (*1, 3, 7, 9, 16, 25*). The most recent of these spectrometric studies was carried out by Hirt and Epstein (*12*), who reported finding no variations in the Ca^{48}/Ca^{40} ratio in a suite of samples outside their error limits of ±0.8%.

The procedure described in this paper employs two separate measurements for determining the ratio of Ca^{48}/(total calcium)—a precision neutron activation analysis for Ca^{48} and an EDTA weight titration with a spectrophotometrically determined end point for total calcium. These techniques are based on principles outlined in experiments by Corless and Winchester (*6–8*). This first series of analyses, which suggested that measurable variations existed but at times yielded values for variations which were either too large or not reproducible, indicated that consistently reliable measurements could be made if the procedure were revised and a better counting system was secured. Continued developmental studies have led to the procedure described below.

EXPERIMENTAL

Apparatus. The beta decay curves were measured using a specially adapted Baird-Atomic counting assembly which consisted of an end-window gas flow detector, preamplifier, amplifier with live-time gate, sample changer, scaler, electronic timer, power supply, time-of-day clock, data translator, and printer. The sample changer was modified by the addition of a wooden support which placed the detector 6 inches above the planchet.

The EDTA titration was carried out using a standard Beckman DU spectrophotometer with plug-in power supply and was modified by the addition of a second standard DU cell compartment in tandem with the first and of a flexible cloth and tape cover with light-tight holes for the microburet and stirring tube. Titration cells measuring 4.5 × 3.25 × 9.25 cm. were made from $^3/_8$-inch Lucite. A polyethylene weight buret was prepared by inserting the tip of a polyethylene pipet in the cap of a 60-ml. polyethylene bottle. A microburet of 2-ml. capacity graduated in divisions of 0.01 ml. was used for completing the titrations.

The ion exchange columns were fabricated from lengths of $^1/_{16}$-inch glass tubing of 1-inch o.d. to a length of 20 inches with a 2-inch tip of $^3/_{16}$-inch i.d. drawn at one end. They were filled with Dowex 50W-X8, 200 to 400 mesh, resin to a height of 11 inches (2*M* HCl).

Reagents and Solutions. In addition to standard reagent grade chemicals and distilled-demineralized water, some special chemicals were used. Murexide (ammonium purpurate, powder) and piperidine (hexahydropiperidine, purified) were used with 0.005*M* EDTA for the titrations. The indicator solution was prepared by dissolving 15 mg. of murexide in 25 ml. of a 3 to 1 ethanol-water mixture. Highly enriched Ca^{45} radiotracer (Oak Ridge National Laboratory Catalog No. Ca-45-P-3) and high purity iron sponge (Johnson, Matthey Co., Catalog No. JM 847), dissolved in 0.1*M* HNO_3 to a concentration of 0.5 mg. of Fe per ml., were used in the pre-irradiation processing. A europium working solution was prepared daily from a stock solution containing 7.4 mg. of high purity Eu_2O_3 (Lindsay Chemical Co., Catalog No. 1014.92) in 250 ml. of 6*M* HNO_3 by diluting 0.050 ml. of the stock solution to 50 ml. with 0.1*M* HNO_3. $Ca^{48}CO_3$ (95.6% Ca^{48}) was obtained from Oak Ridge National Laboratory.

Procedure. Measure out an amount of sample or reference standard containing approximately 40 mg. of calcium. Dissolve carbonate and phosphate samples in a minimal amount of 2*M* HCl, and take silicates into solution with HF and $HClO_4$. Filter, if necessary. If iron or aluminum is present, dilute to 250 ml. with H_2O, adjust the pH to 8 with NH_4OH, filter off the hydroxides, take the filtrate to dryness, and take up the residue in a few milliliters of 2*M* HCl. Add approximately 5 μc. of Ca^{45}, and mount the sample on the column. Elute with 2*M* HCl, following the calcium by previous column calibration and by beta counting of individual drops. Collect the calcium fraction, generously cut to include all of the Ca^{45} radioactivity, take to dryness, and take up the residue in 5 ml. of 2*M* HCl. Repeat the column separation twice, and take the calcium fraction to

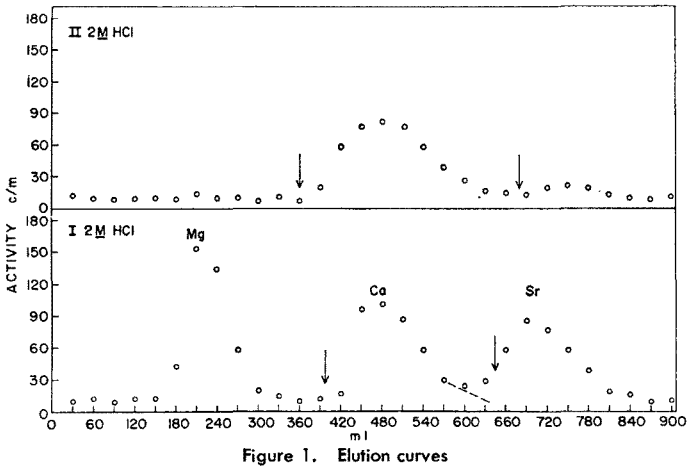


Figure 1. Elution curves

Sample, which initially contained 70 mg. Mg, 40 mg. Ca, and 5 mg. Sr, on first (I) and second (II) passes through column of Dowex 50W-X8, 200-400 mesh

dryness. Take up the residue in 5 ml. of concentrated HNO_3, evaporate to dryness, and repeat the HNO_3 evaporation 5 times. After the final evaporation, take up the residue in 10 ml. of H_2O, add 1 ml. of the high purity $Fe(NO_3)_3$ solution, and slowly bubble NH_3 gas through the solution until the $Fe(OH)_3$ precipitates. Filter, take the filtrate to dryness, and take up the residue in 30 ml. of 0.1*M* HNO_3. Divide into four portions—three of approximately 2 grams each and one of approximately 24 grams—where the portions are weighed to the nearest 0.1 mg.

Titrate the three 2-gram aliquots. Add a few milliliters of H_2O to the cell, and adjust the pH to approximately 11.6 with piperidine. Add 1 ml. of the indicator, and quantitatively transfer the sample to the cell. Weigh the polyethylene buret, titrate to a visual end point, and reweigh the buret. Transfer the cell to the spectrophotometer, and finish the titration, using the microburet.

Spike (weighing to the nearest 0.1 mg.) the large portion with 2 ml. of the europium working solution. Evaporate the solution to a volume of approximately 0.5 ml. under an infrared lamp, package in a sealed polyethylene tube, and irradiate for 2 hours. After a 2-hour wait, open the tube, and transfer the solution to a test tube. Rinse the tube and the pipet with two 0.5-ml. portions of 0.1*M* HNO_3, and add the rinses to the sample solution. Adjust the volume to 4 ml. with H_2O, and add 1 ml. of a $Fe(NO_3)_3$ carrier solution containing 0.5 mg. of Fe per ml. Precipitate the $Fe(OH)_3$ by the dropwise addition of 2*M* NH_4OH (avoid an excess). Swirl and warm gently. Filter under suction through a fine grade sintered-glass filter, and wash the precipitate with three 2-ml. portions of 0.0005*M* NH_4OH. Dissolve the precipitate with two 2-ml. portions of 4*M* HNO_3. Transfer to a small beaker, and evaporate to a volume of 1 ml. Using a dropper, transfer the sample to a planchet, and evaporate to thorough dryness. Count for 48 hours.

DISCUSSION

Procedure. Throughout the entire procedure natural samples and reference standards are treated in precisely the same manner; both are put through the same series of separation and purification steps as a check against the eventuality of isotopic fractionation caused by the chemical processing.

The Ca^{45} tracer permits the monitoring of the calcium as it is eluted from the cation exchange column; and to ensure complete recovery of the calcium from the column, the 10 ml. of the eluent just preceding the activity and the 10 ml. just following the activity are also collected as a part of the calcium fraction. Complete recovery in this step is deemed essential, in order to negate any possibility of isotopic fractionation introduced by the ion exchanger. This step separates calcium from the other alkaline earths as well as from most other elements (*22*). Since the calcium-strontium separation is not ideal [K_d = 12.2 for Ca^{+2} *vs.* 17.8 for Sr^{+2} and 6.2 for Mg^{+2} (*22*)] and since many samples will contain a considerable excess of magnesium over calcium, this column step is repeated in order to achieve a complete separation. Standards are put through twice and natural samples a minimum of three times. The elution curves shown in Figure 1 were constructed by monitoring the tracers Mn^{54} [K_d = 6.0 for Mn^{+2} (*22*)], Ca^{45}, and Sr^{85}. In Figure 1 the dashed line indicates the trend of the tail of the calcium fraction and the arrows indicate the collecting limits. Three passes through the column have been found adequate for samples with a Ca/Sr mole ratio of 20 to 1.

The titration for total calcium utilizing murexide and a spectrophotometrically determined end point was carried out as described by Carpenter (*5*). Usually three aliquots of each sample are titrated. The replicate titrations customarily agree to within ±0.05% or better.

The irradiations were performed in the pneumatic tube facility of the M.I.T. reactor, where the neutron flux was approximately 8×10^{12} n/sq. cm. sec., and a cadmium ratio using europium as the monitor was 75. The samples were packaged in 5-cm. lengths of $^3/_{16}$-inch polyethylene tubing and three of these tubes packed tightly in a polyethylene capsule.

The postirradiation chemistry is carried out 2 hours after the end of the irradiation, sufficient time for essentially all of the 8.8-minute Ca^{49} to decay to Sc^{49}. The pertinent nuclear reactions are:

$$Ca^{48} \xrightarrow[\sigma = 1.1\ \text{lb.}]{(n,\gamma)} Ca^{49} \xrightarrow{8.8\ \text{min.}} Sc^{49} \xrightarrow[E\beta_{max} = 2.0\ \text{Mev.}]{57.5\ \text{min.}} Ti^{49}$$

$$Eu^{151} \xrightarrow[\sigma = 1700\text{b}]{(n,\gamma)} Eu^{152}m_1 \xrightarrow[E_{\beta max} = 1.9\ \text{Mev.}]{9.29\text{h}} Gd^{152}$$

The 9.29-hour half life of $Eu^{152}m_1$, the internal standard, is short enough to establish the half life in each experiment accurately but long enough to be resolved easily and accurately from 57.5-minute Sc^{49}. Because of the small cross section the recently reported 96-minute isomer, $Eu^{152}m_2$ (*23*), does not present a problem. A number of recent measurements have shown, however, that the choice of europium as the internal standard may be less than ideal, because of the large number of neutron capture resonances of Eu^{151} just above the thermal range. Although the 19-hour half life of Pr^{142} is approximately a factor of 2 longer than is required of the internal standard, the neutron capture and precipitation characteristics would appear to make praseodymium a good substitute for europium in future studies.

The postirradiation hydroxide precipitation removes Na^{24}, Cl^{38}, Br^{80}, and Br^{82}, which are always present subsequent to irradiation, the Ca^{45} tracer, and the small amounts of Ca^{41}, Ca^{45}, and Ca^{47} which are produced by neutron capture on other isotopes of calcium. The precise maintenance of the Sc/Eu ratio during this precipitation is essential and can be a problem. In some early experiments scandium and eu-

Table I. Half-Life Determinations of Sc^{49} and $Eu^{152}m_1$

Nuclide	Previous determinations	This study
Sc^{49}	57.5 ± 0.1 minutes (*19*)	57.5 ± 0.1 minutes
$Eu^{152}m_1$	9.3 ± 0.2 hours (*4*) 9.2 hours (*11*)	9.29 ± 0.02 hours

ropium carriers were used to scavenge the Sc^{49} and Eu^{152}, but this combination of $Sc(OH)_3$ and $Eu(OH)_3$ was found to be less reliable than $Fe(OH)_3$ for quantitatively precipitating the two radionuclides. This may be related to the amphoteric properties of $Sc(OH)_3$ (*24*).

A counting standard of long-lived Eu^{152} + Eu^{154} and the three irradiated samples are repeatedly counted in sequence over a 48-hour period. This usually amounts to counting each sample about 150 times. An initial activity of approximately 250,000 counts per minute has been found convenient. Sensitivity changes in the counting system of about 1% over the 48-hour period are compensated for by normalizing the counting rates of the samples to that of the counting standard. To prevent the counting of any Ca^{45} which might be carried through the postirradiation chemistry, an aluminum absorber of 85 mg. per sq. cm. is mounted over the face of the detector.

The counting data and required constants are punched onto cards and combined with the FRANTIC program for the resolution and statistical analysis of exponential growth and decay curves (*20*). Three pieces of information required by the program for the resolution of the decay curves are accurate values for the half lives of Sc^{49} and $Eu^{152}m_1$ and for the "dead time" of the counting system. Half-life determinations were performed for these two nuclides, and the values obtained, together with values previously reported in the literature, are presented in Table I. Repeated measurements of the dead

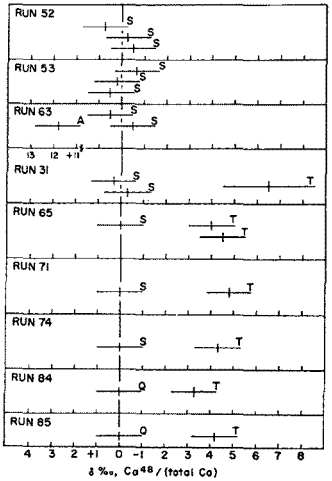


Figure 2. Determinations of Ca^{48}/(total Ca) ratio

time of the system over the range 20,000 to 300,000 counts per minute yielded a value of 2.0 ± 0.4 microseconds.

The principal source of uncertainty in this procedure has been found to be in the counting statistics and in the resolution of the two-component decay curve. With an initial activity of about 250,000 counts per minute and an initial $Sc^{49}/Eu^{152}m_1$ decay ratio of 5/1, this comes out to be of the order of ±0.1%. As stated above, the uncertainty introduced by the total calcium determination is ±0.05%. The actual data from run 65 are presented in Table II, where A_{Sc} and A_{Eu} are the activities of Sc^{49} and $Eu^{152}m_1$ at $t = 0$, W_{Eu} is the weight of the Eu spike, W_{EDTA} is the weight of the titrant, W_t is the weight of the aliquot titrated, and W_I is the weight of the irradiated aliquot. The values for the Ca^{48}/(total Ca) ratio in the last column of Table II are not absolute values of the ratio but relative experimental numbers.

Results. The results of several determinations are presented graphically in Figure 2. The reference standard (a bottle of $CaCO_3$, Mallinckrodt primary standard, lot 7715-X-H) is designated by the letter S. Runs 52 and 53 each consisted of three samples of the standard. Run 63 consisted of two normal samples of the standard and a third sample (*A*) of the standard to which an approximately 1% addition of Ca^{48} had been made. Runs 31, 65, 71, and 74 were analyses of a composite of ten whole human teeth (*T*) relative to the reference standard. Runs 84 and 85 included samples of the tooth composite and of the shell of the local hard-shell clam, *Mercenaria mercenaria* (*Q*). In Figure 2 the Ca^{48}/(total Ca) ratios are plotted in terms of the quantity δ, where

$$\delta(‰) = \left[\frac{Ca^{48}/(\text{total Ca})\ \text{sample}}{Ca^{48}/(\text{total Ca})\ \text{standard}} - 1\right] \times 10^3$$

The δ values for the human teeth analyses are summarized in Table III.

Table III. Tabulation of Tooth Analyses

Run No.	δ, ‰
31	−6.5 ± 2.3
65	−4.0 ± 1.5 −4.5 ± 1.5
71	−4.8 ± 1.5
74	−4.3 ± 1.5

Discussion of Results. Both the agreement among replicate samples and sensitivity achieved appear satisfactory for an isotopic method. The larger uncertainty in the tooth analysis in run 31 is due to irradiating too little sample. This depletion of Ca^{48} in the teeth relative to the standard and the clam shell has appeared consistently in our analyses and is considered to be real. These analyses suggest that further studies into the isotope geochemistry of calcium should prove fruitful.

ACKNOWLEDGMENT

The technical assistance of L. Donald Roy and Nancy Butler and the cooperation of the personnel of the Computation Center and the nuclear reactor facility of the Massachusetts Institute of Technology are gratefully acknowledged.

Table II. Data from Run 65

Sample	$A_{Sc}/A_{Eu} \times W_{Eu}$(g.) = Ca^{48}			$\frac{W_{EDTA}}{W_t} \times W_I$(g.) = total Ca			$\frac{Ca^{48}}{\text{total Ca}} \times 10^5$
S	4.042 ± 0.004	1.9048	7.699	5.331 ± 0.003	23.756	126.64	6079 ± 7
T1	3.998 ± 0.004	1.9303	7.717	6.275 ± 0.003	20.310	127.45	6055 ± 7
T2	3.986 ± 0.004	1.9035	7.587	5.450 ± 0.002	23.003	125.37	6052 ± 7

LITERATURE CITED

(1) Aston, F. W., *Nature* **57**, 684 (1934).
(2) Aumann, D. C., Born, H. J., *Naturwissenschaften* **51**, 159 (1964).
(3) Backus, M. M., Pinson, W. H., Herzog, L. F., Hurley, P. M., *Geochim. Cosmochim. Acta* **28**, 735 (1964).
(4) Bothe, W., *Z. Naturforsch.* **1**, 179 (1946).
(5) Carpenter, J. H., *Limnol. Oceanog.* **2**, 271 (1957).
(6) Corless, J. T., Ph.D. dissertation, Massachusetts Institute of Technology, 1963.
(7) Corless, J. T., Rahn, K. A., Winchester, J. W., *Trans. Am. Geophys. Union* **44**, 69 (1963).
(8) Corless, J. T., Winchester, J. W., Proceedings of Symposium on Isotopic Mass Effects in Chemistry and Biology, I.A.E.A., Vienna, 1963; *Pure Appl. Chem.* **8**, 317 (1964).
(9) Dempster, A. J., *Phys. Rev.* **20**, 631 (1922).
(10) Filby, R. H., ANAL. CHEM. **36**, 1597 (1964).
(11) Hayden, R. J., Reynolds, J. H., Ingram, M. G., *Phys. Rev.* **75**, 1500 (1949).
(12) Hirt, B., Epstein, S., *Trans. Am. Geophys. Union* **45**, 113 (1964).
(13) Hunt, L. H., Miller, W. W., ANAL. CHEM. **37**, 1269 (1965).
(14) Ingerson, E., *Bull. Geol. Soc. Am.* **64**, 301 (1953).
(15) Merz, E., Herr, W., *Proc. 2nd Intern. Conf. Peaceful Uses Atomic Energy, Geneva* **28**, 491 (1958).
(16) Nier, A. O., *Phys. Rev.* **53**, 282 (1938).
(17) Rankama, K., "Progress in Isotope Geology," Interscience, New York, 1963.
(18) Reed, G. W., Proceedings of Symposium on Radioactivation Analysis, I.A.E.A., Vienna, 1959, Butterworths, London, 1960.
(19) Rezanka, I., Frana, J., Vobecky, M., Mastalka, A., *J. Inorg. Nucl. Chem.* **18**, 13 (March 1961).
(20) Rogers, P. C., Laboratory for Nuclear Science, M.I.T., Tech. Rept. **76** (1962).
(21) Rona, E., *Trans. Am. Geophys. Union* **38**, 754 (1957).
(22) Strelow, F. W. E., ANAL. CHEM. **32**, 1185 (1960).
(23) Takahashi, K., McKeown, M., Scharff - Goldhaber, G., *Phys. Rev.* **137**, B763 (1965).
(24) Vickery, R. C., *J. Chem. Soc.* **1955**, 251.
(25) White, J. R., Cameron, A. E., *Phys. Rev.* **74**, 991 (1946).
(26) Wyttenback, A., von Gunten, H. R., Scherle, W., *Geochim. Cosmochim. Acta* **29**, 467 (1965).

RECEIVED for review March 5, 1964. Resubmitted January 4, 1966. Accepted March 17, 1966. Presented in part before the Division of Nuclear Chemistry and Technology, 150th Meeting, ACS, Atlantic City, N. J., September 1965. Investigation supported by the U. S. Atomic Energy Commission under Contract AT(30-1)3369 and the Office of Naval Research under Contract 396(08).

Application of Lithium-Drifted Germanium Gamma-Ray Detectors to Neutron Activation Analysis

Nondestructive Analysis of a Sulfide Ore

J. F. LAMB, S. G. PRUSSIN, J. A. HARRIS, and J. M. HOLLANDER

Lawrence Radiation Laboratory, University of California, Berkeley, Calif.

▶ **Lithium-drifted germanium gamma-ray spectrometers have been used for the nondestructive analysis of a sulfide ore by neutron activation. The concentrations of ten elements have been determined in the range 1.8 × 10^5 p.p.m. (iron) to 2.0 p.p.m. (gold). The analytical sensitivity obtained with available Ge(Li) detectors was compared with sodium iodide scintillators for the estimation of manganese in the ore. The various detector properties which effect sensitivities are discussed.**

THE APPLICATION OF HIGH-RESOLUTION, lithium-drifted germanium gamma-ray detectors to nondestructive neutron activation analysis has been reported by Prussin, Harris, and Hollander (*13*) for the study of trace impurities in aluminum and by Girardi, Guzzi, and Pauly (*2*) for the determination of minor amounts of hafnium in zirconium oxide. These studies illustrated the benefits to be gained from high resolution gamma-ray spectra in the special case of noninterfering bulk material. In many practical analyses, however, minor and trace constituent concentrations are desired for samples in which the activation of major constituents may contribute a high gamma-ray background. In such cases the sensitivity of analysis for a given component may be severely limited by the complexity of the gamma-ray spectra as well as by the masking effect of the radiations from the activated bulk material. The masking effect is of particular concern in the application of available lithium-drifted germanium detectors since the ratio of Compton to photopeak efficiencies for these detectors is considerably larger than the corresponding ratio for the commonly used 3- × 3-inch (diameter) sodium iodide detectors.

In this paper we report the results of the application of lithium-drifted germanium detectors to the nondestructive analysis of minor and trace constituents in a sample of a sulfide ore in which the major constituents iron, zinc, and copper have substantial neutron activation cross sections and yield (n,γ) products with reasonably long half-lives. Results are given for analysis of a number of elements in the ore in the concentration range 1.7 × 10^5 p.p.m. (iron) to 2 p.p.m. (gold). Sensitivities for analysis of manganese in the ore were estimated from gamma-ray spectra obtained with two Ge(Li) detectors of different active volumes and with a very good 3- × 3-inch (diameter) sodium iodide scintillator. This comparison suggests that sensitivities obtained with gamma-ray spectra from available germanium detectors are comparable to sensitivities obtained using spectra from sodium iodide detectors.

EXPERIMENTAL

Spectrometers. The construction and general characteristics of the lithium-drifted germanium detectors and detector assemblies are described in References *1*, *3*, *4*, *6*, and *11*. The two Ge(Li) detectors used in this study had dimensions of about 2 sq. cm. × 7 mm. (active thickness) and 6 sq. cm. × 10 mm. (active thickness). The resolutions of these detectors for the 122-k.e.v. gamma ray of Co^{57} were approximately 2 k.e.v. (FWHM) and 4 k.e.v. (FWHM), respectively. The associated electronics consisted of a low-noise, low-capacity preamplifier and a linear-amplifier, biased amplifier system designed by Goulding and Landis (*5*) and constructed at this laboratory. The 3- × 3-inch (diameter) sodium iodide (thallium) detector system was a Harshaw integrally-mounted unit which exhibited a resolution (FWHM) at 662 k.e.v. of slightly less than 46 k.e.v. (7%). Pulses from the various detector systems were routed to a Victoreen, SCIPP 1600-channel pulse-height analyzer for sorting.

Sample Preparation. The bulk sulfide ore was ground to a fine powder and mixed to ensure homogeneity of sampling in the range of 50–100 mg. Weighed samples were then sealed in polyethylene film or quartz tubing for irradiation. Quantitative analyses were performed by comparison of photopeak intensities of activities induced in the ore to those induced in appropriate standards. To minimize neutron flux variations between samples and

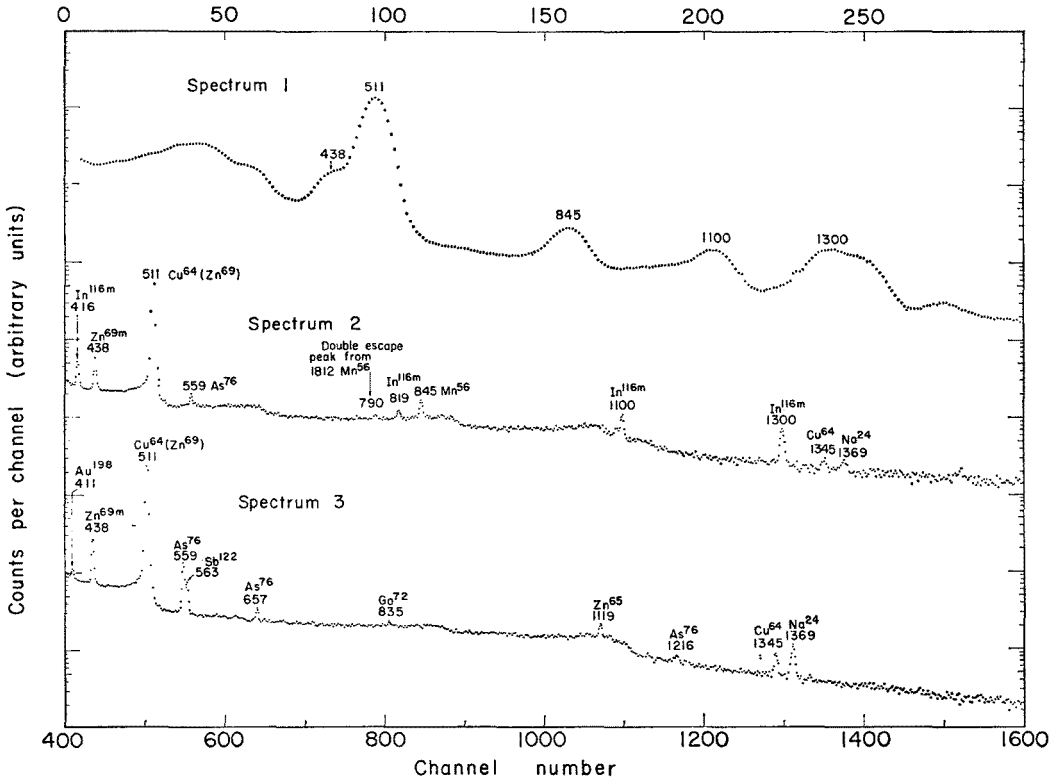


Figure 1. Gamma-ray spectra of activated sulfide ore

Spectrum 1 represents 60 minute data accumulation using the 3- × 3-inch (diameter) sodium iodide scintillator 5.2 hours after a 2-hour irradiation of 62.9 mg. of sulfide ore. Spectrum 2 represents 60 minute data accumulation using the smaller Ge(Li) detector 4 hours after a 2-hour irradiation of 62.9 mg. of the ore. Spectrum 3 represents 120 minute data accumulation using the smaller Ge(Li) detector 24 hours after a 49-hour irradiation of 50 mg. of the ore

standards, the latter were prepared by evaporating aliquots of stock solutions onto thin polyethylene films and heat-sealing a polyethylene cover film over the deposit. The volume occupied by the standards was thereby minimized, permitting the positioning of standards close to the samples within the irradiation capsules.

Irradiations. Neutron irradiations were carried out at the Livermore LPTR nuclear reactor. The thermal neutron flux at the irradiation position was approximately 5×10^{12} n./sq. cm.-second, and the neutron spectrum exhibited a cadmium ratio of approximately 11. Irradiation periods ranged from 2 hours to 72 hours, and samples were available for counting within 2 to 4 hours after the end of irradiation.

RESULTS AND DISCUSSION

Analytical. The qualitative identification of the radioisotopes induced in irradiated ore samples was made through determination of photopeak energies and half-lives and by comparison of experimental gamma-ray relative intensities to literature values for isotopes yielding more than one photon in their decay.

A sample of sulfide ore of approximately 150 mg. was irradiated for 2 hours in the LPTR facility to provide gamma-ray spectra of the shorter-lived activities induced in the sample. The spectra were obtained with the smaller Ge(Li) detector [2 sq. cm. × 7 mm. (active thickness)] using an energy interval of approximately 1 k.e.v. per channel. Data were accumulated for 60 minutes (live time) at two-hour intervals over a period of twelve hours. The first spectrum, taken 4.5 hours after the end of the irradiation, is shown in Figure 1 (Spectrum 2). For comparison we have included a spectrum of the ore obtained with the sodium iodide scintillator (Spectrum 1). Photopeak energies and half-lives were estimated from the Ge(Li) spectra, and isotope assignments were made by comparing these data to literature values (*7, 8, 12*). Assignments were confirmed, where possible, with relative intensity measurements. These data indicated the presence of In^{116m}, Mn^{56}, Zn^{69m} Sb^{122}, and Na^{24} in the activated sample. In Table I are listed the experimental measurements together with the literature values of each quantity. It is interesting to note that much of the relative intensity data obtained from NaI(Tl) gamma-ray spectra may be subject to greater experimental uncertainties than those obtained through the germanium spectra. The Ge(Li) intensity data are estimated to have uncertainties of 5–10% for the more intense lines in the spectra. This was checked by using the relative intensities of photopeaks in a spectrum from an irradiated indium standard. These values are shown in Table I in parentheses beside the literature values.

Enhancement of radioisotopes of longer half-lives was obtained through a 49-hour irradiation of 50 mg. of the sulfide ore. After a decay period of 24 hours, spectra were obtained over a two-

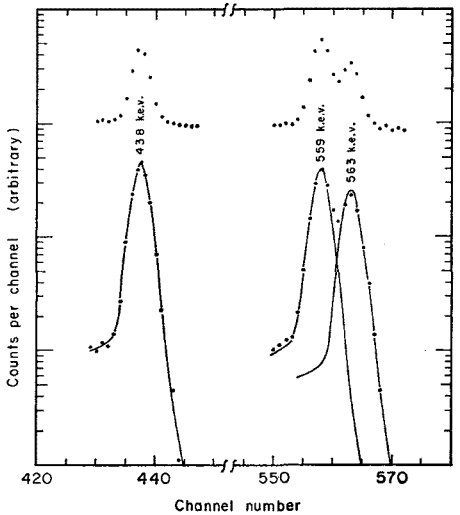


Figure 2. Peak-shape fit for the 559-k.e.v. gamma-ray line of As^{76} and 563-k.e.v. gamma-ray line of Sb^{122} in the activated sulfide ore

The spectra were obtained with the smaller Ge(Li) detector. The energy interval is approximately 1 k.e.v. per channel. The upper spectra represent the total counts in the regions of the photopeaks and the lower spectra represent the counts in the photopeak ($N_t - N_b$)

day period at intervals of four hours. A typical spectrum representing data accumulation for 120 minutes (live time) is shown as Spectrum 3 of Figure 1. These spectra indicated the presence of Au^{198}, Ga^{72}, Fe^{59}, and Zn^{65} in the activated ore in addition to those isotopes listed above. Pertinent data for assignments to these isotopes have been included in Table I.

Quantitative estimation of the elements in the ore giving rise to these activities was obtained through subsequent irradiations of similar samples. These data are given in Table II.

The simplicity of both qualitative and quantitative analysis afforded by the use of Ge(Li) detectors is well demonstrated by considering the neighboring 559-k.e.v. gamma-ray line of As^{76} and the 563-k.e.v. line of Sb^{122}. It is obvious from Figure 1 that accurate resolution of these photopeaks in the sodium iodide spectrum would be difficult, if not impossible, because of the large 511-k.e.v. annihilation photopeak from the β^+ decay of Cu^{64}. The difficulty is intensified by the necessity of interpolating the complex background beneath these photopeaks over an energy range of approximately 200 k.e.v. (40 channels). Figure 2 shows this energy region of a Ge(Li) spectrum obtained with the smaller detector. The spectrum from which Figure 2 was prepared represents a 500-minute count of 19 mg. of the ore, taken 36 hours after a 72-hour irradiation. Peak-shape resolution of the two lines was accomplished for each spectrum, in a decay sequence as shown in Figure 2, by using the single 438-k.e.v. gamma-ray line of Zn^{69m} in the same spectrum as the standard peak shape (line widths increase by less than 0.5 k.e.v. over this energy range). The analytical data shown in Table II for arsenic and antimony were obtained by this method.

Sensitivity. The value of the germanium detector for nondestructive activation analysis rests in large part upon the analytical sensitivity obtained with its use. In order to provide a basis for judging relative merit, we have made measurements on the same samples of the ore with Ge(Li) detector systems and with the commonly used 3- × 3-inch (diameter) sodium iodide scintillator. The major characteristics of the systems which must be considered in such a com-

Table I. Isotope Assignments for Activities Induced in Sulfide Ore

	Experimental			Literature[a]		
Isotope	$T_{1/2}$	E_γ (k.e.v.)	Rel. inten.	$T_{1/2}$	E_γ (k.e.v.)	Rel. inten.
In^{116m}	54 m	137	14.2	54 m	135	12 (14.8)
		416	100[b]		406	100 (100)
		819	39.1		820	... (43.2)
		1100	233		1085	216 (221)
		1300	320		1270	300 (318)
Mn^{56}	2.7 h	845		2.6 h	845	
Cu^{64}	12.5 h	1345		12.8 h	1340	
		511 (annihilation)				
Zn^{69m}	14 h	438		13.8 h	439	
Zn^{65}	...	1119		245 d	1119	
Ga^{72}	14.4 h	835		14.3 h	835	
Na^{24}	15.5 h	1369		15 h	1368	
As^{76}	26 h	559	100[b]	26.3 h	559	100
		657	14.6		657	14.6
		1216	...		1216	9.7
Sb^{122}	~60 h	563		67.2 h	566	
		686			686	
Au^{198}	~60 h	411		64.8 h	412	
Fe^{59}	...	1095		45 d	1100	
		1292			1290	

[a] Nuclear Data Sheets (*12*).
[b] Relative intensities normalized to this value.

Table II. Results of Quantitative Analysis of Sulfide Ore

Element	μg. found	Sample weight, mg.	Irradiation time, hours	Eγ, k.e.v.	p.p.m.[a]
Mn	6.0	62.9	2	845(Mn^{56})	95 ± 7
In	7.6	62.9	2	1300(In^{116m})	120 ± 5
Ga	3.8	62.0	2	835(Ga^{72})	61 ± 16
Zn	3020	24.5	24	438(Zn^{69m})	(1.20 ± 0.01) × 10^5
As	60	19.0	72	559(As^{76})	(3.16 × 0.04) × 10^3
Sb	8.2	19.0	72	563(Sb^{122})	430 ± 6
Cu	1240	19.0	72	511(Cu^{64})[b]	(6.50 ± 0.01) × 10^4
Na	16	19.0	72	1369(Na^{23})	840 ± 25
Fe	3370	19.0	72	1095(Fe^{59})	(1.78 ± 0.01) × 10^5
Au	0.038	19.0	72	411(Au^{198})	2.0 ± 0.2

[a] Errors shown represent statistical counting error only.
[b] Copper concentration corrected for contribution to 511-k.e.v. annihilation photopeak from decay of Zn^{69} and Na^{24}.

parison are the overall efficiencies, relative photopeak to Compton efficiencies, and the resolutions of the detectors. It is obvious that the vastly improved resolution of the germanium systems will improve sensitivities in complex spectra when the major limitation of importance is the ability to resolve cleanly two or more gamma-ray lines which lie close in energy. Clean resolution of such lines will also improve the accuracy of analysis in cases where the spectrum exhibits gamma-rays of similar energies and half-lives. In order to assess the effects of resolution and efficiencies upon sensitivity in the general case, it is necessary to examine the error in the estimation of a photopeak which is superimposed upon a large background from higher-energy gamma rays in the spectrum. For the present purposes we consider only the statistical counting error in such a determination (*9*).

The standard deviation in the measurement of the number of counts, N_p, in a photopeak may be approximated by

$$\sigma_p = \sqrt{\sigma_t^2 + \sigma_b^2} = \sqrt{N_p + 2N_b} \quad (1)$$

where the subscripts t and b refer to total and background counts in the region of the photopeak, and $N_p = N_t - N_b$. If it is required that the photopeak intensity be known within some specific error limit, then

$$\sigma_p = KN_p \quad (2)$$

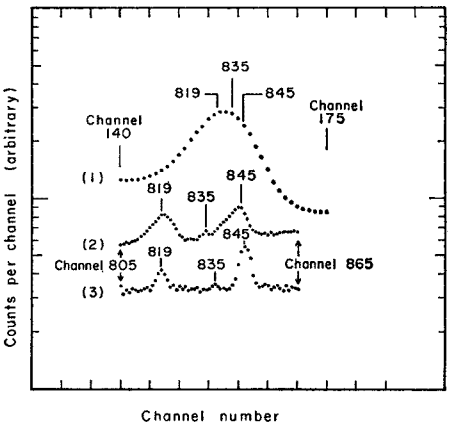


Figure 3. Energy region of the 845-k.e.v. photopeak of Mn^{56}

Spectrum 1 was obtained with the sodium iodide scintillator Spectra 2 and 3 were obtained with the larger and smaller Ge(Li) detectors, respectively. Data were accumulated over 60-minute counting intervals

The number of counts in the photopeak necessary to give rise to this limit of error for a given background, N_b, is

$$N_p = \frac{1}{2K^2}\left[1 + \sqrt{1 + 8K^2N_b}\right] \quad (3)$$

It is seen from Equation 1 that N_b will introduce a major contribution to the error in N_p when the intensity of Compton distributions from higher-energy lines is comparable to the photopeak intensity. The error in the estimation of a photopeak will be reduced by factors which tend to increase the ratio N_p to N_b and which tend to increase the total number of counts accumulated.

There are several response characteristics of Ge(Li) and NaI(Tl) detectors that will affect the errors discussed above. The higher resolution of the Ge(Li) detectors tends to increase the ratio of N_p to N_b since the background under a photopeak is summed over a smaller energy interval than required in sodium iodide spectra. However, the higher ratio of photopeak to Compton efficiencies characteristic of NaI(Tl) scintillators will tend to produce a more intense photopeak and thereby increase the ratio of N_p to N_b relative to germanium. The ratios of the photopeak efficiencies and linewidths of NaI(Tl) relative to Ge(Li) both increase with increasing gamma-ray energies, and these effects will tend to compensate for one another. As a result, the major difference in detector characteristics of importance is in total detection efficiencies. The high efficiency of a 3- × 3-inch (diameter) sodium iodide scintillator will result in greater total counts than that obtained with the small germanium detectors for given experimental conditions.

The above considerations are illustrated by the estimation of the sensitivity for the determination of manganese in the sulfide ore using the two Ge(Li) detectors and the 3- × 3-inch (diameter) sodium iodide detector. Gamma-ray spectra obtained with each

Table III. Data for Comparison of Sensitivities between Ge(Li) Detectors and 3- × 3-Inch (Diameter) NaI(Tl) Scintillator

Sample weight: 62.9 mg.
Irradiation time: 2 hours
Counting interval: 60 minutes
Flux: 5×10^{12} n./sq. cm.-sec.
Detector: small Ge(Li)

Time	N_p ($\times 10^{-3}$)	N_b ($\times 10^{-3}$)	(100 σ)/(N_p)
4.0	2.98	10.0	5.07
6.3	1.55	3.76	6.14
8.5	0.923	2.24	7.96
10.7	0.592	1.89	11.20
13.0	0.240	1.13	20.80

Sample weight: 62.0 mg.
Irradiation time: 2 hours
Counting interval: 60 minutes
Flux: 5×10^{12} n./sq. cm.-sec.
Detector: large Ge(Li)

Time	N_p ($\times 10^{-3}$)	N_b ($\times 10^{-3}$)	(100 σ)/(N_p)
2.0	38.85	209.3	1.74
5.0	16.34	45.0	2.00
7.4	9.27	25.0	2.63
9.7	4.63	17.0	4.24
12.1	2.30	14.0	7.58
14.3	1.26	11.0	12.15

Sample weight: 62.9 mg.
Irradiation time: 2 hours
Counting interval: 60 minutes
Flux: 5×10^{12} n./sq. cm.-sec.
Detector: 3- × 3-inch NaI(Tl)

Time	N_p ($\times 10^{-3}$)	N_b ($\times 10^{-3}$)	(100 σ)/(N_p)
5.2	209.4	310.3	0.43
7.4	102.3	182.0	0.67
9.6	59.3	125.0	0.94
11.9	32.9	94.3	1.43
14.1	18.5	82.4	2.32

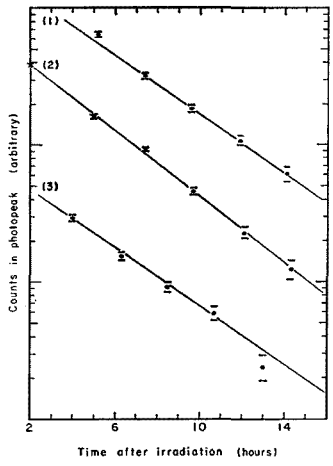


Figure 4. Decay curves for 2.6-hour Mn^{56} in the activated sulfide ore

Curve 1 represents data obtained with the sodium iodide scintillator. Curves 2 and 3 represent data obtained with the larger and smaller Ge(Li) detectors, respectively

detector in the region of the 845-k.e.v. photopeak of Mn^{56} are shown in Figure 3. The photopeak in the NaI(Tl) spectrum (Spectrum 1) covers an energy range of about 175 k.e.v. and appears to be single, while the spectrum from the larger Ge(Li) detector (Spectrum 2) shows complete resolution of the 819-k.e.v. line from In^{116m}. The spectrum obtained with the smaller Ge(Li) detector (Spectrum 3) shows, in addition, the complete resolution of the 835-k.e.v. line of Ga^{72}.

The decay of 2.6-hour Mn^{56} was followed by using each of the three detectors and the resulting decay curves are shown in Figure 4. The data from which this figure was prepared are given in Table III. Because of the difficulty in peak-shape analysis, the complex photopeaks in the sodium iodide spectra were treated as single photopeaks. The initial portion of the NaI(Tl) decay curve is then in error to the extent of contribution from the 54-minute In^{116m}. The error caused by the inclusion of the 835-k.e.v. photopeak from Ga^{72} is negligible. The error bars in Figure 4 represent $\pm 1\sigma$ limits as determined from Equation 1.

The quantity $(100\ \sigma_p)/(N_p)$ as a function of time after irradiation has been determined for the three Mn^{56} decay curves and is shown in Figure 5. These curves clearly show the effects of the level of Compton background upon the error in photopeak determinations. In the curves for the two Ge(Li) spectra, the decrease in error at early times is due to the rapid decay of the In^{116m}, which increases the ratio of N_p to N_b. The apparent linearity in the sodium iodide data during this time interval is due to the inclusion of the In^{116m} photopeak. In all three sets of data the error increases roughly exponentially for times long compared to the half-life of In^{116m}. In this region a reasonable comparison of the sensitivity for estimation of manganese may be attained by comparing the relative photopeak intensities for a given statistical error limit. In the present case, we have determined the fraction of manganese remaining at the times corresponding to the error limit $\sigma_p = 0.1\ N_p$. The corresponding limits of manganese concentration were determined from these data to be 21 p.p.m. (small Ge(Li)), 4.4 p.p.m. (large Ge(Li)), and 0.73 p.p.m. (NaI(Tl)).

It should be noted that the statistical treatment presented here has neglected several sources of error which are of particular importance for the sodium iodide data. The unresolved 835-k.e.v. line of Ga^{72} will contribute significantly to the apparent Mn^{56} photopeak near the sensitivity limit and decrease this limit from the statistical estimate. Although the interpolation of a background under the narrow photopeaks in germanium spectra can generally be performed with certainty, the interpolation over the large energy interval required in the sodium iodide spectra can contribute greatly to the error in estimation of the photopeak intensity.

The sensitivity limits set for the less efficient Ge(Li) detectors are strongly dependent upon the counting interval and sample size in the experiments reported here. With reasonable increases in these variables, the total counts accumulated with the germanium detectors may be increased and sensitivities comparable to sodium iodide can be obtained.

The results of this study show the applicability of available lithium-drifted germanium gamma-ray spectrometers to nondestructive neutron activation analysis of samples in which the major constituents as well as the minor and trace constituents are activated. The simplicity of the spectra obtained with these semiconductor detectors allows rapid and accurate estimation of constituents whose concentrations may vary over a very wide range. Similar treatment of data obtained using sodium iodide scintillators would be very difficult and, in many instances, totally impractical. In the present work, for example, the simplest photopeak in the sodium iodide spectra (845-k.e.v.) was seen to be composed of three gamma-ray lines superimposed on a complex background.

The analytical sensitivities obtained with the various detectors for the particular case of estimation of manganese in the ore indicate that the larger

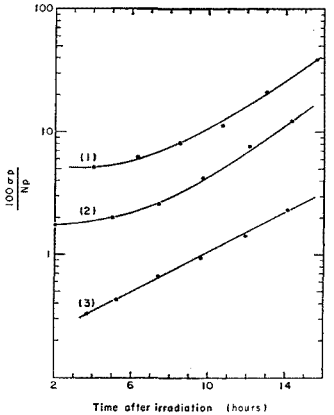


Figure 5. Per cent standard deviation in photopeak intensity vs. time after irradiation for the 845-k.e.v. gamma-ray of Mn^{56}

Curves 1 and 2 represent $(100\ \sigma_p)/(N_p)$ for the smaller and larger Ge(Li) detectors, respectively. Curve 3 is for the NaI(Tl) data

Ge(Li) detector is capable of yielding sensitivities comparable to the sodium iodide detector. This comparison shows the sodium iodide system at its best; in that the gamma-ray line studied was fairly well resolved from other lines in the spectrum. It is clear that the relative sensitivities obtained with the germanium detector would be much better for many of the gamma-ray lines which are not so well resolved in the NaI(Tl) spectra. Also it should be noted that the conditions of sample size, counting interval, and counting geometry could be optimized for use with Ge(Li) spectrometers. The data in Table III show that the sample activity used in the sensitivity comparison is near the practical limit for the sodium iodide detector, while a much more active sample could be used with the less efficient germanium systems. Although it is true that higher counting rates will cause some loss in resolution, the deterioration in the quality of the spectra is not great. It has been our experience that resolving power of the germanium detector systems suffers less from increased counting rates than the sodium iodide detector systems.

As a final note we wish to point out that the small volumes of available Ge(Li) detectors have been set by the techniques used in fabrication and not by the intrinsic properties of the system. Recently Malm, Tavendale, and Fowler (*10*) have reported the construction of a Ge(Li) detector of about 16 cc. (active volume) by a new drifting technique. The efficiency reported for this detector was 2.5% at 1300 k.e.v., comparable to a 1- × 1-inch (diameter)

NaI(Tl) scintillator. The detector resolution was 3.3 k.e.v. (FWHM) and 4.8 k.e.v. (FWHM) at 122 and 1333 k.e.v., respectively. The new drifting technique should make available Ge(Li) detectors of excellent resolution with several times the volume of this detector.

ACKNOWLEDGMENT

The authors acknowledge the kind assistance of R. E. McCracken and the crew of the Livermore LPTR nuclear reactor for help in obtaining irradiations.

LITERATURE CITED

(1) Ewan, G. T., Tavendale, A. J., *Can. J. Phys.* **42**, 2286 (1964).
(2) Girardi, F., Guzzi, G., Pauly, J., *Radiochim. Acta* **4** (2), 109 (1965).
(3) Goulding, F. S., Lawrence Radiation Laboratory *Rept.* **UCRL-11302** (1964).
(4) Goulding, F. S., Hansen, W. L., Lawrence Radiation Laboratory *Rept.* **UCRL-11261** (1964).
(5) Goulding, F. S., Landis, D., "Proceedings of Conference on Instrumentation Techniques in Nuclear Pulse Analysis, Monterey, April 1963," NAS-NRC Publication **1184**.
(6) Hansen, W. L., Jarrett, B. V., Lawrence Radiation Laboratory *Rept.* **UCRL-11589** (1964).
(7) Hawkings, R. C., Edwards, W. J., McLeod, E. M., "Tables of Gamma Rays from The Decay of Radionuclides," Vol. **1** and **2**, **CRDC-1007**, Atomic Energy of Canada Ltd., Chalk River, Ontario, 1961.
(8) Heath, R. L., "Scintillation Spectrometry Gamma-Ray Spectrum Catalog," Vol. **I** and **II** (**IDO-16880-1**).
(9) Lyon, W. S., ed., "Guide to Activation Analysis," Van Nostrand, Princeton, N. J., 1964.
(10) Malm, H. L., Tavendale, A. J., Fowler, I. L., *Can. J. Phys.* **43**, 1173 (1965).
(11) Miner, C. E., Lawrence Radiation Laboratory *Rept.* **UCRL-11946**, (1965).
(12) Nuclear Data Sheets, K. Way, *et al.*, Printing and Publishing Office, National Academy of Sciences-National Research Council, Washington, D. C.
(13) Prussin, S. G., Harris, J. A., Hollander, J. M., ANAL. CHEM. **37**, 1127 (1965).

RECEIVED for review January 24, 1966. Accepted March 28, 1966. This work was performed under the auspices of the United States Atomic Energy Commission Contract No. W-7405-eng-48.

Reactor Neutron Activation Analysis

Instrumental Sensitivities in Six Matrix Materials

HERBERT P. YULE[1]

General Atomic Division/General Dynamics Corporation, San Diego, Calif.

▷ **Radioactivation of major, and sometimes minor, sample constituents often precludes the possibility of instrumental neutron activation analysis for desired trace elements—even though their anticipated concentrations are well above known detection limits. Knowledge of sample composition may be inadequate for accurate prediction of feasibility of the analysis. One way to overcome this difficulty is to assemble data on elemental detection limits in various matrices. This paper presents experimentally determined matrix sensitivities of over 65 elements in six matrix materials commonly encountered in activation analysis. These results enable the analyst to determine immediately the feasibility of a particular analysis in one of these materials, and it seems likely that extrapolation to similar materials should be both easy and quite successful.**

PLANNING of reactor neutron activation analysis often requires a careful evaluation of how the desired results may best be obtained. Past experience with the material to be analyzed may obviate the need for an evaluation, or knowledge of sample composition may be complete enough to make the evaluation quite simple. For nonroutine analyses, however, this knowledge is often lacking.

Lukens (*3*) has suggested the problem be approached by determining, for a number of matrix materials commonly encountered in activation analysis studies, the minimum instrumentally-detectable amounts of those elements having good neutron activation analysis sensitivities.

This paper presents experimental results of 72 elements in each of six different matrices: whole blood, urine, milk, tap water, "pure" water, and polyethylene.

EXPERIMENTAL

Experiments were conducted along the lines set forth by Lukens (*4*, *5*). Several samples of each matrix material were weighed and encapsulated in polyethylene vials obtained from Olympic Plastics Corp., Los Angeles, Calif. Either 2/5-dram or 2-dram vials were used, depending on sample size. (Polyethylene vials are hereafter referred to as vials.) Three samples were irradiated in the rotary specimen rack of the General Atomic TRIGA Mark I nuclear reactor (thermal-neutron flux, 1.8×10^{12} $n/cm.^2$-sec.) for 30 minutes, and counted after delays of 1 hour, 1 day, and 8 days. The activated sample to be counted after a delay of 1 hour was transferred (and weighed) into a fresh, unirradiated vial, eliminating Ar^{41} activity (from argon in the air in the original vial). Two samples were irradiated using the pneumatic tube to transport them in and out of the reactor core (*6*, *7*), where the thermal-neutron flux was 4.3×10^{12} $n/cm.^2$-sec. The first sample was irradiated for 15 seconds and counted for 18 seconds, allowing 15 seconds to elapse between irradiation end and count start. The 15-second irradiation feature described above is not described by Lukens; it is merely an extension of his calculation method to these conditions. The remaining sample was irradiated for 1 minute, allowed to decay 1 minute, and counted for 1 minute. Counting was done with systems described in references (*6–8*) using gain settings of 15 k.e.v./channel to emphasize gamma-ray energies above 500 k.e.v., and 3.75 k.e.v./channel for energies below 500 k.e.v. Thus, each of the samples was counted twice for each delay time. The samples irradiated in the pneumatic-tube were counted only once, since they were expected to decay rapidly. A second count on one of these samples could be too late to approximate the spectrum at its designated time. Counts at the other gain setting were taken with fresh samples in separate experiments.

The matrix materials studied were whole blood, urine, milk, local tap water, "pure" water, and polyethylene vials. The whole blood was treated with a little sodium heparin as an anticoagulant, but was otherwise typical whole blood. The urine sample was collected during mid-day, and no attempt was made to collect the urine at different times to average any diurnal effect (*2*). Tap water was local San Diego water just as it came from the faucet. Milk was a commercially available local brand, stated by the dairy to be ho-

[1] Present address, Activation Analysis Research Laboratory, Texas A&M University, College Station, Texas 77843.

mogenized and have 400 USP units of vitamin D added. "Pure" water was distilled at this laboratory, and then run through a demineralizing column.

Selection of sample size was important—so that the sample would not be too radioactive to count in the standard geometry, nor contain too little activity. The first step in determining optimum sample size was to learn as much as possible about the sample composition. Rather complete data on biological samples are available (*2*), but information on other samples was largely unavailable, and had to be determined in preliminary experiments. For each element known in the sample, the photopeak yields listed in references (*6*) and (*7*) were adjusted for the weight of a given element in 1 ml. of total sample, for irradiation time, decay time, and, for the samples irradiated in the rotary rack, the lower neutron flux (*6*). Summing these corrected yields over all anticipated isotopes gave the expected total photopeak counting rate. The sample size was then adjusted so that the expected total photopeak counting rate was in the range of 5000 to 10,000 c.p.m. This procedure usually meant milligram-size samples for the pneumatic-tube irradiations, and three different-sized samples irradiated in the rotary rack—a few milligrams to be transferred to a "cold" polyvial and counted 1 hour after irradiation end, 0.01 to 1 gram to be counted 24 hours afterward, and several-gram samples to be counted 8 days afterward.

Discussion and calculation of argon, nitrogen, and oxygen are omitted from this study because most samples are contaminated with these elements.

ANALYSIS OF THE DATA

The first step is to identify the components in the gamma-ray spectra, and calculate the amounts of these elements present in the sample. This calculation compares photopeak areas in the present sample with those listed in reference (*6*)—accounting, of course, for any different experimental conditions (flux differences, different irradiation periods, and counting geometries). This approach, although not as accurate as the approach utilizing comparator standards, is sufficiently accurate for the present purposes.

The upper-limit calculations are done by the General Atomic IBM-7044 computer, following the scheme of Lukens (*4*). The raw data are corrected for dead-time counting losses and converted to counts per minute. Provision is also made to correct for geometry differences for samples too radioactive to count in the standard position or for samples larger than the defined 1-ml. volume (*4*). For those spectra at gains of about 3.75 k.e.v. per channel, the corrected counts per channel are summed into five ranges: 0–100, 100–200, 200–300, 300–400, and 400–500 k.e.v. Similarly, those spectra taken at a gain setting of 15 k.e.v. per channel are summed by 100-k.e.v. units, starting at 300 k.e.v. Sums are taken over those channels which most nearly approximate these energy ranges; interpolation to provide sums over exactly defined energy ranges is regarded as an unnecessary refinement.

Table I. Approximate Concentrations of Identified Components (in p.p.m.)

Element	Matrix: Whole blood	Urine	Milk	Tap water	"Pure" water	Polyethylene vials
Na	1400	1900	620	57	...	0.27
Al	140	~ 100	~100	4	<0.5	0.23
Cl	2400	2600	780	110	...	...
K	...	...	~ 70	...	...	...
Mn	...	...	...	...	...	0.0072
Co	1.0	...	...	...	...	...
Cu	...	...	...	...	0.31	...
Zn	...	...	...	...	...	...
Br	2.3	~ 1	1.9	...	...	...
Ag	...	...	...	...	0.54	...

An example of the upper-limit calculation is appropriate. Suppose one wishes to calculate an upper limit for lutetium, using the spectrum taken on a gain setting of 3.75 k.e.v. per channel after a delay of 8 days. Lukens' Table 4 (*4*) gives the following information:

(1) The most sensitive means of determining lutetium at this delay is through the 0.208-m.e.v. gamma ray emitted by Lu^{-177} (half life 6.8 days). This procedure assumes that the radioactivities in the matrix do not emit gamma rays which interfere with the chosen gamma ray of 0.208 m.e.v. To overcome this problem would require that detailed information on many gamma-ray spectra of reactor induced radioactivities be included as input information to the program. The computer could then decide on the proper gamma ray to use as a comparison basis. This refinement has not been included because the necessary data were not available in a form compatible with the needs of this program. Reactor thermal neutron products have over 400 detectable peaks, using NaI(Tl) detectors. For each peak, information would be required on peak energy, intensity, boundaries, etc.

(2) If the number of counts in the spectrum between 0.2 and 0.3 m.e.v. is 1000 counts, then the upper limit to the missing peak's size is 100 counts.

(3) The amount of lutetium corresponding to 100 c.p.m. is 0.28 μg. Suppose that our spectrum contains 500 counts between 0.2 and 0.3 m.e.v. The upper limit to the lutetium concentration is

$$\frac{500}{1000} \times 0.28 \times 0.1 = 0.014\ \mu g.$$

For each spectrum, the computer calculates limits for each element listed in Lukens' table, provided the raw data cover the appropriate energy range.

When the computer finishes calculating upper limits from all the spectra of a given material, it then summarizes the calculations by presenting for each element the best (least) upper-limit value obtained. For many elements several upper limits are obtained, although only one limit may be obtained at a given delay time. Upper limits obtained at different delay times are almost always different, because radioactivities in the sample decay away with time, and because different reference activities are often used at different delay times.

Only one upper limit for each element is calculated from one spectrum even though several isotopes produced from that element may be present. Following Lukens' scheme, the isotope giving most sensitive detection limits, exclusive of possible interferences, is used as a basis for calculation. This isotope may be a reactor fast-neutron product, but in most cases it is a thermal-neutron product.

Sample size does not affect the results, for the upper limit expressed in parts per million is unchanged for different sample sizes, just as the concentration of an element is the same for all sample sizes. Correction factors were applied to all samples to account for sample size. Clearly, some samples cannot be treated in this way because their activities are lower than, or comparable to, background. With low-activity samples, long counts were taken, and observed activities were quite low even after correction for sample size. Lukens' scheme (*4*) breaks down under these conditions, and the computer adjusts the data so that upper limits are calculated consistently with minimum detectable counting rates. The overall effect of sample size and count rate adjustments gives approximately the minimum detectable quantities under ideal conditions (*6*) at the same decay time.

A typical calculation of one set of spectra takes about 10 seconds of computer time, exclusive of loading time, unloading time, etc.

RESULTS AND DISCUSSION

The concentrations of identified components in urine, and blood, in Table I, are in good agreement with available literature values (*2*). The milk data are in poor agreement with the values

listed in reference (*2*). The differences are probably due to dietary and processing differences; fairly large concentration fluctuations in potassium content have been observed (*3*). For the other matrix materials, little information on composition is available and these results appear to be reasonable. The value for aluminum in distilled-deionized water is given as an upper limit, since variability in the aluminum content of the polyvials makes it difficult to distinguish accurately between aluminum in the sample and in the polyvial.

Upper limits for elements not detected in the matrix materials are given in Table II. Results are quoted only to one significant figure, since the calculation is not exact, and results may be in error by factors of two to five (*4*).

The results in Table II indicate that for the biological materials the minimum instrumentally-detectable amounts of many elements correlate with the sodium (and to a smaller extent, the chloride) content of the matrix. This correlation is well known to those engaged in reactor neutron activation analysis work—indeed sodium seems to be ubiquitous.

Comparing tap water and "pure" water, the measurable amounts of sodium and chloride (Table I) in tap water are effectively reduced, in the purified water, to quite low concentrations, as indicated by the upper limits in Table II. The silver and copper concentrations are probably also reduced.

Vials show small concentrations of aluminum, sodium, and manganese. The vial upper limits are generally not as good as those for the "pure" water, since the water samples were heavier. A few hours after irradiation, the gamma-ray spectra of "pure" water and vials were quite similar, giving roughly the same sensitivity in micrograms, but not in parts per million. To achieve the best limits in a sample with a low yield of activities, transfer of the sample to a vial that has not been irradiated may be required.

It is of interest to examine the relationships between the instrumental sensitivities in the various matrices in Table II, and the corresponding ideal matrix (interference-free) sensitivities, in which only the radioactivity of interest is produced by neutron irradiation. The best instrumental sensitivities are found for those matrix materials producing little or no activity, especially if the half lives of the radionuclides generated from the matrix are only an hour or less. Good instrumental sensitivities are obtained when the half life of the radionuclide sought is either much longer or much shorter than the half lives of the principal matrix activities. If the gamma ray of interest is hi her in energy than all, or most, of the gamma rays from the matrix activities, good instrumental sensitivities are obtained—if the sample is not too radioactive to be counted at high geometry (about 30% or so). The poorest instrumental sensitivities are obtained when half lives and gamma-ray energies of the radionuclide sought and the matrix radionuclides are comparable. Under these circumstances, instrumental sensitivities are often several hundred or a thousand times the interference-free sensitivities.

Table II. Limits of Detection of 72 Elements in Six Different Matrix Materials

	Sensitivities in parts per million for					
Element	Whole blood	Urine	Milk	Tap water	"Pure" water	Polyethylene vials
Ag	0.6	0.2	0.09	0.06	...[a]	0.01
Al	...	...	...	...	...	...
As	4	7	1	0.3	0.05	0.01
Au	0.002	0.005	0.0009	0.0003	0.00009	0.0001
Ba	12	5	4	1	0.03	0.06
Br	...	...	...	0.1	0.04	0.01
Ca	200	90	100	8	1	2
Cd	500	20	200	40	0.1	0.2
Ce	2	3	0.8	0.2	0.07	0.2
Cl	...	...	...	...	0.0007	0.02
Co	...	0.2	0.05	0.02	0.06	0.09
Cr	3	5	1	0.4	0.1	0.3
Cs	0.4	0.7	0.1	0.04	0.004	0.009
Cu	40	30	9	2	...	0.008
Dy	0.06	0.0003	0.02	0.002	0.0002	0.0004
Er	20	2	9	2	0.004	0.006
Eu	1	1	0.3	0.4	0.0002	0.0002
F	30	30	10	3	2	0.2
Fe	300	700	80	20	8	10
Ga	300	100	70	6	0.05	0.04
Gd	60	2	20	8	0.02	0.03
Ge	50	0.2	10	2	0.3	0.3
Hf	0.2	0.4	0.09	0.03	0.002	0.006
Hg	20	4	20	2	0.02	0.03
Ho	0.4	2	1	0.06	0.001	0.002
I	4	0.1	2	0.3	0.0009	0.002
In	0.1	0.1	0.03	0.004	0.00006	0.00009
Ir	0.006	0.01	0.002	0.0008	0.0003	0.0006
K	1000	900	...	50	0.009	0.1
Kr	21	0.04	3	0.2	0.0009	0.002
La	0.05	0.1	0.01	0.04	0.0003	0.001
Lu	0.006	0.01	0.003	0.0008	0.0002	0.0006
Mg	800	400	200	20	9	10
Mn	0.9	1	0.3	0.04	0.0001	...
Mo	2	3	2	0.3	0.08	0.1
N	[b]	100	400,000	2000	6000	6000
Na	...	...	...	...	0.03	...
Nb	1000	60	300	100	3	0.009
Nd	6	0.2	2	0.5	0.05	0.3
Ne	500	5	200	10	11	5
Ni	8000	10,000	2000	400	0.04	0.02
Os	30	60	9	2	0.004	0.006
P	1000	1000	600	50	20	40
Pb	200,000	200,000	60,000	10,000	40	10,000
Pd	3	0.4	0.5	0.3	0.07	0.05
Pr	8	20	2	3	0.002	0.008
Pt	3	2	2	0.4	0.02	0.04
Rb	7	9	2	0.5	0.1	0.3
Re	4	0.03	1	0.1	0.001	0.002
Rh	4	0.03	1	0.09	0.2	0.03
Ru	2	4	0.8	0.2	0.05	0.09
S	6000	3000	3000	300	30	50
Sb	0.08	0.2	0.03	0.007	0.003	0.005
Sc	0.04	0.01	0.01	0.003	0.0009	0.002
Se	4	0.2	1	0.5	0.2	0.09
Si	500	400	200	16	7	10
Sm	0.04	0.07	0.04	0.005	0.0005	0.0008
Sn	300	5	200	20	0.1	0.2
Sr	40	2	20	3	0.009	0.02
Ta	0.1	0.2	0.02	0.009	0.03	0.04
Tb	0.2	0.4	0.1	0.03	0.01	0.02
Te	3	2	1	0.4	0.03	0.08
Ti	200	2	72	5	5	2
Tl	300,000	600,000	100,000	40,000	20,000	30,000
Tm	2	6	5	0.2	0.1	0.2
V	0.8	0.6	0.2	0.03	0.01	0.02
W	2	0.1	0.6	0.2	0.003	0.001
Xe	8	15	4	1	0.2	0.3
Y	10	6	3	1	1	0.3
Yb	0.2	0.4	0.08	0.03	0.01	0.02
Zn	2000	80	500	100	0.3	0.4
Zr	20,000	13,000	4000	800	4	2

[a] Three dots indicate a known component.
[b] High matrix activation makes nitrogen undetectable at any concentration.

CONCLUSIONS

The upper limits in Table II provide useful information on the feasibility of instrumental neutron activation analysis in six different matrix materials. Consider, for example, the element selenium, which is of considerable biological interest. According to Table II, the instrumental limit of detection, under the conditions employed, is about 4 p.p.m. for blood, and hence the instrumental determination of selenium in subparts per million concentration range would require considerable additional effort (*1*). One obvious way to improve the sensitivity is to employ longer irradiations to build up the amount of long-lived Se^{75}; this approach may be prohibitively expensive, however. Table II supplies the answer to step two in the evaluation procedure: selenium will be difficult to determine instrumentally, in blood, in concentrations below about 4 p.p.m. Gold, on the other hand, would be easily detectable in blood, even in the parts-per-billion range.

It must be emphasized that the limits in Table II are only approximate, and that they do not represent ultimate limits which cannot be improved. It is hoped that the data presented here will be interesting and useful to those engaged in nonroutine neutron activation analysis. Higher neutron fluxes and longer irradiations will give much improved limits for many elements. Other beneficial counting techniques will undoubtedly emerge as time passes. The approach used here may be modified to optimize results for particular matrices; in its present form it attempts to provide a general solution for any matrix.

ACKNOWLEDGMENT

The author thanks Lavon Todt of the Mathematics and Computing Department of General Atomic for programming the upper-limits calculations.

LITERATURE CITED

(1) Fleishman, D. M., Guinn, V. P., *Trans. Am. Nucl. Soc.* **7**, (2), 327 (1964).
(2) Long, C. A., Ed., "Biochemists' Handbook," Van Nostrand, Princeton, N. J., 1961.
(3) Lukens, H. R., Jr., General Atomic Division/General Dynamics Corp., San Diego, Calif., private communication, 1965.
(4) Lukens, H. R., Jr., *Rept.* **GA-5896**, General Atomic Division/General Dynamics Corp., San Diego, Calif., 1964.
(5) Lukens, H. R., Jr., *Trans. Am. Nucl. Soc.* **8**, (1), 83 (1965).
(6) Yule, H. P., ANAL. CHEM. **37**, 129 (1965).
(7) Yule, H. P., Lukens, H. R., Jr., Guinn, V. P., *Nucl. Instr. Methods* **33**, 277 (1965).
(8) Yule, H. P., Lukens, H. R., Jr., Guinn, V. P., *Rept.* **GA-5978**, General Atomic Division/General Dynamics Corp., San Diego, Calif., 1964.

RECEIVED for review September 13, 1965. Accepted April 8, 1966.

Determination of Trace Amounts of Carbon, Oxygen, and Nitrogen in Metals by Spark Source Mass Spectrometry

W. L. HARRINGTON, R. K. SKOGERBOE, and G. H. MORRISON

Department of Chemistry, Cornell University, Ithaca, N. Y.

▶ **The simultaneous determination of trace amounts of C, O, and N in metals by spark source mass spectrometry has been accomplished. Reduction of the instrument blank for these elements to <0.5 p.p.m. by weight and prevention of blank fluctuations are the results of cryosorption pumping in the source chamber. The micro-sampling of the rf spark is shown to provide reliable localized concentrations which can be used for impurity distribution studies. A sample scanning technique is suggested which gives a good estimate of bulk concentrations as well as an indication of sample homogeneity.**

ONE of the most critical problems in the analytical chemistry of metals has been the quantitative determination of the impurities carbon, oxygen, and nitrogen. Tolerance levels for these impurities in many metallurgical materials have been steadily reduced to the point where a concentration of 1 p.p.m. or less is of current interest. This has been generated by the fact that concentrations of these impurities in the range of 1–10 p.p.m. exert significant effects on the physical properties of many metals.

The importance of this problem has promoted extensive research on the determination of these elements by vacuum fusion (*3*, *5*, *8*), inert gas fusion (*3*, *4*, *8*), emission spectrometric (*3*, *8*, *13*), nuclear activation (*1*, *2*, *8*), isotope dilution (*8*), and wet chemical (*8*) methods. In general, all of these methods are subject to the same primary limitations: the magnitude and inconsistency of the operating blank, the restriction, in all cases except vacuum fusion, to one element in a particular determination, losses due to gettering, nonquantitative recovery, etc., the lack of standards at low concentrational levels, and the large amount of sample required. The optimum range of measurement for these techniques generally lies above 10 p.p.m., but determinations in the 1–10 p.p.m. range can be achieved if sufficiently large samples are available to produce a signal significantly greater than the operating blank.

Although the spark source mass spectrographic method of analysis has shown the capability to minimize most problems of this type for metallic and some nonmetallic impurities, the limited published results on the determination of carbon, oxygen, and nitrogen by this method have essentially been negative. Some results have been reported by Roboz (*11*) and Henry, (*7*) but precision, accuracy, and limits of detection have suffered, presumably due to inadequate blank control. Socha and Willardson (*12*) have shown reduction in residual gases in the source and collector sections of a mass spectrograph by N_2 flushing, cryogenic pumping, and cathodic etching; however, they do not report quantitative data on the determination of C, O, and N using these techniques.

The success in this laboratory of reducing hydrocarbon interferences as well as the C, O, and N blank by cryosorption pumping (not to be confused with cryogenic pumping) in the chamber of a spark source mass spectrograph (*6*) has allowed this method to be extended to the analysis of metals for C, O, and N over a wide concentration range. The method reported here allows the possibility of simultaneous determination of C, O, and N (as well as

all other impurities) in metal samples with a limit of detection better than 0.5 p.p.m. In addition to smaller sample consumption, as compared with other techniques, this mass spectrographic method provides average bulk concentrations or localized concentrations for distribution studies.

EXPERIMENTAL

Apparatus. The mass spectrographic facilities and parameters have been previously described (*6*). With the exception of magnetic field strength, the same parameters were used for all matrices. Unless otherwise noted, all values are expressed in p.p.m. by weight to facilitate comparison with other analytical techniques. Experimental conditions for inert gas fusion and combustion–chromatographic analyses are described in Tables I and II, respectively.

Preliminary Blank Experiments Before attempting to analyze metals for low concentrations of C, O, or N by spark source mass spectrometry, it was necessary to reduce the instrument blank for these elements to a constant value lower than the level of the purest samples to be investigated.

Prior observations of hydrocarbon removal by cryosorption pumping (*6*) presented the possibility that the instrument blank for C, O, and N could be reduced by this method. For an iron sample containing 20 p.p.m. C, 30 p.p.m. O, and 10 p.p.m. N, mass spectral data with and without cryosorption pumping were compared. All calculations were referenced to NBS standard iron sample #465 as explained in the following section. Without cryosorption pumping, C, O, and N values were 55 ± 14 p.p.m., 57 ± 23 p.p.m., and 17 ± 5 p.p.m., respectively. Under identical sparking conditions, but with cryosorption pumping, C, O, and N concentrations were reduced to 25 ± 7 p.p.m., 30 ± 7 p.p.m., and 11 ± 2 p.p.m. To find out more about the nature and magnitude of the remaining blank, a dilution of residual gases in the spark chamber was attempted. The chamber was evacuated to 10^{-6} torr and then brought up to atmospheric pressure with purified argon. This procedure was repeated three times, and finally the chamber was evacuated to 2×10^{-7} torr with cryosorption pumping following the established procedure for analysis. Values for C, O, and N of 26 ± 4 p.p.m., 25 ± 8 p.p.m., and 12 ± 3 p.p.m., respectively, showed no significant difference in the values without argon purging. Thus, residual gases did not contribute to a discernible background when cryosorption pumping was used.

Since most blank contamination probably exists as adsorbed gases on surfaces surrounding the sparking sample, baking these surfaces while employing cryosorption pumping was tried. Again, no reduction of C, O, or N intensity was observed, leading to the conclusion that cryosorption pumping had brought the blank down to a constant low level suitable for analysis of low concentration samples. An estimate of this blank level will be presented after discussion of analysis results.

Mass Spectrographic Data Reduction. Calculations of impurity concentrations from mass spectrographic data were referenced to a standard of each matrix type, Fe, Cu, and Ag. For each sample an exposure ratio E_m/E_i, where m and i refer to matrix and impurity, respectively, was determined from probability *vs.* exposure curves as reported by McCrea (*10*). Probability, in this context, is a cumulative normal distribution function which expresses the percentage of light absorbed during the densitometric process by the relation $P = (OD_m/OD_{sat\ m}) \cdot 100$, where OD_m represents optical density at peak maximum for mass m, and $OD_{sat\ m}$ represents the saturation value of optical density for the same mass m. Since saturation absorption varies with mass and energy of the incident ions, optical density at saturation was determined for each mass under consideration. Plotting matrix line probability values on a probability axis *vs.* log monitor exposure produced a straight line from which the exposure ratio E_m/E_i could be obtained. This ratio was then converted directly to concentration by reference to the sample taken as standard.

Due to the large number of tungsten samples being processed at the time of this work, a computer program by Kennicott (*9*) was used to obtain similar fractional values which could be converted to concentration by comparison with a standard.

Standards. A high concentration sample was chosen as the standard for each matrix, and the reference data obtained from each were used in all subsequent calculations. The samples designated as standard in Table III were analyzed for C and O by combustion–chromatographic and inert gas fusion analyses in our laboratory. Other than being relatively high in concentrations of C, O, and N, these samples were chosen for reference because of sufficient amounts available for replicate combustion analyses and reasonable homogeneity as demonstrated by both mass spectrographic and fusion–chromatographic results. Any inaccuracy in the values of the combustion analyses of these standards is necessarily reflected as an uncertainty in the mass spectrographic results referenced to them.

Nitrogen values for the W, Cu, and Ag standards were obtained by micro-Kjeldahl determination through a com-

Table I. Experimental Conditions for Determination of Oxygen in Fe, Cu, Ag, and W by Inert Gas Fusion

Analysis facility	
Furnace	Leco 537-100
Analyzer	Leco gas chromatograph 589-400
Crucible assembly	Leco carbon crucible 534-352; Leco crucible thimble 537-236; Leco carbon black packing 501-92
For Fe, Cu, Ag	Crucible conditioned with 1–2 grams of similar matrix material before adding sample
For W	1–2 grams low-oxygen Pt added to crucible; Pt added with each sample to maintain flux—sample ratio >1
Carrier gas	Purified helium at flow rate of 1 liter/minute
Calibration	KHP in Sn capsules
Extraction temperature	2400° C.
Extraction–collection time	4 minutes
Sample preparation	
For Fe, Cu, Ag	0.05 to 2.5-gram chunks abraded to bright surface with degreased file, rinsed in acetone, and air dried
For W	0.1 to 1.0 gram powder (<40 mesh), etched in aqua regia, washed with distilled water, acetone, and air dried

Table II. Experimental Conditions for Determination of Carbon in Fe, Cu, Ag, and W by Combustion–Chromatographic Technique

Analysis facility	
Furnace	Leco 521-100
Analyzer	Leco gas chromatograph 589-400
Crucible	Leco aluminum oxide 528-35 with 528-42 cover
Oxygen flow rate	2 liters/minute
Susceptor material	
For Fe	2 grams Sn granules used only when sample size insufficient to ensure coupling (<0.5 g.)
For Cu, Ag	2-gram Sn granules
For W	$\frac{1}{2}$ inch diameter × $\frac{1}{32}$ inch thick Pt sheet on bottom of crucible (*4*)
Calibration	KHP in Sn capsules
Combustion–collection time	4 minutes
Sample preparation	
For Fe, Cu, Ag	0.08 to 1.8-gram amounts cut in 2 mm.² (<10 mesh) pieces, etched in 6*N* acid, washed with distilled water, acetone, and air dried
For W	0.2 to 1 gram powder (<40 mesh), etched in aqua regia, washed with distilled water, acetone, and air dried

mercial analytical laboratory. The value for the Fe standard was taken as the noncertified analysis provided by the U. S. National Bureau of Standards. The unavailability of sufficient sample limited the Kjeldahl nitrogen data that could be compared with mass spectrographic results.

RESULTS AND DISCUSSION

To show the applicability of spark source mass spectrometry for the determination of C, O, and N in metals, analyses for these elements in matrices of Fe, W, Cu, and Ag over a wide concentration range were performed. Table III compares the mass spectrographic results with those obtained by combustion–chromatographic, inert gas fusion, and micro-Kjeldahl nitrogen analyses. Unless otherwise noted, the mass spectrographic values are the results of a single graded series of exposures from which 3–8 exposures per impurity could be used.

Although the general agreement of these results is very favorable, there are some gross differences which need be pointed out and some facets of the mass spectrographic technique which should be explained in more detail.

Sample Homogeneity and Bulk Analysis. There are two cases where the values compared either do not coincide or are not truly representative of the situation—oxygen in Electrolytic Grade Cu, and carbon in 5-9's Fe. Due to a large difference in sample consumption between mass spectrographic and combustion analyses, inhomogeneity of materials can make a comparison of the results between the techniques misleading. For concentrations <10 p.p.m. C or O, combustion–chromatographic methods under ideal conditions require a minimum of 0.1 gram to as much as 8 grams sample size (*4*). The gas content reported from such an analysis will necessarily be an average bulk value. On the other hand, mass spectrographic exposures necessary to detect <10 p.p.m. C or O consume only 0.1–10 mg. of sample depending on the type of matrix. This micro sample may or may not be representative of the bulk concentration depending on the degree of sample homogeneity. Several iron samples used in this study offered a useful illustration of these generalizations and an explanation for the disagreement between techniques for the cases cited.

Combustion–chromatographic determinations of carbon in 5–9's Fe resulted in randomly distributed values ranging from 6 to 70 p.p.m. An average bulk concentration of 57 ± 4 p.p.m. C was obtained from duplicate analyses of the electrodes actually used for the mass spectrographic analyses. Thus, 57 ± 4 p.p.m. C was used as the comparative combustion value in this case. Examination of crucible contents after combustion revealed complete combustion in all replicates, and random analyses of NBS Fe standards run concomitant with the analyses of 5–9's Fe agreed with the NBS certified values to better than ±15%. On the basis of these results, a high degree of inhomogeneity with respect to carbon in 5–9's Fe was suspected. With regard to oxygen content, however, inert gas fusion analyses on this sample indicated a somewhat more uniform distribution.

As an example of contrast, NBS vacuum melted Fe was shown to be very homogeneous in oxygen by inert gas fusion analyses. Five $1/4'' \times 2''$ long rods of this sample were sampled five times each for a total of 25 inert gas fusion determinations. The average oxygen concentration was 25 ± 3.4

Table III. Comparative Analyses of Metals for Carbon, Oxygen, and Nitrogen

Sample	C (p.p.m.) Mass spec.[a]	C (p.p.m.) Combust.–Chrom.	No. runs	O (p.p.m.) Mass spec.[a]	O (p.p.m.) Inert gas fusion	No. runs	N (p.p.m.) Mass spec.[a]	N (p.p.m.) Kjeldahl
Iron matrix								
NBS ingot Fe #465	366*	336 ± 6*	5	35*	35 ± 7*	3	50*	50*[b]
NBS ingot Fe #466	630	659 ± 37	6	47	45 ± 12	6	55	60[b]
NBS vacuum melted Fe	...	...	...	29	25 ± 2	5	...	...
Zone refined Fe	24	17	1	45	49	1	14	...
H_2 reduced chips	<2[c]	<4[d]	4	76	61 ± 55	3	8	...
Commercial 5–9's Fe	64[e]	57 ± 4	2	25	22 ± 6	6	25	...
Vacuum melted Fe	41	23 ± 18	2	50	26	1	12	...
Tungsten matrix								
Welding rod	18*	20 ± 7[f]	6	19*	19 ± 4*	5	7*	7*[g]
Unzoned rod (1)	22*	20 ± 7[f]	6	4	...	...	4	...
Zoned rod, Section 9	7	8	1	6	...	...	4	...
Zoned rod, Section 7	4	6	1	5	...	...	2	...
Zoned rod, Section 6	4	...	...	6	5	1	1	...
Zoned rod, Section 4	9	11	1	2	...	...	0.4	...
Zoned rod, Section 3	18	15	1	3	...	...	1	...
Zoned rod, Section 1	15	9	1	4	...	...	2	...
Unzoned rod (2)	24	16	1	20	...	...	10	...
Zoned rod	15	10	1	8	...	...	12	...
Copper matrix								
Commercial 6–9's Cu	76*	76 ± 9*	4	5*	5 ± 4*	5	7*	7*[h]
Johnson-Matthey CC-5	16	21	1	2	4 ± 2	2	2	...
Johnson-Matthey CC-2	38	38 ± 14	2	6	6 ± 2	2	28	...
Electrolytic grade Cu	6	8 ± 2	2	6	378 ± 20	3	3	...
Silver matrix								
Commercial 6–9's splatters	2*	2 ± 1*	3	69*	69 ± 10*	3	<0.3	...
Asarco 5–9's + bar	2	1.7	1	2	0.9 ± 0.2	3	<1*	<1*[h]

* Reference standard.
[a] Average value from single graded series of exposures unless noted otherwise.
[b] Uncertified NBS value.
[c] $^{13}C^{+}$ not discernible from $^{26}Mg^{+2}$ interference at longest exposure used. Less than value based on just detectable signal at longest exposure level.
[d] Signal not discernible from blank. Less than value determined from least detectable signal from blank at 95% confidence level.
[e] See Table IV.
[f] Standard taken as average of two samples.
[g] Average batch analysis supplied by manufacturer.
[h] Commercial laboratory report based on duplicate analyses.

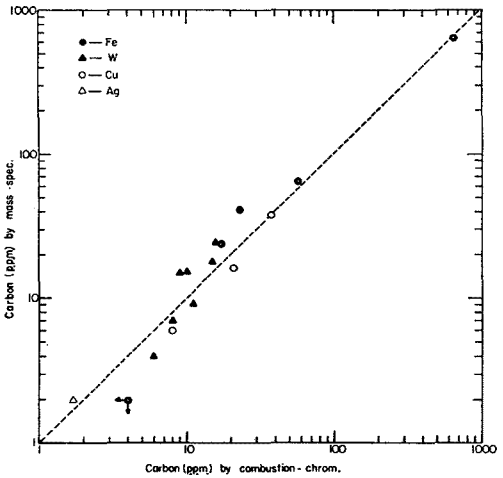


Figure 1. Comparison of mass spectrographic and combustion–chromatographic results for the determination of carbon in metals

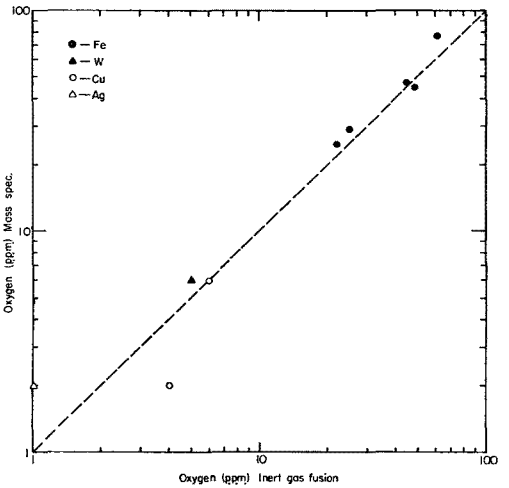


Figure 2. Comparison of mass spectrographic and inert gas fusion results for the determination of oxygen in metals

p.p.m., and the particular 2″ section from which the mass spectrographic sample was taken produced 25 ± 2 p.p.m. O.

Thus, to point out the ability of the mass spectrograph to detect inhomogeneity, five separate mass spectrographic analyses were run on the two Fe samples described above as well as on the standard NBS # 465. The results are summarized in Table IV. The data from plate numbers 1 and 2 represent localized concentrations obtained by running a graded series of exposures for each plate while holding the electrodes stationary with respect to each other. The data from plate numbers 3, 4, and 5 was obtained by running replicate exposures while moving the electrodes between each exposure to systematically scan over the sample length, thereby producing data for the estimation of an average bulk concentration and the degree of inhomogeneity. In all cases care was taken to maintain a constant solid angle with respect to the primary slit.

Several pertinent observations are apparent from this data. The two stationary localized analyses of 5–9's Fe produced reproducible carbon concentrations over a series of exposures, but the average concentrations calculated from these two determinations are significantly different at the 95% confidence level. In addition, neither of these values agrees well with the combustion value obtained from the same electrodes. The scanning analysis of 5–9's Fe, however, shows agreement with the combustion data for carbon, but exhibits very poor reproducibility on replicate exposures taken at different points along the sample. Since the scanning technique resulted in good precision (as well as good accuracy) on the more homogeneous samples, it must be concluded that the poor reproducibility observed for 5–9's Fe is due to a high degree of inhomogeneity.

The oxygen content of 5–9's Fe, indicated to be more homogeneously distributed by inert gas fusion analysis, does not show a significant concentration change at the 95% confidence level in any of the three analyses. However, the significantly poorer reproducibility observed for the scanning determination does imply a greater degree of inhomogeneity than was inferred by the fusion analysis. Again, this is to be expected when relative sample sizes are considered.

In general, these results have the following implications: spark source mass spectrometry gives an accurate representation of concentration for the particular sample region covered; and bulk concentrations and a guide to the degree of homogeneity can be reliably obtained by using a systematic scanning technique.

It is interesting to note that the total p.p.m. of C, O, and N in the 5–9's Fe sample exceeds the level of a 5–9's designation by about a factor of ten. Similar observations can be made on 6–9's Cu and 6–9's Ag. It has been apparent throughout this study that such purity claims may not include the elements C, O, or N, and that many suppliers of these "pure" materials do not specify these elements as exceptions to the X–9's label.

Instrument Blank. Since the instrument blank for C, O, and N will eventually determine the limit of detection for these elements, it is important to obtain an estimate of the blank concentration and thus an

Table IV. Results of Scanning Method for Indication of Homogeneity

Sample	Plate #	Sparking method	Av. C (p.p.m.)	Rel. std. dev.	Av. O (p.p.m.)	Rel. std. dev.	Av. N (p.p.m.)	Rel. std. dev
5–9's Fe	1	Stationary	149 ± 28	18.8	25 ± 5	20.0	25 ± 8	32.0
5–9's Fe	2	Stationary	78 ± 13	16.8	38 ± 14	36.8	22 ± 5	22.6
5–9's Fe	3	Scanning	64 ± 80	125.0	22 ± 16	72.8	23 ± 7	30.4
NBS #465	4	Scanning	370 ± 50	13.5	35 ± 5	14.4	50 ± 9	18.0
NBS vacuum melted Fe	5	Scanning	315 ± 20	6.4	29 ± 2	7.0	16 ± 2	12.5

evaluation of the efficiency of cryosorption pumping for this purpose. A plot of carbon concentration determined by mass spectrometry *vs.* that obtained by the combustion–chromatographic technique for all sample types investigated is presented in Figure 1. A similar plot for oxygen is presented in Figure 2. These plots do not contain points for the standard sample of each matrix. Over a range of 2 to 659 p.p.m. C and <1 to 69 p.p.m. O there is no indication that an instrument blank is interfering with low concentration analyses. That is, no significant deviation or curvature from the theoretical 1:1 relation is apparent over the range of concentrations investigated. These plots also indicate that using one standard to reference concentrations over several orders of magnitude is valid.

To accurately characterize the blank, it would be necessary to have samples with C, O, or N completely absent. After expending considerable effort toward this goal, no such metal sample has been located to date. A limiting value of the blank, however, can be obtained by considering the precision of the measurements below the 10 p.p.m. level and extrapolating from the lowest samples analyzed. The relative standard deviation for determining exposure ratios at this level was 20–30%. Considering the lowest concentration samples in this study (2 p.p.m. C and 0.9 p.p.m. O), the instrument blank would have to be $\geq$0.6 p.p.m. C and $\geq$0.3 p.p.m. O to cause significant curvature in the plots presented. Although insufficient data are available for nitrogen, the lowest value calculated was <0.3 p.p.m. Since concentration is expressed in p.p.m. by weight, the value of the blank will vary with the mass of the matrix. Assuming the lower limits for silver, the average blank value for C, O, and N for all matrices studied can therefore be estimated to be less than 0.5 p.p.m. Since this method of estimation produces only an upper limit, the true blank may in reality lie considerably below this value. With the availability of purer samples it should be possible to better characterize the magnitude of the blank.

Inorganic Interferences. Even with a low, constant blank for C, O, and N determinations, a very important limitation of the mass spectrographic technique is posed by inorganic interferences. The extremely common impurities Mg, Si, and S offer serious interference due to their +2 species. Similarly, many matrix materials such as Ni, Ti, Ge, Fe, Zn, and Cu, among others, have multiply-charged ions which will mask out one or more of the C, O, or N isotopes from M/e = 12 to 18.

The samples chosen for analysis in this study offer good illustrations of these interferences. An iron matrix precluded the use of $^{14}N^+$ due to the $^{56}Fe^{+4}$ ion and also ruled out $^{18}O^+$ due to the $^{54}Fe^{+3}$ ion. In addition, the iron samples varied considerably in Mg and S concentrations so that $^{13}C^+$, $^{17}O^+$, and $^{15}N^+$ proved to be better choices for these analyses. Although there was visual resolution of these interferences from the more abundant isotopes, the high intensity level of the interferences caused extreme variance in values calculated from $^{12}C^+$ and $^{16}O^+$. Reduction in both impurity and interference intensity at the less abundant isotopes allowed sufficient resolution for analysis purposes.

Constant, very low amounts of Mg, Si, and S in the tungsten samples allowed the use of the most sensitive isotopes of C, O, and N in these analyses.

Copper, however, provided interference at M/e = 13 due to $^{65}Cu^{+5}$, but again, low values of Mg in these samples allowed the use of $^{12}C^+$. There was considerable variation in Si and S concentrations, however, so that $^{18}O^+$ and $^{15}N^+$ were found to give more consistent results.

The high purity of the silver samples allowed the use of the most sensitive isotopes for analysis.

These interferences can be serious enough to preclude the determination of one or more of the elements C, O, or N in a given sample. The possibility of having such interferences should be realized when using the mass spectrographic technique, and isotopes having the best resolution from these interferences should be employed.

Localized Analysis. The microsampling property of the rf spark can be used to a great advantage where not only the concentration, but the distribution of impurities is important. A distribution study carried out on a zone refined tungsten rod illustrates the type of information that can be obtained.

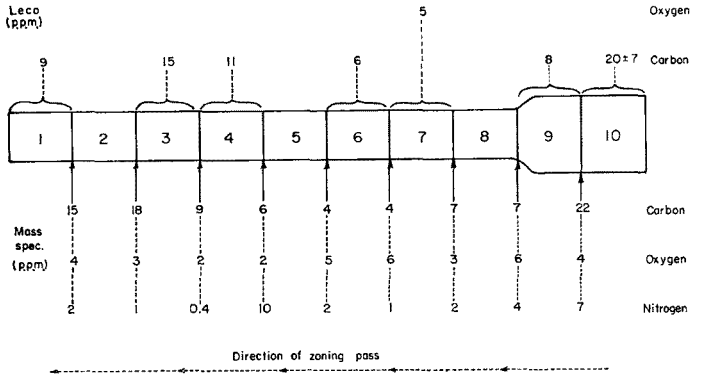


Figure 3. Localized analysis of zone refined tungsten rod

A commercial grade tungsten welding rod was zone refined and chemically etched to remove surface layers. To evaluate the efficiency of the zoning technique, a profile of impurities, the most important metallurgically being carbon, was needed. The rod was sectioned as indicated in Figure 3. At each interface a mass spectrographic analysis was performed, and then these same samples were analyzed for C or O by the combustion technique for comparison. Although many other impurities were simultaneously determined by the mass spectrographic procedure, only C, O, and N are of interest here, with carbon displaying a significant zoning trend. For the combustion analysis there was sufficient sample in any one section for either C or O analysis, but not both. The combustion values represent an average of each section, whereas the mass spectrographic values are confined to the section interfaces. Mass spectrographic carbon values presented in Figure 3 show the zone refining trend. Before the zoning started, after section 10, the carbon value at the 9–10 interface was the same as most "as received" welding rods. Interface 8–9 shows a definite decrease in C as the zoning starts, and the C concentration remains essentially constant through interface 4–5, after which the C builds up toward the end of the zone refining process as evidenced by interfaces 3–4, 2–3, and 1–2.

Although concentrations of oxygen along the zone refined rod are significantly lower than most unzoned welding rods (~20 p.p.m.), there is no migration or movement as in the carbon case. At the 95% confidence level there is no difference between the oxygen values over the entire length of the rod with the average concentration being 4 ± 1.5 p.p.m. (±35%). Thus, within the reproducibility of the method at this level, the "apparent" distribution coefficient of oxygen in tungsten is unity at the zoning speed employed. Apply-

ing this same magnitude of reproducibility to the carbon values, sections 4–5 to 8–9 are statistically identical (6 p.p.m. ±35%), whereas sections to either side of these show a significant increase in concentration.

CONCLUSIONS

Since no particular difficulty in the determination of C, O, and N was posed by the widely different matrices (Fe, W, Cu, and Ag) used in this study, it is concluded that the proposed method of analysis can be extended to metals of all types.

Calibration for corrective sensitivity factors can be performed on available high p.p.m. samples with confident linear extrapolation to low concentrations of C, O, and N.

With the materials available for this study no instrument blank level was apparent that would adversely affect linear extrapolation to concentrations of C, O, and N in the p.p.b. range.

Because other blank lowering procedures such as extensive baking are time consuming and apparently non-reproducible, the faster method of cryosorption pumping in the source chamber is especially valuable in lowering and controlling the level of C, O, and N, as well as hydrocarbon species. The time required for a determination of these elements using the cryosorption method is no different from that for normal spark source procedures where presparking is employed. That is, analysis of a metal for C, O, and N from sample preparation through data reduction would require about 3 hours. Dividing instrument operation and data processing between two people would increase the daily sample throughput by a factor of three.

Although average bulk concentration values are useful in many applications, the degree of homogeneity or the impurity distribution is more important to most metallurgical problems. The scanning method presented here offers a guide to the degree of homogeneity, and the localized sampling of the rf spark is shown to produce an accurate, precise representation of impurity distribution.

ACKNOWLEDGMENT

The authors thank Professor E. Scala, Materials Science and Engineering Department, Cornell University, for supplying the zone refined tungsten rod used in this study.

LITERATURE CITED

(1) Albert, P., *Proc. Int. Conf.: Modern Trends in Activation Analysis*, pp. 78–85, College Station, Texas, 1961.
(2) Bate, L. C., *Nucleonics* **21**, 72–5 (1963).
(3) Fassel, V. A., Dallmann, W. E., Skogerboe, R. K., Horrigan, V. M., ANAL. CHEM. **34**, 1364 (1962).
(4) Gordon, W. A., Graab, J. W., Tumney, Z. T., *Ibid.*, **36**, 1396 (1964).
(5) Goward, G. W., *Ibid.*, **37**, 117R (1965).
(6) Harrington, W. L., Skogerboe, R. K., Morrison, G. H., *Ibid.*, **37**, 1480 (1965).
(7) Henry, W. M., "Development of Anal. Tech. for the Detn. of Minute Quantities of Selected Elements in Beryllium," Battelle Memorial Institute Final Report, July 22, 1963.
(8) Iron and Steel Institute Special Report, **68**, "The Detn. of Gases in Metals," London, 1960.
(9) Kennicott, P. R., "A Computer Program for the Quantitative Interpretation of Mass Spec. Plates," Report No. **64-RL-3766G**, Research Information Section, General Electric Research Laboratory, Schenectady, N. Y., 1964.
(10) McCrea, J. M., "Developments in Applied Spectroscopy," Vol. 4, E. N. Davis, Ed., p. 501, Plenum Press, N. Y., 1965; *Spectrochim. Acta* **21**, 1014 (1965).
(11) Roboz, J., in "Trace Anal.: Physical Methods," G. H. Morrison, Ed., p. 497, Interscience, New York, 1965; Proc. XI Ann. Conf. Mass Spectrometry and Allied Topics, Paper 103, San Francisco, 1963.
(12) Socha, A. J., Willardson, R. K., XI Annual Conf. on Mass Spectrometry and Allied Topics, Paper 84, San Francisco, 1963.
(13) Winge, R. K., Fassel, V. A., ANAL. CHEM. **37**, 67 (1965).

RECEIVED for review March 7, 1966. Accepted April 11, 1966. Research supported by the Advanced Research Projects Agency.

Quantitative Separation of Mercury–Thallium Mixtures

R. G. DOSCH

Sandia Laboratory, Albuquerque, N. M.

▷ Two methods for quantitative separation of Hg and Tl are described: a cation exchange method using $HClO_4$ eluent with a separation time of 3 hours, and a reduction procedure using SO_2 to reduce Hg(I) and Hg(II) to Hg° with a separation time of 15 minutes. Procedures were applied to mixtures ranging from Hg(II)–Tl(I) ratios of 20:1 to Tl(I)–Hg(II) ratios of 5:1.

INTEREST in low temperature switch materials has initiated compatibility studies between Hg–Tl amalgams and a number of different materials. Collection and reduction of data obtained from these studies require quantitative chemical analyses to determine initial and final compositions of the Hg–Tl amalgams used in the experiments.

Several methods have been used to separate Hg from Tl prior to analysis. Foley and Osyany (*2*) used formic acid to reduce Hg(II) from solution as Hg°, the thallium remaining in solution as Tl(I). The method of Richards and Daniels (*8*) involves bubbling air through the amalgam to form thallous oxide and free mercury, followed by selective dissolution of the oxide with dilute sulfuric acid. Korenman (*5*) suggests precipitation of thallium as Tl_2CrO_4 in ammoniacal media in the presence of KCN. The Hg(II) ion forms a stable complex with KCN and does not react with K_2CrO_4.

Bhatnager and Trivedi (*1*) used sodium nitrite to elute Hg(II) in a cation exchange separation of Hg(II)–Tl(I) mixtures. The Tl(I) was subsequently eluted with sodium sulfate solution.

The purpose of this work was to find a rapid procedure to effect a quantitative chemical separation of mercury and thallium applicable to the analysis of Hg–Tl amalgams. The previously described methods were considered to be undesirable for this purpose due to lengthy reduction and oxidation procedures, incomplete separation, or large eluent volumes.

This paper describes two procedures for quantitatively separating Hg–Tl mixtures: a cation exchange procedure using $HClO_4$ as the eluent and a reduction procedure using SO_2 to reduce Hg(I) or Hg(II) to Hg°. Quantitative recovery of mercury and thallium was obtained in both procedures using mixtures ranging from Hg(II)–Tl(I) ratios of 20:1 to Tl(I)–Hg(II) ratios of 5:1.

ION EXCHANGE SEPARATION OF MERCURY–THALLIUM MIXTURES

Experimental. COLUMN PREPARATION. The borosilicate glass ion exchange columns were 30 × 1 cm. (i.d.). The resin used was Dowex

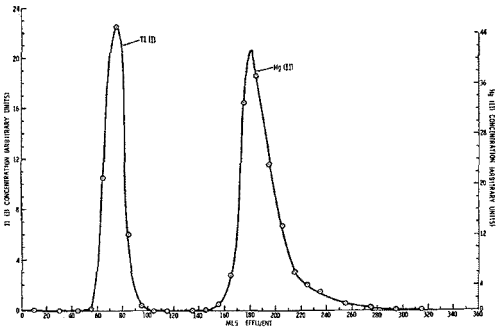


Figure 1. Elution curves of thallium and mercury, 12.5% $HClO_4$, flow rate 2 ml. per minute

AG-50WX8, 100- to 200-mesh, hydrogen form. Twenty-seven grams of resin, dry weight, were used in the columns. The resin was washed several times with distilled water, and the finest particles were decanted after each washing. The resin then was washed with 1*N* HCl, followed by distilled water washing until a negative chloride test was obtained.

REAGENTS. Mercury and thallium standard solutions were prepared from triply distilled mercury and A. R. grade thallous nitrate, respectively. Solutions were standardized using standard analytical methods (*3*, *4*). The 2.5% $HClO_4$ eluent was prepared by dilution of A. R. grade 70% $HClO_4$ to desired volume.

A 91.75% Hg–9.25% Tl amalgam was obtained from Taylor Instrument Co., Tulsa, Okla., in a sealed container. The container was opened and stored in an argon atmosphere containing less than 1 p.p.m. O_2 and less than 10 p.p.m. H_2O.

PROCEDURE. Samples of the amalgam were placed in quartz ampoules, evacuated, and sealed before removal from the argon atmosphere. To prevent error in sample weight due to air oxidation of the thallium in the amalgam, the ampoules were broken under distilled H_2O after the weight of the ampoule plus amalgam was obtained. Dissolution of the amalgam in a minimum amount of HNO_3 was done by covering the amalgam with H_2O, heating to near boiling, and adding HNO_3 dropwise until the reaction was complete. The resulting solution was filtered to remove the quartz, the weight of which was subtracted from the weight of ampoule plus amalgam. A coldfinger was used during dissolution of the amalgam to prevent loss of mercury by volatilization.

The Hg–Tl solutions obtained from the dissolution of amalgam and from standard solutions were diluted until the HNO_3 concentration was less than 1% and were put on the column at a flow rate of 2 ml. per minute. Both mercury and thallium were eluted with 12.5% $HClO_4$ at a flow rate of 2 ml. per minute.

Elution curves for mercury and thallium, Figure 1, were determined by standard techniques. Ten-milliliter fractions were collected and the mercury and thallium were analyzed polarographically using a Davis Differential Cathode Ray Polarograph, Model A 1660, obtained from Southern Analytical, Ltd., England.

With the exception of elution curve data, all mercury analyses were done volumetrically by a complexometric titration with thiocyanate (*4*). All thallium analyses were done polarographically.

Results and Discussion. Figure 1 is an elution curve for a solution containing 50 mg. of Ti(I) and 100 mg. of Hg(II). The solution containing less than 1% HNO_3 was put on the column and eluted with 12.5% $HClO_4$ at a flow rate of 2 ml. per minute. Failure to keep the HNO_3 concentration below 1% when putting the Hg(II)–Tl(I) solutions on the resin causes the subsequent elution of Tl(I) to tail badly, and Tl(I) elution is not complete before Hg(II) appears in the eluent.

An attempt was made to determine the cause of thallium tailing when put on the resin in greater than 1% HNO_3 solutions. In discussing the behavior of Tl(I) on cation exchange resin, Bhatnagar and Trivedi (*1*) state that thallium put on a cation column as Tl(I) is eluted as Tl(III) by 5% HNO_3 solution. Attempts to reproduce their observation in this laboratory proved unsuccessful as no evidence of oxidation of Tl(I) to Tl(III) by 5% HNO_3 solutions on the resin was found.

A Hg(II)–Tl(I) solution put on the column in 0.5% HNO_3 was eluted using 5% HNO_3. Tl(I) appeared in the eluent after 10 column volumes had been collected, and Hg(II) was eluted shortly thereafter, giving a very slight separation. Separation of Hg(II)–Tl(I) may be possible using HNO_3 on cation resin by changing parameters such as flow rate, column size, etc. However, practical use of such a procedure would be undesirable from a time consideration. The tailing shown by Tl(I) when put on the resin in 5% HNO_3 has not been explained; however, the effect is completely eliminated by reducing the HNO_3 concentration to less than 1%.

Table I. Analysis of Hg–Tl Mixtures

Tl, mg.		Hg, mg.	
Present	Found[a]	Present	Found[a]
10.4	10.4	21.1	20.9
52	51.7	105.6	105
104	104	211.3	210

[a] Each number represents the average of three determinations obtained by taking the given listed amount of Tl or Hg and varying the Hg or Tl concentration to give solutions of approximate Hg:Tl ratio of 20:1, 1:1, 1:5.

Table I contains data obtained from Hg–Tl mixtures separated prior to analyses of the constituents using the ion exchange procedure.

REDUCTION PROCEDURE

The use of H_2SO_3 in reducing solutions of Hg(I) and Hg(II) to Hg seems to be omitted in current analytical chemistry literature and reference material. While a reference to this reduction applicable to analytical use was found (*6*), no conditions for the reduction were given, and no statement relating to the completeness of reaction was found.

Although the ion exchange procedure described above was an improvement on existing methods from our standpoint and was used satisfactorily in this laboratory, the separation times for Hg–Tl solutions were 1 to 1.5 hours for thallium elution and another 2 hours for mercury elution. A procedure is described in this section by which quantitative separation of Hg–Tl solutions is achieved in a total time for both elements of 10 to 15 minutes. Recovery of both mercury and thallium is quantitative.

Experimental. REAGENTS. The mercury and thallium solutions and the Hg–Tl amalgam used in this procedure are described in the reagent section above. The source of SO_2 (anhydrous) was a lecture bottle supplied by The Matheson Co.

PROCEDURE. Hg–Tl solutions containing approximately 1% HNO_3 were prepared from standard Hg and Tl solutions and by dissolution of Hg–Tl amalgam. Aliquots of these solutions were bubbled with SO_2 for approximately 2 minutes. A white precipitate is formed initially and rapidly goes to a light gray in color. The solutions were boiled gently, using a coldfinger to prevent Hg loss, until the precipitate was converted to shiny metallic Hg. If the solutions remained cloudly after two minutes of boiling, they were allowed to cool at room temperature until the supernatant liquid was clear. The solutions were then passed through Whatman No. 41H filter paper to remove the mercury. The filter paper containing the Hg was placed in a flask

Table II. Analysis of Hg–Tl Mixtures

Tl, mg.		Hg, mg.	
Present	Found[a]	Present	Found[a]
10.4	10.3	211.3	210.9
52	51.7	105.65	105.4
104	104	21.13	20.92

[a] Each number represents the average of three determinations obtained by taking the given listed amount of Tl or Hg and varying the Hg or Tl concentration to give solutions of approximate Hg:Tl ratios of 20:1, 1:1, and 1:5.

and the Hg was redissolved in HNO_3, and the solution was again passed through Whatman No. 41H filter paper to remove the original filter. The filtrate containing the Tl was boiled for 5 minutes to remove excess SO_2.

The analyses of the resulting Hg and Tl solutions were done as previously described in the procedure section.

Results and Discussion. The HNO_3 concentration of the Hg–Tl solution had no observable effect on reduction of Hg in the range of 1% to 10% HNO_3. However, the HNO_3 was held to a practical minimum to prevent redissolution of Hg.

The white precipitate observed initially in the SO_2 reduction of Hg(II) from Hg–Tl solutions was also observed in the SO_2 reduction of standard Hg(II) solutions. A quantity of the white precipitate was filtered from the solution, washed with acetone, and air dried. Examination of the precipitate by emission spectrographic and x-ray diffraction techniques showed a crystalline compound containing Hg as the only cation present. When the compound was heated in aqueous solution, the decomposition products identified were Hg metal, sulfur dioxide, and sulfate ion.

The chemical behavior of the compound corresponded to that of a sulfitomercurate(II), M_2 $[Hg(SO_3)_2]$, as described by Remy (*7*). When warmed, these salts decompose according to the equation $[Hg(SO_3)_2]^- \rightarrow Hg + SO_2 + SO_4^-$. Further heating causes the initial finely divided Hg to coalesce and form larger drops of mercury.

Recovery of mercury and thallium, after separation using this procedure, was quantitative. Emission spectrographic analysis of the Tl and Hg solutions after separation was unable to detect any cross-contamination of the two materials.

Table II contains data obtained from Hg–Tl mixtures separated prior to determination of the constituents, using this procedure.

LITERATURE CITED

(1) Bhatnagar, R. P., Trivedi, R. G., *Jour. Indian Chem. Soc.* **42**, 53 (1965).
(2) Foley, W. T., Osyany, J. M., ANAL. CHEM. **33**, 1657 (1961).
(3) Kolthoff, I. M., Elving, P. J., ed., "Treatise on Analytical Chemistry," Part II, Vol. 2, Section A by H. Onishi, p. 91, Interscience, New York, 1962.
(4) Kolthoff, I. M., Elving, P. J., ed., "Treatise on Analytical Chemistry," Part II, Vol. 3, Section A by J. F. Coetzee, p. 306, Interscience, New York, 1962.
(5) Korenman, I. M., "Analytical Chemistry of Thallium," pp. 51–53, Israel Program for Scientific Translations, Jerusalem, 1963.
(6) McAlpine, R. K., Soule, B. A., "Qualitative Chemical Analysis," p. 173, Van Nostrand, New York, 1933.
(7) Remy, H., "Treatise on Inorganic Chemistry," Vol. II, p. 473, Elsevier, New York, 1956.
(8) Richards, T. W., Daniels, F., *J. Am. Chem. Soc.* **41**, 1732 (1919).

RECEIVED for review February 1, 1966. Accepted March 28, 1966. Work supported by the United States Atomic Energy Commission.

Continuous Electrolytic Determination of Small Quantities of Gaseous Ammonia

NEIL S. SEGAL[1] and ROBIN WODLEY-SMITH[2]

Department of Chemistry, University of the Witwatersrand, Jan Smuts Ave., Johannesburg, South Africa

▷ **An apparatus for the continuous determination of small amounts of ammonia in a gas stream is described. The ammonia is absorbed in an aqueous solution and the resulting solution titrated with electrolytically-generated hydrogen ions. A constant pH is thereby maintained in the titration cell. The current required to do this is, by Faraday's law, directly proportional to the flow rate of the ammonia and this current is monitored as a measure of the ammonia flow rate. The apparatus has been successfully used in analyzing flow rates of ammonia from about 10^{-6} to 10^{-3} mg. per second.**

In investigating the catalytic synthesis of ammonia using a continuous flow system, it was necessary to analyze the ammonia content of the exit gases continuously. Ammonia can be very accurately estimated by coulometric titration with hypobromite using amperometric end point detection (*1*, *6*, *10*), but this type of end point detection does not lend itself to a continuous, automatic procedure. A coulometric titration where the equivalence point is detected potentiometrically has often found application in such cases, and it is a technique of this type which is described here. The method is based upon the methods used for the determination of mustard gas in air (*3*, *4*, *12*) and of acidic or basic components of process gas streams (*5*).

Bogoslovskii *et al.* (*2*) have recently published a method for the determination of ammonia in a stream of gas using a conductometric technique. The gas is bubbled into a special cell containing 0.3*N* sulfuric acid, and the decrease in hydrogen ion concentration as ammonia is dissolved causes the resistance of the solution to change. This change in electrical resistance, which is a function of the ammonia concentration, is measured using an alternating current. Bogoslovskii's method (*2*) came to the attention of the present writers only after work on the system described here had commenced, but in any event, it is not sufficiently sensitive for the low rates of ammonia with which this study is concerned.

Continuous Coulometric Titration. A schematic diagram of the titration apparatus is shown in Figure 1. The ammonia-containing gas is bubbled into an aqueous solution, the pH of which is initially set in the region of the equivalence point of the NH_3–H^+ neutralization reaction. The dissolution of ammonia causes the pH of the solution to rise, this being detected by a pair of pH-sensitive electrodes. The potential developed by these electrodes relative to the previously set value is used as the input to a d.c. amplifier, the output of which is applied to two

[1] Present address, Department of Chemistry, Imperial College of Science and Technology, South Kensington, London S.W. 7

[2] Address, Department of Electrical Engineering, University of the Witwatersrand, Jan Smuts Ave., Johannesburg, South Africa

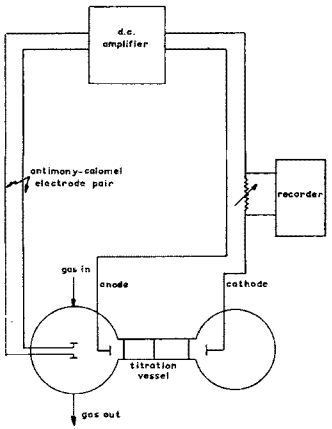


Figure 1. Schematic diagram of analyzer

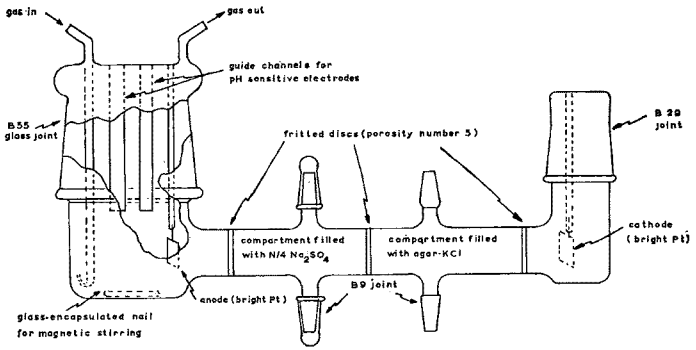


Figure 2. Titration vessel

bright platinum electrodes, one of which is in the original solution and the other in a separate solution which is in direct electrical contact with the former solution. The electrode polarities are so arranged that hydrogen ions are generated in the titration compartment (anode) in order to compensate any pH changes brought about by the absorption of ammonia, while hydroxyl ions are generated in the auxiliary compartment (cathode).

The suggested electrode reactions are as follows:

$$\text{cathode} \quad 4H_2O + 4e = 2H_2 + 4OH^-$$

In this compartment there is a steady increase in hydroxyl ion concentration as the protons are discharged electrically.

$$\text{anode} \quad 2H_2O = O_2 + 4H^+ + 4e$$

Here the incoming ammonia immediately reacts with hydrogen ions to form ammonium ions (NH_4^+), and the electrolytically liberated hydrogen ions stiochiometrically replace the hydrogen ions consumed. In this way the pH is maintained constant and the ammonia is titrated coulometrically.

The potential drop across a standard resistance placed in series in the current generating circuit is measured continuously on a potentiometric recorder. The generating current is proportional to the rate of liberation of hydrogen ions and thus to the rate of dissolution of ammonia.

EXPERIMENTAL

Titration Vessel. The requirements of titration vessels have often been discussed (*7*, *8*, *16*), but seldom with reference to long term continuous work. Briefly, the problem is that at the auxiliary generating electrode there occurs the reverse of the desired electrode reaction; in the present case the excess hydroxyl ions generated at the cathode provide a sufficient concentration gradient for hydroxyl ions to diffuse into the titration chamber, thus causing erroneous readings.

The cell design eventually used to counteract this diffusion is shown in Figure 2. It is based partly on the work of Taylor and Smith (*16*).

Electrolyte. An aqueous solution of about 0.25*N* sodium sulfate is used in both compartments. About 40–50 ml. is placed in the titration chamber.

Detecting Electrodes. A saturated calomel electrode is used as reference electrode. A sleeve-type is preferable to a wick-type for long term use as the latter tends to become clogged and the liquid cannot drain. However, it is important with a sleeve-type electrode that the potassium chloride should not drain too fast as the pH-sensitive antimony electrode (see below) may be poisoned by excess of chloride.

The choice of the pH-sensitive electrode presents some difficulties. The glass electrode has a fast response and attains equilibrium rapidly. But, as the input stage of the amplifier (see below) consists of a pentode with an input impedance of approximately 1 megohm and as a glass electrode has an impedance of between 10 and 100 megohms, its use with this particular amplifier is clearly impossible.

An antimony electrode proves successful, despite the fact that it has been criticized as being unreliable (*11*). This criticism, however, is primarily because the electrode does not give precise values of the absolute pH, and this is of no concern in the present work. Because of its low resistance, this electrode is insensitive to noise and this is a great advantage in a system such as the one under discussion. The general behavior of the antimony electrode has been discussed with reference to the pretreatment, the effect of oxygen, the effect of stirring, chemical interferences, the temperature coefficient, and so on (*13*).

In the present work the electrode pretreatment proceeds as follows. A stick of technical, cast antimony is cleaned and polished using a very fine emery cloth, leaving as smooth a surface as possible, and then well washed with distilled water and wiped with a soft cloth. The clean electrode is allowed to stand in distilled water for about two days to oxidize slightly (*9*), after which it is ready for use. If the electrode is removed from the measuring cell and wiped with a soft cloth once a day, it can be used for at least a few months. If, however, the oxide layer becomes

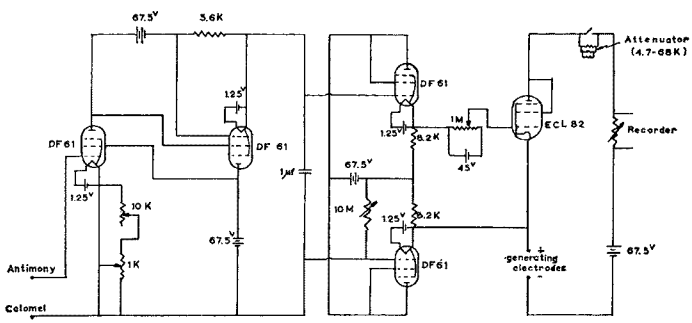


Figure 3. Circuit diagram of amplifier

thick, the electrode response is then sluggish and it should be replaced with a freshly prepared electrode.

To obtain as short a response time as possible, the solution is well stirred by a magnetic stirrer. In addition, the gas inlet is directed away from the detecting electrodes as any bubbles adhering to them give rise to spurious potentials.

Amplifier. The three-stage d.c. amplifier is based on the design of Shaffer *et al.* (*3, 4, 12*). The circuit diagram is given in Figure 3.

The first stage is a series balance voltage amplifier, providing a voltage gain of 700 and having under steady conditions a very high input impedance compared with the impedance of the detecting electrodes. The output impedance of this stage is 1.8 megohms, and together with the 1-μf. capacitor across its output, a low-pass filter is obtained, the gain of which is -3 db. at 0.1 c.p.s. and -20 db. at 1.0 c.p.s. This is a simple yet effective method of attenuating higher frequency noise present at the input and still providing a dynamic response capable of following system variations. (The time constant of the whole system is about 2 seconds.)

The second stage is a balanced cathode follower amplifier which provides the necessary isolation between detecting and generating electrodes. Thus a potential difference existing between the calomel reference electrode and the positive generating electrode appears across the 10-megohm grid leak resistance, affecting both tubes equally and producing no variations in the output voltage.

The final stage supplies the current necessary to neutralize the incoming ammonia.

The bank of resistances in the generating circuit provides a simple yet effective attenuation system. This helps not only to mask the effect of fluctuations in potential in the solution on the record obtained, but also to prevent the over-generation of hydrogen ions at the start of analysis. This latter effect is the result of the unusual resistance characteristics of the titration system: the resistance of the cell is high for no current flowing, but it decreases rapidly as current starts to flow and consequently far more hydrogen ions are generated than are actually necessary to neutralize the ammonia.

Procedure. Since the ammonia will cause the pH of the electrolyte to rise and in order to achieve as sensitive a response to pH changes as possible, the electrolyte is set initially at a pH corresponding to the start of the steep region of the conventional titration curve. This is done simply by using a d.c. source to generate H^+ or OH^- as required, and the actual value of the pH is about 6. The coarse- and fine-control (10 kilohm and 1 kilohm) potentiometers in the first stage are now adjusted so that for this particular pH setting there is no output from the amplifier. As soon as ammonia is absorbed by the solution, the input potential to the amplifier is changed, the amplifier is now off-balance, and current is generated in the output circuit.

RESULTS AND DISCUSSION

The performance of the amplifier is extremely good, there being no noticeable drift even over long periods. It is simple, easy to construct, and inexpensive. It must be pointed out, however, that far more refined systems have been developed which are undoubtedly electronically superior to that used here (*5, 14, 15*). In this laboratory F. Fisher has extended the method described here for use in a more conventional (and costly) coulometric titration apparatus consisting of a glass-calomel electrode pair, a standard pH meter as preamplifier, and a commercial high-gain amplifier.

To determine whether (in the range of ammonia rates with which this work has been concerned) all the ammonia is dissolved, a separate experiment was carried out. After bubbling through the titration chamber, the gas stream was led into a second vessel containing an aqueous solution with some Nessler's reagent. For the normal range of ammonia rates (about 10^{-4} to 10^{-5} mg. per second) there was no noticeable color change in the second solution during 12 hours of bubbling. Provided the titration solution is changed sufficiently often, all the ammonia is dissolved. In practice, the solution was changed at least once every 24 hours.

This analytical system has been used continuously for about 18 months in the range of generating current from about 0.01 to 5 ma., corresponding to a flow rate of ammonia from about 1.75×10^{-6} to 9×10^{-4} mg. per second. The carrier gas, normally a 3:1 mixture of hydrogen and nitrogen, has flowed at a rate usually between 1 and 5 liters (S.T.P.) per hour. All ammonia rates have been found to be within 4% of values obtained on sampling and analysis by conventional chemical means (absorption in a 2% boric acid solution followed by titration with standard hydrochloric acid).

Normal ambient temperature variations have not caused undue difficulties with the apparatus and, while this has not been studied, it is felt that any such fluctuations probably lie within the overall limits of accuracy of the whole procedure.

The convenience of this method suggests that it could find application in industry, in biological studies, or as here, in studies of catalysis and reaction kinetics.

LITERATURE CITED

(1) Arcand, G. M., Swift, E. H., ANAL. CHEM. **28**, 440 (1956).
(2) Bogoslovskii, Y. N., Kudrashov, V. I., Luzyanin, B. P., Makarov, G. N., Muzychenko, L. A., *Zavodsk. Lab.* **29**, 158 (1963); *Engl. transl.* **29**, 139 (1963).
(3) Briglio, A., Brockman, J. A., Schlinger, W., Shaffer, P. A., *U. S. Dept. Comm. Office Publ. Board OSRD Rept.* **6047**, PB 5925, 1945.
(4) Briglio, A., Brockman, J. A., Shaffer, P. A., *Ibid.*, **6183**, PB 5940, 1945.
(5) Burnett, R. L., Klaver, R. F., ANAL. CHEM. **35**, 1709 (1963).
(6) Christian, G. R., Knoblock, E. C., Purdy, W. C., *Ibid.*, **35**, 2217 (1963).
(7) Einsel, D. W., Trumit, H. J., Silver, S. D., Steiner, E. C., *Ibid.*, **28**, 408 (1956).
(8) Epstein, J., Sober, H., Silver, S., *Ibid.*, **19**, 675 (1947).
(9) King, N. J., IND. ENG. CHEM., ANAL. ED. **5**, 323 (1933).
(10) Krivis, A. F., Supp, G. R., Gazda, E. S., ANAL. CHEM. **35**, 2216 (1963).
(11) Mattock, G., "pH Measurement and Titration," Heywood, London, 1961.
(12) Shaffer, P. A., Briglio, A., Brockman, J. A., ANAL. CHEM. **20**, 1008 (1948).
(13) Stock, J. T., Purdy, W. C., Garcia, L. M., *Chem. Revs.* **58**, 611 (1958).
(14) Takahashi, T., Nilu, E., Sakurai, H., *J. Electroanal. Chem.* **3**, 373 (1962).
(15) Takahashi, T., Sakurai, H., *Ibid.*, **3**, 381 (1962).
(16) Taylor, J. K., Smith, S., *J. Res. Natl. Bur. Std.* **63A**, 153 (1959).

RECEIVED for review August 31, 1965. Accepted November 12, 1965. Thanks are expressed to the South African Council for Scientific and Industrial Research and to the South African Atomic Energy Board for a bursary to R.W.S. and N.S.S., respectively.

Determination of Diphenhydramine and Certain Related Compounds by Ultraviolet Spectrophotometry

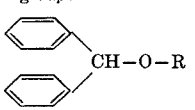
JACK E. WALLACE, JOHN D. BIGGS, and ELMER V. DAHL

Forensic Toxicology Branch, USAF Epidemiological Laboratory, Lackland Air Force Base, Texas

▷ **A rapid method for determining diphenhydramine and some related compounds permits analysis for those substances in biological materials in the presence of other alkaline drugs without preliminary separation. In the procedure, acid hydrolysis of the ether linkages in the compounds is followed by oxidation of the resulting secondary alcohol to yield steam-distillable products which, in contrast to the original compounds, have a high molar absorptivity and a well-defined absorption maximum in the ultraviolet region. The method is specific for a group of compounds which have a diphenylmethyl ether functional group and are extractable as bases. It is sufficiently sensitive to determine concentrations of the drugs in urine after therapeutic doses.**

THE ANTIHISTAMINES have a wide medical use. Most of them have a low toxicity but they do, nevertheless, frequently demand attention in a forensic toxicology laboratory and there is a need for analytical methods which permit specific identification and quantitative determination of these compounds in biological materials.

This report concerns a spectrophotometric method of analysis for diphenhydramine (Benadryl), [2-(benzohydryloxy)-*N*, *N*-dimethylethylamine hydrochloride], and the related compounds bromodiphenhydramine (Ambodryl) and diphenylpyraline (Diafen). Dimenhydrinate (Dramamine) differs from diphenhydramine only in that it is the 8-chlorotheophyllinate rather than the hydrochloride of the same organic base, and will not be considered separately. Each of the compounds has a structure which includes a diphenylmethyl ether functional group:



Many analytical methods have been devised for determining these compounds. Some of the methods are suitable for assaying the drugs in pharmaceutical preparations. Others are sufficiently sensitive for use on biological materials but lack the specificity necessary for identification of the substance measured. Thus, many nitrogenous bases other than the drugs in question give a positive reaction in the colorimetric method of Dill and Glazko (*7*), in the modification of that method for fluorometric assay (*6*), and in the nonaqueous titration techniques described in several reports (*8*, *12*, *13*, *17*, *18*, *21*, *22*).

Various chromatographic means have been adapted for determining the antihistamines. Paper chromatography (*1*, *2*, *4*, *11*, *15*, *24*), thin layer chromatography (*5*, *9*), and gas chromatography (*10*, *14*, *16*) have all been used to separate, identify, and quantitate these compounds. The chromatographic procedures are sensitive, but many of them lack an ability to provide the positive identification from biologic samples which is required in a forensic toxicology laboratory.

Diphenhydramine and its related compounds absorb ultraviolet radiations weakly, and for that reason ultraviolet spectrophotometric methods are not sufficiently sensitive for the direct determination of these drugs in therapeutic concentration in biologic materials (*3*, *23*). Further, direct ultraviolet spectrophotometric methods are subject to interference by other alkaline drugs which absorb in the region of 260 mμ.

The method to be described is rapid, sensitive, and is group specific for diphenhydramine and those related compounds which extract as bases and which have a diphenylmethyl ether functional group. Preliminary separation from other alkaline drugs is unnecessary. In the determination, acid hydrolysis of the ether linkage is followed by oxidation of the resulting benzhydrol to benzophenone in acid dichromate. The benzophenone is steam distilled from the reaction flask for final spectrophotometric assay. The method and its results will be described for diphenhydramine, with notation of the differences which apply when it is used for bromodiphenhydramine.

EXPERIMENTAL

Apparatus. A Beckman DK-2A ratio - recording spectrophotometer with linear presentation, settings and operation routine, was used for the ultraviolet absorption measurements. The sample path length was 10 mm. throughout. A Beckman IR-4 double beam infrared spectrophotometer was used for infrared spectral characterization of the reaction products. These were purified and prepared for infrared analysis by extraction of an appropriate steam distillate with methylene chloride, evaporation of the organic solvent in a rotary vacuum evaporator, and suspension of the residue in anhydrous potassium bromide.

Procedure. Ten-milliliter amounts of whole oxalated blood or serum, or 20- to 50-ml. amounts of urine containing the compound or suspected of containing the compound, are placed in a separatory funnel to which 5 ml. of 1*N* NaOH and 200 ml. of ether are added. This mixture is shaken vigorously for 5 minutes, after which the organic and aqueous phases are allowed to separate. The lower aqueous layer is removed and discarded. The ether layer is transferred from the separatory funnel and is filtered through Whatman No. 541 filter paper into a graduated cylinder. The volume of ether recovered is recorded. Complete recovery of the ether should not be attempted, but a correction for the lost ether must be included in the final calculations. Ten milliliters of 1*N* H_2SO_4 are added to the filtered ether. This mixture is shaken for 5 minutes. After the ether and aqueous layers have separated, 9 ml. of the aqueous layer are transferred to a 1000-ml. round-bottom flask to which a steam distillation assembly can be connected. Ten milliliters of 0.1*N* potassium dichromate in 10*N* H_2SO_4 are added to the flask. Distillation is initiated by allowing steam to pass into the intact assembly. The distillate should appear at a rate of approximately 5 ml. per minute. Fifty milliliters of distillate are collected and read against a blank at 257 mμ except for bromodiphenhydramine, which is read at 267 mμ. The blank should be a distillate obtained by subjecting 10 ml. of blood or 20–50 ml. of urine containing no drug to the same procedure outlined above.

If the spectrophotometric reading indicates a concentration of reaction product in the distillate equivalent to less than 2.5 μg. of drug per ml., then the following concentration procedure should be carried out. Fifty milliliters of distillate are extracted by vigorous shaking with 10 ml. of methylene chloride, in which the reaction products are preferentially soluble. After the

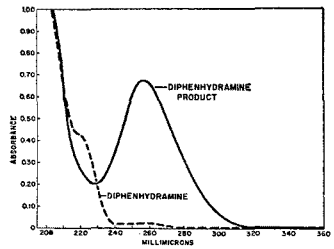


Figure 1. Ultraviolet absorption spectra of diphenhydramine 10 μg. per ml. of water and of the steam-distilled diphenhydramine reaction product corresponding to a sample of equivalent concentration

phases have separated, 8 ml. of the methylene chloride are placed in a 125-ml. flask which is then attached to a rotary vacuum evaporator. The solvent is evaporated by vacuum while the flask rotates at room temperature, with no heat applied. The vacuum is released as soon as the methylene chloride is completely removed. The residue is dissolved in 2, 4, or 8 ml. of water, depending on the absorbance previously observed for the unextracted distillate.

The content of diphenhydramine or related drug in the sample is calculated from a standard curve prepared from aqueous solutions of the drugs in appropriate concentrations carried in identical fashion through the procedures which have been outlined, including the concentration technique for solutions containing only small amounts of drug.

Table I. Standard Curve of Steam Distilled Diphenhydramine Reaction Product

Diphenhydramine in sample, μg./ml.	Absorbance of steam distillate	Absorbance / concentration
20	1.37	0.068
15	1.00	0.067
10	0.66	0.066
5	0.33	0.066
2	0.12	0.060

RESULTS AND DISCUSSION

The ultraviolet absorption curve of the steam-distilled reaction product of diphenhydramine is well defined. It has an absorption maximum at 257 mμ and a minimum at 228 mμ. The high absorbance at 257 mμ, illustrated in Figure 1, provides the increase in sensitivity of the present method over that of techniques which rely on direct ultraviolet spectrophotometric analysis of unconverted diphenhydramine. Bromodiphenhydramine yields a steam-distillable product whose ultraviolet absorption curve has a maximum at 267 mμ and a minimum at 233 mμ (Figure 2). The ultraviolet absorption curves of the steam-distilled products of diphenhydramine and of diphenylpyraline are identical except that the

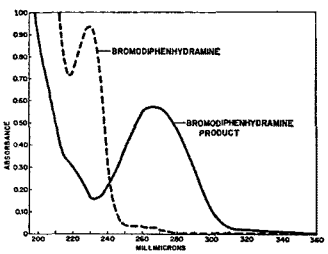


Figure 2. Ultraviolet absorption spectra of bromodiphenhydramine 15 μg. per ml. of water, and of the steam-distilled bromodiphenhydramine reaction product corresponding to a sample of equivalent concentration

curve for diphenylpyraline yields lower values per unit concentration of drug in the original sample.

Inability of the method to distinguish between diphenhydramine and diphenylpyraline is considered to be no serious defect. The medical use and pharmacologic effect of the two drugs is similar.

Absorbance of the steam-distilled reaction product has a linear relationship, at the levels investigated, to concentration of drug in the original

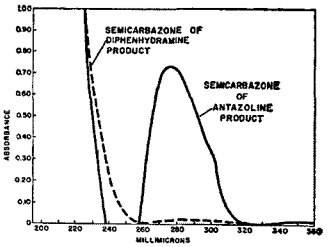


Figure 3. Ultraviolet absorption spectra of the semicarbazones of steam-distilled reaction products of antazoline and diphenhydramine, each derived from aqueous solutions corresponding to 20 μg. of drug per ml.

sample. Table I shows this relationship for diphenhydramine.

Table II, summarizes the recovery of diphenhydramine which had been added in known amounts to whole blood, urine, and homogenized liver. The average recovery was greater than 90% in each case.

In four adult human males, each of whom received 100 mg. of Benadryl by mouth, the concentration of diphenhydramine in the urine was found to be 0.55 to 2.90 (average 1.36) μg./ml. in samples collected at the end of the first 4 hours following ingestion of the drug. Samples collected at the end of the second 4-hour interval contained from 0.56 to 2.09 (average 1.36) μg./ml.; and those from the third 4-hour interval, 0.11 to 2.63 (average 1.73) μg./ml. Samples from the interval 12 to 24 hours after taking the drug contained from 0.37 to 3.51 (average 1.59) μg./ml. While the diphenhydramine concentration in the individual samples varied considerably from person to person, the total amount excreted in the urine by the four subjects during the first 24 hours was less variable: 1.38 to 1.59 (average 1.49) mg.

Other drugs, including numerous antihistamines, which might be given to patients together with diphenhydramine or its related compounds were investigated for interference. Each substance was added to whole blood and carried through the procedure outlined. Only antazoline produced a steam-distillable product with significant absorbance at 257 mμ (Table III). That product had an ultraviolet absorption maximum at 247 mμ and a minimum at 222 mμ. Antazoline (Antistine) is not used internally; it is used topically as eye drops. If, under unusual circumstances, there is a question of the presence of this drug, it can be determined quantitatively, even in the presence of diphenhydramine, by conversion of the steam-distilled antazoline reaction product to a semicarbazone which has an ultraviolet

Table II. Recovery Studies of Diphenhydramine

Diphenhydramine added, μg./ml.	Recovery, mean ± std. dev. (μg./ml.) Whole blood	Urine	Homogenized liver
50.0	45.7 ± 1.1	48.5 ± 0.7	46.0 ± 1.1
25.0	23.5 ± 0.8	23.4 ± 0.5	22.5 ± 0.9
10.0	9.0 ± 0.2	9.8 ± 0.3	9.0 ± 0.2
5.0	4.4 ± 0.2	4.6 ± 0.2	4.7 ± 0.2
2.5	2.2 ± 0.1	2.4 ± 0.2	2.3 ± 0.2
Average recovery	90.2%	95.2%	91.5%

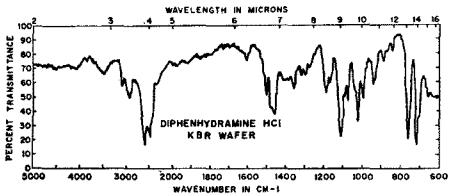


Figure 4. Infrared absorption spectrum of diphenhydramine hydrochloride, 2 mg. in 400 mg. of potassium bromide

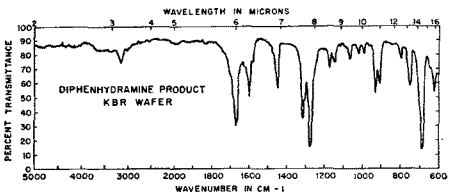


Figure 5. Infrared absorption spectrum of the steam-distilled diphenhydramine reaction product, 2 mg. in 400 mg. of potassium bromide

absorption maximum at 278 mμ. For this specific determination of antazoline, 4 ml. of the steam distillate and 1 ml. of 0.5*M* semicarbazide in phosphate buffer at pH 7.0 are permitted to react at 100° C. for 10 minutes, a time sufficient to achieve equilibrium. The reaction mixture is cooled and read at 278 mμ against a blank prepared by the addition of 1 ml. of distilled water to 4 ml. of the steam-distilled reaction product. No significant semicarbazone formation by the diphenhydramine product takes place under these conditions (Figure 3).

Sulfuric acid is the acid of choice for extraction and hydrolysis in this procedure. Other acids decrease the specificity of the method by permitting hydrolysis of linkages besides that of the diphenylmethyl ether group concerned here.

Comparison of the infrared absorption spectra of diphenhydramine (Figure 4) and of its steam-distilled reaction product (Figure 5) shows several distinct differences, among them a strong carbonyl absorption band at 1660–1680 cm.$^{-1}$ which is present in the product but not in the parent compound. This carbonyl band is in the approximate region reported for the stretching vibrations of carbonyl groups with two aryl groups directly attached (*19*, *20*). Conjugation of the carbonyl group with aromatic rings would account for the increased ultraviolet absorptivity of the steam-distilled products.

The close similarity of the ultraviolet and infrared absorption spectra of diphenhydramine (Figures 1 and 4) with those of benzophenone (Figures 6 and 7) suggests that the reaction product is benzophenone. Its formation may be thought to include acid hydrolysis of the ether linkage followed by oxidation of the resulting secondary alcohol to a carbonyl grouping. Calculations from the ultraviolet absorption curves indicate that 96% of the diphenhydramine in the sample is converted to benzophenone. It is assumed that bromodiphenhydramine is converted to a para-bromo derivative of benzophenone.

Table III. Compounds Investigated for Interference with the Determination of Diphenhydramine[a]

Compound	Absorbance of steam distillate[b]	Compound	Absorbance of steam distillate[b]
Diphenhydramine	1.37	Meclizine	0.02
Bromodiphenhydramine (267 mμ)	0.72	Meperidine	0.01
Diphenylpyraline	0.62	Meprobamate	0.01
Blank	0.01	Methyl Phenidate	0.01
Acetylsalicylic acid	0.01	Morphine	0.01
Amitriptyline	0.02	Phenindamine	0.01
Amphetamine	0.01	Pheniramine	0.01
Antazoline (247 mμ)	0.92	Phenyramidol	0.05
Atropine	0.01	Pilocarpine	0.01
Azacyclonal	0.01	Pipradol	0.01
Buclizine	0.02	Prochlorperazine	0.01
Caffeine	0.01	Propoxyphene	0.02
Captodiamine	0.02	Thenyldiamine	0.04
Carbinoxamine	0.01	Thonzylamine	0.06
Chlorcyclizine	0.06	Tripelennamine	0.03
Chlorothen	0.05	Triprolidine	0.01
Chlorpheniramine	0.01		
Clemizole	0.01		
Cyclizine	0.09		
Doxylamine	0.01		
Ephedrine	0.01		
Hydroxyzine	0.04		
Lidocaine	0.01		

[a] Each compound was determined from whole blood, to which it had been added. The level in the distillate corresponds to a concentration of 20 μg. of the compound per ml. of sample. Each value is the average of three determinations.
[b] Read at 257 mμ unless otherwise indicated.

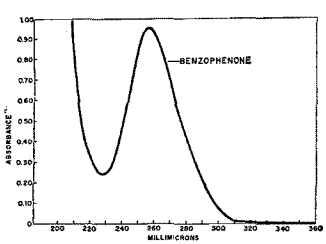


Figure 6. Ultraviolet adsorption spectrum of benzophenone, 10 μg. per ml. of water

LITERATURE CITED

(1) Baruffini, A., *Farmaco (Pavia) Ed. Prat.* **13**, 459 (1958).
(2) Belles, Q. S., Sievert, H. W., *J. Lab. Clin. Med.* **46**, 628 (1955).
(3) Brandstätter-Kuhnert, M., Hoffman, R., Senn, M., *Microchem. J.* **7**, 357 (1963).
(4) Curry, A. S., Powell, H., *Nature* **173**, 1143 (1954).
(5) Daly, J. W., Cochin, J., *J. Pharmacol. Exp. Therap.* **139**, 160 (1963).
(6) Dill, W. A., Glazko, A. J., *Federation Proc.* **21**, 269 (1962).

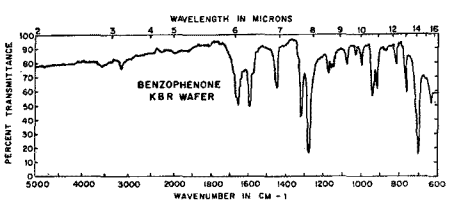


Figure 7. Infrared absorption spectrum of benzophenone, 2 mg. in 400 mg. of potassium bromide

(7) Dill, W. A., Glazko, A. J., *J. Biol. Chem.* **179**, 395 (1949).
(8) Ekeblad, P., *J. Pharm. Pharmacol.* **4**, 636 (1952).
(9) Fike, W. W., Sunshine, I., ANAL. CHEM. **37**, 127 (1965).
(10) Fontan, C. R., Smith, W. C., Kirk, P. L., *Ibid.*, **35**, 591 (1963).
(11) Goldbaum, L. R., Kazyak, L., *Ibid.*, **28**, 1289 (1956).
(12) Jasinski, T., *Acta Polon. Pharm.* **14**, 45 (1957).
(13) Kashima, T., Kano, K., *J. Pharm. Soc. Japan* **76**, 931 (1956).
(14) Kazyak, L., Knoblock, E. C., ANAL. CHEM. **35**, 1448 (1963).
(15) Kitamura, M., Okajima, S., *Yakkyoku* **6**, 837 (1955).
(16) MacDonald, A., Pflaum, R. T., *J. Pharm. Sci.* **52**, 816 (1963).
(17) Mainville, C. A., Chatten, L. G., *Ibid.*, **53**, 154 (1964).
(18) Murata, T., Ochiai, T., *Kumamoto Pharm. Bull.* **4**, 15 (1959).
(19) Randall, H. M., Fowler, R. G., Fuson, N., Dangel, J. R., "Infrared Determination of Organic Structures," p. 16, Van Nostrand, New York, 1949.
(20) Rasmussen, R. S., Tunnicliff, D. D., Brattain, R. R., *J. Am. Chem. Soc.* **71**, 1068 (1949).
(21) Rink, M., Riemhofer, M., *Mitt. Deut. Pharm. Ges.* **31**, 197 (1961).
(22) Selles, E., Rodriguez, A. M., *Galencia Acta (Madrid)* **9**, 33 (1956).
(23) Sunshine, I., Gerber, S. R., "Spectrophotometric Analysis of Drugs Including Atlas of Spectra," p. 39, Chas. C Thomas, Springfield, Ill., 1963.
(24) Vecerkova, J., Sulcova, M., Kacl, K., *Pharmazie* **17**, 22 (1962).

RECEIVED for review January 5, 1966. Accepted March 21, 1966.

Ultra Sensitive, Specific Method for Cyanide Using p-Nitrobenzaldehyde and o-Dinitrobenzene

GEORGE G. GUILBAULT and DAVID N. KRAMER

Defensive Research Department, Research Laboratories, U. S. Army Edgewood Arsenal, Md.

▷ **p-Nitrobenzaldehyde reacts with cyanide specifically to give an active reductant, which is capable of effecting the reduction of various compounds to form highly colored products. The intermediate cyanohydrin reacts with o-dinitrobenzene to give a highly colored purple compound, the dianion of o-nitrophenyl hydroxylamine, or with triphenyl tetrazolium chloride to produce a red dye, triphenyl formazan. Because cyanide is regenerated, a catalytic reaction occurs, with corresponding increase in sensitivity. Adding isonitroso benzoyl acetone, as little as 1.3 × 10^{-9} gram of cyanide per ml. of total solution (3 nanograms total CN^-) may be detected. Only p-nitro- and p-cyanobenzaldehyde of over 30 aldehydes tested react at an appreciable rate to form the reductive cyanohydrin. Only cyanide of more than 35 anions tested is detectable by this procedure.**

IN A PREVIOUS paper (*5*), we described a specific method for the detection and determination of cyanide using various quinone derivatives. Further experiments were conducted, in attempts both to improve the sensitivity of detection and to develop a water soluble system which might be applicable to enzymatic reactions.

Feigl (*2*) reported that a variety of reductants was capable of effecting the reduction of 1,2-dinitrobenzene(III) in the presence of alkali to *o*-nitrophenyl hydroxylamine. This reaction served as the basis for qualitative spot tests for such compounds as hydroquinone, ascorbic acid, benzoic acid hydrazide, and reducing sugars. See Reactions (1) and (2).

It was thought that a catalytic reaction involving aromatic aldehydes and cyanide would result in a benzoin condensation, whose products would reduce *o*-dinitrobenzene. The formation of the characteristic blue color of the *o*-nitrophenylhydroxylamine dianion (IV) could then be used to monitor the reaction. Aldehydes incapable of undergoing the benzoin condensation due to substitution by electron withdrawing groups (*p*-Br, *p*-NO_2), would not, therefore, be expected to participate in the reduction of *o*-dinitrobenzene (*3*, *4*). Nevertheless, it was found that *p*-nitrobenzaldehyde, in the presence of cyanide ion, rapidly effects this reduction.

p-Nitrobenzaldehyde readily forms a cyanohydrin (*1*) but does not undergo the benzoin condensation. Preliminary experiments indicated that this reaction can serve as the basis for a sensitive, specific method for the detection of cyanide. The cyanohydrin produced (II) reacts with *o*-dinitrobenzene(III) to give the highly colored blue compound(IV). Because cyanide is regenerated, a catalytic reaction occurs, with increased sensitivity.

Isonitrosobenzoyl acetone(IBA) serves as a further source for the production of the catalyst cyanide, permitting the determination of as little as 1.3 nanograms of cyanide. Only *p*-nitro and *p*-cyano benzaldehyde of over 30 aldehydes tested react at an appreciable rate to form the cyanohydrin, and only cyanide of over 35 anions tested is detectable by this procedure. No other ions interfere in concentrations up to 0.1*M*.

EXPERIMENTAL

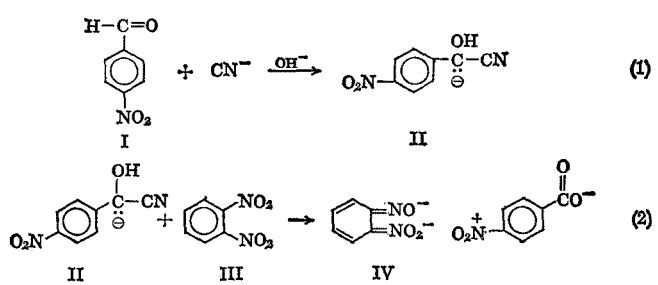
Reagents. All experiments were performed with reagent grade chemicals and pure solvents. All anions tested were added in the form of the C.P. sodium or potassium salt.

p-Nitrobenzaldehyde and *o*-dinitrobenzene solutions, 0.1*M*, were prepared by dissolving the C.P. compounds (Eastman Organics, Rochester, N. Y.) in methyl cellosolve.

Triphenyl tetrazolium chloride, 0.1*M* solution in tris (hydroxymethyl)amino methane buffer, 0.1*M*, pH 8.5, was obtained from the Nutritional Biochemical Corp.

Isonitrosobenzoyl acetone solution, 0.02*M*, was prepared by dissolving the pure compound [prepared in these laboratories by the method of Wolf (*10*)] in pH 8.5 borax buffer, 0.1*M*.

Preparation of Pure *o*-Nitrophenyl Hydroxylamine Monoacetate. Two grams of *o*-dinitrobenzene (Aldrich Chemical Co.) (0.012*M*) was dissolved in 50 ml. of tetrahydrofuran with



slight heat and stirring. Zinc dust (2.0 grams) and ammonium chloride (3.0 grams) were then added and the stirring was continued for 3 hours at room temperature. The initial pale yellow solution turned deep brownish yellow. The suspension was filtered and 15 ml. of acetic anhydride–pyridine (3:1) was added. The solution now became yellow. After 0.5-hour acetylation time, 10 volumes of ice water were added and 1.8 grams (83% yield) of a yellow solid was obtained, which upon recrystallization from ether–petroleum ether (40–60° C. fraction), melted at 44–5° C. (uncorr.). The purity of the compound was checked by infrared (N—H, 3.01 microns, ester carbonyl 5.72 microns), and elemental analysis ($C_8H_8O_4N_2$, Calcd.: C, 48.9; H, 4.08. Found, C, 48.4; H, 3.9). Repeated attempts to obtain stable preparations of *o*-nitrophenylhydroxylamine by the method of Kuhn and Weigand (*7*) were unsuccessful.

The bisulfite addition product of *p*-nitrobenzaldehyde was prepared by conventional means.

Isolation of Product of Reaction of *o*-Dinitrobenzene, *p*-Nitrobenzaldehyde, and Cyanide. The products of reactions 1 and 2 have been shown (*6*) to be *p*-nitrobenzoic acid and *o*-nitrophenylhydroxyamine. Thus, it was reasoned that the reaction must proceed as per reactions 1 and 2.

Apparatus. A Beckman model DB spectrophotometer was used in all experiments. A constant temperature of 25° C. was maintained using a constant temperature room.

Procedure. Qualitative Detection of Cyanide. To a reagent solution, containing 1 ml. of 0.1*M* *o*-dinitrobenzene, 1 ml. of 0.1*M* *p*-nitrobenzaldehyde, 0.1 ml. of 0.02*M* IBA and 0.1 ml. of 0.50*M* sodium hydroxide, is added 0.1 ml. of the unknown ion (containing at least 3×10^{-9} gram of the anion to be tested). If a purple color develops, cyanide is present.

Determination of Cyanide. A mixture consisting of 1 ml. of 0.1*M* *p*-nitrobenzaldehyde, 1 ml. of 0.1*M* *o*-dinitrobenzene, and 0.1 ml. of 0.5*M* NaOH is placed in each of two cuvettes in a spectrophotometer, and the absorbance is adjusted to read zero. At zero time, 0.1 ml. of a solution of the cyanide to be determined (containing 0.1 to 1.0 μg. of cyanide) is added. The rate of change in the absorbance with time is then measured, and from calibration plots of $\Delta A/\Delta t$ *vs.* cyanide concentration (45-450 nanograms per ml. of solution used), the amount of cyanide present can be calculated.

DISCUSSION AND RESULTS

Detection of Cyanide Using Reduction of *o*-Dinitrobenzene. A number of substituted benzaldehydes were screened for their ability to effect the reduction of *o*-dinitrobenzene in the presence of cyanide to *o*-nitrophenyl hydroxylamine. The rates of reduction were followed spectrophotometrically by monitoring the change in the absorbance at 560 mμ, ascribed to the di-aci-form of *o*-nitrophenylhydroxylamine(II) [(*7*) (Table I)].

p-Nitrobenzaldehyde reacted 20 times faster than *o*-nitrobenzaldehyde. The rate of reaction of the meta nitro derivative was immeasurably slow, but the rate is faster with higher concentrations of cyanide. The remaining aldehydes did not enter into the reaction, except for the *p*-cyano benzaldehyde, which had a rate approximately $^2/_3$ that of the *p*-nitro derivative. The 4-chloro-*m*-nitro derivative reacted at about the same rate as the *m*-nitro. The *p*-bromo and *p*-fluoro benzaldehydes did not react with cyanide at any appreciable rate to give a compound that effects the reduction of *o*-dinitrobenzene.

A kinetic study of the reaction (*6*) revealed a first order dependence on *p*-nitrobenzaldehyde and cyanide ion, and a zero order dependence on *o*-dinitrobenzene (Table II). In addition, the reaction is dependent on the amount of base present, being optimum at pH 9. The rate was measured by following the change with time of the absorbance at 560 mμ, which is the wavelength of maximum absorbance of the *o*-nitrophenylhydroxylamine anion.

Using the optimum concentrations of *p*-nitrobenzaldehyde and *o*-dinitrobenzene (0.1*M* added) and sodium hydroxide (0.1 ml. of 0.5*M* = pH 9), the reaction was found to be approximately proportional to the cyanide concentration, allowing the determination of this anion with a deviation of about 8%. Under these conditions, a $1.7 \times 10^{-6}M$ (45 nanograms per ml. of solution) concentration of cyanide could be assayed.

Over 30 anions were tested for possible reaction with *p*-nitrobenzaldehyde to form a compound that might effect the reduction of *o*-dinitrobenzene. None of the ions tested had any effect on either the qualitative or the quantitative determination of cyanide: iodide, chloride, bromide, sulfite, carbonate, cyanate, bicarbonate, phosphite, tungstate, bisulfate, bismuthate, arsenite, arsenate, perborate, iodate, molybdate, ferricyanide, ferrocyanide, phthalate, thiosulfate, chlorite, chlorate, thiocyanate, fluoride, silicate, bromate, sulfate, perchlorate, citrate, tartrate, nitrate, hypochlorite, sulfide, tellurite, and various nitriles and isocyanates. Some of the compounds had slight solubilities under the reaction conditions described, giving a moderately high initial absorbance caused by cloudiness. In the presence of dichromate, the color of the cyanide detection reaction is purple-black, the color being slightly obscured by the yellow color of dichromate. All materials were tested in

Table I. Relative Rates of Reduction of o-Dinitrobenzene by Substituted Benzaldehydes in Presence of Cyanide Ion

[*o*-Dinitrobenzene] = 0.1*M*; [Aldehyde] = 0.1*M*; [CN^-] = $5 \times 10^{-6}M$

[Aldehyde]	Δ Absorbance/Min.[a]
p-Nitro	0.20
o-Nitro	0.010
p-Cyano[b]	0.14
p-Me_2N; *p*-Et_2N; *m*-OH; 2,4,6-trihydroxy; 2-Cl, 4-Me_2N; *p*-isopropyl; *p*-H; *p*-methoxy; *p*-ethoxy; *p*-benzyloxy; 3,4 dimethoxy; 3,4,5 trimethoxy; *p*-acetimido; 2,4 dimethoxy; *p*-bromo; 2,4,6 trinitro[c]; 2,6 dichloro; *m*-methoxy; 2,4,6 trimethyl; 2-ethoxy 3-methoxy; *m*-fluoro; *p*-fluoro; 4-chloro 3-nitro[d]; *m*-nitro[d]; *o*-chloro	0

[a] A rate of zero indicated no reaction, regardless of the amount of cyanide added.
[b] Compound displays a green fluorescence.
[c] Turns red because of a pH effect.
[d] $2 \times 10^{-6}M$ cyanide needed to effect reaction.

Table II. Variation of Rate of Reaction Expressed as ΔA/min. on Concentration of o-Dinitrobenzene, p-Nitrobenzaldehyde, Cyanide, and pH (T = 23°C.).

o-Dinitrobenzene, *M*	*p*-Nitrobenzaldehyde, *M*	Cyanide, *M*	pH	Δ*A*/min.
5×10^{-2}	5×10^{-5}	5×10^{-6}	9	0.01
5×10^{-2}	1×10^{-4}	5×10^{-6}	9	0.02
5×10^{-2}	5×10^{-4}	5×10^{-6}	9	0.10
5×10^{-2}	5×10^{-2}	5×10^{-6}	9	0.60
2.5×10^{-5}	5×10^{-2}	5×10^{-6}	9	0.60
2.5×10^{-4}	5×10^{-2}	5×10^{-6}	9	0.60
5×10^{-2}	5×10^{-2}	5×10^{-7}	9	0.010
5×10^{-2}	5×10^{-2}	2.5×10^{-6}	9	0.040
5×10^{-2}	5×10^{-2}	5.0×10^{-6}	9	0.083
5×10^{-2}	5×10^{-2}	1.0×10^{-5}	9	0.17
5×10^{-2}	5×10^{-2}	2.0×10^{-5}	9	0.40
5×10^{-2}	5×10^{-2}	5×10^{-6}	8[a]	0.070
5×10^{-2}	5×10^{-2}	5×10^{-6}	7[a]	0.008
5×10^{-2}	5×10^{-2}	5×10^{-6}	9	0.70

[a] No correction was made for the effect of pH on molar absorptivity of the *o*-nitrophenylhydroxylamine. Also, at the lower pH values, the concentration of the cyanohydrin ion is lower.

Table III. Dependence of Rate of Reduction (ΔA/min.) of o-Dinitrobenzene by Cyanohydrin of p-Nitrobenzaldehyde Produced from the Spontaneous Decomposition of IBA

o-Dinitrobenzene = $5 \times 10^{-2}M$; *p*-nitrobenzaldehyde = $5 \times 10^{-2}M$ pH = 9.0, no cyanide added

IBA, M	ΔA/min.	Time for cyanide production, min.[a]
8.6×10^{-5}	0.015	20
1.7×10^{-4}	0.030	14
3.4×10^{-4}	0.060	10
6.8×10^{-4}	0.120	9
8.7×10^{-4}	0.150	7

[a] Time required for first appearance of color.

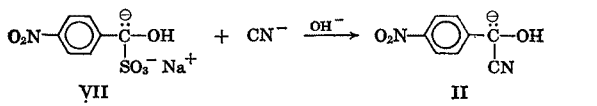
concentrations up to $10^{-1}M$. Thus, the method is specific for cyanide.

Molar Absorptivity of Dye. In order to measure the molar absorptivity of the blue dye produced from the reduction of the *o*-dinitrobenzene by the cyanohydrin of *p*-nitrobenzaldehyde, a pure sample of *o*-nitrophenyl hydroxylamine monoacetate was prepared as described in the experimental section. Known concentrations of the purified monoacetate were then hydrolyzed with excess base to form the blue compound, and the absorbance was determined at different pH's at various time intervals until stable, maximum values were obtained. The absorbance increased with increasing pH, reaching a maximum at about pH 10, and remained constant over the range 10–14. A pK was calculated for the Dianion of 8.5, and at a pH of 9.0 (the pH at which all determinations were made), a molar absorptivity of 2.3×10^3 was obtained. Although the molar absorptivity at pH 9 is only about 70% of that at 10 (3.5×10^3), the instability of the blue color at pH's > 9 necessitated the use of a below maximum pH.

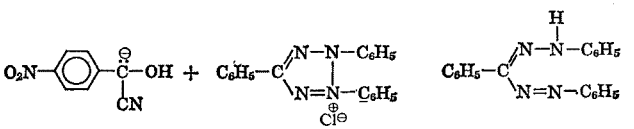
Addition of IBA. The sensitivity of the *o*-dinitrobenzene–*p*-nitrobenzaldehyde reaction for cyanide was found to be increased by the addition of the oxime isonitrosobenzoyl acetone (IBA). Adding 0.1 ml. of $0.02M$ IBA (overall $M = 8.7 \times 10^{-4}M$) to 1 ml. of $0.1M$ *p*-nitrobenzaldehyde and 1 ml. of $0.1M$ *o*-dinitrobenzene at a pH of 9, 1.30 nanograms of cyanide per ml. of total solution (3 nanograms total CN^- in the 2.3 ml. of solution used) can be detected. Catalysis by IBA(V) is believed due to the reaction of cyanide with IBA to form benzoyl and acetyl cyanide (reactions 3, 3a, and 3b). The hydrolysis of these two compounds then produces two molecules of cyanide for each original cyanide, or a further catalytic effect (*9*).

One disadvantage in the use of IBA as a sensitizer for the detection of cyanide, is that it is spontaneously decomposed at pH 9 to liberate cyanide after some time. The dependence of the rate of reduction of *o*-dinitrobenzene upon IBA, together with the time required for spontaneous production of cyanide, is indicated in Table III. Using the concentration of IBA recommended in the procedure for the most sensitive detection of cyanide, $8.7 \times 10^{-4}M$, 7 minutes is required before any significant purple color is observed to form in the absence of cyanide added. This is sufficient time to allow an analysis of cyanide. Also, the rate of reaction, ΔA/min., appears proportional to the concentration of IBA, thus providing a possible method for the assay of this compound (Table III).

Reduction of Triphenyl Tetrazolium Chloride. In attempting to apply the cyanohydrin reduction of *o*-dinitrobenzene procedure for detecting cyanide to the monitoring of enzymatic reactions that liberate cyanide, a completely water soluble system was sought. Compounds I and III are water insoluble, and could not be used. Hence a bisulfite addition product of I was prepared (VII), and the soluble dye triphenyl tetrazolium chloride(VIII) was used:

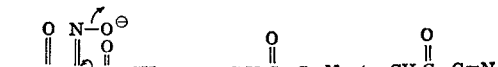


(4)

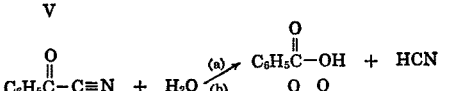


(5)

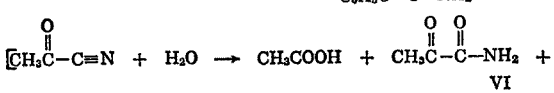
Triphenyl tetrazolium chloride(VIII) is reduced by II to a red colored compound (IX), triphenyl formazan (*8*). Using the optimum conditions for analysis [1 ml. of $0.1M$(VIII) in tris buffer, $0.1M$, pH 8.5; 1 ml. of $0.01M$(VII) in water and 0.1 ml. of $0.50M$ NaOH, overall pH 8.50], as little as $5 \times 10^{-6}M$ cyanide can be detected. Because this procedure is not so sensitive as the reduction of *o*-dinitrobenzene method ($2 \times 10^{-7}M$ cyanide detectable), further work on it was not pursued.



(3)



(3a)



(3b)

LITERATURE CITED

(1) Baleer, A. *et al.*, *J. Chem. Soc.*, **1949**, p. 1089.
(2) Feigl, F., "Spot Tests in Organic Analysis," pp. 131–2, Elsevier, New York, 1956.
(3) *Ibid.*, pp. 205–6.
(4) Gould, E. S., "Mechanism and Structure in Organic Chemistry," pp. 396–7, Holt, Reinhart, and Winston, New York, 1962.
(5) Guilbault, G. G., Kramer, D. N., ANAL. CHEM. **37**, 1395 (1965).
(6) Kramer, D. N., Guilbault, G. G., *J. Org. Chem.*, in press.
(7) Kuhn, R., Weigand, F., *Ber.* **69** (2), 1969 (1936).
(8) Lakon, A., *Compt. Rend. Assoc. Intern. Essais Semences* **1**, 1 (1940).
(9) Poziomek, E., Crabtree, E., Edgewood Arsenal Rept., U. S. Army Edgewood Arsenal, Md., in press.
(10) Wolf, L., *Ann.* **325**, 136 (1902).

RECEIVED for review November 8, 1965. Accepted December 27, 1965.

Apparatus and Procedures for Rapid Extraction and Identification of Pesticides by Single and Multiple Distribution in Binary Solvent Systems

MORTON BEROZA

Entomology Research Division, Agricultural Research Service, U. S. Department of Agriculture, Beltsville, Md.

MALCOLM C. BOWMAN

Agricultural Research Service, Tifton, Ga.

▷ A new apparatus capable of performing many simultaneous extractions rapidly extracts small volumes of one liquid phase with another. Equilibration of a solute between the phases is usually complete after 20 seconds of mechanical agitation because of the large interfacial contact between the small volumes. Because new, highly sensitive instrumental methods of analysis require only very small samples and use highly purified solvents, extractions with small volumes are desirable to avoid wasting these expensive solvents. The time-consuming evaporation of extracts to small volumes is also minimized. The value of extractions with unequal volumes of the two solvent phases, especially for identification purposes, was demonstrated. Mathematical equations and graphs relating the distribution of a solute between equal and unequal phase volumes to its p-value are presented.

APPARATUS for the rapid extraction of one liquid phase with another immiscible one, especially in small volumes, was devised and applied to the analysis of pesticides. The apparatus permits the extraction of many samples simultaneously. The utility of the *p*-value [fraction of solute partitioning into upper phase (*1*, *2*)] for the identification of pesticides, as derived from a single extraction, has been extended—through the use of unequal volumes of the two phases—to give more accurate and useful extraction data for pesticides having low or high *p*-values. These results have been compared with those obtained by multiple extraction with equal phase volumes. Mathematical formulas are given for calculating the amount of solute in each layer from the *p*-value, or vice versa.

The *p*-values, which can be determined within 0.02, are sufficiently different to allow their use in identifying pesticides, even if only nanogram amounts are being analyzed, as in electron-capture gas chromatography (*1*). To aid such identifications the *p*-values of 131 pesticides in six solvent systems have been reported (*3*). For identification purposes the amount of pesticide need not be known, only its ratio in the two phases. At the high dilutions employed in gas chromatographic analysis the *p*-value is rarely concentration-dependent (*2*). These advantages make the *p*-value method easy to use.

p-Values have also been utilized for determining the number of extractions needed to extract a given amount of pesticide (*2*, *3*).

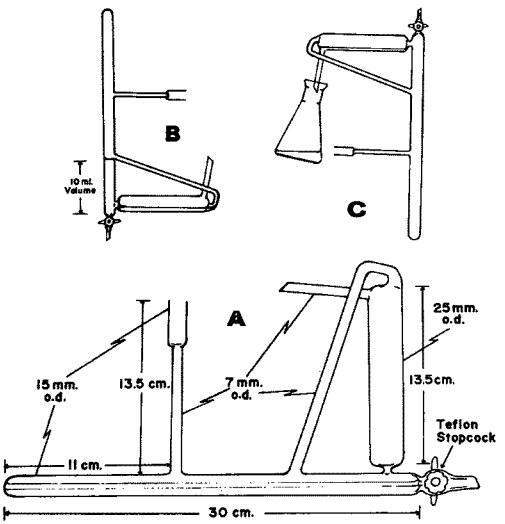


Figure 1. Positions of multiple extraction tube
A. Equilibration
B. Transfer of upper phase to reservoir (decant)
C. Transfer of reservoir contents to flask

EXPERIMENTAL

All extractions were carried out with solvents equilibrated at 25° ± 0.5° C. Solvents were distilled reagent-grade liquids purified as described previously (*2*, *3*). Analyses were made by electron-capture gas chromatography, as previously reported (*2*). Pesticides are identified in a previous publication (*3*).

Apparatus for Multiple Extraction. The extraction unit is Craig's glass countercurrent distribution cell (*4*) modified to deliver upper phase (usually 10 ml.) to a 50-ml. reservoir and equipped with a stopcock made of Teflon (Du Pont) to permit recovery of the lower phase (10 ml.). The unit is shown in Figure 1 in the three basic positions of operation. Figure 2 shows a battery of five such units [mounted on a rack that is fastened to a shaker (W. H. Curtin Co., Houston, Texas #19013H)] in the equilibration (horizontal) and decant positions. Each unit can be quickly and easily removed while it is held in the equilibration position by lifting off its spring-loaded retainer ring *A* (Figure 3) from the stopcock delivery tube and pulling the cell

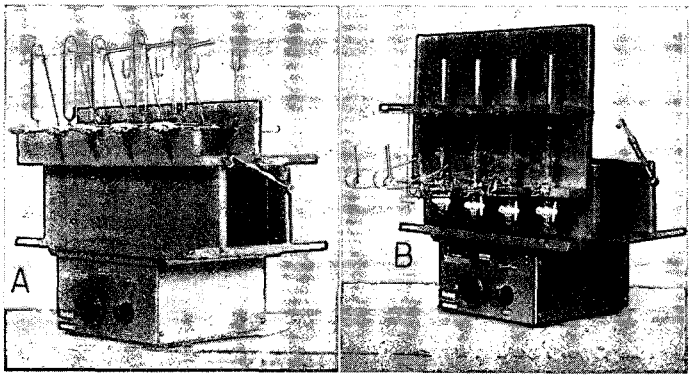


Figure 2. Battery of five extraction units on shaker

A. Equilibration position
B. Decant position

forward. The long tube of each cell must be level during the equilibration process. Ring *A* not only holds the tube level, but, by holding the addition tube (11 cm. from end of long tube, Figure 1*A*) in the vertical 3/8-inch diameter groove (Figure 3), it maintains the cell upright, as shown in Figure 2*A*. Figure 3 gives a front and rear view of the rack with dimensions; none of these are critical but the volume of the lower phase should be 10 ml. after transfer of the upper phase.

A shaker may be constructed with as many extraction units as desired.

Apparatus for Single Extraction. A 10- or 15-ml. glass-stoppered graduated centrifuge tube is used, as appropriate. The equilibrated phases are added by means of volumetric pipets.

Multiple Extractions of Lower Phase with Upper Phase. With the cell in the horizontal position (Figure 1*A* or 2*A*) the 10-ml. portions of each phase (containing the pesticide) are added through each addition tube. The shaker, set to oscillate about 175 times a minute, is turned on for about 20 seconds to equilibrate the phases. After the phases separate (usually after about 30 seconds), the rack of tubes is tilted forward to the 45° position (rack rests on turnbuckle *F* as shown in Figure 3, rear view); then when the layers appear well separated, the rack is brought to the decant position (Figure 1*B* or 2*B*) to transfer the upper phases to the reservoirs. To bring the rack to the decant position, it is released by removing spring *D* from hook *G* (Figure 3 rear view), tilted forward as far as it will go, and held there for 10 seconds. The rack is then returned to the original horizontal position, and spring *D* is replaced. Fresh 10-ml. portions of upper phase are added, and the equilibration, transfers, and solvent additions are repeated for as many as five extractions of lower phase with upper phase. The lower phases are removed via the stopcocks after the last transfer of upper phases to the reservoirs. The combined upper phase is recovered by removing each tube from the rack, rotating it to position C of Figure 1, and emptying the reservoir contents into the desired vessel. The tubes may be rinsed with acetone or other solvent and dried before the next extraction.

Although the volume of the upper phase may be varied, that of the lower phase is fixed at 10 ml. with the cell described.

Multiple Extraction of Upper Phase with Lower Phase. After the phases are equilibrated and separated as described above, the rack is brought to the 45° position (no flow of upper phase to the reservoir occurs); the lower layer of each tube is then drawn off into a flask set under each stopcock. The tubes are returned to the horizontal position, fresh lower phase is added, and the procedure is repeated for the desired number of extractions. The lower phases are accumulated in the flasks, and eventually the upper phase is withdrawn separately. The reservoirs are not used when the upper phase is extracted, and the volume of upper and

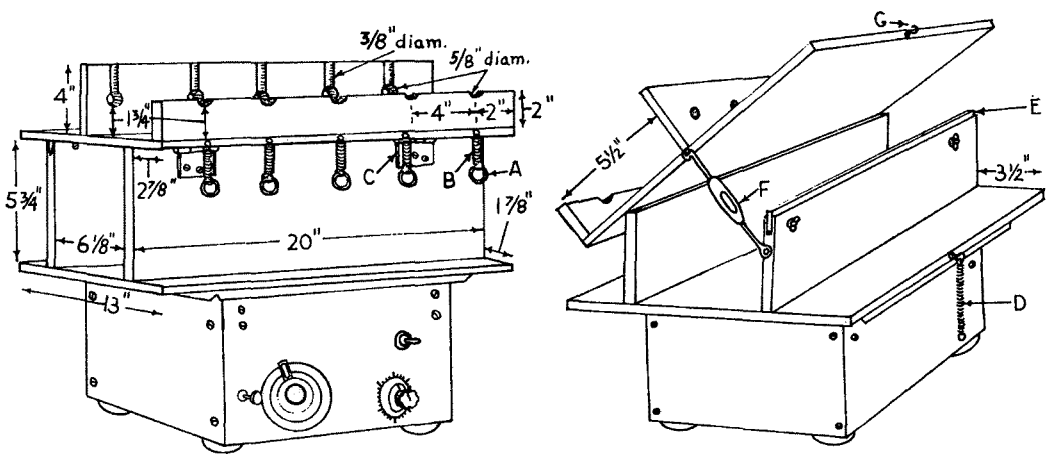


Figure 3. Front and rear view of rack mounted on shaker. Rack is made of ¾-inch plywood and finished with two coats of solvent-resistant epoxy paint

A. 0.5-inch i.d. plastic rings
B. 0.25-inch diam. × 1-inch spring
C. Hinge
D. 0.25-inch diam. × 3.5-inch spring
E. Leveling device (0.25 inch thick) is held tight with wing nuts. Either end is adjustable to maintain tubes level. Rack holds tubes in horizontal position when spring *D* is fastened to hook *G*
F. Turnbuckle (about 6.5 inches long) is adjusted to hold rack at 45° angle

lower phases may be varied since one does not depend on decantation to a set height.

Procedure for Single Extraction with Unequal Phase Volumes. A 5-μl. aliquot of upper phase containing the pesticide is analyzed. The upper phase is then extracted with the appropriate volume of lower phase in a 10- or 15-ml. glass-stoppered centrifuge tube by shaking the phases vigorously for 1 minute. A 5-μl. aliquot of the upper layer is again analyzed in exactly the same way. The ratio of the second analysis (amount of pesticide in upper phase) to the first (total amount) is the fractional amount in the upper phase (or E_u). (This ratio becomes the p-value when the phase volumes are equal.) Should an emulsion occur, the tube is centrifuged to separate the layers.

RESULTS

The multiple extraction apparatus was used to determine the fractional quantities (E_u) of 10 insecticides in the combined upper phase after making two and four extractions of lower phase with equal-volume portions of the upper one. The results obtained with hexane–acetonitrile and isooctane–dimethylformamide are given in Table I. Table II presents E_u values for seven insecticides obtained similarly, except that the upper phase was extracted with equal-volume portions of the lower one, and isooctane–80% acetone and heptane–90% ethanol were the solvent systems.

Data on the fractional amount of insecticide in the upper layer after a single extraction with unequal phase volumes when $\alpha = 5$ and 10 (α = ratio of upper to lower phase volumes) are given in Table III for 10 insecticides in two solvent systems; data are given in Table IV for seven insecticides in two other solvent systems when $\alpha = 0.2$ and 0.1.

CALCULATIONS

Included in parentheses in the four tables are the fractions of solute in the upper phase (E_u) calculated from the experimentally determined p-values. Calculations were made as follows:

For multiple extractions with phases of equal volume, the following equations were used to calculate the fractional amount of solute in each layer from the p-value, or vice versa.

Lower phase extracted with upper phase n times

$$E_u = 1 - (1 - p)^n \text{ or } p = 1 - (1 - E_u)^{1/n} \quad (1)$$

$$E_l = (1 - p)^n \text{ or } p = 1 - (E_l)^{1/n} \quad (2)$$

Upper phase extracted with lower phase n times

$$E_u = p^n \text{ or } p = (E_u)^{1/n} \quad (3)$$

$$E_l = 1 - p^n \text{ or } p = (1 - E_l)^{1/n} \quad (4)$$

where

E_u = fractional amount of solute in upper phase
E_l = fractional amount of solute in lower phase
p = p-value
n = number of extractions

For a single distribution between unequal phase volumes, the following equations were used to calculate the fractional amount of solute in each phase from the p-value, or vice versa:

$$E_u = \frac{\alpha p}{\alpha p - p + 1} \text{ or } p = \frac{E_u}{\alpha - E_u(\alpha - 1)} \quad (5)$$

$$E_l = 1 - \frac{\alpha p}{\alpha p - p + 1} \text{ or } p = \frac{1 - E_l}{E_l(\alpha - 1) + 1} \quad (6)$$

where $\alpha = \dfrac{\text{volume of upper phase}}{\text{volume of lower phase}}$

Table I. Fractional Quantities of Insecticides in Combined Upper Phase (E_u) after Two and Four Extractions of 10 ml. of Lower Phase with 10-ml. Portions of Upper Phase with Two Solvent Systems[a]

Multiple extraction apparatus was used

	Hexane–acetonitrile			Isooctane–dimethylformamide		
Insecticide	p-Value	$n = 2$	$n = 4$	p-Value	$n = 2$	$n = 4$
γ-Chlordane	0.42	0.64 (0.66)	0.88 (0.89)	0.15	0.29 (0.28)	0.45 (0.48)
p,p'-DDT	0.40	0.63 (0.64)	0.89 (0.87)	0.080	0.14 (0.15)	0.25 (0.28)
Diazinon	0.29	0.50 (0.50)	0.74 (0.74)	0.14	0.23 (0.26)	0.41 (0.44)
Dieldrin	0.35	0.57 (0.58)	0.82 (0.82)	0.13	0.23 (0.24)	0.40 (0.42)
EPN	0.042	0.088 (0.082)	0.16 (0.16)	0.015	0.027 (0.029)	0.061 (0.060)
Heptachlor	0.57	0.80 (0.81)	0.95 (0.97)	0.22	0.40 (0.39)	0.64 (0.63)
Lindane	0.13	0.25 (0.24)	0.44 (0.43)	0.049	0.091 (0.096)	0.16 (0.18)
Methyl Trithion	0.081	0.15 (0.16)	0.28 (0.29)	0.022	0.040 (0.044)	0.083 (0.084)
Parathion	0.048	0.10 (0.094)	0.19 (0.18)	0.031	0.058 (0.061)	0.11 (0.12)
Telodrin	0.49	0.74 (0.74)	0.94 (0.93)	0.18	0.31 (0.32)	0.52 (0.54)

[a] E_u values in parentheses are calcd. from experimentally determined p-values shown in table. n = number of extractions.

Table II. Fractional Quantities of Insecticides in Combined Upper Phase (E_u) after Two and Four Extractions of 10 ml. of Upper Phase with 10-ml. Portions of Lower Phase with Two Solvent Systems[a]

Multiple extraction apparatus was used

	Isooctane–80% acetone			Heptane–90% ethanol		
Insecticide	p-Value	$n = 2$	$n = 4$	p-Value	$n = 2$	$n = 4$
Aldrin	0.97	0.91 (0.93)	0.87 (0.88)	0.77	0.58 (0.59)	0.37 (0.35)
γ-Chlordane	0.95	0.88 (0.90)	0.80 (0.81)	0.59	0.33 (0.35)	0.12 (0.12)
Dieldrin	0.91	0.81 (0.83)	0.68 (0.68)	0.58	0.34 (0.34)	0.12 (0.11)
p,p'-DDT	0.93	0.86 (0.86)	0.76 (0.75)	0.61	0.39 (0.37)	0.15 (0.14)
Heptachlor	0.96	0.93 (0.92)	0.83 (0.85)	0.73	0.53 (0.53)	0.28 (0.28)
Heptachlor epoxide	0.90	0.81 (0.81)	0.65 (0.66)	0.58	0.33 (0.34)	0.12 (0.11)
TDE	0.91	0.85 (0.83)	0.70 (0.69)	0.48	0.23 (0.23)	0.057 (0.053)

[a] Same as in Table I.

DISCUSSION

The introduction and widespread use of new instrumentation have markedly altered the extraction requirements for analytical purposes. Previous reliance on comparatively insensitive colorimetric and other procedures in pesticide residue analysis made it necessary to extract large amounts of starting material, usually with conventional separatory funnels and large volumes of solvent. The new methods, many of which rely on electronic measuring devices that are extremely sensitive, may require for an analysis only a few microliters of a very dilute solution (or a few nanograms of solute). They also usually require solvents of extremely high purity, which are expensive.

To meet present analytical needs we have devised a multiple extraction apparatus capable of extracting small volumes rapidly. Extraction takes place by mild rotatory oscillation of the tubes in a horizontal position; equilibration of the solute between phases is achieved rapidly (usually within 20 seconds) because the comparatively large interface and small volume facilitate rapid exchange of solute. Inasmuch as only 10-ml. phases are employed, the use of excessive amounts of expensive solvent is avoided. Time is saved because many extractions may be run simultaneously and because the need to evaporate down large volumes of solvent is eliminated. Extractions are accomplished with a minimum of manipulations. Another advantage of the new apparatus is that emulsions are frequently avoided because shaker oscillation is much less vigorous than the shaking required to equilibrate phases in a separatory funnel. Shaker action may be slowed to any degree to avoid emulsification, but a longer shaking period is then required to attain equilibrium.

Tables I and II present data obtained with the multiple extraction apparatus after two and four extractions. The values in parentheses, calculated from experimentally determined p-values by using Equations 1 and 3, are in excellent agreement with E_u values determined experimentally with the multiple extraction apparatus, deviations usually being 0.02 or less. The achievement of practically theoretical results indicates that equilibration of the solute between the phases was attained and that the apparatus was performing satisfactorily.

The data of Tables III and IV, obtained by single extraction with unequal volumes, likewise show excellent agreement between the E_u values calculated from experimentally determined p-values by using Equation 5 and those obtained directly by trial.

Accordingly, knowledge of the p-value enables the analyst to calculate the distribution of solute in the upper and lower phase in multiple extractions with equal phase volumes or in single distributions of unequal phase volumes.

One major objective of this study was to overcome the difficulty in distinguishing pesticides having high or low p-values that are close together. This problem arose because many pesticides have very low p-values in some of the binary solvent systems that are most widely used in pesticide analyses (*3*). For example, the p-values of parathion (0.031) and Methyl Trithion (0.022) in the isooctane–dimethylformamide system are not distinguishable with any degree of certainty, since we can determine p-values only within 0.02. An examination of the E_u values in Table I shows that the E_u values of parathion and Methyl Trithion are not distinguishable after two and four extractions with phases of equal volume (0.058 *vs.* 0.040 and 0.11 *vs.* 0.083), nor after an extraction employing unequal volumes with $\alpha = 5$ (0.12 *vs.* 0.10). However, the E_u values are sufficiently different in an extraction with $\alpha = 10$ (0.22 *vs.* 0.17). These data show that both multiple extractions and extractions with unequal phases can spread or magnify small differences in p-value to the point that these differences may be-

Table III. Fractional Quantities of Insecticides in Upper Phase (E_u) after a Single Distribution between Unequal Phase Volumes When $\alpha = 5$ and 10[a]

Insecticide	Hexane–acetonitrile			Isooctane–dimethylformamide		
	p-Value	$\alpha = 5$	$\alpha = 10$	p-Value	$\alpha = 5$	$\alpha = 10$
γ-Chlordane	0.42	0.80 (0.79)	0.90 (0.88)	0.15	0.47 (0.47)	0.66 (0.64)
p,p'-DDT	0.40	0.76 (0.77)	0.89 (0.87)	0.080	0.30 (0.31)	0.48 (0.47)
Diazinon	0.29	0.67 (0.67)	0.80 (0.80)	0.14	0.43 (0.45)	0.62 (0.62)
Dieldrin	0.35	0.73 (0.73)	0.86 (0.84)	0.13	0.45 (0.43)	0.63 (0.60)
EPN	0.042	0.19 (0.18)	0.33 (0.31)	0.015	0.076 (0.075)	0.11 (0.135)
Heptachlor	0.57	0.90 (0.87)	0.95 (0.93)	0.22	0.61 (0.59)	0.76 (0.74)
Lindane	0.13	0.43 (0.43)	0.61 (0.60)	0.049	0.19 (0.21)	0.35 (0.35)
Methyl Trithion	0.081	0.32 (0.31)	0.49 (0.47)	0.022	0.10 (0.10)	0.17 (0.19)
Parathion	0.048	0.21 (0.20)	0.35 (0.34)	0.031	0.12 (0.14)	0.22 (0.245)
Telodrin	0.49	0.84 (0.83)	0.93 (0.91)	0.18	0.54 (0.53)	0.71 (0.69)

[a] E_u values in parentheses are calcd. from the experimentally determined p-values shown in table. α is ratio of upper to lower phase volumes; 10:2 and 10:1 phase volumes in milliliters were used.

Table IV. Fractional Quantities of Insecticides in Upper Phase (E_u) after a Single Distribution between Unequal Phase Volumes When $\alpha = 0.2$ and 0.1[a]

Insecticide	Isooctane–80% acetone			Heptane–90% ethanol		
	p-Value	$\alpha = 0.2$	$\alpha = 0.1$	p-Value	$\alpha = 0.2$	$\alpha = 0.1$
Aldrin	0.97	0.84 (0.87)	0.75 (0.76)	0.77	0.39 (0.40)	0.25 (0.25)
γ-Chlordane	0.95	0.76 (0.79)	0.65 (0.66)	0.59	0.22 (0.22)	0.13 (0.13)
Dieldrin	0.91	0.65 (0.67)	0.51 (0.50)	0.58	0.23 (0.23)	0.13 (0.13)
p,p'-DDT	0.93	0.75 (0.73)	0.58 (0.57)	0.61	0.25 (0.24)	0.14 (0.14)
Heptachlor	0.96	0.81 (0.83)	0.68 (0.70)	0.73	0.34 (0.35)	0.20 (0.21)
Heptachlor epoxide	0.90	0.66 (0.64)	0.50 (0.48)	0.58	0.22 (0.22)	0.13 (0.12)
TDE	0.91	0.68 (0.67)	0.53 (0.51)	0.48	0.16 (0.16)	0.087 (0.085)

[a] Same as in Table III except that upper to lower phase volumes in milliliters were 2:10 and 1:10.

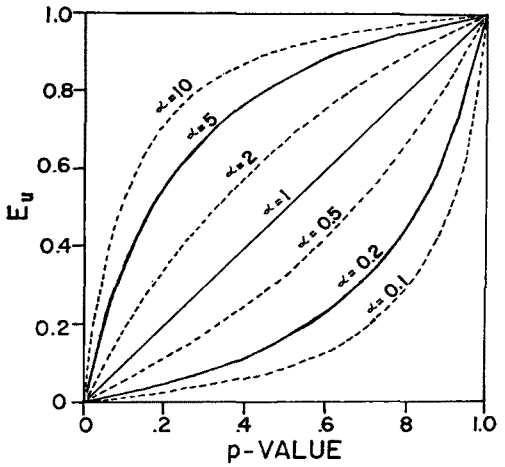


Figure 4. Extraction with unequal phase volumes: fractional amount in upper phase (E_u) vs. p-value

α is ratio of upper to lower phase volumes

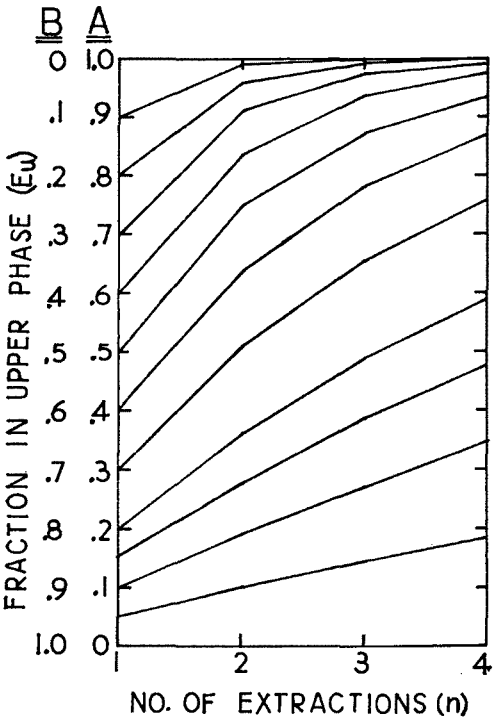


Figure 5. Extraction with phases of equal volume

Scale A: number of extractions vs. fraction of solute extracted into upper phase after lower phase is extracted with upper phase.
Scale B: number of extractions vs. fraction remaining in upper phase after upper phase is extracted with lower phase. One extraction equals p-value

come useful. Since it is quicker and easier to run a single extraction than multiple extractions, the single extraction with unequal phase volumes appears to be preferable for identification.

For single extractions with phases of unequal volume (Tables III and IV), the difference in E_u values becomes greater for solutes with low p-values when α is increased; for solutes with high p-values, the difference becomes greater when α is decreased. These relationships are further demonstrated in Figure 4 which relates p-value, E_u, and α. With such a graph tedious calculations of these values may be eliminated.

For multiple extractions with phases of equal volume, the difference in E_u values becomes greater for solutes with low p-values as the number of extractions of lower phase with upper one increases; for solutes with high p-values the difference becomes greater as the number of extractions of upper phase with lower one increases. This effect can be readily seen in Figure 5, part of which was previously reported (*2*). The graph allows p-values and E_u values to be approximated from each other without tedious calculation. For an exact value, the appropriate equation (1–4) is used.

Figure 5 may be useful for identification when multiple extractions are used, but it will probably find greater application in guiding residue extraction processes and cleanup operations. Several extractions of one phase with another are used routinely in pesticide and other analyses to separate the unwanted from the wanted material. With knowledge of the p-value the number of extractions necessary to separate a given fraction of solute may be read off the graph. In this connection the 771 pesticide p-values in six solvent systems, available from a previous study (*3*), may be helpful to the pesticide analyst.

It is apparent that modifications of the basic apparatus described here may be made readily. We made a useful modification by attaching a reservoir to units of two, three, or four Craig cells (cells available from H. O. Post Instrument Co., Middle Village, Long Island, N. Y., reservoir is attached to last cell). This arrangement is meant for cleanup of pesticide residues which require a distribution of several plates to achieve separation of the residue from interferences. [Details of this general approach are given in (*2*).] The multiple-plate arrangement serves the same purpose as a very different and more complex apparatus described by L. Martin (*5*) for removal of fat in the analysis of chlorinated pesticide residues in food.

Although operation of the multiple extraction unit is illustrated for pesticide residue analysis, it may be equally useful for other analyses that require extraction with separatory funnels.

ACKNOWLEDGMENT

The technical assistance of F. G. Crumley is gratefully acknowledged.

LITERATURE CITED

(1) Beroza, M., Bowman, M. C., ANAL. CHEM. **37**, 291 (1965).
(2) Beroza, M., Bowman, M. C., *J. Assoc. Offic. Agr. Chemists* **48**, 358 (1965).
(3) Bowman, M. C., Beroza, M., *Ibid.*, **48**, 943 (1965).
(4) Craig, L. C., ANAL. CHEM. **22**, 1346 (1950).
(5) Martin, L., *Food Tech. in Australia* **16**, 456 (1964).

RECEIVED for review January 19, 1966. Accepted April 11, 1966. Presented in part at the 79th Annual Meeting of the Association of Official Agricultural Chemists on October 12, 1965 at Washington, D. C. Mention of a proprietary product is for identification only and does not constitute an endorsement by the U. S. Department of Agriculture.

Characterization of Position Isomers of Secondary Straight-Chain Alcohols and Their 3,5-Dinitrobenzoate Derivatives by Nuclear Magnetic Resonance

CHARLES E. GODSEY

Research and Development Department, Continental Oil Co., Ponca City, Okla.

▷ **Proton chemical shifts of methyl groups have been determined for all position isomers of secondary straight-chain octanols, decanols, and dodecanols, and their 3,5-dinitrobenzoate derivatives. These chemical shifts are correlated empirically with the number of C—C bonds between the carbon of the methyl group and the carbon adjacent to the functional group. Correlation data from the 3,5-dinitrobenzoate derivatives may be used to characterize the 2-through 6-position isomers of the secondary alcohols.**

DESHIELDING effects induced by electron withdrawing groups substituted on aliphatic hydrocarbons, such as alkylhalides, alcohols, or esters, are generally considered to be negligible at protons more than 2 or 3 C—C bonds away. We have studied a number of these structures and find that deshielding can be detected at protons of methyl groups up to 6 C—C bonds away from the functional group. These deshielding effects provide useful information about the structure of substituted aliphatic hydrocarbons. Secondary straight-chain alcohols were selected for the present study because of their growing commercial importance as detergent intermediates (*4*).

Nuclear magnetic resonance (NMR) signals from methyl protons of secondary straight-chain alcohols may be used to characterize position isomers. The chemical shift of the methyl protons can be correlated with the number of C—C bonds between the methyl carbon and the carbon adjacent to the hydroxyl group. This correlation is independent of chain length. However, if the hydroxyl group is near the center of the chain (4-octanol, 5-decanol, 6-dodecanol), signals from the two methyl groups are not resolved.

This problem can be overcome by converting the alcohol to the 3,5-dinitrobenzoate and using a correlation similar to that for alcohols. We have been successful in characterizing all position isomers of secondary octanols, decanols, and dodecanols by this method.

All position isomers of secondary alcohols below octanols may be characterized by inspection of signal shapes in their NMR spectra. However, chemical shifts of methyl groups of all shorter chain-length secondary alcohols and their 3,5-dinitrobenzoate derivatives have been found to agree with the correlation data in Table I. Only one exception has been found. Chemical shifts of the ω-methyl groups of 2-position isomers of the 3,5-dinitrobenzoates are consistently higher than values for equivalent methyl groups of other position isomers. The difference is about 2 c.p.s. for the 2-butyl derivative and decreases to 0.4 c.p.s. for the 2-octyl derivative.

Esterification of the alcohol also provides a method for determining relative amounts of primary and secondary alcohols and ethers in mixtures or in certain polyhydric alcohols or hydroxy ethers (*3*).

EXPERIMENTAL

Proton NMR spectra were recorded at 60 m.c.p.s. using a Varian Associates DP 60 high resolution NMR spectrometer. Tetramethylsilane was used as an internal reference. Chemical shifts were measured by superimposing an audio-frequency sideband signal from the tetramethylsilane line on the peak to be measured and adjusting the frequency of the modulated signal to attain maximum peak height. Alcohols which were not commercially available were prepared from ketones by reduction with $LiAlH_4$ (*6*). The 5-decanol was prepared by Grignard synthesis. The 3,5-dinitrobenzoates were prepared by reaction of the alcohol with reagent grade 3,5-dinitrobenzoyl chloride (*5*). All samples were analyzed as 0.1 to 0.3 molar solutions in carbon tetrachloride. Variations in the chemical shift of the methyl proton with changes in the concentration in this range were observed to be within the limits of uncertainty of the chemical shift meas-

Table I. Chemical Shifts of Methyl Groups

Alcohol	Methyl group[a]	Number of C—C bonds between methyl carbon and R_2CHOH carbon	Chemical shift relative to TMS (c.p.s.)	
			Alcohol	3,5-Dinitrobenzoate
2-Octanol	α	1	67.1	85.4
2-Decanol	α	1	67.0	85.6
2-Dodecanol	α	1	67.3	85.6
3-Octanol	α	2	54.8	60.1
3-Decanol	α	2	54.8	60.0
3-Dodecanol	α	2	54.8	60.1
4-Octanol	α	3	55.2[b]	58.9
4-Decanol	α	3	55.8	59.0
4-Dodecanol	α	3	55.5	58.9
4-Octanol	ω	4	55.2[b]	56.0
5-Decanol	α	4	54.7[b]	56.0
5-Dodecanol	α	4	54.9	55.8
3-Octanol	ω	5	53.9	54.1
5-Decanol	ω	5	54.7[b]	54.0
6-Dodecanol	α	5	53.6[b]	54.1
4-Decanol	ω	6	53.4	53.3
6-Dodecanol	ω	6	53.6[b]	53.1
3-Decanol	ω	7	53.1	52.4
5-Dodecanol	ω	7	53.3	52.4
4-Dodecanol	ω	8	53.2	52.4
3-Dodecanol	ω	9	53.1	52.2
2-Octanol	ω	6	53.7	53.7[c]
2-Decanol	ω	8	53.3	52.7[c]
2-Dodecanol	ω	10	53.4	52.5[c]

[a] The methyl group in the number 1 position according to conventional naming rules is labeled (α). The methyl group at the opposite end of the chain is labeled (ω).
[b] Signals from the two methyl groups were not resolved.
[c] Chemical shifts of ω-methyl groups of all 2-position isomers were found to be consistently high.

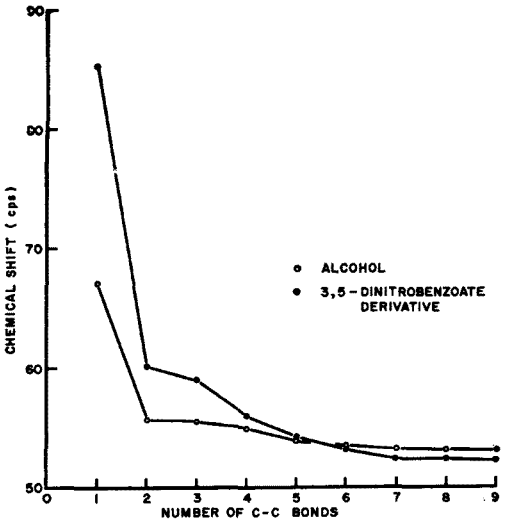


Figure 1. Proton chemical shifts of methyl groups of secondary straight-chain alcohols and their 3,5-dinitrobenzoate derivatives vs. number of C—C bonds between the methyl carbon and the carbon adjacent to the functional group

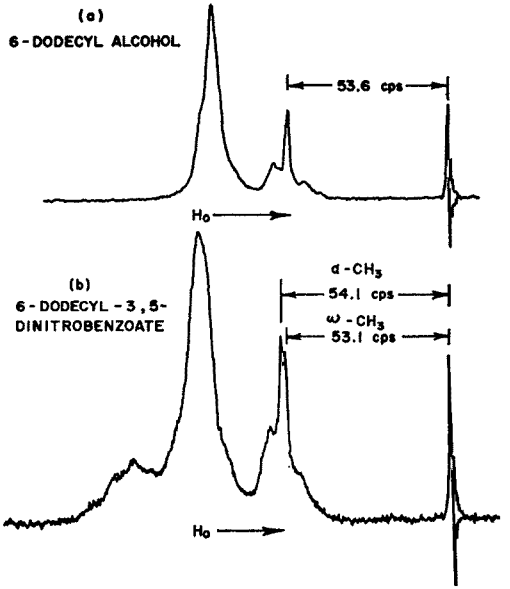


Figure 2. Proton NMR spectra of the methyl and methylene groups of (a) 6-dodecanol and (b) 6-dodecyl-3,5-dinitrobenzoate as 0.1 M solutions in carbon tetrachloride with TMS as an internal reference

urement, ±0.2 c.p.s. The chemical shifts are listed in Table I.

RESULTS AND DISCUSSION

The hydroxyl group appears to induce deshielding at methyl groups up to 6 C—C bonds away (7-position isomers) (Figure 1). Each position isomer of the even-carbon-number secondary straight-chain alcohols has two nonequivalent methyl groups. Their NMR spectra should show two methyl proton signals. However, if the number of C—C bonds between the hydroxyl group and the two methyl groups differs by only one (4-octanol, 5-decanol, 6-dodecanol), signals from the two methyl groups are not resolved.

Derivatization of the alcohol to form the 3,5-dinitrobenzoate offers several advantages to this method. At 60 m.c.p.s. the 2- through 6-position isomers of secondary straight-chain 3,5-dinitrobenzoates may be characterized. Since the ester group induces a greater deshielding effect than the hydroxyl group, resonance signals from methyl groups of different position isomers are better resolved. Signals from the two methyl groups of 6-dodecyl 3,5-dinitrobenzoate are resolved sufficiently to be measured separately. The NMR spectra of 6-dodecanol and 6-dodecyl 3,5-dintrobenzoate are shown in Figure 2, *a* and *b*.

It can be seen from Figure 1 that the range of the deshielding effect induced by the 3,5-dinitrobenzoate group appears to be about the same as that of the hydroxyl group, about 6 C—C bonds. However, signals from protons of methyl groups more than 6 C—C bonds away from the 3,5-dinitrobenzoate appear at higher field than signals from methyl groups of corresponding alcohols. This appears to be due to the long-range diamagnetic shielding induced perpendicular to the aromatic ring. When the 3,5-dinitrobenzoate group is substituted near the center of a long chain, rotation about the axis of the ring may be hindered slightly so that conformations in which methyl groups lie over the ring are favored. The consistently high values of chemical shifts of ω-methyl groups of 2-position isomers may indicate more equal population of the various conformations. In other experiments we have found that chemical shifts of methyl groups of primary alcohols are the same as that of their 3,5-dinitrobenzoate derivatives for alcohols longer than octanol, indicating free rotation of the 3,5-dinitrobenzoate group.

Detergency performance of secondary alcohol derivatives decreases markedly as the position of substitution is moved toward the center of the chain. This effect appears to be greatest for alcohol sulfates. Cotton detergency ratings for 7-tridecyl and 7-pentadecyl sulfates have been reported to be about one-half and two-thirds, respectively, compared with the corresponding primary alcohol sulfates (*2*).

The rate of biodegradation of secondary alcohol derivatives also decreases markedly as the position of substitution is moved toward the center of the alkyl chain. The rate of biodegradation of ethoxylated primary dodecanol has been reported to be about twice the rate for the 4-position isomer and nearly ten times the rate for the 6-position isomer (*1*).

Detergency performance and biodegradability could be predicted from information about the position isomer distribution of the alcohol. We have not attempted to analyze mixtures of position isomers, but empirical correlation of signal shapes with isomer distribution appears to be possible.

LITERATURE CITED

(1) Blankenship, F. A., Piccolini, V. M., *Soap Chem. Specialties* 39, 75 (1963).
(2) Finger, B. M., Gillies, G. A., Hartwig, G. M., Ryder, E. E., Jr., Sawyer, W. M., "The Effect of Alcohol Structure and Molecular Weight on Surfactant Properties," 38th AOCS meeting, Chicago, October 1964.
(3) Goodlett, V. W., ANAL. CHEM. 37, 431 (1965).
(4) Myerly, R. C., Rector, J. M., Steinle, E. C., Vath, C. A., Zika, H. T., *Soap Chem. Specialties* 40, 78 (1964).
(5) Shriner, R. L., Fuson, R. C., "Identification of Organic Compounds," p. 165, Wiley, New York, N. Y., 1953.
(6) Weissberger, A., "Techniques of Organic Chemistry," 5, 253, Interscience, New York, N. Y., 1958.

RECEIVED for review December 22, 1965. Accepted March 23, 1966.

Kinetics of Bromination of Certain Substituted 8-Quinolinols

GEORGE O'DOM and QUINTUS FERNANDO

Department of Chemistry, University of Arizona, Tucson, Ariz.

▷ **A constant current generator and an amperometric indicator system have been used to measure the rates of bromination of 8-quinolinol and its 4-methyl, 5-bromo, 5-chloro, and 5-fluoro derivatives in acid solutions in the presence of bromide ions. An analog computer has been used to obtain the rate constants for the stepwise bromination of 8-quinolinol and 4-methyl-8-quinolinol and for the monobromination of the 5-halo derivatives. There is no evidence of steric hindrance to substitution in the 5-position of 4-methyl-8-quinolinol. In all the 8-quinolinols studied, the bromine molecule was the active brominating agent when bromination occurred in the 5-position, whereas, in every case bromination in the 7-position was accomplished by the tribromide ion as well as by molecular bromine.**

THE QUANTITATIVE DIBROMINATION of the chelating agents, 8-quinolinol and 2-methyl-8-quinolinol is the basis for the determination of metal ions which form chelates with these ligands. The metal chelates are precipitated, washed free of excess ligand, dissolved in acid, and the liberated ligand is determined by a bromometric titration. The application of this method to metal chelates formed by other substituted 8-quinolinols has received little attention. Recently, Corsini and Graham (*2*), reported that the dibromination of 4-methyl-8-quinolinol is a relatively slow reaction and takes about twenty minutes to go to completion. The slowness of the reaction was attributed to steric hindrance by the methyl group in 4-position to the monobromination reaction which usually occurs in the 5-position, the position para to the phenolic group. The 4-methyl group might, on the other hand, sterically hinder the introduction of the second bromine atom in the 5-position, if the monobromination reaction occurred in the 7-position. It was decided therefore to resolve this question by carrying out a detailed study of the kinetics of bromination of 4-methyl-8-quinolinol.

In a previous investigation of the kinetics of bromination of 8-quinolinol and 2-methyl-8-quinolinol, the tribromide ion was postulated to be an active brominating species in the second bromination step of 8-quinolinol but not in the first (*4*). In this study, the kinetic data for the bromination of 8-quinolinol have been re-examined with the help of an analog computer, and the kinetics of bromination of a series of 5-substituted 8-quinolinols have been investigated to determine whether the tribromide ion is indeed an active brominating species whenever electrophilic substitution occurs in the 7-position in 8-quinolinol.

EXPERIMENTAL

Apparatus. The apparatus used in this work has been described in detail in a previous paper (*5*). In addition, an E.A.I. Pace Analog Computer Model T.R. 10 and a Moseley Autograph X-Y recorder were used in this study.

Reagents and Solutions. Analytical reagent grade perchloric acid and sodium hydroxide, were used in this work without further purification and were also used to prepare sodium perchlorate. Analytical Reagent grade sodium bromide was heated in a muffle furnace for 8–12 hours at about 605° C. before use.

Analytical Reagent grade 8-quinolinol was purified by sublimation under reduced pressure (m.p. 72.5–73.5° C.). 4-Methyl-8-quinolinol was prepared from methyl vinyl ketone and *o*-aminophenol by the Doebner von Miller reaction. The product was recrystallized from ethanol and sublimed under reduced pressure (m.p. 137–8° C.). 5-Bromo-8-quinolinol was prepared by bromination with *N*-bromosuccinimide (*7*), separated from any dibromo compound by selective precipitation and recrystallized from ethanol (m.p. 125° C.). 5-Chloro-8-quinolinol was obtained from Aldrich Chemical Co. and recrystallized from ethanol (m.p. 122° C.). 5-Nitro-8-quinolinol was prepared from 5-nitroso-8-quinolinol, obtained from Aldrich Chemical Co., by the method of Petrow and Sturgeon (*6*) (m.p. 178° C.). 5-Fluoro-8-quinolinol which was obtained from Dr. H. Gershon at the Boyce Thompson Institute, Yonkers, N. Y., was prepared by the Schiemann reaction. The compound was purified by recrystallization from methanol (m.p. 109–10° C.; % C, 65.8 (found), 66.2 (calcd.); % H, 3.60 (found), 3.07 (calcd.); % N, 8.58 (found), 8.59 (calcd.). The NMR spectrum of this compound in trifluoroacetic acid was consistent with that expected for 5-fluoro-8-quinolinol.

All solutions were made as previously described (*5*) and the ionic strength of the solutions used in this study was maintained at a value of 1.35 by the addition of sodium perchlorate.

Rate Equations. The reaction scheme can be represented by two parallel consecutive second-order reactions

$$A + B \xrightarrow{k_{1obs}} C \qquad (1)$$

$$C + B \xrightarrow{k_{2obs}} D \qquad (2)$$

where $[A]$ is the total concentration of unreacted 8-quinolinol,

$$[A] = [HOx] + [H_2Ox^+] \qquad (3)$$

$[C]$, the total concentration of monobrominated 8-quinolinol,

$$[C] = [HOxBr] + [H_2OxBr^+] \qquad (4)$$

and $[D]$ the total concentration of the dibrominated substrate,

$$[D] = [HOxBr_2] + [H_2OxBr_2^+] \qquad (5)$$

The following differential equations can be obtained from the reaction scheme:

$$\frac{d(B)}{dt} = R - k_{1obs}[A][B] - k_{2obs}[C][B] \qquad (6)$$

$$-\frac{d[A]}{dt} = k_{1obs}[A][B] \qquad (7)$$

$$-\frac{d[C]}{dt} = k_{2obs}[B][C] - k_{1obs}[A][B] \qquad (8)$$

where R is the rate of generation of bromine, B, which is present in solution as molecular bromine and tribromide ions. These equations can be readily solved on an analog computer, and from a knowledge of the concentration, $[B]$, at any time t, the rate constants, k_{1obs} and k_{2obs} can be obtained.

Voltage and Time Scaling on the Analog Computer. The program used in this study is shown in Figure 1. The difference in the magnitude of $[A]$ and $[B]$ necessitates voltage scaling. The basic variables, $[A]$, $[B]$, $[C]$ and R were scaled. The variable $[B]$ was underscaled since, with the slow reactions, large concentrations of both $[A]$ and $[B]$ are present initially and cause overloading at the amplifier following the multiplier, since amplification by a factor of ten is required. $[B]$ was therefore multiplied by ten before the signal was fed into the multi-

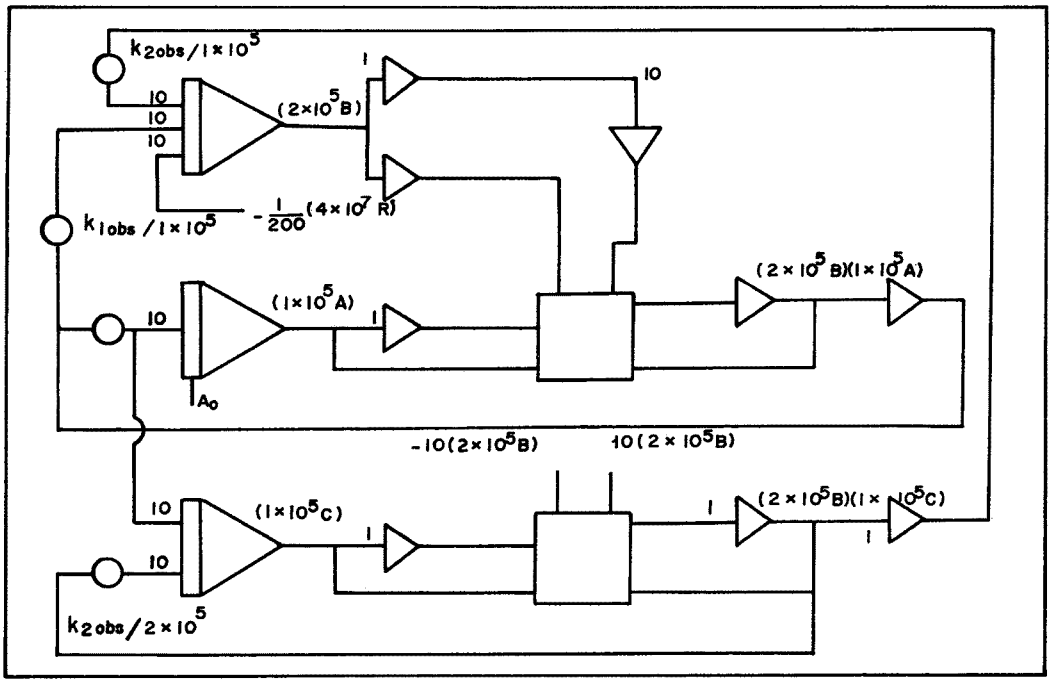


Figure 1. Analog computer program for consecutive parallel second order reactions

pliers to ensure that sufficient voltage was present at the multipliers. The voltage scaling used for the kinetic study of the bromination of 8-quinolinol is shown in Table I. The scaled variable was substituted for the corresponding variable in the differential Equations 6, 7, and 8 to obtain the scaled equations and the concentration–time curves were converted into voltage–time curves which were plotted on an X–Y recorder synchronized with the computer.

In each kinetic experiment, data were recorded for about 400 seconds. Since drift in the computer can occur during such long periods, time scaling was used. A reduction in time by a factor of ten was obtained by increasing the gain across all integrators by a factor of ten.

Determination of Rate Constants. The rate constants were obtained from the computer by a method of curve fitting. The concentration–time data were converted into voltage–time data by means of the scale factor for $[B]$ and the resulting curve was plotted on the recorder chart. The initial concentration of A was set on the computer and the attenuators were adjusted until a good fit was obtained with the experimental curve. The attenuation was determined by feeding a reference voltage into the input of the loaded attenuator system and measuring the voltage drop between the attenuator arm and ground by means of a Minneapolis-Honeywell Model 2730 potentiometer. The rate constant was readily calculated from this voltage drop.

Table I. Voltage Scaling for the Analog Computer Kinetic Study of 8-Quinolinol

Variable	Max. value	Scale factor	Scaled variable
B	$5 \times 10^{-5}M$	$10V/5 \times 10^{-5}M$	$[2 \times 10^{5}B]$
A	$1 \times 10^{-4}M$	$10V/1 \times 10^{-4}M$	$[1 \times 10^{5}A]$
C	$1 \times 10^{-4}M$	$10V/1 \times 10^{-4}M$	$[1 \times 10^{5}C]$
R	$2.5 \times 10^{-7}M$/sec.	$10V/2.5 \times 10^{-7}M$/sec.	$[4 \times 10^{7}R]$

The rate constants $k_{1_{obs}}$ and $k_{2_{obs}}$ given in Equation 6 can be defined in the following manner:

$$k_{1_{obs}} = \frac{v_1}{([H_2Ox^+] + [HOx])([Br_2] + [Br_3^-])} \quad (9)$$

$$k_{2_{obs}} = \frac{v_2}{([H_2OxBr^+] + [HOxBr])([Br_2] + [Br_3^-])} \quad (10)$$

where v_1 and v_2 are the rates of decrease of the total bromine concentration, in the first and second bromination steps, respectively. These rates can also be written in terms of specific rate constants which will be illustrated for the monobromination step.

$$v_1 = k_1[Br_2]([H_2Ox^+] + [HOx]) + k_2[Br_3^-]([H_2Ox^+] + [HOx]) \quad (11)$$

$$v_1 = k_3([Br_2] + [Br_3^-])[HOx] + k_4([Br_2] + [Br_3^-])[H_2Ox^+] \quad (12)$$

Equations 11 and 12, therefore, serve to define the rate constants involved. The same equations can be written for the dibromination step, and the specific rate constants for this reaction are primed—i.e., k_1', k_2', k_3', and k_4'.

The above equations are valid for the high acid and bromide ion concentrations used in these experiments, since it can be assumed that only Br_2 and Br_3^- are the possible brominating species and that 8-quinolinol is present only in the neutral and protonated forms, the concentration of the anionic form being negligible in these highly acidic solutions.

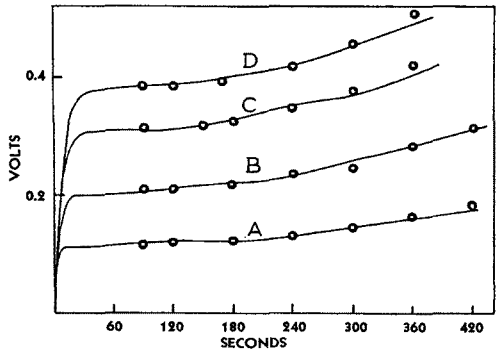


Figure 2. Analog computer curves obtained for the bromination of 8-quinolinol in 0.64*M* NaBr
o—experimental values
A: 0.05*M*, B: 0.12*M*, C: 0.23*M*, D: 0.35*M* $HClO_4$

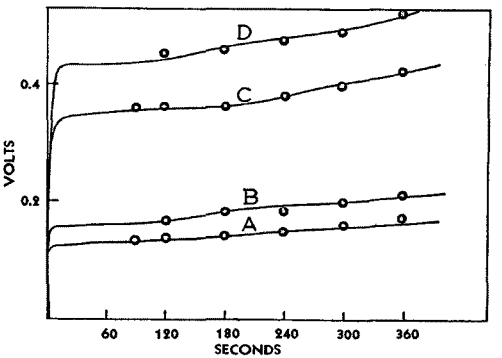


Figure 3. Analog computer curves obtained for the bromination of 4-methyl-8-quinolinol in 0.12*M* $HClO_4$
o—Experimental values
A: 0.12*M*, B: 0.24*M*, C: 0.64*M*, D: 0.80*M* NaBr

From data obtained at constant hydrogen ion concentration and varying bromide ion concentration the rate constants k_1 and k_2 can be obtained from a plot of $k_{1_{obs}}(1 + K[Br^-])$ *vs.* $[Br^-]$

$$K = \frac{[Br_3^-]}{[Br_2][Br^-]} = 17 \qquad (13)$$

In a similar manner k_3 and k_4 are obtained from data at constant $[Br^-]$ and varying $[H^+]$. A plot of $k_{1_{obs}}$ *vs.* $K_{a_1}/[H^+]$, where K_{a_1} is the first acid dissociation constant of the 8-quinolinol and $K_{a_1}/H^+ \ll 1$ will give k_3 and k_4. The rate constants for the second bromination step can be obtained in exactly the same manner. Therefore the computer values for $k_{1_{obs}}$ and $k_{2_{obs}}$ can be used to determine specific rate constants for the reaction.

All kinetic data for the bromination of the 8-quinolinols, except that for the 5-nitro-8-quinolinol were simulated on the analog computer. The fit of the experimental data with the values obtained for the computer is quite good as shown in Figures 2 and 3 for 8-quinolinol and its 4-methyl derivative. The reproducibility of the computer rate constants is illustrated by the data in Table II for 8-quinolinol. The precision with which $k_{1_{obs}}$ can be determined is $\pm 0.1 \times 10^3$ or better and $k_{2_{obs}}$ can be determined with a precision of about $\pm 0.3 \times 10^3$. Furthermore, a comparison of the $k_{2_{obs}}$ obtained for 8-quinolinol with $k_{2_{obs}}$ for 5-bromo-8-quinolinol in most cases shows good agreement. Thus it appears that the experimental data fit the proposed mechanism and the assumption that electrophilic substitution occurs first in the 5-position of 8-quinolinol and then in the 7-position is justified.

In Tables III and VII two observed constants are listed—i.e. $k_{1_{obs}}$ (computer) and $k_{1_{obs}}$ (calcd.). The calculated values of $k_{1_{obs}}$ were obtained from an analysis of the current-time curves which is valid for simple second order reaction kinetics (*3*). The rate of bromination of 5-nitro-8-quinolinol was quite rapid and an approximate value of the overall rate constant, $k_{2_{obs}}$, for the monobromination reaction was found to be $2.0 \times 10^{-1} M^{-1}$ second^{-1} in 0.35*M* $HClO_4$ and $1.4 \times 10^{-4} M^{-1}$ second^{-1} in 0.45*M* $HClO_4$. The effects of varying bromide ion and hydrogen ion concentrations on the kinetics of bromination of 8-quinolinol is shown in Table III. The kinetic data obtained for the 4-methyl compound are

Table II. Analog Computer Results for 1.00×10^{-4}M 8-Quinolinol

Initial Concentration of $HClO_4$ = 0.23*M*

[NaBr]		Trial 1	Trial 2	Average
0.24	$10^{-3}k_{1_{obs}}$	3.48	3.50	3.49
	$10^{-3}k_{2_{obs}}$	3.38	3.28	3.33
0.64	$10^{-3}k_{1_{obs}}$	1.65	1.85	1.75
	$10^{-3}k_{2_{obs}}$	1.55	1.31	1.43
0.80	$10^{-3}k_{1_{obs}}$	1.34	1.40	1.37
	$10^{-3}k_{2_{obs}}$	1.30	1.21	1.25
1.00	$10^{-3}k_{1_{obs}}$	1.16	1.15	1.16
	$10^{-3}k_{2_{obs}}$	0.94	0.96	0.95

Initial Concentration of NaBr = 0.64*M*

$[HClO_4]$		1	2	Average
0.05	$10^{-3}k_{1_{obs}}$	4.60	4.60	4.60
	$10^{-3}k_{2_{obs}}$	3.30	3.00	3.15
0.12	$10^{-3}k_{1_{obs}}$	2.60	2.60	2.60
	$10^{-3}k_{2_{obs}}$	1.84	2.04	1.94
0.23	$10^{-3}k_{1_{obs}}$	1.65	1.85	1.75
	$10^{-3}k_{2_{obs}}$	1.55	1.31	1.43
0.35	$10^{-3}k_{1_{obs}}$	1.34	1.35	1.35
	$10^{-3}k_{2_{obs}}$	1.30	1.31	1.31

Table III. The Effect of Bromide and Hydrogen Ions on the Bromination of 1.00×10^{-4}M 8-Quinolinol

$[HClO_4]$	[NaBr]	$10^{-3}\overline{k_{2_{obs}}}$ Calcd.	$10^{-3}\overline{k_{2_{obs}}}$ Computer	$10^{-3}k_{2_{obs}}(1 + K \times [Br^-])$	$10^6 K_{a_1}/[H^+]$
0.23	0.24	3.91	3.49	17.7	...
0.23	0.64	1.97	1.75	20.8	...
0.23	0.80	1.60	1.37	20.0	...
0.23	1.00	1.97	1.16	20.9	...
0.05	0.64	5.48	4.60	...	13.88
0.12	0.64	3.02	2.60	...	5.78
0.23	0.64	1.97	1.75	...	3.02
0.35	0.64	1.74	1.35	...	1.98

$K_{a1} = 6.94 \times 10^{-6}$

Table IV. The Effect of Bromide Ion Concentration on the Bromination of 1.36 × 10^{-4}M 4-Methyl-8-Quinolinol

[$HClO_4$]	[NaBr]	$10^{-3}k_{1obs}$ Calcd.	$10^{-3}k_{1obs}$ Computer	$10^{-4}k_{1obs}$ / (1 + K [Br^-])
0.12	0.12	7.88	7.30	2.22
0.12	0.24	6.59	5.89	2.99
0.12	0.64	3.00	2.74	3.26
0.12	0.80	2.54	2.10	3.07
0.12	1.00	2.03	1.62	2.92
0.23	0.12	7.00	6.36	1.93
0.23	0.24	5.00	4.11	2.09
0.23	0.64	2.05	1.65	1.96
0.23	0.80	1.61	1.32	1.93
0.23	1.00	1.24	1.02	1.84
0.35	0.12	6.33	5.17	1.57
0.35	0.24	4.10	3.41	1.73
0.35	0.64	1.61	1.35	1.60
0.35	0.80	1.23	1.01	1.48
0.35	1.00	1.00	0.78	1.40

Table V. The Effect of Hydrogen Ion Concentration on the Bromination of 1.36 × 10^{-4}M 4-Methyl-8-Quinolinol in 0.64M NaBr

[$HClO_4$]	$10^{-3}k_{1obs}$ Calcd.	$10^{-3}k_{1obs}$ Computer	$10^{6}K_{a1}/[H^+]$	$10^{-4}[H^+]/K_{a1}$
0.05	4.77	4.05	54.00	1.85
0.07	4.02	3.57	38.57	2.59
0.095	3.25	2.92	28.46	3.52
0.12	3.00	2.69	22.50	4.44
0.23	2.05	1.65	11.74	8.52
0.35	1.61	1.35	7.71	12.96
0.47	1.36	1.12	5.74	17.40

$K'_{a1} = 2.7 \times 10^{-6}$

summarized in Tables IV to VII. The specific rate constants obtained from these data are compared in Table VIII.

DISCUSSION

An analysis of the data for 8-quinolinol shows that the plot of k_{1obs} (1 + K [Br^-]) *vs.* [Br^-] is a straight line of zero slope. Furthermore, it is seen that the rate constant for the bromination of the neutral species is about 10^4 times greater than that of the protonated species. This is in agreement with a previous study of some 8-quinolinols (*4*).

The results obtained for the 4-methyl compound are quite unexpected in view of the work reported by Corsini and Graham (*2*). Little difference was found between the behavior of 8-quinolinol and its 4-methyl derivative. The values of k_{1obs} and k_{2obs} for 4-methyl-8-quinolinol are approximately equal to one another and to those obtained for 8-quinolinol. The data for the monobromination of 4-methyl-8-quinolinol show that the tribromide ion is not an active brominating species and here again the neutral species is much more reactive than the protonated species.

The neutral species also brominates with a rate constant which is much larger than that for the protonated species in the bromination of the halo substituted compounds. The rate constant for the neutral species of 8-quinolinol, furthermore, was about 10 times that for the 5-bromo derivative. These rate constants, however, refer to bromination at different sites (the 5 and the 7 position) and the difference may not, therefore, be entirely due to halogen deactivation. Furthermore, the rate constants for the neutral halo substituted 8-quinolinols follow the order bromo~chloro>fluoro.

Table VI. The Effect of Bromide Ion Concentration on the Second Bromination Step of 1.36 × 10^{-4}M 4-Methyl-8-Quinolinol

[$HClO_4$]	[NaBr]	$10^{-3}k_{2obs}$	$10^{-3}k_{2obs}$ / (1 + K[Br^-])
0.12	0.12	4.28	13.0
0.12	0.24	3.09	15.7
0.12	0.64	2.29	27.2
0.12	0.80	2.04	29.8
0.12	1.00	1.90	34.0
0.23	0.12	3.93	11.9
0.23	0.24	3.41	17.3
0.23	0.64	1.60	19.0
0.23	0.80	1.37	20.0
0.23	1.00	1.18	21.2
0.35	0.12	3.95	12.0
0.35	0.24	2.86	14.5
0.35	0.64	1.28	15.2
0.35	0.80	1.12	16.3
0.35	1.00	0.84	15.1

Table VII. The Effect of Hydrogen Ion Concentration on the Second Bromination of 1.36 × 10^{-4}M 4-Methyl-8-Quinolinol in 0.64M NaBr

[$HClO_4$]	$10^{-3}k_{2obs}$	$10^{-4}K'_{a1}/[H^+]$	$10^{-2}[H^+]/K'_{a1}$
0.05	4.26	23.2	4.31
0.07	3.35	16.57	6.02
0.095	2.99	12.21	8.19
0.12	2.29	9.67	10.34
0.23	1.59	5.04	19.83
0.35	1.28	3.31	30.17
0.47	1.04	2.47	40.52

$K'_{a1} = 2.7 \times 10^{-6}$

An interesting result which has emerged from this work is that the tribromide ion is not an active brominating species in the first bromination step of 8-quinolinol or the 4-methyl compound. In the second bromination step of the two compounds, however, as well as in the bromination of the 5-chloro and 5-fluoro compounds, the tribromide ion is an active brominating species. In all cases a positive slope is obtained when values of k_{2obs} (1 + K [Br^-]) are plotted against [Br^-]. These slopes increase when the hydrogen ion concentration is decreased. In all cases, however, the rate constant for

Table VIII. Summary of Rate Constants

	$10^{-4} \times k_1$ or $10^{-4} \times k_1'$			$10^{-2} \times k_2$ or $10^{-2} \times k_2'$			$10^{-6} \times k_3$ or $10^{-6} \times k_3'$	$10^{-2} \times k_4$ or $10^{-2} \times k_4'$
Molarity of $HClO_4$	0.12	0.23	0.35	0.12	0.12	0.35		
8-Quinolinol	...	2.0	...	...	0	...	26	8
5-Bromo-8-quinolinol	2.4	1.6	...	7	2.4	...	2.0	1
4-Methyl-8-quinolinol	3.1	1.6	...	...	...	...	75	7.5
4-Methyl-5-bromo-8-quinolinol	1	1.6	1.3	14	3	1.5	1.5	8
5-Chloro-8-quinolinol	1.6	...	...	9	...	...	1.6	2.5
5-Fluoro-8-quinolinol	...	0.4	...	...	0.7	...	0.65	1.7

tribromide bromination is about 1–2% that of molecular bromine. Therefore tribromide ion is a less reactive brominating agent than molecular bromine as was found previously for aromatic bromination (*1*). The above results for tribromide ion activity in substituted 8-quinolinols agree with a previous observation (*4*), that in 8-quinolinols substitution in the seven position occurs *via* the attack of the tribromide ion as well as by molecular bromine, whereas substitution in the 5-position takes place only via attack of a bromine molecule.

LITERATURE CITED

(1) Bell, R. P., Rawlinson, D. J., *J. Chem. Soc.* **1961**, 63.
(2) Corsini, A., Graham, R. P., *Anal. Chim. Acta* **28**, 583 (1963).
(3) Kozak, G. S., Fernando, Q., *J. Phys. Chem.* **67**, 811 (1963).
(4) Kozak, G. S., Fernando, Q., Freiser, H., ANAL. CHEM. **36**, 296 (1964).
(5) O'Dom, G., Fernando, Q., *Ibid.*, **37**, 893 (1965).
(6) Petrow, V., Sturgeon, B., *J. Chem. Soc.* **1954**, 570.
(7) Prasad, R., Coffer, H. L. D., Fernando, Q., Freiser, H., *J. Org. Chem.* **30**, 1251 (1965).

RECEIVED for review December 9, 1965. Accepted March 16, 1966. Work supported by the National Institutes of Health.

Intermolecular Energy Transfer as a Means of Chemical Analysis

Sensitization of Rare Earth Emission in Dilute Solution by Aromatic Carbonyl Compounds

W. J. McCARTHY and J. D. WINEFORDNER

Department of Chemistry, University of Florida, Gainesville, Fla.

▷ **The fluorescence emission of terbium, europium, samarium, and dysprosium ions is selectively sensitized by various aromatic carbonyl compounds. The system is excited by monochromatic light at the wavelength of maximum absorption for the phosphorescence transition of the carbonyl compound, and emission is measured at the wavelength corresponding to the rare earth ion emission line. The influence of donor-acceptor concentration on the emission intensity of the rare earth ion is studied, and limits of detection for the rare earths are given. An empirical equation is developed to facilitate prediction of sensitization by a specific aromatic carbonyl compound for a specific rare earth. The analytical possibilities of the new phenomenon are discussed with regard to sensitivity, selectivity, and speed of analysis and other analytically important considerations.**

AN INVESTIGATION of the emission of several rare earth ions in chelates by the method of intramolecular energy transfer resulted in the discovery of a new phenomenon. This phenomenon, the intermolecular energy transfer from excited organic compounds to rare earth ions in solution (*7, 9, 10 13*), seems to possess great analytical possibilities for several reasons: The method should be nearly as selective as any atomic emission procedure because the line emission from an ion in solution is being measured, and even more selectivity should arise because various organic compounds transfer their energy with widely different efficiencies to different rare earth ions.

Analytical considerations such as speed, accuracy, precision, and convenience have not been previously studied for the phenomenon and were included in this investigation. Commercially available instrumentation is used for these studies.

THEORY

The phenomenon of intramolecular energy transfer in rare earth chelates is well known, but it has received little attention from an analytical standpoint, probably because of the stoichiometric dependence of the sensitized emission. The process of intramolecular energy transfer has been described in the past few years in detail by Weissman (*21*) and Crosby and coworkers (*4–6, 8*). The ligand molecules are raised to the first excited singlet state by absorption of a photon which approximately corresponds in energy to the absorption energy of the uncomplexed ligand; the spectral shift is, of course, due to the presence of the ligand in the chelate rather than simply the uncomplexed ligand. After a radiationless crossover to the triplet state of the ligand, energy is transferred to the metal ion in the chelate, raising the metal ion to an excited (luminescent) level. As the excited ion undergoes a radiational deactivation to the ground state, the sensitized emission of the metal ion is observed. This type of energy transfer has been applied to a number of cases of analytical interest. Two articles (*2, 18*) have reviewed the state of the method through 1962; recently a new method utilizing intramolecular energy transfer has been developed for the determination of Sm, Tb, Dy, and Eu (*1*).

Recently, however, sensitized emission from nonchelated rare earth ions in solution has been observed. Matovick and Suzuki (*13*) observed that $Eu(NO_3)_3$ and $Tb(NO_3)_3$ fluoresce strongly in solutions of acetophenone, propiophenone, and benzophenone when irradiated with long wavelength ultraviolet light (3000 to 4000 A.). They found that water strongly quenched the emission of the rare earth ions. They concluded that the mechanism of excitation for the rare earth ion was through a weakly bonded ketone complex. They suggested that the process was probably endothermic, which would account for the observed rise in the quantum efficiency with increased temperature.

El-Sayed and Bhaumik (*7*) observed that benzophenone efficiently transferred its energy to an europium chelate (europium trishexafluoroacetylacetonate) at room temperatures. They suggested initial intermolecular transfer of triplet state energy from the benzophenone to the ligand and subsequent intramolecular transfer of energy to the europium ion as the mechanism of the process. A tenfold increase in europium ion emission upon addition of the benzophenone donor was reported by these authors. Because of temperature variations of the intensity of rare earth emission, a diffusion-controlled process was shown to exist rather than the weak

chelate previously suggested for the mechanism of energy transfer. Similar results have been obtained by Gallagher, Heller, and Wasserman (*9*) in studying the nonradiative resonance exchange process (*19*) from terbium to europium ions after initial transfer of energy from 4,4′ -dimethoxybenzophenone. The authors found that other rare earth ions would not participate in this two-step type of mechanism.

Heller and Wasserman (*10*) have performed an extensive investigation of direct transfer of triplet state energy from various organic carbonyl compounds to rare earth ions in solution. A qualitative examination of the efficiency of transfer from 25 organic compounds to europium and terbium in dilute solutions was presented. The possibility of a chelate formation mechanism for energy transfer was shown to be improbable, because no changes in emission spectra are observed from one donor to another. The criteria for efficient energy transfer were qualitatively discussed, and, of greatest importance, the lack of dependence of rare earth emission on the stoichiometry of the system was also considered. They also suggested that a second-order diffusion-controlled process was the probable mechanism for excitation of the rare earth ions.

It has been shown for a limited number of systems (*10*) that the process observed under the experimental conditions described above is the transfer of triplet state energy from the donor to the acceptor. This process may be schematically represented as shown in Figure 1. The donor absorbs incident radiation and is excited to the lowest energy excited singlet state. The molecule then crosses over to the lowest energy triplet state. After an encounter with a rare earth ion which has an absorption level of slightly lower energy than the energy of the triplet state of the donor, energy is transferred. This transfer of energy populates one of the luminescent levels of the rare earth ion. Finally, emission of energy as the line fluorescence of the rare earth ion (*10*) results. Hence, in an analytical study, the system would be excited at the absorption maximum for production of the lowest energy triplet state of the donor molecule, and the emission would be measured at the fluorescence wavelength of the rare earth ion emission line (or, where there is more than one line, at the most intense line). Experimental evidence supports this type of process (*7, 9, 10, 13, 19*):

Excitation occurs at the wavelength maximum for the excitation of the phosphorescence of the donor.

Emission occurs at the wavelength(s) for rare earth ion luminescence.

There are no shifts in the rare earth ion emission spectrum from one donor to another, which is expected if a chelate is present.

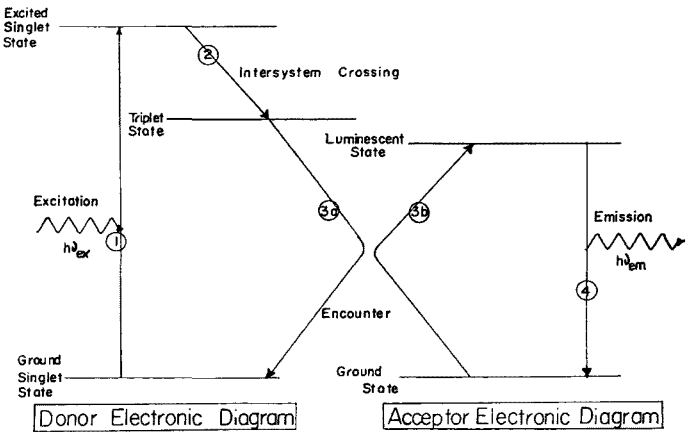


Figure 1. Schematic representation of mechanism for intermolecular energy transfer from aromatic carbonyl donor compound to rare earth acceptor

Step 1. Absorption of photon, $h\nu_{ex}$, to produce excited singlet state of donor
Step 2. Radiationless crossover from excited singlet state to triplet state of donor
Step 3a. Upon collision of donor with acceptor, donor loses its energy by a radiationless deactivation to the ground singlet state
Step 3b. Rare earth accepts energy lost by donor in step 3a and is raised to its luminescent electronic level(s)
Step 4. Rare earth loses its energy by emitting a photon, $h\nu_{em}$. This produces the emission spectrum of the rare earth.
Other radiational and radiationless processes are involved but are not important in the transfer mechanism, although they affect the efficiency of energy transfer

The process as described above in spin-invariant in the transfer step—i.e., the donor multiplicity changes by 2 [from 3 to 1 (triplet to singlet)]—and the rare earth ion multiplicity also changes by two—e.g., trivalent Tb absorption at 491 mμ is $^7F_6 \rightarrow {}^5D_4$.

The efficiency of transfer increases with temperature—i.e., the number of encounters increases.

The process of intermolecular energy transfer from organic molecules to rare earth ions is very similar to the transfer of energy between organic molecules in solution (*14–17, 20*). Application of intermolecular energy transfer between molecules to analysis has been discussed by Parker, Hatchard, and Joyce (*17*).

EXPERIMENTAL

Apparatus. An Aminco-Bowman spectrofluorometer (American Instrument Co., Silver Spring, Md.) equipped with an Aminco solid sample accessory (Catalog No. C73-62140), an Aminco-Kiers phosphoroscope attachment (Catalog No. C27-62140), a potted RCA 1P28 multiplier phototube, and an X-Y recorder (Model 1620-814, manufactured for American Instrument Co., by Electro Instruments, Inc., San Diego, Calif.) were used for obtaining all spectra. The source was a high pressure xenon arc powered by the solid state power supply provided with the instrument. Relative emission intensities were obtained directly from the Aminco photomultiplier - microphotometer also supplied with the instrument.

Luminescence decay times for molecules with relatively long lifetimes (greater than 0.2 second) were measured by manually terminating the excitation beam with the aid of a blank slit placed in the excitation path. For species with short luminescence decay times—i.e., less than 0.2 second—the multiplier phototube was powered by batteries, and the photoanodic current of the multiplier phototube was amplified by a Textronix Type 122 low level preamplifier (Textronix, Inc., Portland, Ore.). The output of the preamplifier was displayed on a Textronix Type 545 oscilloscope, equipped with Type L plug-in preamplifier and the decay of the species during the repetitive cycles of the phosphoroscope was recorded on Polaroid 3000 speed Type 47 film using a Textronix trace-recording camera (Type C-12).

Reagents. The oxides of cerium, praseodymium, neodymium, samarium, lanthanum, europium, gadolinium, terbium, dysprosium, holmium, erbium, thulium, ytterbium, and lutetium, (Rare Earth Division, American Potash and Chemical Corp., West Chicago, Ill.) were obtained in purities of 99.9% or better, except for Dy and Ho which were of 99% minimum purity. Reagent grade acetic anhydride was used as the solvent. All donor organic carbonyl compounds were reagent grade and were readily available from several sources. Stock solutions of all donor compounds were made to be 0.02*M* with acetic anhydride as the solvent.

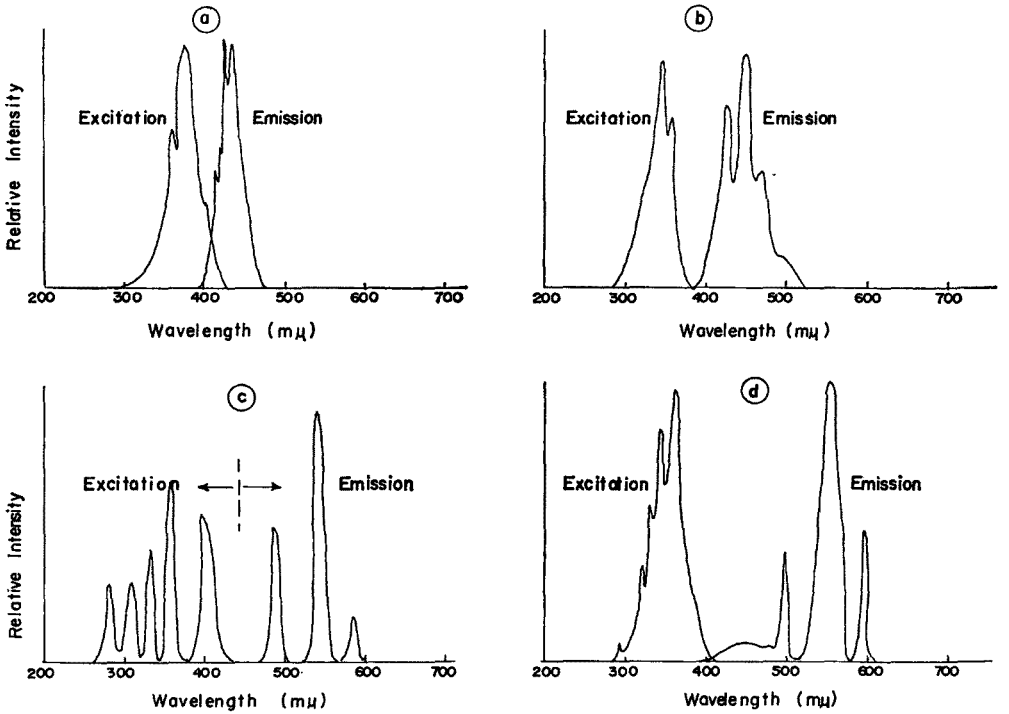


Figure 2. Luminescence spectra of 4,4′-dimethoxybenzophenone (donor) and terbium(III) ions

a. Fluorescence excitation and emission spectra for donor at room temperature ($2 \times 10^{-2}M$)
b. Phosphorescence excitation and emission spectra of donor at 77° K. ($2 \times 10^{-5}M$)
c. Line spectrum of Tb^{+3} at room temperature ($2 \times 10^{-2}M$)
d. Excitation and emission spectra for donor and Tb^{+3} together at room temperature. (Donor at $10^{-2}M$ and terbium ions at $10^{-2}M$)
No intended correlation from plot to plot of relative intensities

The rare earth oxides were dissolved in HCl or HNO_3 and evaporated to dryness on a hot plate. The rare earth chloride or nitrate was then dissolved in acetic anhydride with the aid of deionized distilled water with care to prevent spattering due to localized heat production. In this manner, stock solutions of the rare earth ions were prepared to be $0.02M$ in the rare earth ion.

Procedure. Relative emission intensity signals of the rare earth-donor systems were obtained by adding 1 ml. of the stock solution of the donor and 1 ml. of the stock rare earth solution to a 1-sq. cm. quartz cell after deoxygenating with a stream of nitrogen gas. Oxygen is well known as a quencher for the triplet state and Heller and Wasserman discuss the necessity for deoxygenating solutions (*10*). This procedure produced a $0.01M$ solution of both donor and rare earth ion. The mixture in the quartz cell was placed in the solid sample cell compartment, and the relative emission intensity signal of the rare earth-donor system was determined.

Phosphorescence excitation and emission spectra were obtained as previously described (*12*, *22*) for the donor molecules in ethanol solvent at 77° K. Phosphorescence decay times were also measured as previously described (*12*) for the systems with lifetimes greater than 0.2 second and as mentioned above for systems with lifetimes less than 0.2 second.

Fluorescence excitation and emission spectra were obtained similarly at room temperature of the donors alone and for the donor-acceptor systems.

RESULTS AND DISCUSSION

The use of intermolecular energy transfer as an analytical tool depends upon the knowledge of several factors which influence a determination. The optimum excitation wavelength for any donor-acceptor system is the wavelength at which the donor is excited to the state which allows it to transfer its energy to the acceptor. The optimum wavelength of emission is the wavelength at which the acceptor emits the greatest amount of its energy devoid of interfering lines. The excitation spectrum of the mixed system is a superposition of the phosphorescence excitation spectrum and the rare earth excitation spectrum (*10*).

In Figure 2, the energy transfer process is more clearly demonstrated. Four spectra are shown: fluorescence excitation and emission spectra of the donor at room temperature; phosphorescence excitation and emission spectra of the donor at 77° K.; the line spectrum of the rare earth ion at room temperature; and the excitation and emission spectra of the donor-acceptor system at room temperature. The great increase in the emission intensity of the rare earth ion in the presence of a donor as compared to the emission in the absence of the donor is a direct result of the transfer of energy from the triplet state of the aromatic carbonyl to the rare earth ion. Intermolecular energy transfer is not the only means of excitation, as can be seen from Figure 2, *d*. The excitation spectrum of the rare earth emission is a combination of the phosphorescence excitation spectrum of the donor and a line absorption spectrum of the rare earth, and so some direct excitation of the rare earth should also occur.

Direct demonstration of intermolecular energy transfer can be made by referring to Figure 3, where three

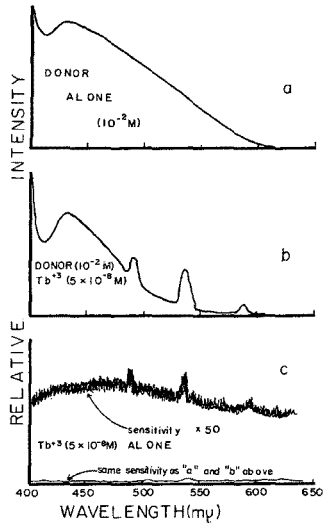


Figure 3. Illustration of sensitized rare earth ion emission due to aromatic carbonyl compound

Donor is 4,4′-dimethoxybenzophenone and RE acceptor is Tb^{+3}

a. Fluorescence spectrum of donor ($10^{-2}M$) alone at room temperature

b. Emission spectrum of donor ($10^{-2}M$) and acceptor ($5 \times 10^{-8}M$) at room temperature

c. Lower curve. Emission spectrum of acceptor alone at $5 \times 10^{-8}M$ obtained at same instrumental sensitivity as used for *a* and *b*

Upper curve. Emission spectrum of acceptor alone at same concentration but at 50 times greater sensitivity, both spectra taken at room temperature

Table I. Enhancement Factors for Various Rare Earth Ion-Donor Systems and Phosphorescence Lifetimes of the Donors

Donor	Phosphorescence lifetime, sec.[a,b]	Enhancement factor[c,d] Eu^{+3}	Tb^{+3}	Sm^{+3}	Dy^{+3}
Benzophenone	0.008	3.3	150	12	2
4,4′-Dimethoxybenzophenone	0.035	7.3	1100	23	17
2-Acetonaphthone	0.90	2.0	0	0	0
2-Bromoacetophenone	0.038	8.0	37	0	2.0
Vanillin	0.025	2.7	14	23	2.0
Veratraldehyde	0.22	2.0	2.0	33	0
2-Bromo-4′-phenylacetophenone	0.028	27	10	21	0
2,4′-Dibromacetophenone	0.008	4.7	23	0	0
9-Fluorenone	...[e]	0	0	0	0
7,8-Benzoflavone	2.9	0	5	0	0
o-Nitrobenzaldehyde	2.2	2.3	0	0	0
4′-Bromoacetophenone	0.004	3.3	76	2.0	2.5
Benzaldehyde	0.020	25	425	0	3.5
Anisaldehyde	0.14	2.0	50	6.0	19
o-Tolualdehyde	0.022	28	370	10	8
m-Tolualdehyde	0.034	20	480	0	11
1-Acetonaphthone	0.6	10	0	0	0
Acetophenone	0.036	9.3	195	3	8
p-Chloroacetophenone	0.022	5.0	44	4	2.5

[a] All lifetimes measured in an ethanol solution at 77° K.
[b] Lifetimes greater than 0.2 sec. measured on recorder; lifetimes less than 0.2 sec. measured with oscilloscope.
[c] Enhancement factor is defined as ratio of RE intensity to background intensity at wavelength of maximum RE emission.
[d] Concentration of all donors and acceptors is $10^{-2}M$ in acetic anhydride solvent. Front surface illumination used to obtain maximum intensity. All enhancement factors measured at room temperature (293° K.).
[e] No phosphorescence observed.

spectra are shown: emission of a solution containing no acceptor, of a solution containing donor at $0.01M$ and acceptor at a concentration 5 times the concentration at the limit of detection, and of a solution containing no donor but containing an acceptor at 5 times the concentration as at the limit of detection—i.e., limit of detection resulting when donor is present. These spectra also indicate the relative ease with which one may make quantitative measurements of rare earth emission in the presence of a fluorescent donor.

Quantitative measurements of the degree of enhancement of the rare earth ion emission by various donors are presented in Table I, in terms of the enhancement factor obtained by dividing the relative intensity of the rare earth ion emission in the presence of the donor by the relative intensity of the background at that wavelength. This is an analytically important value because the limit of detection is defined as an enhancement factor of unity—i.e., the limit of detection is that concentration which produces a luminescence signal exactly equal to the background signal. Actually this is a very conservative definition for the limit of detection. In most isolated experimental cases, a considerably lower limit of detection can be obtained. Also included in Table I are the measured triplet state lifetimes at 77° K. The lifetimes at room temperature are much shorter. Even so, there is an inverse correlation between the enhancement factor and the triplet state lifetime. This observation seems o contradict the energy transfer scheme which has been invoked for an explanation of the phenomenon. However, because the energy transfer process is both collision and lifetime-limited, the contradiction fades—i.e., the time for a collision must in the cases studied here be much less than the lifetime of the triplet state, and so the more triplet singlet transitions, the greater the enhancement of the rare earth emission.

Acetic anhydride was the so'vent used for all measurements except the phosphorescence spectra. Although the energy transfer process under examination here has been reported (*10*) to occur in other less objectionable solvents (ethyl alcohol, methanol, pyridine, acetic acid, and dimethylformamide), the greatest emission intensities were observed in acetic anhydride. The presence of water in the solvent system decreased the efficiency of sensitization because water in the coordination sphere of the rare earth ion probably prevented an intimate encounter with the donor.

Wide variation is observed in the efficiency of energy transfer for various systems. In an attempt to explain this in terms of physical parameters characteristic of each system, a multiple regression analysis of experimental data was performed by means of the stepwise multiple regression with variable transformation computer program (ERMPR 3) obtained from SHARE distribution number 1194 modified for the University of Florida IBM 709 digital computer.

The program produces an empirical equation relating input parameters to the enhancement factor. The programmer determines which of the factors produce the best fit by examining such statistical information as simple correlation coefficients between the various parameters and the standard error of the input data and the resulting equation. The reliability of the equation produced by this procedure is measured by examining the multiple correlation coefficient and the F level. From a consideration of the standard errors and multiple correlation coefficients obtained from over 20 trials, the best empirical equation for predicting the enhancement factor appears to be:

$$\ln E_f = -18.7 - 0.085\left(\frac{1}{T}\right) + 1.5\left(\frac{1}{T}\right)^{1/2} + 2.8 \times 10^3\left(\frac{1}{M_A}\right) +$$

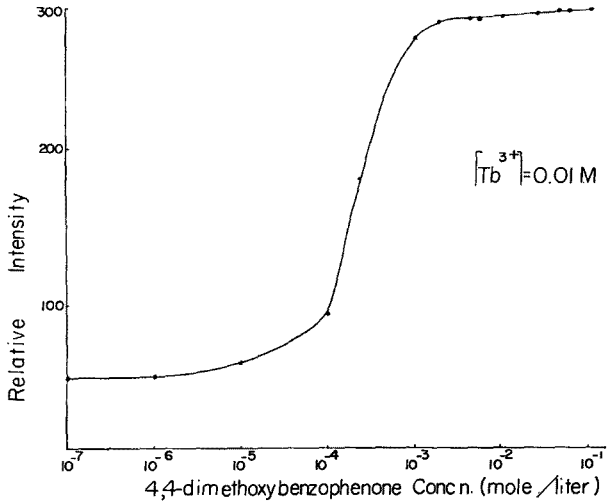


Figure 4. Variation of terbium(III) ion luminescence with changes in donor (4,4′-dimethoxybenzophenone) concentration

Terbium concentration 0.01 M at all points. Data taken at room temperature with front surface illumination

$$1.9 \times 10^5 \left(\frac{1}{M_D}\right)^2 + 1.3 \times 10^8 \left(\frac{1}{M_A M_D}\right)^2 - 1.1 \times 10^2 \left(\frac{1}{M_A M_D}\right)^{1/2} + 1.5 \left(\frac{1}{TM_A M_D}\right)^2 - 1.0 \times 10^{-5} \times \left(\frac{1}{TM_A M_D}\right)^{1/2}$$

where E_f is the enhancement factor, T is phosphorescence decay time in seconds, M_A is the atomic weight of the acceptor, and M_D is the molecular weight of the donor.

The equation can be used to predict approximate values of the enhancement factor for a specific donor-acceptor system. Only the decay time and the molecular weights prove significant in determining E_f. Various functional relationships between phosphorescence and fluorescence excitation and emission wavelengths were constructed, but all were of little significance in determining E_f. By determining the decay time and the two weights, an approximate enhancement factor can be predicted. The standard error of ln E_f is ±1.10—i.e., the standard error of E_f is ±3.1. The above equation was calculated to have a multiple correlation coefficient equal to 0.65 and an F level of 3.52; both of these statistical measures place the equation well within a 95% confidence interval, assuming a normal distribution.

Only europium, terbium, samarium, and dysprosium were found to display any sensitized emission. The effect of donor concentration on the acceptor luminescence was studied. With the concentration of the terbium held constant, the concentration of the donor, 4,4′-dimethoxybenzophenone, was varied. The results of this study are shown in Figure 4. The relative intensity of the terbium emission remained nearly constant over about a 500-fold range of donor concentrations; further decrease in donor concentration resulted in a rapid decrease in terbium emission with concentration. This observation should be of great importance in analytical studies, because small changes in donor concentration from sample to sample would not greatly affect the rare earth emission. Also, the mechanism of a diffusion-controlled encounter is supported by these data; if chelate formation were the mechanism, a wide variation of intensity of emission would be expected for donor concentrations less than acceptor concentrations (see Figure 4).

Analytical curves were prepared for the rare earth ions which were found to be useful acceptors by varying the rare earth ion concentration while holding the donor concentration constant (Figure 5). All points are the averages of duplicate or multiplicate readings. The relative standard deviation for all concentrations tenfold greater than the limit of detection was less than 10%. In all cases the analytical curves were determined with the donor concentration at 0.01M; the donor for the rare earth ions is in each case the one which most efficiently sensitized the rare earth emission (Table I). Initially very poor sensitivities were obtained for the systems while the conventional fluorescence cell arrangement was used—i.e.,

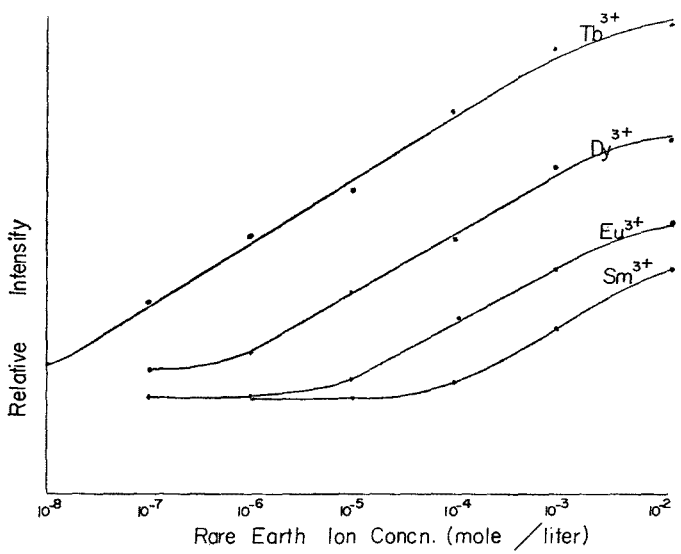


Figure 5. Analytical curves for terbium(III), dysprosium(III), europium(III), and samarium(III) ions

Donors. 4,4′-Dimethoxybenzophenone; anisaldehyde; o-tolualdehyde; and veratraldehyde, respectively, held at 0.01 M for all measurements. All analytical curves taken at room temperature with front surface illumination

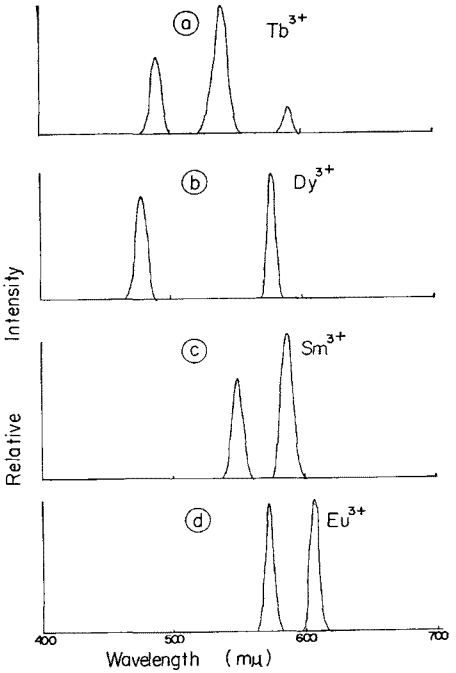


Figure 6. Luminescence spectra of ions in acetic anhydride

a. Terbium
b. Dysprosium
c. Samarium
d. Europium

No indended correspondence of relative intensity from one spectrum to another. Concentration of all RE ions $10^{-2}M$, spectra taken at room temperature

observing emission at right angles to illumination. Great increases in sensitivities were obtained when front surface illumination was used because the $0.01M$ solutions of the donors are optically thick in most cases. Analytical curves were measured for terbium and 4,4′-dimethoxybenzophenone; dysprosium and anisaldehyde; europium and *o*-tolualdehyde; and samarium and veratraldehyde. Limits of detection were found to be $10^{-8}M$, $8 \times 10^{-7}M$, 5×10^{-6}, and $2 \times 10^{-5}M$ for Tb^{+3}, Dy^{+3}, Eu^{+3}, and Sm^{+3}, respectively; the useful ranges of the analytical curves were over a 10,000-, 1000-, 1000-, and 100-fold concentration range, respectively (see Figure 5) for Tb^{+3}, Dy^{+3}, Eu^{+3}, and Sm^{+3}.

Extraneous ions present in the sample were found to quench the energy transfer process in relation to their concentration, as expected. This effect is probably due to a collisional competition between the extraneous ion and the rare earth ion to be sensitized. Consequently, if a system for analysis has other ions present, a standard addition technique should be employed. Such studies were extensively investigated by Alberti and Massucci (*1*).

Simultaneous determination of the four rare earth ions which exhibit sensitized emission should be possible. An examination of the emission spectra of the ions (Figure 6) shows that with suitable adjustment of the emission monochromator, the various lines may be isolated. For quantitative work, standard addition would be necessary to determine the amount of each ion present. Further selectivity is available to the analyst by judicious choice of the donor (Table I)—for example, a donor which efficiently sensitizes the emission of terbium but completely quenches the emission of other rare earth ions would be an obvious choice if terbium were to be determined in the presence of other rare earth ions.

CONCLUSIONS

Intermolecular energy transfer appears to hold great promise for the determination of trace amounts of terbium, dysprosium, europium, and samarium in samples containing rare earth ions. Large useful concentration ranges are available for quantitative work. Great selectivity is a natural consequence of both the transfer process and the line nature of the rare earth ion emission. The low limits of detection for the rare earth ions should permit microtechniques to be used for small samples. The lack of a great dependence of emission intensity on donor concentration reduces possible gross errors in the method. The procedure for analysis is extremely fast and simple, except that acetic anhydride is an objectionable solvent.

It is conceivable that emission intensities can be increased even more (perhaps as much as 20-fold) by using deuterated solvents (*8*, *11*). Further studies of donor molecules should yield useful enhancement factors. The empirical equation for enhancement factor given above is by no means intended as a final result but rather as an initial indication of preliminary results.

ACKNOWLEDGMENT

The authors thank the University of Florida Computing Center and Jim Marcum for help in obtaining the computer program.

LITERATURE CITED

(1) Alberti, G., Massucci, M. A., ANAL. CHEM. **38**, 214 (1966).
(2) Bartholomew, R. J., *Rev. Pure Appl. Chem.* **8**, 265 (1958).
(3) Borkowski, R. P., Forest, H., Grafstein, D., *J. Chem. Phys.* **42**, 2974 (1965).
(4) Crosby, G. A., Kasha, M., *Spectrochim. Acta* **10**, 377 (1958).
(5) Crosby, G. A., Whan, R. E., Alire, R. M., *J. Chem. Phys.* **34**, 743 (1961).
(6) Crosby, G. A., Whan, R. E., Freeman, J. J., *J. Phys. Chem.* **66**, 2493 (1962).
(7) El-Sayed, M. A., Bhaumik, M. L., *J. Chem. Phys.* **39**, 2391 (1963).
(8) Freeman, J. J., Crosby, G. A., *J. Phys. Chem.* **67**, 2717 (1963).
(9) Gallagher, P. K., Heller, A., Wasserman, E., *J. Chem. Phys.* **41**, 3921 (1964).
(10) Heller, A., Wasserman, E., *Ibid.*, **42**, 949 (1965).
(11) Kropp, J. L., Windsor, M. W., *Ibid.*, **42**, 1599 (1965).
(12) McCarthy, W. J., Winefordner, J. D., *J. Assoc. Offic. Agr. Chemists* **48**, 915 (1965).
(13) Matovick, E., Suzuki, C. K., *J. Chem. Phys.* **39**, 1442 (1963).
(14) Parker, C. A., *Proc. Roy. Soc.* **A, 276**, 125 (1965).
(15) Parker, C. A., Hatchard, C. G., *Proc. Chem. Soc.* **1962**, 386.
(16) Parker, C. A., Hatchard, C. G., *Proc. Roy. Soc.* **A 269**, 574 (1962).
(17) Parker, C. A., Hatchard, C. G., Joyce, T. A., *Analyst* **87**, 1 (1965).
(18) Parker, C. A., Rees, W. T., *Ibid.*, **87**, 83 (1962).
(19) Peterson, G. E., Bridenbaugh, P. M., *J. Opt. Soc. Am.* **53**, 1129 (1963).
(20) Porter, G., *Proc. Chem. Soc.* **1959**, 291.
(21) Weissman, S. I., *J. Chem. Phys.* **10**, 214 (1942).
(22) Winefordner, J. D., Moye, H. A., *Anal. Chim. Acta* **32**, 278 (1965).

RECEIVED for review February 1, 1966. Accepted March 30, 1966. Research carried out as part of a study on the phosphorimetric analysis of drugs in blood and urine, supported by a grant from the U. S. Public Health Service (GM-11373-03). W. J. McCarthy held a Gulf Oil fellowship during the academic year 1965–66 at the University of Florida.

Rapid Determination of Primary Hydroxyl Content of Poly(Oxyalkylene) Glycols and Poly(Oxyalkylene) Sorbitols by Pseudo First-Order Differential Reaction Kinetics

FRISO WILLEBOORDSE and R. L. MEEKER

Chemicals Division, Union Carbide Corp., Technical Center, South Charleston, W. Va.

▷ **The conventional procedure for the determinaton of primary hydroxyl content in polyols, the logarithmic extrapolation method based on the differential kinetic analysis of the hydroxyl group reacting with either acetic anhydride or phenyl isocyanate, is cumbersome with respect to duration of analysis and method of calculation. A differential pseudo first-order reaction rate approach is described which only requires a fraction of the analysis time of the extrapolation method, and does not need a calculation procedure. The primary hydroxyl content of the polyol is obtained by determination of the effective fractional life time in the urethanation reaction and usage of a predetermined calibration curve. The procedure can be applied to any other binary system of active-hydrogen-containing compounds when simultaneous reactions with phenyl isocyanate occur under sufficiently differential rate constant conditions.**

An increasing number of analytical techniques for the determination of mixtures of organic compounds which contain the same functional group have been based upon differences in reaction rates with a common reagent (*5*, *7*). With reference to mixtures of hydroxyl compounds this approach was recently successfully applied under irreversible second-order reaction conditions to determine binary mixtures of alcohols and primary/secondary hydroxyl contents in polyether polyols with reagents such as acetic anhydride (*3*) or phenyl isocyanate (*9*). In addition, three non-kinetic methods have been developed. One approach employing the reaction between primary alcohols and trityl chloride (*4*) is quite time-consuming and does not resolve secondary and tertiary alcohols. Another one involves an esterification reaction of primary alcohols with 3-nitrophthalic anhydride (*2*), but secondary hydroxyl groups interfere because of partial esterification. A third method (*1*) is based on the absorption spectra of nitrites of hydroxyl compounds in the ultraviolet region. However, the absorption band maxima of the nitrites of primary alcohols differ only by 1–2 mμ from those of secondary alcohols. For polyglycols the method has to be carried out under nitrogen, and includes a filtration step and a correction for background absorption.

A recently published kinetic method (*9*) will determine the primary hydroxyl content in ω,ω'-polyether glycols and in mixtures of isomeric alcohols. This method is not restricted to two-component systems. The technique presented in this paper is based on the same reaction—i.e., between the hydroxyl compounds and phenyl isocyanate—which is followed by observing the disappearance of the NCO band at 4.42 microns in the infrared region of the spectrum. However, instead of employing the second-order logarithmic extrapolation technique (*9*), the present method is based on pseudo-first order kinetics, thus circumventing the two inconvenient features of the extrapolation technique—i.e., length of reaction time and the calculation procedure. Apart from the analytical desirability and convenience of the pseudo first-order approach, the method can be utilized to determine (by extrapolation) the reaction rate constants of single functional groups in polymeric substances. In the underlying case, it was possible to determine the rate constants of the primary alcohol groups and those of the secondary alcohol groups in poly(oxyalkylene) compounds with phenyl isocyanate in the urethanation reaction, and with acetic anhydride in the acetylation reaction. However, this approach is by no means limited to the above-mentioned cases, but can generally be applied for any other type of system where the simultaneous reactions of various molecules with the same functional group can lead to differential kinetic analysis (*5*). The pseudo first-order approach has in addition the advantage of overcoming nonintegral kinetic orders in reaction rate studies which has been recognized and utilized long ago by Roberts and Regan (*8*).

The present method is extremely rapid, requiring 10 minutes per analysis, and is not subject to interference by finite mixing times. Reaction conditions are mild and do not effect fragmentation of polyether linkages. The procedure is applicable to binary mixtures of alcohols whose rate constant ratios are as low as 1.97 to 1, and to glycol-based or sorbitol-based polyhydric alcohols in their entire molecular weight region between 200 and 5000.

The procedure requires the construction of a predetermined calibration curve employing either the two constituents or, in the case of polyols, known mixture compositions. The method should be industrially of significant applicability for routine use since the end-result is obtained by simple read-out from the calibration curve.

EXPERIMENTAL

Reagents and Apparatus. *N,N*-Dimethylformamide (DMF). Redistill or dry DMF (Du Pont) with Linde Molecular Sieve, Type 5A, until the water content is less than 0.01%. Store in a capped bottle.

Toluene. Redistill the solvent from stannous octoate (catalyst T-9 from M and T Corp.), 100 grams per gallon of toluene. The water content should be less than 0.008%. Store in a capped bottle.

Phenyl Isocyanate, reagent grade, boiling point 60° to 62° C. at 20 mm. (Matheson Coleman and Bell). Add 10.0 ml. (10.95 grams) of phenyl isocyanate to 50 ml. of dry toluene, dilute to 100 ml. with additional toluene, and mix thoroughly. Store in the volumetric flask. Discard the reagent if any crystalline precipitate is formed upon standing.

Alcohols. Use reagent grade chemicals as standards.

Catalyst. Add 4.480 grams of 1,4-diazabicyclo(2.2.2)-octane (DABCO, Houdry Process and Chemical Co.),

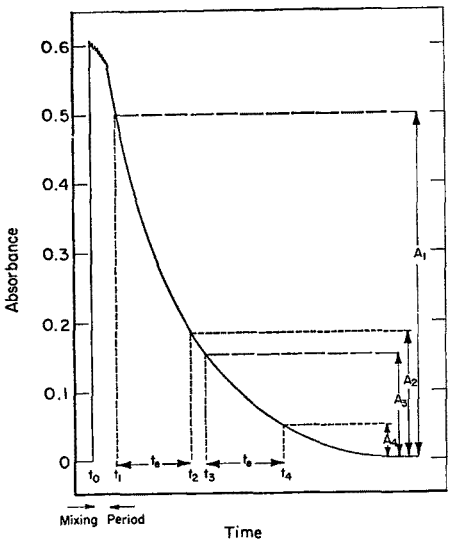


Figure 1. Rate curve for decrease of isocyanate absorbance vs. time

$A_1/A_2 = A_3/A_4 = e$
(A_1 and A_3 arbitrarily selected)

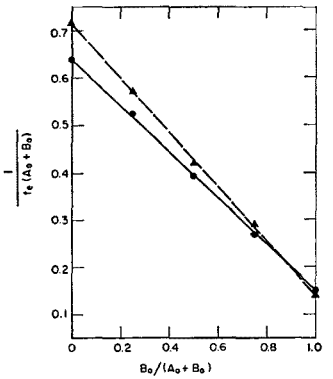


Figure 2. Calibration curves for binary mixtures of alcohols

A = Faster reacting component
B = Slower reacting component
O A = 1-PrOH; B = 2-PrOH
Δ A = 1-BuOH; B = 2-BuOH
(catalyzed by 0.200M DABCO)

also known as triethylenediamine, to 100 ml. of dry toluene, dilute to 200 ml. with additional toluene, and mix thoroughly. The concentration of this solution is 0.200M. The amine content is determined by titrimetric analysis with perchloric acid in glacial acetic acid medium. The catalyst solution can be kept without any detrimental effect for three days at the most.

Infrared Spectrophotometer. Use a Beckman Model IR 5A or equivalent. The absorption cells are 0.10-mm. CaF_2 cells. CaF_2 cells are preferred rather than NaCl cells because of the elimination of possible complications due to the water content in polyols.

Principle. Reilley, *et al.* (*6*) presented a generally applicable method for simultaneous reactions of two components A and B with a common reagent R, where the concentration of R with time was followed and where R may be detected with high sensitivity. If the concentration of A and B are each much greater than that of R, the rate expression for an irreversible second-order reaction becomes that of a pseudo first-order reaction. The rate of disappearance of R is given by:

$$-\frac{d[R]}{dt} = k_A[A][R] + k_B[B][R] \quad (1)$$

where

$$k_m = k_A[A]_o + k_B[B]_o \quad (2)$$

and k_A and k_B are the second-order rate constants of A and B reacting with R. The latter part of Equation 1 is valid only when the values of $[A]_o$ and $[B]_o$, the initial concentrations, are equal to A and B, respectively, throughout the entire reaction period—i.e., when $[R]_o \ll [A]_o$ and $[B]_o$. The integrated form of Equation 1 can be written as (*6*):

$$\frac{[A]_o}{[M]_o} = \frac{\ln\{[R]_t/[R]_o\}}{(k_B - k_A)[M]_o t} + \frac{k_B}{k_B - k_A} \quad (3)$$

where $[M]_o$ is the total initial concentration of the mixture, equal to $[A]_o + [B]_o$. Equation 3 refers to molar concentration values. However, in this method where the concentration of R (phenyl isocyanate) is followed spectrophotometrically as a function of time, the infrared absorbance value can be plotted instead. The linearity of the phenyl isocyanate absorbance *vs.* concentration dependence in a solvent system of 10% dimethyl formamide in toluene (v./v.) has been established previously (*9*).

Accordingly, the first-observed absorbance value A_1 at time t_1 from the start of the reaction is plotted *vs.* t_1, then A_2 *vs.* t_2, etc., as represented in Figure 1. A smooth curve depicts the decrease in isocyanate absorbance as the reaction proceeds. The absorbance *vs.* time curve becomes a straight line on semi-logarithmic graph paper.

Equation 3 stipulates that a plot of $1/[M]_o t$ *vs.* $[A]_o/[M]_o$, the mole fraction of A, at *a given fraction* of reagent reacted, $[R]_t/[R]_o$, yields a straight line which can serve as a calibration curve for the determination of binary mixtures. Reilley (*6*) pointed out that the most reliable measurements are made when the fraction $[R]_t/[R]_o$ is chosen to be $1/e$. Thus, in Figure 1, the time intervals t_e for fractional absorbance decreases of $1/e$, are used in constructing the calibration curve.

In a case where both of the components are available in pure form, the calibration curve can simply be determined by application of the abovementioned operations for single compound A to yield the value $1/(t_e[A]_o)$ and for B to yield $1/(t_e[B]_o)$, and by connecting these two data points by means of a straight line. Known binary compositions should serve to check the pseudo first-order straight-line relationships. Figure 2 represents a typical plot experimentally obtained for mixtures of two aliphatic alcohols, the combinations primary/secondary propanol, and primary/secondary butanol. However, in those cases where a component of the binary mixture is not available in pure form, mixtures of predetermined composition (by second-order rate approach) are analyzed to construct the calibration curve. Such is the case with polymeric compounds like poly(oxyalkylene) glycols and poly(oxyalkylene) sorbitols.

Choice of Catalyst and Reagent. If synthetic samples are made of various polyols and the purely ethoxylated polymer Carbowax PEG-200 with varying composition ratios in much the same way as published earlier (*9*), one can experimentally determine the value of $1/(t_e[B]_o)$ by extrapolation to nil primary hydroxyl content. From these values the corresponding (secondary hydroxyl group) reaction rate constants can be calculated. The results are summarized in Table I employing acetic anhydride (*3*) as reagent, and also phenyl isocyanate (*9*) as reagent with three different catalysts, stannous octoate, dibutyltin(IV)-dilaurate, and triethylenediamine, all known to markedly promote the hydroxyl-isocyanate reaction. When one singles out a particular case—whether acetic anhydride is the reagent or one of the three catalysts is

Table I. Rate Constants for Secondary Hydroxyl Group Reactions

$k \times 10^2$, liter mole^{-1} minute^{-1}

Alcohol	Av. mol. wt. of polyol	Ac_2O reagent, 25° C. noncatalyzed	PhNCO reagent, 25° C. catalyzed[f] by		
			Stannous octoate	Dibutyltin-dilaurate	DABCO
2-Propanol		14.3	5.07	2.33	0.918
2-Butanol		13.7	5.64	2.15	0.870
2-Ethylhexanol			3.22		0.606
NIAX Polyol PPG-2025[a]	2010	11.9	6.41	2.85	0.528
NIAX Polyol LG-56[a]	2890	12.4	6.60	2.28	0.529
Voranol CP 3000[b]	2940	12.1	6.76		0.521
Actol 31-56[c]	3040	11.8	6.43		0.534
Poly-G 4031 PG[d]	3820	12.3	6.27		0.539
NIAX Polyol LC-45[a]	3950	12.3	6.85	2.63	0.537
Pluracol TPE 4542[e]	4700	12.0	6.37		0.530
Polyether polyols, av. value and std. dev.	2000 to 5000	12.1 ± 0.23	6.53 ± 0.22	2.59 ± 0.29	0.531 ± 0.007

[a] Union Carbide Corp.
[b] Dow Chemical Co.
[c] Allied Chemical Co.
[d] Olin Mathieson Chemical Corp.
[e] Wyandotte Chemicals Corp.
[f] Catalyst concn. is $^1/_{200}$ of alcohol concn.

used in the isocyanate reaction—it appears that the extrapolated (to nil primary hydroxyl content) reaction rate constants of a variety of polyglycols are the same within experimental error. Hence, an average rate value and standard deviation range has been calculated for each of the four different procedures. These data are included as the last line in Table I, and summarize the secondary constants of the polyols investigated. This comparative investigation was meant to furnish the kinetically most reliable method for polyglycols which are either difunctional or trifunctional, and have an average molecular weight range anywhere between about 2000 to 5000. These requirements cover practically the entire field of polyglycols for flexible foam. The similarity in rate values can be interpreted as follows. If it were experimentally possible to polymerize a low-molecular-weight multifunctional alcohol such as propylene glycol, glycerine or trimethylpropane, with pure propylene oxide, to a polyol with only secondary hydroxyl groups, the reactivity of these hydroxyl groups is the same whether it is a 2000 mole weight species or a 5000 mole weight molecule.

The dibutyltin dilaurate-catalyzed reactions between polyether polyols and tolylenediisocyanate have been extensively investigated by Wissman, Rand, and Frisch (*10*). Although their system is kinetically more involved than the one under consideration because of the difunctionality of the isocyanate, their data are essentially in good agreement with the findings of the constancy of the extrapolated, secondary rate constants. They too observe that the reactivity of the terminal hydroxyl groups appears to be independent of the chain length of the oligomer. However, Table I reveals that dibutyltin dilaurate is the least attractive catalyst from an analytical point of view since it shows the widest range of k values. DABCO yields by far the greatest precision in extrapolated k values for polyols. Therefore, this catalyst was employed in the further evaluation of the primary hydroxyl determination procedure.

Procedure. The catalyst solution, DMF and toluene are all placed in a constant temperature bath (24.9° ± 0.1° C. in our work) for about 30 minutes before the reaction is started. A sample containing a total of 12.48 mmoles of hydroxyl is transferred to a 50-ml. volumetric flask and is diluted to almost 25 ml. with toluene. For polyols in particular, the sample size in grams can be more easily calculated as the quotient of 700 over the relevant hydroxyl number value. Ten milliliters of DMF are pipetted into the flask, and then 10 ml. of the catalyst solution are added. The time is noted as soon as 0.6 ml. of the phenyl isocyanate solution (0.55 mmole) are added, and the reaction mixture is rapidly diluted to volume with toluene. The volumetric flask too is kept in the constant-temperature bath. At intervals of about 90 seconds, small aliquots (ca. 1 ml.) are withdrawn with a hypodermic syringe, injected into the infrared cell, and the absorbance is measured at 4.42 microns. The absorbance values, A_n, measured during the course of the analysis are plotted *vs.* time values, t_n, and the time interval t_e for a specified fractional life A_2/A_1 (or A_4/A_2) = $(1/e)$ is determined from this plot. The fractional life time, t_e, and a knowledge of the value $[M]_o$ are necessary to determine the quotient $1/(t_e[M]_o)$, which is then referred to a calibration curve to read off either the mole fraction $[A]_o/[M]_o$ in a binary mixture or the primary hydroxyl content of a polyol.

DISCUSSION AND RESULTS

Solvent System. Phenyl isocyanate is not only very reactive toward compounds or solvent systems with active hydrogen atoms, it also exhibits self-condensation reactions in many solvents. Unless a suitable solvent system is employed, a correction factor nullifying the reaction rates besides those between hydroxyl and isocyanate has to be determined. However, in our attempts to eliminate this factor, an anhydrous, binary solvent system, consisting of 9:1 (v./v.) toluene/dimethylformamide, was observed to be particularly suitable for this purpose. It is stable toward the isocyanate, and appears to completely suppress the isocyanate's self-condensation reaction (mostly dimerization). In addition, it is an excellent solvent medium for urethane compounds which are formed as products of the alcohol–isocyanate reactions, and it allows an absorbance determination of the 4.42-micron peak without interference.

Catalyst Concentration. In order to establish optimum conditions for the procedure—i.e., fulfilling the requirement of a rapid analysis—the response of the calibration curve to the magnitude of the catalyst concentration was studied first. The concentration of catalyst cannot be chosen too high as it would result in a very fast reaction, which would be detrimental to the accuracy of the spectrophotometric measurements. Accordingly, three concentration levels of the DABCO solution—i.e., 0.125M, 0.200M, and 0.250M—were found to be very suitable for the analysis of most of the binary mixtures of primary and secondary alcohols, and for the primary hydroxyl content determination of polyhydric alcohols. The calibration curves for polyether polyols are pictured in Figure 3. The slopes of the curves are in good agreement with the relevant catalyst concentrations. The 0.200M DABCO concentration level was found to be generally useful, and should be

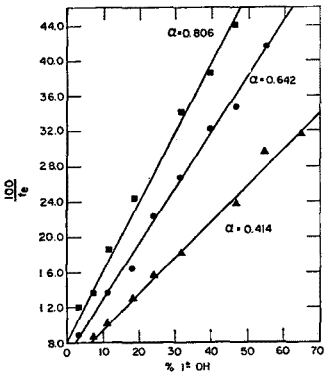


Figure 3. Calibration curves for primary hydroxyl content in polyoxyalkylene glycols

Catalyst concn.
▲ 0.125M DABCO
○ 0.200N DABCO
■ 0.250M DABCO

recommended for routine purposes. The 0.125M DABCO concentration solution can be used if an accurate study of polyols with a relatively high primary-hydroxyl content is required, whereas the 0.250M DABCO solution is appropriate in those cases where the percentage of primary hydroxyl groups is small.

Other Conditions for Pseudo First-Order Differential Kinetics Analysis. The hydroxyl concentration and the temperature were specified in the Procedure section. However, these factors are considered somewhat arbitrary as long as they are kept constant throughout the entire calibration and binary mixture analysis procedure.

Although the application of pseudo first-order kinetics requires mathematically an infinite excess of hydroxyl reactant, a reactant/reagent ratio of more than 15 was found to be satisfactory from a practical standpoint. When the hydroxyl/isocyanate ratio becomes less, a nonlinearity in the absorbance *vs.* time semi-logarithmic plot is observed, indicating a deviation from ideal pseudo first-order behavior. Another implication of the reactant/reagent ratio requirement is that the determination of binary mixtures with either less than about 10% of most reactive hydroxyl or more than about 90% of most reactive hydroxyl becomes inaccurate. The remainder of the composition region can adequately be determined by the present procedure which constitutes a far wider applicability than the slope method (*3*, *9*). For example, polyglycols with a primary hydroxyl content larger than 55% cannot be accurately determined by the slope method, but offer no problems for the pseudo first-order approach. However, in the few cases that an accurate reading on a polyol with a primary hydroxyl content of less than 10% is required, the slope method should be preferred.

Analysis of Binary Mixtures of Alcohols. The calibration curves for a number of selected mixtures of primary and secondary alcohols were determined and found to be linear within experimental error, as predicted by Equation 3. Table II summarizes the results of the analyses of five binary mixtures when DABCO was used at a 0.200M concentration level. Mixtures 3 and 4 are particularly interesting since they both constitute mixtures of primary alcohols as components. The deviations of the experimental results in case 3 with reference to the calculated content of faster reacting component (1-octanol) are undesirable; the inaccuracy is most probably due to the relatively low ratio of reaction rate constants. A k_a/k_b ratio of 2.0 should be considered the lowest value under which this differential kinetic technique can be applied.

Determination of Primary Hydroxyl Content in Polyoxyalkylene Glycols and Polyoxyalkylene Sorbitols. Again, 0.200M DABCO solution was used as catalyst, and the calibration curve with slope 0.642 was utilized to determine the primary hydroxyl

Table II. Determination of Hydroxyl Compounds by Triethylenediamine Catalyzed Reaction with Phenyl Isocyanate

Mixture	Most reactive hydroxyl,[a] % Calcd.	Found	Ratio of, rate constants, k_A/k_B
A. 1-Propanol	24.9	23.9	4.16
B. 2-Propanol	50.2	49.8	
	75.3	76.2	
A. 1-Butanol	25.0	25.8	4.92
B. 2-Butanol	50.0	48.5	
	75.0	74.8	
A. 1-Octanol	25.0	26.2	1.97
B. 2-Ethylhexanol	50.0	49.3	
	75.0	73.7	
A. 1-Propanol	25.3	25.6	6.30
B. 2-Ethylhexanol	50.7	51.0	
	74.8	74.6	
A. 1-Butanol	15.7	15.5	4.66
B. 2-Propanol	32.8	33.1	
	46.9	47.4	
	64.6	66.0	
	81.5	82.3	

[a] Compound A is the most reactive alcohol in the binary mixture.

Table III. Determination of Primary Hydroxyl Content in Alkoxylated Polymers of Propylene Glycol, Glycerine, Trimethylolpropane, and Sorbitol

Sample	OH No. (NCO, corr.)	Primary hydroxyl, % Slope method	Pseudo first-order method
NIAX Polyol PPG-2025[a]	55.9	4.9	5.5
Pluronic L61[b]	47.2	33.4	34.7
NIAX Polyol LG-56[a]	58.3	6.7	7.0
Voranol CP 3000[c]	57.2	5.8	7.2
NIAX Polyol LC-60[a]	57.1	45.0	44.1
Actol 31-56[d]	55.5	6.3	5.4
NIAX Polyol 11-48[a]	47.8	38.1	37.3
Poly-G 4031 PG[e]	44.2	37.3	40.5
NIAX Polyol LC-45[a]	42.7	54.9	55.6
Pluracol TPE 4542[b]	35.9	31.3	32.9
Hexol S-500[f]	648	27.8	33.4
Atlas G-2406[g]	641		27.5
Atlas G-2579[g]	502		18.7
Pluracol SP-760[b]	497		18.9
NIAX Polyol LS-490[a]	492	14.6	16.8
Atlas G-2410[g]	486		19.2

[a] Union Carbide Corp.
[b] Wyandotte Chemicals Corp.
[c] Dow Chemical Co.
[d] Allied Chemical Co.
[e] Olin Mathieson Chemical Corp.
[f] Jefferson Chemical Co.
[g] Atlas Chemical Industries.

content of the polymeric, polyhydric alcohols derived from polymerization starters propylene glycol, glycerine, and trimethylolpropane. For polyols derived from sorbitol, a new calibration curve was determined because of the different nature of the starter product. The calibration curve was constructed by measuring the reaction rates of known blends of NIAX polyol LS-490 and Carbowax polyethylene glycol PEG-200; LS-490 is a hexafunctional, about 680 molecular weight, propylene oxide adduct of sorbitol with a primary hydroxyl content of 14 to 20%, whereas PEG-200 is a 200 molecular weight oxyethylene diol with an assumed primary hydroxyl content of 100%. The slope value for these synthetic samples was 0.628, only marginally lower than the corresponding value for the dihydric and trihydric polyols. To confirm the validity of the pseudo first-order approach, the primary hydroxyl content of a variety of polymeric diols, triols, and hexols was determined by the second-order slope method (*9*) and the present procedure. The results on these commercially available poly(oxyalkylene) glycols and poly(oxyalkylene) sorbitols are compared in Table III; the data substantiate a satisfactory accuracy equivalence of the two methods.

Interferences. Nonapplicability of this method can be caused by two sources of interference, (a) the presence of a substance which reacts with phenyl isocyanate or affects the reagent otherwise, and (b) the presence of any substance which catalytically affects the rate of the hydroxyl–isocyanate reaction. Source (a) has been discussed in a previous communication (*9*). With regard to source (b), some acids, bases, and organometallic compounds influence the rate of the urethane formation reaction if present in significant quantities (more than 100 p.p.m.). Thus, one has to be watchful for contaminations of this nature in the hydroxyl compounds to be analyzed. One of the possible sources of interference, commonly present in polyols—i.e., the presence of parts-per-million quantities of a stabilizer, phosphoric acid—was investigated. However, no catalytic effect or other interference could be found if this acid was present in a 0- to 30-p.p.m. concentration range. In a way, this might be explained by the "neutralizing" basicity features of one of the components of the solvent system, *N*,*N*-dimethylformamide.

CONCLUSIONS

The advantages of the present method are obvious; it is an extremely rapid and simple approach for the determination of binary mixtures of hydroxyl compounds because the mathematical framework requires that only a negligible fraction of the two components react. In addition, the experimental simplicity is apparent from the procedure. The determination is made by pipetting a small amount of the reagent, the exact quantity of which is irrelevant as long as it is negligibly small in comparison to that of the two components in the sample. Once the reacting mixture is injected into the calcium fluoride cell the whole analysis is followed without any further changes by simply reading off the absorbance as a function of time, and without concern for a predetermined t_o. The method is thus easily adaptable to automatic recording.

Another advantage of the method is that the interference from possible side reactions is substantially suppressed because only a negligible quantity of the original components reacts—e.g., simultaneous reactions which might become of different kinetic order or otherwise complex in the advanced stages will stay pseudo first-order throughout the analysis period in the present approach. This is particularly important in the case of polyols, because they invariably contain a small amount of water which reacts with phenyl isocyanate in a complex manner in latter stages.

The present method is not only useful for the analysis of binary mixtures of hydroxyl compounds but should be adaptable to any other binary system of active-hydrogen-containing compounds in which simultaneous reactions occur with phenyl isocyanate with sufficiently different specific rate constants.

ACKNOWLEDGMENT

The authors express their appreciation to C. N. Reilley of the University of North Carolina, Chapel Hill, N. C., for the recommendation of the pseudo first-order rate approach which initiated this investigation, and to Mrs. D. K. Elder and J. S. Bodenschatz, both of Union Carbide Corp., Chemicals Division, Charleston, W. Va., for helpful discussions and the regression analysis evaluation.

LITERATURE CITED

(1) Crummett, W. B., ANAL. CHEM. **34,** 1147 (1962).
(2) Floria, J. A., Dobratz, I. W., McClure, J. H., *Ibid.*, **36,** 2053 (1964).
(3) Hanna, J. G., Siggia, S., *J. Polymer Sci.* **56,** 297 (1962).
(4) Hendrickson, J. G., ANAL. CHEM. **36,** 127 (1964).
(5) Mark, H. B., Papa, L. J., Reilley, C. N., "Advances in Analytical Chemistry and Instrumentation," C. N. Reilley, ed., Vol. 2, pp. 313–359, Wiley, New York, 1963.
(6) Papa, L. J., Patterson, J. H., Mark, H. B., Reilley, C. N., ANAL. CHEM. **35,** 1889 (1963).
(7) Rechnitz, G. A., *Ibid.*, **36,** (5) 456R (1964).
(8) Roberts, J. D., Regan, C., *Ibid.*, **24,** 360 (1952).
(9) Willeboordse, F., Critchfield, F. E., *Ibid.*, **36,** 2270 (1964).
(10) Wissman, H. G., Rand, L., Frisch, K. C., *J. Appl. Polymer Sci.* **8,** 2971 (1964).

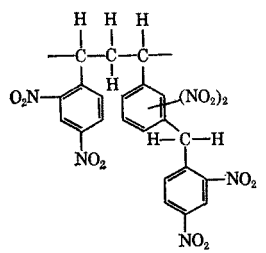
RECEIVED for review November 23, 1965. Accepted March 30, 1966. Presented in part at the 16th Pittsburgh Conference on Analytical Chemistry and Applied Spectroscopy, March 1965.

Synthesis of Tetranitrobenzylpolystyrene Resin for Chromatographic Stationary Phase

JAMES T. AYRES and CHARLES K. MANN
Department of Chemistry, Florida State University, Tallahassee, Fla. 32306

▶ **The synthesis of a nitrated polystyrene resin is reported. It consists of Friedel-Crafts benzylation of cross-linked divinylbenzene–polystyrene copolymer, followed by nitration. Results of IR, NMR, and elemental analysis indicate that the degree of benzylation is about 0.5 and that an average of two nitro groups is introduced on each ring. The reaction sequences are reproducible and result in production of about 30 mole % of intact beads in the final product. The resin is stable to heat to at least 160° C., not affected by prolonged exposure to the atmosphere, and exhibits the chemical properties of 2,4-dinitrophenyls. The swelling properties of the resin in a number of solvents are reported.**

IN A PRELIMINARY REPORT (*1*) the authors described the use of tetranitrobenzylpolystyrene (TNBP) resin as a stationary phase for column chromatography. This is a detailed report of the synthesis, and properties of TNBP resin. A discussion of the chromatographic evaluation of the resin will follow (*2*). A more exact structure and nomenclature for TNBP are shown below:



poly[3-(2,4-dinitrobenzyl)-dinitrostyrene resin]

The molecular complexes between polynitro aromatic compounds (PNAC) and polycyclic aromatic hydrocarbons (PAH) have been used as a basis of separation, purification, and identification. Therefore, a polynitro matrix such as TNBP resin is a logical stationary phase for the chromatographic fractionation of PAH mixtures. PNAC–PAH molecular complexes are described as charge-transfer (*CT*) complexes (*6*) in which PNAC functions as a Lewis-acid electron acceptor and PAH behaves as an electron donor. One of the most characteristic features of this type of complex is the *CT* absorption spectrum. The excitation energy of the *CT* spectral transition is a function of both the electron affinity of the acceptor and the ionization potential of the donor; the stability of the complex also depends upon these two quantities (*3*, *5*).

TNBP resin has a soluble linear analog (linear TNBP) and numerous small molecule analogs such as 2,4-dinitrotoluene and 2,2′, 4,4′-tetranitrodiphenylmethane (TNDPM), which facilitate extrachromatographic studies as to the nature of the chromatographic adsorption mechanisms on TNBP resin; chromatographic behavior on TNBP resin should parallel the *CT* equilibria typical of both the macromolecular and micromolecular analogs. Thus, TNBP resin is a chromatographically active, pi-acid stationary phase which contains a well characterized electron acceptor (a PNAC moiety) as an integral part of the molecular structure. As expected, TNBP resin displays activity toward PAH and related donor molecules.

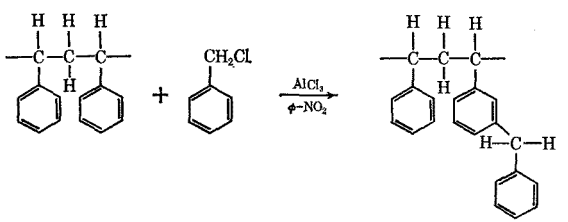
SYNTHESIS OF TNBP

TNBP was prepared by Friedel-Crafts benzylation of divinylbenzene-polystyrene resin using benzyl chloride in nitrobenzene solvent, followed by nitration with a fuming acid mixture.

Benzylation. In a typical experiment, 0.96 mole (100 grams) of 50–100 mesh 2% divinylbenzene–polystyrene resin was swelled for 4 hours at room temperature in 400 ml. of nitrobenzene contained in a 1-liter, 3-necked flask equipped with a stirrer, condenser, dropping funnel, and drying tube. The reaction mixture was cooled to 0° C., and 0.26 mole of anhydrous $AlCl_3$ added. The contents were vigorously stirred for 1 hour at this temperature to allow diffusion of the catalyst into the resin beads. A mixture of 1.4 moles of reagent grade benzyl chloride and 140 ml. of nitrobenzene was added dropwise over a period of 3 hours at 0° C. The reaction was continued for an additional hour after removal of the ice bath; reaction was evidenced by discharge of HCl. These moderate conditions are necessary to minimize the $AlCl_3$-catalyzed cross-linking of the product; higher temperatures favor complete decomposition.

The reaction was quenched by pouring the mixture into 1 liter of methanol; the product settles as a viscous mass contaminated with the benzyl chloride self-condensation products. The methanol was decanted, and the product stirred with benzene to remove the by-products. The benzylated resin was then collected in a filtering funnel and further washed with benzene, and then with a dioxane–HCl solution to remove residual catalyst. The resin was washed with methanol to cause shrinkage, air dried with an aspirator, and then dried overnight in vacuo at 80° C. The yield was 150 grams. A sample of low molecular weight linear polystyrene was benzylated in like manner pursuant to the synthesis of linear TNBP.

The weight increase (50 grams) on going from polystyrene resin to poly(benzylstyrene) resin indicates a degree of benzylation of approximately 0.5. There was no evidence of *para* substitution in the infrared spectra of the benzylated products. The NMR spectrum (*4*) of the linear poly(benzylstyrene) indicated that substitution did not occur in the *ortho* position. The product can then be more accurately described as shown below:



poly (*m*-benzylstyrene) resin

Table I. Swelling Ratios of TNBP Resin in Various Solvents

Solvent	Approximate swelling ratio
Dimethylsulfoxide	3.0
Dimethylformamide	3.0
Nitromethane	2.0
Acetone	2.0
Tetrahydrofuran	1.8
3:1 Dioxane-acetonitrile	1.4
Acetone 0.5*F* in $NaClO_4$	3.3
Tetrahydrofuran 0.5*F* in $NaClO_4$	2.7
Tetrahydrofuran at 0° C. *vs.* 25° C.	1.1

Nitration. In a 2-liter, 3-necked flask equipped as before, 1000–1200 ml. of 90% HNO_3 was cooled to about −50° C. with a dry ice bath. To this vigorously stirred cold solution was then added 0.33 mole (100 grams) poly(*m*-benzylstyrene) resin (polystyrene resins react exothermically with rapid swelling in fuming HNO_3 at room temperature). The dry ice bath was removed, and the contents were allowed to reach room temperature. The contents were heated to 35° C. to ensure complete swelling. The mixture was again cooled as before, and 300 ml. of fuming sulfuric acid, 65% added dropwise; the addition rate and stirring rate were maintained at the level necessary for effective heat dissipation. The mixture was slowly brought to a temperature of 80° C.; reaction was continued at this temperature for 6 hours.

The contents were again cooled with dry ice, and then poured into 4 liters of crushed ice. The product settles as nitrated beads contaminated with degradation products (such as carboxy acids and low molecular weight nitropolymer). Most of the acids and by-products were removed by decantation washing with water. The product was collected on a filter and thoroughly washed with acetone; this solvent readily swells TNBP resin and readily dissolves residual acids and degradation fragments. The resin was washed with methanol to cause shrinkage, air dried, and then dried overnight in vacuo at 100° C. A yield of 0.28 mole of TNBP resin was obtained. A sample of linear poly(*m*-benzylstyrene) was nitrated in like manner to form linear TNBP.

The resin was free of bead fragments; initial bead fragmentation during nitration is evidently followed by complete degradation to an acetone-soluble form. Any nitrating medium that swells polystyrene resin can be used with equal effectiveness. Polystyrene has not been nitrated beyond the dinitro stage; exhaustive nitration results in degradation.

The infrared spectrum of TNBP had bands at 1540, 1350, 1070, 915, and 840 $cm.^{-1}$ which are characteristic of 2,4-dinitrophenyls (*7*). The average of duplicate elemental analyses are as follows: calculated, 48 59% C, 2.84% H, and 14.78% N; found, 49.13% C, 3 18% H, and 14.45% N. The elemental analyses and spectral data support the designated TNBP structure. The reaction sequences are reproducible.

PROPERTIES OF TNBP RESIN

TNBP resin is composed of rust-colored spherical beads which are chemically and thermally stable to at least 160° C. The dry density is 1.38 grams/ml. These beads are quite rigid, but can be pulverized with a mortar. TNBP exhibits behavior typical of 2,4-dinitrophenyls, such as the blue color formation with methanolic base. Prolonged contact with various solvents, and standing for one year in contact with the atmosphere, produced no change in its infrared spectrum. Nitrogen bases are strongly adsorbed, but can easily be removed with HCl. The resin swells, and linear TNBP dissolves, in the solvents listed in Table I.

The swelling ratio is expressed as the swelled volume/dry volume. Swelling is also effected by nitroaromatics, amides, and related polar solvents. Dioxane–acetonitrile mixtures swell TNBP, but not the neat solvents. Mixtures composed of nonpolar solvents and those listed in Table I will swell TNBP to some extent. TNBP will not swell in hydrocarbons, halocarbons, alcohols, esters, or carboxy acids. The addition of electrolytes enhances swelling in acetone and tetrahydrofuran, but does not affect swelling in dimethylsulfoxide or dimethylformamide.

TNBP is hydrophobic. Particles acquire static charges during manipulation; sizing is best accomplished by a water–methanol washing technique. Static charges persist even when the resin is in contact with hexane; the resin exists as lumps rather than discrete particles. However, this tendency is not present when higher dielectric solvents such as acetone are used.

In the chromatographic studies on TNBP resin, acetone and acetone–hexane solutions were used as eluents. Dry TNBP resin will swell in acetone and acetone-rich eluents, but not in hexane-rich eluents. In the chromatographic conditioning process, the acetone-swelled state was produced first and then the swollen resin was allowed to equilibrate with the given eluent prior to packing the column. Thus, the swelling was always unidirectional, from the acetone-swelled state to the eluent-swelled state. The swelling ratio, internal volume per unit weight of resin, determined under chromatographic conditions is plotted as a function of the eluent composition in Figure 1. The portion of the curve below mole fraction 0.84 represents the region in which swelling behavior is irreversible. Dry resin will not swell in solvent mixtures in this range, but previously swelled resin does not lose all occluded solvent. Above mole fraction 0.84, behavior is reversible. The same results are obtained, whether one starts with dry or swelled resin.

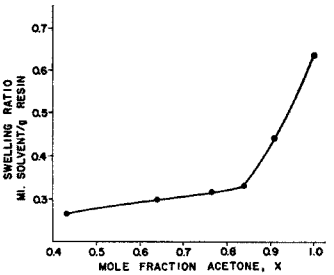


Figure 1. TNBP swelling ratio as a function of eluent composition

ACKNOWLEDGMENT

The authors thank The Dow Chemical Co. for the divinylbenzene–styrene copolymer.

LITERATURE CITED

(1) Ayres, J. T., Mann, C. K., ANAL. CHEM. **36**, 2185 (1964).
(2) Ayres, J. T., Mann, C. K., *Ibid.*, **38**, 861 (1966).
(3) Basu, S., *Chem. & Ind. (London)* **1956**, 764.
(4) Bovey, F. A., Tiers, G. V. D., Filipovich, G., *J. Polymer Sci.* **38**, 73 (1959).
(5) Chakrabarti, S. K., Basu, S., *Trans. Faraday Soc.* **60**, 465 (1964).
(6) Mulliken, R. S., *J. Am. Chem. Soc.* **72**, 600 (1950); *Rec. Trav. Chim.* **75**, 845 (1956).
(7) Pristera, F., Halik, M., Castelli, A., Fredericks, W., ANAL. CHEM. **32**, 495 (1960).

RECEIVED for review October 7, 1965. Accepted March 21, 1966. Work supported under grant 536A from the Petroleum Research Fund and grant GM 10064 from the National Institutes of Health, U. S. Public Health Service.

Column Chromatography with Tetranitrobenzylpolystyrene Resin Stationary Phase

JAMES T. AYRES and CHARLES K. MANN

Department of Chemistry, Florida State University, Tallahassee, Fla. 32306

▶ **The use of tetranitrobenzylpolystyrene resin as stationary phase in column chromatography is described. The curve for acetone elution of a mixture of tetraphenylethylene, *m*-terphenyl and phenanthrene is presented. A study of solvent effects with acetone and acetone–hexane eluents has been made. Chromatographic *R* values are presented to describe elution characteristics of 26 compounds. The mechanism of chromatographic sorption is discussed.**

IN THE PRECEDING PAPER (*2*), the synthesis and properties of poly-[3 - (2,4 - dinitrobenzyl) - dinitrostyrene] resin were described. This resin will be designated as tetranitrobenzylpolystyrene (TNBP) resin. The chromatographic behavior of TNBP will be discussed.

Organic pi-acids have received rather limited application as chromatographic stationary phases. Polynitro aromatic compounds (PNAC) have been used as stationary phase impregnants in the chromatography of polycyclic aromatic hydrocarbons (PAH) and related electron donors. Godlewicz (*5*) fractionated PAH mixtures on silica gel impregnated with trinitrobenzene (TNB) and picric acid. Klemm *et al.* (*10*) chromatographed PAH on PNAC-impregnated alumina and silica gel, and postulated that chromatographic behavior should correlate with the PNAC–PAH equilibrium constants. However, these workers did not investigate the role of the PNAC. Recently Tye and Bell (*15*) studied the partition chromatography of PAH on a Columpak support impregnated with a Carbowax-TNB solution. TNB was shown to be the essential component of the stationary phase; Carbowax alone produced no separation. Good resolution was obtained with this system. There was also good agreement between the chromatographic and the extrachromatographic distribution coefficients.

The preliminary communication (*1*) on TNBP resin was the first report of the chromatography of PAH on a macromolecular PNAC stationary phase. In TNBP resin, the PNAC moiety is an integral part of the molecular structure of an insoluble, chemically and thermally stable polymer matrix. Such a system has advantages over an impregnated stationary phase in that the effluent is free of sorbent-induced impurities, and there is no deactivation on continued use. Also, impregnated stationary phases (such as impregnated alumina and silica gel) are bifunctional adsorbents; this impairs the understanding of chromatographic behavior. The retardation mechanism on TNBP resin can be considered in terms of the PNAC moiety alone if allowance is made for gel filtration. TNBP resin also has an advantage over conventional inorganic adsorbents in that TNBP has a soluble linear form and numerous micromolecular analogs, which facilitates extrachromatographic studies and correlations. TNBP resin can be easily synthesized, and it is compatible with chromatographically functional solvent systems.

The effect of eluent composition on chromatographic behavior was investigated by chromatographing 15 compounds on TNBP using acetone and five acetone-hexane solutions as eluents; 11 other compounds were chromatographed with neat acetone eluent. The resin swells in acetone and acetone-rich eluents; retardation on swelled TNBP is due to a combination of adsorption and gel filtration. Spectrometric equilibrium constants (K_c) for several solutes were determined with linear TNBP. These constants and the ionization potentials of the solutes were correlated with the corresponding chromatographic data. Separation efficiencies were calculated from elution curves. The chromatographic behavior of PAH and related compounds was studied within this context.

EXPERIMENTAL

Materials. Spectroquality acetone and *n*-hexane were used without further purification. All solid solutes were reagent grade chemicals that had been further purified by crystallization from methanol, benzene, hexane, or methanol–benzene mixtures. When purity was in doubt, charcoal treatments and multiple crystallizations were employed. Liquid solutes were reagent grade chemicals which were used without further purification.

Apparatus and Instruments. A conventional reservoir [topped with a 45/50 male joint and capped with the 45/50 female joint and attached anhydrous $Mg(ClO_4)_2$ drying tube], glass frit, 1.23 cm. i.d. column (bed depth 48.5 ± 0.5 cm.) was used to obtain all data. The flow rate was controlled by a grooved Teflon stopcock. A luer from a hypodermic syringe was sealed to the column exit. The drip-tip consisted of a No. 23 hypodermic needle attached to the luer, which afforded a dead volume of 0.35 ml. The tip was recessed in a shield of tubing to minimize eluent evaporation; this tip delivered an average of 215 drops/ml. Fractions were collected at time intervals with an automatic fraction collector. A 3600 A. ultraviolet lamp, a Beckman DB spectrophotometer, and a flame ionization gas chromatograph were used in solute detection.

Conditioning TNBP for Chromatographic Use. The resin was ground in a mortar and then thoroughly wet-screened with methanol–water mixtures to 250–270 mesh; any remaining small particles were removed by suspension flotation. Microscopic examination revealed a high degree of uniformity in particle size. This very uniform batch of 250–270 mesh resin was used in all chromatographic experiments. After sizing, the resin was placed in a conventional fritted disk column and slowly washed with acetone until the effluent was colorless (the preliminary washing following synthesis did not remove all the occluded impurities). The purified resin was stored under acetone. Prior to packing the column the resin was equilibrated with the eluent.

The vertically aligned column was bottom filled with eluent. With the stopcock open, the column was wet packed to the desired depth by adding small portions of resin while tapping the column. The resin bed was rigid, uniform, and free of air pockets. The bed was then washed with 100 ml. of eluent at a flow rate of about 6 ml./hr. to effect the final conditioning; the bed was now ready for use.

A single resin bed, packed and conditioned in this manner, could be used for an entire chromatographic study provided that the eluent was not changed. One resin bed was used daily for 30 days without a noticeable change in appearance or behavior. When the eluent was to be changed, the resin was removed from the column, dried at 80° C. in vacuo, weighed, washed

with acetone and then equilibrated with the next eluent. The packing and conditioning process was then repeated. Since TNBP swelling ratios differ in each eluent, voids in the column packing result if the eluent is changed without removal of the resin.

The Chromatographic Method. The flow rate was determined by calibrating the drop size from the No. 23 needle. The periodic fluctuations in drop rate and drop size (0.5% per degree) due to fluctuations in ambient temperature (the average fluctuation in ambient temperature for one experiment was 23 ± 3° C.) were corrected by monitoring both the drop rate and temperature during a run. By this method R values were reproducible to ±1%.

Solute samples consisting of 3–6 mg. of each component in 0.3 ml. eluent were applied to the top of the resin bed. Small increments of eluent were carefully added until the zone had penetrated the bed to a depth of about 1.5 inches. The reservoir was then carefully filled, and elution allowed to proceed under gravity flow at a normal flow rate of 5 ml./hr. Eluate fractions of about 0.5-ml. volume were collected at discrete time intervals until the last solute component appeared. The remainder of the solute was then eluted and the drip-tip was cleaned; the column was now ready for the next experiment.

The eluate fractions were carefully evaporated. Some detection method (visual, fluorescence, ultraviolet spectra, odor, gas chromatography) was now used to detect the breakthrough point. Thus, breakthrough volumes were determined relative to the zone front. The breakthrough volumes of paraffin or Nujol were used as the void volumes; high molecular weight aliphatic hydrocarbons are not retarded by TNBP. The TNBP density was determined by chromatographing paraffin with hexane as the eluent (TNBP does not swell in hexane); the volume of the resin was obtained by subtracting the void volume from the total bed volume. When acetone–hexane solutions were used as eluents, the internal volumes of swelled resin beds were obtained by subtracting the sum of the void and resin volumes from the total bed according to Equation 1:

$$V_t = V_o + V_i + V_s \qquad (1)$$

The terms denote, in sequence, the total bed volume, the void volume, the internal volume and the resin volume. The eluents were acetone and five different acetone–hexane solutions. Some of the operational parameters, expressed as functions of the mole fraction acetone, X, in the acetone–hexane eluent, are given in Table I.

The R values and specific retention volumes, were calculated according to Equations 2 and 3:

$$R = \frac{V_o}{V_b} \qquad (2)$$

$$R^o = \frac{V_b - V_o}{W} \qquad (3)$$

Here V_b is the breakthrough volume. Breakthrough volumes for 15 solutes are presented as functions of mole fraction of acetone in acetone–hexane in Table II. Supplemental data for 11 other solutes determined with neat acetone eluent are given in Table III. The partition constant, K, was calculated by multiplying R^o by the resin density ($K = 1.38\ R^o$). Values calculated in this way from breakthrough volumes will differ slightly from values calculated from mid-peak volumes. All data were reproducible to ±1%. The overall accuracy is postulated to be within ±2%. R values were independent of the length of time a given resin had been in use; the ambient temperature fluctuations also had little or no effect. Accuracy and precision were limited primarily by the degree of uncertainty in flow rate measurements and solute detection methods.

Elution curves with acetone eluent were determined for tetraphenylethylene, m-terphenyl and phenanthrene. Eluate fractions were collected at 6

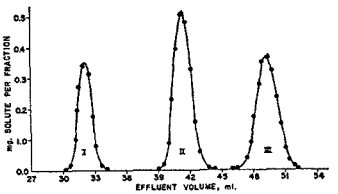


Figure 1. Elution curve for a chromatographic separation on TNBP resin

Peak	Compound	Weight, mg.	HETP, cm.
I.	Tetraphenylethylene	1.50	0.207
II.	m-Terphenyl	2.31	0.0839
III.	Phenanthrene	2.27	0.0645

Table I. Operational Parameters Expressed as Functions of Mole Fraction of Acetone (X) in Acetone–Hexane Mixtures

	X					
	0.430	0.638	0.766	0.841	0.909	1.00
Total bed volume, ml.	57.9	57.9	56.5	57.9	57.9	57.3
Void volume, ml.	22.9	23.0	23.1	23.7	23.9	24.1
Wt. resin in column, grams	35.3	34.2	32.2	32.4	29.3	24.5
Volume resin in column, ml.	25.6	24.8	23.3	23.5	21.2	17.8
Internal volume, ml.	9.40	10.1	10.1	10.7	12.1	15.4
Internal volume/wt. resin, ml./g.	0.266	0.295	0.314	0.330	0.437	0.628

Table II. Acetone–Hexane Elution

Effect of Changing Eluent Composition

Mole fraction acetone	0.430	0.638	0.766	0.841	0.909	1.00
	Breakthrough volumes (ml.)					
Chrysene	78.2	57.0	47.1	44.2	47.2	50.0
Pyrene	66.2	54.4	46.2	45.9	51.4	56.1
Fluoranthene	61.6	50.3	42.8	42.2	47.4	51.7
Tetracene		47.2	41.5	41.1	44.3	52.2
Phenanthrene	56.3		40.8	39.4	42.5	47.3
Anthracene	54.8	46.6	40.5	39.8	42.2	47.9
Carbazole	64.2	47.8	39.1	37.6	39.9	44.0
2-Methoxynaphthalene	49.3	43.4	37.5	37.1	39.8	42.6
Naphthalene	43.7	40.1	35.9	36.2	38.2	43.2
Biphenyl	38.5	36.8	33.7	33.7	36.7	40.0
2-Methylnaphthalene	39.8	37.1	33.7	34.9	37.8	42.1
trans-stilbene	43.2	37.5	32.6	33.0	36.1	40.2
m-Terphenyl	37.3	34.1	30.6	30.9	35.4	40.1
Triphenylmethane	26.2	26.9	25.7	26.6	30.2	34.8
Tetraphenylethylene	23.3		23.1	23.8	27.0	31.1

Table III. Acetone Elution

Compound	R	R^o, ml./g.
N,N-dimethylaniline	0.445	1.22
Acenaphthene	0.535	0.854
Fluorene	0.564	0.758
1-Bromonaphthalene	0.572	0.733
Tetranitrodiphenylmethane	0.574	0.700
Diphenylamine	0.637	0.537
Benzene	0.641	0.529
Mesitylene	0.651	0.525
Cyclohexane	0.699	0.406
Tetraphenylbutadiene	0.751	0.315
3,4-Dimethylphenol	0.754	0.308

minute intervals, evaporated to dryness, extracted into hexane and then assayed by ultraviolet spectrometry. The curves are presented in Figure 1. HETP were calculated by the method of James and Martin (7). An elution curve for fractionation of a mixture of anthacene and pyrene with an acetone–hexane eluent is presented elsewhere (1).

RESULTS

Chromatographic Behavior and TNBP Swelling. Representative R values determined from the data in Table II are plotted as functions of mole fraction of acetone in Figure 2. A comparison of Figure 2 with the swelling ratio plot (Figure 1, reference 2) shows that the inflection in each curve occurs at the same eluent composition. This indicates that the sudden change in chromatographic behavior, which occurs at mole fraction 0.84, is related to the sudden change in swelling ratio. R values increase linearly with mole fraction between 0.43 and 0.84, peak at 0.84, and then decrease from 0.84 to 1.0 (100% acetone).

The solvent effect can be interpreted in the following manner. Assuming that the pore size of TNBP between mole fraction 0.43 and 0.84 is small enough to exclude these solute molecules, the increase in R is due entirely to the increase in eluent strength. However, the sudden increase in swelling on going from mole fraction 0.84 to 1.0 is accompanied by a parallel increase in porosity; the solute molecules are now no longer excluded by the pore structure. Thus, the solute is partitioned between the internal and the external solvent. Therefore, when liquid phase composition is in the range of mole fraction 0.84 to 1.0, solute movement is retarded by a combination of surface adsorption, gel filtration, and gel filtration followed by internal adsorption; only surface adsorption occurs below mole fraction 0.84. The increase in eluent strength on going from 0.84 to 1.0 does not compensate for the gel filtration effect; thus, R values are smaller with acetone than with mole fraction 0.84 mixture. For the same reason, some R^o values are larger at mole fraction 1.0 than at 0.43. In support of this, it was demonstrated by an independent experiment that the pore size of acetone-swelled TNBP was large enough to accommodate all the solutes studied.

The role of gel filtration is further indicated by the chromatographic behavior of several compounds. Tetraphenylethylene has an R value of 1.00 at mole fraction 0.766; an increase in eluent strength alone certainly would not change this value. However, the R value is 0.884 at 0.91 and 0.777 at 1.0. Likewise, the R value for triphenylmethane is 0.900 at mole fraction 0.78, but decreases to 0.693 at 1.0. Since increases in eluent strength favor increases in R, this converse behavior indicates retarding mechanisms other than simple adsorption.

Cyclohexane would not be expected to have any affinity for TNBP; however, the R value is 0.699 with pure acetone; that for benzene is 0.641. It is also of significance that the R of cyclohexane is smaller than that of tetraphenylethylene. If neither compound has an adsorption affinity for TNBP, then the differences in R indicate a differential penetration into the porous sorbent based on molecular size; therefore, swelled TNBP functions as a gel filter. On swelled TNBP, compounds can be separated on the basis of differences in both their molecular size and their adsorption affinity. All small molecules should have R values less than unity on highly swelled TNBP. Only large molecules which have no surface adsorption tendencies, and which are excluded from the matrix (such as paraffin), would have R values approaching unity.

If one assumes that R would increase linearly with mole fraction of acetone from 0.0 to 1.0 in the absence of gel filtration, then the linear portions of the plots in Figure 2 can be extrapolated to pure acetone to resolve the gel filtration effects from the adsorption effects. Extrapolated data are presented in Table IV.

Thus, K_a (adsorption) and K_i (gel filtration) values should provide a quantitative estimation of the contributions of each retarding mechanism in pure acetone. On the basis of this extrapolation, gel filtration is the dominant retarding mechanism with acetone eluent for all compounds except chrysene.

Chromatographic Efficiency. In some of the exploratory studies, 50–100 mesh and 120–150 mesh batches of resin were also used. Fluorescent compounds such as anthracene were chromatographed and observed under ultraviolet light. As the mesh size and the mesh range were reduced, there was a very noticeable improvement in zone widths and zone shapes. The uniformity of the 250–270 mesh batch of resin virtually eliminated eddy and convection effects; the shapes of the elution curves and the HETP values in Figure 1 support this.

No attempt was made to determine the optimum flow rate. However, anthracene was chromatographed at flow rates between 2.5 and 6.5 ml./hr. and observed under ultraviolet light. There was no appreciable change in the width and shape of the zone within these flow rate limits. In one experiment a zone was held stationary at the midpoint of the column for 18 hours to isolate the diffusion effects; the zone

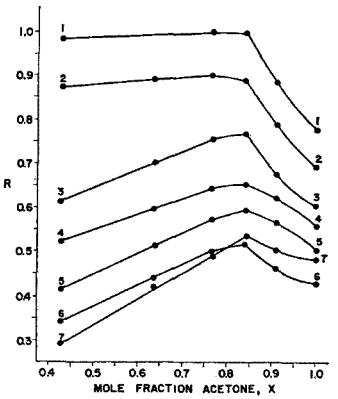


Figure 2. Acetone–hexane elution

1. Tetraphenylethylene
2. Triphenylmethane
3. *m*-Terphenyl
4. Naphthalene
5. Anthracene
6. Pyrene
7. Chrysene

Table IV. Extrapolated Chromatographic Data

Compound	R_o[a]	R_a[b]	K_a[c]	K_i[d]
Chrysene	0.040	0.629	0.805	0.754
Pyrene	0.143	0.610	0.872	1.07
Fluoranthene	0.157	0.657	0.715	0.967
Tetracene	0.270	0.645	0.750	0.961
Phenanthrene	0.203	0.679	0.640	0.765
Anthracene	0.222	0.677	0.646	0.798
Carbazole	0.051	0.756	0.444	0.779
2-Methoxynaphthalene	0.260	0.724	0.523	0.601
Naphthalene	0.368	0.728	0.512	0.650
Biphenyl	0.467	0.753	0.450	0.505
2-Methylnaphthalene	0.432	0.765	0.421	0.682
trans-Stilbene	0.290	0.838	0.623	0.741
m-Terphenyl	0.432	0.855	0.230	0.773
Triphenylmethane	0.838	0.918	0.124	0.552
Tetraphenylethylene	0.960	1.00	0.00	0.450

[a] R extrapolated to $X = 0.0$ (100% *n*-hexane). Tailing prohibits the determination of data below $X = 0.43$.
[b] R extrapolated to $X = 1.0$.
[c] K determined from R_a.
[d] K based on V_i computed from $R - R_a$.

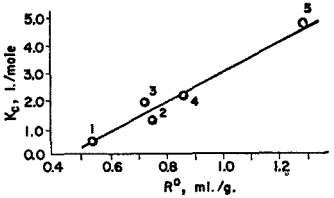


Figure 3. Correlation of complex formation on linear TNBP with chromatography on TNBP resin

1. Diphenylamine
2. 2-Methoxynaphthalene
3. 2-Methylnaphthalene
4. Acenaphthene
5. Pyrene

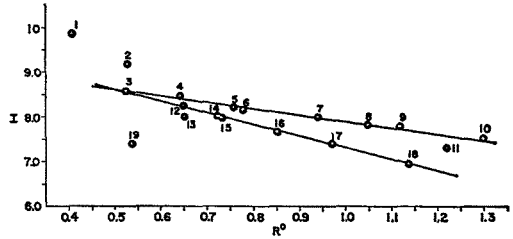


Figure 4. Ionization potential vs. specific retention volume

1. Cyclohexane
2. Benzene
3. Mesitylene
4. Biphenyl
5. Fluorene
6. Naphthalene
7. Phenanthrene
8. Chrysene
9. Fluoranthene
10. Pyrene
11. Dimethylaniline
12. *m*-Terphenyl
13. *trans*-Stilbene
14. 2-Methylnaphthalene
15. 1-Bromonaphthalene
16. Acenaphthene
17. Anthracene
18. Tetracene
19. Diphenylamine

changed very little in width or shape. Thus, diffusion should contribute little to zone spreading for reasonable experimental times. Since the careful sizing and packing processes minimized eddy, convection, and diffusion effects, zone spreading should be a function of primarily the shapes of the adsorption isotherms and the extent of local nonequilibrium. Based on these assumptions, the flow rate should be just large enough for practical operation. Consequently, flow rates of 4–6 ml./hr. seemed reasonable.

Zone spreading increased as mole fraction of acetone decreased. Tailing became so pronounced that accurate data could not be obtained below mole fraction 0.43. Fluoranthene tailed to some extent in all eluent compositions except neat acetone. R values diverged as acetone concentration decreased. However, resolution decreases as acetone concentration decreases. The divergence of the R values does not compensate for the increased tailing. As a result, resolution is drastically impaired below mole fraction 0.841. In this solvent system, the optimum eluent composition lies between 0.84 and 1.0. Although the range of R values for this series of compounds is only 0.347 in neat acetone, the solute zones are very compact. For example, anthracene has a total zone width of only 4 cm. after traversing a 48-cm. column when neat acetone is the eluent, as compared to a zone width of 8 cm. when acetone mole fraction is 0.77. Any two PAH that differ in R by 0.05 can be fractionated on a 48-cm. column of 250–270 mesh TNBP when acetone is the eluent. For example, a mixture of tetraphenylethylene, triphenylmethane, *m*-terphenyl, naphthalene, anthracene, and pyrene can be fractionated in one chromatographic run. The HETP values in Figure 1 are comparable to those obtained with moderately efficient gas chromatographic columns.

R^0 and K_c Correlations. If the chromatographic adsorption mechanism is based entirely on CT complexation, the R^0 is the chromatographic equivalent of K_c; therefore R^0 should correlate with K_c. However, solubility restrictions necessitate the use of acetone as the solvent in the determination of K_c with linear TNBP; consequently these data must be correlated with R^0 values that pertain to acetone as the eluent. Since gel filtration contributes to R^0 under these conditions, the retarding mechanism on TNBP resin is not identical to the complexing mechanism in linear TNBP solutions. Also the relative number of complexing sites would be much greater in a linear TNBP solution. R^0 and K_c correlations are further restricted by the limited number of solutes that are amenable to spectrometric K_c determinations. These restrictions make it impossible to calculate chromatographic constants from data obtained by equilibration experiments on the linear polymer. However, if the mechanism of chromatographic retardation involves charge transfer complex formation, then a correlation between chromatographic and equilibration experiments might be expected.

The spectrophotometric equilibrium constants for linear TNBP with several donors were determined in acetone by use of the Ketelaar (*8*) relationship. A discussion of the study of charge-transfer spectra of macromolecular systems has been given by Smets, Balogh, and Castrille (*12*).

K_c values for linear TNBP are plotted against appropriate R^0 values in Figure 3. The linear relationship obtained seems to support the suggestion of the role charge-transfer complex formation in the retardation mechanism.

R^0 and I Correlations. Since the stability of a complex is related to the electron-acceptor and the electron-donor strengths of the components, then the stability should also be related to electron affinities and ionization potentials I. Therefore, the stabilities of the complexes with a given acceptor (the electron affinity is fixed) should increase as the I's of the donors decrease. The observations of Chakrabarti and Basu (*4*) support this. Furthermore, LeRosen *et al.* (*11*) demonstrated that chromatographic behavior could be predicted from the relative donor and acceptor strengths of the sorbent, solvent, and solute. Therefore, with a given adsorbent and eluent, the adsorption affinity should vary as the electron-donor strength of the solute. Consequently, in the absence of perturbing factors (such as steric hindrance, hydrogen bonding, unusual adsorption configurations, etc.) the adsorption affinity should vary inversely as the I of the solute.

In Figure 4 the I values from various sources (*3, 6, 9, 13, 14, 16*) are plotted against corresponding R^0. Angular PAH and those free of steric effects fall on one line; acenes and substituted PAH generate another line. On TNBP resin, the angular PAH is adsorbed more strongly than the acene isomer. This is inconsistent with differences in ionization potentials but consistent with differences in resonance energies (*17*). Ionization potential values may not have the same donor strength connotation as applied to all PAH systems.

LITERATURE CITED

(1) Ayres, J. T., Mann, C. K., ANAL. CHEM. **36**, 2185 (1964).
(2) Ayres, J. T., Mann, C. K., *Ibid.*, **38**, 859 (1966).
(3) Briegleb, G., Czekalla, J., *Z. Electrochem.* **63**, 6 (1959).
(4) Chakrabarti, S. K., Basu, S., *Trans. Faraday Soc.* **60**, 465 (1964).
(5) Godlewicz, M., *Nature* **164**, 1132 (1949).
(6) Hedges, R. M., Matsen, F. A., *J. Chem. Phys.* **28**, 950 (1958).
(7) James, A. T., Martin, A. J. P., *Biochem. J.* **50**, 679 (1952).
(8) Ketelaar, J. A. A., Van DeStolpe, C., Gersmann, H. R., *Rec. Trav. Chim.* **70**, 499 (1952).

(9) Kinoshita, M., *Bull. Chem. Soc. Japan* **35**, 1609 (1962).
(10) Klemm, L. H., Reed, D., Miller, L. A., Ho, B. T., *J. Org. Chem.* **24**, 1468 (1959).
(11) LeRosen, A. L., Monaghan, P. H., Rivet, C. A., Smith, E. D., ANAL. CHEM. **23**, 730 (1951).
(12) Smets, G., Balogh, V., Castrille, Y., *J. Polymer Sci.*, pt. C, **4**, 1467 (1964).
(13) Spotswood, T., *Australian J. Chem.* **15**, 278 (1962).
(14) Streitwieser, A., *J. Am. Chem. Soc.* **82**, 4123 (1960).
(15) Tye, R., Bell, Z., ANAL. CHEM. **36**, 1612 (1964).
(16) Watanabe, K., *J. Chem. Phys.* **26**, 542 (1957).
(17) Wheland, T. W., "Resonance in Organic Chemistry," pp. 75–152, John Wiley and Sons Inc., New York, N. Y., 1955.

RECEIVED for review October 7, 1965. Accepted March 21, 1966. Work supported under Grant A 536 from the Petroleum Research Fund and Grant GM 10064 from the U. S. Public Health Service, National Institutes of Health.

Electrolysis with Constant Potential

Diffusion Currents for the Formation of an Amalgam at a Hanging Mercury Drop Electrode

WILLIAM G. STEVENS and IRVING SHAIN
Chemistry Department, University of Wisconsin, Madison, Wis.

▷ **The effect of the spherical nature of the hanging mercury drop electrode on the diffusion current of a reaction in which an amalgam is formed has been verified for the potentiostatic reduction of Cd(II) near the formal $E°$ of the system Cd(II)/Cd(Hg). The spherical correction term to the diffusion current equation changes sign, and the experimental results are in excellent agreement with the theory.**

In a previous study of the potentiostatic reduction of thallous ion at a hanging mercury drop electrode (*7*), it was observed that at potentials near the formal $E°$ for this reversible system, the magnitude of the spherical correction term in the characteristic current–time equation varied; and at the formal $E°$, the spherical correction term changed sign. Thus, at potentials cathodic of $E°$, the observed current was higher than would have been expected for a plane electrode of the same area, while at potentials anodic of $E°$, the currents were smaller. It was suggested that this was related to the convergent nature of the diffusion process within the spherical mercury electrode, which would lead to higher concentrations of the thallium amalgam at the surface of the electrode than would have been obtained for a linear diffusion case. This suggestion was qualitatively in accord with an approximate limiting solution to the boundary value problem which was obtained by considering the convergent diffusion process within the electrode under conditions where the amalgam concentration is very low. A more general solution could not be obtained because of the complexity of the mathematics encountered when an attempt was made to account for both the convergent diffusion and the finite volume of the drop.

Recently, in a careful study of the effect of the formation of an amalgam in a.c. polarography, similar spherical correction term effects were observed by Delmastro and Smith (*3*). They published a rigorous solution to the boundary value problem for a.c. polarography in which the convergent diffusion was considered but the finite volume of the drop was ignored, an approach first suggested by Reinmuth (*6*). The equations describing the a.c. polarography experiment include the result for a constant potential experiment, and an explicit equation for the potentiostatic case can be obtained by taking Equations 1 and 50 from Reference (*3*), and combining them with the Nernst Equation for the reaction $O + ne \rightleftharpoons R$:

$$i = nFAD_OC_O^*[1/(1 + \gamma\theta)\sqrt{\pi D_O t} + 1/r_o(1 - \gamma^2\theta) - \theta(\gamma + 1)^2(e^{\beta^2 t}\,\mathrm{erfc} \times \beta\sqrt{t})/r_o(1 - \gamma^2\theta)(\gamma\theta + 1)^2] \quad (1)$$

a result obtained independently in this laboratory (*10*). In Equation 1,

$$\beta = \sqrt{D_O}(\gamma^2\theta - 1)/r_o\,\gamma(\gamma\theta + 1) = (\theta D_O - D_R)/r_o(\theta\sqrt{D_O} + \sqrt{D_R})$$

and all other terms are as defined previously (*7*, *8*). It should be noted that Equation 1 is the same as that derived previously (*8*) for the case in which both O and R are soluble in the solution, except for the different signs in the second and third terms in the brackets.

There are several limiting forms of Equation 1 which are of importance. First, for very cathodic potentials, $\theta \rightarrow 0$, and Equation 1 reduces to

$$i = nFAD_OC_O^*[1/\sqrt{\pi D_O t} + 1/r_o] \quad (2)$$

which is the result expected for this case where diffusion of substance O is the controlling factor in the rate of the reaction (*2*). On the other hand, for a reduction taking place at potentials significantly anodic of $E°$, θ becomes large, and since the third term in brackets in Equation 1 is a function of $1/\theta^2$, while the second is a function of $1/\theta$, the third term becomes small more rapidly than the second. Under these conditions, Equation 1 reduces to

$$i = nFAD_OC_O^*\,[1/\gamma\theta\sqrt{\pi D_O t} - 1/\gamma^2\theta r_o] \quad (3)$$

Equation 3 is of the same form as the result obtained previously on the basis of qualitative considerations [Equation 14, in Reference (*7*)].

The third case of interest is at potentials near the $E°$ for the system, since it is in this region that the spherical correction term changes sign as predicted previously from experimental results (*7*). From Equation 1, the spherical contribution to the current is time dependent, and in general, for any particular potential in this range, the spherical correction term decreases as a function of time. This can be evaluated from Equation 1 by expanding the function $\exp \beta^2 t\ \mathrm{erfc}\ \beta\sqrt{t}$ as a series, using the form valid for small values of the argument (since the argument never exceeds unity for realistic values of the experimental parameters). When the first two terms of the series are used, the spherical correction term, σ—i.e., the last two terms in Equation 1—becomes:

$$\sigma = [1/r_o(1 + \gamma\theta)^2][1 - \theta - \theta(\gamma + 1)^2 \times 2\sqrt{D_O t}/\gamma r_o\sqrt{\pi}(1 + \gamma\theta)] \quad (4)$$

At $t = 0$, σ is positive at potentials cathodic of $E°$, and negative at poten-

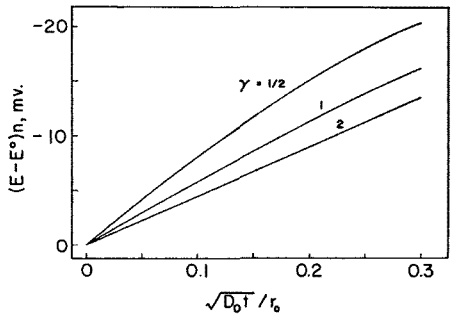


Figure 1. Time and potential dependence of the vanishing point of the spherical correction term

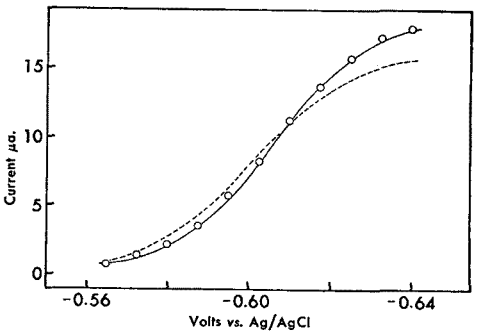


Figure 2. Current flowing 5 seconds after start of electrolysis. Comparison of plane and spherical electrodes

Solution: $1.00 \times 10^{-3}M$ Cd(II) in 1.0M KCl, 0.1M Na acetate 0.1M acetic acid
Electrode radius, 0.0659 cm.
Points, experimental; solid line, theoretical for a spherical electrode (Equation 1); dashed line, theoretical for a plane electrode

tials anodic of E°. In all cases, σ decreases with time; the time dependence being the largest at E°.

The time dependence of the point at which the spherical contribution to the current vanishes can be obtained from Equation 4 by setting $\sigma = 0$:

$$\sqrt{D_0 t}/r_0 = \sqrt{\pi}\gamma(1-\theta) \times (1+\gamma\theta)/2\theta(1+\gamma)^2 \quad (5)$$

This relation between the potential, the ratio of the diffusion coefficients, and the parameter $\sqrt{D_0 t}/r_0$ is shown in Figure 1. Any specific set of experimental parameters will determine a point on this graph. If the point lies above the line for the appropriate value of γ, σ will be positive, if below, σ will be negative.

In the normal case, the potential dependence of potentiostatic experiments is demonstrated by plotting the current flowing at some fixed time after the start of the electrolysis as a function of potential. The point at which the spherical correction term vanishes will always be cathodic of E° in such a plot, and the exact potential can be obtained from Figure 1.

To verify these theoretical relations, extensive potentiostatic studies were carried out on the reduction of Cd(II) in 1.0M potassium chloride, 0.1M sodium acetate, 0.1M acetic acid, pH 4.7.

EXPERIMENTAL

All experiments were carried out on an instrument based on operational amplifiers. The circuit was the same as that described previously in Figure 9 of Reference (*13*), except that the controller amplifier did not include a booster amplifier. In addition (using the previous notation) the analog integrator, I, and the associated recorder, M-2, were not used. PS-1 and PS-2 were battery-operated low voltage power supplies. M-1 was a Leeds and Northrup Speedomax G Series 6000 recorder with a chart speed of 27.9 ± 0.2 inches/minute, a full scale sensitivity of 10 mv., and a nominal full scale response of 0.4 second.

The cell was similar to that described previously (*1*), except that the holes in the Teflon lid were provided with neoprene "O" rings to help keep out air. The counter electrode was 2 inches of 18-gauge platinum wire, mounted on the mercury transfer scoop. The reference electrode was Ag–AgCl, placed directly in the cell. All experiments were carried out at 25.0° ± 0.1° C., and the cell and thermostat were mounted on a 60-lb. slab of concrete (supported by semi-inflated plastic balls) to minimize vibration. High purity nitrogen was passed through a vanadous sulfate solution, washed, and then passed through each solution for at least 15 minutes to remove oxygen. All chemicals were reagent grade and were used without further purification. The electrode area was determined after each experiment by collecting the individual hanging mercury drop and weighing it on a micro balance.

The working electrodes were made from 6-mm. glass tubing and were provided with convection shields as described previously (*1*). To minimize the effects of shielding of the electrode by the glass (*7*), the tip of the electrode was carefully ground to a point, so that very little glass remained around the platinum-glass seal. In all calculations, the area of the electrode was corrected by subtracting that portion subtended by the platinum and the glass support (generally of the order of 0.0013 sq. cm.).

RESULTS AND DISCUSSION

Current–time curves were obtained for the reduction of $10^{-3}M$ Cd(II) solutions over the potential range from −0.5 v. to −0.7 v. *vs.* Ag–AgCl, using hanging drop electrodes ranging from 0.052- to 0.076-cm. radius. By using the equipment as described, useful data were obtained over the time interval from 1 to 30 seconds. The data were treated by plotting $i\sqrt{t}/nFAC^*_0$ as a function of $\sqrt{t}$, as suggested by Lingane (*4*). Straight lines were obtained in each case, with positive slopes at potentials more cathodic than about −0.61 volt *vs.* Ag–AgCl, and negative slopes at more anodic potentials, as predicted by Equation 1.

From curves obtained at very cathodic potentials (−0.725 volt) the diffusion coefficient of Cd(II) in 1M potassium chloride, 0.1M sodium acetate, 0.1M acetic acid was determined to be 0.735×10^{-5} sq. cm./sec., with a relative standard deviation of 2.8%, calculated from both the slope and the intercept of the $i\sqrt{t}$ *vs.* $\sqrt{t}$ curves. This value is somewhat lower than that reported by Skobets and Kavetskii (*9*), although other values have been reported ranging from 0.700 to 0.781 $\times 10^{-5}$ (*5*, *12*). The value reported here is considered reliable within the indicated level of accuracy, since the effects of convection and other uncontrolled variables were minimized. The correlation between values of D calculated from slope and intercept agreed closely, after the area of the electrode was corrected for the portion shielded by the glass and platinum of the support.

When this value of the diffusion coefficient was used, the experimental results were correlated with Equation 1. The excellent agreement is shown in Figure 2 where the current, flowing five seconds after the start of the electrolysis, is plotted as a function of potential. For comparison, the current expected for a plane electrode is also shown, demonstrating the sign change for the spherical correction term at a potential slightly cathodic of E°.

It was previously pointed out (*8*) that for the case in which the product of

the electrode reaction is soluble in the solution, it is possible to obtain independent values of $\gamma\theta$ and $\gamma^2\theta$ from current time curves taken near the formal E° for the system. Since D_O can be determined separately from data obtained at very cathodic potentials, both θ and D_R can be obtained from cathodic experiments only. When substance R is soluble in the mercury, it is possible to make the same calculations using Equation 1. These calculations were carried out for the Cd(II)–Cd(Hg) system used in this work, and a value of $2.303(RT/nF) \log \theta = 0.606$ volt *vs.* Ag–AgCl was obtained. For D_R, a value of 1.6×10^{-5} sq. cm./sec. was obtained, compared with 1.61×10^{-3} sq. cm./sec. obtained from direct anodic dissolution of cadmium amalgams (*11*). This procedure should make it possible to calculate $2.303(RT/nF) \log \theta$ to ± 2 mv., and D_R to about 5% from reduction experiments only. The method should be useful in those cases where it is not feasible to prepare stable amalgam electrodes for direct study.

LITERATURE CITED

(1) Alberts, G. S., Shain, I., ANAL. CHEM. **35**, 1859 (1963).
(2) Delahay, P., "New Instrumental Methods in Electrochemistry," p. 61, Interscience, New York, 1954.
(3) Delmastro, J. R., Smith, D. E., ANAL. CHEM. **38**, 169 (1966).
(4) Lingane, P. J., *Ibid.*, **36**, 1732 (1964).
(5) Macero, D. J., Rulfs, C. L., *J. Am. Chem. Soc.* **81**, 2942 (1959).
(6) Reinmuth, W. H., ANAL. CHEM. **33**, 185 (1961).
(7) Shain, I., Martin, K. J., *J. Phys. Chem.* **65**, 254 (1961).
(8) Shain, I., Polcyn, D. S., *Ibid.*, **65**, 1649 (1961).
(9) Skobets, E. M., Kavetskii, N. S., *Zh. Fiz. Khim.* **24**, 1486 (1950).
(10) Stevens, W. G., Ph.D. Thesis, University of Wisconsin, 1966.
(11) Stevens, W. G., Shain, I., *J. Phys. Chem.* (in press).
(12) Turnham, D. S., *J. Electroanal. Chem.* **10**, 19 (1965).
(13) Underkofler, W. L., Shain, I., ANAL. CHEM. **35**, 1778 (1963).

This work was performed in part while W. G. Stevens held an NSF predoctoral fellowship, and also was supported in part by funds received from the U. S. Atomic Energy Commission under Contract No. AT(11-1)-1083.

The Depletion Effect in Pulse Polarography with Stationary Electrodes

K. B. OLDHAM[1] and E. P. PARRY

North American Aviation Science Center, Thousand Oaks, Calif. 91360

▶ Normal pulse polarography involves the application of voltage pulses of gradually increasing amplitude to an electrode which is held at a potential (resting potential) more positive than that at which reduction occurs. The pulse duration is at least 50 times smaller than the time between pulses. With reversible systems reoxidation occurs during the time between pulses so that the reductant is fully regenerated. With irreversible systems, no reoxidation occurs, and a depletion effect is observed in unstirred solutions. This paper describes the depletion effect from both a theoretical and experimental point of view and points out its rather wide occurrence. Both stirring and proper choice of resting potential can eliminate this effect in applications of normal pulse polarography.

IN NORMAL PULSE POLAROGRAPHY a succession of voltage pulses is applied to an electrode of constant area. The interval between pulses T exceeds the duration τ of each pulse by a factor of 50 or greater. When employed analytically to study the electrode reaction

$$Ox + ne \rightarrow Red \qquad (1)$$

the applied potential during the pulses steadily increases as shown in Figure 1*a*, so that initially the potential is inadequate to cause the reduction of Ox. However, toward the end of the experiment the electrode is completely concentration polarized with respect to Ox during all pulses. Between pulses the electrode potential is returned to a resting value at which reaction (1) does not proceed from left to right. All of the theory and many of the experiments described in this communication are, however, concerned with one or other of the situations shown as *b* or *c* in Figure 1, in which the potential of the first pulse is already sufficient to cause complete polarization with respect to Ox. The current measurement in pulse polarography is the difference between the instantaneous cell current measured toward the end of each potential pulse and immediately prior to the pulse. Measured currents are true diffusion-limited currents if the potential pulses are as in Figures 1*b* or 1*c*.

Normal pulse polarography can be used to advantage with solid electrodes. It has been shown, for instance, that in the reduction of silver ion at a platinum electrode, the same curves can be obtained if the electrode is in stirred solution or is in a quiet solution (*4*). This is as expected since the silver is reduced for only the very brief period of the pulse but the electrode is kept for a much longer period at a potential where the silver metal is reoxidized so that no net deposit of metal accumulates on the electrode surface. Since the diffusion layer during pulses is thinner than the shear layer in a stirred solution, stirring has essentially no effect on the polarogram obtained (*4*). The foregoing is completely valid if the resting potential is chosen so that the metal on the electrode surface is completely oxidized between pulses. However, in an unstirred solution and for a sufficiently irreversible system where a resting potential cannot be chosen at which oxidation takes place a net depletion will occur during the very short pulse which will not be eliminated during the much longer waiting period between pulses. In spite of the fact that the interval between pulses exceeds the pulse duration 50 to 100 times, this depletion effect is quite significant. The object of the present work is to describe this effect both experimentally and theoretically and show its wide applicability. The effect has been qualitatively observed in the reduction of nickelous, chromate and iodate ions, and in the oxidation of ascorbic acid at the hanging mercury drop, in the reduction of gold(III) at the pyrolytic graphite electrode, and lead ion at the platinum electrode. Since adequate stirring eliminates the depletion effect, pulse polarographic analyses of irreversible systems should be carried out in the presence of stirring.

THEORY

Prior to the first pulse, a uniform concentration C_∞ of Ox exists throughout the cell. Subsequently, the Ox concentration at a distance x from the

[1] Present address, Chemistry Department, The University, Newcastle-upon-Tyne, England.

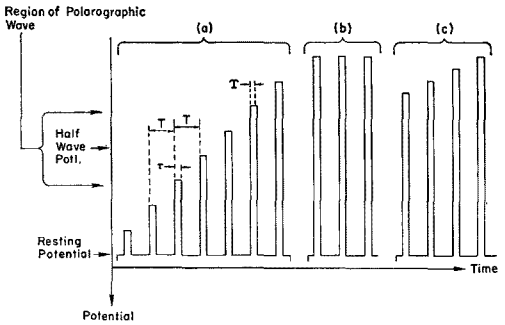


Figure 1. Diagram, not to scale, showing the time-dependence of potential in normal pulse polarography:

(a) As usually employed for analytical purposes
(b) As treated in the theoretical section of this article and in the quantitative experiments described herein
(c) Also covered by the theoretical treatment

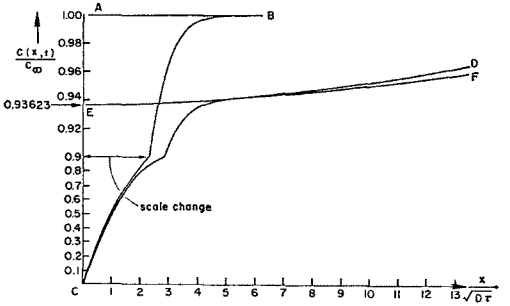


Figure 2. Concentration profiles: *AB*, at time $t = 0$; *BC*, at time $t = \tau$; *DE* at time $t = T$ according to Equation 6; *EF* at time $t = T$ according to Equation 10; *CD* at time $t = T + \tau$ according to Equation 11

In calculating these profiles, the ratio $T/\tau = 100$ has been used. Note the tenfold change of scale at $C(x,t)/C_\infty = 0.90$

electrode and at a time t after the imposition of the first pulse is given by (2)

$$\frac{C(x,\, O < t \leq \tau)}{C_\infty} = \text{erf}\left\{\frac{x}{2\sqrt{Dt}}\right\} \quad (2)$$

In this equation, D is the diffusion coefficient of Ox and erf denotes the error function.

The current at any instant during the first pulse is readily calculated as

$$i(O < t \leq \tau) = nAFD\frac{\partial C}{\partial x} \times$$

$$(O,\, O < t \leq \tau) = nAFC_\infty\sqrt{\frac{D}{\pi t}} \quad (3)$$

which will be recognized as the familiar Cottrell expression (2). Equation 3 ignores any contribution to the current due to migration and to nonfaradaic processes: experimental conditions during pulse polarography should decrease the importance of these two effects. Integration of Equation 2 between $x = 0$ and $x = \infty$ gives the total number of moles of Ox reduced during the first pulse as

$$\Delta N_1 = 2AC_\infty\sqrt{\frac{D\tau}{\pi}} \quad (4)$$

Figure 2 includes a plot of Equation 2 and shows that virtually all of these ΔN_1 moles are removed from a zone of thickness no greater than $5\sqrt{D\tau}$.

At $t = \tau$ the first pulse ends and the current immediately falls to zero. The steep concentration profile shown as *BC* in Figure 2 now commences to decay as Ox diffuses toward the electrode from the bulk of the solution. We are now interested in determining the concentration profile during the interval between the first and second pulses, and in particular at $t = 1$. We can write this as a MacLaurin expansion, in the distance variable, as follows:

$$C(x,T) = C(O,T) + x\frac{\partial C}{\partial x}(O,T) +$$

$$\frac{x^2}{2}\frac{\partial^2 C}{\partial x^2}(O,T) + \frac{x^3}{6}\frac{\partial^3 c}{\partial x^3}(O,T) +$$

$$\frac{x^4}{24}\frac{\partial^4 C}{\partial x^4}(O,T) + \ldots \quad (5)$$

The evaluation of the first four coefficients in the series is discussed in Appendix A. In view of T's being a large time interval in comparison with τ, no acute curvature can be expected anywhere in the concentration profile when $t = T$, so that little approximation is introduced for moderate x values in neglecting from Equation 5 the term in x^4 and those in higher powers of the distance variable. Therefore, from the relations derived in Appendix A, we have

$$\frac{C(x,T)}{C_\infty} = \frac{2}{\pi}\arctan\sqrt{\frac{T-\tau}{\tau}} + \frac{x^2}{2\pi DT}\sqrt{\frac{\tau}{T-\tau}} \quad (6)$$

Equation 6 is an approximation valid at small x and is exact for $x = 0$. We now proceed to derive a second approximation for $C(x,T)$ which is the more valid the greater the ratio T/τ. In the interval between the first and second pulses the concentration profile changes from a steep deep curve close to the electrode to one which becomes increasingly flat and shallow. In terms of a concentration *vs.* distance graph, the area enclosed by the lines $C = C_\infty$, $x = 0$, and $C = C(x,t)$ remains constant and equal to $\Delta N_1/A$. Since T is so much greater than the pulse width τ it might be expected that the concentration profile at $t = T$ will be virtually identical with that which would have resulted had ΔN_1 moles of Ox been removed instantaneously from $x = 0$ at a time $t = t^*$ close to the time $t = 0$ when the first pulse was initiated. Diffusion theory gives the profile resulting from the decay of this Dirac delta function to be of the following Gaussian form:

$$C(x,t) = C_\infty - \frac{\Delta N_1}{A\sqrt{\pi D(t-t^*)}} \times \exp\left\{\frac{-x^2}{4D(t-t^*)}\right\} \quad (7)$$

To determine t^* we identify $C(O,T)$ according to Equation 7 with the exact expression provided by Equation 6. This yields

$$\frac{t^*}{\tau} = \frac{T}{\tau} - \arcsin^{-2}\sqrt{\frac{\tau}{T}} \quad (8)$$

or, using a power series expansion for arcsin:

$$t^* = \frac{\tau}{3}\left[1 + \frac{\tau}{5T} - \frac{691}{1680}\frac{\tau^2}{T^2} + \ldots\right] \quad (9)$$

Hence, under all conditions of pulse polarographic interest, t^* is almost precisely equal to one third of the pulse width. Adopting this value, Equation 7 becomes, for $t = T$:

$$\frac{C(x,T)}{C_\infty} = 1 - \frac{2}{\pi}\left(\frac{T}{\tau} - \frac{1}{3}\right)^{-1/2} \times \exp\left\{\frac{-3x^2}{4D(3T-\tau)}\right\} \quad (10)$$

Figure 2 compares the expressions 6 and 10: evidently the agreement is excellent except at the highest values of x, where Equation 6 is known to be erroneous.

At time $t = T$ the second pulse commences. This pulse will generate a concentration profile very similar to that which was generated during the first pulse and which is described by Equation 2. However, there are two differences: first, the concentration of Ox adjacent to the electrode is not as

great at time $t = T$ as it was at time $t = 0$; and second, the concentration profile at $t = T$ is slightly curved. These differences are apparent in comparing curves AB and DE in Figure 2 and are reflected in the first and second terms on the right hand side of the following equation which describes the concentration profile during the second pulse and which is derived in Appendix B,

$$\frac{C(x,T<t\leq T+\tau)}{C_\infty} = \left[1-\frac{2}{\pi}\left(\frac{T}{\tau}-\frac{1}{3}\right)^{-1/2}\right]\operatorname{erf}\times\left\{\frac{x}{2\sqrt{D(t-T)}}\right\}+\left(\frac{t-T}{\pi\tau}\right)\times\left(\frac{T}{\tau}-\frac{1}{3}\right)^{-3/2}\left[1+\frac{x^2}{2D(t-T)}-4i^2\operatorname{erfc}\left\{\frac{x}{2\sqrt{D(t-T)}}\right\}\right] \quad (11)$$

Figure 2 includes a graph of this expression. The current flowing during the second pulse may be derived analogously to Equation 3 for the first pulse; hence we have (see Appendix B)

$$i(T<t\leq T+\tau) = nAFD\frac{\partial C}{\partial x}\ (O,T<t\leq T+\tau) = nAFC_\infty\sqrt{\frac{D}{\pi(t-T)}}\left[1-\frac{2}{\pi}\times\left(\frac{T}{\tau}-\frac{1}{3}\right)^{-1/2}+\frac{2}{\pi}\left(\frac{t-T}{\tau}\right)\times\left(\frac{T}{\tau}-\frac{1}{3}\right)^{-3/2}\right] \quad (12)$$

The number of moles of Ox reduced during the second pulse may be most easily calculated by integration of Equation 12 over the limits $t = T$ to $t = T + \tau$, followed by division by nF. This yields

$$\Delta N_2 = 2AC_\infty\sqrt{\frac{D\tau}{\pi}}\left[1-\frac{2}{\pi}\left(\frac{T}{\tau}-\frac{1}{3}\right)^{-1/2}+\frac{2}{3\pi}\left(\frac{T}{\tau}-\frac{1}{3}\right)^{-3/2}\right] \quad (13)$$

Between times $t = T + \tau$ and $t = 2T$, the electrode is held at the resting potential and the profile once more undergoes a period of decay. Toward the end of this interval, the concentration profile will be virtually identical with that which would have resulted from a Dirac delta function of magnitude ΔN_1 at time $t = {}^1/_{3}\tau$ and a similar function of magnitude of ΔN_2 at $t = T + {}^1/_{3}\tau$. Since the effects of these two events will be strictly additive, we have:

$$C(x,T+\tau<t<2T) = C_\infty - \frac{\Delta N_1}{A\sqrt{\pi D\tau}}\left(\frac{t}{\tau}-\frac{1}{3}\right)^{-1/2}\exp\left\{\frac{-x^2}{4D\tau}\times\left(\frac{t}{\tau}-\frac{1}{3}\right)^{-1}\right\}-\frac{\Delta N_2}{A\sqrt{\pi D\tau}}\times\left(\frac{t}{\tau}-\frac{T}{\tau}-\frac{1}{3}\right)^{-1/2}\exp\left\{\frac{-x^2}{4D\tau}\times\left(\frac{t}{\tau}-\frac{T}{\tau}-\frac{1}{3}\right)^{-1}\right\} \quad (14)$$

analgous to Equation 7. Equation 14 will be a better approximation the closer t is to $2T$; for $t = 2T$ it may be written

$$\frac{C(x,2T)}{C_\infty} = 1-\frac{2}{\pi}\left(\frac{2T}{\tau}-\frac{1}{3}\right)^{-1/2}\times\exp\left\{\frac{-x^2}{4D\tau}\left(\frac{2T}{\tau}-\frac{1}{3}\right)^{-1}\right\}-\frac{2}{\pi}\frac{\Delta N_2}{\Delta N_1}\times\left(\frac{T}{\tau}-\frac{1}{3}\right)^{-1/2}\exp\left\{\frac{-x^2}{4D\tau}\left(\frac{T}{\tau}-\frac{1}{3}\right)^{-1}\right\} \quad (15)$$

Equation 15 describes conditions immediately before the third pulse just as Equation 10 describes the concentration profile immediately prior to the second pulse. Equation 15 may therefore be handled just as was Equation 10, to generate the following relationships applicable to the third pulse:

$$i(2T<t\leq 2T+\tau) = nAFC_\infty\times\sqrt{\frac{D}{\pi(t-2T)}}\left[1-\frac{2}{\pi}\left(\frac{2T}{\tau}-\frac{1}{3}\right)^{-1/2}+\frac{2}{\pi}\left(\frac{t-2T}{\tau}\right)\left(\frac{2T}{\tau}-\frac{1}{3}\right)^{-3/2}-\frac{2}{\pi}\frac{\Delta N_2}{\Delta N_1}\times\left(\frac{T}{\tau}-\frac{1}{3}\right)^{-1/2}+\frac{2}{\pi}\frac{\Delta N_2}{\Delta N_1}\left(\frac{t-2T}{\tau}\right)\times\left(\frac{T}{\tau}-\frac{1}{3}\right)^{-3/2}\right] \quad (16)$$

and

$$\Delta N_3 = 2AC_\infty\sqrt{\frac{D\tau}{\pi}}\left[1-\frac{2}{\pi}\times\left(\frac{2T}{\tau}-\frac{1}{3}\right)^{-1/2}+\frac{2}{3\pi}\left(\frac{2T}{\tau}-\frac{1}{3}\right)^{-3/2}-\frac{2}{\pi}\frac{\Delta N_2}{\Delta N_1}\left(\frac{T}{\tau}-\frac{1}{3}\right)^{-1/2}+\frac{2}{3\pi}\frac{\Delta N_2}{\Delta N_1}\times\left(\frac{T}{\tau}-\frac{1}{3}\right)^{-3/2}\right] \quad (17)$$

This procedure may now be repeated indefinitely, resulting in the following general formulae for the j^{th} pulse:

$$i(jT-T<t<jT-T+\tau) = nAFC_\infty\sqrt{\frac{D}{\pi(t-jT+T)}}\left[1-\frac{2}{\pi}\times\sum_{k=1}^{k=j-1}\frac{\Delta N_{j-k}}{\Delta N_1}\left(\frac{kT}{\tau}-\frac{1}{3}\right)^{-1/2}+\frac{2}{\pi}\left(\frac{t-jT+T}{\tau}\right)^{k=j-1}_{k=1}\sum\frac{\Delta N_{j-k}}{\Delta N_1}\times\left(\frac{kT}{\tau}-\frac{1}{3}\right)^{-3/2}\right] \quad (18)$$

and

$$\frac{\Delta N_j}{\Delta N_1} = 1-\frac{2}{\pi}\sum_{k=1}^{k=j-1}\frac{\Delta N_{j-k}}{\Delta N_1}\times\left(\frac{kT}{\tau}-\frac{1}{3}\right)^{-1/2}+\frac{2}{3\pi}\sum_{k=1}^{k=j-1}\times\frac{\Delta N_{j-k}}{\Delta N_1}\left(\frac{kT}{\tau}-\frac{1}{3}\right)^{-3/2} \quad (19)$$

Equations 3, 12, 16, and 18 are expressions for the currents throughout the first, second, third, and j^{th} pulses. Experimentally, however, pulse polarographic currents are not monitored throughout the pulses, but are measured only at a fixed instant during each pulse. We shall denote by Υ ($O<\Upsilon<\tau$) the time after the beginning of each pulse at which the current is measured. Hence from Equations 3 and 18 we can derive the ratio of the measured current for the j^{th} pulse to that for the first pulse as

$$\frac{i_j}{i_1} = \frac{i(jT-T+\Upsilon)}{i(\Upsilon)} = 1-\frac{2}{\pi}\times\sum_{k=1}^{k=j-1}\frac{\Delta N_{j-k}}{\Delta N_1}\left(\frac{kT}{\tau}-\frac{1}{3}\right)^{-1/2}+\frac{2\Upsilon}{\pi\tau}\sum_{k=1}^{k=j-1}\frac{\Delta N_{j-k}}{\Delta N_1}\left(\frac{kT}{\tau}-\frac{1}{3}\right)^{-3/2} \quad (20)$$

Equation 20 provides a quantitative basis for the theoretical interpretation of the depletion effect. It has been used, together with the iteration formula 19 and the experimentally accessible values of the time parameters, τ, T, and Υ to construct Table I.

EXPERIMENTAL

The pulse polarograph used in this investigation was constructed in this laboratory. For purposes of this paper it is generally similar to the instrument described by Barker (*1*).

Table I. Values of i_j/i_1 Calculated by the Use of Equations 19 and 20

The times $\tau_1 = 46.2$ milliseconds, $\Upsilon = 40.3$ milliseconds were employed, together with the listed T values

j	$T = 2.95$ sec.	$T = 4.62$ sec.	$T = 13.80$ sec.
1	1.0000	1.0000	1.0000
2	0.9212	0.9368	0.9633
3	0.8714	0.8959	0.9386
4	0.8339	0.8647	0.9192
5	0.8035	0.8390	0.9029
6	0.7779	0.8171	0.8888
7	0.7557	0.7979	0.8761
10	0.7024	0.7513	0.8446
15	0.6393	0.6946	0.8044
20	0.5935	0.6524	0.7731

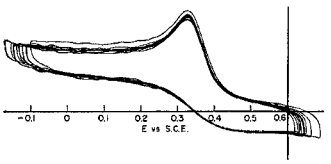


Figure 3. Cyclic sweep for the system $1 \times 10^{-4}M$ Au(III) in 2M HCl at a pyrolytic graphite electrode

All solutions were made from reagent grade chemicals. The gold(III) chloride solution was prepared by weighing gold foil, dissolving in aqua regia, evaporating the solution to near dryness, and repeating the evaporation after the addition of hydrochloric acid. A stock solution of gold(III) chloride was made from this by dilution with acid.

A Beckman platinum inlay electrode (Cat #39273) and a Kemula type hanging drop electrode (Brinkmann Instruments Co., Westbury N. Y.) were used. The construction of the pyrolytic graphite electrode will be described in a future publication (*5*).

RESULTS AND DISCUSSION

The reduction of auric gold at the pyrolytic graphite electrode will be described in some detail later (*5*) but it provides an interesting example of the depletion effect. Figure 3 shows a current–voltage curve which results from the rapid cyclic sweep of a stirred solution containing $1 \times 10^{-4}M$ Au(III) and $2M$ HCl. The peak at +0.33 volt represents reduction to the metal. Notice that the oxidation of gold does not occur in the potential range scanned. Other experiments have shown that the gold is reoxidized near +1.0 volt. If the resting potential chosen for a normal pulse polarographic scan for the reduction of gold(III) is chosen between +0.5 volt and +0.9 volt a depletion effect should be observed. Figure 4 shows three normal pulse polarograms for the gold(III) reduction. The two upper curves were recorded with different degrees of stirring. The curve recorded in the absence of stirring shows a significant depletion effect. Figure 5 shows two curves recorded in the absence of stirring. The time interval T from one pulse to the next is 2.95

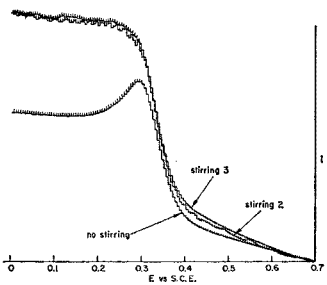


Figure 4. Normal pulse polarograms for the reduction of Au(III) at a pyrolytic graphite electrode, without stirring, with mild stirring ("stirring 2") and with more violent agitation ("stirring 3")

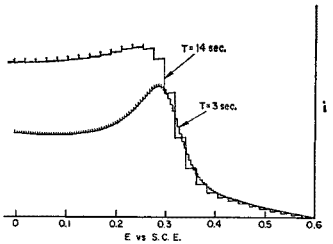


Figure 5. Normal pulse polarograms, obtained in the absence of stirring, for the reduction of Au(III) at a pyrolytic graphite electrode.

In both cases the pulse width was nominally 50 milliseconds (actually 46.2 ms.), but the time lapse between pulses was nominally as indicated (actually 13.8 sec. and 2.95 sec.)

seconds for the lower curve and 13.8 seconds for the upper curve; the difference is qualitatively as expected.

Experimental data were obtained by applying pulses similar to those shown in Figure 1*b* to the electrodes to compare with the theoretically calculated current ratios. The data are tabulated in Tables II and III together with the theoretical values. Most of the experimental current ratios do not fall quite as rapidly with successive pulses as do the theoretical values. This is attributed to convection effects. No precautions were taken in our experiments to eliminate convective transport. Data taken on successive days showed that the reproducibility of the measurements was never better than 1 to 4% relative. Inspection of the data also shows that the agreement is good for the first two or three pulses but the deviation from theory generally becomes larger with successive pulses. If one remembers

Table II. Comparison of Experimental Ratio of i_j/i_1 of Several Systems with Theoretical Values

$$\frac{T}{\tau} = 64.2$$

	Experimental								
	[a]Reduction of Au(III) at P.G.E.			[b]Reduction of Ni(II) at hanging Hg drop		[c]Oxidation of ascorbic acid at hanging Hg drop			
j Value	Set 1	Set 2	Set 3	Set 1	Set 2	Set 1	Set 2	Set 3	Theoretical
1	1.0	1.0	1.00	1.0	1.0	1.0	1.0	1.0	1.0
2	0.923	0.916	0.879	0.918	0.928	0.925	0.914	0.928	0.921
3	0.876	0.874	0.806	0.871	0.886	0.880	0.863	0.888	0.871
4	0.840	0.843	0.764	0.838	0.857	0.850	0.824	0.860	0.834
5	0.810	0.820	0.729	0.812	0.831	0.825	0.800	0.835	0.804
6	0.788	0.800	0.702	0.790	0.815	0.805	0.778	0.816	0.778
7			0.679	0.774	0.800	0.785	0.760	0.800	0.756
8			0.661	0.758				0.790	0.736
9								0.780	0.718

[a] Gold: Solution approximately $3 \times 10^{-5}M$ Au^{+3} in $1M$ HCl.
Sets 1 & 2—two runs showing reproducibility; resting potential at +0.55 volt *vs.* S.C.E. Step 0.3 volt.
Set 3—Resting potential +0.65 volt. Step 0.5 volt.

[b] Nickel: $6 \times 10^{-4}M$ nickel in
Set 1—Slightly ammoniacal $0.1M$ $NaNO_3$. Average 4 runs.
Set 2—$1M$ NH_4NO_3-NH_3 buffer pH = 8. Average 2 runs.

[c] Ascorbic acid: $0.1M$ phosphate buffer pH 6.6 as supporting electrolyte.
Set 1—Approximately $10^{-3}M$ ascorbic acid; resting potential −0.1 volt; Step 0.2 volt
Set 2—Approximately $5 \times 10^{-4}M$ ascorbic acid; resting potential −0.1 volt; Step 0.2 volt
Set 3—Approximately $5 \times 10^{-4}M$ ascorbic acid; resting potential −0.3 volt; Step 0.4 volt

Table III. Comparison of Experimental i_j/i_1 Ratio with Theoretical Value

$$\frac{T}{\pi} = \frac{13.8}{0.046} = 298$$

	Experimental		
j Value	[a]Reduction of gold(III) at P.G.E.	[b]Oxidation of ascorbic acid at hanging Hg drop	Theoretical
1	1.0	1.0	1.0
2	0.958	0.971	0.963
3	0.936	0.954	0.939
4	0.917	0.940	0.919
5	0.914	0.932	0.902
6	0.910	0.925	0.889
			0.876

[a] Approximately $3 \times 10^{-6}M$ Au^{+3} in $1M$ HCl. Resting potential +0.55 volt; Step 0.3 volt. Average of 2 runs.

[b] About $10^{-3}M$ ascorbic acid in phosphate buffer of pH 6.6. Resting potential −0.1 volt; Step 0.2 volt.

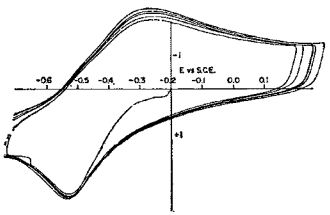


Figure 6. Cyclic voltammograms for the system $3 \times 10^{-4}M$ Pb(II) in 0.1M KNO_3 at a platinum inlay electrode

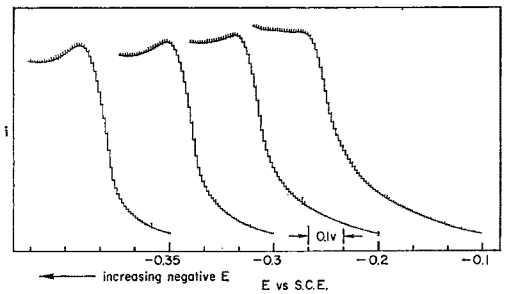


Figure 7. Normal pulse polarograms for the unstirred system $9 \times 10^{-4}M$ Pb(II) in 0.1M KNO_3 at a platinum inlay electrode

The resting potentials differed in the four cases shown and were, reading from the left, −0.35 volt, −0.30 volt, −0.20 volt, and −0.10 volt *vs.* S.C.E.

that any error or deviation is cumulative with successive pulses, a relative difference of 10 to 15% from theoretical after 7 or 8 pulses is considered good agreement.

It should be emphasized that the largest contribution to the deviation from the theoretical values is probably convection although other effects may be of some significance. However, the general agreement between theory and experiment is satisfying and establishes the concept of depletion under pulse polarographic conditions.

Data for the reduction of gold(III) at the pyrolytic graphite electrode are in good agreement if the resting potential is +0.55 volt *vs.* S.C.E. but the current falls more rapidly than it should if the potential is a more positive value. (See Set 3 for gold.) These data are quite reproducible and the effect is real. It has also been observed that in a stirred solution and when the resting potential is +0.6 volt or greater, the current for the first pulse is always significantly higher than that for subsequent pulses. It would be logical to advance an adsorption explanation of these effects but further study is needed to positively identify the extraneous factor responsible for this behavior.

Comparison of Sets 2 and 3 for ascorbic acid oxidation suggests that the back reaction is insignificant under conditions of our experiment since there is no dependence of current ratio on the value of the resting potential. This is in agreement with the observation that dehydroascorbic acid is not reduced at the dropping mercury electrode (*3*).

Many reductions at solid electrodes (and many organic reactions at mercury electrodes) are not completely reversible and some depletion may be encountered. Figure 6 shows rapid cyclic sweep of a solution of approximately $3 \times 10^{-4}M$ Pb^{+2} in $0.1M$ KNO_3 at a platinum electrode. It is clear that under these experimental conditions the lead couple is not reversible. One therefore would expect a depletion effect if the resting potential chosen were in the vicinity of −0.4 volt, and perhaps at more positive potentials if the reoxidation is sufficiently slow. Figure 7 shows a series of normal pulse polarographic curves for the reduction of approximately $9 \times 10^{-4}M$ Pb^{+2} starting from different resting potentials. As the resting potential becomes more negative the depletion effect becomes greater. Even from a resting potential of −0.2 volt a depletion is found. The reoxidation of lead is apparently slow. The details of this system are complicated presumably because of alloy formation, but the effect of depletion can be easily observed qualitatively.

In many systems examined by normal pulse polarography the depletion effect can give rise to decreasing currents in the limiting current region. The reason for these decreasing currents should be recognized and means for avoiding or minimizing them should be understood. Both stirring and proper choice of resting potential are effective in eliminating this effect.

APPENDIX A

A solution to the equations expressing Fick's second law is sought subject to the conditions

$$C(x,\tau) = C_\infty \text{erf}\left\{\frac{x}{2\sqrt{D\tau}}\right\} \quad \text{(A1)}$$

$$\frac{\partial C}{\partial x}\,(O,\tau < t \leq T) = 0 \quad \text{(A2)}$$

and

$$C(\infty,t) = C_\infty \quad \text{(A3)}$$

Taking the Laplace transforms of the last two equations

$$\frac{d\bar{C}}{dx}\,C\,(O,s) = 0 \quad \text{(A4)}$$

$$\bar{C}(\infty,s) = C_\infty/s \quad \text{(A5)}$$

where $\bar{C}$ and $1/s^2$ are the Laplace transforms of C and $(t - \tau)$, respectively. Similarly, the transform of Fick's law in linear coordinates reads

$$D\,\frac{d^2\bar{C}}{dC^2}\,(x,s) = s\bar{C}\,(x,s) - C(x,\tau) \quad \text{(A6)}$$

Equations (A1, A4, A5, and A6 may be solved by the "variations of parameters" method (*6*), to yield

$$\frac{2s}{C_\infty}\,\bar{C}(x,s) = 2\,\text{erf}\left\{\frac{x}{2\sqrt{D\tau}}\right\} + 2\exp\left\{s\tau - x\sqrt{\frac{s}{D}}\right\}\text{erfc}\times\left\{\sqrt{s\tau}\right\} - \exp\left\{s\tau - x\sqrt{\frac{s}{D}}\right\}\text{erfc}\times\left\{\sqrt{s\tau} - \frac{x}{2\sqrt{D\tau}}\right\} + \exp\times\left\{s\tau + x\sqrt{\frac{s}{D}}\right\}\text{erfc}\left\{\sqrt{s\tau} + \frac{x}{2\sqrt{D\tau}}\right\} \quad \text{(A7)}$$

Substituting $x = 0$ into A7 and taking the inverse Laplace transform gives

$$C(O,\tau < t \leq T) = \frac{2C_\infty}{\pi}\arctan\sqrt{\frac{t-\tau}{\tau}} \quad \text{(A8)}$$

Repeated differentiation of A7 with respect to x, followed by setting $x = 0$ and inversion yields

$$\frac{\partial C}{\partial x}\,(O,\tau < t \leq T) = 0 \quad \text{(A9)}$$

$$\frac{\partial^2 C}{\partial x^2}\,(O,\tau < t \leq T) = \frac{C_\infty}{\pi Dt}\sqrt{\frac{\tau}{t-\tau}} \quad \text{(A10)}$$

$$\frac{\partial^3 C}{\partial x^3}\,(O,\tau < t \leq T) = 0 \quad \text{(11A)}$$

These last four equations provide the MacLaurin coefficients required for Equation 5.

APPENDIX B

Curve DE in Figure 2 is an approximation to $C(x, T)$ which is the more valid the smaller x, being exact for $x = 0$. Curve EF is based upon a completely different approximation and becomes exact as the ratio τ/T approaches zero. The two curves coincide at $x = 0$ because EF has been "fitted" at this point. However, no such fit has caused the coincidence of the curves at non-zero x values, yet the figure shows that the two curves are virtually identical out to about $x = 7\sqrt{D\tau}$. The agreement of these two quite independent approximations for $0 < x < 7\sqrt{D\tau}$ and $\tau/T = 0.01$ strongly suggests that both correspond very closely to the true $C(x, T)$ under these conditions.

Recall that the depletion caused by the first pulse did not extend beyond about $5\sqrt{D\tau}$ (Figure 2). One is justified therefore, in expecting that only that section of the concentration profile lying well within the range $0 < x < 7\sqrt{D\tau}$ at time $t = T$ will have any bearing on the depletion caused by the second pulse. This is just the region for which Equations 6 and 10 (and thereby curves DE and EF) are coincident. Moreover, since Equation 10, which is of the form $C(x,T)/C_\infty = 1 + \gamma \exp\{\delta x^2\}$, is mirrored so closely by Equation 6, which has the form $C(x,T)/C_\infty = \alpha + \beta x^2$, it follows that $1 + \gamma + \gamma\delta x^2$ must be both an adequate expansion of Equation 10 and a valid approximation of 6. Writing out the γ and δ terms:

$$\frac{C(x,T)}{C_\infty} = 1 - \frac{2}{\pi}\left[\frac{T}{\tau} - \frac{1}{3}\right]^{-1/2} + \frac{x^2}{2\pi D\tau}\left[\frac{T}{\tau} - \frac{1}{3}\right]^{-3/2} \quad \text{(B1)}$$

We now seek a solution to the equation expressing Fick's second law subject to B1 as an initial condition. This solution will be valid for times $T < t \leq T + \tau$—i.e., during the second pulse. Equation A3 still holds but A2 is replaced by

$$C(x, T < t \leq T + \tau) = 0 \quad \text{(B2)}$$

The Laplace transform method is again of value. The solution of the transform of the equation for Fick's second law (analogous to A6) subject to the transforms of Equations B1, B2, and A3 is

$$\frac{\bar{C}(x,p)}{C_\infty} = \frac{x^2}{2\pi D\tau p}\left[\frac{T}{\tau} - \frac{1}{3}\right]^{-3/2} + \left\{1 - \exp\left[-x\sqrt{\frac{p}{D}}\right]\right\}\left\{\frac{1}{p} - \frac{2}{\pi\tau p^2} \times \left[\frac{T}{\tau} - \frac{1}{3}\right]^{-1/2} + \frac{1}{\pi\tau p^2}\left[\frac{T}{\tau} - \frac{1}{3}\right]^{-3/2}\right\} \quad \text{(B3)}$$

where $1/p^2$ is the transform of $(t - T)$. This inverts to give Equation 11 in which i^2 erfc denotes the second integral of the error function complement. Differentiation of 11 yields

$$\frac{1}{C_\infty}\frac{\partial C}{\partial x}(x, T < t \leq T + \tau) = \frac{x}{\pi D\tau}\left[\frac{T}{\tau} - \frac{1}{3}\right]^{-3/2} + \left\{1 - \frac{2}{\pi} \times \left[\frac{T}{\tau} - \frac{1}{3}\right]^{-1/2}\right\}\{\pi D(t - T)\}^{-1/2} \times \exp\left\{\frac{-x^2}{4D(t - T)}\right\} + \frac{2}{\pi\tau}\frac{t - T}{D} \times \left[\frac{T}{\tau} - \frac{1}{3}\right]^{-3/2} i\text{erfc}\left\{\frac{x}{2\sqrt{D(t - T)}}\right\} \quad \text{(B4)}$$

which readily generated Equation 12 and in which $i$erfc represents the first integral of the error function complement.

ACKNOWLEDGMENT

We are indebted to J. H. Christie for assistance in some experimental work and to R. A. Osteryoung for helpful discussions and for writing the computer program from which Table I was obtained.

LITERATURE CITED

(1) Barker, G. C., Gardner, A. W., *A.E.R.E.* C/R 2297 Harwell Report 1958.
(2) Delahay, P., "New Instrumental Methods in Electrochemistry," p. 50, Interscience, New York, 1954.
(3) Kalousek, M., *Collection Czech. Chem. Commun.* **13**, 105 (1948).
(4) Parry, E. P., Osteryoung, R. A., ANAL. CHEM. **36**, 1366 (1964).
(5) Parry, E. P., unpublished data, 1966.
(6) Sokolnikoff, I. S., Sokolnikoff, E. S., "Higher Mathematics for Engineers and Physicists," p. 318, McGraw-Hill, New York, 1941.

RECEIVED for review February 21, 1966. Accepted March 28, 1966. Division of Analytical Chemistry, Winter Meeting, ACS, Phoenix, Ariz., January 1966.

Polarographic Study of the Iodine-Iodide Couple at the Rotating Platinum Electrode

E. CLIFFORD TOREN, Jr., and CHARLES P. DRISCOLL[1]

Department of Chemistry, Duke University, Durham, N. C.

▷ The oxidation of iodide in 0.1*M* $HClO_4$ has been investigated voltammetrically at the rotating platinum electrode (RPE) at 25° C. Results indicate that the formation of triiodide must be considered in the polarographic equation. An anodic maximum due to the formation of solid iodine is observed for iodide concentrations greater than 2.5m*M*. A polarographic peak in the cathodic wave of ca. millimolar iodine-iodide solutions indicates the presence of adsorbed iodine. The peak is investigated as a function of sweep rate, pretreatment, and potential. A potential-coverage isotherm is presented. Results indicate the utility of polarography at the RPE to the investigation of potential-dependent adsorption processes.

KOLTHOFF and Jordan (*7*) have described the polarographic behavior of the iodine-iodide system at the rotating platinum electrode (RPE) in 0.1*M* $HClO_4$. They report a reversible 2-electron oxidation of iodide to iodine which obeys the following polarographic equation in dilute iodide solutions:

$$E = \text{const} - 0.030 \log \frac{(i_{l_a} - i)^2}{i}, \quad \text{at 25° C.} \quad (1$$

where E is the applied potential of the RPE, and i_{l_a} is the anodic limiting current.

The authors observed that the polarographic oxidation of iodide did not obey Equation 1 in more concentrated iodide solutions.

Iodide may be oxidized to either I_2 or I_3^- in the same potential region (*9*).

$$I_3^- + 2e^- = 3I^-;\ E^\circ = 0.290 \text{ volt } vs. \text{ SCE} \quad \text{(I)}$$

$$I_{2(s)} + 2e^- = 2I^-;\ E^\circ = 0.2897 \text{ volt } vs. \text{ SCE} \quad \text{(II)}$$

Jordan and Javick (*5*) report that the molecularity of iodide oxidation is 2 in the principal electrode process under conditions which favor iodine as the principal product.

Consideration of the iodide-iodine-triiodide equilibrium (*6*),

$$I_3^- = I_2 + I^-;\ K_{eq} = 1.27 \times 10^{-3},$$

[1] Present address, Celanese Corp. of America, Box 1000, Summit, N. J.

at 25° C. in 0.1*M* $HClO_4$ (III)

reveals that I_2 may be formed initially at the electrode surface with subsequent reaction with I^- to form I_3^- in solutions more concentrated than described by other workers (*5*, *7*).

While performing coulometric titrations using amperometric indication with internally generated I_2, Malmstadt and Toren (*12*) have observed a prolonged, cathodic indicator current which persists even in the presence of large excesses of $Na_2S_2O_3$ and As(III).

Early work by Lorenz and Mühlberg (*11*) demonstrates that the I_2-I_3^--I^- system undergoes potential dependent adsorption on platinum black electrodes. Toth (*19*) has also shown that iodine adsorption occurs on platinum electrodes, especially if the surface is cathodically pretreated. The saturation value is reached rapidly and is independent of the total iodide concentration.

Osteryoung (*14*), using current-reversal chronopotentiometry, finds that iodine is adsorbed on bright platinum electrodes. Similar conclusions are reached using integration of single sweep polarograms (*16*, *17*) and by radiotracer experiments (*15*). Osteryoung and coworkers further demonstrate that although both iodine and iodide are adsorbed, only iodine is electroactive in the region of the reversible I_2/I^- potentials (*15*).

The polarographic investigation presented herein elucidates anomalous anodic and cathodic peak behavior at the RPE. A polarographic equation is derived for the oxidation of relatively concentrated iodide solutions in 0.1*M* $HClO_4$.

EXPERIMENTAL

A three-electrode system using operational amplifiers was employed in this investigation. The basic instrumentation was a modification of circuits designed by DeFord (*4*).

The current was obtained as a function of the cell potential with an X-Y recorder, Houston Instrument Corp., Houston, Texas, Model HR-96T. Since a linear ramp was used for the sweep voltage, the current-time curve was indirectly recorded.

The cell is shown in Figure 1. The auxiliary compartment was separated from the reaction chamber by a sodium perchlorate–agar salt bridge and glass frit. The reference compartment, containing the saturated calomel electrode (SCE), was separated from the reaction chamber by a glass frit and KCl-saturated agar. The center section, containing the RPE and the solution under study, had a total volume of ca. 60 ml. A two-way stopcock permitted selection of two gas inlets. The one shown at the bottom of the cell has been drawn into a capillary for deaeration of the solution. After the solution was purged, the upper inlet was activated to cover the solution

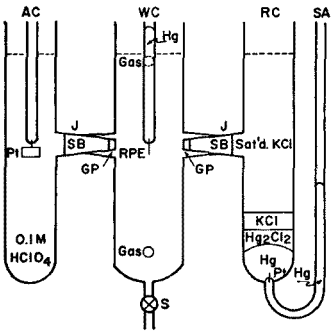


Figure 1. Three-electrode cell

- AC. Auxiliary compartment, 18 × 150 mm., borosilicate glass
- GP. Glass frit (fine)
- J. Ground glass joint, ⅌ 14/35
- RC. Reference compartment, 18 × 150 mm., borosilicate glass
- S. Stopcock
- SA. Side arm
- SB. Salt bridge
- WC. Working compartment, 30 × 150 mm., borosilicate glass

with an inert atmosphere of water-pumped, prepurified nitrogen.

Electrodes. The platinum-flag auxiliary electrode was a Sargent, Type S-30515. The RPE was constructed by sealing platinum wire into 7-mm. soft glass tubing. The glass-platinum seal was checked for continuity, since anomalous results are obtained with cracked electrodes (*7*). Care was taken to keep the glass tubing and platinum wire straight, since irregularities produce undesirable stirring effects when the electrode is rotated. RPE (*a*), used in the anodic studies, had a smooth surface and a geometric area of 2.70×10^{-2} sq. cm. RPE (*b*), used in the cathodic studies, was prepared by grinding the platinum wire flush to the tubing with pumice. The geometric area of RPE (*b*) was 7.40×10^{-3} sq. cm. The electrodes were stored in a reducing solution of acidified Fe(II) to prevent surface oxidation (*1*). The RPE was driven by a Sargent, Type S-76485 synchronous rotator at 600 r.p.m. in all cases unless otherwise noted. A Sargent, Type S-76445 cone-driven stirrer was used as a variable speed rotator.

Solutions. All solutions were prepared with reagent grade chemicals. In all cases 0.1*M* $HClO_4$ was the supporting electrolyte. I_2-I_3^--I^- solutions were prepared by adding standard KIO_3 to excess KI in the supporting electrolyte. The temperature of the solutions was 25° ± 2° C.

THEORY

Under conditions in which both I_2 and I_3^- are present at the electrode surface, the over-all process may be considered as

$$Ox + 2e = xI^- \qquad \text{(IV)}$$

where Ox represents $I_2 + I_3^-$ and x is the ratio of I^- to Ox.

The Nernst equation may be approximated as

$$E = E^{o\prime} + \frac{2.303\,RT}{2F} \log \frac{[Ox]_o}{[I^-]_o^x} \qquad (2)$$

where $E^{o\prime}$ is the formal potential of the system and $[Ox]_o$ and $[I^-]_o$ represent the surface concentrations. All other terms have their usual significance.

For a reversible process, the current at a given potential will be governed by the rate of mass transport and is proportional to the concentration gradient across the effective diffusion layer. With only I^- initially present,

$$i = -k_{ox}[Ox]_o = -k_{red}([I^-] - [I^-]_o) \qquad (3)$$

where k_{ox} and k_{red} are the cathodic and anodic polarographic constants, respectively, defined as

$$i_{la} = -k_{red}[I^-];\ i_{lc} = k_{ox}[Ox] \qquad (4)$$

$$i - i_{la} = k_{red}[I^-]_o \qquad (5)$$

where i_{la} is the anodic limiting current and i_{lc} is the cathodic limiting current when Ox is initially present.

Kolthoff and Jordan (*7*) report that $D_{I_2} = D_{I_3^-} = 1.11 \times 10^{-5}$ sq. cm. per second; therefore, k_{ox} is independent of the actual species.

Upon substitution of Equations 3 and 5 into 2

$$E - \frac{2.303\,RT}{2F} \log(-i) = K - x\frac{2.303\,RT}{2F} \log \frac{(i - i_{la})}{k_{red}} \qquad (6)$$

where $K = E^{o\prime} - \frac{2.303\,RT}{2F} \log k_{ox}$.

By plotting the left-hand side of Equation 6 *vs.* $\log (i - i_{la})/k_{red}$ at various potentials along the wave, x may be determined from the slope.

The extension of Equation 6 to

$$E - \frac{2.303\,RT}{2F} \log(i_{lc} - i) = K - x\frac{2.303\,RT}{2F} \log \frac{(i - i_{la})}{k_{red}} \qquad (6a)$$

is doubtful because k_{red} is found to vary when Ox is initially present. Equations 3 to 5 assume that only I^- is the diffusing reductant. This assumption may lead to appreciable errors when I_3^- is present in the bulk in the determination of x from Equation 6a. Negligible errors are expected in the application of Equation 6, because the concentration gradient of I^- greatly exceeds that of I_3^- at potentials near the plateau of the anodic wave.

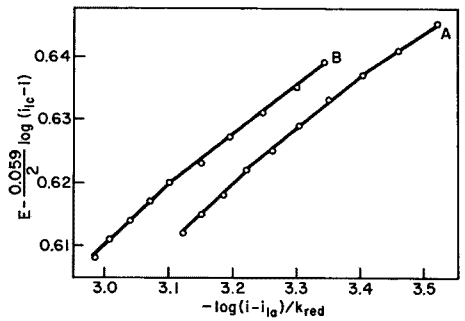


Figure 2. Plots used to evaluate x in Equation IV

RPE (a) at +5 mv./sec.
A. 1.05mM I^-, $i_{la} = -13.0$ μa., $i_{lc} = 0$
B. 0.635 mM I^-, 0.500mM $I_2 + I_3^-$, $i_{la} = -9.27$ μa., $i_{lc} = 6.90$ μa., $k'_{red} = 1.16 \times 10^{-2}$ amp. liter mole^{-1}

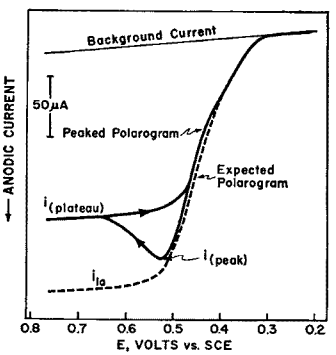


Figure 3. Comparison of typical, peaked anodic polarogram and expected polarogram

RPE (a) at ca. 1000 r.p.m., +2mv./sec. sweep rate, 4.68mM I^-

RESULTS AND DISCUSSION

Data to support the form of Equations 6 and 6a are presented in Figure 2. Since the oxidation of solutions containing iodide alone is simpler, it is discussed first.

Iodide Solutions. Using Equation 6 to plot anodically swept polarograms in Figure 2, *A*, an x value of 2.8 was found for potentials near the center of the rising portion of the wave. This indicates that both Reactions I and II are occurring, but that Reaction I predominates.

At more anodic potentials x attains a value of 2.2; and at more cathodic potentials x becomes 3.1. This behavior may be explained by consideration of the iodine-triiodide-iodide equilibrium(III). At the foot of the anodic wave, one can establish by using Equation 3 that the surface concentration of iodide does not differ greatly from the bulk, and that the oxidant concentration at the surface is small; thus triiodide is the favored product and x becomes ca. 3. Conversely, near the anodic plateau the surface concentration of iodide becomes small, thus favoring the formation of iodine near the surface. Therefore, x becomes ca. 2. Similar results at different concentrations are obtained with an average of $x = 2.74$ near the center of the wave. In all cases x decreases at more anodic potentials and increases at more cathodic potentials.

Iodide-Iodine-Triiodide Solutions. For solutions initially containing I_3^-, I_2, and I^-, the anodic polarographic constant, k_{red}, defined by Equation 4 varies with the relative concentrations of the three species. Table I illustrates that k_{red} increases as $[I_2] + [I_3^-]$ increases and as $[I^-]$ decreases according to Reaction III. A more reasonable polarographic constant, $k'_{red} = -i_{la}/[I^-] + [I_3^-]$, is also shown in Table I. That k'_{red} is more constant and in better agreement with k_{red} obtained in solutions containing iodide alone, is qualitatively explained by the oxidation of I_3^- to I_2 on the anodic plateau.

Using Equation 6a with $k'_{red} = 1.16 \times 10^{-2}$ amp. liter mole^{-1}, an x value of 2.8 results for potentials near the center of the wave as obtained from the plot of Figure 2, *B*. In the present case, the slope also increases at more cathodic potentials and decreases at more anodic potentials. An average x value of 2.84 results from similar plots using different concentrations. Since k_{red} is not constant in a mixture of all three species, the agreement between Equations 6 and 6a is perhaps fortuitous owing to the insensitivity of the logarithmic terms.

Large Concentrations of Iodide. An anodic maximum appears when the iodide concentration exceeds 2.5m*M*. The authors believe that the diffusion of the principal product at plateau potentials—i.e., I_2—is inhibited by the formation of solid I_2 on the electrode surface. A similar phenomenon at the dropping mercury electrode has been reported by Miller (*13*, *18*) in the anodic depolarization of chloride solutions greater than 1m*M*. Figure 3, a typically peaked polarogram, illustrates that neither the peak nor the plateau current attains the expected anodic limiting current as calculated from Equation 4.

To strengthen the hypothesis that the normal transport process is inhibited at large bulk iodide concentrations, a potential-step technique was employed. After standard pretreatment of the RPE, anodic step potentials were applied and the resulting current was observed as a function of time. In solutions of millimolar iodide, the currents at all potentials were the same as those described by the normal polarogram, even over very long time intervals. With large iodide concentrations the initial currents corresponded to those values which would be attained by a normal polarogram calculated from Equations 3 and 4; however, these currents decayed with time to coincide with the abnormal or peaked polarogram. The rate of change of the current was greater at more anodic potentials, as is particularly evident in the plateau region. These results indicate that, initially, the diffusing species has free access to the electrode surface; however, at high bulk iodide concentrations the mass transport process is inhibited. It appears reasonable to attribute this interference to the accumulation of the product, I_2, at the platinum surface. No peak occurs if the polarogram is scanned in the cathodic direction, as

Table I. Variation of k_{red} with Oxidant Concentration

RPE (*a*) at +5 mv./sec. sweep rate

$([I_2] + [I_3^-]) \times 10^4 M$	$[I_3^-]_{calcd.} \times 10^4 M$	$[I^-]_{calcd.} \times 10^4 M$	$-i_{la}/[I^-]_{calcd.}$, $\times 10^2$ amp.-l./mole	$-i_{la}/[I^-] + [I_3^-]$, $\times 10^2$ amp.-l./mole
5.00	1.65	6.35	1.46	1.16
10.0	2.90	5.10	1.55	1.00
20.00	4.40	3.60	2.22	1.01
...	...	5.23[a]	1.21	1.21
...	...	10.46[a]	1.23	1.23

[a] Actual iodide concentration.

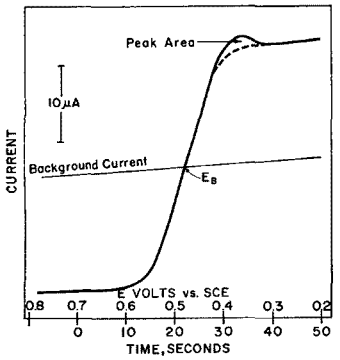


Figure 4. Typical polarogram indicating cathodic peak

RPE (b) at −10 mv./sec. sweep rate, 1.00mM I^- and 1.00mM $I_2 + I_3^-$, anodized 1 min. at 0.8 volt

seen in Figure 3, because solid I_2 has already been formed at these very anodic initial potentials.

A series of polarograms was obtained to determine the concentration limit for anodic peak formation by plotting the iodide concentration against the peak height, $i_{(peak)} - i_{(plateau)}$, and extrapolating to zero peak height. The results given in Table II yielded an average intercept of 2.54mM I^-.

At potentials in the vicinity of the peak $[I^-]_o$ approaches zero as $[I_2]_o$ approaches one half $[I^-]$. Therefore, $[I_2]_o$ at the critical iodide concentration is 1.27mM, which is in good agreement with 1.30mM, the reported solubility of iodine in 0.1M $HClO_4$ (*6*).

The expected polarogram is more closely approached with increasing sweep rates, decreasing iodide concentration, and decreasing electrode rotation speeds. With a sweep rate of +2 mv. per second, the peak height is greater than at a sweep rate of +5 mv. per second, as shown in Table II. At a sweep rate of +20 mv. per second the expected polarogram is approached. The potential step experiments demonstrate that the initial currents correspond to the expected anodic limiting current calculated from Equation 4. At faster sweep rates an extensive buildup of solid I_2 is not possible because fewer faradays are passed in the same potential range. At an electrode rotation speed of 600 r.p.m., the peak height is diminished because of smaller diffusion currents over the same time interval.

Cathodically Swept Polarograms. The following experiments demonstrate that even in solutions with I^- below the critical value for anodic peak formation, large quantities of surface-held oxidant are found on the RPE.

Figure 4 illustrates a typical polarogram obtained in the presence of both oxidized and reduced forms of the I_2/I^- couple. The area, in microcoulombs, indicated in Figure 4 was obtained by graphical integration of the current-time curve. The dashed line was obtained by sweeping the cathodic polarogram at slow sweep rates where the peak current is effectively obscured by the large polarographic current. The peak current exceeds the normal limiting current and does not resemble the behavior of the anodic peak. Regardless of the cathodic peak behavior, $i_{lc}/[I_2] + [I_3^-]$ remains constant within experimental error. No irregularities were observed in the background-current polarograms using identical pretreatment procedures in the supporting electrolyte only. No anodic peaks were obtained in the anodically swept polarograms in I_2-I^- solutions unless the critical concentration to produce solid I_2 was exceeded. Surface-held I_2 is apparently reformed at anodic potentials, but is completely obscured by the normal polarographic current.

Figure 5 illustrates the variation of peak area (with respect to the geometric

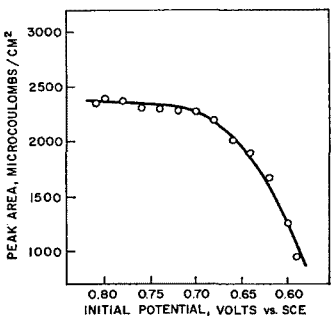


Figure 5. Peak area as a function of initial potential

RPE (b) at −10 mv./sec. sweep rate, 1.00mM I^- and 1.00mM $I_2 + I_3^-$
Pretreatment. 2 min. at −0.2 volt, 1 min. at initial potential

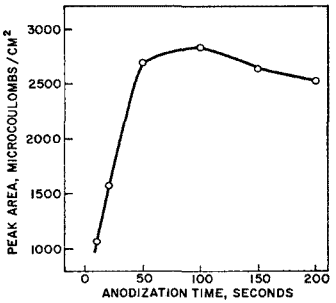


Figure 6. Peak area as a function of anodization time

RPE (b) at −10 mv./sec. sweep rate, 1.00mM I^- and 1.00mM $I_2 + I_3^-$
Pretreatment. −0.2 volt for 2 min., 0.8 volt for variable times

area of the RPE) as the initial anodic potential is varied. An apparent limiting coverage of 2400 μcoulombs per sq. cm. is reached at ca. 0.7 volt. Similar results were obtained when the time of anodization was varied at an initial potential of 0.80 volt as shown in Figure 6. An apparent limiting coverage of 2700 μcoulombs per sq. cm. was noted after 50 seconds. No significance is attached to the maximum at 100 seconds.

Cathodic peaks were observed even in 1mM I^- solutions which do not contain bulk iodine. After the peak, the current became identical with the cathodically swept background current.

The peak area remained essentially constant at relatively fast sweep rates of −10 to −5 mv. per second. With sweep rates less than −1 mv. per second, the peak effectively disappeared. This is explained by the relatively small currents produced by the surface-held oxidant which become obscured by the normal polarographic current at slow sweep rates. Furthermore, at slower sweep rates the electrode is necessarily held cathodic for longer times in the rising portion of the wave, during which

Table II. Determination of Minimum Iodide Concentration for Peak Formation

RPE (*a*) at ca. 1000 r.p.m.

$[I^-] \times 10^3 M$	$-i_{(peak)}$, μa.	$-i_{(plateau)}$, μa.	$-[i_{(peak)}, -i_{(plateau)}]$, μa.
4.68[a]	186	139	47
5.15[a]	200	140	60
5.62[a]	218	145	73
5.85[b]	234	162	72
6.08[a]	234	151	83
6.32[b]	248	175	93
6.55[a]	253	158	95
6.79[b]	268	175	93
7.02[a]	262	161	101
7.26[b]	284	181	103

[a] Sweep rate = +2 mv./sec.
[b] Sweep rate = +5 mv./sec.

a larger fraction of the surface-held oxidant is reduced. On this basis a sweep rate of −10 mv. per second was selected. The abnormally large coverages compared to the results of ca. 300 μcoulombs per sq. cm. obtained by other workers (*15–17*) prompted further studies under less severe anodic conditions.

Figure 7 illustrates the peak area as a function of the overpotential from E_B, the background-current potential. E_B was obtained by halting the sweep at the intersection of the previously determined background-current polarogram as demonstrated in Figure 4. Because E_B varied with iodide concentration, it was determined for each series of experiments.

A plateau of 1380 μcoulombs per sq. cm. was attained between +0.03 and 0.05 volt *vs.* E_B. At anodic overpotentials greater than indicated in Figure 7, the peak area increased rapidly. At +0.10 volt *vs.* E_B the area was greater than 2700 μcoulombs per sq. cm. From four other determinations in which the iodide concentration was varied between 1 and 3m*M*, plateau values between 1700 and 1400 μcoulombs per sq. cm. were observed. Similar results were obtained with longer equilibration times, at both E_B and the specific overpotential.

The limiting coverages observed in Figures 5 and 6 are much larger than the plateau coverage illustrated in Figure 7. I_2 is deposited on the electrode surface if the iodide concentration exceeds 2.54m*M*. In the present case, it is observed that large quantities of I_2 are held on the surface at anodic overpotentials of 0.10 volt, indicating that multilayer deposits are also possible, if it is assumed that monolayer coverage is ca. 1400 μcoulombs per sq. cm. (geometric surface area) as indicated by the plateau in Figure 7.

The authors feel that the plateau in Figure 7 which was reproduced in many similar experiments at different concentrations, represents monolayer coverage greater than that on bright platinum due to the extreme roughness of the pumice-ground electrode. Unground wire electrodes produced lower, but more erratic, results due to electrode wobble and to the difficulty in distinguishing the adsorption current from the normal polarographic current. If the roughness factor is considered, results in accord with other workers (*3, 14–17*) are obtained. Laitinen and Enke (*8*) report a roughness factor of 1.12 for bright platinum. Breiter (*2*) believes a roughness factor of 2 or 3 is not unlikely. Finally, de Levie (*10*) infers that roughness factors greater than 10 are possible. An electrode

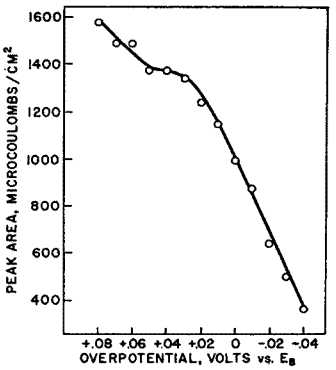


Figure 7. Extent of adsorption as a function of overpotential

RPE (b) at −10 mv./sec. sweep rate, 4.00m*M* I^- and 1.00m*M* $I_2 + I_3^-$, 2 min. at initial potential of 0.7 volt *vs.* SCE, halt sweep at E_B for 2 min., equilibrate 2 min. at overpotential, continue sweep
Pretreatment. 2 min. at −1.0 volt *vs.* SCE, 2 min. at open circuit in 0.1 *M* $HClO_4$

roughness factor of ca. 3 is estimated from Figure 7. At E_B, the coverage is 996 μcoulombs per sq. cm. Osteryoung *et al.* (*3, 14–17*) obtained results of ca. 300 μcoulombs per sq. cm. at open-circuit; however, it is difficult to compare this effect, since their results were obtained in 1*M* H_2SO_4.

That I_2 is strongly adsorbed on platinum electrodes is clearly indicated, because the peak disappears only at very slow sweep rates. It must therefore be more difficult to reduce than bulk I_2. The reduction of adsorbed iodine proceeds only slowly at potentials more cathodic than E_B. Adsorbed iodine is reduced between 0.33 and 0.44 volt *vs.* SCE as indicated in Figures 4 and 7.

As the iodide concentration decreases, it is qualitatively observed that the peak area increases; however, gross variations in the iodide concentration have not been attempted. This tends to indicate that I_2 is the adsorbed species, in agreement with other workers (*15*). Approximately millimolar concentrations of oxidized and reduced forms were used in this study, because it is inferred that saturation is attained at millimolar levels (*15*). Further work is in progress to determine the effects of variations in both I^- and $I_2 + I_3^-$ concentrations.

A cyclic-voltammetric technique further illustrated that the cathodic peak formation is due to adsorbed I_2. The RPE was soaked at open circuit in a solution containing I_2-I_3^--I^-. After 4 minutes the electrode was removed, rinsed several times with distilled water, and placed in a solution of supporting electrolyte. After deaeration, a scan from 0.80 to 0.20 volt was applied. At 0.20 volt the sweep was reversed. A peak was observed on the first cathodic cycle but did not reappear on successive cycles, which indicates that the adsorbed species is reduced on the first cathodic cycle and is lost to the bulk of the solution or that the adsorbed species is reduced to adsorbed, nonelectroactive iodide. The anodic cycles exhibited no irregularities and were identical with curves obtained in the supporting electrolyte. The peak area is comparable in magnitude to the polarographic peak and is essentially independent of sweep rate except at slow sweep rates where it is difficult to distinguish the peak from the background current. Further work is in progress using this technique.

LITERATURE CITED

(1) Anson, F. C., ANAL. CHEM. **33**, 934 (1961).
(2) Breiter, M. W., *Electrochim. Acta* **8**, 925 (1963).
(3) Christie, J. H., Lauer, G., Osteryoung, R. A., *J. Electroanal. Chem.* **7**, 60 (1964).
(4) DeFord, D. D., mimeographed notes, from a paper presented at 133rd meeting, American Chemical Society, San Francisco, 1958.
(5) Jordan, J., Javick, R. A., *Electrochim. Acta* **6**, 23 (1962).
(6) Katzin, L., Gebert, E., *J. Am. Chem. Soc.* **77**, 5814 (1955).
(7) Kolthoff, I. M., Jordan, J., *Ibid.*, **75**, 1571 (1953).
(8) Laitinen, H. A., Enke, C. G., *J. Electrochem. Soc.* **107**, 733 (1960).
(9) Latimer, W. M., "Oxidation Potentials," 2nd ed., Prentice-Hall, Englewood Cliffs, N. J., 1952.
(10) Levie, R. de, *Electrochim. Acta* **10**, 113 (1965).
(11) Lorenz, W., Mühlberg, H., *Z. Elektrochem.* **59**, 736 (1955).
(12) Malmstadt, H. V., Toren, E. C., University of Illinois, Urbana, Ill., unpublished results, 1960.
(13) Miller, C. S., Ph.D. thesis, University of Minnesota, Minneapolis, 1940.
(14) Osteryoung, R. A., ANAL. CHEM. **35**, 1100 (1963).
(15) Osteryoung, R. A., Anson, F. C., *Ibid.*, **36**, 975 (1964).
(16) Osteryoung, R. A., Lauer, G., Anson, F. C., *Ibid.*, **34**, 1833 (1962).
(17) Osteryoung, R. A., Lauer, G., Anson, F. C., *J. Electrochem. Soc.* **110**, 926 (1963).
(18) Swofford, H. S., Holifield, C. L., ANAL. CHEM. **37**, 1515–16 (1965).
(19) Toth, G., *Radiokhimiya* **5**(4), 411 (1963); *Chem. Abstr.* **59**, 14894*b* (1963).

RECEIVED for review November 22, 1965. Accepted March 23, 1966. Southeast-Southwest Regional Meeting, ACS, Memphis, Tenn., December 1965. Research supported by the North Carolina Board of Science and Technology. Preliminary investigations supported by the Duke University Council on Research.

Coulometric Generation of Hydrogen Ions in Water and Methanol Using Hydrogen-Permeable Membrane Electrodes

THOMAS R. BLACKBURN and ROSALIND B. GREENBERG
Department of Chemistry, Wellesley College, Wellesley, Mass. 02181

▶ **The usefulness of hydrogen-permeable membrane electrodes for coulometric generation of hydrogen ions is explored through current–voltage curves and coulometric titrations of a primary standard base in water and methanol. Satisfactory currents, present only when the electrode is supplied with hydrogen, are observed in both solvents. The overall titration efficiency of constant-current coulometric titrations is 99.7% in water and 99.6% in methanol. No previous coul metric titration of bases in strictly nonaqueous solvents has been reported. An easily fabricated membrane electrode is described.**

In 1935, Szebelledy and Somogyi (*8*) introduced coulometric titration of bases in water solutions via the half-reaction

$$H_2O \rightarrow {}^1/_2\,O_2 + 2H^+ + 2e^-$$

Streuli (*7*) generated hydrogen ions in acetonitrile by oxidation of a small amount of water added to the solvent. While this method may, in principle, be extended to many solvents compatible with water, it is not suitable for rigorously nonaqueous systems or for solvents easier to oxidize than water. By exploiting the permeability of palladium and palladium–silver membranes to hydrogen, we have constructed a proton-generating electrode whose functioning does not depend on the solvent.

The electrode's efficiency as a transmitter and oxidizer of hydrogen is greatly improved by surface pretreatment as described below. However, this improvement is fairly short-lived, probably because of loss of catalytic activity for the dissociation of H_2 and for adsorption and desorption of H atoms. Chloride ions and other complexants for Pd(II) limit the useful range of operating potentials by promoting anodic dissolution of the palladium and loss of current efficiency for proton generation.

As an illustration of the analytical potentialities of the electrode, a primary standard base, 2-amino, 2-(hydroxymethyl) - 1,3 - propanediol (*6*) has been titrated in water and in methanol.

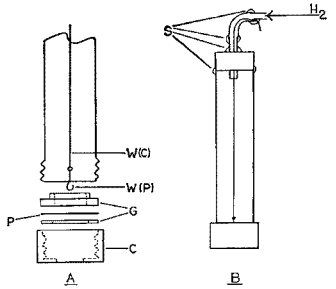


Figure 1. Construction of hydrogen-permeable membrane electrode

A: Exploded view. *C:* Bakelite cap; *G:* rubber gaskets; *P:* palladium or Pd–Ag foil, thickness 0.004 cm., exposed area 1 cm.^{2}; *W(P):* platinum wire; *W(C):* copper wire
B: Assembled electrode. *S:* Black Glyptal seals

EXPERIMENTAL

Primary standard 2-amino,2-(hydroxymethyl)-1,3-propanediol (AHPD) was obtained from Fisher Chemical Co., under the trivial name tris-(hydroxymethyl)aminomethane, or THAM. Water was boiled or deionized before use to minimize interference due to CO_2. A basic impurity was present in the methanol (Baker's analyzed reagent grade), necessitating pretitration of the cell solution to a potentiometric end point before the sample was introduced. Pure palladium and 70% Pd–30% Ag alloy foil was supplied by Baker Platinum Division of Englehard Industries.

A Beckman Duostat power supply was used as a constant-current source. The slow 0.1 to 0.2% drift in the output of this instrument was compensated manually, by monitoring the iR drop across a precision resistor with a potentiometer. Potential and pH readings were made with a Corning Model 7 pH meter. Time was registered by a Standard Electric Time Co. Model S-10 stopclock, which was operated simultaneously with the electrolysis current by a DPST relay. Other circuitry was of ordinary design (*5*). Oxygen was removed from the cell by sweeping with prepurified nitrogen to avoid its reaction with the palladium–hydrogen electrode.

Electrode Construction. Figure 1 shows the construction of the electrode used in this study. The glass, rubber, and bakelite components of the electrode are parts from an ordinary borosilicate glass condenser. Because of the frequent necessity for rejuvenation of the electrode surface, it is desirable to be able to dismantle the electrode and remove the palladium foil easily. The tube was flushed thoroughly with H_2 before use, and the hydrogen pressure was maintained at 1–2 p.s.i.g. during use. According to studies by Jewett and Makrides (*4*), the rate of transfer of hydrogen through a palladium membrane is not a strong function of pressure at pressures at or above 1 atm.

Choice of Membrane Composition. Early work in this study, and some of the titrations reported in this paper, were carried out using a pure palladium electrode. However, the palladium–silver alloy offers several advantages:

The system Pd–H exhibits two crystalline modifications (α and β), with different thermodynamic properties, depending on the H content of the palladium (*9*). While the electrode is being used in the dynamic process of hydrogen ion generation, it is not convenient to control the foil's hydrogen content which, in any case, may have a gradient from back to front. Thus the current–potential behavior of the electrode is poorly reproducible. The 30% Ag–70% Pd alloy's crystalline form is independent of hydrogen content, and the electrode shows much more reproducible current–voltage curves for hydrogen ion generation than pure palladium.

Constant cycling of the palladium–hydrogen electrode through the α–β phase transition during use results in warping, embrittlement and, finally, cracking of the foils. The alloy foils are sturdier than pure palladium at the outset and do not grow brittle with use, though they do undergo some distortion when they absorb hydrogen.

The hydrogen permeability of 30% Ag–70% Pd is less by a factor of about 5 than that of pure palladium (*4*). Since our hydrogen ion generation currents correspond to effective permeabilities much lower than those observed by Jewett and Makrides, other factors (probably surface poisoning) limit the overall rate of hydrogen transport. We observed somewhat larger current densities with alloy foils than with pure palladium.

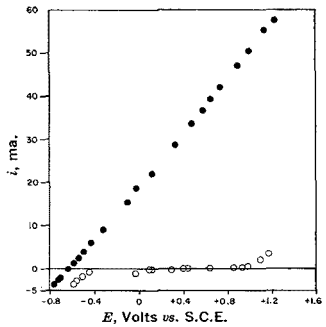


Figure 2. Current–voltage curves for Pd–Ag membrane electrode in aqueous phosphate buffer, pH 7

● Electrode supplied with hydrogen
○ Hydrogen absent

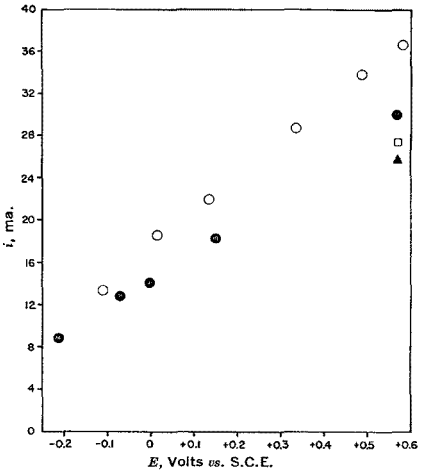


Figure 3. Decay of proton generation at an electrode after initial activation (see text)

○ Immediately after activating pretreatment
● After 48 hours exposure to air
□ After 20 minutes exposure to pH 7 phosphate buffer
▲ After 30 minutes

RESULTS

Current–Voltage Curves. Figure 2 shows current–voltage curves for a palladium–silver alloy electrode in an aqueous phosphate buffer with, and without, hydrogen present. The electrode had been heated in a muffle furnace to about 700–900° C. for 2 hours to coat the surface with an oxide film, and this film reduced electrolytically to produce a finely divided surface (*1*, *2*, *4*). Just prior to the current–voltage curves of Figure 2, the electrode had been further pretreated on both sides by cathodic deposition of a layer of palladium black from a Pd(II) nitrate–nitric acid solution. A recent publication of Cleary and Greene (*2*) discusses in a thorough and systematic way the treatment of pure palladium foils to obtain larger and longer-lived currents for hydrogen oxidation than those reported here.

When freshly treated as described above, the electrode is a relatively efficient transmitter of hydrogen and exhibits reversible behavior with respect to the solution; however, exposure to laboratory air or, more severely, to solutions of ordinary cleanliness results in a shift of the curve to smaller currents at a given potential. Note that in Figure 2, the current–voltage curve for the freshly treated electrode passes through the potential axis at the reversible potential without inflection. Figure 3 shows the decay of the current–voltage curve to less reversible behavior with use and the passage of time. In view of this decay, the oxidation–reduction treatment was given to each new foil, and the palladium black coating renewed before each use of the electrode.

Figure 4 shows current–voltage curves for a pure palladium electrode with, and without, hydrogen present, in methanol buffered with 0.1*M* each acetic acid and sodium acetate. Although the proton-generation currents obtained in methanol were generally less than those shown in Figure 2 for water, they are still usefully large. The anodic currents flowing at the extreme anodic end of the curve in the absence of hydrogen probably result from the oxidation of the solvent to formaldehyde, formic acid, or a mixture. During long electrolysis at this potential, the pH of the electrolyte shows a slow decrease, and the characteristic odor of formic acid is obvious. This reaction is not suitable for titrating bases; in a single experiment, the titration curve for the titration of AHPD was poorly developed with the maximum pH drop occurring at about 50% beyond the theoretical equivalence point, calculated assuming 100% current efficiency for the oxidation of methanol to formic acid.

Coulometric Titrations. Using currents chosen on the basis of the observed current–voltage curve to avoid oxidation of the solvent, the current efficiency for hydrogen ion generation in water and methanol was determined by coulometric titration of AHPD. For titrations in water, the auxiliary electrolyte compartment was filled with 0.5*M* $AgNO_3$ so that the cathode reaction would not interfere with the titration. This precaution was unnecessary for titrations in methanol.

A glass electrode–aqueous S. C. E. pair was used for potentiometric end point detection in both water and methanol. We are aware that the apparent pH readings in methanol have no absolute significance, but assumed that the equivalence point coincided

Table I. Coulometric Titrations of AHPD in Water

Supporting electrolyte: 0.5*M* $NaNO_3$

AHPD taken, mmoles	Generating current, ma.	Base found, meq.	Rel. error, %
0.3084	20	0.3106	+0.7
0.3084	20	0.3096	+0.4
0.2815	25	0.2807	−0.3
0.2815	25	0.2824	+0.3
0.2470	20	0.2479	+0.4
0.2470	20	0.2481	+0.4

Table II. Coulometric Titrations of AHPD in Methanol

Supporting electrolyte: 0.25*M* $NaNO_3$

AHPD taken, mmoles	Generating current, ma.	Base found, meq.	Rel. error, %
0.1576	11	0.1585	+0.6
0.1440	12	0.1437	−0.2
0.1440	12	0.1445	+0.4
0.1440	12	0.1451	+0.7

For the titrations in water, the average error is +0.3%, standard deviation = 0.3%; in methanol, the average error is +0.4%, standard deviation = 0.4%.

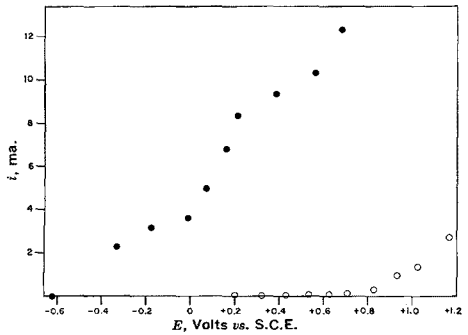


Figure 4. Current–voltage curves for pure Pd membrane in methanol, buffered with 0.1M each acetic acid–sodium acetate

● Electrode supplied with hydrogen
○ Hydrogen absent

with the maximum rate of change of pH with generation time (t). This latter was located by the method of Gran (*3*) as the intersection of linear plots of $\Delta t/\Delta$pH for short increments of t around the equivalence point. A summary of results is presented in Tables I and II.

The small but significantly positive titration errors shown in Tables I and II may be restated as negative deviations from 100% titration efficiency; failure to achieve 100% current efficiency for hydrogen ion generation is the most likely cause. The small anodic residual currents which flow in the absence of hydrogen (Figures 2 and 4) are of the same order of magnitude as the apparently inefficient portion of the generating current used in titrations. However, since the current–voltage performance of a given electrode changes with time in contact with solutions, there seems no exact way to correct for the residual current. Consequently, we have reported errors based on the total current.

There is no *a priori* reason that the method reported here should not have application for the titration of bases in any electrolytic solvent in which the potentials for the oxidations of hydrogen, palladium, and the solvent bear the same relationship to each other that they do in water and methanol.

ACKNOWLEDGMENT

The authors thank A. C. Makrides and D. N. Jewett and their colleagues for helpful discussions.

LITERATURE CITED

(1) Blackburn, T. R., Ph.D. thesis, Harvard University, Cambridge, Mass., 1962.
(2) Cleary, H. J., Greene, N. D., *Electrochim. Acta* **10**, 1107 (1965).
(3) Gran, G., *Acta Chem. Scand.* **4**, 559 (1950).
(4) Jewett, D. N., Makrides, A. C., *Trans. Faraday Soc.* **61**, 932 (1965).
(5) Lingane, J. J., "Electroanalytical Chemistry," 2nd ed., Interscience, New York, 1958.
(6) Riddick, J. A., *Ann. N. Y. Acad. Sci.* **92**, 357 (1961); *C.A.* **56**, 10884*d* (1962).
(7) Streuli, C. A., ANAL. CHEM. **28**, 130 (1956).
(8) Szebelledy, L., Somogyi, Z., *Z. Anal. Chem.* **112**, 395 (1935).
(9) Vasile, M. J., Enke, C. G., *J. Electrochem. Soc.* **112**, 865 (1965).

RECEIVED for review February 2, 1966. Accepted April 11, 1966. Work supported by National Science Foundation grant GP-3510 and by Wellesley College work scholarship to R. B. G.

Reversible Charge Transfer at the Tubular Platinum Electrode

W. J. BLAEDEL and L. N. KLATT

Department of Chemistry, University of Wisconsin, Madison, Wis.

▶ **Current–potential equations for the reversible charge transfer at the tubular platinum electrode (TPE) have been theoretically derived and experimentally verified with the ferricyanide–ferrocyanide system. At steady state, the dependences of the concentration profile upon distance along the tube and upon axial linear velocity are shown graphically. For flow rates of a few milliliters per minute in a 1-cm. × 0.05-cm. diameter tube, the diffusion layer at steady state is comparable to that obtained in a potentiostatic experiment for times less than 1 second. For a given system, the half wave potential at the TPE differs slightly but definitely from that at the dropping mercury electrode.**

HYDRODYNAMIC electrochemical systems, where transport of the electroactive material occurs principally by convection, are of two general types: moving electrode systems, such as the rotating platinum wire electrode (*14, 17*), the rotating disk electrode (*6, 8*), and the streaming mercury electrode (*7*); and moving solution systems, containing such electrodes as stationary wire electrodes (*9, 27*), a micro-bypass electrode (*25*), plane electrodes (*19*), spherical electrodes (*13, 28*), a micro-conical electrode (*12*), and tubular electrodes (*4, 5, 10*). Much of the work on these systems has been empirical or has been based upon the Nernst diffusion layer concept, which assumes a linear concentration gradient. Only a few cases have been treated rigorously, usually in the diffusion-limited region.

Hydrodynamic electrochemical systems have great analytical and practical capabilities; however, a more extensive theory of the convective transport process and of the associated charge transfer is required to understand the fundamental processes occurring at hydrodynamic electrodes. The following work is concerned with a theoretical description and experimental confirmation of the reversible charge transfer at the tubular platinum electrode (TPE).

THEORY

Derivation of Equations. The general equation for mass transfer of a chemical species, C_i, in a tube of circular cross section, with radius ρ and length X, and with a laminar velocity regime is given by Levich (*20*).

$$v_x \frac{\partial C_i}{\partial x} = D_i \frac{\partial^2 C_i}{\partial y^2} \qquad (1)$$

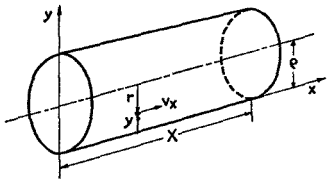


Figure 1. Coordinate system and tube parameters

The coordinate system and tube parameters are depicted in Figure 1.

In the laminar flow regime, the velocity profile is of the form

$$v_x = v_a\left(1 - \frac{r^2}{\rho^2}\right) \tag{2}$$

where v_a is the axial linear velocity. If the diffusion layer is very thin—i.e., $r \cong \rho$—the introduction of the variable $y = \rho - r$ gives

$$v_x = \frac{2v_a y}{\rho} \tag{3}$$

Equations 1 and 3 may be combined to give the equation for convective transport in a tube with laminar flow

$$\frac{2v_a y}{\rho} \cdot \frac{\partial C_i}{\partial x} = D_i \frac{\partial^2 C_i}{\partial y^2} \tag{4}$$

For the reversible reduction of an oxidized species O to a reduced species R,

$$O + ne \rightleftharpoons R \tag{5}$$

occurring at a tubular electrode, the following boundary value problem must be considered.

$$\frac{2v_a y}{\rho} \cdot \frac{\partial C_O}{\partial x} = D_O \frac{\partial^2 C_O}{\partial y^2} \tag{6}$$

$$\frac{2v_a y}{\rho} \cdot \frac{\partial C_R}{\partial x} = D_R \frac{\partial^2 C_R}{\partial y^2} \tag{7}$$

$$y \to \infty : C_O \to C_O^*;\ C_R \to C_R^* \tag{8}$$

$$y = 0:\ D_O \frac{\partial C_O}{\partial y} + D_R \frac{\partial C_R}{\partial y} = 0 \tag{9}$$

$$y = 0:\ C_O/C_R = \exp \frac{nF}{RT}(E - E^0) \tag{10}$$

C_O and C_R are the molar concentrations of substances O and R; C_O^* and C_R^* are the bulk molar concentrations of substances O and R; D_O and D_R are the diffusion coefficients; n is the number of electrons; E^0 is the formal electrode potential; and R, T, and F have their usual thermodynamic significance.

Equations 6–10 may be solved by defining a new variable

$$\eta = (v_a/x\rho)^{1/3} y \tag{11}$$

This change of variable reduces Equations 6 and 7 to second-order differential equations which may be solved by methods applicable to first-order differential equations, as shown in the appendix. The solution gives the explicit dependences of C_O and C_R upon v_a, ρ, x, and y:

$$C_O = \frac{C_O^* - C_{O(y=0)}}{1.4743\ D_O^{1/3}} \sum_{j=0}^{\infty} \frac{\left(\frac{2}{9}\right)^j \left[\left(\frac{v_a}{x\rho}\right)^{1/3} y\right]^{3j+1}}{j!\ (3j+1) D_O^j} + C_{O(y=0)} \tag{12}$$

$$C_R = \frac{C_R^* - C_{R(y=0)}}{1.4743\ D_R^{1/3}} \sum_{j=0}^{\infty} \frac{\left(\frac{2}{9}\right)^j \left[\left(\frac{v_a}{x\rho}\right)^{1/3} y\right]^{3j+1}}{j!\ (3j+1) D_R^j} + C_{R(y=0)} \tag{13}$$

The fluxes of O and R to the wall of the tube may be found by differentiating Equations 12 and 13 with respect to y and evaluating at $y = 0$.

$$D_O\left(\frac{\partial C_O}{\partial y}\right)_{y=0} = 0.6782\ D_O^{2/3}\left(\frac{v_a}{x\rho}\right)^{1/3}(C_O^* - C_{O(y=0)}) \tag{14}$$

$$D_R\left(\frac{\partial C_R}{\partial y}\right)_{y=0} = 0.6782\ D_R^{2/3}\left(\frac{v_a}{x\rho}\right)^{1/3}(C_R^* - C_{R(y=0)}) \tag{15}$$

Combining Equations 14 and 15 according to Equation 9 gives

$$C_R^* - C_{R(y=0)} = (D_O/D_R)^{2/3} C_{O(y=0)} - (D_O/D_R)^{2/3} C_O^* \tag{16}$$

which expresses the conservation of mass at the electrode surface, and which relates the surface concentrations to the bulk concentrations.

The current i due to Reaction 5 may be obtained from the flux of substance O.

$$i = nF(2\pi\rho)\int_0^X D_O\left(\frac{\partial C_O}{\partial y}\right)_{y=0} dx \tag{17}$$

$$i = 2.035\ \pi n F D_O^{2/3} v_a^{1/3} X^{2/3} \rho^{2/3} \times \left(\frac{C_O^* - \theta C_R^*}{1 + k\theta}\right) \tag{18}$$

In Equation 18, θ is an abbreviation for the exponential term in Equation 10, and k is $(D_O/D_R)^{2/3}$. For the purposes of measurement, it is convenient to use a volume flow rate V which may be expressed in terms of ρ and v_a.

$$V = \int_0^\rho 2\pi r v_a dr \tag{19}$$

$$V = \pi\rho^2 v_a/2 \tag{20}$$

The current may now be expressed in terms of volume flow rate.

$$i = 5.306 \times 10^5 n D_O^{2/3} X^{2/3} V^{1/3} \cdot \frac{C_O^* - \theta C_R^*}{1 + k\theta} \tag{21}$$

When D_O is in cm.²/second, X in cm., and V in cm.³/second, i is in ma.

The relation between the current and the potential may be obtained directly from Equation 21 by substitution of the exponential form of θ and rearranging.

$$E = E^0 - \frac{RT}{nF} \ln (D_O/D_R)^{2/3} + \frac{RT}{nF} \ln \frac{i_{dc} - i}{i - i_{da}} \tag{22}$$

In Equation 22, i_{dc} and i_{da} are the limiting currents approached at highly cathodic potentials (θ approaches zero in Equation 21) and at highly anodic potentials (θ approaches infinity in Equation 21), respectively. The first two terms on the right side of Equation 22 correspond to the half-wave potential.

$$E_{1/2} = E^0 - \frac{RT}{nF} \ln (D_O/D_R)^{2/3} \tag{23}$$

Concentration Profiles. Equations 12 and 13 give the dependence of the concentrations of substances O and R upon the independent variables x and y, and upon the experimentally controllable parameters v_a and ρ. Figure 2 indicates how the concentration profile (C_O/C_O^* or C_R/C_O^* *vs.* y) changes with distance (x cm.) along the tube. Also given with each curve is the value of the parameter $v_a/x\rho$ (cm. second)$^{-1}$ from which the effect of v_a and ρ upon the concentration profiles may be determined by simply evaluating this parameter for various values of v_a and ρ.

Figure 2 shows that the thickness of the diffusion layer ranges from 0.002 to 0.006 cm., or from 4 to 12% of the electrode radius. Examination of Equation 3 reveals that it is an excellent approximation for the velocity profile near the electrode surface, where molecular diffusion dominates relative to the linear velocity, and that the error of this approximation is under 5%, even for distances as far out as 0.006 cm.

The times required to establish diffusion layers of comparable thickness in potentiostatic experiments are rather short, calculable as 0.1–1 second for $D_O = 10^{-5}$ cm.²/second (7). Thus, there may be some advantage in studying electrode reaction kinetics at steady

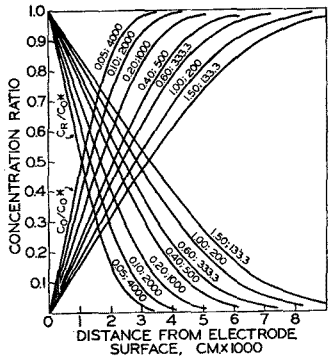


Figure 2. Concentration profiles

The pair of numbers associated with each curve represents x (cm.) and the value of the parameter $v_a/x\rho$ (cm. second)$^{-1}$. Profiles are calculated for $D_o = 10^{-5}$ cm.^{2}/second, $v_a = 10$ cm./second, $\rho = 0.05$ cm., and $C_R^* = 0$

state with the TPE rather than with stationary electrodes in quiescent media, because of the experimental simplicity that may be achieved.

Variation of the Flux along the Electrode. Because the flux at the surface of the electrode depends inversely upon the cube root of x, the flux does not change very rapidly with distance along the electrode. From Equation 14, with the same conditions as in Figure 2, and with $C_O^* = 10^{-4}M$, the relative fluxes of substance O at distances x of 0.1, 0.5, 1.0, and 2.0 cm. are 1.24, 0.73, 0.58, and 0.46, respectively.

According to Equations 14 and 15, the fluxes are undefined at $x = 0$, and this entire theory does not apply in the region near $x = 0$.

The Half-Wave Potential. Unlike the thermodynamic standard potential, the half-wave potential is not a fundamental property of the chemical system alone, but depends upon the electrode at which it is measured. At the TPE, the half-wave potential depends upon $(D_O/D_R)^{2/3}$, whereas at the dropping mercury electrode (DME) the half-wave potential depends upon $(D_O/D_R)^{1/2}$ (*23*). Thus, the half-wave potentials at the TPE and DME differ by:

$$E_{1/2,\ \mathrm{DME}} - E_{1/2,\ \mathrm{TPE}} = \frac{RT}{6nF} \ln (D_O/D_R) \qquad (24)$$

Even if the diffusion coefficients of O and R differed by an order of magnitude, the half-wave potentials would differ by only about 10 mv. at 25° C., which makes experimental verification of this difference quite difficult.

Table I. Summary of Log *i*–Log *V* Plots at Various Potentials[a]

Potential	Slope
0.285	0.352
0.275	0.362
0.250	0.361
0.225	0.334
0.200	0.343
0.175	0.343
	mean = 0.349

[a] Data taken from Figure 4.

EXPERIMENTAL

Apparatus. The current–potential measurements were made with a Sargent Model XXI polarograph, and all potential measurements were checked with a precision potentiometer (Rubicon Co., Philadelphia, Pa.). A peristaltic pump (Model 000–1200, Harvard Apparatus Co., Dover, Mass.) powered by a regulated variable-speed motor ($^1/_{15}$ h.p., Type NSH-34RH, S47 motor control; B and B Motor and Control Corp., 96 Spring St., New York, N. Y.) was used to control the flow rate of the solutions.

Figure 3 depicts the electrode assembly. The body consisted of two $2 \times 1^1/_4 + {}^1/_2$-inch Plexiglas blocks (Rohm and Haas Co., Philadelphia, Pa.), into which were milled $1^1/_4 \times {}^3/_8 \times {}^3/_8$-inch mirror-image channels. These channels formed the working and reference electrode compartments, when separated with an anion exchange membrane (A-104-EC Series, American Machine and Foundry Co., Springdale, Conn.).

The platinum tube was cut from seamless platinum tubing (0.010-inch wall thickness), and the ends were finished squarely and smoothly. The platinum tube was then press-fitted into 0.003-inch undersize holes in the Plexiglas and heated slightly, softening the Plexiglas and forming a tight seal. Electrical contact to the TPE was made by a soldered platinum wire before assembly. After assembly, the exposed portion of the TPE was completely encased in epoxy cement to provide mechanical strength.

The reference electrode was an Ag–AgCl electrode of geometric area approximately 50 times greater than the TPE, prepared according to the procedure of Ives and Janz (*11*). The reference electrode electrolyte was $1M$ KCl saturated with silver chloride. The resistance of the cell, filled with $1M$ KCl, was 230 ohms, measured with a conductance bridge (Model RCM 15B1, A. H. Thomas Co., Philadelphia, Pa.).

Except for the ball joint, inlet and outlet tubes were $^1/_{32}$-inch i.d. Tygon tubing (U. S. Stoneware Co., Akron, Ohio), press fitted with cyclohexanone into the Plexiglas. All solution channels upstream from the TPE were constructed from 2 mm. i.d. glass capillary tubing.

Materials. All chemicals were of reagent grade quality, used without further purification. All solutions were prepared from triply distilled water, the second distillation being from alkaline permanganate. The solutions were deaerated, prior to and during use, with nitrogen gas purified with respect to oxygen by passage through a zinc–vanadium column (*23*). The $K_3Fe(CN)_6$ and the $K_4Fe(CN)_6$ solutions were prepared fresh daily.

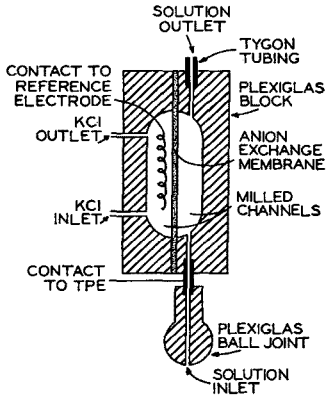


Figure 3. Electrode assembly

Experimental Procedure. To minimize pulsing, the solutions were pumped simultaneously through both channels of the Harvard pump, which was located downstream from the electrode assembly.

The TPE was pretreated according to the procedure suggested by Anson (*2*) before each experiment to minimize surface oxide film effects and to attain reproducible behavior of the TPE.

The current–potential data were obtained in the following manner: A particular potential was applied, and then the blank and ferricyanide solutions were each alternately pumped to steady state through the TPE. This procedure minimized interferences due to platinum oxide film formation or dissolution (*15*). Various flow rates, electrode lengths, and concentrations of both $K_4Fe(CN)_6$ and $K_3Fe(CN)_6$ were studied.

All experiments involving verification of the theoretical parameters were performed with a supporting electrolyte of $1M$ KCl, $0.01M$ NaH_2PO_4, and $0.01M$ Na_2HPO_4, unless stated otherwise. The analytical solution consisted of this electrolyte plus $10^{-4}M$ $K_3Fe(CN)_6$ and/or $10^{-4}M$ $K_4Fe(CN)_6$, unless otherwise stated. All the solutions were thermostated at 25° ± 0.02° C.

Flow rates were obtained from the time required to collect a 5-ml. fraction in a 10-ml. buret graduated in 0.05 ml.

RESULTS AND DISCUSSION

Dependence of Current upon Flow Rate. The manner in which the current–potential curve changes with flow rate V is shown in Figure 4. According to Equation 21, a log-log plot of current *vs.* flow rate at a given potential should theoretically be linear with a slope of $^1/_3$. Such plots, prepared from data of Figure 4, were good straight lines with slopes in excel-

lent agreement with the theoretical value, as summarized in Table I.

Equation 22 for the current–potential curve is independent of flow rate, with a particular electrode, and a plot of potential *vs.* log $[(i_{dc} - i)/(i - i_{da})]$ should be linear with a slope at 25° C. of $0.0591/n$ volts, and an intercept which gives the half-wave potential. The curves of Figure 4 plus a few not shown may be analyzed in this way to obtain values of $E_{1/2}$ and $0.0591/n$ that are independent of flow rate, as shown in Table II. The average value of 0.063 volt for the slope is in good agreement with theory for a one-electron reversible charge transfer (*18, 21, 22, 24, 26*).

Dependence of Current upon Electrode Length. The experimental dependence of current upon electrode length was established in a manner similar to the dependence upon flow rate. The average experimental value for the exponent of X is 0.617, with a variance of 0.053, which is in good agreement with the theoretical value of 2/3. Since the exponent of X had to be obtained from data with different electrodes, its precision was not as good as the precision with which the exponent of V was determined.

Table II. Summary of Log $\frac{i_{dc} - i}{i - i_{da}}$ vs. E Plots at Various Flow Rates[a]

V, ml./minute	Intercept $E_{1/2}$, volts	Slope, $0.0591/n$, volts
2.07	0.225	0.0633
3.13	0.231	0.0654
4.29	0.231	0.0639
5.58	0.225	0.0662
6.45	0.224	0.0619
8.55	0.228	0.0636
10.17	0.225	0.0584

[a] $K_3Fe(CN)_6$ is $10^{-4}M$. TPE is 1.81 cm. × 0.204 cm. diameter.

Analysis of current–potential curves obtained with electrode lengths ranging from 1.09 to 2.33 cm. gave an average slope for the E *vs.* log $[(i_{dc} - i)/(i - i_{da})]$ plots of 0.065 volt with a variance of 0.0014 volt, and an intercept ($E_{1/2}$) of 0.228 ± 0.002 volt. This value is in good agreement with the formal potential of 0.458 volt *vs.* NHE reported by Kolthoff and Tomsicek (*16*) and 0.20 volt *vs.* NCE reported by Zuman (*29*).

Dependence of the Current-Potential Curves upon Concentration. Slopes and intercepts of plots of log $[(i_{dc} - i)/(i - i_{da})]$ *vs.* potential for solutions of $K_3Fe(CN)_6$ and/or $K_4Fe(CN)_6$ at concentrations from $10^{-5}M$ to $10^{-3}M$ are summarized in Table III. Reversible behavior is indicated for all concentrations within the range 10^{-5}–$10^{-3}M$. Currents at concentrations below $10^{-5}M$ were too small ($i_d < 0.5$ μa) for accurate measurement.

Uncorrected current–potential data gave slopes and intercepts that deviated slightly but increasingly from the reversible values at concentrations above $10^{-4}M$. Measurements on systems with differing concentrations of KCl and other electrolytes (1.0M $NaClO_4$, 0.333-M $CaCl_2$, 0.333M K_2SO_4) showed that these deviations were due to ohmic resistance, which when determined and corrected for resulted in the slopes and half-wave potentials shown in Table III.

At high currents, cell resistance causes deviation from reversible behavior. Because of the tubular geometry and laminar flow, a symmetric working-counter electrode arrangement cannot be achieved, making it difficult to minimize ohmic potential losses. In fundamental studies, therefore, it appears advisable to work at current levels low enough to keep ohmic potentials negligible. In most analytical applications, where measurements are made in the diffusion-limited region, ohmic drops are usually of little consequence and do not materially diminish the usefulness or sensitivity of the tubular electrode.

Table III. Summary of Log $\frac{i_{dc} - i}{i - i_{dc}}$ vs. E Plots at Various Concentrations

Solute	Molarity (×10⁴)	Intercept, $E_{1/2}$, volts	Slope, volts
$K_4Fe(CN)_6$	1	0.238	0.0668
$K_4Fe(CN)_6$ and $K_3Fe(CN)_6$	1	0.230	0.0682
$K_3Fe(CN)_6$[a]	0.1	0.231	0.0593
$K_3Fe(CN)_6$[a]	0.3	0.229	0.0676
$K_3Fe(CN)_6$	0.5	0.228	0.0628
$K_3Fe(CN)_6$[a]	1	0.233	0.0646
$K_3Fe(CN)_6$[a]	3	0.224[b]	0.0675[b]
$K_3Fe(CN)_6$	5	0.224[b]	0.0671[b]
$K_3Fe(CN)_6$	10	0.230[b]	0.0642[b]

[a] TPE is 1.81 cm. × 0.204 cm. diameter, except in these experiments, where the TPE is 1.45 cm. × 0.204 cm. diameter.
[b] Corrected for ohmic resistance.

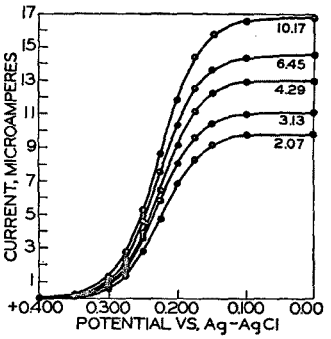


Figure 4. Current–potential curves

$K_3Fe(CN)_6$ is $10^{-4}M$. TPE is 1.81 cm. × 0.204 cm. diameter. Number on each curve represents flow rate in ml./minute

APPENDIX

Derivation of Equations 12 and 13. After applying elementary differentiation theorems to Equation 11, the boundary value Equations 6–10 may be expressed in terms of η.

$$\frac{\partial^2 C_O}{\partial \eta^2} + \frac{2}{3D_O}\eta^2 \frac{\partial C_O}{\partial \eta} = 0 \qquad (A\text{-}1)$$

$$\frac{\partial^2 C_R}{\partial \eta^2} + \frac{2}{3D_R}\eta^2 \frac{\partial C_R}{\partial \eta} = 0 \qquad (A\text{-}2)$$

$$\eta \to \infty: \quad C_O \to C_O^*; \quad C_R \to C_R^* \qquad (A\text{-}3)$$

$$\eta = 0: \quad D_O\left(\frac{\partial C_O}{\partial \eta}\right) + D_R\left(\frac{\partial C_R}{\partial \eta}\right) = 0 \qquad (A\text{-}4)$$

$$\eta = 0: \quad C_O/C_R = \exp\frac{nF}{RT}(E - E^0) \qquad (A\text{-}5)$$

Equations A-1 and A-2 are second order differential equations with the dependent variable absent, and may be solved by methods applicable to first order differential equations. The solutions are:

$$C_O = \frac{C_O^* - C_{O(\eta=0)}}{\int_0^\infty \exp\left(-\frac{2\eta^3}{9D_O}\right) d\eta} \int \exp\left(-\frac{2\eta^3}{9D_O}\right) d\eta \qquad (A\text{-}6)$$

$$C_R = \frac{C_R^* - C_{R(\eta=0)}}{\int_0^\infty \exp\left(-\frac{2\eta^3}{9D_R}\right) d\eta}$$

$$\int \exp\left(-\frac{2\eta^3}{9D_R}\right) d\eta \quad (A\text{-}7)$$

Applying the transformation

$$s = \eta^3/D \quad (A\text{-}8)$$

to Equations A-6 and A-7 the definite integrals may be recognized as the gamma function

$$\frac{D^{1/3}}{3}\int_0^\infty s^{-2/3} \exp\left(-\frac{2}{9}s\right) ds = \frac{D^{1/3}}{3} \cdot \left[\frac{\Gamma(1/3)}{(2/9)^{1/3}}\right] \quad (A\text{-}9)$$

The properties of this function are discussed in a monograph by Artin (*3*). Values of $\Gamma(\chi)$ are tabulated in standard mathematical tables (*1*).

The indefinite integrals are defined for all values of η greater than zero. Evaluation of these integrals may be accomplished by expanding the exponential as a power series and integrating termwise. Then by expressing the series in terms of x and y, Equations 12 and 13 are obtained.

LITERATURE CITED

(1) Abramowitz, M., Stegum, A., eds., "Handbook of Mathematical Functions," National Bureau of Standards, Washington, D. C., 1964.
(2) Anson, Fred, ANAL. CHEM. **33**, 934 (1961).
(3) Artin, Emil, "The Gamma Function," Holt, Rinehart, and Winston, New York, 1964.
(4) Bazan, J. C., Arvia, A. J., *Electrochim. Acta* **9**, 17 (1964).
(5) Blaedel, W. J., Olson, C. L., Sharma, L. R., ANAL. CHEM. **35**, 2100 (1963).
(6) Cochran, W. G., *Proc. Cambridge Phil. Soc.* **30**, 365 (1934).
(7) Delahay, Paul, "New Instrumental Methods in Electrochemistry," Interscience, New York, 1954.
(8) Fried, I., Elving, P. J., ANAL. CHEM. **37**, 464 (1965).
(9) Gubel'bank, S. M., Lavrinova, E. N., *Isvest. Vysshykh Ucheb. Zavedeni, Khim. ikhim. Tekhnol.* **5**, 195 (1958).
(10) Gurinov, Va. S., Gorbachev, *Zh. Fiz. Khim.* **38**, 2245 (1964).
(11) Ives, D. J. G., Janz, G. J., "Reference Electrodes, Theory and Practice," Academic Press, New York, 1961.
(12) Jordan, J., Javick, R. A., Ranz, W. E., *J. Am. Chem. Soc.* **80**, 3846 (1958).
(13) Kimla, A., *Collection Czech. Chem. Commun.* **28**, 2696 (1963).
(14) Kolthoff, I. M., Jordan, J., *J. Am. Chem. Soc.* **76**, 3843 (1954).
(15) Kolthoff, I. M., Tanaka, N., ANAL. CHEM. **26**, 632 (1954).
(16) Kolthoff, I. M., Tomsicek, W. J., *J. Phys. Chem.* **39**, 945 (1935).
(17) Laitinen, H. A., Kolthoff, I. M., *Ibid.*, **45**, 1079 (1941).
(18) Laitinen, H. A., Taebel, W. A., IND. ENG. CHEM., ANAL. ED. **13**, 825 (1941).
(19) Levich, V. G., *Acta Physiochem., U.R.S.S.* **17**, 257 (1942).
(20) Levich, V. G., "Physiochemical Hydrodynamics," Prentice-Hall, Englewood Cliffs, N. J., 1962.
(21) Lingane, J. J., *J. Am. Chem. Soc.* **61**, 2099 (1939).
(22) Meites, Louis, *Ibid.*, **72**, 184 (1950).
(23) Meites, Louis, "Polarographic Techniques," Interscience, New York, 1955.
(24) Meites, Louis, Lingane, J. J., *J. Am. Chem. Soc.* **73**, 2165 (1951).
(25) Muller, O. H., *Ibid.*, **69**, 2992 (1947).
(26) Onsott, E. I., *Ibid.*, **74**, 3773 (1952).
(27) Ozak, T., Nakayama, T., *Nippon Kagaku Zasshi* **81**, 98 (1960).
(28) Strafelda, F., Kimla, A., *Collection Czech. Chem. Commun.* **28**, 1516 (1963).
(29) Zuman, P., *Ibid.*, **19**, 602 (1954).

RECEIVED for review December 3, 1965. Accepted April 11, 1966. Financial support for work from National Science Foundation Grant No. GP-3190.

Twin-Electrode Thin-Layer Electrochemistry

Determination of Chemical Reaction Rates by Decay of Steady-State Current

BRUCE McDUFFIE,[1] LARRY B. ANDERSON, and CHARLES N. REILLEY

Department of Chemistry, University of North Carolina, Chapel Hill, N. C.

▶ **A continuous monitor of the concentration of an electroactive species is provided by the steady-state current attainable with a twin-electrode thin-layer cell. If the concentration is disturbed by a chemical reaction, the rate of appearance or decay may be followed directly and continuously by recording the current. This principle has been applied to the study of the rate of the benzidine rearrangement under varying conditions of acidity and ethanol concentration. Results covering a range of pseudo-first-order rate constants from 1.1×10^{-1} to 2.2×10^{-3} sec.$^{-1}$ indicate general agreement with various other electrochemical methods and with a classical kinetic method. Limitations in determining rate constants outside this range are discussed. The method appears to be generally applicable in studying the rates of first- or higher-order chemical reactions following (or preceding) electron transfer.**

IN TWO recent papers (*1*, *2*) thin-layer electrochemistry using a twin-electrode cell has been discussed, with particular reference to the study of rate processes. One method suggested (*2*) for determining chemical reaction rates is developed further here: the use of the decay of a quasi-steady-state current to monitor the rate of a chemical reaction which follows a charge-transfer step.

For a pseudo-first-order chemical reaction, the system in question can be represented by the equation:

$$O \underset{-ne}{\overset{+ne}{\rightleftharpoons}} R \xrightarrow{k} P \quad (1)$$

where O and R are the oxidized and reduced species, respectively, of an electrochemical couple involving a transfer of n electrons, and P is the product formed from R by the chemical reaction of rate constant k.

Several voltammetric relaxation methods have been used to measure the rates of such following reactions. These techniques were reviewed recently (*14*) and classified either as one-step methods, such as polarography, based on the extent of displacement of the electrode equilibrium during a voltammetric curve, or two-step methods, such as current-reversal chronopotentiometry where the reverse transition time is shortened by the extent of the chemical reaction. In an extension of the chronopotentiometric method, Christensen and Anson (*4*) developed a delayed current-reversal technique suitable for studying relatively slow reactions using a thin-layer cell which confined the reacting species to a solution layer near the electrode. Schwarz and Shain (*14*) used a step-functional controlled potential approach at a hanging mercury drop electrode, taking as a model system the reduction of azobenzene, O, to hydrazobenzene, R, which undergoes the pseudo-first-order benzidine rearrangement in acidic media.

This same chemical system was used by Oglesby, Johnson, and Reilley (*12*) to compare several two-step electrochemical techniques. In the course of that work, reaction rates were also determined by two thin-layer techniques.

In contrast to the methods indicated

[1] On leave from State University of New York at Binghamton.

above, the steady-state current decay method presented in this work is a more direct technique, since it provides a means of continuously monitoring the reactant concentration with time. The method is illustrated by application to a model system, the benzidine rearrangement.

DESCRIPTION OF METHOD

The steady-state current is generated in the following manner. An azobenzene solution of known acidity, ionic strength, and ethanol concentration is introduced into the thin-layer cell. A limiting steady-state current is generated through the cell if the two facing electrodes are made sufficiently cathodic and anodic, thus maintaining the concentrations of O and of R at zero at the respective electrode surfaces (Figure 1). This current then decays exponentially with time as species R is removed by the irreversible pseudo-first-order rearrangement, P being in this case a mixture of products (benzidine and diphenyline) electroinactive in the potential range employed.

The limiting steady-state current, i_{ss}, in amperes, is related to the concentrations of electroactive species present by Equation 2 (*1*)

$$i_{ss} = \frac{2nFAC}{l}\left(\frac{D_O D_R}{D_O + D_R}\right) \qquad (2)$$

where $C = C_O + C_R$, the sum of the concentrations (averaged from 0 to l) of O and R in the thin layer, in moles per cc.; l = the thickness of solution layer, in cm.; A = the area of each working electrode, in sq. cm.; D_O and D_R = the diffusion coefficients of O and R, respectively; n = the number of electrons transferred; and F = the Faraday. Thus, the measurement of i_{ss} *vs.* time affords a direct and continuous monitor of the course of any chemical reaction disturbing the concentrations of R and O in the thin layer.

Derivation of Rate Expression. In the system under consideration, the interconversion of O and R takes place at opposing electrode faces. The rate of mass transfer from one face to the other is assumed to be rapid relative to the rate of the chemical rearrangement—i.e., $(D/l^2) >> k$, where $D = D_O = D_R$. With this condition, the concentration profiles of O and R between the two electrodes will be essentially linear, a condition of quasi-steady state [see Figure 2 of (*2*)]. Edge-effect diffusion (discussed below) is considered negligible in this derivation.

The rate expression for the first-order chemical reaction can be represented by the equation

$$\frac{dC_P}{dt} = -\frac{dC}{dt} = kC_R \qquad (3)$$

where C_P is the total concentration of products at time t.

The flux at both electrodes is essentially equal at quasi-steady state; hence, $D_O C_O = D_R C_R$. Thus, C_R, which equals $C - C_O$, may be expressed as

$$C_R = \frac{C}{1 + \left(\frac{D_R}{D_O}\right)} \qquad (4)$$

Substitution of this expression in Equation 3 and integration yields the rate equation

$$\ln\left(\frac{C}{C^\circ}\right) = -\frac{kt}{1 + \left(\frac{D_R}{D_O}\right)} \qquad (5)$$

where C° is the total concentration of O plus R at $t = 0$. Substituting Equation 2 into Equation 5 gives an expression for the decay of the quasi-steady-state current as substance R is removed by chemical reaction:

$$\ln(i_{ss}/i_{ss}^\circ) = -\frac{kt}{1 + \left(\frac{D_R}{D_O}\right)} \qquad (6)$$

where i_{ss}° is the initial steady-state current—i.e., that which would flow in the absence of the decay reaction.

The rate constant for steady-state current decay is, thus, $k/(1 + K)$, where K is the ratio D_R/D_O, equivalent to the ratio C_O/C_R in the thin layer. A similar rate expression is obtained for a first-order reaction that follows a relatively fast chemical-equilibrium step of equilibrium constant K—i.e., $A \underset{K}{\rightleftharpoons} B \xrightarrow{k} P$.

The ratio, D_R/D_O, which must be known, can be determined readily by using the thin-layer cell (*1*). If $D_R = D_O$ (an assumption verified below for the species O and R of the present study), the current-decay rate constant becomes $k/2$ and a plot of $\log i_{ss}$ *vs.* t will be a straight line of slope $-k/4.606$ for pseudo-first-order reactions.

Thus, the determination of k by steady-state current decay is independent of thin-layer parameters l and A, as well as independent of the initial concentration of reactant, provided the signal i_{ss} is of measurable magnitude. The half life of the reaction under these conditions of steady-state decay has the value $1.386/k$, twice the normal half life for first-order decay processes.

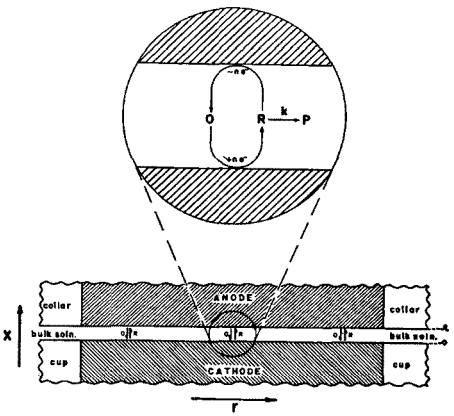


Figure 1. Schematic cross section of twin-electrode cell for steady-state current decay method

r. Radial direction
x. Axial direction

EXPERIMENTAL

Twin-Electrode Cell. The micrometer-type thin-layer cell described by Oglesby, Omang, and Reilley (*13*) was equipped for this work with twin mercury-coated platinum electrodes, each with a projected surface area, A, of 0.28 sq. cm. The detachable micrometer anvil, faced with platinum and suitably coated with mercury, constituted the lower electrode, whose working surface was flush with the inner bottom of the Teflon cup. This electrode was insulated from the upper electrode on the micrometer spindle by means of a ceramic anvil (installed on the micrometer by L. S. Starrett Co., Athol, Mass.) between the detachable anvil and the micrometer body (*1*).

Absolute solution layer thicknesses for this cell were established in the usual manner (*1*) from the linear plot of $1/i_{ss}^\circ$ *vs.* micrometer setting, where the values of i_{ss}° were obtained by extrapolation of the log i_{ss} *vs.* t curves to zero time. Moreover, a simpler method of calibrating the twin-electrode cell, particularly suitable if i_{ss} is decaying, gave an excellent check on the l-zero intercept. In this method, the resistance of a dilute electrolyte solution—e.g., $10^{-3}M$ $NaClO_4$—was measured in the cell at several thickness settings and extrapolated to the point of zero resistance. The solution resistance was determined

by passing a 50-kHz alternating current, of constant RMS amplitude, through the twin-electrode cell to ground and measuring the potential drop between the two electrodes. This method is satisfactory, provided the measured resistance is much greater than the capacitative reactance of the cell, due primarily to the electrode double layers.

Sample Solutions. Six different solution conditions were used, covering a 50-fold range in rate constants. The solutions were all 1 m*M* in azobenzene, 0.25 in ionic strength, and of sufficient acidity to maintain pseudo-first-order conditions.

Sample solutions 1 through 4 (Table I), 35.5 weight % in ethanol and of varying $HClO_4$ and $NaClO_4$ molarities, were stock solutions used in a previous study (*12*). Results with these solutions provided a basis for direct comparison between the method under study and the methods of the previous work.

Solutions 5 and 6 (Table I) were freshly prepared from recrystallized *trans*-azobenzene (m.p. 68.0° C.), commercial absolute ethanol, standardized $HClO_4$ solution, and reagent grade $NaNO_3$ and $NaClO_4$. The 44 weight % ethanol concentration was achieved by mixing 250 ml. of absolute ethanol (containing the azobenzene) with an equal volume of the appropriate aqueous reagent solution, diluting to 500 ml. finally with 44 weight % ethanol-water mixture.

Salt Bridge and Presaturation Train. A low-resistance S.C.E. reference electrode was connected to the cell solution via a beaker of $NaNO_3$ solution and a salt bridge of deaerated sample solution. This arrangement prevented precipitation of $KClO_4$ at the S.C.E. tip and minimized concentration changes in the small volume (2 to 3 ml.) of cell solution. Also, in this way chloride ions were excluded from the cell, so that spurious anodic current would not arise from the oxidation of mercury at the potentials employed.

Sample solutions were deaerated with N_2, and the cell was filled and protected from the atmosphere using techniques described previously (*13*). The N_2 stream was presaturated, before entering the special deaeration bottle, by passage through two gas-saturator bottles, the first containing an ethanol-water mixture of the same weight per cent ethanol as the sample and the second containing a large volume of the solution under study.

Circuit. An operational-amplifier circuit similar to that of Anderson and Reilley [(*1*), Figure 1, top] was used for independent potential control of the twin working electrodes, *W*1 and *W*2, with current measurement at that electrode, *W*1, held at virtual ground. The auxiliary electrode was a platinum gauze ring.

Preliminary Operations. The cell was held at 25.0° ± 0.5° C. for all the experiments.

Before each series of runs with a given solution, the presaturation train and S.C.E. salt bridge were prepared, and the mercury coatings were renewed. Excess mercury was removed from the electrode surfaces by suction through a fine capillary, but this was not a critical operation in the present work, the actual thickness of the solution layer not seriously affecting the relative shapes of the current decay curves.

After the cell was positioned, covered, and filled, a solution-layer thickness of 20 to 50 microns was set with the micrometer spindle. Attempts to set thinner layers often resulted in shorting of the twin electrodes, depending on the thicknesses of the mercury coatings.

Between successive runs with a given portion of sample solution, the upper electrode was raised about 0.1 inch, then reset, thus bringing fresh solution into the thin-layer volume element.

Procedure. To start a run, the tip of the salt bridge was inserted in the cell solution, the initial potential was set at a value, *E*1, too anodic to reduce azobenzene, and both working electrodes were connected. A current transient through electrode *W*1 quickly decayed to <0.1 μa. Then at zero time, a potential difference, ΔE, sufficient to establish the limiting steady-state current was applied between electrode *W*2 and electrode *W*1, the latter being held at the potential *E*1 *vs.* S.C.E. The IR drop between the two working electrodes is assumed to be negligible compared to ΔE. With potential *E*2 of electrode *W*2 held at the value $E1 + \Delta E$, the observed current signal through *W*1 was recorded. After a sufficient time period—i.e., 2 to 7 half lives—the potentials were turned off to terminate the run.

The azobenzene - hydrazobenzene couple is polarographically reversible in acidic media (*10*, *15*) with an $E_{1/2}$ value of approximately 0.0 volt *vs.* S.C.E. at the hydrogen ion concentrations used in these experiments. Thus, *E*1 and *E*2 values of +0.15 and −0.15 volt, respectively, *vs.* S.C.E. were sufficient to establish the limiting steady-state current in this study. In some experiments potentials of ±0.20 and ±0.30 volt were used, without apparent change in the current-time response curve.

In the typical procedure above, electrode *W*1 (either the upper or the lower electrode) was the anode for the electrochemical reaction. When ΔE was applied, a sudden rise and fall of anodic current was observed, probably associated with switching transients, capacity currents, and IR drop between *W*1 and the auxiliary electrode. This was followed by a rapid increase in anodic current to a maximum value (around 25 μa.), and then, after a descending inflection point (at $t > 6$ seconds), the expected exponential decay as the rearrangement of species *R* proceeded. If the solution layer was thicker than about 40 microns or if slow reaction conditions were used (solutions 3 through 6), a longer time lag (12 to 30 seconds) was evident before the condition of steady-state current decay was reached.

Alternatively, the kinetics could be followed by measuring the decay of steady-state current at the cathode. In this case, a large cathodic current is observed as soon as ΔE is applied, corresponding to the initial reduction of azobenzene in the thin layer. Furthermore, a higher background current is observed at the cathode than at the anode. Thus, the decay of the anodic current was preferred for measuring *k* values with the present chemical system.

Both currents could be recorded simultaneously by using the circuit reported previously (*1*), which employs two differential amplifiers.

Diffusion Coefficients. The diffusion coefficient, D_R, and the ratio of coefficients, D_R/D_O, were determined using the coulometric methods described previously (*1*). A thin layer of solution at the condition of steady-state current was analyzed for substance *R* by disconnecting the cathode and measuring the integral of current at the anode, Q_a. In a parallel experiment, substance *O* was determined by disconnecting the anode and measuring the integral of current at the cathode, Q_c. The ratio Q_c/Q_a equals the ratio D_R/D_O. For these experiments, solution 6 was used, as it had the slowest decay rate, and each *Q*-value was corrected for the amount of decay that occurred in establishing the steady-state condition prior to the measurement of *Q*. By collecting data at several values of *l*, the individual diffusion coefficients also were estimated, using the reciprocal slopes of the *Q vs. l* and the $1/(i_{ss}^{\circ})$ *vs. l* plots (*1*).

RESULTS AND DISCUSSION

Typical plots of log i_{ss} *vs. t*, made from experimental steady-state current decay curves, are shown in Figure 2. The plots for the more rapid rates of decay (solutions 1 to 3) are linear for several half lives, as expected for pseudo-first-order decay processes. Curvature becomes apparent under slower reaction conditions, at times longer than 2 to 5 minutes (solutions 4 to 6). This nonlinearity is attributed to diffusional transfer of material into the thin layer from the bulk solution at the edge. For such cases, the rate constant was calculated from the slope of the logarithmic decay curve at short times, when it is more nearly linear, corresponding to the period just past the maximum in the recorded current-time curve. Justification of this procedure is given below in the discussion of edge effects.

For the redox system of solution 6, the experimentally determined ratio, Q_c/Q_a, gave a D_R/D_O ratio of 1.00 ± 10%. Thus, the rate constant for steady-state current decay had the value $k/2.00$ in the present case, within 5%. (The determination of Q_a was more accurate than that of Q_c, because of a relatively high cathodic background current.) The experimental value of

D, the common diffusion coefficient, was determined as 0.40×10^{-5} sq. cm. per second, in agreement with the value 0.34×10^{-5} sq. cm. per second found by Schwarz and Shain for D_O in a 50 weight % ethanol medium (*14*).

The experimentally determined first-order rate constants, which cover a 50-fold range, are summarized in Table I. Each rate constant was calculated from the average slope of the logarithmic plot over the period indicated. The incremental slope was constant to ±3% during the chosen period (time increments used for testing the constancy of the logarithmic slopes were 6, 12, 24, 60, 90, and 120 seconds, respectively, for the data of solutions 1 through 6).

The experimental rate constants are found to be reproducible to about 3% for successive runs on the same portion of solution. However, differences between rate constants determined on successive portions of the same solution were occasionally as large as 10%. The observed deviations are not surprising in view of the fact that the rate of the benzidine rearrangement is sensitive to fluctuations in temperature and ethanol concentration. The data of Croce and Gettler (*6*) indicate that, under our solution conditions, an increase in k of about 10% would be expected per degree increase in temperature or per 1% decrease in ethanol concentration.

Occasional anomalous decay curves were recorded, perhaps caused by changes in the distribution of mercury on the electrode surfaces. Thus, at least two runs were made on each solution.

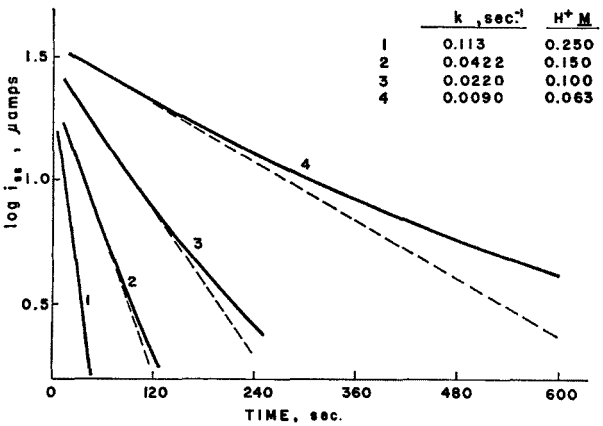


Figure 2. Steady-state current decay curves

——Experimental data
– – –Limiting slopes

In Figure 3, the results obtained for solutions 1 to 4 are compared with the results obtained by Oglesby *et al.* (*12*) using four different two-step techniques. The comparison shows good agreement between the steady-state method and the two-step methods. Apparently, the many successive redox cycles completed by the average hydrazobenzene molecule before it rearranges have not affected its decay rate. This "turnover number" for the steady-state current-decay method is equal to $2D/kl^2$, a dimensionless expression obtained by taking the ratio of the steady-state flux to the decay rate, in moles per second. Taking D as 0.40×10^{-5} sq. cm. per second and l as 3.0×10^{-3} cm., the turnover number ranged from 8 to 100 for solutions 1 to 4 in the present experiments.

Fast Reaction Limit. An upper limit for the determination of k by the present method is set by the provision that the rate of mass transfer must be rapid compared with the rate of the chemical reaction. This limit is apparently reached in the case of solution 1, at least with the present electrodes and cell design. Table II shows that the rate constant, calculated under the assumptions of quasi-steady-state decay, drops off significantly for this relatively fast reaction at solution thicknesses greater than about 40 microns. If considerable decay of R occurs in the time required for it to traverse the thin layer, the axial concentration profiles of O and R will be curved (in opposite directions) such that the ratio C_O/C_R will always be greater than 1. Thus, the current-decay rate constant, which in the limiting case can be written $k/(1 + C_O/C_R)$, will be less than the assumed value $k/2$, and the calculated values of k will be low. Because little change is evident between 38 and 28

Table I. Rate Constants for Benzidine Rearrangement by Steady-State Current Decay Method

Soln. No.[a]	Concn. of $HClO_4$,[b] M	Period of constant slope (in log i_{ss} vs. t plot) Sec.	Half lives	Rate constant[c] (pseudo-first-order), sec.$^{-1} \times 10^3$ Portion A	Portion B
1[d]	0.250	6–30	0.5–2.5	111 115 — 113 ± 3	118 113 111 114 ± 3
2[d]	0.150	12–60	0.4–2.0	41.4 42.2 43.7 45.7 43.2 ± 1.9	46.4 47.2 48.3 48.0 47.5 ± 0.9
3[d]	0.100	12–120	0.2–2.0	21.8 22.0 22.4 21.8 23.2 22.3 ± 0.6	
4[d]	0.063	15–135	0.10–0.9	9.0 9.0 8.9 9.0 ± 0.1	
5[e]	0.075	18–240	0.06–0.75	4.35 4.00 4.35 4.23 ± 0.20	4.50 4.45 — 4.48 ± 0.04
6[e]	0.040	30–330	0.05–0.5	2.30 2.02 2.16 ± 0.20	

[a] All solutions 1 mM in azobenzene; temperature 25° C.
[b] Ionic strength made constant at 0.25 by addition of $NaClO_4$ as necessary, except solution 5 which had $NaNO_3$ added.
[c] Several runs made on each portion taken and average result and standard deviation calculated.
[d] 35.5 wt. % ethanol; identical with solutions of Oglesby *et al.* (*12*).
[e] 44.0 wt. % ethanol; comparable to solutions used by Blackadder and Hinshelwood (*3*).

microns, the values given in Table I for solution 1 are thought to be accurate within 10%, though probably on the low side.

If it becomes feasible to use thinner solution layers, the determination of rate constants larger than 0.1 sec.$^{-1}$ by this method would be limited by the time required to overcome IR drop in establishing the correct limiting concentration profiles.

A different twin-electrode steady-state method, based on measuring the ratio of anodic to cathodic currents (where the cathodic current is held constant in the presence of a large excess of species O) has been suggested (*2*) for faster reactions. In that case, one is actually measuring the extent of decay as R diffuses from cathode to anode.

Slow Reactions. Comparison of Methods. The rate of rearrangement of hydrazobenzene is much slower at higher alcohol and lower hydrogen ion concentrations. Under such slow conditions, classical kinetic methods involving sampling, quenching, and analysis have been used. For example, Blackadder and Hinshelwood (*3*), using a spectrophotometric method of analysis, determined the rearrangement rate under solution conditions identical to those of solutions 5 and 6, except that HCl instead of $HClO_4$ was used as the acid. The results presented here for those solutions illustrate the application of the present method to slow reactions and also provide a basis for comparison of electrochemical and classical rate methods.

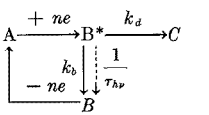
The rate constants found for solutions 5 and 6 (0.0043 and 0.0022 sec.$^{-1}$, respectively) are in fair agreement with Blackadder and Hinshelwood's values of 0.0031 and 0.0010 sec.$^{-1}$ for comparable solutions. Both methods had a reproducibility of approximately ±10% in k. Thus, there exists more discrepancy between the electrochemical and spectrophotometric techniques than the internal precision seems to warrant. Some of this observed discrepancy may be attributed to slight differences in concentrations or temperature in the two studies as well as to the fact that different acids were used. In any event, if the heterogeneous nature of the electron-transfer process or the presence of a large surface-volume ratio has any influence on the rate of this particular following reaction, it cannot be a gross effect.

There is some additional evidence that surface effects, such as catalysis, do not significantly affect the kinetics. In the steady-state current decay method, under conditions of relatively rapid mass transfer, a large change in the surface-volume ratio (change of l from 20 to 90 microns) had no significant effect on the observed rate constant. Furthermore, the thin-layer methods outlined in this work and in the previous study (*12*) are in general agreement with the methods employing chronopotentiometry at a mercury pool (*12*). If surface phenomena significantly influenced the rate, such agreement would not be expected between techniques employing unrestricted diffusion and those using a finite boundary to confine the reactants to the vicinity of the electrode surface.

Study of Excited States Formed at Electrodes. A turnover number of around 400 is calculated for the slowest reaction studied. With a thinner solution layer, and perhaps some correction for edge-effect diffusion, a first-order process with rate constant as small as 10^{-4} sec.$^{-1}$ could be studied, with a corresponding turnover rate of the order of 10^5. Such a large turnover rate might provide conditions for studying the characteristics of "hot" molecules formed at the electrodes in the electron-transfer process.

Suppose that with a particular redox system, $A \underset{-ne}{\overset{+ne}{\rightleftharpoons}} B$, a potential difference, ΔE, is applied which is much greater than that needed to establish the limiting steady-state current. The power input to the thin-layer cell will be $\Delta E \times i_{ss}$, but only a small fraction of this power will be used by the mass-transfer process. The remaining power provides excess energy for the electron-transfer process—23 kcal./mole/volt—which may result in the formation of significant concentrations of excited states, particularly at the cathode. Marcus (*9*) has indicated that it is energetically possible to produce even electronically excited species if the reduction potential is sufficiently large.

If an excited state, B^*, were produced at the cathode with 100% efficiency, the system could be represented as follows:



(7)

where k_b and $1/\tau_{h\nu}$ are the rate constants for nonradiative and radiative decay, respectively, of B^* to B, and k_d is the rate constant for irreversible chemical decay of B^* to C. If $[k_b + (1/\tau_{h\nu})] >> k_d$, the average molecule will undergo the redox cycle many times before changing to C (presumed here to be electrochemically inert). The rate constant for steady-state current decay will be approximately $(k_d/2)f_{B^*}$ where f_{B^*} is the average fraction of time that B spends as the excited state B^*.

Suppose B^* is restricted to a vibrationally excited state and the possibility of light emission is neglected. Taking k_b^{-1} second as the lifetime of B^*, and l^2/D second as the relatively long time required for diffusion of B across the thin layer, f_{B^*} will be the ratio, $k_b^{-1}/(l^2/D)$, and the steady-state decay rate constant will be equal to $(k_d/2k_b)(D/l^2)$. This becomes approximately $10^{-10}\ k_d$ sec.$^{-1}$ if $k_b \cong 10^{10}$ sec.$^{-1}$ and if $l^2/D \cong 0.5$ second. Thus, if a steady-state rate constant as small as 10^{-4} sec.$^{-1}$ can be measured, it follows that a chemical decay of B^* with k_d of 10^6 sec.$^{-1}$ or larger could be studied by this technique. Since D and l may be known, the ratio, k_d/k_b, could be measured as a function of ΔE or solution conditions, and the magnitude of k_d could be determined if k_b were known independently.

Table II. Test for Quasi-Steady-State Current Decay for Fast Reaction

(Solution 1 at 23° C.)

l, microns	Apparent k, sec.$^{-1}$ × 10^3	Difference, %
28	102	(0)
38	98	−4
64	88	−14
89	77	−24

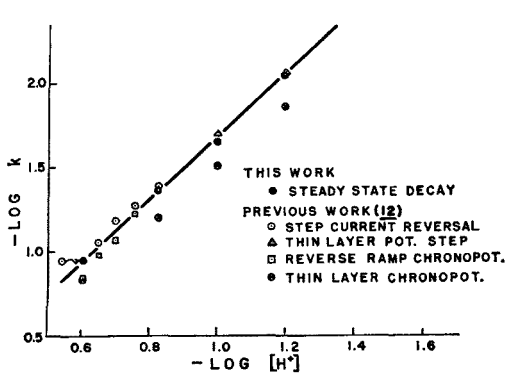


Figure 3. Comparison of rate constants for benzidine rearrangement

Edge Effects. Edge effects impose a lower limit on the magnitude of the rate constant that may be determined by the steady-state current decay technique. The net flux of material into the cylindrical thin-layer volume element introduces an error in the slope of the log i_{ss} *vs.* t plot. Obviously, the resultant error in the rate constant will be serious if the increase in i_{ss} during a given time interval caused by the edge effect is significant compared to the decrease in i_{ss} caused by chemical decay during the same time interval. An estimate of the magnitude and time-dependence of this error current can be made and is useful in order to delineate further the range of applicability of the method.

Curvature becomes pronounced in the logarithmic decay curve of solution 6 (k = 0.0022 sec.$^{-1}$). The period of relatively constant slope is from 30 to 330 seconds or from 0.05 to 0.5 half lives. Such a decay period is so short that there is an added uncertainty in the determination of k.

At times long compared to the half life, the current reaches a region of very slow decay. This phenomenon appears when the rate of decay of hydrazobenzene is nearly balanced by diffusional transport of additional electroactive material into the thin layer. Because the edge geometry approximates a shielded cylindrical section, this "terminal" current should disappear at extremely long times (*8*). The experimental data are in qualitative agreement with this analysis. The magnitudes of the currents at seven half lives were 0.2, 0.4, 0.6, 1.2, 2.0, and 5.0 μa. for solutions 1 through 6, respectively; and slight decay of the current was still observable in each case.

With some modification of procedure, this terminal current could be used to relate the rate of the decay quantitatively to the rate of mass transport. Use of electrodes of much smaller radius, a very thin collar, and a rapidly stirred solution outside the collar would allow attainment of a truly constant terminal current. This arrangement would provide conditions favorable to high amplification of the signal (small l values) and might be used to measure rather large values of k. However, it does reintroduce the rate of diffusion (diffusion coefficient) into the rate expression.

Derivation of Approximate Error Current. The error in steady-state current caused by edge-effect diffusion is proportional to the total excess number of moles, N_{excess}, of species O and R in the thin layer at any time t. This quantity, N_{excess}, will depend on the net rate of diffusion through the cylindrical edge from the bulk solution, which in turn will depend on the extent of first-order decay in the thin-layer region. Consideration must also be given to interconversion of O and R at the opposing electrodes and to the fact that material which enters from the bulk solution is subject to decay for a shorter time than material initially in the thin-layer region. A complete solution of this complicated boundary value problem is not attempted. Instead, the solution for a simplified model is used to approximate the error-current function and to estimate its magnitude.

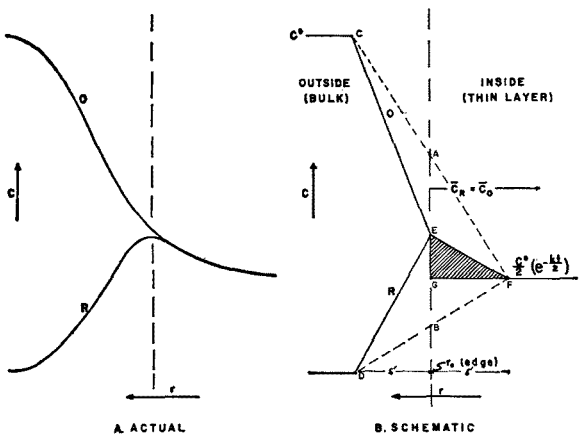


Figure 4. Edge effect, radial concentration profiles

Shortly after the potential difference, ΔE, is applied, the average concentrations of both O and R in the thin layer are equal to $C^\circ/2$, and there is no net flux of material into the thin layer. (The fact that the fluxes of O-in and R-out at the cathode side of the edge are greater than at the anode side of the edge is ignored, the profiles in the radial direction not being affected appreciably by changes in the x-direction profiles.)

After a time, t, the concentration may be represented by Figure 4 for points near the edge of the thin-layer volume element of radius r_o. The concentration profiles shown are those at the x-coordinate, $l/2$. These profiles approximate the average concentrations in the x-direction. In the central part of the thin-layer region, the concentrations of R (and O) have decayed exponentially, undisturbed by edge-effect diffusion. In the schematic drawing, the excess material, N_{excess}, is assumed to be in a concentration ring represented by the shaded triangle EGF, extending inward from the edge a distance δ'.

This ring constitutes the inner part of a modified Nernst diffusion layer, centered approximately at the edge of the thin-layer volume element. Actually, the diffusion layer may be somewhat thinner inside the edge than outside because of chemical decay of the material which enters at the edge.

Figure 4 is drawn to indicate that the concentration profiles of O and R are perturbed because of the requirement that C_O equal C_R at any radial distance, r, less than r_o. Thus, O and R do not have schematic concentration profiles that follow the dotted lines CAF and DBF, respectively, but rather have profiles that follow the solid, bent lines CEF and DEF, respectively.

For one-dimensional semi-infinite diffusion with a constant concentration gradient, ΔC, a schematic profile constructed with the usual Nernst layer thickness, δ [(*7*), inset of Figure 44.1], does not generate a triangle of area equal to the amount transferred in time t, per unit area of surface. To construct such a triangle, a layer of slightly greater thickness, $(4/\pi)\delta$ or $4(Dt/\pi)^{1/2}$, is required. However, such a layer is not appropriate when the height of the concentration gradient, ΔC_t, is a function of t exponentially approaching a constant value, as in the present system. This increasing ΔC_t has the effect of keeping the gradient steeper, which implies a thinner diffusion layer. Empirically, if a factor of 0.5 is introduced in the present case, the calculated error currents agree with those estimated from the experimental decay curves, at least during the period from 0 to 2 half lives. This empirical factor seems reasonable because the increasing ΔC_t [equal to $C^\circ - C^\circ e^{-(k/2)t}$] has a time-average value of 0.5 ΔC_t at 0.1 half life and 0.6 ΔC_t at 2.0 half lives. Thus, the factor 0.5 is used, and δ' then has the value $2(Dt/\pi)^{1/2}$ for the approximation represented by Figure 4,*B*. [The fact that diffusion is through a cylindrical rather than a planar boundary will not appreciably affect the thickness of the diffusion layer for periods up to 20 minutes if r_o is 0.30 cm. and D has the value 0.40 $\times$ 10^{-5} sq. cm. per second (*7*).]

The region of excess concentration has a volume $\pi l[r_o^2 - (r_o - \delta')^2]$ or $\pi l\delta'$-

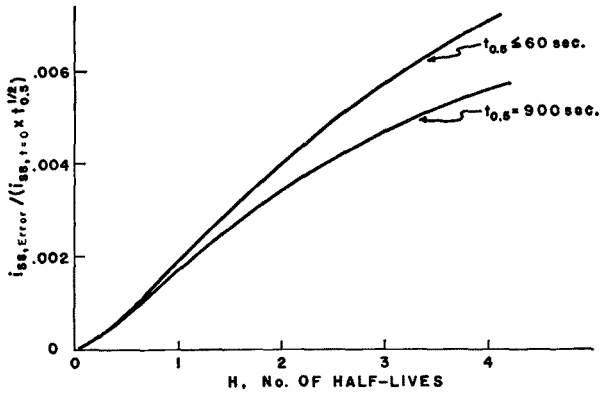


Figure 5. Normalized edge-effect correction ratio

$(2r_o - \delta')$. In this ring, there is an excess concentration of O, represented by the area of triangle EGF, and an equal excess concentration of R. The total average excess concentration of O plus R, C_{excess}, can be represented by the equation

$$C_{excess} = (C_{edge} - C_{center})/2 \quad (8)$$

where C_{edge} and C_{center} are total average concentrations of O plus R at $r = r_o$ and $r = 0$, respectively. From the geometry of Figure 4,B, where point E is taken as the average of points A and B, and from the realization that the values of C_R or C_O at point E must be doubled to obtain C_{edge}, it can be demonstrated that

$$C_{edge} = (C^\circ + C_{center})/2 \quad (9)$$

Then, because $C_{center} = C^\circ e^{-(k/2)t}$, it follows that

$$C_{excess} = \frac{C^\circ}{4} [1 - e^{-(k/2)t}] \quad (10)$$

where the term in brackets is equal to the fractional amount of first-order steady-state decay expected in time t.

The quantity, N_{excess}, is now obtained by multiplying this excess concentration by the volume of the ring containing it.

$$N_{excess} = \frac{C^\circ}{4} [1 - e^{-(k/2)t}] \pi l \delta' (2r_o - \delta') \quad (11)$$

This equation can be normalized by dividing both sides by the initial number of moles in the thin layer, N°, or $C^\circ \pi l r_o^2$, giving the expression

$$\frac{N_{excess}}{N^\circ} = [1 - e^{-(k/2)t}] \left(\frac{\delta'}{2r_o}\right) \left(1 - \frac{\delta'}{2r_o}\right) \quad (12)$$

From the proportionality between the limiting steady-state current and the number of moles in the thin layer (*1*), and substituting the approximate expression for δ', the error current ratio can be written

$$\frac{i_{ss,error}}{i_{ss}^\circ} = [1 - e^{-(k/2)t}] \times \left(\frac{Dt}{\pi r_o^2}\right)^{1/2} \left[1 - \left(\frac{Dt}{\pi r_o^2}\right)^{1/2}\right] \quad (13)$$

This is seen to be an equation in $t^{1/2}$, modified by the exponential term and the final term in brackets, a consequence of the cylindrical geometry.

It is convenient to normalize Equation 13 for reactions of different half lives by making the substitutions $t = H \times t_{0.5}$ and $(k/2)t = 0.69\ H$ where $t_{0.5}$ is the half life and H is the number of half lives at time t. This gives, on rearranging, an expression for the normalized correction ratio, $i_{ss,error}/(i_{ss}^\circ \times t_{0.5}^{1/2})$, as a function of H and $t_{0.5}$

$$\frac{i_{ss,error}}{i_{ss}^\circ \times t_{0.5}^{1/2}} = \left[1 - \left(\frac{1}{2}\right)^H\right] \times (0.0038 H^{1/2})(1 - 0.0038 H^{1/2} t_{0.5}^{1/2})] \quad (14)$$

where the term $(D/\pi r_o^2)^{1/2}$ has the value 0.0038 sec.$^{-1/2}$ in the present case.

In Figure 5, this normalized correction ratio is plotted against H for relatively fast reactions ($t_{0.5} \leq 60$ seconds) where the cylindrical correction term vanishes and for a relatively slow reaction of $t_{0.5}$ equal to 900 seconds.

The sigmoid shape of the correction curves provides a justification for using the limiting slopes of the logarithmic plots in calculating k values. The tendency of the correction curve to level off for slow reactions corresponds to a pile-up of material in the center, in qualitative agreement with the observed terminal currents at long times. Also, the curves of Figure 5 are similar in general shape to those presented by Crank (*5*) as exact solutions for a somewhat analogous problem in cylindrical diffusion.

In Figure 6, the logarithmic plot for solution 6 is shown, together with a plot corrected by Equation 14. The logarithmic plot of the corrected current is essentially straight for at least two half lives, with a slope very close to the limiting slope of the uncorrected plot. This result suggests that it would be profitable to apply a similar edge effect correction to data obtained by the related technique, thin-layer potential scan coulometry (*11*).

Technique for Eliminating Edge Effect. Edge-effect diffusion can be avoided if a quantity of solution just sufficient to fill the thin-layer space, of volume Al, between the two working electrodes is used. With our cell, because of the small volume, elimination of the external reference and auxiliary electrodes and use of the method of two-electrode steady-state voltammetry suggested earlier (*1*) would be convenient. In a chloride medium, with mercury-coated working electrodes, the anode of the pair may then serve as

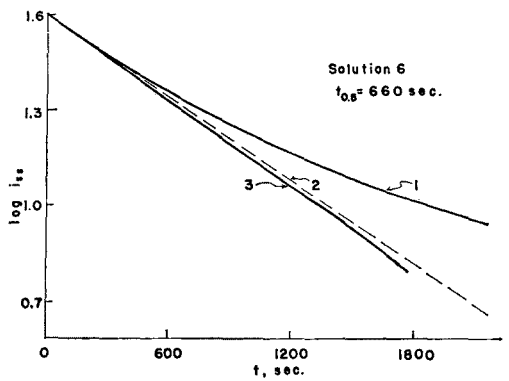


Figure 6. Edge-effect correction applied to slow reaction

1. Experimental data
2. Limiting slope of experimental curve
3. Corrected data

an "internal" calomel reference electrode (*2*), minimizing IR drop problems and facilitating potential control. If the Cl^- concentration is millimolar, the anode potential will be poised at approximately +0.20 volt *vs.* S.C.E.

Preliminary studies, using the slow reaction conditions of solution 6 with 3 m*M* Cl^- added, indicate that the two-electrode system eliminates the edge effect in steady-state decay and yields rate constants of satisfactory accuracy. The solution in the thin layer was isolated by the Teflon cup and collar from the bulk solution. A feature of the two-electrode system is that background currents at the working electrodes must be negligible compared to the initial steady-state current, $i_{ss}°$. Thus, to exclude oxygen as well as to avoid evaporation of ethanol (with consequent changes in rate), several milliliters of deaerated solution was placed in the cell as usual, except that the Teflon cup was elevated about 50 microns above the surface of the lower electrode. Then, when the upper electrode was screwed down until the Teflon collar hit the cup, the solution in the thin layer (ca. 1.5 μl.) was effectively trapped between the mercury-coated electrodes. A potential difference of + 0.35 volt was applied between the anode, *W*2, and the cathode, *W*1, at the circuit ground potential, and the current decay at the cathode was recorded. The condition of exponential steady-state current decay was reached after a few minutes and continued for about 70 minutes (seven half lives), the current dropping practically to zero except for a background current of approximately 2% $i_{ss}°$.

With a solution initially 100% in species *O*, a transient current had to flow at the cathode to reduce half the *O* to *R* in establishing the steady-state condition. This transient current was balanced by oxidation of mercury to $HgCl_2$ at the anode, another reason for adding Cl^- to the solution in the two-electrode method as applied to the present chemical system. Apparently hydrazobenzene is oxidized readily at the calomel surface.

CONCLUSIONS

The method of steady-state current decay with the twin-electrode thin-layer cell should be generally applicable to first- or higher-order chemical reactions following (or preceding) electron transfer. It is a direct method, analogous to the usual methods employed in homogeneous solution kinetics. For higher-order cases, the advantage of this technique over transient electrochemical techniques (handled most expeditiously through computer programs) is obvious.

Preliminary studies in this laboratory of systems exhibiting catalytic and disproportionation behavior polarographically, indicate that the kinetics of such systems may be studied conveniently by this new electrochemical method.

LITERATURE CITED

(1) Anderson, L. B., Reilley, C. N., *J. Electroanal. Chem.* **10**, 295 (1965).
(2) *Ibid.*, p. 538.
(3) Blackadder, D. A., Hinshelwood, C., *J. Chem. Soc.* **1957**, 2898.
(4) Christensen, C. R., Anson, F. C., ANAL. CHEM. **36**, 495 (1964).
(5) Crank, J., "The Mathematics of Diffusion," pp. 67–8, Oxford, London, 1956.
(6) Croce, L. J., Gettler, J. D., *J. Am. Chem. Soc.* **75**, 874 (1953).
(7) Delahay, P., "Chronoamperometry and Chronopotentiometry," "Treatise on Analytical Chemistry," I. M. Kolthoff and P. J. Elving, eds., Part I, Vol. 4, Chap. 44, pp. 2235–40, Interscience, New York, 1963.
(8) Delahay, P., "New Instrumental Methods in Electrochemistry," Chap. 3, Interscience, New York, 1954.
(9) Marcus, R. A., *J. Chem. Phys.* **43**, 3477 (1965).
(10) Nygard, B., *Arkiv Kemi* **20**, 163 (1963).
(11) Oglesby, D. M., Anderson, L. B., McDuffie, B., Reilley, C. N., ANAL. CHEM. **37**, 1317 (1965).
(12) Oglesby, D. M., Johnson, J. D., Reilley, C. N., *Ibid.*, **38**, 385 (1966).
(13) Oglesby, D. M., Omang, S. H., Reilley, C. N., *Ibid.*, **37**, 1312 (1965).
(14) Schwarz, W. M., Shain, I., *J. Phys. Chem.* **69**, 30 (1965).
(15) Wawzonek, S., Fredrickson, J. D., *J. Am. Chem. Soc.* **77**, 3985 (1955).

RECEIVED for review February 1, 1966. Accepted March 31, 1966. Division of Analytical Chemistry, Winter Meeting, ACS, Phoenix, Ariz., 1966. Research supported in part by the Advanced Research Projects Agency and by the Directorate of Chemical Sciences, Air Force Office of Scientific Research Grant AF-AFOSR-584-64.

Comprehensive Computer Program for Electron Probe Microanalysis

JAMES D. BROWN

Bureau of Mines, College Park Metallurgy Research Center, U. S. Department of the Interior, College Park, Md.

▷ **A computer program for calculating composition from x-ray data measured with an electron probe microanalyzer is described. This program can be used with several calculation procedures, including absorption corrections due to Philibert and as modified by Duncumb and Shields, fluorescence corrections of Castaing and Wittry, and Thomas' atomic number correction. The program facilitates the comparison of calculation procedures as well as the evaluation of errors associated with uncertainties in the parameters used.**

IN HIS thesis, Castaing (*2*) outlined the principles of quantitative electron probe microanalysis using pure elements as standards. Several reviews (*3*, *6*, *10*) provide a good basis for understanding the problems of quantitative electron probe microanalysis. Corrections for absorption, secondary fluorescence, and atomic number effects must be applied to the relative intensities to obtain the composition of a sample. Many equations have been proposed for these corrections. All are time-consuming to use, particularly when many areas are analyzed or when more than two elements are present in the sample. Computer programs provide the logical means of reducing the personnel time used for these calculations. For maximum utility, data from any sample measured by any type of electron probe microanalyzer should be compatible with the program. A previous report (*1*) described such a computer program for calculating compositions from measured x-ray intensities using Philibert's absorption correction (*5*) and Castaing's fluorescence correction (*2*). The present report describes a more extensive program which includes several absorption, fluorescence, and atomic number corrections. Besides permitting rapid calculation of sample compositions, the program has proved useful in comparing the various correction procedures.

PROGRAM OUTLINE

Figure 1 is a flow diagram of the computer program. The procedures used in the calculations can be visualized by reference to it.

The x-ray intensities measured from sample and standards are read into the computer. Dead time and background corrections are applied to both the

standard and sample intensities. If a compound is used as standard, the standard intensity is corrected to that which would be measured from the pure element. Measured relative intensities are then obtained by calculating the ratio of the sample to standard intensities. The initial estimate of the composition of the sample is obtained by normalizing the measured relative intensities. This composition is used on the first iteration. Absorption, fluorescence, and, if necessary, atomic number corrections applied to concentrations of each element in the sample yield calculated relative intensities. New concentrations are then calculated for each element, using the expression

$$C_n = \frac{I_{\text{meas}d}}{I_{\text{calcd}}} \times C_{n-1} \qquad (1)$$

where C_n is the concentration of the nth iteration, C_{n-1} is the concentration of the previous iteration, and $I_{\text{meas}d}$ and I_{calcd} are measured and calculated relative intensities, respectively.

The new concentrations are normalized to 100% and compared with the previous estimate of composition. If the agreement is sufficiently good, the results are written out and the next set of measured relative intensities is treated. If not, the procedure is repeated, after adjusting measured relative intensities if the background intensity from the sample is calculated as a function of composition. The criterion used for agreement of composition on successive iterations is that the concentration of each element should differ by not more than 0.1% of the amount present.

If some element in the sample is not analyzed—for example, oxygen in an oxide—its concentration can be determined by difference. The iterative procedure proceeds as before, except that after the first iteration no normalization is carried out. Instead, the concentrations of the elements for which x-ray intensities have been determined are summed and the unmeasured element is determined by difference. If more than one element is not determined but the ratio of their concentrations is known, a fictitious atomic number and atomic weight corresponding to the ratio of the elements can be used, and the calculations performed. For example, if the sample is known to be a carbonate, the average atomic number for CO_3 would be 7.5 and the atomic weight 15.

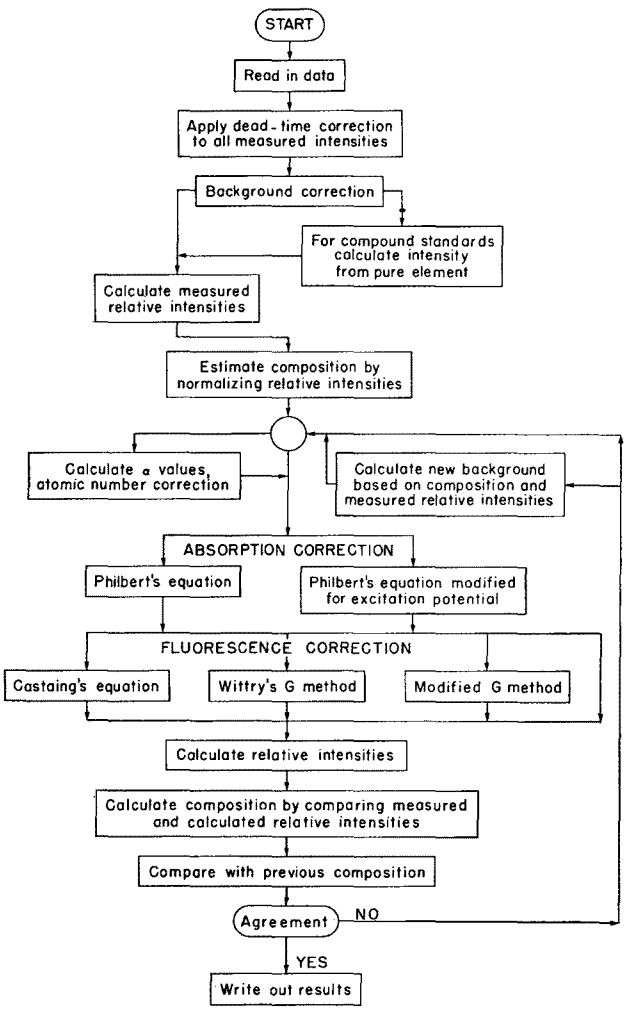


Figure 1. Flow diagram of computer program

Calculation of Relative Intensities. To use intensities as measured by an electron probe microanalyzer, corrections must be applied to the raw intensity data for dead time, instrumental drift, and background.

Dead Time. The dead time correction equation programmed is

$$N_t = \frac{N_o}{1 - N_o T} \qquad (2)$$

where N_t is the true counting rate, N_o is the measured counting rate, and T is the dead time for the entire counting system.

The dead time correction is applied to all measured intensities, including the background measurements.

Instrumental Drift. By measuring standard intensities before and after the sample measurements are made, the magnitude of the instrumental drift during the period of analysis can be determined. Using these standard intensities, a correction for drift is calculated, assuming that the drift is linear with time and that each analysis requires an equal amount of time. A drift correction is also applied to the background measurements. This latter correction becomes important when small concentrations are measured, even though the drift in background intensities may be only a few counts per second.

Background. As in the previous program (*1*) the background can be calculated in one of two ways. Either a constant background is subtracted which for each spectral line is invariant with composition or the background is calculated as a function of composition. The constant background method will introduce negligible error, provided peak to background ratios are large. For small concentrations and low peak to background ratios backgrounds should be calculated as a function of composition. A background measurement is made for each element for each spectral line. The total background is then calculated on each iteration as the product of the background for each

element times its weight fraction summed over the composition.

Any or all of these corrections to the intensity data can be circumvented. The dead time correction will not be applied if a dead time of 0 microsecond is used. No drift correction will be calculated if initial and final standard intensities are set equal. Finally, no background correction will be subtracted if everywhere in the data the background is zero. In this way, it is possible to use relative intensity data as input to the program. Dead time, drift, and background corrections are set equal to zero, while initial and final standard intensities for each element are set at 1.0. If then the relative intensities are read in as sample intensities, the computer will use these relative intensities directly to calculate the composition of the sample.

Absorption Corrections. The computer program provides two methods of calculating the absorption correction: the method of Philibert (*5*), or this method as modified by Duncumb and Shields (*4*). The absorption correction is selected by index values in the data input. According to Philibert, in the absence of secondary fluorescence and atomic number effects, the concentration, C_A, of element A in a sample is given by

$$C_A = \frac{I_A{}^S}{I_A{}^A} \frac{F_A(\chi_A)}{F_S(\chi_S)} \tag{3}$$

where $I_A{}^S/I_A{}^A$ is the relative intensity of the characteristic line of element A from the sample to the intensity of that same line from the pure element measured under identical conditions.

$F_A(\chi_A)$ and $F_s(\chi_s)$ are the "F of χ" values for the pure element and sample, respectively. $F(\chi)$ is given by the expression

$$F(\chi) = \frac{1}{\left(1 + \frac{\chi}{\sigma}\right)\left[1 + h\left(1 + \frac{\chi}{\sigma}\right)\right]} \tag{4}$$

χ is defined by the expression

$$\chi = \frac{\mu}{\rho} \csc \psi$$

where μ/ρ and ψ are the mass absorption coefficient and x-ray take-off angle, respectively. σ is a parameter dependent on the electron accelerating voltage. Values of σ are given by Philibert (*5*). Finally,

$$h = 1.2 \frac{A}{Z^2} \tag{5}$$

where A is atomic weight and Z is atomic number. The values of μ/ρ and h for the sample composition are calculated by summing the product of the variable times its weight fraction for the composition being considered. Thus, average values for μ/ρ, atomic number Z, and atomic weight A are calculated on each iteration of the program. In this way, the $F(\chi)$ value is adjusted to correspond to the curve with the proper value of average atomic number and weight. $F(\chi)$ does contain a small atomic number correction, since when $\chi = 0$, $F(\chi) = 1 + h$. The absorption correction alone is normally used when no significant atomic number correction is necessary. Under these conditions there is little difference in the use of $F(\chi)$ or $f(\chi)$ in the absorption correction. For those who prefer to use $f(\chi)$, a minor change to three statements in the computer program can be made.

Duncumb and Shield's (*4*) modification to the Philibert absorption correction was to replace the Philibert σ, which is dependent only on the electron-accelerating voltage, by the expression

$$\sigma = \frac{2.39 \times 10^5}{E_0{}^{1.5} - E_C{}^{1.5}} \tag{6}$$

where E_0 is the electron-accelerating voltage and E_C is the absorption edge energy, both in kilovolts. The value of σ is thereby different for each element which is determined. The expression for $F(\chi)$ remains the same except for substitution of the new values for σ.

For electron probes in which the sample surface is tilted relative to the electron beam, the x-rays are generated nearer to the surface than with a normal incidence beam. To allow for this sample tilt, the value of σ is increased according to the expression

$$\sigma_T = \sigma_N \sec \theta \tag{7}$$

where σ_T is the value of σ for the tilted specimen, σ_N is the value given by Philibert or the expression of Duncumb and Shields, and θ is the angle between the normal to the surface of the specimen and the electron beam. The factor sec θ is simply the geometrical factor relating the path length for electrons with nonnormal incidence to the depth in the sample along the normal.

Fluorescence Corrections. When fluorescence effects are important, Equation 3 for calculating composition from x-ray intensities must be modified so that

$$C_A = \frac{I_A{}^S}{I_A{}^A} \frac{F_A(\chi_A)}{F_S(\chi_S)} \frac{1}{(1 + K_f)} \tag{8}$$

where $K_f = I_f/I_d$ is the ratio of the intensity, I_f, of the fluorescence radiation to the intensity, I_d, of the same spectral line directly excited by electrons. Several methods have been proposed for calculating this ratio. Three methods have been included in the computer program. The specific method chosen for a given set of data is determined by index values which are part of the input data.

CASTAING'S METHOD. Castaing's equation (*2*) for secondary fluorescence is

$$K_f = \frac{I_f}{I_d} = C_B \frac{1}{2}\left(\frac{r_K{}^A - 1}{r_K{}^A}\right) \omega^B{}_K \times \frac{\lambda^B}{\lambda^A} \frac{\mu_B{}^A}{\mu_B{}^S} \frac{A_A}{A_B}\left[\frac{\ln(1+u)}{u} + \frac{\ln(1+v)}{v}\right] \tag{9}$$

where A and B are the excited and the exciting elements, respectively. In Equation 9 C_B and $\omega_K{}^B$ are the weight fraction and the fluorescent yield, respectively, for the exciting element. $r_K{}^A$ is the absorption jump ratio for the excited element. λ refers to the wavelength at the absorption edge related to the excited or exciting wavelength. A_A and A_B are atomic weights. $\mu_B{}^A$ and $\mu_B{}^S$ are the mass absorption coefficients for characteristic radiation from element B in pure element, A, and in the composite sample, S, respectively. Subscripts refer to the spectral line, superscripts to the absorber. u and v are given by the equations

$$u = \frac{\mu_A{}^S}{\mu_B{}^S} \csc \psi \qquad v = \frac{\sigma}{\mu_B{}^S} \sec \theta \tag{10}$$

Castaing's equation was derived for the fluorescence of K lines of one element due to absorption of K lines of a second element. For fluorescence involving L lines, the same expression can be used, but some adjustment must be made for the difference in intensity of the L lines relative to that of the K lines. Reed (*8*) measured some of these intensities and gives the necessary factors for calculating fluorescence corrections when L lines are used.

WITTRY'S METHOD. Wittry developed three equations for secondary fluorescence corrections (*11*). These equations have not been programmed because of the inaccuracy of the simplest equation and the close similarity to Castaing's expression of the more complex expressions. The use of the most refined equation of Wittry is complicated by a lack of knowledge of the values of parameters b and Z_0 in his expression. In 1962, Wittry (*12*) published another correction procedure for secondary fluorescence which has become known as Wittry's G method. This equation is simpler to use but still includes the effects of x-ray take-off angle and electron-accelerating voltage. His original equation was written in terms of a binary alloy, but this can be extended to multielement systems. Equation 11 is Wittry's equation as modified to apply to systems of more than two elements. To keep the notation the same as for Castaing's expression, A is the excited and B the exciting element. Then Wittry's equation is

$$K = \frac{I_f}{I_d} = \left[\frac{U_B \ln U_B - U_B + 1}{U_A \ln U_A - U_A + 1}\right] \times \left[\frac{0.425\,\omega_K{}^B(r_K{}^A - 1)}{\csc \psi}\right] \times \left[\frac{C_B \ln (1+u)}{X_B{}^{7.6} \sum_i (C_i X_i{}^3 r_i{}^B)}\right] \quad (11)$$

In Equation 11, U_A and U_B are the ratio E_O/E_K of the electron-accelerating voltage, E_O, to the appropriate critical absorption edge energy E_K,

$$X_i = \frac{Z_i}{Z_A}$$

where Z is atomic number and $r_K{}^A$ is the absorption jump ratio for the excited element. u is defined by the equation

$$u = \left[\frac{\sum_i C_i X_i{}^3 r_i{}^B}{\sum_i C_i X_i{}^3 r_i{}^A}\right] \csc \psi \quad (12)$$

where $r_i{}^A$ and $r_i{}^B$ are constants, equal to unity or the absorption jump ratio.

In Equations 11 and 12 Wittry approximated the mass absorption coefficients by a λ^3 law. The law holds only between absorption edges, so that where an analytical line lies on the short wavelength side of an absorption edge for one element but on the long wavelength side for a second element, the absorption jump ratio must be used to obtain the proper relative values for the mass absorption coefficients. The values used for $r_i{}^A$ and $r_i{}^B$ can be illustrated by considering an iron-chromium sample. In the denominator of Equation 11 and the numerator of Equation 12 the sum refers to the absorption coefficient for Fe$K\alpha$. This wavelength lies on the long wavelength side of the absorption edge of Fe but on the short wavelength side for Cr. Therefore $r_{Fe}{}^{FeK\alpha}$ will be 1 while $r_{Cr}{}^{FeK\alpha}$ will be equal to the absorption jump ratio for the CrK edge. In the denominator of Equation 12 for the Cr$K\alpha$ line, the wavelength lies on the long wavelength side of the absorption edges of both Fe and Cr. Therefore $r_{Fe}{}^{CrK\alpha}$ and $r_{Cr}{}^{CrK\alpha}$ will both equal 1. This leads to the general rule that $r_i{}^A$ or $r_i{}^B$ is unity if the characteristic line is on the long wavelength side of the absorption edge but is equal to the absorption jump ratio if it is on the short wavelength side.

Wittry's equations can be used for K lines with elements close in atomic number, but become almost unworkable for other systems.

Modification of Wittry's Method. The approximations used by Wittry to obtain ratios of mass absorption coefficients in terms of atomic number simplify the solution of his equation if graphs are used but, unfortunately, complicate the solutions from the standpoint of computer techniques. A modified version of Wittry's equation [equation 12 in (*12*)] has therefore been used in which the approximation to the mass absorption coefficients has been removed. Wittry's equation then becomes

$$K = \frac{I_f}{I_d} = \left[\frac{U_B \ln U_B - U_B + 1}{U_A \ln U_A - U_A + 1}\right] \times \left[0.425\,\frac{\omega_K{}^B(r_K{}^A - 1)}{r_K{}^A}\,\frac{A_B}{A_A}\left(\frac{E_K{}^B}{E_K{}^A}\right)^{0.3}\right] \times \left[C_B \frac{\mu_B{}^A}{\mu_B{}^S}\,\frac{\ln (1+u)}{u}\right] \quad (13)$$

where u now has the same value as in Castaing's equation. Comparison of the modified form of this equation with that of the Castaing equation shows that the essential differences are in the treatment of the dependence on the electron-accelerating voltage and the penetration of the electrons into the sample.

Atomic Number Correction. To take into account atomic number effects, the method of Thomas (*9*) is used. Including an atomic number effect, Equation 3 becomes

$$C_A = \frac{I_A{}^S}{I_A{}^A}\,\frac{F_A(\chi_A)}{F_S(\chi_S)}\,\frac{\sum_i C_i \alpha_{iA}}{C_A \alpha_{AA}} \quad (14)$$

where α_{iA} and α_{AA} are the alpha values for the characteristic line of element A. α is defined as S/R where S is the stopping power and R the effective current factor. Graphs for determining S and R are given by Thomas.

In the procedure outlined by Thomas, the x-ray absorption term is also modified to take into account the change in depth of x-ray production with the change of average atomic number. This is accomplished by substituting for the χ value

$$\chi = \frac{\sum \left(\frac{\mu}{\rho}\right)_{iA} C_i \csc \psi}{\sum C_i \frac{\alpha_{iA}}{\alpha_{AA}}} \quad (15)$$

and using a value of h equal to that for the pure element for all composition. In the computer program, parallel routes for calculating χ and h for the Philibert equation are used, depending on whether an α correction is required or not. The Duncumb and Shields modification to σ should not be used with the Thomas equation.

Because of the mixing of the atomic number effect and the absorption correction by using the more or less arbitrary Equation 15 for calculating χ, the Thomas method has theoretical weaknesses. However, justification rests on the observed agreement between known and calculated compositions from x-ray measurements of 150 binary samples. The x-ray data used to justify the Thomas correction include measurements by a number of laboratories, over a range of electron-accelerating voltages and x-ray take-off angles. A comparison with other correction procedures (*7*) shows a considerably smaller average error between measured and known compositions for the Thomas method.

Table I. Computer Output for a Typical Analysis

```
PROBLEM NUMBER   62
 MODIFIED PHILIBERT ABSORPTION
 CASTAING FLUORESCENCE CORRECTION

OBS. ITER.     CONCENTRATIONS, WEIGHT PERCENT
   AT NO*** 28.0       26.0       16.0
 1    5    5.8010    40.7460    53.4530    1.0108
 2    5    5.8779    40.7078    53.4143    1.0224
 3    5    5.6624    41.5300    52.8076    1.0280
 4    5    5.6371    41.1743    53.1885    1.0283
 5    5    5.7748    41.0075    53.2177    1.0157
```

THE PROGRAM

The computer program is written in FORTRAN and consists of a general program with three subroutines for the fluorescence corrections. (A listing of the program along with a description of the input requirements can be obtained by writing the author.) Compilation time on an IBM 7094 computer is less than 2 minutes. Actual calculation of data has seldom required more than 1 minute regardless of the amount or complexity of the data.

Table I gives the output from the computer for a typical analysis. Under the problem number are listed the correction procedures which have been used in calculating the compositions which follow. The first two columns of numbers give the observation number and the number of iterations required to obtain the necessary convergence. If the composition has not converged by the twentieth iteration, the largest percentage difference in concentration for any of the components between the nineteenth and twentieth iteration is printed out along with the composition calculated on the last iteration. The concentrations in weight per cent which are printed in Table I under the atomic number for the element are normalized

to 100%. The right-hand column gives the sum of the weight fractions before normalization. This sum can serve as a check on the analysis since, ideally, it should be 1.0000 if all elements have been analyzed and the correction procedures are exact. Results in which the sum differs from 1.0 by more than a few per cent point toward the presence of unsuspected elements in the sample or poor data. At the same time, the unwary must be warned about placing too much confidence in this sum. Each of the correction procedures tends to give compositions which sum to 100%, although the concentrations of individual components can vary considerably from one procedure to another.

CONCLUSIONS

The major advantages of using a computer program such as the one described are the reductions in both personnel time consumed in the calculations and possible human errors. Data from more complicated systems can be treated quantitatively. Calculation of composition of a four-component system using a desk calculator is a formidable task.

Since several correction procedures have been programmed, comparison of these methods is easy. Intelligent use of the program can yield a feeling for the magnitudes of the differences in the correction procedures. The development of this computer program by the addition of published procedures will continue. In particular, programming of a correction for fluorescence by the continuum is planned. The magnitude of the effect of changes in mass absorption coefficients on composition can be determined by substitution of different mass absorption coefficients. In this way, a more concrete estimate of the accuracy of electron probe microanalysis of complex systems can be obtained. This estimation of accuracy may be the most important benefit of such computer programs.

LITERATURE CITED

(1) Brown, J. D., U. S. Bur. Mines, Rept. Invest. 6648 (1965).
(2) Castaing, R., Ph.D. thesis, University of Paris, 1951 (English trans. Rept. WAL 142159-7).
(3) Duncumb, P., Shields, P. K., *Brit. J. Appl. Phys.* 14, 617 (1963).
(4) Duncumb, P., Shields, P. K., "The Electron Microprobe," T. D. McKinley *et al.*, eds., p. 284, Wiley, New York, 1966.
(5) Philibert, J., "X-Ray Optics and X-Ray Microanalysis," H. H. Pattee *et al.*, eds., p. 379, Academic Press, New York, 1963.
(6) Philibert, J., L'Institut de Recherches de la Sidérurgie, Saint-Germain-en-Laye (S. & O.) France, IRSID Publications, Ser. B, No. 51 (1965).
(7) Poole, D. M., Thomas, P. M., "The Electron Microprobe," T. D. McKinley *et al.*, eds., p. 269, Wiley, New York, 1966.
(8) Reed, S. J. B., *Brit. J. Appl. Phys.* 16, 913 (1965).
(9) Thomas, P. M., U. K. At. Energy Auth. Research Group, Metallurgy Div., AERE, Harwell, Berkshire, Eng., Rept. **AERE-R4593** (1964).
(10) Wittry, D. B., *Advan. X-Ray Anal.* 7, 395 (1964).
(11) Wittry, D. B., Ph.D. thesis 188, California Institute of Technology, 1957.
(12) Wittry, D. B., University of Southern California Engineering Center, Rept. 84-204 (1962).

RECEIVED for review December 22, 1965. Accepted March 21, 1966. Trade names are used for information only, and endorsement by the Bureau of Mines is not implied.

Optical and Electron Microscope Studies of Thin Fuel Cell Electrode Structures

WILLIAM R. LASKO and GERALD P. McCARTHY

United Aircraft Research Laboratories, East Hartford, Conn.

▷ **Light and electron microscope cross-sectional and surface techniques were employed to characterize the physical structure of platinum–Teflon catalyzed grid-type electrodes. Surface analysis showed that the platinum part of the electrode consisted of loosely packed flocculates intermixed with fibrils of Teflon and spherical-shaped particles of Teflon. Cross-sectional examinations showed a similar catalyst arrangement throughout the entire electrode structure with the fibrils apparently acting as a binder for the flocculates. Due to the composite arrangement of the platinum and Teflon, very little occlusion of the platinum by the Teflon was indicated. Improvements in the specimen preparation techniques permitted a tentative working model to be established revealing one of the possible sources for the observation of fibrils in thin electrodes by replication techniques.**

A NUMBER of companies are currently engaged in the development of lightweight high performance electrodes for application in practical H_2–O_2 fuel cells (*1*, *2*). Currently the work is being directed toward asbestos matrix type cells with catalyzed grid structures as electrodes (*3*). The electrodes consist of Pt catalysts supported on Ni or Ta screens, bonded and waterproofed with Teflon (Du Pont). To make visible the overall detail of the Pt catalyst and particles of Teflon, it was necessary to make several modifications to the conventional replication methods as applied to the study of cross-sections of thin fuel cell electrodes. This paper deals with an exploratory light and electron microscope study of catalyzed thin electrodes undertaken with the view that the techniques employed could be of considerable value in revealing the physical makeup of thin electrodes, the degree of catalyst dispersion and the amount of catalyst occlusion by the Teflon.

EXPERIMENTAL PROCEDURE

The thin fuel cell electrodes analyzed in this study were prepared by applying Pt–Teflon mixtures onto a single side of a sealed (immersed in a dilute suspension of Teflon) Ni or Ta screen in the range of 50 to 100 mesh, followed by vacuum drying with typical Pt loading varying between 8 and 10 mg./sq. cm.

A number of techniques were employed to delineate the physical makeup of the electrodes. Cross-sectional light microscopy examinations were made to reveal the overall electrode morphology, while cross-sectional replication electron microscopy techniques were applied to reveal the distribution of the catalyst in the electrode containing a mixture of Pt–Teflon. In all cases the electrode received for analysis was inspected visually for representative areas and small sections 0.5-inches-square were removed with the aid of a sharp scissor. To preserve the integrity of the electrode structure, each square for cross-sectional analysis was vacuum impregnated with Bakelite resin BR-0014 prior to mounting by a technique which will be discussed in detail in a paper submitted for publication (*4*). After impregnation the electrode sections were mounted in a thermal setting resin (diallyl phthalate) and cured at 150° F. for 3–5 minutes. Prior to polishing, the micro was ground to a depth of 1/8 inch, thus eliminating the distorted area introduced during cutting. Polishing was initiated on 240-grit SiC paper with H_2O lubrication and was con-

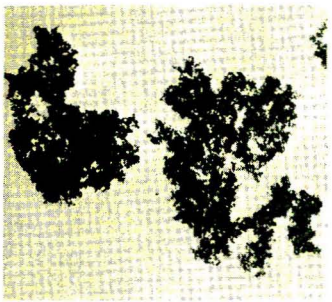


Figure 1. Platinum-black catalyst

(44,000×)

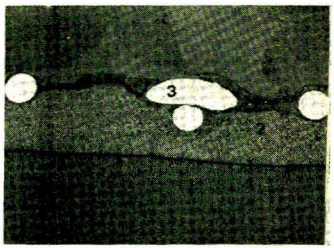
tinued on 320, 400, and 600 papers. Final polishing was achieved on 6-micron diamond followed by 0.3-micron Al_2O_3 powder and H_2O. Normally the entire polishing operation took approximately 10 hours. To aid in distinguishing the morphological makeup and distribution of the catalyst from the impregnating resin by eliminating the masking effect introduced by the loose catalyst flocculates adhering to the initial replica, the highly polished micro was immersed in hot aqua regia for 1–2 minutes followed by repeated rinses in distilled water and alcohol. When the mount was completely dry, the surface was studied by replication electron microscopy.

A negative two-stage collodion Pt–C replication technique was employed exclusively throughout this study. Briefly, the technique consists in flooding the sample surface with a solution of collodion in amyl acetate, placing a specimen screen in the solution, drying in a horizontal position, stripping with the aid of scotch tape and moisture, coating with Pt–C at a suitable angle, evaporating a C reinforcing layer and solubilizing the primary collodion replica in acetone leaving the negative C–Pt–C replica in place on the specimen screens.

The replication technique was also applied directly to the electrode surface to show the flocculated nature of the Pt-black catalyst adhering to the initial replica. In addition, transmission studies were undertaken of Pt–Teflon mixtures sprayed on glass surfaces in an attempt to determine the wetting characteristics of Pt and Teflon.

RESULTS AND DISCUSSION

An electron micrograph of the Pt-black catalyst employed in the thin electrodes investigated in this study is shown in Figure 1. The black is somewhat flocculated with a base particle size at <50 A. The flocculated nature of this catalyst when mixed with Teflon is more clearly shown in the replica (Figure 2) of the surface of a Pt-catalyzed thin fuel cell electrode. The opaque clusters of Pt shown in the micrograph represent sections of the electrode which adhered to the primary replica during stripping of the collodion from the electrode surface. Fibrils as well as spherical-shaped particles of Teflon can also be observed in the background. To determine if the catalyst exists in a flocculated state throughout the entire electrode structure, cross-sectional studies were instituted of a select group of thin electrodes.



(100×)



Figure 3. Optical polished cross-sections of typical thin fuel cell electrode

(250×)

Typical cross-sectional optical micrographs of a thin fuel cell electrode structure are shown in Figure 3. The micrographs have been labeled with

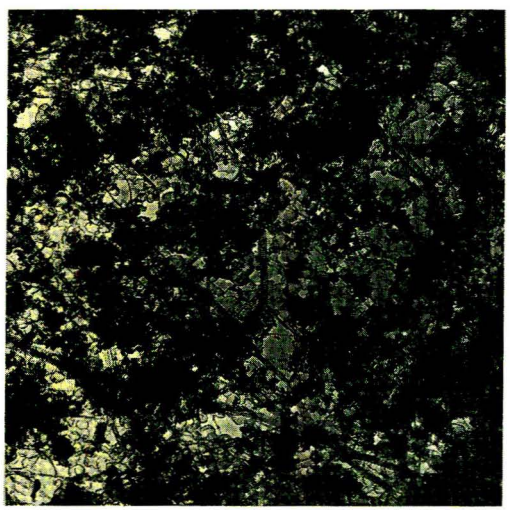


Figure 2. Replica of surface of platinum catalyzed thin electrode

(9200×)



Figure 4. Replica of cross-section of thin electrode in platinum–Teflon layer

(5100×)

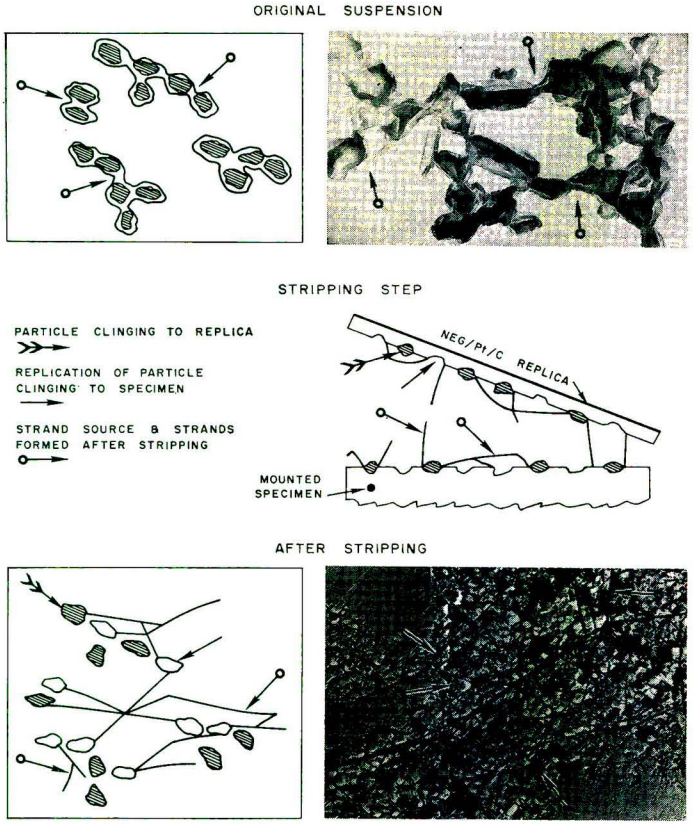


Figure 5. Schematic drawing illustrating the formation of strands



Figure 6. Replica of etched cross-section of thin electrode in platinum–Teflon layer

(5000 ×)

numbers 1, 2, and 3, to indicate the Teflon, Pt–Teflon, and screen areas, respectively. A relatively good distribution of the catalyst is indicated; however, the bond between the Teflon particles and Pt-black is not readily discernible due to the limitation in resolution of the light microscope. In an attempt to improve the resolution, replication electron micrographs were prepared at or near the middle of the Pt–Teflon layer and studied in the electron microscope. Numerals 1, 2, and 3 on the micrograph in Figure 4 indicate the Teflon, Pt, and Pt–resin regions, respectively. The opaque areas typify Pt flocculates which have adhered to the initial replica during the stripping step. Fibrils of Teflon are also in evidence (labeled #4) which have been shown by other workers (*3*) and postulated to be the bonding medium for the Pt-black. The micrograph also clearly shows a large amount of open structure (Pt–resin impregnated areas) (*3*), which is effectively linked by the fibrils of Teflon. It is difficult to discern the Pt particles in these areas by conventional techniques. Some concept of the shape and size of the particle of Teflon is also indicated.

It is not clearly understood at this time how the fibrils originate, since it is possible for fibril development to occur in the electron fabrication process through expansion of the Teflon during sintering, application of the Pt–Teflon mixture to the screen or in the replication process as depicted schematically and photographically in Figure 5. In this case it is hypothesized that in the stripping of the replica from the electrode surface, the connecting linkages or the transparent regions observed in the original suspension (shown by untailed arrows in the upper micrograph) are subjected to stretching as clusters and individual particles of Teflon become separated (stripping step). The ultimate results of this stretching process develop into a complex network of interconnecting fibrils which interwind and bind isolated flocculates of Pt-black and Teflon (lower

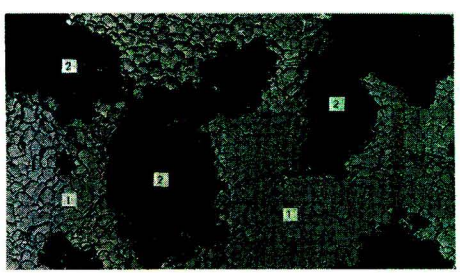


Figure 7. Platinum–Teflon suspension sprayed on glass

(5000 ×)



Figure 8. Platinum–Teflon suspensions sprayed on glass

(52,000×)

micrograph). Loose opaque particles clinging to the replica as well as replications of bound clusters of Teflon are also depicted by appropriate arrows in the micrograph.

Because it is difficult to distinguish the morphological makeup of the Pt-black in resin-impregnated thin electode cross-sections except for the loose Pt-black that adheres to the replica, several were etched with aqua regia to delineate the structural makeup of the Pt-black. An example of a typical etched cross-section is shown in Figure 6. To aid in the overall analysis of the replica, the platinum (Pt), Teflon (T), and resin (R) areas are appropriately labeled on the micrographs. This analysis clearly shows that the Pt-black is dispersed as discrete flocculates with Teflon stringers bridging across the various Pt flocculates. The micrograph also clearly demonstrates that the Teflon does not occlude any large amount of the Pt-black as both the Pt and Teflon appear to exist as separate discrete units indicating poor wetting of the Teflon by the Pt-black.

In an attempt to demonstrate this effect of poor wetting more clearly, suspensions of Pt and Teflon were thoroughly mixed in a Waring Blendor and sprayed onto the surface of a glass slide. From the micrograph illustrated in Figure 7, the flocculated nature of the Pt-black as well as the poor bond between the Teflon and black is readily demonstrated by the extent of the opaque deposits which have adhered to the replica. A high magnification electron micrograph (52,000×), shown in Figure 8 also was prepared to show the difference in size between the Teflon and Pt-black particles (shown by untailed arrows). The mottled structure observed on the surface of the particles of Teflon may be due to granulation or poor wetting of the shadow-casting metal at the Teflon surface (*4*).

LITERATURE CITED

(1) Barber, W. A., Woodberry, N. T., *J. Electrochem. Tech.* **3**, 194 (1965).
(2) Grubb, W. T., Michalske, C. J., *J. Electrochem. Soc.* **111**, 477 (1964).
(3) Haldeman, R. G., Colman, W. P., Langer, S. H., Barber, W. H., "Advances in Chemistry Series, Number 47," "Fuel Cell Systems," R. F. Gould, ed., pp. 106–15, ACS, Washington, D. C., 1965.
(4) Lasko, W. R., United Aircraft Research Laboratories, East Hartford, Conn., private correspondence, 1966.

RECEIVED for review February 18, 1966. Accepted March 28, 1966.

Photochemical Determination of Oxalate

WILLIAM M. RIGGS and CLARK E. BRICKER

Department of Chemistry, University of Kansas, Lawrence, Kan.

▶ The photochemical decomposition of ferric oxalate complexes in aqueous acidic solution has been utilized as the basis of new analytical techniques for the determination of oxalate. Two indirect methods are described; one which is applicable to traces of oxalate (detection limit of 5 μg. of $Na_2C_2O_4$), and another which is useful in the milligram range. A number of organic acids have been investigated for possible interference with each of the methods. Better than 3% accuracy is obtained for traces of oxalate in the absence of interferences. Accuracy and precision are both 2 parts per thousand or better with larger amounts of oxalate.

THE PHOTOCHEMICAL ACTION of light has received only limited attention from analytical chemists. Bricker and Schonberg (*2*) suggested the technique of "photonometric" titration using carefully calibrated light sources. Using this technique, the amount of material titrated is proportional to the time of exposure to the light. Bricker and Schonberg determined vanadium (V) and chromium(IV) by this technique and Kuwana (*5*) later applied it to an oxygen determination. Beattie, Bricker and Garvin (*1*) determined traces of organic materials in water by photosensitized oxidation followed by mass spectrometric measurement of the CO_2 produced. G. G. Rao and coworkers (*10, 12, 13*) describe indirect methods for determination of uranium (VI) and iron(III) using photoreduction of these ions by various organic materials followed by titration of the reduced species with sodium vanadate. Rao and Aravamudan (*11*) also report the determination of oxalic acid by photosensitized oxidation with iron(III). Part of the work reported here is an extension of this idea.

The photoactivity of iron(III) oxalate in solution was first observed by Dobereiner (*4*) who detected iron(II) in a solution of potassium trisoxalatoferrate (III) which had been exposed to sunlight. In subsequent years the reaction has been extensively studied. Photo-

Table I. Method I. Oxalate Determination

$Na_2C_2O_4$, mg. Added	Found	Std. dev.	Rel. error, %
13.34	13.35	0.05	0.10
26.68	26.65	0.07	0.10
40.02	40.01	0.13	0.03
53.36	53.43	0.05	0.13

Table II. Extent of Reaction with Time of Irradiation

Irradition time (min.)	Amount reacted, %
5.0	87.3
7.0	95.8
9.0	98.0
10.0	99.3
15.0	100.2
20.0	99.9

(26.68 mg. sodium oxalate present)

chemical action has been observed with light of wavelengths from 579 to 254 mμ (*6*). The quantum yield is low at long wavelengths and has a value of 1.00 or more [based upon iron(II) production] only at wavelengths shorter than 436 mμ. Recently Parker and Hatchard (*6*, *7*) pointed out the usefulness of the reaction as a chemical actinometer. They also suggested a reaction mechanism (*8*) and later, after a more detailed study using flash photolysis (*9*), they modified their suggestions somewhat. Some details of the mechanism are still in doubt.

Iron(III) forms mono-, di-, and trioxalato complexes in solution, all of which are photochemically active. The overall reaction may be represented by Equation 1, with the monoxalate species as the example.

$$2Fe(C_2O_4)^{+} \xrightarrow{h\nu} 2Fe^{+2} + 2CO_2 + C_2O_4^{-2} \quad (1)$$

The analytical methods described in this report are based on this reaction. The first of these (Method I) depends upon titrating the photochemically produced iron(II) with dichromate. It is applicable to quantities of sodium oxalate in the 10- to 100-mg. range. Method II rests upon the spectrophotometric determination of the iron(II) by formation of the 1,10-phenanthroline complex and measurement of the intensity of the red color formed. This method works well with samples of 5 to 150 μg. of $Na_2C_2O_4$.

EXPERIMENTAL

Apparatus. The light source used throughout was a 100-watt medium pressure mercury vapor lamp from Ultra-Violet Products Inc. The radiation from this lamp was filtered through a soft glass plate which effectively eliminated wavelengths shorter than 305 mμ. Spectrophotometric measurements were made with a Bausch and Lomb Spectronic 20 except for an absorption spectrum of the above-mentioned glass plate which was obtained on a Bausch and Lomb Spectronic 505. For Method I the sample vessel was a 125-ml. Erlenmeyer flask equipped with a side arm at the bottom so that the solution could be de-aerated with nitrogen. After irradiation, titrations were performed directly in this vessel. Sample containers for Method II were 50-ml. beakers also fitted with side arms near the bottom for de-aeration with nitrogen. Solutions were stirred with a Teflon covered magnetic stirring bar.

Reagents. Standard dichromate solutions were prepared from Fisher Certified Reagent potassium dichromate, dried overnight at 110° C. and stored in a desiccator over calcium chloride. Standard oxalate solutions were prepared from Mallinckrodt analytical reagent grade sodium oxalate, dried and stored in the same manner. Standard iron(III) sulfate solutions were prepared from reagent grade material, and were standardized by the stannous chloride reduction–dichromate titration method (*3*). Sodium diphenylaminesulfonate indicator solution was prepared by dissolving 0.3 gram of barium diphenylaminesulfonate in 100 ml. of water, adding excess 0.1*M* sodium sulfate and decanting the solution after the precipitate settled. Orthophenanthroline solution (0.1%) was prepared by dissolving the solid in hot water. Standard iron(II) solutions were prepared by weighing G. F. Smith primary standard ferrous ethylenediammonium sulfate tetrahydrate. The compounds used in the interference studies were of various grades depending upon availability. This caused no trouble except in the case of formic acid which appeared to have a small amount of oxalate impurity. All other reagents used were analytical reagent grade. Solutions were de-aerated when necessary with tank nitrogen.

Procedures. A. Analyses of sodium oxalate by Method I were carried out as follows: The sodium oxalate was prepared as a 0.0100*M* solution, which was also 1*N* H_2SO_4. Amounts varying from 10.00 to 40.00 ml. were pipetted into the reaction flask. A 3- to 5-fold excess of ferric iron was added from a buret as 1–2 ml. of 0.1*M* solution of iron(III) in 1*N* sulfuric acid. The solution was swept for 5 minutes with nitrogen and then irradiated for 20 minutes with constant stirring and continued nitrogen sweeping. The mercury vapor lamp was approximately 6 inches from the surface of the solution. After irradiation, 2 ml. of 85% phosphoric acid and 5 drops of sodium diphenylaminesulfonate indicator were added to the flask, and the iron(II) present was titrated with 0.0100*N* dichromate. Compounds studied as possible interferences were added to the mixture before irradiation in the form of 0.1 gram/ml. solutions in 1*N* sulfuric acid.

B. The general procedure for Method II was as follows: A standard curve was obtained by dissolving 0.0684 gram of ferrous ethylenediammonium sulfate tetrahydrate in water and diluting to 1 liter with 1*N* H_2SO_4. This solution contained 0.010 mg./ml. of iron(II). Further dilutions were made by pipetting amounts varying from 1.00 to 50.00 ml. into 100-ml. volumetric flasks. Ten milliliters of 0.1% orthophenanthroline was added, the pH was adjusted to about 5 with sodium acetate, and the solution was diluted to volume. The absorbance was read at 508 mμ. Samples for analysis were prepared and analyzed by pipetting amounts varying from 0.10 ml. to 10.00 ml. of $1.00 \times 10^{-4}M$ sodium oxalate solution into the irradiation vessel, adding 5.00 ml. of $1 \times 10^{-3}M$ iron(III) solution and enough 1*N* H_2SO_4 to bring the volume to 20.00 ml. The solutions were stirred and swept with nitrogen for 5 minutes in the dark and then for 20 minutes under irradiation with the lamp positioned about 6 inches from the surface of the solution. At the end of this time a 5.00-ml. aliquot of the irradiated solution was pipetted into a 10.00-ml. volumetric flask; 2 ml. of orthophenanthroline were added, and the pH was adjusted to about 3.5 with sodium formate solution. The solution was then diluted to volume and the absorbance determined *vs.* the appropriate blank. For interference studies, appropriate solutions were added before the irradiation.

RESULTS AND DISCUSSION

Method I. The results of the analysis of several different solutions of sodium oxalate are presented in Table I. The precision and accuracy are good and are of the magnitude of ordinary volumetric errors. This supports the hypothesis that the photochemical reaction is quantitative and stoichiometric under these conditions. Experiments carried out without nitrogen de-aeration gave low and erratic results due to air oxidation of iron(II). The solution acidity is not critical as long as it is high enough to prevent precipitation of ferrous oxalate or ferric hydroxide. The recommended concentration of acid is 0.1 to 1.0*N*. Sulfuric rather than hydrochloric acid should be used since HCl prevents the reaction from going to completion in a reasonable period of time. This is due to the chloro- complexes of iron(III) which form in HCl solution and absorb a large proportion of the incident radiation. Results are independent of the iron(III) concentration provided at least 2 moles of iron (III) are present for each mole of oxalate. The time of irradiation required is somewhat dependent upon the amount of oxalate in the sample as well as upon the lamp intensity and geom-

etry. With the lamp and geometry used here, 15 minutes was found to be a sufficiently long irradiation time over the oxalate concentration range studied. For a sample containing 26.68 mg. of sodium oxalate, the percentage found as a function of irradiation time is shown in Table II.

Attempts were made to analyze sodium oxalate in the presence of a variety of other compounds. Table III gives a list of these compounds and a tabulation of the concentration levels at which interference was found. The slight interference found with formate is believed to be due to traces of oxalate impurity in the formic acid used. All of the hydroxy acid anions studied form photochemically active complexes and interfere by producing iron(II) in a competing reaction.

Table III. Interference Studies in the Determination of Oxalate by Method I

	$Na_2C_2O_4$, mg. added	$Na_2C_2O_4$ mg. found, Oxalate:interference ratio 1:1	1:10	1:100
Formate	26.67	26.68	26.76	27.69
Acetate	26.67	26.62	...	26.64
Propionate	26.67	26.62	...	26.68
Malonate	26.67	26.68	...	26.74
Succinate	26.67	26.66	...	26.66
Maleate	26.67	26.66	26.67	[a]
Acrylate	26.67	26.58	[b]	...
Citrate	26.67	38.41	...	...
Tartrate	26.67	[a]	...	...
Lactate	26.67	31.45	...	...
Mannitol	26.67	32.50	...	...

The amount present of the compound being studied as a possible interference is expressed as the ratio: moles oxalate/moles interference.

[a] No end point color change occurs in the dichromate titration.
[b] Acrylate polymerizes under these conditions upon exposure to light.

Method II. This method is essentially an extension of Method I, with spectrophotometric determination of iron(II) replacing the titrimetric method. As with Method I, the amount of iron(II) produced is found to be directly proportional to the amount of oxalate initially present. A plot of absorbance of the ferrous *o*-phenanthroline solution *vs.* amount of sodium oxalate in the sample is linear. It is in excellent agreement with a similar plot prepared using iron(II) solutions prepared from primary standard ferrous ethylenediammonium sulfate with the assumption that two iron(II) ions will be produced per oxalate ion. Thus, entirely satisfactory calibration curves may be prepared using this convenient standard. The same restrictions regarding the absence of atmospheric oxygen and the proper solution acidity apply in this case as in Method I. Twenty minutes was found to be sufficient irradiation time for complete reaction in all cases. Fifteen-minute irradiations sometimes gave low results.

Compounds which interfere with Method I also interfere in this case for the same reason. Compounds which do not interfere at the levels investigated with Method I may interfere at the higher concentrations which might be encountered when attempting to analyze traces of oxalate in other materials. This possibility was investigated in the case of formate, acetate, propionate, and malonate. In the presence of formate, high, consistent results were obtained which were, as with larger amounts of oxalate, probably due to oxalate impurities in the formate. Assuming that the high results obtained in the presence of formate are due to oxalate impurity, the per cent of oxalate impurity calculated to be in the formate varied between 0.06 and 0.13%. Results were less than 3% off in the presence of a 250-fold excess of acetate, a 125-fold excess of propionate, and a 5000-fold excess of malonate. Accuracy of ±10% could be obtained in the presence of a 1250-fold excess of acetate, a 2500-fold excess of propionate, and a 10,000-fold excess of malonate. In these experiments the interference was in the direction of production of *less* iron(II) than that corresponding to the amount of oxalate added. However, irradiation of solutions with interfering ion but no oxalate present produces small yields of iron(II), the amount of which increases with time over a wide range. It is thus apparent that at least two types of interference are operative; one which inhibits the iron (III) oxalate reaction and another, less important one which produces iron(II) in a side reaction. The exact nature of these processes is far from clear and deserves further study.

Conclusions. Using techniques described in this paper, it is now possible to determine rapidly, milligram to microgram quantities of oxalate with good accuracy and precision. These indirect techniques have certain definite advantages over the direct titrimetric methods for oxalate which are presently in common use. For example, the standard dichromate solutions used in the back-titration of iron (II) are stable and can be prepared directly by weighing. This is in contrast to permanganate which is not stable indefinitely in solution and which should be standardized before use. Ceric nitrate and perchlorate solutions are also unstable on standing, although sulfate solutions are stable. The iron(II)–dichromate titration can be carried out at room temperature without catalysts, and the indicator color change is sharp. On the other hand, permanganate and ceric titrations of oxalate must be carried out at elevated temperatures or with a catalyst present, or both. The indicators used with ceric titrations must be added just before the end point is reached, or if the yellow color of the ceric ion is used as the end point indication, a blank must be used. Furthermore, most organic substances interfere with permanganate and ceric titrations because of the strong oxidizing nature of the titrants. However, the presence of many of these organic compounds can be tolerated in large excess with the photochemical method.

The spectrophotometric technique described makes it possible to determine oxalate in microgram quantities with good accuracy. No other method is presently available which is applicable to such small amounts of oxalate. This trace determination may be successfully carried out in the presence of large excesses of some compounds.

LITERATURE CITED

(1) Beattie, J., Bricker, C. E., Garvin, D., ANAL. CHEM. **33**, 1890 (1961).
(2) Bricker, C. E., Schonberg, S. S., *Ibid.*, **30**, 922 (1958).
(3) Day, R. A., Underwood, A. L., "Quantitative Analysis," pp. 116, 121, Prentice-Hall, Inc., Englewood Cliffs, N. J., 1958.
(4) Dobereiner, J., *Schweigg. Journal* **62**, 19 (1831).
(5) Kuwana, T., ANAL. CHEM. **35**, 1398 (1963).
(6) Hatchard, C. G., Parker, C. A., *Proc. Roy. Soc.* (*London*) **A235**, 518 (1956).
(7) Parker, C. A., *Ibid.*, **A220**, 104 (1953).
(8) Parker, C. A., *Trans. Faraday Soc.* **50**, 1213 (1954).
(9) Parker, C. A., Hatchard, C. G., *J. Phys. Chem.* **63**, 22 (1959).
(10) Rao, G. G., Aravamudan, G., *Anal. Chim. Acta* **13**, 328 (1955).
(11) *Ibid.*, p. 415.
(12) Rao, G. G., Rao, V. P., Rao, M.V. R., *Ibid.*, **15**, 97 (1956).
(13) Rao, G. G., Rao, V. P., Venkatamma, N. C., *Z. Anal. Chem.* **150**, 178 (1956).

RECEIVED for review February 2, 1966. Accepted April 7, 1966.

Determination of Dissolved Polonium-210 in Water by Coprecipitation with Tellurium by Stannous Chloride

D. E. RUSHING

Colorado River Basin Water Quality Control Project, U. S. Department of Health, Education, and Welfare, 1750 South Redwood Road, Salt Lake City, Utah 84104

▷ **The efficient coprecipitation of polonium-210 with tellurium by stannous chloride as precipitant is applied to the determination of polonium-210 in water. The doubly precipitated tellurium–polonium-210 precipitates are alpha counted on 0.22-micron membrane filters. A short-cut single-precipitation method is also given. Methods were tested at six levels of polonium-210 activity (0.06 to 1636 pc. per liter); in this range, the weighted average recovery was 98.8% for both methods. Radiochemical specificity is very good; there are no interferences from stable substances in samples whose compositions approach drinking water standards. The methods have sufficient sensitivity to permit their use in the determination of lead-210 in water by polonium-210 ingrowth.**

In studies of the radioactive pollution of the Colorado River Basin, it became necessary to determine ^{210}Pb and ^{210}Po concentrations in natural and polluted waters and in uranium mill effluents. The permissible concentrations for ^{210}Po for such media are high as compared to those of ^{210}Pb (*4, 9*), but the accurate determination of low concentrations of ^{210}Po is important since ^{210}Pb can be determined by the ingrowth of ^{210}Po. The 30-day ingrowth of ^{210}Po from ^{210}Pb is 10.9% if ^{210}Bi is absent and 13.9% if the ^{210}Pb to ^{210}Bi ratio is 1:1; therefore, sensitive ^{210}Po methods are needed for this approach to ^{210}Pb determinations.

From acid solutions, ^{210}Po deposits to some extent by displacement on many metals—e.g., Ag, Ni, Fe, Au, Pt, and Cu—and methods based on this principle are quite popular (*1, 2, 5–8, 12, 13*). Although excellent results usually can be obtained by the methods on chemically simple samples, the methods require the control of a large number of variables and may require preliminary separation of the ^{210}Po from a chemically complicated mixture. Broadly speaking, organic matter, oxidants, and elements which also deposit on the metal tend to interfere. Some of these interferences can be masked or eliminated by valance changes; other interferences require preliminary separations or treatments. In the writer's experience, recoveries of ^{210}Po on silver foil have varied from 85 to 100% without obvious reason for the lower recoveries. "This ease of deposition. . . .has probably hindered the development of procedures based on newer methods. . . ." (*6*). The writer agrees.

Frisch and Feldman inferred from limited data that the deposition on silver is highly dependent upon temperature and that the bath temperature must be 97° C. or higher (*8*). This temperature is not reached by boiling water in many mountainous locations.

Bismuth-210 and ^{210}Pb are deposited on some of the baser metals used in some methods (*3*). While these radionuclides are beta-emitters, they decay to alpha-emitting products. For this reason, the deposited ^{210}Po must be alpha-counted immediately after its isolation if ^{210}Pb and ^{210}Bi are present in significant amounts. The writer has observed unidentified alpha growth on silver foil used to deposit ^{210}Po.

Both Te and Se, when precipitated with $SnCl_2$, can carry ^{210}Po quantitatively. Under some conditions, the writer has observed that Se does not carry ^{210}Po; this behavior seems to be associated with the prevailing digestion conditions. Such failures have not been observed with Te. Both elements seem to carry some Sn with them physically or in chemical combination.

Rundo coprecipitated ^{210}Po with Te using NaH_2PO_2 as the precipitant, but completed the analysis by plating the ^{210}Po. Recoveries of ^{210}Po from biological samples averaged about 85% (*10*). In 1954, the writer observed that ^{210}Po was coprecipitated essentially quantitatively with Te if $SnCl_2$ was the precipitant. A limited study on urine samples showed promise, but was given up for the lack of a suitable mounting technique. Further limited work has been reported (*11*). Lindner recovered about 98.8% of the ^{209}Po coprecipitated with several mg. of Te from 0.3*N* to 3.0*N* HCl, using $SnCl_2$ as the precipitant (*6*). Since he centrifuged, it is likely that some of the loss was mechanical.

The aims of this investigation were to develop a method for ^{210}Po in water which would be applicable to other more complex media and to check the sensitivity, accuracy, and precision of the method with the idea of using it for ^{210}Pb determinations also.

EXPERIMENTAL

The experimental work consisted principally of the following: (a) tests of various mounting techniques; (b) analyses of water samples containing added ^{210}Po by the recommended procedure and of doubly precipitated standards: (c) analyses of 1-liter water samples containing added ^{210}Po using a single cold precipitation of the Te–Po; (d) tests to determine ^{210}Po losses into filtrates and on glassware; (e) tests to determine the effects of various substances on the solubility of ^{210}Po; and (f) periodic recounting of Te–Po precipitates to establish the specificity of the method.

Apparatus. Nuclear Measurements Corp. Model PC-3B internal proportional counters were used for α-counting. The counters were new, had a hemispherical detector, and would accommodate a $2^1/_4$-inch planchet. Their efficiencies were checked with a National Bureau of Standards ^{210}Po source; all counters agreed to within ±0.3% of the average of the four. Their geometries averaged 1.984 π. The counting gas was 90% argon–10% methane. NMC No. Sp-4 2-inch stainless steel planchets were used.

Reagents. Particulate matter in distilled water and reagents may find its way into the final precipitate. Care should be taken to see that a significant amount of foreign material is not introduced in this way.

Distilled Water. Distilled water must be free of ^{210}Po and ^{222}Rn. If purification is necessary, redistill; discard the distillate collected during the first ten minutes.

Acid Mixture. Pour 800 ml. of 1:1 H_2SO_4 into 400 ml. of H_2O, cool, transfer to plastic bottle, and add 400 ml. of HF (48%) and 400 ml. of HNO_3. Store in polyethylene or Teflon bottle.

Lead–Bismuth–Tellurium Carrier Solution. Prepare a solution containing 1.00 mg. each of Pb, Bi, and Te(IV) in 3.00 ml. of 1:3 HCl and no nitrate.

Lead–Bismuth Carrier. Prepare a solution containing 0.5 mg. each of Pb and Bi per ml. in 1:3 HBr and no nitrate.

Stannous Chloride Solution. Dissolve 10 grams of $SnCl_2 \cdot 2H_2O$ in 1*N*

HCl and dilute to 100 ml. with 1*N* HCl. Filter through a 0.22-micron membrane filter. Prepare every few days. Filter daily.

WASH SOLUTION. Add 0.1 ml. of 10% $SnCl_2 \cdot 2H_2O$ to 100 ml. of 1*N* HCl. Prepare daily.

HYDROCHLORIC ACID–BROMINE SOLUTION. Dissolve 5 ml. of bromine in a liter of 1*N* HCl.

PRESSURE - SENSITIVE ADHESIVE. Krylon pressure-sensitive adhesive No. 1080. Spray into a 400-ml. beaker; add ethyl acetate to dissolve. The solution should contain about 10 mg. dry adhesive per ml. Place about 0.75 ml. on a 2-inch planchet with a dropper, rotate planchet to spread solution uniformly, air-dry, and dry under lamp for 5 minutes to remove solvent.

HYDROXYLAMINE HYDROCHLORIDE SOLUTION. Dissolve 20 grams of $NH_2OH \cdot HCl$ in 1*N* HCl and dilute to 100 ml. with same solution. (Used in short-cut method only.)

BORIC ACID SOLUTION. Dissolve 50 grams H_3BO_3 in a liter of distilled water. (Used in short-cut method only.)

POLONIUM-210 SOLUTIONS. If a reliable standard solution is not available, prepare an active solution from aged ^{210}Pb solution using recommended procedure and standardize. Prepare suitable dilutions in 6*N* HNO_3. Nitric acid must be removed before precipitation step.

Procedures. STANDARDIZATION OF POLONIUM-210 SOLUTIONS. Transfer at least four small aliquots (about 50 μl.) of the strong ^{210}Po solution to the centers of 2-inch stainless steel planchets and evaporate to dryness at approximately 100° C. Alpha-count long enough to give the appropriate statistical precision. Compare with a standard solution of ^{210}Po, if one is available.

Alternatively, the count rates of the planchets are compared with a National Bureau of Standards ^{210}Po source mounted on a 1-inch Monel disk. The author assumed a 2% correction for backscattering. The results were 2.6% too high as compared to an International Atomic Energy Agency standard solution, which had an estimated uncertainty of ±2%.

PRETREATMENT OF WATER SAMPLE. Filter water sample through a 0.45-micron membrane filter as soon as possible after it is received. Add 2% by volume of concentrated HCl. Store in a polyethylene container. Analyses should be started as soon after receipt of sample as is practicable, because of slow ingrowth of ^{210}Po from ^{210}Pb and ^{210}Bi.

RECOMMENDED METHOD. Add, in increments if necessary, 1020 ml. of the acidified water sample to a Teflon beaker (400 to 1000 ml.) and evaporate in a boiling steam bath. When all the sample has been added and space is available in the beaker, add 50 ml. of the acid mixture and 3.0 ml. of Pb–Bi–Te carrier solution and continue evaporation until essentially only the H_2SO_4 remains. Cool. Add 100 ml. of 1:9 HNO_3 and evaporate overnight in steam bath. While solution is still warm, pour it into a 400-ml. glass beaker containing approximately 1 gram solid H_3BO_3. Transfer to a hot plate and fume gently (200° C.) to remove fluorides. While solution is fuming, oxidize organic matter by adding small amounts of KNO_3. Cool. Rinse Teflon beaker twice with H_2O from a fine-tipped wash bottle and add washings to the glass beaker. Mix and evaporate to remove H_2O. Transfer to hot plate (200° C.) and fume gently to remove HNO_3; cool. Dilute with about 5 ml. H_2O. While the evaporation in the glass beaker is proceeding, add 10 ml. of 1:3 HBr to the Teflon beaker, cover, and warm in steam bath. When the HNO_3 has been evaporated, transfer the contents of the Teflon beaker to the glass beaker, mix, and evaporate on steam bath to remove HBr. (This treatment reduces Te and removes traces of HNO_3.) Transfer to hot plate (200° C.) and fume gently. Cool.

To the beaker, add 67 ml. of 1:3 HCl and warm to dissolve soluble salts. Dilute with 133 ml. of H_2O; heat until solution is complete. In some samples $CaSO_4$ may remain undissolved. If $CaSO_4$ persists, heat nearly to boiling, stir, and continue heating for about an hour. Once the $CaSO_4$ goes into solution, it does not precipitate on cooling. If it persists after the hour of heating, add additional 1*N* HCl and repeat heating process until solution is effected. While solution is very hot (incipient boiling) and while stirring, add 5 ml. of $SnCl_2$ solution in excess of that required to reduce any Fe present as judged by the color change. Cover beaker, digest on steam bath for one hour, and cool in water. Record date and time of this precipitation.

Filter through a 25-mm. membrane filter (0.22-micron). Rinse beaker and funnel once with 1*N* HCl–$SnCl_2$. Do not let filter run dry during filtration. No oxidizing fumes should be in room air. Remove funnel and filter to original precipitation beaker, cover, and set aside until all samples are filtered. Discard filtrate unless ^{210}Pb is to be determined. Dissolve the Te–Po precipitate in 50 ml. of 1*N* HCl–Br_2 by pouring the latter over the funnel. Add 1 ml. of Pb–Bi carrier. Cover beaker, let stand a few minutes, swirl, heat nearly to boiling, and let stand for 15 minutes. Rinse and remove cover, funnel, and membrane filter. Place beaker on steam bath and evaporate contents until dry spot just appears in center of beaker.

Add 33 ml. of 1:3 HCl, cover beaker, heat contents just to boiling, cool, add 67 ml. of H_2O, while stirring add 5 ml. of $SnCl_2$ solution, let stand one hour, filter on a 47-mm. membrane filter (0.22-micron), and wash well as previously described. Do not scrub beaker.

Using tweezers, transfer membrane filter to a 2-inch planchet which has been coated previously with pressure-sensitive adhesive. The filter will lie flat while moist. Use a blunt glass rod to press down the border of the filter at 180°-, 90°-, and 45°-points. Finally, press down the entire periphery by running the glass rod around the edge of the filter. Allow to air-dry for about 2 minutes. Expose the planchet to gaseous NH_3 for 5 minutes in a desiccator containing 1:1 NH_4OH. Dry *gently* under a lamp for 5 minutes. A thermometer, in sample position, read 100° C. Alpha-count in a low-background proportional counter on the following day or later. Correct count rate for background. Record date and time of counting.

Calculate the ^{210}Po concentration in the water sample. Decay correction beyond the first precipitation is complicated by possible presence of other radionuclides which produce ^{210}Po. Decay tables are given in the literature (*11*).

SHORT-CUT METHOD. Add 1000 ml. of water sample (or 1020 ml. of water acidified with 2% by volume of 12*N* HCl) to a 1500-ml. beaker. Add sufficient HCl to make the solution 1*N*. Add 3.0 ml. of Pb–Bi–Te carrier. Add 5 ml. of 20% $NH_2OH \cdot HCl$ solution and let sample stand 10 minutes. Add 20 ml. of 5% H_3BO_3 solution, add 1 ml. (20 drops) of 48% HF, and mix. Add 25 ml. of 10% $SnCl_2$ solution and let stand for 1 hour. Filter on a 47-mm. membrane filter (0.22-micron) and wash with 1*N* HCl–$SnCl_2$ as described previously. Mount and count the filter as directed in the recommended procedure. If the activity is high enough to warrant positive identification, treat the filter as directed in the following paragraph.

WET-ASHING OF MEMBRANE FILTERS. Moisten the filter on the planchet with $CHCl_3$ and transfer it to a 250-ml. beaker; add 10 ml. of 1:1 HCl plus Br and 1.0 ml. of Pb–Bi carrier; evaporate to dryness on a steam bath; add 10 ml. of 1:1 HNO_3; evaporate to dryness on a steam bath; add 10 ml. of 60% $HClO_4$, cover and heat on hot plate (200° C.) until acid just darkens; add HNO_3 drop by drop (or KNO_3) until the acid clears and the dark color disappears; digest on the hot plate for 1 hour; cool, remove cover, and rinse it and sides of beaker with a little H_2O; add 5 ml. of 1:3 HBr and evaporate on steam bath until the $HClO_4$ becomes decolorized and golden crystals appear. Add a few mls. of H_2O and evaporate to $HClO_4$ on steam bath. Add 67 ml. 1:3 HCl, heat nearly to boiling, cool, add 133 ml. of H_2O, and reprecipitate the Te with 5 ml. of 10% $SnCl_2$ solution. Continue as in the previous paragraph. Polonium-210 will not volatilize under the conditions of the wet-ashing, but the result will be low by an average of 1.4% because the second loss on glassware is not compensated for by the standards.

CONCENTRATION OF FILTRATES. Sometimes it is desirable to reduce the volume of the filtrates by evaporation. This can be done if the $SnCl_2$ is oxidized first with Br. Ordinarily, evaporation is not required except when ^{210}Pb is to be determined by ^{210}Po ingrowth.

DECONTAMINATION OF GLASSWARE. Compared to most other radionuclides, ^{210}Po is difficult to remove from glassware. Chromic–sulfuric acid is suit-

able for cleaning filter funnels between samples which do not vary in ^{210}Po content by more than a factor of ten. Glassware and Teflon beakers are cleaned as follows: Arrange the items in a drainable position in a 4-liter covered beaker; use two desiccator plates with feet as supports. Use perforated beakers for rods and other small items. Add concentrated HNO_3 until its level is about 5 mm. below the bottom plate. Boil vigorously until the vapors condense freely on the items and the cover glass. Cool 15 to 20 minutes. Repeat twice. Remove and rinse items.

Table I. Variations in and Reproducibilities of Mounting Techniques

Set no.	Source, treatment, and conditions	No. of replicates	Counting σ^a %	Average deviation from mean %	Range of deviations %
	(Weightless)				
I.	^{210}Po solution, weightless, evap. on planchets, well-centered.	4	1.0	0.5	0.4–0.6
II.	^{210}Po solution (50-λ), weightless, evap. on planchets, well-centered.	4	0.3	1.0	0.2–1.8
III.	Same treatment as II.	4	0.3	2.6	2.0–3.3
IV.	^{210}Pb + ^{210}Bi + ^{210}Po solution, weightless, evap. on planchets, well-centered.	4	0.4	2.1	0.5–4.2
V.	^{210}Po solution, weightless, evap. on planchets, not well-centered.	4	1.0	8.6	7.5–9.6
	(Ponderable: recommended method)				
VI.	^{210}Po separated from ^{210}Pb + ^{210}Bi + ^{210}Po solution by double precipitation, mounted as directed in procedure.	4	0.3	0.9	0.1–1.6
VII.	^{210}Po solution (standards), twice precipitated, mounted as directed in procedure.	4	1.0	1.6	0.6–3.1
VIII.	Same treatment as VII.	4	0.2	0.3	0.2–0.5
IX.	Same treatment as VII.	4	0.07	0.8	0.2–1.7
	(Ponderable: miscellaneous)				
X.	^{210}Po solution + 1 mg. Te (in soln.) evap. on planchets, not well-centered.	4	1.0	2.6	2.0–3.2
XI.	^{210}Po solution, through entire procedure, filtered through fritted glass, Te dissolved and evap. on planchets, not well-centered.	4	1.2	5.3	1.6–9.0
XII.	Same treatment as XI, but used Se instead of Te, Se removed with HBr, not well-centered.	3	1.1	1.1	0.8–1.7

[a] σ for an individual counting.

Table II. Recovery of Polonium-210 from Standards and from Water Samples by Recommended and Short-Cut Methods

Polonium-210 added pc./l.	Approx. σ of counting %	Recovery of polonium-210, %		
			Water samples	
		Precipitated standards	Recommended method	Short-cut method
0.000	10	(0.050 pc./l.)	(0.056 pc./l.)	(0.132 pc./l.)
		(0.035 pc./l.)	(0.033 pc./l.)	(0.132 pc./l.)
0.056	20	92.9	78.6	122.1
		94.6	98.6	107.9
0.186	6	99.5	101.1	109.3
		96.8	93.5	102.5
1.86	2	101.6	102.7	101.9
		100.0	104.8	103.1
18.6	0.6	98.9	100.0	100.0
		101.1	99.5	100.6
163.6	0.2	99.4	101.1	94.8
		99.2	99.6	99.8
		99.6		100.4[b]
		99.8		99.6[b]
				97.4[b]
				97.8[b]
1636	0.07	99.0	97.5	97.2
		101.8	99.7	95.4
		99.9		101.5[b]
		100.0		100.3[b]
				99.9[b]
				98.5[b]
Weighted av.		100.1[a]	98.8	98.8

[a] Standardization of solution included other solutions not shown here.
[b] Boric and hydrofluoric acids not added.

TESTS, RESULTS, AND DISCUSSION

Mounting and Counting. A number of mounting techniques were investigated. The techniques and results are outlined in Table I. Mounting the ^{210}Po with Te on a membrane filter results in a reproducibility which compares favorably with the technique of evaporation of carrier-free ^{210}Po solution. Although no information on self-absorption is given in the table, this was a serious factor in Sets X, XI, and XII. Hence, despite the reproducibility indicated for Set XII, the technique was not considered to be as good as that used in the recommended method.

The fractions of samples obtained in the experimental work can be placed in three categories: (a) the main Te precipitate containing the major portion of the ^{210}Po; (b) the Te precipitate containing the ^{210}Po recovered from filtrates; and (c) the Te precipitate containing the ^{210}Po recovered from the glassware used in the final precipitation and filtration of the main Te precipitate. The main precipitates were counted at least 24 hours no matter what their activities were; precipitates from the other two categories usually were counted 24 hours, but in some cases shorter counting periods were used. Repeated countings with the same planchet-counter combinations showed that other factors affected the high count rates much more than the counting statistics did. At the higher activities, results have been rounded to four digits; this procedure is justified by the statistics of counting but not by the absolute accuracy of the standardization of the ^{210}Po solutions.

Analyses of Samples Containing Added Polonium - 210. Known amounts of ^{210}Po were added, as indicated in Table II, to replicate aliquots of the water sample of the chemical composition shown in Table III and the resulting solutions were analyzed by the recommended and short-cut methods. Duplicate portions of the standard ^{210}Po solutions were doubly precipitated, mounted, and counted. The water originally contained less than 0.02 pc. of ^{210}Po per liter. As judged by the weighted averages, the recoveries from samples are 98.8% by both methods and are 1.3% less than the average of the standards. To within the experimental error, the reproducibilities of the two methods and the standards are equal.

Losses. Obviously, some self-absorption losses occur with samples and standards because of the mass of the counted precipitate. Comparison of the standards and samples in Table II indicates that the average additional

self-absorption loss for samples is not more than 1.3%.

Standards containing 0, 1, and 10 mg. of Bi or Pb, or both, were carried through single and double precipitations to determine the effect of varying the amount of these carriers. The effect was very slight (<1%) if it existed at all.

Polonium-210 losses into the filtrates were determined by slowly adding, with stirring, 20 ml. of Te solution (1 mg./20 ml.) to the filtrates immediately after filtration. An additional 5 ml. of $SnCl_2$ was added if the sample had been heated. The resulting precipitates were analyzed as in the recommended method. The data in Table IV show that occasional losses into the filtrates of up to 2.6% were observed, but, normally, these losses are in the hundredths or thousandths of a per cent. Corresponding samples of the 6-series and 7-series were known to differ only in ^{210}Po content; since losses were much lower in the 7-series, the losses in the 6-series have to be attributed to untested variables such as whether or not the filter ran dry for a significant time, exposure to oxidizing fumes, nonretention by the filter, and other factors. The data in Table IV are not typical; out of 70 filtrates (from water, bone, and interferences tested), only seven showed losses of over 0.1%. Solubility losses at the second (cold) precipitation step are also in the thousandths of a per cent as judged by the results of analyses of composited filtrates.

In spite of the higher dilutions, samples analyzed by the short-cut method showed filtrate losses approximately equal to those in the recommended method.

The physical characterisitcs of the precipitated Te depend greatly upon chemical and physical conditions during its precipitation. A 0.45-micron membrane filter will not always retain the precipitate quantitatively; in fact, a trace of Te sometimes can be observed on a 0.1-micron filter after filtration through a 0.22 micron filter. Unfortunately, organic matter from membrane filters seems to cause losses if the solution is evaporated to dryness prior to the final precipitation. Fine-fritted glass was used for the filtration in the preparation of the ^{210}Po solution, but the recovery was not quantitative.

Polonium-210 losses on the glassware were determined by refluxing the funnel used for final filtration with 1:1 HCl plus Br_2, using the precipitation beaker, cover, and rod. Lead–bismuth–tellurium carrier was added, the acid was evaporated, and the test sample was analyzed as described in the procedure. From Table IV, ^{210}Po losses on the glassware averaged 3.8% with a range of 2.9 to 4.8%; this error is fairly reproducible and is compensated for, somewhat, by the use of standards precipitated and filtered in the same way as the samples. Many other tests were made with essentially the same results. The losses on glassware in the short-cut method were about the same as in the recommended method.

When the precipitate and filter from the short-cut method were wet-ashed and the tellurium was reprecipitated, the average loss of ^{210}Po from 40 samples was 1.4%. This figure is not compatible with that given for the loss on glassware. One explanation is that the $HClO_4$ digestion removes grease from the beaker, thus lowering the tendency of the Te to adhere to the glassware. Also, the final precipitation is done from twice the volume used in the recommended procedure and is done in the presence of $HClO_4$. These factors probably affect the physical characteristics of the precipitate. A noticeable amount of the Te clings to the funnel, the amount depending significantly upon the exact washing technique. The loss can be made fairly reproducible with a little experience.

Effects of Stable Substances. The observation that comparatively large filtrate losses (0.6–2.6%) occurred in samples W-6A, W-6B, W-6E, and W-6F (Table IV) prompted a special series of tests to determine whether or not certain variables influenced the solublity of the ^{210}Po. The individual effects of Fe, Mn, H_2SO_4, $HClO_4$, H_3BO_3, H_3BO_3–HF, solids from the water, and precipitation temperature were investigated. With the exceptions of tests 9 and 10 in Table V, the substance tested was added to ^{210}Po solution carried through the precipitation procedure. The medium was 200 ml. of 1*N* HCl. None of the variables checked had any significant influence on the completeness of precipitation. Furthermore, the results on the 7-series in Table IV indicate no significant losses from samples corresponding to those of the 6-series. However, in the 7-series special attention was paid to the temperature of precipitation, because two of the four samples showing significant losses in the 6-series had been precipitated in Teflon and boiling of these samples was not practical. In the 7-series, corresponding samples were preheated in the steam bath with occasional stirring for an hour prior to precipitation.

Table III. Chemical Analysis of Water Used as Test Sample

Constituent	Milligrams per liter
Calcium	82
Magnesium	28
Sodium	13
Potassium	1.2
Bicarbonate	242
Sulfate	124
Chloride	14
Silica	9
Hardness (as $CaCO_3$)	322
Total dissolved solids	413
Iron^{+3} (added)	5
Manganese^{+2} (added)	5
Sucrose (added)	5
Chlorine (added)	1

Table IV. Losses of Polonium-210 in Filtrates and on Glassware: Standards and Water Samples

Sample no.	Polonium-210, % First filtrate (hot digestion)	Second filtrate (cold digestion)	Glassware Second precipitation (cold digestion)
	(163.6 pc. ^{210}Po in Sample)		
Std-6C	0.02		
Std-6D	0.03		
Std-6X	0.02		
Std-6Y	0.00		
W-6A	0.56		
W-6B	1.63		
W-6C	0.04		
W-6D	0.01		
W-6E	2.39		
W-6F	2.60		
	(1636 pc. ^{210}Po in sample)		
Std-7C	0.001		4.0
Std-7D	0.002	(C, D, X, Y, combined)	3.2
Std-7X	0.000	0.0001	3.4
Std-7Y	0.002		3.5
W-7A	0.001	(A, B combined)	4.5
W-7B	0.003	0.002	4.8
W-7C	0.005		2.9
W-7D	0.006	(C, D, E, F combined)	4.2
W-7E	0.001	0.002	3.1
W-7F	0.11		4.0
			Av. 3.8

Table V. Effects of Various Substances and Factors on Recovery and Solubility of Polonium-210

Test no.	Substances added[a] and conditions	Recovery of polonium-210, % Main precipitate	Filtrate
1	None	103.0	0.06
2	None	100.2	0.005
3	5 mg. Fe^{+3}	102.9	0.006
4	5 mg. Mn^{+2}	102.1	0.003
5	10 ml. conc. H_2SO_4	102.3	0.005
6	1 g. H_3BO_3	100.4	0.02
7	1 g. H_3BO_3, 1 ml. 48% HF, precipitated at boiling temperature	101.3	0.02
8	Same as 7, but precipitated at steam bath temperature	101.9	0.006
9	Solids from 1 liter of test water, evaporated with HCl, then filtered after dilution	100.2	0.02
10	Same as 9, but added 5 mg. Fe^{+3}, 5 mg. Mn^{+2}, 10 ml. conc. H_2SO_4, 1 g. H_3BO_3. (Essentially equivalent to sample ashed and fumed as in recommended procedure.)	99.4	0.03
11	10 ml. 70% $HClO_4$	102.8	0.04

[a] All test samples contained 200 ml. 1*N* HCl and 163.6 pc. ^{210}Po when precipitated first time.

The normal macro constituents of potable water, up to the concentrations shown in the analysis of the test samples (Table III), do not cause significant losses of ^{210}Po. The occasional observed losses are believed to be caused by factors not investigated. It is known, for example, that Te can be lost through oxidation during filtration especially if it is finely divided. With solutions containing essentially Te and ^{210}Po only (second precipitation), no losses into the filtrate were observed.

Samples of very high calcium content may present a solubility problem, but no difficulty was experienced with the samples used in these tests. If $CaSO_4$ does not dissolve after an hour, additional 1*N* HCl is added; large volumes are permissible because of the extremely small ^{210}Po solubility loss. The behaviors of $BaSO_4$ and $PbSO_4$ are discussed in the section on radiochemical interferences.

Elements which are precipitated from acid solution by $SnCl_2$ are rare; the most common one is Se. Selenium can be removed by boiling the original sample or the dissolved Te precipitate with concentrated HBr. Selenium does not interfere with the precipitation of ^{210}Po, but causes low results because of increased self-absorption losses. Water containing significant amounts of Se is not potable.

Radiochemical Interferences. The coprecipitation of ^{210}Po with Te by $SnCl_2$ is unusually selective chemically and radiochemically. Although the data are not presented here, the writer has used the technique on many types of effluents from uranium mills; the decay of the isolated activities could not be distinguished from that of pure ^{210}Po. Similar results for natural water samples have been obtained but the data are not as conclusive, because the relatively low activities involved resulted in larger counting errors.

Approximate minimum decontamination factors for alpha-emitters as determined on uranium mill effluents are: 1600 for ^{226}Ra, 166,000 for ^{238}U or ^{234}U, and 990,000 for ^{230}Th. The decay products of ^{222}Rn up to ^{210}Pb showed no detectable interference.

Other naturally occurring Po isotopes do not interfere seriously because of their short half lives (longest, 3.05 minutes). If samples are counted on the day following the filtration, interference will be negligible. This waiting period is necessary with samples of low activity, so that decay products of ^{222}Rn, filtered from the air, will die out.

Hold-back carriers, other than Pb and Bi, are not needed. Any reasonable amount of $Ba(Ra)SO_4$ which might precipitate in the first precipitation will be redissolved before the second precipitation. In the recommended method, 7.8 mg. of $BaSO_4$ and 400 mg. of $PbSO_4$ will dissolve. Nearly all of the $BaSO_4$ dissolves after the first precipitation, while the $PbSO_4$ dissolves roughly in proportion to the solution volumes at the two precipitation steps.

Sensitivity and Related Subjects. The data presented in Tables II, IV, and V indicate that (a) ^{210}Po is quantitatively precipitated over the entire range of concentrations (0.06 to 1636 pc. per liter) studied and (b) the lower limit of detection is determined by counting statistics, sample size, and the size and reproducibility of the blanks rather than by any failure of the chemical reactions. The lowest activity used in the experiments was taken deliberately to be equal to the anticipated blank.

The blanks could be reduced somewhat by precipitating ^{210}Po from the $SnCl_2$ solution with Te. Two batches of $SnCl_2$ were found to contain 0.03 and 0.09 pc. ^{210}Po per 25 ml. 10% solution. A possible source of ^{210}Po in reagents is distilled water used for preparing them. The likelihood of the occurrence of ^{210}Po in distilled water varies greatly from area to area and from time to time. The ^{210}Po concentration in our distilled or tap water did not exceed 0.02 pc. per liter. Depending upon the chemical treatments used in preparing Te or its compounds, ^{210}Po might or might not be expected to be found in the Te used as a carrier. Precipitation of Te with $N_2H_4 \cdot 2HCl$ should eliminate ^{210}Po (*10*).

Application of Methods. The recommended method is applicable to a wide variety of samples. Provision has been made for the destruction of all but the most resistant organic matter. No assumption as to the form of the ^{210}Po needs to be made other than that its complexes are destroyed by the ashing technique. The method has been used on waters and uranium mill effluents. With minor modifications, it is applicable to urine. Precipitations were successfully carried out when $HClO_4$ was substituted for H_2SO_4. With this change, bone samples can be analyzed also.

The short-cut method is predicated on the assumption that the ^{210}Po is in ionic form and that the water contains no significant interferences. This method is rapid and should find application as a routine screening test where a large majority of the samples pass the test. The minority of questionable samples can be examined further rather easily. The only data pertinent to this method are given in Table II.

Both methods for ^{210}Po in water are sufficiently sensitive to serve as indirect methods for ^{210}Pb.

ACKNOWLEDGMENT

The author is indebted to J. G. Connor and the Inorganic Chemistry Unit of this laboratory for the analysis given in Table III, and to Bernd Kahn for furnishing the IAEA standard ^{210}Po solution.

LITERATURE CITED

(1) Baxter, R., Wood, D., "Apparatus for Plating Out Polonium for Analysis," *Univ. of Rochester At. Energy Project Rept.* **UR-269**, Rochester, N. Y., August 1953.
(2) Black, Stuart C., "Low Level Polonium Determination of Tissue and Urine," *Univ. of Rochester At. Energy Project Rept.* **UR-463**, Rochester, N. Y., October 1956.
(3) Blanchard, R. L., ANAL. CHEM. **38**, 189 (1966).

(4) Code of Federal Regulations, Title 10, Part 20, "Standards for Protection Against Radiation," June 1, 1962.
(5) Eutsler, B. C., Milligan, M. F., Robbins, M. C., "The Determination of Polonium in Urine," *Los Alamos Scientific Laboratory Rept. No.* **LA-1904,** Los Alamos, N. M., April 1955.
(6) Figgins, P. E. (Ed.), "The Radiochemistry of Polonium," *NAS–NS Rept. No.* **3037,** OTS, Department of Commerce, Washington, D. C., 1961.
(7) Fink, R. M. (Ed.), "Biological Studies with Polonium, Radium, and Plutonium," *NNES* **VI-3,** McGraw-Hill, New York, N. Y., 1950.
(8) Frisch, M., Feldman, I., "A Note on Precision Plating of Polonium," *Univ. of Rochester At. Energy Project Rept.* **UR-426,** Rochester, N. Y., February 1956.
(9) National Bureau of Standards, "Maximum Permissible Body Burdens and Maximum Permissible Concentrations of Radionuclides in Air and in Water for Occupational Exposure," Handbook 69, Washington, D. C., June 5, 1959.
(10) Rundo, J., "The Analysis of Biological Samples for Polonium," *AERE* **HP/R-627,** Harwell, England, 1950.
(11) Rushing, D. E., Garcia, W. J., Clark, D. A., "The Analysis of Effluents and Environmental Samples from Uranium Mills and of Biological Samples for Radium, Polonium, and Uranium," Radiological Health and Safety in Mining and Milling of Nuclear Materials, Vol. II, pp. 187–230, *Intern. At. Energy Agency,* Vienna, Austria, 1964.
(12) Scott, R. G., Stannard, J. N., "Modified Procedure for Analysis of Polonium-210 in Biological Materials," *Univ. of Rochester At. Energy Project Rept.* **UR-235,** Rochester, N. Y., March 1953.
(13) Smith, F. A., Della Rosa, R. J., Casarett, L. J., "Analytical and Autoradiographic Methods for Polonium-210," *Univ. of Rochester At. Energy Project Rept.* **UR-305,** Rochester, N. Y., November 1955.

RECEIVED for review December 1, 1965. Accepted March 28, 1966. Mention of trade names is not to be construed as endorsement of the products by the Federal Water Pollution Control Administration.

SCIENTIFIC COMMUNICATIONS

Liquid–Liquid Extraction of Anionic Americium and Europium Complexes of Hydroxyethylethylenediaminetriacetic Acid and Diethylenetriaminepentaacetic Acid

SIR: A number of new liquid–liquid extraction systems (*2*) were recently described, based on the power of various high-molecular-weight amines to extract anionic chelate complexes of many metal ions from aqueous solutions of most organic acids. Several EDTA–amine systems were among the more interesting ones considered to have great potential in separations chemistry. The writer now reports that the anionic chelate complexes of americium and europium with *N*-hydroxyethylethylenediaminetriacetic acid (HEDTA) and diethylenetriaminepentaacetic acid (DTPA) exhibit similar extractability. Interestingly, these very large anions were previously thought to be inextractable. Unlike the EDTA complexes, the DTPA complexes do not sorb readily on anion exchange resins (*1*); no work has been reported for the anion resin behavior of the HEDTA complexes.

EXPERIMENTAL

Apparatus. A NaI(Tl) well-type gamma scintillation counter, 1.75 × 2 inches, was used. Interchangeable aluminum and lead absorbers (1.88 inches high, 0.75-inch o.d., and 0.4-inch i.d.) were used for selective counting.

An internal sample methane flow proportional counter was used.

Reagents. Aliquat 336-S (tricaprylmethylammonium chloride) is a quaternary ammonium chloride available from General Mills, Inc., Kankakee, Ill.

The 20% (w./v.) Aliquat 336-S-Cl-xylene was prepared by dissolving 200 grams of Aliquat 336-S in 1 liter of reagent grade xylene. It was then stored in a glass bottle.

The 20% Aliquat 336-S-DTPA-xylene was prepared by mixing 20% Aliquat 336-S-Cl-xylene for 2 minutes with an equal volume portion of 0.1*M* Na_5DTPA. The aqueous phase was discarded, and the treatment was repeated twice. The organic solution was centrifuged for several minutes and then decanted into a glass bottle for storage.

The 20% Aliquat 336-S-HEDTA-xylene was prepared by mixing 20% Aliquat 336-S-Cl-xylene for 2 minutes with an equal volume portion of 0.3*M* Na_3HEDTA. The aqueous phase was discarded and the treatment was repeated twice. The organic solution was centrifuged for several minutes and then decanted into a glass bottle for storage.

Diethylenetriaminepentaacetic acid pentasodium salt (Na_5DTPA) and *N*-hydroxyethylethylenediaminetriacetic acid trisodium salt(Na_3HEDTA) are

Table I. Liquid–Liquid Extraction of the HEDTA Complexes of ^{241}Am and $^{152-4}Eu$ Tracers with 20% Aliquat 336-S-Xylene Solution

Aqueous phase pH[a]	Solvent	Tracer extracted, % ^{241}Am	Tracer extracted, % $^{152-4}Eu$
	20% Aliquat		
1.7	336-S-Cl-xylene	<1.0	<1.0
2.3		<1.0	<1.0
3.0		7.1	5.8
4.9		20.1	12.1
8.3		65.6	77.9
9.2		67.2	75.6
9.6		67.7	75.9
	20% Aliquat		
3.9	336-S-HEDTA-xylene	30.8	27.8
4.8		50.2	41.7
5.1		53.6	44.6
6.0		79.1	68.1
8.7		94.5	90.1
10.1		91.1	88.9
10.3		84.3	84.9

[a] Each aqueous phase contained 0.013*M* HEDTA before extraction.

Table II. Liquid–Liquid Extraction of the DTPA Complexes of ^{241}Am and $^{152-4}Eu$ Tracers with 20% Aliquat 336-S-Xylene Solution

Aqueous phase pH[a]	Solvent 20% Aliquat	Tracer extracted, % ^{241}Am	Tracer extracted, % $^{152-4}Eu$
1.2	336-S-Cl-xylene	<1.0	<1.0
1.6		<1.0	<1.0
1.8		11.5	8.9
2.2		40.8	36.5
2.3		43.4	39.3
2.6		46.5	42.6
3.7		43.2	39.8
7.7		36.6	37.2
9.9		45.6	39.5
10.2		39.8	35.6
2.5	20% Aliquat 336-S-DTPA-xylene	24.7	22.6
2.9		64.0	61.8
3.2		66.8	62.4
3.5		63.5	59.0
4.2		57.9	53.8
6.2		52.2	48.2
8.6		33.7	32.4
9.3		31.3	29.0

[a] Each aqueous phase contained 0.004*M* DTPA before extraction.

available from The Dow Chemical Co., Midland, Mich.

Procedure. Five milliliters of the indicated aqueous phase was extracted at room temperature with an equal volume portion of the various solvents in 50-ml. heavy-duty glass centrifuge tubes. Two-minute mixing periods were selected arbitrarily. High-speed-motor stirrers equipped with glass paddles were satisfactory for the extractions. After extraction, the tubes were centrifuged in a clinical centrifuge for 2 minutes. Each phase was then analyzed for ^{241}Am and $^{152-4}Eu$ by counting 1-ml. aliquots in a well-type gamma scintillation counter. The weak ^{241}Am gamma ray (0.0596 m.e.v.) is completely absorbed in the lead absorber used while the $^{152-4}Eu$ counting rate is reduced only about one half. Thus, a convenient method for studying the chemistry of these two nuclides simultaneously in the same solution is to count through the aluminum and lead absorbers.

RESULTS AND DISCUSSION

The extractions of americium and europium HEDTA and DTPA complexes with 20% Aliquat 336-S-xylene as a function of pH are shown in Tables I and II, respectively. The listed pH's represent the equilibrium value after extraction. These systems are not necessarily the best but simply indicate the potential of the method. In general, these systems are similar to the EDTA–amine system (*2*) but somewhat less efficient. The americium and europium complexes with HEDTA and DTPA exhibit good extractability, especially from alkaline solution. Because of their greater solubility in acid solution, HEDTA and DTPA probably will replace EDTA in some extraction systems.

It is most surprising that these bulky anionic species extract at all into organic solvents. The fact that the DTPA complexes do not sorb readily on anion exchange resins is probably related to problems inherent in the diffusion of very large ions into resin beads. Very little work has been done in this area.

It is anticipated that other actinide, lanthanide, and metal ions in general will be extractable in these HEDTA and DTPA systems; indeed, it seems probable that the phenomenon will apply to most aminopolycarboxylic acid systems. Separations based on differences in metal stability constants and ionic radii and on amine class and organic diluent are under investigation. Detailed studies in this promising area will be reported in the near future.

ACKNOWLEDGMENT

The author gratefully acknowledges the capable assistance of G. I. Gault in the experimental work.

LITERATURE CITED

(1) Baybarz, R. D., Oak Ridge National Laboratory, *Unclassified Rept.* **ORNL-3739**, 7 (1965).
(2) Moore, F. L., ANAL. CHEM. **37**, 1235 (1965).

FLETCHER L. MOORE
Oak Ridge National Laboratory
Oak Ridge, Tenn.

RECEIVED for review February 16, 1966. Accepted March 28, 1966. Research sponsored by the U. S. Atomic Energy Commission under contract with the Union Carbide Nuclear Corp.

Spectrophotometric Determination of Tertiary Aromatic Amines in the Presence of Primary and Secondary Amines by Complexation with Tetracyanoethylene

SIR: Few colorimetric or spectrophotometric methods are available for the selective determination of a given tertiary aromatic amine in the presence of primary and secondary aliphatic or aromatic amines. The 3-methyl-2-benzothiazolone hydrazine method of Sawicki, Stanley, Hauser, Elbert, and Noe (*10*) can be applied to tertiary aromatic amines but it also measures primary and secondary aromatic amines as well. The same can be said for the 4 - azobenzenediazonium fluoroborate method of Sawicki, Noe, and Fox (*9*); however, these authors did show that acetic anhydride could prevent the interference of primary and secondary amines in the colorimetric determination of *N,N*-dimethylaniline. The Lauth reaction using PbO_2 as employed by Jan, Kolsek, and Perpar (*8*) also determines all three classes of aromatic amines. Specific methods for individual tertiary aromatic amines are available: the Fujiwara reaction, for example, is used for the determination of pyridine (*8*). Methods of this type cannot be applied to the determination of other tertiary amines, however.

Studies of the molecular complexes of tetracyanoethylene (TCNE) (*5, 11*) and the use of TCNE by Peurifoy and Nager (*7*) for the estimation of many amines on paper suggested that TCNE might be used for the determination of tertiary aromatic amines. The very high molar absorptivity (ϵ = 10,500) of the pyridine –TCNE complex (*5*) and other TCNE complexes indicates that the absorption of light causes a charge-transfer type of electronic transition. However, it does not appear to be clearly established (*1*) whether complexation of a tertiary aromatic amine in the ground state involves the nonbonding electrons on nitrogen (*n* donor) or the π electrons of the aromatic ring (π donor). Some evidence indicates that *N,N*-dimethylaniline and pyridine function as *n* donors toward iodine (*1*), a markedly different acceptor than TCNE.

The most serious analytical problem is that some tertiary aromatic amines and most primary and secondary amines tend to react with TCNE to give colored 4-substituted or *N*-substituted tricyanovinyl derivatives (*4*). The reaction with *N,N*-dimethylaniline is:

$$C_6H_5NMe_2 + (NC)_2C{=}C(CN)_2 \rightarrow HCN + (NC)_2C{=}C(CN){-}C_6H_4NMe_2 \quad (1)$$

Fortunately this reaction is base-catalyzed (*4*) and its rate is negligible in weakly acid solution during analytical measurements. The complexation and reaction of TCNE with primary and secondary amines can be drastically reduced by acetylation (*11*). The use of acetic anhydride raised the question of whether the anhydride would interfere by complexing the tertiary amine as follows:

$$R_3N: + \underset{\displaystyle Me}{\overset{\displaystyle O}{\overset{\|}{C}}}{-}O{-}\underset{\displaystyle Me}{\overset{\displaystyle O}{\overset{\|}{C}}} \rightleftharpoons R_3N: \rightarrow \underset{\displaystyle Me}{\overset{\displaystyle O}{\overset{\|}{C}}}{-}O{-}\underset{\displaystyle Me}{\overset{\displaystyle O}{\overset{\|}{C}}} \quad (2)$$

Such a complex has been detected by physical measurement in mixtures of acetic anhydride and the aliphatic amine triethylenediamine, but not in anhydride–pyridine mixtures (*13*). Such complexation would certainly be deleterious if the tertiary amine acted as an *n* donor.

The method described below was designed to determine a given tertiary aromatic amine in the presence of primary and secondary amines after acetylation of the latter at different concentrations of acetic anhydride, using TCNE. An alternate reagent, 2,4,7-trinitrofluorenone (TNF) was also investigated since TNF complexes more strongly with large ring aromatic amines (*12*), even in the presence of excess perchloric acid.

EXPERIMENTAL

Apparatus. These determinations were carried out using a Beckman DB Spectrophotometer with 1.0-cm. cells and a Bausch and Lomb Spectronic 20 colorimeter using 1.17-cm. cells.

Reagents. Tetracyanoethylene (TCNE) was obtained from the Eastman Kodak Co. and was sublimed at 120° C. under vacuum to obtain a white solid which was stored in a desiccator over sodium hydroxide pellets. Since it is used in large excess, TCNE need not be sublimed for routine work. For careful work, a reagent blank should be used to set 100% T.

TCNE solutions were saturated solutions in methylene chloride. The concentration is about 0.09 to 0.1*M* after heating (*11*). The solutions were used for 1 to 2 weeks. If the solution was not colorless, a reagent blank was used to set 100% T for careful work.

Acetic anhydride and methylene chloride were reagent grade. Aromatic amines and phenols were Eastman White Label or comparable quality.

Procedure. TERTIARY AROMATIC AMINES IN PRESENCE OF PRIMARY AND SECONDARY AMINES. The sample is weighed accurately into a 25-ml. or larger volumetric flask and dissolved in methylene chloride. From this is taken a 1- to 20-ml. aliquot containing about 5×10^{-3} mmoles of tertiary amine (see Table I for exact values). The aliquot is transferred to a 50-ml. volumetric flask. Two ml. of acetic anhydride is added to the flask for every estimated 5×10^{-3} mmoles of primary or secondary amine. The flask is shaken and allowed to stand for 5 minutes. (Fifteen minutes acetylation time was allowed for 2,5-dimethylpiperazine.) A two- or threefold excess of TCNE is added by pipetting 5 ml. of saturated TCNE solution into the flask, giving a final TCNE concentration of about 0.009 to 0.01*M*. (More TCNE may be added in the case of weakly colored π complexes.) The solution is diluted to 50 ml. with methylene chloride and allowed to stand for 10 to 25 minutes, or until the optimum absorbance is reached.

(In the case of pyridine, color development is slower and dependent on temperature. The calibration curve should be controlled within ±0.5° C. Different calibration curves were obtained by measurements after 35, 75, and 120 minutes at 24° and 26° C. with higher sensitivity at higher temperatures and longer times. Readings were more stable after 35 minutes than those obtained after 10 minutes. The determination of pyridine in the presence of aniline and similar amines is limited to equimolar concentrations to avoid upward curvature of the calibration curve in the initial portion of the curve.)

The absorbance is determined at the appropriate wavelength (Table I) and the concentration is read from a standard curve prepared from known concentrations of the tertiary amine containing acetic anhydride at the same concentrations used for the unknowns.

TERTIARY AROMATIC AMINES IN PRESENCE OF PHENOLS BY EXTRACTION. The sample is weighed accurately into a volumetric flask and dissolved in pentane, preferably, or less preferably in pentane–methylene chloride or methylene chloride alone. From this is taken an aliquot of 1 to 5 ml. containing no more than 2 ml. of methylene chloride, to avoid water pickup in the extraction. The aliquot should contain about 1×10^{-3} mmole of tertiary aromatic amine and no more than 0.1 mmole of phenol. The aliquot is transferred to a 50- to 100-ml. separatory funnel, 10 ml. of 10% aqueous sodium hydroxide is added and contacted for 30 seconds, and 10 ml. of dry pentane is added and contacted for one minute. The aqueous layer is withdrawn, and the sides of the funnel are rinsed twice with 2-ml. portions of pentane. Any aqueous layer collected is then withdrawn. The contents of the funnel is emptied into a 50-ml. volumetric flask, and the funnel is rinsed twice with 2-ml. portions of pentane. (Some problems with water carryover were avoided by pouring the pentane out of the top of the funnel occasionally.) The total volume of the solution at this point should be no more than 23 ml. to permit addition of sufficient methylene chloride to keep TCNE in solution.

If no primary or secondary amine is present, 10 ml. of saturated TCNE in methylene chloride is added, and methylene chloride is used to dilute to volume. The absorbance is read at the appropriate wavelength (Table I). A standard curve is prepared using the same proportions of pentane and methylene chloride as used in the unknown extraction and dilution procedure.

N,N-dimethylaniline and carbazole were determined in this manner in the presence of 2,6-dimethoxyphenol, *p*-methoxyphenol, *tert*-amylphenol, and Shell "Ionox R" polyringed phenol. Heterocyclic amines such as pyridine required a higher concentration of sodium hydroxide—i.e., 25% aqueous solution—to ensure proper extraction.

WEAKLY BASIC AMINES: DETERMINATION WITH 2,4,7-TRINITROFLUORENONE. Weakly basic amines were determined by dissolving the appropriate amount of sample (Table II) in 0.1*M* perchloric acid–triethyl phosphate solvent (*12*) and adding a 1- to 4-ml. aliquot to 126 mg. of purified 2,4,7-trinitrofluorenone (*12*) in a 5-ml. volumetric flask. The solution was diluted to the mark with 0.1*M* perchloric acid–triethyl phosphate, and the absorbance was read on the Spectronic 20 at 450 mμ. A standard curve is prepared in the same manner.

RESULTS AND DISCUSSION

Solvent Effects. The best experimental results were obtained using methylene chloride as the solvent medium. In the procedure involving extraction of phenols, a mixture of methylene chloride and pentane, not to exceed 45% pentane, was found satisfactory. In general, chlorinated hydrocarbons were preferable to oxygenated or highly polar solvents inasmuch as the latter tended to promote tricyanovinylation of the aromatic amines by TCNE.

Methylene chloride also dissolves up to 0.1*M* TCNE as well as the required experimental level of most aromatic amines and phenols, even those of molecular weight in excess of 500.

Analysis for Tertiary Amines. As shown in Table I, various types of tertiary aromatic amines can be determined by complexation with TCNE. Carbazole, a weakly basic secondary aromatic amine, is unreactive toward acetic anhydride, and can also be determined in the presence of other primary and secondary amines. Apparently the same is true for benzidine. Although 1,10-phenanthroline absorbs ultraviolet light at 310 mμ, its molar absorptivity (*2*) is only one fourth that of the TCNE-1, 10-phenanthroline complex absorbance peak. Beer's law was obeyed for the amines in Table I from the stated lower limit of concentration to a concentration at least seven-fold greater than this limit.

Comprehensive absorbance data in Table I give the minimum level of amine that can be determined in up to 0.4*M* acetic anhydride, where the total primary and secondary aromatic amine interferences are at least equimolar. It should be mentioned here that the complexes of TCNE and aliphatic amines and their decomposition products are only slightly colored so that their interference may be considered minimal above 400 mμ. However, the complexes and the *N*-tricyanovinylamines (*4*) exhibit rather intense absorption bands in the ultraviolet so that if such interference is suspected, a control determination should be undertaken. Tetracyanoethylene itself exhibits considerable absorption at 252 and 244 mμ in methylene chloride.

Concentration of Acetic Anhydride. Although no greater than 1.2 molar acetic anhydride masking agent was found necessary in the room temperature acetylation of primary and secondary amine interferences at equimolar concentrations, excessive quantities (1.6*M*) were found to cause a hypochromic shift. The same effect was observed with a concentration of greater than 45% pentane in methylene chloride in the final solution of amine after the extraction of phenolic interferences. No greater than a tenfold excess of primary and secondary aromatic amine was present at the lower limit of absorbance readings.

Systems of unknown interferences were investigated by plotting total absorbance *vs.* specific increments of anhydride in 0.03*M* TCNE and methylene chloride. In the case of a pure tertiary aromatic amine mixed with primary and

Table I. Lower Limit of Detection of Tertiary Amines

0.01*M* TCNE, 0.4*M* Ac_2O in CH_2Cl_2, A = 0.10

Tertiary amine	Detected by TCNE, *M*; wavelength, mμ	Molar absorptivity[a] of final solution
Triphenylamine	1.6×10^{-4} (342)	7×10^{2}
Pyridine	2×10^{-3} (400[b])	5×10^{1}
2,5-Dimethylpyrazine	5×10^{-4} (460)	2×10^{2}
N,N-Dimethylaniline	8×10^{-4} (640)	1.5×10^{2}
1,10-Phenanthroline	2.9×10^{-5} (310[c])	3.5×10^{3}
Carbazole	1×10^{-3} (600[d])	1×10^{2}
Carbazole–TNF[e]	2×10^{-5} (450)	5×10^{3}
Benzidine	1×10^{-5} (440)	1×10^{4}

[a] These molar absorptivities are the slopes of the Beer's law plots, not the true molar absorptivities as determined by the Benesi–Hildebrand method (*5*).
[b] Measured after 75-minute reaction at 26° C.
[c] The molar absorptivity of 1,10-phenanthroline alone at 310 mμ is 850 (*2*).
[d] Triethyl phosphate solvent.
[e] 0.011*M* TNF in triethyl phosphate solvent.

Table II. Determination of Weakly Basic Amines

0.08*M* TNF, 0.1*M* $HClO_4$–$(EtO)_3PO$ solvent, 450 mμ

Amine	Agreement with Beer's law: Concentration range[a]	Molar absorptivity of final solution
Carbazole	2 to 8 $\times 10^{-4}M$	210
Diphenylamine	0.4 to 2 $\times 10^{-2}M$	10
Triphenylamine	0.3 to 2 $\times 10^{-2}M$	14

[a] The lower figure corresponds to A = 0.05 on the Bausch-Lomb Spectronic 20 colorimeter.

secondary aromatic amine, this curve approaches the absorbance of the tertiary amine-TCNE complex at its absorbance peak.

Acetylated primary and secondary aromatic amines investigated showed essentially 100% transmittance at the absorbance peak of the unacetylated amine–TCNE complex. Any variance in this respect for practical systems may be effectively eliminated by employing a methylene chloride–anhydride-TCNE blank.

It was also found that some tertiary aromatic amines such as 2,5-dimethylpyrazine and 3-picoline exhibited such low molar absorptivities that their TCNE complexes could be effectively masked by a 1.6*M* acetic anhydride. These amines did not interfere with the determination of amines such as *N*,*N*-dimethylaniline. It is possible that complexation of 2,5-dimethylpyrazine and 3-picoline by acetic anhydride (as in Equation 2) prevents these amines from acting as *n* donors (or possibly π donors) towards TCNE, thus masking them. *N*,*N*-dimethylaniline is too hindered to be strongly complexed even by 1.6*M* anhydride and will therefore form a colored complex readily with TCNE. Obviously all the tertiary amines studied, including 2,5-dimethylpyrazine and 3-picoline, are not strongly complexed by 0.4*M* anhydride and can complex with TCNE in the presence of 0.4*M* anhydride.

Effect of Time. Although the colors of these complexes darkened over a period of a day, measurements made within an interval of 10 to 30 minutes after adding TCNE were reproducible and conformed to Beer's law over the concentration ranges studied. Temperatures above 24° to 25° C. tended to shorten this 20-minute interval, especially at the lower concentration limits.

N,*N*-dimethylaniline is known to condense with TCNE to give the deep red 4-tricyanovinyl-*N*,*N*-dimethylaniline (Equation 1) with a peak at 515 mμ. However, it does so rapidly only in basic solvents such as dimethylformamide at 50° to 60° C. (*4*). In acid solution and at room temperature, it forms a blue complex with TCNE with a peak at 640 mμ. The presence of acetic acid in the acetic anhydride used will retard this reaction long enough for the complex to be measured accurately.

The slow increase in absorbance of the pyridine–TCNE system is noteworthy because it was apparently stable enough for its stability constant and molar absorptivity to be measured by Benesi-Hildebrand plots in methylene chloride (*5*). First, 0.4*M* acetic anhydride did cause a 7% decrease in the absorbance of a typical TCNE–pyridine mixture in methylene chloride. This possibly indicates an interaction of anhydride and pyridine (Equation 2). Secondly, whether anhydride was present or not, the absorbance of a typical mixture nearly doubled after standing 35 minutes as compared to the initial absorbance. Fortunately, after 75 minutes, the increase is slow enough to permit accurate analysis.

Table III. Determination of Tertiary Aromatic Amines in the Presence of Primary and Secondary Amines

0.02*M* TCNE + 3° Amine, *M*	1° and 2° Amines, *M*	Absorbance 1° + 2°*N*	Absorbance no 1° or 2°*N*	Molar absorptivity of final soln.
N,*N*-Dimethylamine 1.8×10^{-3}	9.2×10^{-3a}	0.33	0.33	1.8×10^{2}
Pyridine 2.5×10^{-3}	9.2×10^{-3a}	0.17	0.17	6.8×10^{1}
2,5-Dimethylpyrazine 4.6×10^{-3}	9.2×10^{-3a}	0.32	0.32	7.0×10^{1}
N,*N*-Dimethylaniline 2×10^{-3}	7.8×10^{-3b}	0.25	0.25	1.2×10^{2}
Triphenylamine 4×10^{-4}	1.6×10^{-4b}	0.26	0.26	6.5×10^{2}
1,10-Phenanthroline 6×10^{-6}	1.6×10^{-4b}	0.20	0.20	3.3×10^{3}

[a] Mixture contains 2,6-diethylaniline, *N*-methylaniline, and diphenylamine. Final *M* of Ac_2O is 0.4*M*.
[b] Mixture contains 2,5-dimethylpyrazine, 2,5-dimethylpiperazine, aniline, and 3-picoline. Final *M* of Ac_2O is 1.2*M*.

Table IV. Determination of Tertiary Aromatic Amines after Extraction from Phenols

75% CH_2Cl–25% pentane solvent, 0.02*M* TCNE

3° Amine	Phenol interference	Absorbance Extracted	Absorbance No phenols
N,*N*-Dimethylaniline, 0.001*M*	Mixture,[a] 0.001*M*	0.578	0.584
Carbazole,[b] 0.005*M*	2,6-Dimethoxyphenol, 0.002*M*	0.260[c]	0.253

[a] 2,6-Dimethoxyphenol, *p*-methoxyphenol, and *tert*-amylphenol.
[b] Solvent was 75% $(EtO)_3PO$–25% pentane.
[c] The absorbance of the carbazole–2,6-dimethoxyphenol before extraction was 0.97.

Analysis of Amine Mixtures. Table III gives data for the determination of various tertiary amines in the presence of primary and secondary aromatic amines. These amines react rapidly with acetic anhydride at room temperature and are converted to amides which complex only slightly with TCNE. In some cases, a five-fold molar excess of primary and secondary amines could be tolerated after acetylation.

Primary and secondary aliphatic amines are better nucleophiles than aromatic amines and acetylate more rapidly at room temperature. Although they were not tested as interferences, it is apparent from their lack of interferences with the π complexation of TCNE and phenols in acetic anhydride (*11*) that a two-fold excess of these amines can be tolerated without error. Tertiary aliphatic amines interfere with the above complexation and presumably would interfere in this method also. Phenols react very slowly with acetic anhydride at room temperature and would interfere to varying degrees with the determination of tertiary aromatic amines.

Analysis of Amine–Phenol Mixtures. Since acetic anhydride will not prevent phenols from interferring with this method, extraction of phenols with sodium hydroxide was attempted. The extraction scheme worked best with pentane and 10% aqueous sodium hydroxide, leaving the tertiary aromatic amine in the pentane layer. Methylene chloride was added in sufficient quantity to the pentane to keep TCNE in solution.

The extraction procedure was applied of the determination of *N*,*N*-dimethylaniline and carbazole after extraction of various phenols. Table IV shows the results of these determinations. Beer's law was obeyed by the extracted samples.

Since water hydrolyzes TCNE, any water carry-over into the pentane layer would be a possible source of error. Although the experimental data appeared to show no such error, the water level in the pentane was determined by the Karl Fischer method according to the modification of Peters and Jungnickel (*6*). The water concentration was found to be 1.5 p.p.t., corresponding to an error of 0.002 absorbance units.

Weakly Basic Aromatic Amines. TNF has been found to complex more strongly than TCNE with amines and aromatic hydrocarbons having

effectively three or more fused rings (*12*)—e.g., carbazole, diphenylamine, etc. It has also been observed that 0.1*M* perchloric acid–triethyl phosphate solvent prevents complexation of TNF and moderately basic amines but does not prevent complexation of TNF and weakly basic amines like carbazole and diphenylamine (*12*). This suggested a very selective method for determining those amines in the presence of more basic primary, secondary, or tertiary amines. (TNF was used because this phenomenum was not observed with TCNE.)

As shown in Table II, carbazole, diphenylamine, and triphenylamine can be colorimetrically determined over the concentration ranges listed. Previous work (*12*) has already established that amines such as β-naphthylamine, pyridine, and triethylamine should not interfere with this determination. In addition, the interference of 1,10-phenanthroline and quinoline was tested. When present at 0.01*M* levels, neither of these amines caused an increase in absorbance of more than 0.03 units in the absorbance of a solution of TNF–diphenylamine.

LITERATURE CITED

(1) Andrews, L. J., Keefer, R. M., "Molecular Complexes in Organic Chemistry," pp. 18–19, Holden-Day, San Francisco, 1964.
(2) Badger, G. M., Pearce, R. S., Pettit, R., *J. Chem. Soc.* **1951**, 3199.
(3) Jan, J., Kolsek, J., Perpar, M., *Z. Anal. Chem.* **153**, 4 (1956).
(4) McKusick, B. C., Heckert, R. E., Cairns, T. L., Coffman, D. D., Mower, H. T., *J. Am. Chem. Soc.* **80**, 2806 (1958).
(5) Merrifield, R. E., Phillips, W. D., *Ibid.*, **80**, 2780 (1958).
(6) Peters, E. D., Jungnickel, J. L., ANAL. CHEM. **27**, 450 (1955).
(7) Peurifoy, P. V., Nager, M., *Ibid.*, **32**, 1135 (1960).
(8) Ploquin, *Bull. Soc. Chim. France* **1947**, 700.
(9) Sawicki, E., Noe, J. L., Fox, F. T., *Talanta* **8**, 257 (1961).
(10) Sawicki, E., Stanley, T. W., Hauser, T. R., Elbert, W., Noe, J. L., ANAL. CHEM. **33**, 722 (1961).
(11) Schenk, G. H., Santiago, M., Wines, P., *Ibid.*, **35**, 167 (1963).
(12) Schenk, G. H., Vance, P. W., Pietandrea, J., Mojzis, C., *Ibid.*, **37**, 372 (1965).
(13) Schenk, G. H., Wines, P., Mojzis, C., *Ibid.*, **36**, 914 (1964).

GEORGE H. SCHENK
PETER WARNER
WILLIAM BAZZELLE

Department of Chemistry
Wayne State University
Detroit, Mich. 48202

PRESENTED in part at the 12th Anachem Conference, October, 1964. Work supported by Public Health Research Grant GM-07760 from the National Institutes of Health.

Mercurimetric Determination of Organic Disulfides Using Reaction with Butyllithium

SIR: Disulfides are usually estimated by reduction to thiols—e.g., with zinc (*1*), sodium borohydride (*3*) or lithium aluminium hydride (*2*)—followed by estimation of the thiols produced (2 moles per mole of disulfide). For the estimation of thiols, titration with *o*-hydroxymercuribenzoate (HMB) in the presence of thiofluorescein as indicator is extremely well suited (*4*) and the presence of zinc ions does not interfere when excess of EDTA is added.

A drawback of the methods of reduction suggested is that the reduction is carried out in acid solution or the excess of reductor has to be destroyed by acidification, and this means that serious errors may be introduced by evaporation for low-boiling members of the series.

By using butyllithium as the active agent this source of error is eliminated, as the reaction of the solution is kept alkaline all through the estimation.

From the equation

$$RS—SR + C_4H_9Li \rightarrow RSC_4H_9 + RSLi \quad (1)$$

it is seen that 1 mole of thiol is produced per mole of disulfide and at the same time 1 mole of a thioether is formed.

Unfortunately the butyllithium is not quite indifferent toward thioethers and to some extent the reaction

$$C_4H_9Li + RSR \rightarrow C_4H_9R + RSLi \quad (2)$$

may take place. This reaction is, however, very slow in comparison with reaction 1 and usually the quantitative conversion of disulfide according to 1 can be performed without any remarkable interference of 2.

As examples it may be mentioned that after 60 seconds at 70° C. the determination of methyl disulfide results in 107% recovery, of ethyl disulfide in 102% and of benzyl disulfide in 120% recovery. From Table I it is seen that for the estimation of these three disulfides the temperatures of 25° C., 40° C., and 15° C., respectively, are recommended, so that even for benzyl disulfide the influence of reaction 2 is negligible.

The rate of reactions 1 and 2 depends on the reaction compounds. Some disulfides are quickly converted at room temperature, others need short heating for quantitative conversion. Moreover, the rates of reactions 1 and 2 are somewhat parallel—e.g., dimethyl disulfide is converted very readily at room temperature according to reaction 1 without any interference of reaction 2, but at higher temperature the interference of reaction 2 between butyllithium and methyl butyl thioether becomes noticeable. On the other hand, isopropyl disulfide reacts quantitatively with butyllithium only at elevated temperatures. For these reasons it may be difficult to determine the sum of two different disulfides—e.g., the two mentioned, in the same sample. Of course the sum of disulfides of similar reactivity to butyllithium can be estimated without difficulties.

Aromatic disulfides—e.g., phenyl disulfide—react readily according to

Table I. Determination of Organic Disulfides

Disulfide	Reaction with butyllithium: Time, sec.	Temp., ° C.	Taken, mg.	Errors, %	Average recovery, %
Methyl	30	25	1-12	−0.7, +0.6, −1.1, −0.4, −0.8	99.5
Ethyl	60	40	2-12	−0.8, +0.4, −0.6, −0.9, −1.1	99.4
Butyl	60	70	5-25	−0.9, −0.1, −0.6, −0.5, −0.4	99.5
Isopropyl	60	70	5-25	−0.8, 0.0, −0.7, −0.5, +0.4	99.7
Phenyl	60	25	5-25	−1.1, −0.8, −0.6, −1.4, −0.5	99.1
Benzyl	10	15	8-40	+0.2, +0.6, −0.4, 0.0, +0.5	100.2
Trimethylene (1,2-dithiolane)	60	70	4-12	−1.6, −1.7, −1.2, −1.5, −1.6	98.5

reaction 1 and no interference of reaction 2 could be stated either at room temperature or at elevated temperatures.

EXPERIMENTAL

Reagents. Commercially available 6*N* butyllithium in hexane and sodium *o*-hydroxymercuribenzoate (HMB) 0.01*N* are used. Dissolve 3.2 grams of *o*-hydroxymercuribenzoic anhydride in 20 ml. of 1*N* sodium hydroxide and dilute to 1000 ml. with 50% aqueous ethanol. The normality is calculated from the weight of the anhydride.

Indicator. A solution of thiofluorescein in 0.5*N* ammonia in 50% aqueous ethanol is prepared. The blank value of the indicator should be not more than 0.05 ml. of 0.01*N* HMB per 1 ml. of the indicator solution.

Procedure. A sample of organic disulfide is dissolved in 10 ml. of dry benzene and treated with 0.5 ml. of 6*N* butyllithium, the time and temperature being chosen according to the disulfide in question (see Table I). Then 15 ml. of ethanol cooled in ice are added and the solution is titrated with 0.01*N* HMB in the presence of thiofluorescein (1 ml.) indicator until the blue color disappears.

The results are summarized in Table I.

DISCUSSION

Three possible sources of error must be taken into account, *viz.*: the incomplete reaction with butyllithium, the oxidation of thiols by oxygen, and the decomposition of thioethers.

At room temperature the conversion of such disulfides as butyl disulfide could not be carried out with higher recovery than 97%, because the increase of the time of reaction increases the oxidation. In spite of the fact that the disulfide produced by oxidation will react with butyllithium again the thiol content will decrease. Possibly butyllithium, being readily oxidized itself, causes the co-oxidation of thiols. In as short time as one minute the oxidation is negligible at room temperature as well as at elevated temperature.

LITERATURE CITED

(1) Ashworth, M. R. F., "Titrimetric Organic Analysis," part II, pp. 669–81, Interscience, New York-London-Sydney, 1965.
(2) Porter, M., Saville, B., Watson, A. A., *J. Chem. Soc.* **1963**, p. 346.
(3) Stahl, C. R., Siggia, S., ANAL. CHEM. **29**, 154 (1957).
(4) Wrónski, M., *Wiadomosci Chem.* **17**, 1 (1963).

STIG VEIBEL
MIECZYSLAW WRÓNSKI[1]
Department of Organic Chemistry
Technical University
Copenhagen, Denmark

M.W. is indebted to the Danish Ministry of Education for financial support during this work.

[1] Permanent address: Department of Chemical Technology, University of Lódź, Poland.

Spectrophotometric Determination of Copper in Lead, Tin, Aluminum, Zinc, and Their Alloys with Biscyclohexanone Oxalyldihydrazone

SIR: The amount of copper contamination in lead-base and tin-base alloys is of considerable metallurgical interest, particularly in type metals in which only small amounts of copper, not more than 0.13%, can be tolerated because of its effect in forming crystals enriched with copper during the pouring of the types. The production of copper-free lead—e.g., for the manufacture of sheet, pipes, and shot—necessitates close control of the decopperization process. Furthermore, the alloying amounts of copper in bearing metals, tin and its alloys, aluminium and its alloys, and zinc and its alloys meet narrow specification ranges which call for a reliable and sufficiently fast method for the determination of copper in the wide range of 0.05 to 10%.

Neocuproine (2,9-dimethyl-1,10-phenanthroline) (*2*) and sodium diethyldithiocarbamate (*5*) have been recommended for the absorptiometric determination of copper in a variety of materials, but both involve extraction of the copper–organo complex. The recommended method of the American Society for Testing Materials (*1*) involves the use of hydrogen bromide while photometric measurement is taken; it is generally considered as being tedious.

Publications describing the use of biscyclohexanone oxalyldihydrazone in the determination of copper, first suggested by Nilsson (*4*) and later applied to the examination of plant material (*8*), paper (*7*), steel (*3*), and titanium and zirconium alloys (*9*) suggested, because of a large number of noninterfering elements, a possible application to the determination of copper in lead-base alloys and nonferrous alloys generally.

To provide a suitable method for a wide variety of nonferrous metals and their alloys, the biscyclohexanone oxalyldihydrazone procedure has been investigated.

EXPERIMENTAL

Reagents. Hydrogen bromide–bromine mixture. To 180 ml. of hydrogen bromide, add 20 ml. of bromine.

Perchloric acid, 70–72% w./w. Sulfuric acid, 5*N*. Ammonium citrate solution, 20%. Neutral red indicator solution, 0.05%. Sodium hydroxide solution, 10%.

Sodium borate buffer solution. Dissolve 15.45 grams of boric acid in 400 ml. of water and dilute to 500 ml. (solution A). Dissolve 2.0 grams of sodium hydroxide in 90 ml. of water and dilute to 100 ml. (solution B).

To 400 ml. of solution A, add 60 ml. of solution B and mix.

Biscyclohexanone oxalyldihydrazone solution, 0.5%. Dissolve 0.5 gram of the reagent in 100 ml. of ethanol–water mixture (4:3).

Procedure. In general, the procedure as given under Calibration Graph for preparation of the sample solution can be followed.

Calibration graphs covering the ranges 0.003 to 2.0% using appropriate aliquots of a standard copper nitrate solution were identical with those in the presence of the major alloying metals of lead-base, tin-base, aluminum-base, and zinc-base alloys. Tests have shown that the method can be successfully extended to the determination of up to 10% of copper by using a smaller sample weight.

The addition of reagents, noting subsequent color development, and measurement of absorbance have been followed in all cases exactly as given under Absorption.

A 5.0-ml. aliquot of the filtered sample solution has been used throughout the investigation.

ABSORPTION. High purity copper (0.25 gram) was dissolved in 20 ml. of diluted nitric acid (1:1) and the solution boiled for 3 minutes to expel nitrous fumes. It was then cooled, transferred to a 1-liter volumetric flask, and diluted to the mark with distilled water. A 20-ml. aliquot of this solution was then diluted to 500 ml., so that 1 ml. contained 0.01 mg. of copper.

Diluted copper solution (1.5- and 15-ml. portions) was added to two 50-ml. volumetric flasks; 10 ml. of distilled water were added to a separate 50-ml. volumetric flask to serve as a reference solution (blank). To each flask were added 10 ml. of 20% ammonium citrate solution and 2 to 4 drops of 0.05% neutral red indicator solution. A 10% sodium hydroxide solution was then added from a buret until the color of the solution changed from red to yellow; then 1 ml. was added in excess. A 50-ml. capacity semiautomatic buret with plastic reservoir and spring-loaded rub-

ber valve (Dr. Schillings-Burette, Jena GMBH, Mainz, West Germany) was found to be most satisfactory for adding the sodium hydroxide solution. A 5-ml. portion of a sodium borate buffer and 2 ml. of 0.5% biscyclohexanone oxalyldihydrazone in ethanol-water (4:3) were added. After 3 minutes, a suitable portion of the reference solution was transferred to an absorption cell, the spectrophotometer (Unicam SP 600) adjusted, and the absorbance measured in 4-cm. and 1-cm. cells, respectively. Measurements, made at wavelengths between 560 and 640 mμ, confirmed (7) that the maximum absorbance is at 595 mμ.

CALIBRATION GRAPH. Three calibration curves were prepared by transferring appropriate portions of the standard copper nitrate solution into 50-ml. volumetric flasks and reagents added in accordance with the procedure described in Absorption, so that the graph is suitable for amounts of copper in the range 0.003 to 0.1% using 4-cm. absorption cells; for amounts of copper in the range 0.1 to 0.4% using 1-cm. absorption cells; and for amounts of copper in the range 0.4 to 2% using 0.2-cm. absorption cells. A linear calibration curve was obtained on all three curves.

To present a versatile method suitable for a variety of materials, all B.C.S. samples and synthetic compositions listed in Table I were treated in the same manner. A sample of suitable weight, transferred into a 150-ml. conical beaker, was dissolved in 10 ml. of hydrogen bromide–bromine mixture (180 ml. + 20 ml.) by gentle heating avoiding excessive loss of bromine. A 10-ml. portion of perchloric acid was then added, and the beaker was heated in a well ventilated hood while being swirled until all bromides were decomposed and all hydrogen bromide was expelled. In most cases, the volume of solution had to be reduced to about 2 ml. until all bromides formed were decomposed. Finally 10 ml. of sulfuric acid (5*N*) were added and the solution was evaporated to dense white fumes to expel all perchloric acid; heating continued until the volume of solution had been reduced to about 3 ml. The solution was cooled and 30 ml. of distilled water were added. Precipitates—e.g., lead sulfate—which formed were separated by filtering the solution quantitatively through a medium fast filter into a 100-ml. volumetric flask which was filled to the mark with distilled water.

The above weighing, dissolving, and filtration procedure has in all cases been performed in less than 20 minutes. A 5-ml. aliquot was then transferred into a 50-ml. volumetric flask, reagents were added, and the absorbance was measured in accordance with the procedure described in Absorption.

Table I. Determination of Copper in Standard Samples and Synthetic Compositions

		Certified value for copper, %	Copper added, %	Copper by proposed method, %
B.C.S. No. 177/1	Pb, 84.5%; Sb, 10.4%; Sn, 5.09%; Fe, 0.004%; Bi, 0.002%; As, <0.005%; Zn, <0.01%	0.007	...	0.006, 0.0065, 0.006
B.C.S. No. 177/1	Pb, 84.5%; Sb, 10.4%; Sn, 5.09%; Fe, 0.004%; Bi, 0.002%; As, <0.005%; Zn, <0.01%	0.007	0.025	0.031, 0.031, 0.032
B.C.S. No. 177	Pb, 82.6%; Sb, 12.04%; Sn, 4.64%; Fe, 0.06%; Bi, 0.03%; As, 0.06%; Zn, 0.08%	0.33	...	0.315, 0.315, 0.32
B.C.S. No. 178	Sn, 84.0%; Sb, 7.51%; Pb, 3.86%; Zn, 0.40%; Fe, 0.05%; As, 0.04%	4.08	...	4.04, 4.05; 4.04
B.C.S. No. 178	Sn, 84.0%; Sb, 7.51%; Pb, 3.86%; Zn, 0.40%; Fe, 0.05%; As, 0.04%	4.08	0.05	4.09, 4.09, 4.09
B.C.S. No. 178	Sn, 84.0%; Sb, 7.51%; Pb, 3.86%; Zn, 0.40%; Fe, 0.05%; As, 0.04%	4.08	0.90	4.93, 4.94, 4.93
B.C.S. No. 182	Al, by difference; Si, 12.74%; Fe, 0.34%; Mn, <0.005%; Ti, 0.006%	0.003 — <00.1[a]	...	0.004, 0.003, 0.004
B.C.S. No. 182	Al, by difference; Si, 12.74%; Fe, 0.34%; Mn, <0.005%; Ti, 0.006%	0.003 — <0.01[a]	0.10	0.104, 0.104, 0.104
B.C.S. No. 262	Al, by difference; Mg, 10.57%; Si. 0.10%; Fe, 0.18%; Mn, 0.06%; Zn, 0.05%; Cr, 0.06%; Ti, 0.10%	0.027	...	0.025, 0.025, 0.026
B.C.S. No. 216	Al, by difference; Si, 0.71%; Fe, 0.81%; Mn, 0.54%; Zn, 0.26%; Ni, 0.22%; Mg, 0.53%; Ti, 0.08%; Sb, 0.05%; Sn, 0.02%; Cr, 0.07%; Pb, 0.01%	4.15	...	4.15, 4.15, 4.15, 4.18
B.C.S. No. 216	Al, by difference; Si, 0.71%; Fe, 0.81%; Mn, 0.54%; Zn, 0.26%; Ni, 0.22%; Mg, 0.53%; Ti, 0.08%; Sb, 0.05%; Sn, 0.02%; Cr, 0.07%; Pb, 0.01%	4.15	3.45	7.60, 7.61, 7.61, 7.58
No. 33/91[b]	Zn, by difference; Al, 3.06%; Fe, 0.03%; Pb, 0.003%; Sn, 0.01%; Si, 0.01%; Ni, 0.01%; Mn, 0.01%	0.15	...	0.135, 0.135, 0.140
No. 516[b]	Zn, by difference; Al, 3.50%; Fe, 0.01%; Mg, 0.05%; Pb, 0.03%; Sn, 0.01%; Si, 0.01%; Cr, 0.01%; Ni, 0.01%; Cd, 0.001%	2.20	...	2.24, 2.24, 2.24
No. 33/125[b]	Zn, by difference; Al, 7.0%; Fe, 0.08%; Pb, 0.25%; Sn, 0.10%; Si, 0.05%; Ni, 0.01%; Mn, 0.01%; Cd, 0.003%	5.30	...	5.38, 5.32, 5.38, 5.36

[a] Refers to approximate figures issued with certificate.
[b] Refers to synthetic compositions, which have been analyzed by at least one other source.

RESULTS AND DISCUSSION

Initial tests confirmed that the presence of a high concentration of ammonium ions caused low results (7); the sample was, therefore, dissolved in a minimum volume of acid to avoid the formation of excessive amounts of ammonium salts when the solution was neutralized.

It was further established that the blue copper–organo complex formed in a sodium hydroxide–sodium borate buffer was not liable to low and erratic results in the presence of aluminum, iron, tin, and manganese, whereas with an alternative procedure (6), using an ammonium hydroxide–ammonium citrate buffer, such interferences were observed.

Effect of Ammonium Citrate Solution. Amounts of 20% ammonium citrate solution in the range 2 to 10 ml. have a negligible effect on the absorbance. Below 8 ml., precipitation of aluminum occurs when the acid is neutralized. On additions of above 10 ml. of this reagent, the absorbance

decreases with increase in ammonium citrate concentration. In subsequent tests, 10.0 ml. of 20% ammonium citrate solution were used.

Addition of Indicator. Neutral red does not absorb light at 595 mμ, hence no effect on the absorbance could be observed using varying amounts of indicator.

Two to four drops of 0.05% neutral red indicator were used in subsequent tests.

Effect of pH. Different amounts of 10% sodium hydroxide solution were added after neutralization. Amounts between 0.5 and 1.5 ml. had no significant effect, but amounts under 0.5 or over 1.5 ml. of this reagent depress the color development of the complex: the addition of 5 ml. of 10% sodium hydroxide had such a depressing effect that full color development was not achieved before 15 minutes. The color of the complex develops rapidly in the presence of 0.5 to 1.5 ml. of the reagent. Therefore, an excess of 1 ml. of 10% sodium hydroxide solution was added in subsequent tests, the pH being about 9.0; full color development is achieved within 3 minutes.

No significant variation in absorbance occurs when different amounts of sodium borate buffer solution are used. Tests were performed in the range of 2 to 15 ml. of this reagent, and the pH of the solutions ranged from 8.9 to 9.1. The amount of 5 ml. of the buffer solution was used in subsequent tests.

Biscyclohexanone Oxalyldihydrazone Reagent. No effect in the absorbance was observed by using different amounts of this reagent. A 25-fold w./w. (biscyolohexanone oxalyldihydrazone–copper) excess is necessary for full color development. An amount of 2 ml. of this reagent was used in most of the subsequent tests. The reagent is stable over a period of at least three months.

Stability of Color. The color of the organo–copper complex is stable for at least 5 hours; the value of absorbance decreasing only slightly after this period. Satisfactory results were still obtainable after a standing time of 15 hours.

Effect of Temperature. To check the method under extreme conditions, measurements of absorbance were performed at temperatures ranging from 5° to 35° C. No significant variation on the absorbance was observed.

Interference. Aluminum, arsenic, bismuth, calcium, cadmium, lead, magnesium, molybdenum, phosphorous, antimony, silicon, tin, and zinc do not interfere. In the range of up to 10%, the presence of chromium, nickel, and manganese has no significant effect. The color of the copper–organo complex develops slowly if titanium is present above 1%, while the presence of 10% of titanium completely inhibits color development. Iron above 1% causes a sharp decrease in absorbance, but this can be overcome by taking a smaller aliquot of the test solution.

CONCLUSIONS

The proposed method offers a rapid and reliable procedure for a variety of nonferrous metals and alloys and is suitable for determining copper in the range 0.003 to 10%. The method is selective; interference of iron and titanium can be overcome by using a smaller aliquot of the sample solution. A single determination can be carried out within 30 to 40 minutes, while for routine batch-analysis purposes 25 to 30 determinations can be performed in 8 hours by one analyst.

ACKNOWLEDGMENT

The author thanks R. K. Rush for helpful assistance.

LITERATURE CITED

(1) ASTM Standards, Part 32, **1956**, p. 498.
(2) Crawley, R. H. A., *Anal. Chim. Acta* **13**, 373 (1955).
(3) Haywood, L. J. A., Suteliffe, P., *Analyst* **81**, 651 (1956).
(4) Nilsson, G., *Acta Chem. Scand.* **4**, 205 (1950).
(5) Sandell, E. B., "Colorimetric Determination of Traces of Metals," 2nd ed., Vol. III, p. 304, Interscience, New York and London, 1950.
(6) Somers, E., Garroway, J. L., *Chem. Ind. (London)*, **1957**, 395.
(7) Wetlesen, G., Gran, G., *Svensk Papperstid.* **52**, 212 (1952).
(8) Williams, T. R., Morgan, R. R. T., *Chem. Ind. (London)* **1954**, p. 461.
(9) Wood, D. F., Clark, R. T., *Analyst* **83**, 509 (1958).

R. K. ROHDE

W. Brown & Sons (Vic.) Pty., Ltd.
Non-Ferrous Metals Division
Brooklyn Works
Melbourne, Australia

PERMISSION to publish this paper was given by the directors of W. Brown & Sons Proprietary, Ltd.

Determination of Sulfur in Inorganic Sulfides Using Oxygen Flask Combustion

SIR: We wish to report a method for the decomposition of several inorganic sulfides. The procedure developed is simple and the equipment required is inexpensive. The method should be especially suitable for laboratories doing an occasional sulfide analysis and should also prove valuable for routine analysis where combustion equipment is not available. The results obtained with several inorganic sulfides are reported in this paper.

In the procedure developed, the sulfide sample is mixed with a combustion mixture and is burned in an atmosphere of oxygen in a closed flask. The SO_2 and SO_3 formed during the combustion are absorbed in dilute hydrogen peroxide to form sulfuric acid. The analysis of the sulfate is completed by either the usual gravimetric method or the volumetric method developed by Fritz and Yamamura (*2*). The latter method was found to be especially well suited to the procedure described and was, therefore, used for most of the analyses.

EXPERIMENTAL

Apparatus. The combustion apparatus used was similar to the usual commercial oxygen flasks except that the sample holder consisted of a tapered spiral of 18 gauge Chromel A wire and the stopper was neoprene. The combustion flasks consisted of one- or two-liter filtering flasks without tubulation. The Chromel A spiral holder seemed to provide better combustions than platinum gauze holders and was also much more durable under the vigorous combustion conditions used. Since the feasibility of using neoprene stoppers in this apparatus was uncertain, blanks were run. From the results obtained it did not appear that these stoppers should be a source of trouble for the samples being determined.

Reagents. Standard Barium Perchlorate solution, 0.0100*N*. Dissolve 4.0 grams of $Ba(ClO_4)_2 \cdot 3H_2O$ (G. F. Smith) in 400 ml. of distilled water and dilute to 2 liters with reagent grade methanol. Adjust the pH to 3.5 with perchloric acid and standardize with standard 0.00500*N* sulfuric acid solution. Pipet 10.00-ml. aliquots of the standard sulfuric acid solution into 125-ml. Erlenmeyer flasks and dilute with 40 ml. of methanol. Add two drops of Thorin indicator and titrate while constantly stirring the solution with a magnetic stirrer. The color change is from yellow to pink.

Thorin Solution, 0.20%. Dissolve 0.2000 grams of Thorin, 1,-(o-Arsonophenylazo) - 2 - Naphthol - 3,6 - disulfonic acid disodium salt (Eastman No. 6748) in distilled water and dilute to 100 ml. in a volumetric flask.

"Starch Combustion Mixture." Mix

Table I. Effect of Combustion Mixtures on the Determination of Sulfur in Inorganic Sulfides

Sample[a]	Sulfur found, %	Mean
Zinc sulfide		
Starch	32.7, 32.5, 32.7, 32.7, 32.4 32.3, 32.3, 32.4, 32.7	32.5
Starch + magnesium	32.3, 32.6, 32.0, 32.6	32.4
Starch combustion mixture	32.4, 32.8, 33.0, 32.5	32.7
Copper(II) sulfide		
Starch	21.3, 21.1, 22.9, 20.7	21.5
Starch (large excess)	30.7, 30.4	30.6
Starch + magnesium	30.0, 30.0	30.0
Starch combustion mixture	30.2, 29.8, 31.5, 31.7	30.8
Iron(II) sulfide		
Starch	27.1, 28.5	27.8
Starch combustion mixture	30.6, 31.2, 30.6, 30.5 31.5, 30.2	30.8
Cadmium sulfide		
Starch	20.8, 20.8	20.8
Starch combustion mixture	22.2, 22.5, 22.3, 22.2 22.4, 22.3	22.3
Mercury(II) sulfide		
Starch	11.2, 11.5	11.4
Starch combustion mixture	11.8, 13.0, 12.8, 11.5 12.6	12.3

[a] Weights of samples, starch, magnesium and "combustion mixture" were about 25 mg. except where otherwise noted.

Table II. Effect of Starch Content on the Determination of Sulfur in Zinc and Copper(II) Sulfides

Sample	Wt. sample, mg.	Wt. starch, mg.	Sulfur found, %
Zinc sulfide			
1	24.5	26	32.7
2	24.4	110	28.1
3	25.4	212	18.5
4	24.8	415	2.9
Copper(II) sulfide			
1	26.3	26	21.3
2	24.6	51	22.9
3	28.1	86	21.9
4	28.0	219	28.6
5	27.2	312	30.7
6	35.6	503	30.4

together, without grinding, 43 grams of granular tin, 43 grams of powdered iron, 14 grams of thermite and 100 grams of starch.

Procedure. Weigh 25 mg. of the powdered sulfide sample into a filter paper sample cup. The combustion mixture is weighed or measured approximately into this cup with the sulfide sample. After mixing, the sides of the sample cup are tightly folded over the contents and the resulting disk is wrapped in a piece of flag-shaped filter paper. The filter paper and contents are then placed in the combustion holder.

The combustion flask is prepared by adding 5 ml. of 30% hydrogen peroxide to 45 ml. of distilled water contained in the flask. The flask is flushed with oxygen and the sample is burned in the usual manner. After absorption of the SO_2 and SO_3 is complete, the contents of the flask are quantitatively transferred to a beaker and boiled to reduce the volume to about 25 ml. This solution is then passed through a cation exchange column (Dowex 50, H^+ form) which drains into a 100.0-ml. volumetric flask. The column is flushed with small portions of distilled water until the flask is filled to the mark. The sulfate is determined by a titration procedure based on the method developed by Fritz and Yamamura (*2*). A 10.00-ml. aliquot of the solution is pipetted into a 125-ml. Erlenmeyer flask and diluted with 40 ml. of methanol. Two drops of Thorin indicator are added and the sulfate titration with $Ba(ClO_4)_2$ is carried out as previously described under "standardization of $Ba(ClO_4)_2$ solution."

Table III. Summary of Results for the Determination of Sulfur in Inorganic Sulfides

Sample	Sulfur found, % Peroxide method	Flask method	Difference	Std. dev. (flask method)
Zinc sulfide	32.4 (7)	32.5 (9)[a]	+0.1	0.18
		32.4 (4)[b]	0.0	0.29
		32.7 (4)[c]	+0.3	0.28
Copper(II) sulfide	30.4 (8)	30.0 (2)[b]	−0.4	
		30.8 (4)[c]	+0.4	0.94
		30.6 (2)[d]	+0.2	
Iron(II) sulfide	31.1 (4)	30.8 (6)[c]	−0.3	0.49
Cadmium sulfide	22.4 (8)	22.3 (6)[c]	−0.1	0.12
Mercury(II)	13.6 (4)	12.3 (5)[c]	−1.3	

Numbers in parentheses indicate the number of determinations.

[a] Starch + sample.
[b] Starch + magnesium + sample.
[c] Starch + combustion mixture + sample.
[d] Large excess of starch + sample.

RESULTS AND DISCUSSION

An objective of this research was to find a combustion mixture which could be used with different inorganic sulfides to give quantitative yields of sulfur (as SO_2 and SO_3) on combustion in an oxygen atmosphere.

Results of experiments for determining sulfur in zinc sulfide, copper(II) sulfide, iron(II) sulfide, cadmiun sulfide, and mercury(II) sulfide with various combustion mixtures are reported in Table I. Some interesting results obtained by varying the starch content with zinc sulfide and copper(II) sulfide are shown in Table II. These results were rather surprising and no explanation can be given for the opposite trends observed with increasing starch content. The large amount of starch necessary to give satisfactory results with copper(II) sulfide was very difficult to handle and is, therefore, not practical for analytical use. Some mixtures that were tried were magnesium powder and starch; aluminum powder and starch; magnesium, aluminum and starch; thermite; and a mixture of iron powder, granular tin, thermite, and starch. This latter mixture was based on one developed by Cardano and Fantini (*1*) for the determination of carbon and sulfur in steel and cast iron. This mixture provided the most complete burning of any of those tried. However, in most cases additional starch was added to produce a smoother less vigorous combustion.

It can be seen from Table I that similar results were obtained with zinc sulfide regardless of which combustion mixture was used. However, in the case of iron(II) sulfide, the "starch combustion mixture" was the only mixture found to be suitable. It can be seen from the data in Table I and Table III that satisfactory results were obtained with all of the sulfides tested except for the mercury(II) sulfide which gave consistently low results.

The results obtained by the oxygen flask method are compared with those

obtained by the peroxide fusion method in Table III. Since the per cent sulfur in most commercially available sulfides is not reported, the results obtained by the peroxide fusion method are here assumed to represent the theoretical per cent sulfur values.

Although the oxygen flask combustions were generally vigorous, no dangerous situations resulted. However, these combustions were carried out behind a safety shield and the operator wore safety glasses.

The authors believe that the method described in this paper offers a simple, accurate and relatively rapid procedure for the determination of sulfur in many inorganic sulfides. Extensions of this technique to the determination of sulfur in other inorganic compounds, to sulfide ores, and to other types of inorganic substances should also be feasible.

ACKNOWLEDGMENT

The authors thank William A. Sedlacek, George O. Moses, and Franklin G. Doolittle for carrying out portions of the experimental work on this project.

LITERATURE CITED

(1) Cardano, Renato, Fantini, Nicola, to "TERNI" Societa per l'industria e l'elettricita, Ital. Patent **460,119** (Oct. 19, 1950); *C. A.* **46**, 4958*a* (1952).

(2) Fritz, James S., Yamamura, Stanley S., ANAL. CHEM. **27**, 1461 (1955).

(3) Heinrich, B. J., Grimes, M. D., Puckett, J. E. "Treatise on Analytical Chemistry," Part II, Sec. A, Vol. 7, I. M. Kolthoff and P. J. Elving, ed., Interscience, New York, 1961.

(4) Kodama, K., "Methods of Quantitative Inorganic Analysis," Chap. 58, Interscience, New York, 1963.

(5) MacDonald, A. M. G., *Analyst* **86**, 3 (1961).

ARNOLD R. JOHNSON, JR.[1]
GARY B. MCVICKER
Department of Chemistry
University of Wyoming
Laramie, Wyo.

[1] Present address: Department of Chemistry, Minot State College, Minot, N. D. 58701.

Spectrophotometric Determination of Cobalt in Iron and Steel with 2-Nitroso-1-Naphthol

SIR: The method developed by Rooney (*6, 7*), Claassen and Daaman (*4*), and Boyland (*2*), for the determination of cobalt in iron and steel using 2-nitroso-1-naphthol, is simpler and quicker than the American and British standard methods (*1, 3*). Moreover, it is not subject to the losses that can occur with the latter at the zinc oxide separation stage. It also overcomes difficulties noted by Cogan (*5*). However, measurement of absorbance is not made at the most sensitive wavelength, 362 mμ, because of high and erratic blanks in this region. Instead, another wavelength, 530 mμ, is used at which there is less than half the sensitivity, but where blanks have less effect. This deficiency is removed in the method described, and a cupferron separation with subsequent destruction of excess cupferron (*7*) is eliminated.

The method is applicable to a wide variety of irons and steels in the range 0.001 to 0.6% cobalt and, with suitable selection of sample aliquots, to nickel-base alloys.

EXPERIMENTAL

Apparatus. Bausch and Lomb Spectronic 505 and Beckman DU spectrophotometers were used for absorbance measurements with 1- and 2-cm. cells.

Reagents. The size of the reagent blank is directly related to the organic impurity content of the 2-nitroso-1-naphthol and to the amount of reagent required to react with cobalt and other complex forming elements. Rooney (*6, 7*) found that 40 ml. of 1% reagent was the maximum amount he could add and still obtain an acceptable blank at 530 mμ. In experiments to obtain a reagent with a low blank at 362 mμ, vacuum sublimation gave a highly satisfactory product, but the process was too slow to be of practical use. Eventually the following method was developed. Dissolve 10 grams of 2-nitroso-1-naphthol in 400 ml. of acetone, without heating, add 4 grams of activated charcoal, and shake the mixture for 15 minutes. Filter into a large separating funnel, add 500 ml. of redistilled amyl acetate, mix, add 200 ml. of 1*M* NaOH, and shake for 30 seconds. Run off and retain the aqueous layer. Repeat the extraction twice more using 100 ml. of NaOH solution each time. Combine the aqueous extracts and add to 2 liters of 0.3*M* HCl with stirring. Filter off the bright yellow precipitate and dry under vacuum at room temperature. Yield, about 8 grams.

The reagent was used as a (2.5% w./v.) solution in acetone, prepared daily. 2*M* hydrated sodium acetate, 1*M* ammonium fluoride, and 1*M* sodium hydroxide were prepared from analytical grade reagents.

Standard Cobalt Solution. Dissolve 0.5 gram of high purity cobalt in a minimum amount of 12*M* HCl and dilute to 1 liter. Dilute an aliquot of this solution to prepare a working solution containing 2.5 μg. of Co per ml.

Preparation of Calibration Curve. Transfer portions (0, 2, 5, 10, 15, 20, and 25 ml.) of the working solution to 100-ml. separating funnels and add 1 ml. of 12*M* HCl, 20 ml. of sodium acetate solution, and 1 ml. of 2-nitroso-1-naphthol solution. Shake the mixture after each addition and allow the reagent to react for about 2 minutes. Add 25 ml. of amyl acetate and shake for about 30 seconds. Run off and discard the aqueous layer. Wash the organic layer successively with 10-ml. portions of water, 12*M* HCl, water, NaOH solution, water, 12*M* HCl, water, NaOH solution, and water (twice), shaking the mixture for about 15 seconds after each addition, and discarding each aqueous layer. If an emulsion forms at any stage, add a few grams of KCl, shake until the emulsion clears, and continue the washing procedure.

Transfer the organic layer to a 50-ml. graduated flask and dilute to the mark with amyl acetate. Add anhydrous sodium sulfate, shake, and allow to stand for a few minutes. Filter through a medium speed filter paper and measure the absorbance of the solution *vs.* the blank at 362 mμ using 1-cm. cells. Plot a calibration curve.

Procedure. Transfer 0.5 gram of sample to a 150-ml. squat beaker, add 15 ml. of 12*M* HCl, 5 ml. of 16*M* HNO_3, and allow to dissolve, with warming if necessary. Two ml. of 26*M* HF should be added to the acid mixture to assist the decomposition of high silicon irons and to remove silica. When solution of the sample is complete, evaporate to small volume.

For alloys high in chromium, add 5 ml. of 11*M* $HClO_4$ to the solution of the sample and evaporate almost to dryness.

Add 10 ml. of 12*M* HCl and warm to dissolve soluble salts and reduce chromium if present. Cool and dilute to 100 ml. in a graduated flask.

Alloys containing tungsten should be decomposed with a mixture of 5 ml. of 18*M* H_2SO_4, 5 ml. of 16*M* HNO_3, and 1 ml. of 88% phosphoric acid. When the sample has decomposed, add water and warm until solution is complete. Cool and dilute to 100 ml. in a graduated flask.

Allow insoluble material to settle, and pipet a suitable aliquot into a 250-ml. separating funnel. Add water to a total volume of 50 ml.; 25 ml. of sodium acetate solution; ammonium fluoride solution until the color caused by iron has disappeared; and 10 ml. of 2-nitroso-1-naphthol solution. Shake after each addition and allow the final mixture to stand for a minimum of 2 minutes. Add 20 ml. of 12*M* HCl and 25 ml. of amyl acetate, shaking the mixture after each addition (for about 30 seconds in the latter case).

Run off and discard the aqueous layer. Wash the organic layer as described under Preparation of Calibra-

tion Curve. The reagent may be recovered in a pure state from the first NaOH wash-liquor by precipitation with 0.3*M* HCl as described under reagent purification.

Transfer the organic layer to a graduated flask, and, if necessary, dilute with amyl acetate. Dry with anhydrous sodium sulfate and filter. Measure the absorbance of the solution at 362 mμ in an appropriate size of cell *vs.* a blank.

Size of sample solution aliquot, final amyl acetate volume, and size of cell should be selected as:

Cobalt percentage	Solution aliquot, ml.	Amyl acetate volume, ml.	cell size, cm.
0.25 to 0.6	5	100	1
0.04 to 0.3	5	50	1
0.006 to 0.06	10	50	2
0.001 to 0.008	25	25	2

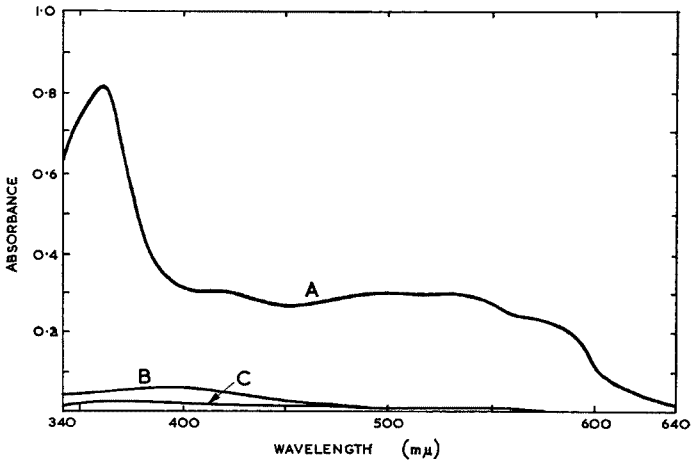


Figure 1. Spectra of cobalt complex and associated blank
A = 1.24 μg. of cobalt/ml.
B = 1.0 μg. of purified reagent/ml.
C = blank
Solvent and reference solutions in all spectra were amyl acetate (1-cm. cells)

Table I. Tests of Cobalt Solutions for Interference from Iron, Chromium, Copper, and Nickel

Cobalt present, μg.	Element and amt. added	Cobalt error, μg.	Volume of 2.5% reagent added, ml.
0	40 mg. Cr	−0.1	10
0	40 mg. Ni	0	10
0	40 mg. Cu	−0.1	10
0	40 mg. Fe	+3.2	10
0	40 mg. Fe	+0.5[a]	10
10	35 mg. Ni	0	10
10	40 mg. Ni	+0.2	10
10	20 mg. Cu	−0.6	10
10	30 mg. Cu	−0.6	10
10	40 mg. Cu	−0.6	10
100	40 mg. Cr	+0.4	10
100	40 mg. Ni	−3.3	10
100	40 mg. Cu	−7.8	10
100	40 mg. Fe	−6.4	10
100	40 mg. Fe	0[a]	10
100	40 mg. Ni	+0.4	15
100	20 mg. Cu	+0.9	15
100	30 mg. Cu	+0.9	15
100	40 mg. Cu	−4.7	15
100	40 mg. Cu	+0.4	20

[a] Sufficient fluoride added to decolorize buffered solution.

RESULTS AND DISCUSSION

Absorbance Curves. Absorption spectra for the cobalt 2-nitroso-1-naphthol complex and its relationship to the reagent and the blank are shown in Figure 1. The cobalt and blank spectra are those which result from a reagent addition of 10 ml. of 2.5% solution and a final amyl acetate volume of 50 ml.

A test of Beer's law showed linearity of the absorbance curve between 0 and 70 μg. of cobalt at 362 mμ and 0 and 100 μg. at 530 mμ. The color intensity is stable for at least 12 hours. The calculated molar absorptivity of the cobalt complex is 3.6×10^4 at 362 mμ and 1.4×10^4 at 530 mμ. The calibration results show standard deviations of 0.6 μg. at 362 mμ and 1.4 μg. at 530 mμ.

Effect of Other Elements. Nickel, chromium, iron, and copper are the only elements, other than cobalt, usually found in iron and steel which form complexes with 2-nitroso-1-naphthol in the pH range of 5 to 6 (*7*). Their complexes are destroyed by hydrochloric acid but the cobalt complex is unaffected. To remove gross amounts of iron in this way would require, however, large amounts of reagent which would have to be extracted subsequently. Rooney avoided these difficulties by a preliminary separation of iron (and copper) with cupferron (*6*, *7*). A simpler method is addition of ammonium fluoride to the buffered solution. This avoids the additional requirement of the destruction of the excess cupferron.

Trivalent chromium precipitates when the sodium acetate buffer solution is added to the sample aliquot. It is said not to interfere (*7*). However, cobalt was occluded when appreciable amounts of chromium(III) precipitated rapidly, the rate of precipitation being proportional to chromium(III) and dissolved silica concentrations. The occlusion was reduced to a negligible amount by delaying the precipitation of chromium until cobalt had reacted with the 2-nitroso-1-naphthol. This was achieved by dehydrating silica, with perchloric acid, and diluting the aliquot to 50 ml. before adding sodium acetate.

The extraction of cobalt into the amyl acetate layer, with only small amounts of the complexes of the other elements, was ensured by the addition of 20 ml. of 12*M* hydrochloric acid to the sample solution after the formation of the 2-nitroso-1-naphthol complexes (*7*). The interfering complexes were removed by the washing procedure, leaving only the cobalt complex dissolved in the amyl acetate. The amounts of reagent re-

Table II. Determination of Cobalt in Standard Analyzed Samples of Iron and Steel and Nickel Base Alloys

Sample[a,b]	Recommended cobalt content and range, %	Cobalt found, %
NBS 55a open-hearth iron	0.008 (0.007 and 0.008)	0.005, 0.006, 0.006
NBS 115a 16Ni-6Cu-2Cr cast iron	0.08	0.079, 0.080, 0.082
NBS 126a 36Ni steel	0.30 (0.29–0.32)	0.292, 0.299, 0.300
NBS 160 19Cr-9Ni-3Mo steel	0.071[c]	0.073, 0.074, 0.074
BCS 220 7W-5Cr-4Mo steel	0.67 (0.64–0.69)	0.658, 0.666, 0.666
BCS 273 mild steel	0.021 (0.020–0.023)	0.020, 0.020, 0.021
BCS 275 mild steel	0.059 (0.055–0.062)	0.057, 0.057, 0.058
NBS 162a 64Ni-31Cu (monel type)	0.076 (0.073–0.078)	0.075, 0.075, 0.076
NBS 169 77Ni-20Cr-1Si	0.19 (0.18–0.21)	0.183, 0.183, 0.183

[a] NBS National Bureau of Standards.
[b] BCS British Chemical Standards.
[c] Revised figure (Private communication from NBS).

quired for different amounts of nickel, copper, and chromium in the presence and absence of cobalt (to a maximum of 100 μg.) are shown in Table I. These results were obtained by following the extraction technique detailed in Procedure, the exceptions being that the iron interference was tested with and without fluoride present and the others were tested with a standard addition of 5 ml. of fluoride. The resistance of the iron complex to complete decomposition (following two acid washes as in Procedure) and the removal of iron interference with ammonium fluoride is also indicated.

The introduction of a second alkali wash removes the free naphthol which is liberated when the last traces of interfering complexes are decomposed by the final acid treatment. This reduces the blank value, particularly at 362 mμ.

The results given in Table I, size of reagent blank, and the sensitivity of the reagent to cobalt, taken together, enabled the construction of the table given in the Procedure which relates cell size, sample aliquot, and amyl acetate volume to the expected cobalt content.

The method can be applied to alloys of nickel and copper by suitable selection of aliquot and reagent volumes (see Tables I and II).

LITERATURE CITED

(1) American Society for Testing Materials, "ASTM Methods of Chemical Analysis of Metals," pp. 54–5, Philadelphia, Pa., 1964.
(2) Boyland, E., *Analyst* **71**, 230 (1946).
(3) British Standard 1121, Part 42, 1961.
(4) Claassen, A., Daamen, A., *Anal. Chim. Acta* **12**, 547 (1955).
(5) Cogan, E., ANAL. CHEM. **32**, 973 (1960).
(6) Rooney, R. C., *Metallurgia* **58**, 205 (1958).
(7) *Ibid.*, **62**, 175 (1960).

MANUEL NEEDLEMAN

Department of Supply
Defence Standards Laboratories
Australian Defence Scientific Service
Maribyrnong, Victoria, Australia

The author thanks the Chief Scientist, Autralian Defence Scientific Service, Department of Supply, Melbourne, Victoria, Australia, for permission to publish this paper.

Spectrophotometric Determination of Cyclohexanone Oxime in Sulfuric Acid Solution of Epsilon-Caprolactam

SIR: Most of the current industrial processes for the production of ε-caprolactam involve the Beckmann rearrangement of cyclohexanone oxime in concentrated sulfuric acid. This reaction proceeds nearly quantitatively and a very small amount of the oxime remains unchanged in the Beckmann rearrangement solution. A number of methods for the quantitative determination of the oxime have been reported—e.g., the gravimetric determination of the oxime by 2,4-dinitrophenylhydrazine (*4*), the spectrophotometric determination of 1-chloro-1-nitrosocyclohexane (*9*) or formhydroxamate (*3*) derived from oxime, and polarography (*10*). However, these methods have many limitations, especially for the determination of trace amounts of the oxime. The present paper reports a novel method for the determination of trace amounts of the oxime in sulfuric acid solution of ε-caprolactam. It is based on the analysis of an azo dye composed of sulfanilamide and *N*-(1-naphthyl)-ethylenediamine, a procedure first used by Shinn (*8*) in the determination of nitrous acid. Also included is a quantitative modification of Feigl's spot test (*2*), in which an azo dye composed of sulfanilic acid and 1-naphthylamine, the Griess-Ilosvay reagent (*5, 6*), is analyzed. A comparison between Shinn's reagent and the Griess-Ilosvay reagent is described.

EXPERIMENTAL

Apparatus. Absorbance measurements were made with a Hitachi EPU-2 spectrophotometer in a 1.000-cm. quartz cell. pH determinations were made with a Hitachi-Horiba M-3 type pH meter with a glass electrode.

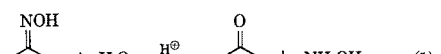
Reagents. A 0.2% sulfonamide solution was prepared by dissolving 0.2 gram of sulfanilamide in about 70 ml. of distilled water on a water bath at 50° C., followed by dilution to 100 ml. with distilled water. A 0.1% *N*-(1-naphthyl)-ethylenediamine dihydrochloride solution was stored in a red bottle. Iodine–acetic acid solution was prepared by adding 1.3 grams of iodine to 100 ml. of glacial acetic acid; the supernatant liquid was used after undissolved iodine settled.

Procedure. Ten grams of the Beckmann rearrangement solution [cyclohexanone oxime is usually rearranged with more than 1.5 molar ratio of sulfuric acid at 110° to 120° C. (*4*)] of cyclohexanone oxime is weighed accurately and then brought to a total volume of 250 ml. with distilled water. The diluted Beckmann rearrangement solution (25 ml.) is pipetted into a conical flask equipped with a condenser, and 1*N* sulfuric acid is added to make the solution contain approximately 1.72 grams total weight of sulfuric acid in order to obtain a suitable pH range in the color reaction. The solution is refluxed for 1 hour. After cooling, 5.0 ml. of the 0.2% sulfonamide solution is added. Then, 5.0 ml. of the iodine–acetic acid solution is added at a temperature below 10° C., followed by the addition of 10 ml. of a 50% aqueous solution of sodium acetate. The solution is kept at a temperature between 14° and 18° C., and excess iodine is decomposed by addition of 0.1*N* sodium thiosulfate solution. Ten milliliters of the 0.1% *N*-(1-naphthyl)-ethylenediamine dihydrochloride solution is added and diluted accurately to 250 ml. with distilled water. The absorbance is read at 540 mμ after 2 minutes. Equivalent amounts of the reagents are added to distilled water in the reference cell.

RESULTS AND DISCUSSION

Color Reaction. The color reaction involved may be indicated by the following successive reactions:

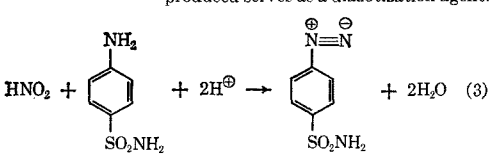
Cyclohexanone oxime is readily hydrolyzed in acidic media to cyclohexanone and hydroxylamine, which is oxidized quickly and quantitatively into nitrous acid by iodine in acetic acid solution.



(1)

$$NH_2OH + 2I_2 + H_2O \longrightarrow HNO_2 + 4HI \quad (2)$$

When Reaction 2 is carried out in the presence of sulfonamide, the nitrous acid produced serves as a diazotization agent.



(3)

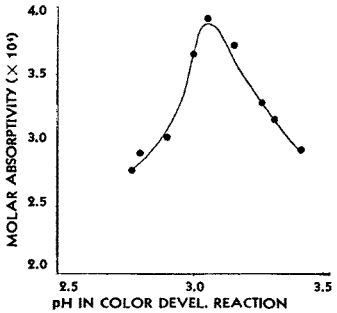


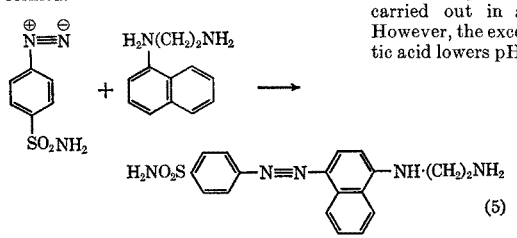
Figure 1. Dependence of molar absorptivity of cyclohexanone oxime on pH in color development reaction

Therefore, Reaction 4 between nitrous acid and hydriodic acid can be suppressed.

$$2NO_2^{\ominus} + 2I^{\ominus} + 4H^{\oplus} \rightarrow I_2 + 2H_2O + 2NO \quad (4)$$

After removal of excess iodine, *p*-sulfamoylbenzenediazonium salt formed is coupled with *N*-(1-naphthyl)-ethylenediamine to produce an azo dye, *p*-{4-[(2-aminoethyl) - amino]azo}benzenesulfonamide.

In order to obtain good precision, accuracy, and high sensitivity, a stable azo dye having high absorbance must be formed.



(5)

In addition, Reaction 4 must be suppressed as completely as possible, for which purpose an easily diazotized aromatic amine must be selected. Satisfying these requests, our method using Shinn's reagent proved to be superior as follows: (1) The time required for color development is decreased to 2 minutes or less. When the Griess-Ilosvay reagent is used, for 10 minutes to half an hour is required to obtain complete coloration. (2) As the color developed is stable, the absorbance remains unchanged for more than 3 hours and good precision is obtained. (3) Both sensitivity and solubility are higher, when compared with the Griess-Ilosvay reagent.

Effect of pH. By changing the quantity of sulfuric acid added, the relationship between molar absorptivity and pH at color development was investigated (Figure 1). Maximum molar absorptivity, the value of which is 3.93×10^4, is observed at pH = 3.05. pH effect can be explained as follows: Although the rate of Reaction 4 is decreased with the decrease of pH (*1*), Reaction 3 is accelerated at a lower pH range because the rate of diazotization is determined by the amounts of both the ammonium form of aromatic amine and the nondissociated form of nitrous acid (*12*). In addition, Reaction 5 does not take place in the ammonium form of the amine (*11*). Therefore, a lower or higher pH range is unsuitable. The results show that maximum molar absorptivity is observed at pH 3.05.

Effect of Acetic Acid Added. Oxidation of hydroxylamine to nitrous acid takes place smoothly only when carried out in acetic acid solution. However, the excessive addition of acetic acid lowers pH at the color development reaction. In the experimental procedure described above, the effect of the quantity of acetic acid added upon the molar absorptivity was investigated. As shown in Figure 2 it is suitable to add 0.5 to 1.0 ml. of acetic acid.

Table I. Dependence of Molar Absorptivity of Cyclohexanone Oxime on the Composition of Sulfuric Acid Solution of ϵ-Caprolactam

Composition of soln. (% by wt.)		
ϵ-Caprolactam	Sulfuric acid	Molar absorptivity
0	100	$3.7–3.8 \times 10^4$
80	20	3.6
90	10	3.3
100	0	3.0

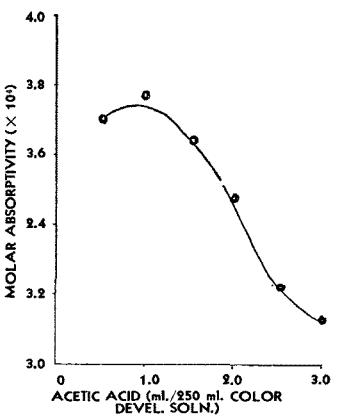


Figure 2. Dependence of molar absorptivity of cyclohexanone oxime on added quantity of acetic acid to color development solution at pH 3.05

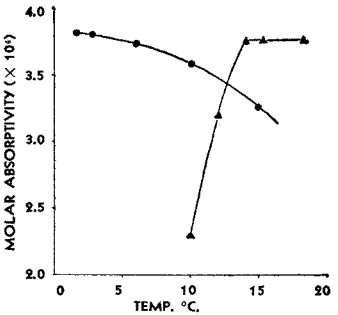


Figure 3. Dependence of molar absorptivity of cyclohexanone oxime on temperature in diazotization and coupling reactions

○ Diazotization
▲ Coupling reaction

Effect of Temperature. The effect of temperature is shown in Figure 3. There is a rapid decrease of molar absorptivity above 10° C. This indicates thermal unstability of the diazonium salt. However, the coupling reaction is too slow at a lower temperature and it must be carried out above 14° C.

Effect of Presence of ϵ-Caprolactam and ϵ-Aminocaproic Acid. To a series of sulfuric acid solutions of ϵ-caprolactam, a known amount of cyclohexanone oxime was added and the molar absorptivities of the solutions were compared. Table I shows that presence of ϵ-caprolactam affects only slightly the molar absorptivity of cyclohexanone oxime. However, no effect is observed by the presence of ϵ-aminocaproic acid. Therefore, the complete hydrolysis of ϵ-caprolactam is recommended.

Effect of Ferrous and Ferric Ions. In the determination of nitrous acid using the Griess-Ilosvay reagent, Rider (*7*) showed 10 p.p.m. of iron formed precipitates with 1-naphthylamine and a 4% deviation was observed in the presence of 40 p.p.m. of ferrous ion. On the other hand, in the determination of the oxime using Shinn's reagent, neither ferric nor ferrous ions affect the molar absorptivity, when present in amounts less than 5,000 p.p.m., respectively.

Measurable Range. Ten to 700 p.p.m. of the oxime can be measured. Contents higher than 700 p.p.m. of cyclohexanone oxime cause precipitation of the azo dye. This defect can be partly improved by the addition of alcohol.

Table II. Precision of the Recommended Procedure

Results, %			Range, %
0.0063	0.0066	0.0066	0.0003
0.0138	0.0146	0.0150	0.0022
0.0158	0.0155	0.0161	0.0006
0.0056	0.0055	0.0055	0.0001
0.0257	0.0258	0.0257	0.0001
0.0564	0.0538	0.0535	0.0029

Quantitativity of Successive Reactions. If Reaction 4 can be suppressed completely, the molar absorptivity of cyclohexanone oxime must be equal to that of nitrous acid.

By adjusting to pH 3.05 at the color reaction and controlling the temperature at the diazotization and the coupling, the same molar absorptivity is obtained when diazotization is carrried out starting from nitrous acid, hydroxylamine, and cyclohexanone oxime.

This means that successive Reactions 1, 2, 3, and 5 proceed quantitatively.

Accuracy and Precision of Recommended Procedure. Known amounts (200–500 p.p.m.) of cyclohexanone oxime added to the mixture composed of 36.5% by weight purified ϵ-caprolactam and 63.5% concentrated sulfuric acid were determined. The maximum error was 8 p.p.m. Good precision was obtained by the procedure and examples are shown in Table II.

In the Beckmann rearrangement of both cyclohexanone oxime and its dihydrochloride using 100% concentrated sulfuric acid (the molar ratio was 2.5) at 115° C., the unchanged oxime was 311–380 and 243–278 p.p.m., respectively.

LITERATURE CITED

(1) Chakravarti, K., Sengupta, K. K., *J. Indian Chem. Soc.* **41**, 861 (1961).
(2) Feigl, F., "Spot Tests in Organic Applications," p. 161, Elsevier, Amsterdam, 1954.
(3) Filippov, M. P., Ruch'eva, N. I., Kodner, M. S., *Zavodsk. Lab.* **29**, 549 (1963).
(4) Fukumoto, O., *Kogyo Kagaku Zasshi* **64**, 1285 (1961).
(5) Griess, P., *Ber.* **12**, 427 (1897).
(6) Ilosvay, L., Ilosvay, N., *Bull. Soc. Chim.* **2**, 247 (1889).
(7) Rider, B. F., Mellon, M. G., IND. ENG. CHEM., ANAL. ED. **18**, 96 (1946).
(8) Shinn, M. B., *Ibid.*, **13**, 33 (1941).
(9) Terent'ev, A. P., Kosin'ski, M., *Zhur. Anal. Chem.* **15**, 234 (1960).
(10) Tur'yan, Ya. I., Smekalova, V. V., *Zavodsk. Lab.* **28**, 423 (1962).
(11) Wistar, W., Bartlett, P. D., *J. Am. Chem. Soc.* **63**, 413 (1941).
(12) Zollinger, H., "Azo and Diazo Chemistry," p. 25, Interscience, New York, 1961.

YOSHINARI KOBAYASHI

Nagoya Research Laboratory
Tôyô Rayon Co.
Nagoya, Japan

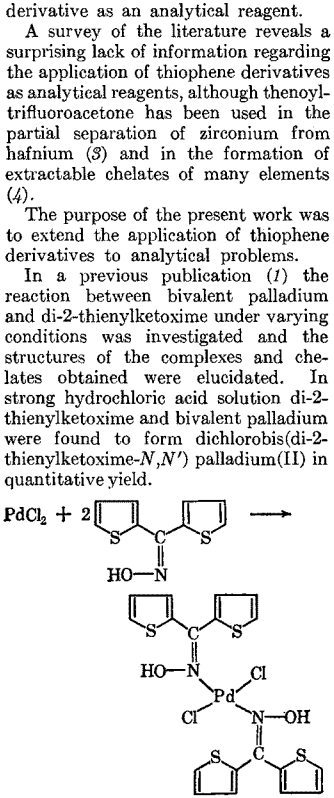
Gravimetric Determination of Palladium with Di-2-Thienylketoxime

SIR: A previous investigation (*5*) of complex formation between bivalent palladium and 2-thienyl *trans*-aldoxime has illustrated the utility of a thiophene derivative as an analytical reagent.

A survey of the literature reveals a surprising lack of information regarding the application of thiophene derivatives as analytical reagents, although thenoyltrifluoroacetone has been used in the partial separation of zirconium from hafnium (*3*) and in the formation of extractable chelates of many elements (*4*).

The purpose of the present work was to extend the application of thiophene derivatives to analytical problems.

In a previous publication (*1*) the reaction between bivalent palladium and di-2-thienylketoxime under varying conditions was investigated and the structures of the complexes and chelates obtained were elucidated. In strong hydrochloric acid solution di-2-thienylketoxime and bivalent palladium were found to form dichlorobis(di-2-thienylketoxime-*N*,*N'*) palladium(II) in quantitative yield.



Further investigation (*2*) proved the utility of the above reaction in the nephelometric determination of trace amounts of bivalent palladium in the presence of other transition metals.

In the present work the above reaction has been applied to the gravimetric determination of bivalent palladium in the presence of a large number of diverse cations and anions (Table I). A statistical comparision has also been made between this procedure and the standard dimethylglyoxime procedure for bivalent palladium.

EXPERIMENTAL

Reagents. Di-2-thienylketoxime was synthesized and purified by the method outlined in a previous publication (*1*). A 2% ethanol solution of this compound was used.

Pure anhydrous palladium(II) chloride dried over sulfuric acid was used in the preparation of known palladium (II) solutions. In the determination of the effect of diverse ions, the solutions used were standardized by the dimethylglyoxime procedure. Sufficient palladium(II) chloride was dissolved in concentrated hydrochloric acid and made up to 1 liter in a volumetric flask such that each milliliter of solution contained an exactly known amount of palladium(II) approximating 1 mg.

Procedure. A volume of the palladium(II) chloride solution containing either approximately 12 or 22 mg. of the palladium(II) ion is transferred by pipet to a 250-ml. beaker. The solution is diluted to approximately 95 ml. with distilled water. The pH is adjusted to 0.8–0.9 by adding 1:1 hydrochloric acid dropwise. The di-2-thienylketoxime solution is added dropwise from a calibrated pipet with vigorous stirring with a magnetic stirrer of 3.5-ml. volume. In solutions containing approximately 12 mg. of palladium(II) a total of 67 mg. of the reagent is added. For solutions containing approximately 22 mg. of palladium(II) a total of 107 mg. of the

Table I. Effect of Diverse Ions

50 mg. of diverse ion added in each case

	Pd(II), mg.		
Diverse ion	Calcd.	Found, av. of 3 results	Dev., mg.
Na^+ ($NaCl$)	20.77	20.75	−0.02
K^+ (KCl)	20.77	20.76	−0.01
NH_4^+ (NH_4Cl)	20.77	20.72	−0.05
Mg^{+2} ($MgCl_2$)	20.77	20.77	0.00
SO_4^{-2} ($MgSO_4$)	20.77	20.77	0.00
Ni^{+2} ($NiCl_2$)	20.77	20.75	−0.02
Rh^{+3} ($RhCl_3$)	20.77	20.75	−0.02
Ca^{+2} ($CaSO_4$)	20.77	20.74	−0.03
Ir^{+3} ($IrCl_3$)	20.77	20.78	+0.01
Pb^{+2} ($Pb[NO_3]_2$)	20.77	20.81	+0.04
NO_3^- ($Pb[NO_3]_2$)	20.77	20.81	+0.04
Co^{+2} ($CoCl_2$)	20.77	20.76	−0.01
Ru^{+2} ($RuCl_2$)	20.77	20.74	−0.03
Pt^{+2} (K_2PtCl_4)	20.77	20.80	+0.03
Ac^- ($NaAc$)	20.69	20.69	0.00
Br^- ($NaBr$)	20.69	20.71	+0.02
PO_4^{-3} (KH_2PO_4)	20.69	20.67	−0.02
Fe^{+2} ($FeCl_2$)	20.51	20.57	+0.06
Cr^{+3} ($CrCl_3$)	23.05	23.05	0.00
Fe^{+3} ($FeCl_3$)	20.69	20.67	−0.02
AsO_4^{-3} [$(NH_4)_2HAsO_4$)	20.51	20.47	−0.04
Os^{+8} (OsO_4)	20.51	20.49	−0.02
Au^{+3} ($AuCl_3$)	20.77	21.37	+0.60
CN^- (KCN)	20.51	No precipitate forms	
Sn^{+2} ($SnCl_2$)	20.51	Pd metal precipitates	
I^+ (NaI)	20.51	PdI_2 precipitates	
Ag^+ ($AgNO_3$)	20.51	AgCl precipitates	
CrO_4^{-2} (K_2CrO_4)	20.51	19.86	−0.64

Table II. Results of Elimination of Interferences

50 mg. of interfering ion taken in each case

Procedure	Pd(II), mg. Calcd.	Found, av. of 3 results	Dev., mg.
(a) CrO_4^{-2} (K_2CrO_4)	23.08	23.08	0.00
(b) CN^- (KCN)	23.08	23.09	+0.01
(c) I^- (KI)	23.08	23.09	+0.01
(d) Ag^+ ($AgNO_3$)	23.08	23.07	−0.01
(e) Au^{+3} ($AuCl_3$)	23.08	23.09	+0.01

reagent is added. Sufficient ethanol is added to make the solution 6% in alcohol content. The solution is stirred for 45 minutes and allowed to stand overnight. The supernatent solution is decanted through a weighed glass filtering crucible leaving the main body of the precipitate and 30 ml. of mother liquor in the beaker. To this is added 20 ml. of an 81.5% ethanol solution for the 22-mg. region sample and 20 ml. of an 80% ethanol solution to the 12-mg. sample and the resulting solution is stirred for 3 hours. The solution is filtered through the glass filtering crucible and the yellow precipitate is washed with 50 ml. of a 5% ethanol solution containing 5 drops of concentrated hydrochloric acid. The precipitate is finally washed with a few milliliters of water, dried at 110°C. for 1 hour, and weighed.

RESULTS

The theoretical value of palladium in pure palladium(II) chloride is 60.01%. In the 22-mg. palladium(II) region, the average value of 20 determinations found by the di-2-thienylketoxime method was 59.97% with a standard deviation of 0.12% and the average value of 20 determinations found by the standard dimethyl glyoxime procedure was 59.84% with a standard deviation of 0.13%. In the 12-mg. palladium(II) region, the average value of 21 determinations found by the di-2-thienylketoxime method was 60.01% with a standard deviation of 0.13% and the average value of 20 determinations found by the standard dimethyl glyoxime procedure was 59.85% with a standard deviation of 0.45%.

From the above results, it is seen that Au^{+3}, CrO_4^{-2}, CN^-, Sn^{+2}, I^-, and Ag^+ interfere. The results of the elimination of these interferences are found in Table II.

ELIMINATION OF INTERFERENCES

(a) CrO_4^{-2} Reduction of CrO_4^{-2} to Cr^{+3} by addition of $FeCl_2$.

(b) CN^- Addition of concentrated HCl to sample solution and boiling.

(c) I^- Bubbling Cl_2 gas through the sample solution to remove I^- as I_2.

(d) Ag^+ Filtering off the precipitated AgCl and adding reagent to filtrate

(e) Au^{+3} Reduction to Au(O) by addition of $NaHSO_3$, filtering off the precipitated Au(O) and addition of reagent to filtrate.

(f) Sn^{+2} No satisfactory method could be found.

LITERATURE CITED

(1) Holland, W. J., Lee, L., *Can. J. Chem.* **41**, 1657 (1963).
(2) *Ibid.*, **42**, 1016 (1964).
(3) Huffman, E., Beaufait, L., *J. Am. Chem. Soc.* **71**, 3179 (1942).
(4) Magnusson, L. B., Anderson, M. L., *Ibid.*, **76**, 6207 (1954).
(5) Trandon, S., Brattacharya, S., ANAL. CHEM. **32**, 194 (1960).

WILLIAM J. HOLLAND
JESSE GERARD

Department of Chemistry
University of Windsor
Windsor, Ontario, Canada

WORK supported by the National Research Council of Canada.

Note on the Determination of Lead in Gasolines by Atomic Absorption Spectrometry

SIR: Difficulties have been encountered in this laboratory in using a high-efficiency total-consumption (HETCO) type burner for the determination of lead in gasolines by atomic absorption spectrometry. Although Robinson (*6*) has been successful in carrying out the analysis with a Beckman total consumption burner, we were unable to use his procedure without obtaining results that were invariably high. Similar troubles with a premix type burner have been reported by Dagnall and West (*3*). We have been unable to find the exact source of the problem but it appears to have been solved by the use of an acetone–isooctane mixed solvent for sample dilutions and standard solutions rather than isooctane alone.

Table I. Mean Lead Content Values of Selected Gasoline Samples

(ml./Imperial gal.)

Gravimetric and/or polarographic[a]	Atomic absorption: Isooctane	Atomic absorption: Acetone–isooctane[b]
2.51[c]	2.75	2.57
1.42	1.55	1.37
1.26	1.42	1.24
3.28	3.70	3.32

[a] References (*1*) and (*2*).
[b] 1:1 mixture of acetone and isooctane used as a sample diluent instead of isooctane alone.
[c] The experimentally determined values for all three methods were found to vary less than 0.025 ml./Imperial gal. from the mean values listed.

EXPERIMENTAL

Analyses were carried out with the Pb 2833 A. line on a Jarrell-Ash Model 82-516 atomic absorption/flame spectrometer equipped with a high efficiency total consumption (HETCO) burner, a four element (Cu-Pb-Zn-Ag) hollow cathode normally operated between 10 ma. and 15 ma., an 1180 groove/mm. grating blazed at 3000 A. and a meter readout. Except under special circumstances the burner was operated on a 2:1 mixture of compressed air and hydrogen.

Tetraethyl lead standards were prepared from Ethyl Corp. commercial tetraethyl lead (TEL) solutions and ranged in concentration from 1 to 3 ml./Imperial gal. (1 ml./Imperial gal. = 86 p.p.m. of Pb approximately). In use they were diluted to values of less than 70 p.p.m. of Pb. Samples were also diluted until they fell within the range of 0 to 70 p.p.m. of Pb.

All solutions were fed to the burner through a 15-cm. length of 0.9-mm. i.d. nylon tubing. Following standard practices in handling TEL solutions, polyethylene tubing was avoided.

RESULTS AND DISCUSSION

Table I is a listing of the lead contents of four selected gasolines as determined by various methods. The gravimetric method (*1*) has been used as a standard method for some time in this laboratory and the polarographic (*2*) method correlates extremely well with it. The atomic absorption methods varied only in the use of isooctane in one and a 1:1 mixture of acetone and isooctane in the other for sample dilution and TEL standard purposes.

In attempting to find some ready and simple explanation for the consistently

high lead values found using isooctane alone, a wide variety of experimental and instrumental factors were investigated. No improvement was found, for instance, in changing the length or diameter of the nylon burner feed tubing or even dispensing with it altogether. The use of oxygen in place of compressed air failed to cause any significant variation in the results as did various instrumental settings such as the photomultiplier voltages, cathode currents, slit widths, etc.

At this point it appeared a certainty that the trouble involved the complex phenomena associated with the vaporization and burning of the lead solutions at the burner tip and in the flame itself. In view of current thinking on the nature of these phenomena (*4*, *5*, *7*), various mixed solvents were tried and a 1:1 mixture of acetone and isooctane was selected on the basis of vastly improved results (Table I).

It is difficult to pinpoint exact reasons for the success of the mixed solvent. Part of the story may lie in the fact that the measured vapor pressure of the isooctane standards is only about one quarter that of raw gasolines. The acetone increases the vapor pressure of the solvent to the point where raw samples, diluted samples, and standards are all nearly identical. On the other hand, the acetone may improve the solubility of the TEL in the solvent, particularly as it emerges from the burner tip, but such an event would be most difficult to study.

ACKNOWLEDGMENT

The author expresses his appreciation to G. deBoer for his valuable assistance in this work.

LITERATURE CITED

(1) Am. Soc. Testing Materials, Standard Method D526-61 (1961), 1965 Book of Standards, part 17, pp. 272–6 Philadelphia, Pa., 1965.
(2) Am. Soc. Testing Materials, Standard Method D1269-61 (1961), 1965 Book of Standards, part 17, pp. 571–6, Philadelphia, Pa., 1965.
(3) Dagnall, R. M., West, T. S., *Talanta* **11**, 1553 (1964).
(4) Menzies, A. C., ANAL. CHEM. **32**, 905 (1960).
(5) Rann, C. S., The Element #9, Aztec Instruments Inc., Westport, Conn., 1965.
(6) Robinson, J. W., *Anal. Chim. Acta* **24**, 451 (1961).
(7) Robinson, J. W., The Element #5, Aztec Instruments Inc., Westport, Conn., 1965.

H. W. WILSON

British American Research and Development Co.
Sheridan Park
Ontario, Canada

Analysis of α-Olefin-Derived Sodium Sulfonates by Ion Exchange and Potentiometric Titrimetry

SIR: A simple, yet rapid, method of analysis was needed for α-olefin-derived sodium sulfonates. These products normally consist of the sodium sulfonates and a few per cent of sodium sulfate. The alkyl sulfonate analysis is usually obtained by ASTM D-1681 (*2*), a variation of two separate methods developed by Epton (*5*) and by Barr, Oliver, and Stubbings (*3*). This method involves titration with a standardized cationic reagent and uses the distribution of methylene blue between two liquid phases for detection of the end point. This method, however, is not applicable to lower molecular weight sulfonates. Sodium sulfate is frequently determined as the alcohol insoluble content (*1*) or by precipitation as barium sulfate after ether extraction to remove the sulfonate. Both of these procedures are quite lengthy for routine application.

Recently an instrumental method based on x-ray fluorescence and infrared spectrometry has been reported (*7*); however, it would require quite expensive equipment for routine plant analyses. The procedure reported here consists of passing an aqueous solution of the sulfonate-sulfate sample through a sulfonic acid ion exchange column, diluting the effluent with acetone, and titrating with tetrabutylammonium hydroxide.

EXPERIMENTAL

Apparatus. Titration curves were obtained with a Sargent Model D automatic recording titrator equipped with a 10-ml. buret and Leeds and Northrup general purpose glass and calomel electrodes without modification.

The ion exchange column was a 1-cm. diameter glass tube, 15 cm. long, with a 3-mm.-bore Teflon stopcock at the bottom and 50-ml. reservoir at the top. It contained 15 ml. of 50- to 100-mesh Dowex 50W-X8, ion exchange resin in the acid form.

Reagents. All chemicals were reagent grade or equivalent. Standard 0.1*N* tetrabutylammonium hydroxide was prepared by diluting 1*N* tetrabutylammonium hydroxide (Eastman Organic Chemicals) 9:1 with a solution of 70% benzene–30% methanol. The titrant was protected from the atmosphere by use of a drying tube containing Ascarite and Drierite and was standardized each day with benzoic acid in a 9:1 acetone–water solvent. Commercial sulfonic acids and the sulfonic acid salt were purchased from Eastman Organic Chemicals and the Aldrich Chemical Co. and used without further purification.

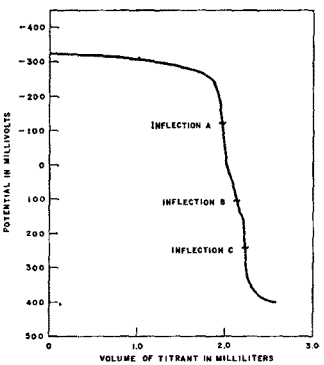


Figure 1. Titration of acids from a typical α-olefin-derived sodium sulfonate with tetrabuylammonium hydroxide

Procedure. The samples were prepared for titration by dissolving 0.45 gram in 50 ml. of water. Because of solubility problems, some of the higher molecular weight sulfonate solutions were maintained at a temperature of 55° C. A 5-ml. aliquot was pipetted into the column reservoir and the stopcock was opened. When the solution level reached the top of the resin bed, washes were added in the following order: two 3-ml. volumes of water and four 6-ml. volumes of acetone. The effluent was collected in a 150-ml. beaker, diluted to 100 ml. with acetone, and titrated automatically with the standard 0.1*N* tetrabutylammonium hydroxide solution. The resin should be immediately regenerated by washing with 50 ml. of 10% hydrochloric acid and then with distilled water until the effluent is neutral. Acetone, when kept in contact with the resin for more than 20 minutes, caused erratically high results.

A typical curve for the titration of the acids obtained by passing a sample of C_{16} α-olefin-derived sulfonate through the ion exchange column is shown in Figure 1. Inflection *A* represents the neutralization of the sulfonic acid and one hydrogen from the sulfuric acid. Inflection *B* represents the neutralization of the second hydrogen from sulfuric acid. Inflection *C* represents impurities and does not enter into the calculations. These impurities are probably in the acetone since the volume of titrant to

Table I. Determination of Sodium Sulfate in a Blended Sulfonate-Sulfate Sample

Sodium sulfate, %			Sodium sulfonate, %		
Calcd.	Found	Error	Calcd.	Found	Error
...	1.6	...	...	85.3	...
3.6	3.7	+0.1	83.5	82.9	−0.6
6.0	6.4	+0.4	81.5	79.8	−1.7
8.8	9.1	+0.3	79.1	78.6	−0.5

Table II. Comparison of Total Sulfur Values for Different Structure Sulfonic Acids Containing Sulfuric Acid

	% Sulfur	
Sample type	Proposed titration technique	High temperature combustion
Methanesulfonic acid (Aldrich)	30.5	30.4
Methanesulfonic acid (Eastman)	32.8	33.7
d-10-Camphorsulfonic acid	12.9	12.8
Benzenesulfonic acid	17.0	17.4
Benzenesulfonic acid (sodium salt)	15.7	16.1

obtain inflection C increases proportionally with the amount of acetone.

The calculations for the percentages of the sulfate and sulfonate salts are given by the following equations:

$$\% \text{ Sodium sulfate} = \frac{(\text{ml. of titrant})\ (\text{normality})\ (142)\ 100}{(\text{sample weight in grams})\ 1000}$$

where milliliters of titrant = (ml. at Inflection *B*) − (ml. at Inflection *A*)

$$\% \text{ Sodium sulfonate} = \frac{(\text{ml. of titrant})\ (\text{normality})\ (\text{molecular weight})\ 100}{(\text{sample weight in grams})\ 1000}$$

where ml. of titrant = (2) (ml. at Inflection *A*) − (ml. at Inflection *B*)

RESULTS AND DISCUSSION

N,N-dimethyl fatty amide (*9*), pyridine (*4*), and acetone (*4, 6, 8*) can be used for the differential titration of sulfonic and sulfuric acids but none of these solvents will dissolve α-olefin-derived sodium sulfonates. Water will dissolve the sulfate and sulfonate salts; however, it will not readily dissolve the resulting sulfonic acid nor will it act as a differentiating solvent. Therefore, a differentiating solvent must be used in conjunction with water to obtain a final titration solvent.

N,N-dimethyl fatty amide (*8*) has been suggested as the best solvent for the titration of sulfonic and sulfuric acids. However, water, in concentrations of more than 4%, leveled the inflection points enough to make them unsuitable for analytical purposes. Pyridine was investigated; however, it did not prove to be as satisfactory as acetone. Acetone (*6*) has been used as a differentiating solvent but Cundiff and Markunas (*4*) reported that it reacts with strong acids and yields nonstoichiometric titrations. To determine if the strong acids react with acetone in the presence of water, a sample of an α-olefin-derived sodium sulfonate containing sodium sulfate was converted to the corresponding acids and allowed to remain in contact with acetone containing about 10% water for various periods of time. The results indicate that there was no significant change in either sulfuric or sulfonic acid concentration over a 6-hour period.

To determine the stiochiometry of acetone–water mixtures, samples of sulfuric acid were titrated in acetone containing increasing concentrations of water. Figure 2 shows these titrations. The titration in acetone results in only two inflections. The first represents the neutralization of one hydrogen of sulfuric acid. The second represents the neutralization of the second hydrogen of sulfuric acid plus impurities in acetone. The addition of water to the acetone causes a differentiation between the neutralization of the second hydrogen of sulfuric acid and the impurities in acetone. As the concentration of water increases, the differentiation between the inflections for the neutralization of sulfuric acid, Figure 2, becomes more poorly defined. However, a solvent containing as much as 20% water yields titration curves which are suitable for analytical purposes. It was found that more acid is titrated between the first and second inflection points than between the second and third inflections, confirming Cundiff and Markunas' (*4*) findings. Since the method is designed for samples containing less than 10% sodium sulfate, the error in the determinations is relatively small.

To determine the accuracy of the titration procedure a specially prepared and purified C_{16} α-olefin-derived sodium sulfonate was analyzed with the following results: carbon, found 58.74%, theory 58.85%, purity 99.8%; hydrogen, found 9.54%, theory 9.57%, purity 99.7%; oxygen, found 14.68%, theory 14.70%, purity 99.9%; sulfur, found 10.02%, theory 9.84%, purity 101.8%. The results obtained by the titration procedure, 0.16% sulfate and 99.2% sulfonate, agree very well with those calculated by elemental analysis.

The effect on the analysis of up to 10% sodium sulfate was determined by adding sodium sulfate to a typical α-olefin-derived sodium sulfonate (Table I). The average error was approximately 1% for the sodium sulfonate and approximately 0.3% for the sodium sulfate.

Five samples of sulfonic acids of widely varying structure, containing small amounts of sulfuric acid, were analyzed. The results, expressed as total sulfur, were compared with sulfur values obtained by high temperature combustion (Table II). These results further indicate that the titration is applicable to the analysis of sulfates and sulfonates in the presence of each other.

Typical samples of α-olefin-derived sodium sulfonates, varying in carbon number from C_8 through C_{20}, were analyzed using the titration procedure. Comparison sulfate values were obtained by ASTM-D-1568 (alcohol insoluble method). The comparison sodium sulfonate results were obtained by ASTM-D-1681 (cationic titration) and, also, by a difference value obtained by subtracting percentages of the

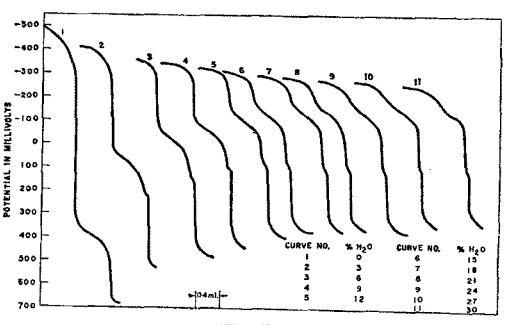


Figure 2. Titration of sulfuric acid in acetone–water mixtures

Table III. Analysis of Typical α-Olefin-Derived Sodium Sulfonates

Carbon No.	Sulfate, % Titration	Sulfate, % Alcohol insoluble	Sulfonate, % Titration	Sulfonate, % ASTM D-1681	Sulfonate, % Difference method
C_8	3.8	4.3	99.4	19.7	91.2
C_{10}	2.6	1.8	94.3	...	94.5
	2.0	1.8	100.2	60.7	95.3
C_{14}	9.5	12.0	81.5	80.7	80.4
	7.8	8.7	83.8	79.8	85.0
	7.0	7.4	76.9	65.4	75.6
	5.8	6.4	87.7	79.5	84.5
	4.4	4.3	81.6	87.4	80.1
	2.2	1.9	94.5	97.0	95.7
C_{16}	8.9	8.4	77.0	86.9	79.6
	2.2	1.6	96.3	96.3	96.7
	1.1	1.0	98.5	...	98.1
C_{18}	1.7	1.0	90.0	81.2	93.3
	3.8	3.5	88.7	72.3	89.7
	3.9	5.0	88.8	87.6	90.5
C_{20}	3.1	3.1	92.1	96.2	93.7
	2.2	1.9	89.8	95.5	89.7
	2.5	3.2	92.6	94.0	92.0

alcohol insolubles, neutral oils, and water from 100%. Representative results are given in Table III. For the sodium sulfonate values, the agreement is generally good between the titration and the difference results, while the cationic titration results are scattered. No sample size dependence was observed with sample sizes varying from 0.3 to 1 gram.

The over-all error of the method appears to be ±1% for the sodium sulfonate at the 90–100% level and ±0.3% for sodium sulfate below the 10% level. The standard deviation for the analysis of approximately 70 α-olefin-derived sulfonate samples was 0.5% for the sodium sulfonate at the 90 to 100% level and 0.1% for the sodium sulfate below the 10% level.

No interferences have been found in the normal production α-olefin-derived sulfonates. However, any salts which would be converted by the ion exchange resin to acids that would be titrated with either of the hydrogens of sulfuric acid would interfere.

LITERATURE CITED

(1) ASTM Std. D1568, American Society for Testing and Materials, Philadelphia, Pa., 1960.
(2) ASTM Std. D1681, American Society for Testing and Materials, Philadelphia, Pa., 1960.
(3) Barr, T., Oliver, J., Stubbings, J., *J. Soc. Chem. Ind.* **76,** 45 (1948).
(4) Cundiff, R. H., Markunas, D. C., ANAL. CHEM. **30,** 1447 (1958).
(5) Epton, S. R., *Trans. Faraday Soc.* Vol. **XLIV,** Part V, p. 226, April 1948.
(6) Gribova, E. A., *Zavodsk. Lab.* **25** (3), 154 (1961), *Anal. Abstr.* No. 3812 (1961).
(7) Kullbom, S. D., Pollard, W. K., Smith, H. F., ANAL. CHEM. **37,** 1031 (1965).
(8) Malmstadt, H. V., Vassallo, D. A., *Ibid.,* **31,** 206 (1959).
(9) Reynolds, C. A., Little, J., Pattengill, M., *Ibid.,* **35,** 973 (1963).

EDWIN H. GRIFFIN, JR.[1]
EDGAR W. ALBAUGH
Gulf Research & Development Co.
Pittsburgh, Pa.

[1] Present address, Philip A. Hunt Chemical Corp., Wayland Chemical Division, Lincoln, R. I.

A Simple and Accurate Calibration Model for Hydrogen-Content, Beta-Particle Transmission Gauges

SIR: In our recent work on the simultaneous use of beta-particle transmission and backscatter gauges for the analysis of three-component liquids (*2*), we had occasion to examine the calibration models previously used. The original calibration methods used by Smith and Otvos (*6*) and Jacobs, Lewis, and Piehl (*3*) and later refined by Rowan (*5*) are trial-and-error methods based on somewhat arbitrary mathematical models. An alternate model is proposed here that does not require a trial-and-error analysis and still gives an adequate fit of the data.

PREVIOUS MODELS

Smith and Otvos (*6*) proposed the calibration model:

$$R = K_1 + K_2A + K_3A^2 \qquad (1)$$

where R is the beta-particle transmission gauge response; K_1, K_2, and K_3 are constants to be determined by a least-squares analysis of data; and A is the total cross section. A is defined by

$$A = \rho\sum_i w_iS_i/A_i \qquad (2)$$

where ρ is liquid density, w_i is the weight fraction of element i in the liquid, S_i is the relative absorption cross section of element i, and A_i is the atomic weight of element i. To use this calibration model, one assumes that the value of S for hydrogen is unity and then makes experimental measurements on liquids containing only hydrogen and carbon in known amounts. One then assumes various values of S for carbon and does a least-squares analysis of data on Equation 1 for each assumed value of S for carbon. The minimum variance obtained for A dictates the correct value of S for carbon.

Jacobs, Lewis, and Piehl (*3*) used the model:

$$R = K_1\rho\sum_i w_iS_i/A_i + K_2 \qquad (3)$$

These authors chose to standardize on the S value for carbon and choose various values of the S value for hydrogen to best fit Equation 3 in the same manner used by Smith and Otvos. Rowan (*5*) described a graphical trial-and-error method and a combination trial-and-error and least-squares method for determining the constants of Equation 3.

PROPOSED MODEL

The calibration model proposed here is

$$R = 10^{K_1 + K_2\rho \sum_i w_iZ_i/A_i + K_3\rho \sum_i w_iZ_i^2/A} \qquad (4)$$

where Z_i is the atomic number of element i.

The reasoning behind this model is that the cross sections for the four major interactions of beta particles with matter are given approximately by $\rho \sum_i w_iZ_i/A_i$ and $\rho \sum_i w_iZ_i^2/A_i$ when beta-particle energy and sample thickness are held constant (cf. Ref. 1). It is well known that the transmission of beta particles empirically follows the Beer-Lambert law over a wide range of absorber thicknesses. Our model simply combines this empirical law for beta particle transmission with the appropriate cross sections for the four major interactions of beta particles.

To obtain a least-squares analysis for this model one simply takes the

Table I. Beta-Particle Transmission Gauge Results of Smith and Otvos

Sample	Empirical formula	Relative beta-particle transmittance at 37.2° C. volts amplifier output, R	Density gram/ml. at 37.2° C., ρ
n-Hexane	C_6H_{14}	30.29	0.6435
2,2,4-Trimethylpentane	C_8H_{18}	27.46	0.6777
Methylcyclopentane	C_6H_{12}	23.05	0.7324
Cyclohexane	C_6H_{12}	20.53	0.7615
Benzene	C_6H_6	15.40	0.8607
o-Xylene	C_8H_{10}	14.36	0.8622
Decalin	$C_{10}H_{18}$	11.46	0.8791
Tetralin	$C_{10}H_{12}$	7.15	0.9560
1,6-Dimethylnaphthalene	$C_{12}H_{12}$	5.39	0.9895
Diisopropyl ether	$C_6H_{14}O$	24.79	0.7112
Ethyl alcohol	C_2H_6O	18.68	0.7757
Ethyl acetate	C_4H_8O	11.80	0.8793
Water	H_2O	0.00	0.9932
Diethylamine	$C_4H_{11}N$	26.31	0.6906
Di-*n*-butylamine	$C_8H_{19}N$	21.40	0.7461
Piperidine	$C_5H_{11}N$	13.66	0.8457
Pyridine	C_5H_5N	7.53	0.9659

Table II. Results of Different Calibration Models on Data of Smith and Otvos[5]

Sample	Weight fractions of hydrogen: Experimental	Calcd. by method of Smith and Otvos from Equations 7 and 2	Calcd. with proposed model from Equation 8
n-Hexane	0.1638	0.1655	0.1671
2,2,4-Trimethylpentane	0.1588	0.1573	0.1563
Methylcyclopentane	0.1437	0.1499	0.1424
Cyclohexane	0.1437	0.1442	0.1412
Benzene	0.0774	0.0765	0.0759
o-Xylene	0.0950	0.0950	0.0942
Decalin	0.1269[a]	0.1266	0.1258
Tetralin	0.0915	0.0916	0.0938
1,6-Dimethylnaphthalene	0.0774	0.0770	0.0804
Standard error		±0.0010	±0.0023

[a] This value was obtained by a standard hydrogen analysis when it was found that the sample of decalin was impure.

logarithm to the base 10 of both sides of Equation 4 to obtain:

$$\log R = K_1 + K_2\rho\sum_i w_iZ_i/A_i + K_3\rho\sum_i w_iZ^2_i/A_i \quad (5)$$

Equation 5 is linear in log R and one can do a least-squares analysis directly without recourse to a trial-and-error method. It is also quite simple to solve this equation, once it has been established, for the weight fraction of hydrogen when experimental values of R and ρ taken on a liquid containing only hydrogen and carbon.

Table III. Beta-Particle Transmission Gauge Results of Piehl

Sample	Wedge position in inches, N	Density, gram/ml., ρ
Benzene	1.233	0.8741
Benzene	1.249	0.8759
Cumene	1.248	0.8591
Cumene	1.237	0.8580
sec-Butylbenzene	1.273	0.8587
sec-Butylbenzene	1.277	0.8592
Ethylbenzene	1.244	0.8624
Ethylbenzene	1.250	0.8630
Toluene	1.201	0.8631
Toluene	1.206	0.8637
Decalin	1.657	0.8826
Decalin	1.657	0.8828
n-Decane	0.368	0.7266
n-Decane	0.372	0.7267

COMPARISON OF RESULTS

To evaluate the effectiveness of the proposed model in relation to the previous ones, we have used the data given by Smith and Otvos (*6*), some unpublished data furnished by Piehl (*4*), and the data of Rowan (*5*). Unfortunately, all of these authors used sophisticated two-cell techniques in which the current obtained from an ion chamber measuring the absorption through a sample of water or a standard absorber was balanced against an identical ion chamber measuring the absorption through the sample. We therefore had to modify our model somewhat for these specific cases. Since Smith and Otvos measured the net current between the two ion chambers, the modification of our model for this case is:

Table IV. Beta-Particle Transmission Gauge Results of Rowan

Sample	Wedge position in inches, N	Density, gram/ml., ρ
Toluene	1.1325	0.86222
Benzene	1.1656	0.87331
Cumene	1.1858	0.85907
Ethylbenzene	1.1851	0.86296
sec-Butylbenzene	1.2010	0.85766
Cyclohexane	0.6700	0.77362

$$R = K_4 + 10^{K_1 + K_2\rho\sum_i w_iZ_i/A_i + K_3\rho\sum_i w_iZ_i^2/A_i} \quad (6)$$

where K_4 is the response of the gauge for water. Since K_4 was not given by Smith and Otvos, a least-square analysis of Equation 6 must be done by a trial-and-error method which assumes various values of K_4 and determines the minimum variance by a least-squares determination of the remaining constants.

The data given by Smith and Otvos are presented in Table I. Using this data they found the best calibration model to be:

$$R = 101.05 - 197.97A + 61.68A^2 \quad (7)$$

where S for carbon is 6.80, S for nitrogen is 8.17, and S for oxygen is 9.55. We found the best fit for our calibration model to be:

$$R = -88.20 + 10^{2.3036 - 0.55390\rho\sum_i w_iZ_i/A_i - 0.013157\rho\sum_i w_iZ_i^2/A_i} \quad (8)$$

The calculated or measured values of the weight fraction of hydrogen were backcalculated from Equations 7 and 2 and Equation 8 for the 9 samples that contain only hydrogen and carbon. These values are compared to the actual experimental values in Table II. The standard error is found to be ±0.0010 for the method used by Smith and Otvos and ±0.0023 for the method proposed here. This demonstrates that the calibration model proposed here has about the same accuracy as that used by Smith and Otvos. They reported an accuracy of 0.1% absolute for hydrogen which is consistent with our calculation. Our model was also tested for fitting the liquid samples that also contained nitrogen and oxygen and was found to fit as well as for liquids containing only hydrogen and carbon. We obtained a standard deviation on R of ±0.105 when samples containing only hydrogen and carbon were used. This compares well to the standard deviation of ±0.116 when all 17 samples were included in the least-squares analysis.

Jacobs, Lewis, and Piehl (*3*) and Rowan (*5*) used a two-cell gauge in which

the current from an ion chamber measuring the absorption of beta particles through a standard invar absorber was bucked against an ion chamber measuring the absorption through the sample and an adjustable wedge absorber. In this case the readout consisted of the wedge position that would give a zero net current between the two chambers. Assuming that the absorbance of the wedge is linear with wedge position gives the following relationship between wedge position and amount of wedge absorbance.

$$WA = K_5(K_6 + N) \quad (9)$$

WA is wedge absorbance in grams / sq. cm., N is wedge position in inches, and K_4 and K_6 are empirical constants. Since the net current is zero, our calibration model is modified for this case to:

$$0 = K_4 + 10^{K_1 + K_2\rho \sum_i w_i Z/A_i + K_3 \sum_i w_i Z_i^2/A_i + K_7 K_5 (K_6 + N)} \quad (10)$$

where K_4 is the current in the standard cell and K_7 is the absorption coefficient for the wedge material. Equation 10 can be obtained in the form:

$$N = \frac{-(\log K_4 + K_1)}{K_7 K_5} - K_6 - \frac{K_2}{K_7 K_5} \rho \sum_i w_i Z_i/A_i - \frac{K_3}{K_7 K_5} \rho \sum_i w_i Z_i^2/A_i \quad (11)$$

If we define new constants as $L_1 = \frac{-(\log K_4 + K_1)}{K_7 K_5} - K_6$, $L_2 = -K_2/K_7K_5$, and $L_3 = -K_3/K_7K_5$, then we obtain the relationship:

$$N = L_1 + L_2\rho \sum_i w_i Z_i/A_i + L_3\rho \sum_i w_i Z_i^2/A_i \quad (12)$$

which is a simple linear equation that can be easily fitted to experimental data to obtain the calibration constants L_1, L_2, and L_3. This has been done for the data of Piehl in Table III and the data of Rowan in Table IV. For the data of Piehl the resulting equation is:

$$N = -6.3285 + 15.344\rho \sum_i w_i Z_i/A_i + 0.14103\rho \sum_i w_i Z_i^2/A_i \quad (13)$$

For the data of Rowan the equation is:

$$N = -6.5070 + 15.708\rho \sum_i w_i Z_i/A_i + 0.11825\rho \sum_i w_i Z_i^2/A_i \quad (14)$$

The backcalculated values of hydrogen for this data are reported in Tables V and VI and compared with the values obtained by Piehl and Rowan. The standard error of ±0.00038 obtained by our calibration method compares favorably with the value of ±0.00028 obtained by Piehl. The standard error of ±0.00039 obtained by our method on the data of Rowan does not compare as well with his standard error of ±0.00003. However, he also reports an estimated standard error for a large number of experimental results of ±0.00010 to ±0.00020 which gives a reasonable check with our value.

Table VI. Results of Different Calibration Models on Data of Rowan

Sample	Weight fractions of hydrogen: Exptl.	Calcd. by method of Rowan	Calcd. with proposed method from Eq. 14
Toluene	0.08752	0.08754	0.08767
Benzene	0.07743	0.07738	0.07773
Cumene	0.10064	0.10063	0.10028
Ethylbenzene	0.09495	0.09498	0.09480
sec-Butylbenzene	0.10513	0.10511	0.10460
Cyclohexane	0.14373	0.14373	0.14327
Standard error		±0.00003	±0.00039

DISCUSSION

Even though the accuracy demonstrated is not quite as good for the calibration model proposed here as that used by the previous authors, the other advantages of this model would appear to compensate for this small discrepancy in accuracy. The model proposed here contains only three constants when background can be neglected or obtained experimentally (the usual case), and these constants can be determined by a straightforward least-squares analysis. Even when the two-cell technique of Smith and Otvos is used and a trial-and-error technique must be employed to find the additional required constant, the model proposed here is simpler when elements other than hydrogen and carbon are present in the samples to be measured. Recall that the relative absorption cross section must be determined individually by a trial-and-error method in the other methods.

The use of the calibration model to measure hydrogen weight fraction is also more straightforward than that proposed by Smith and Otvos. To use their model one must first solve a quadratic equation for A (Equation 7), and then solve Equation 2 for the value of the hydrogen weight fraction. Since the model proposed here is linear in hydrogen weight fraction, it can be solved directly.

If greater accuracy than that demonstrated here is desired, one could employ multiple calibration curves which are appropriate only to limited regions of hydrogen densities.

Table V. Results of Different Calibration Models on Data of Piehl

Sample	Weight fractions of hydrogen: Exptl.	Calcd. by method of Jacobs, Lewis, and Piehl	Calcd. with proposed model from Eq. 13
Benzene	0.07743	0.07727	0.07726
Benzene	0.07743	0.07733	0.07731
Cumene	0.10064	0.10047	0.10042
Cumene	0.10064	0.10026	0.10021
sec-Butylbenzene	0.10514	0.10502	0.10498
sec-Butylbenzene	0.10514	0.10495	0.10492
Ethylbenzene	0.09495	0.09518	0.09514
Ethylbenzene	0.09495	0.09529	0.09526
Toluene	0.08752	0.08736	0.08731
Toluene	0.08752	0.08732	0.08728
Decalin	0.13125	0.13168	0.13183
Decalin	0.13125	0.13140	0.13155
n-Decane	0.15587	0.15576	0.15501
n-Decane	0.15587	0.15634	0.15558
Standard error		±0.00028	±0.00038

LITERATURE CITED

(1) Evans, R. D., "The Atomic Nucleus," p. 608, McGraw-Hill, New York, 1955.
(2) Gardner, R. P., Dunn, J. W., III, ANAL. CHEM. **37**, 528 (1965).
(3) Jacobs, R. B., Lewis, L. G., Piehl, F. J., *Ibid.*, **28**, 324 (1956).
(4) Piehl, F. J., private communication, American Oil Co., 2500 New York Ave., Whiting, Ind. 46394, 1966.
(5) Rowan, R., Jr., ANAL. CHEM. **31**, 558 (1959).
(6) Smith, V. N., Otvos, J. W., *Ibid.*, **26**, 359 (1954).

ROBIN P. GARDNER
KENNETH F. ROBERTS

Measurement and Controls Laboratory
Research Triangle Institute
Post Office Box 490
Durham, N. C. 27702

WORK done under the auspices of the U. S. Atomic Energy Commission.

Extraction of Metal Pyridine Azides

Spectrophotometric Determination of Copper, Nickel, and Palladium

SIR: Complexes with pyridine and thiocyanate have been used for the extraction and determination of some transition metals (*1*, *5*). The azide and thiocyanate ions are isoelectronic and show many similarities in their abilities to form colored complexes with transition elements, and so one may expect similarities between pyridine-azide and pyridine-thiocyanate solutions in their chemical behavior. Metal pyridine azides have apparently not been reported previously, and it was thought to be of some interest to investigate possible analytical uses of such compounds. The efficiencies of extraction into chloroform of pyridine azide complexes of eleven metals are presented here and spectrophotometric methods are reported for determining copper, nickel, and palladium in the optimum ranges of about 30 to 100 μg., 50 to 200 μg., and 20 to 80 μg., respectively.

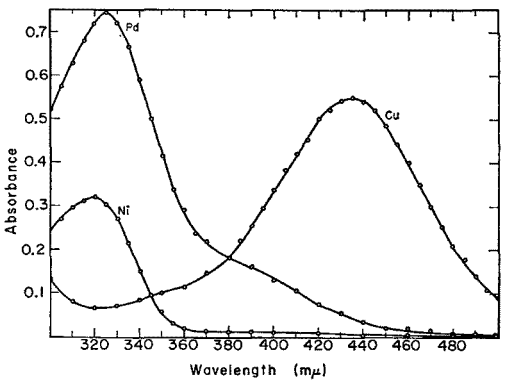


Figure 1. Absorption spectra of chloroform extracts

Aqueous phase: 0.2M azide; 1.1M pyridine; 70 μg. Cu^{+2}, 90 μg. Ni^{+2}, or 82 μg. Pd^{+2} per 10 ml. Readings vs. extracts of blanks containing all reagents

EXPERIMENTAL

Materials and Analyses. The apparatus used has been described before (*2*, *4*), except for a Leeds and Northrup Type E Electro-Chemograph.

All materials used were of reagent grade unless otherwise specified. The preparation of the palladium and gold solutions has been given previously (*2*, *4*). Platinum and manganese were used as their chlorides, and uranyl nitrate was prepared from U_3O_8. All other metals were used as their perchlorate salts. Sodium azide (Fisher's Purified) was found to assay 99.2% (*3*).

Selected methods of analysis, listed elsewhere (*7*), were used in obtaining the extraction efficiencies.

Preliminary Tests. Iron, cobalt, nickel, copper, palladium, platinum, gold, and uranium were observed to be extracted from nearly neutral solutions containing both pyridine and azide, as evidenced by the transfer of color from the aqueous to the chloroform phase. The presence of pyridine alone or azide alone did not cause the color transfer. Zinc and cadmium were found to be but slightly extracted when only pyridine or azide was present, but the extractions were greatly enhanced by the presence of both pyridine and azide. Neither chromium(III) nor vanadium(V) was extracted, based on visual observations, when both pyridine and azide were present.

Recommended Procedures for Copper, Nickel, and Palladium. Add the weakly acidic solution (pH 1–2) containing 30–100 μg. of copper, 50–200 μg. of nickel, or 20–80 μg. of palladium to a 125-ml. separatory funnel; add 1 ml. of pyridine and 2 ml. of 1.00*M* sodium azide, and adjust the volume to 10 ml. Adjust the pH in the range from 5 to 7 for copper or from 8.5 to 11 for nickel. If the palladium sample contains no other buffering agent, add 12 drops (about 0.3 ml.) of concentrated sulfuric acid, which will give a pH of 4.67 ± 0.10. If a foreign buffer ion is present, adjust the pH using a narrow range pH paper. Pipet 10 ml. of chloroform and shake for 30 seconds.

Drain a sufficient amount of the chloroform extract to fill a 1.00-cm. absorbance cell through a small cotton tuft supported on a micro-funnel. Measure the absorbance of the extract at 435 mμ for copper, 320 mμ for nickel, or 325 mμ for palladium against a blank extract prepared in the same manner. Prepare a calibration curve by carrying known amounts of metal ion through the same procedure.

RESULTS

Extraction. The concentrations of pyridine and azide, 1.12*M* and 0.200*M*, respectively, used throughout the extraction studies, were those sufficient to give optimum color development with copper, nickel, and palladium. In all instances the volume ratio of chloroform to aqueous phase was 1:1, before equilibration, and the pH was adjusted with either sodium hydroxide or sulfuric acid.

After equilibration the metal-poor phase was taken for analysis. Consistent results were obtained in all cases, except for platinum, using a 30-second equilibration time. Shortly after the addition of the reagents to a chloroplatinate solution, a turbidity appeared. After shaking and phase separation, a clear solution was first obtained, but the turbidity gradually reappeared in the aqueous layer. It was necessary to shake the chloroplatinate solution with the chloroform a total of nine times, 30 seconds each, over a period of one half hour in order to reach equilibrium. This behavior probably allows a cleaner separation of palladium and gold from platinum than would be expected from the equilibrium extraction values shown in Table I. Data for the last column were obtained by equilibration of 10 ml. each of the organic and aqueous phases containing no extractable metal ions. The gold extracts must be sampled soon after equilibration, since gold is reduced on standing.

Color Development. The details of color development were studied for only copper, nickel, and palladium; spectral scans for chloroform extracts of these three elements are shown in Figure 1.

To study the effect of pH on absorbance, pyridine and azide were held at 1.12*M* and 0.200*M*, respectively, concentrations found sufficient to give optimum color development for all three metals. The pH was adjusted with concentrated sulfuric acid or 10*M* sodium hydroxide. After equilibration of the solutions for 30 seconds with an equal volume of chloroform, the absorbances of the organic phases were obtained. The results are shown in Figures 2, 3, and 4. It seems likely that a number of different complexes exist in the chloroform phase, since the variation in absorbance cannot be explained in terms of volume change, blank variation, or amount of metal extracting. The peak at pH 5.5 in Figure 3 is reproducible.

Copper and nickel exhibit absorbance

Table I. Percentage Extraction of Various Ions into Chloroform as Metal Pyridine Azides

pH	Extraction, %												$V_{aq}:V_{org}$
	Mn^{a}	Fe^{+3}	Co^{a}	Ni^{+2}	Cu^{+2}	Zn^{+2}	Pd^{+2}	Cd^{+2}	Pt^{+4}	Au^{+3}	UO_2^{+2}	N_3^-	
2	0.0	0.0	0.2	<0.1	<0.1	0.0	98.8	0.0	79.9	92.0	<0.1	47	9.5:10.5
3	0.0	0.0	0.4	0.1	1.8	0.0	98.9	0.0	92.4	98.2	<0.1	41	9.5:10.5
4	0.0	0.6	0.8	0.3	72.8	0.0	98.9	0.8	95.5	98.4	<0.1	37	9.4:10.6
5	0.0	50.0	2.5	51.6	98.1	2.9	99.4	7.4	94.6	98.9	<0.1	25	9.2:10.8
6	<0.1	ppt.	84.0	98.7	99.4	73.2	99.7	85.0	85.9	98.9	1.1	19	8.8:11.2
7	0.1	...	95.0	99.9	99.5	93.3	99.8	91.4	75.6	98.9	ppt.	2	8.7:11.3
8	0.2	...	95.7	>99.9	99.6	93.7	99.8	91.6	72.3	98.6	...	0.3	8.6:11.4
9	0.2	...	95.4	>99.9	99.8	ppt.	99.8	90.2	70.9	98.3	...	0.0	8.6:11.4
10	ppt.	...	ppt.	99.6	98.2	...	98.9	89.1	70.1	98.0	...	0.0	8.6:11.4
11	...	...	...	99.5	ppt.	...	97.6	ppt.	68.7	97.6	...	0.0	8.6:11.4
mg./10 ml.	10.64	2.00	5.00	4.67	2.03	10.00	4.00	4.00	2.79	5.00	10.00 as U	84.0	

[a] Oxidation state may be +2 or higher, depending on pH and air oxidation.

plateaus in the pH intervals from 5 to 7 and 8.5 to 11, respectively (Figures 2 and 3). Palladium shows no plateau (Figure 4), but there is a range from pH 4 to pH 6 in which the absorbance variation in about 6%. Both hydrazoic acid and the pyridinium ion have their pK_a values near the middle of the range and, under the conditions for the procedure above, a pH of 4.67 ± 0.10 is attained by the addition of a constant amount of strong acid to both sample and blank.

Absorbance plateaus for both copper and nickel occur at azide concentrations between 0.1*M* and 0.3*M*, with the pH levels held within the optimum limits. A maximum absorbance, with no level region, is found for palladium at 0.2*M* azide. Plateaus also occur for copper and nickel between 0.6*M* and 1.2*M* pyridine and for palladium between 1.1*M* and 2.2*M* pyridine.

Precision and Interferences. The absorptivity for copper in the 30- to 100-μg. range is 0.0697 ± 0.0005 p.p.m.$^{-1}$ cm.$^{-1}$, for nickel in the 50- to 200-μg. range, it is 0.0355 ± 0.0010, and for palladium in the 20- to 80-μg. range it is 0.0913 ± 0.0010, based on the initial 10 ml. of organic phase. The anticipated errors for concentrations covering these absorption ranges are 0.8%, 2.8%, and 1.1%, based upon the respective standard deviations of the absorptivities.

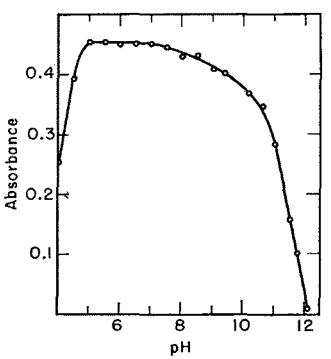


Figure 2. Effect of pH on color development for copper at 435 mμ

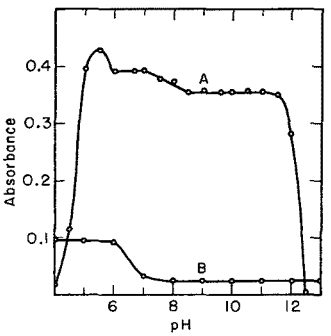


Figure 3. Effect of pH on color development for nickel at 320 mμ

A. Nickel extract vs. blank extract
B. Blank extract vs. chloroform

In Table II are listed the maximum concentrations of anions which will give less than a 3% error in the determinations of the three metals. The volume ratio of aqueous phase to organic phase may be increased to 2:1 for copper, 3:1 for nickel, and 2:1 for palladium and still give an error of less than 3% if the concentrations of reagents are constant and corresponding blank are used.

DISCUSSION

In comparison to the pyridine-thiocyanate reagent, the pyridine-azide reagent has two advantages: there is no change in the absorbance of the blank up to 17 hours, and the excess azide is easily removed. The use of masking agents can undoubtedly be used to improve selectivity. For example, when the aqueous phase is 0.1*M* in tartrate, only 0.4% of iron(III) is extracted at pH 6 and less than 0.1% at all other values from pH 2 to pH 11.

Both cobalt and gold were investigated briefly for possible trace method development. Extracts of these two metals are not sufficiently stable to warrant further investigations; gold is slowly reduced to metal and cobalt(II) is apparently oxidized. If the cobalt is completely oxidized in the aqueous phase, very little extraction occurs.

A spectral scan of an aqueous solution containing 1 × 10^{-4}*M* Cu^{+2} and 0.2*M* N_3^- has the same shape, with maximum absorbance at 385 mμ, as has the scan of a solution which is also 1.1*M* in pyridine. It thus appears that no pyridine-containing complex is present in the aqueous phase, though pyridine is necessary for the extraction of copper. A mole ratio plot using 1 × 10^{-3}*M* Cu^{+2}, with the absorbance peak at 370 mμ, shows a

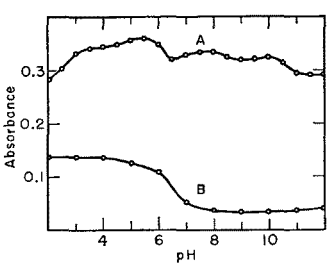


Figure 4. Effect of pH on color development for palladium at 325 mμ

A. Palladium extract vs. blank extract
B. Blank extract vs. chloroform

Table II. Tolerance for Anions

	Max. molarity giving less than 3% error				
	Cl^-	ClO_4^-	PO_4^{-3}	SO_4^{-2}	$C_4H_4O_6^{-2}$
Cu	1.3	0.5	0.6	0.9	0.1
Ni	2.8	0.4	0.5	0.7	0.7
Pd	1.2	0.2	1.2	1.1	0.5

1:4 copper to azide species in the presence of 4.46 × $10^{-2}M$ pyridine. Saini and Ostacoli (*6*) found the same ratio in a mixture of 2-ethyoxyethanol and water, but containing no pyridine. The shift in the maximum absorbance to 385 mμ when the azide concentration is increased 50-fold also indicates the presence of unstable higher complexes of copper.

LITERATURE CITED

(1) Ayres, G. H., Baird, S. S., *Talanta* **7**, 237 (1961).
(2) Clem, R. G., Huffman, E. H., ANAL. CHEM. **37**, 86 (1965).
(3) *Ibid.*, p. 366.
(4) *Ibid.*, p. 1155.
(5) Forsythe, J. H. W., Magee, R. J., Wilson, C. L., *Talanta* **1**, 249 (1958).
(6) Saini, G., Ostacoli, G., *J. Inorg. Nucl. Chem.* **8**, 346 (1958).
(7) UCRL Report 16642, Lawrence Radiation Laboratory, University of California, Berkeley, 1966.

RAY G. CLEM
E. H. HUFFMAN

Lawrence Radiation Laboratory
University of California
Berkeley, Calif.

WORK done under the auspices of the U. S. Atomic Energy Commission, AEC Contract No. W-7405-eng-48.

Use of an Alkali Additive for Gas Chromatographic Analysis of Organic Bases on Open Tubular Columns

SIR: Recently, Grob (*3*) demonstrated the use of open tubular columns for the gas chromatographic analysis of amines. Although the use of free alkali as both a pretreatment and an additive was discussed, the results obtained were not satisfactory. Because of this, it was necessary to prepare polyimines for use as the liquid phase. Our experience has been that, although sometimes difficult, it is possible to coat an open tubular column with a liquid phase that contains an alkali additive.

EXPERIMENTAL

A Perkin-Elmer Model 226 gas chromatograph equipped with a flame ionization detector was used for these studies. The recorder was a Leeds & Northrup Speedomax G with a full-scale span of 5 mv. The columns, fabricated from stainless steel tubing, were 200 feet long, and had a 0.030-inch o.d. and 0.020-inch i.d. The liquid phases which were used were Carbowax 20M and Carbowax 1540 (Union Carbide Corp., New York City), and the additive was potassium hydroxide (Fisher Scientific Co., Pittsburgh, Pa.). The columns were coated under pressure by passing 5 ml. of the coating solution through the tubing with N_2 at 5 p.s.i.g.

The coating solutions were made in the following manner. Ten grams of either Carbowax 20M or 1540 was dissolved in 100 ml. of methylene chloride, and 5 grams of KOH was dissolved in 100 ml. of methanol. To coat the column, 4.9 ml. of the Carbowax solution and 0.1 ml. of the KOH solution were used.

The analyses were carried out under various conditions of temperature programming. The column inlet pressure was 10 p.s.i.g. of N_2, and the split ratio was approximately 50:1.

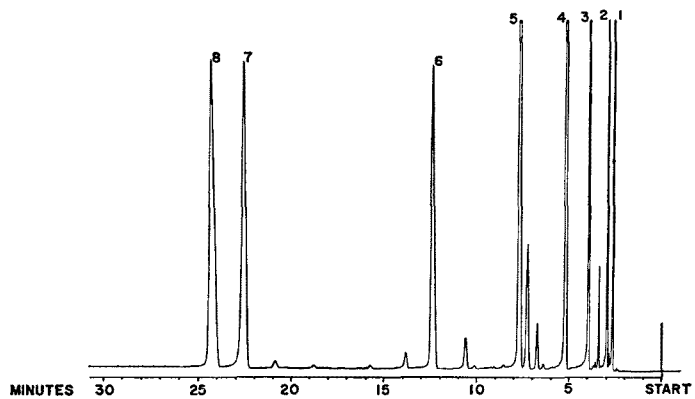


Figure 2. Chromatogram of aliphatic amines on 200-ft. × 0.020-inch i.d. column coated with Carbowax 1540-KOH

Peak identification the same as Figure 1

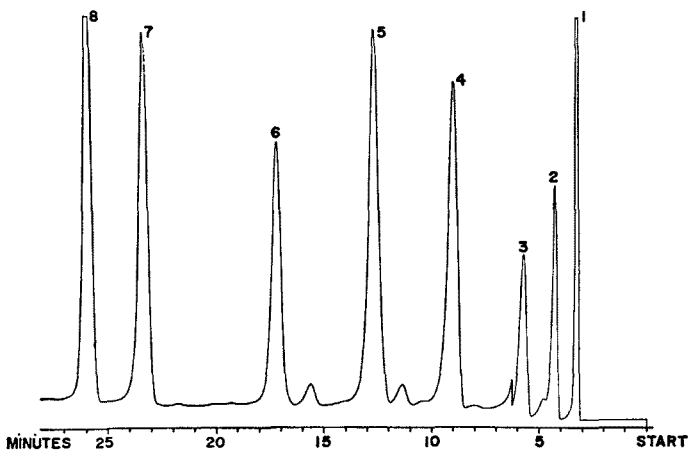


Figure 1. Chromatogram of aliphatic amines on 200-ft. × 0.020-inch i.d. column coated with Carbowax 20M–KOH.

Peaks:
1. Acetone
2. Tripropylamine
3. Dibutylamine
4. Tributylamine
5. Triisopentylamine
6. Tri-*n*-pentylamine
7. Di-*n*-heptylamine
8. Trihexylamine

DISCUSSION

The use of an alkali additive on packed columns has been the subject of many papers (*1*, *2*, *4–7*). Although Grob (*3*) was unsuccessful in its use on open tubular columns, our previous experience in coating these columns with

polar liquid phases led us to believe that it was possible. The first attempt was made using Carbowax 20M and KOH. A synthetic mixture was analyzed on this column, and the resultant chromatogram is shown in Figure 1. Although all the components were resolved, a large degree of peak broadening can be observed.

A column was then coated with Carbowax 1540 and KOH, and the same mixture was analyzed. Figure 2 shows the chromatogram that was obtained. A comparison of this figure with Figure 1 shows that the Carbowax 1540 plus KOH column was more efficient than the Carbowax 20M plus KOH column.

The next materials which were analyzed on this column were a mixture of various pyridines and pyrazines. The solution contained some methyl, ethyl, dimethyl, diethyl, and acetyl pyridines and two diethyl pyrazines. The chromatogram obtained is shown in Figure 3.

While performing the analysis of the pyridines and pyrazines, it was observed that the column used was apparently more temperature stable than a column coated with plain Carbowax 1540. To determine if the column was indeed more stable, a reading of the background current was made at various temperatures. The data obtained for each column was then plotted on semilog paper and is shown in Figure 4. Two straight lines were then drawn through the various points for each of the columns, and the intercept of each plot was noted. This point can generally be taken as the maximum operating temperature for that particular liquid phase. The intercept for the Carbowax 1540 was approximately 130° C., and the intercept for the Carbowax 1540 plus KOH was approximately 210° C. This means that the column with the alkali-additive had a temperature range increase of about 80° C. This is very important in capillary column gas chromatography, where the maximum operating temperature of a liquid phase is usually much lower than that of a packed column.

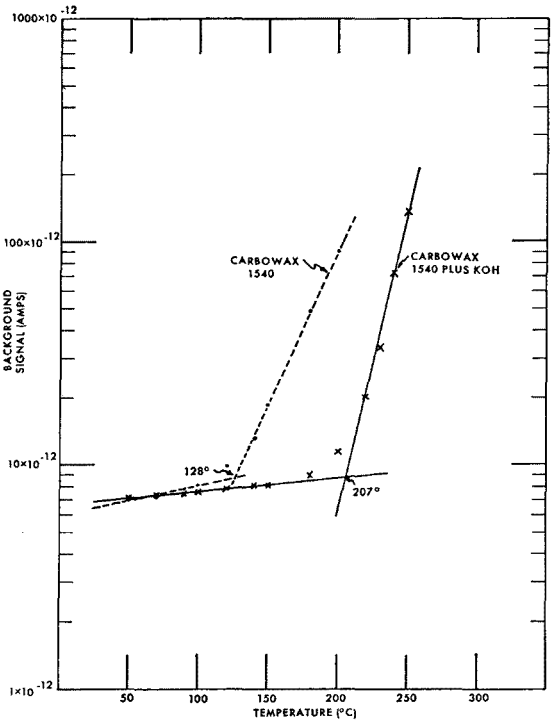


Figure 4. Plot of column background signal *vs.* temperature

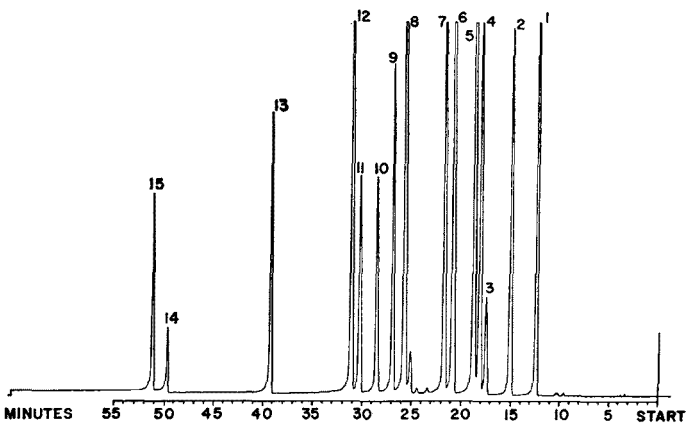


Figure 3. Chromatogram of aromatic amines on 200-ft. × 0.020-inch i.d. column coated with Carbowax 1540-KOH

Peaks:

1. 2-Picoline
2. 2,6-Lutidine
3. 2-Ethylpyridine
4. 3-Picoline
5. 4-Picoline
6. 2,5-Lutidine
7. 2,4-Lutidine
8. 4-Ethylpyridine
9. 3,5-Lutidine
10. 2,6-Diethylpyrazine
11. 2,5-Diethylpyrazine
12. 3,4-Lutidine
13. 2-Acetylpyridine
14. 4-Acetylpyridine
15. 3-Acetylpyridine

ACKNOWLEDGMENT

The author thanks G. C. Bassler of Stanford Research Institute for supplying the samples of the various pyridines and pyrazines.

LITERATURE CITED

(1) Cincotta, J. J., Feinland, R., ANAL. CHEM. **34**, 774 (1962).
(2) Golding, W. E., Townsend, C. A., *Chem. Ind. (London)*, **1960**, p. 1476.
(3) Grob, K., *J. Gas Chromatog.* **2**, 80 (1964).
(4) Link, W. E., Morrissette, R. A., Cooper, A. D., Smullin, C. F., *J. Am. Oil Chemists' Soc.* **37**, 364 (1960).
(5) Ottenstein, D. M., *J. Gas Chromatog.* **1**, 11 (1963).
(6) Parker, K. D., Fontan, C. R., Kirk, P. C., ANAL. CHEM. **34**, 1345 (1962).
(7) Smith, E. D., Radford, R. D., *Ibid.*, **33**, 1160 (1961).

E. W. CIEPLINSKI[1]
Perkin-Elmer Corp.
Norwalk, Conn.

[1] Present address: Olin Research Center, 275 Winchester Avenue, New Haven, Conn. 06504

Polarographic Behavior in the Oxidation of Sodium Formaldehyde Sulfoxylate

SIR: The stability and high reducing strength of sodium formaldehyde sulfoxylate (SFS) have made it particularly attractive for use in the dyeing industry, as a stabilizer for oxygen-sensitive compounds in solution, and for controlled reductions in numerous organic reactions. Therefore the mechanisms of its reactions have been of significant industrial and scientific interest.

Goehring (*5*) reported that under neutral and alkaline conditions at 25° C. the SFS anion, $CH_2(OH)SO_2^-$, remained intact in solution. Oxidation of the ion under these conditions resulted in the formation of formaldehyde and sulfite ion.

Studies by Rinker, Gordon, and Corcoran (*13*) showed that under acidic conditions SFS undergoes decomposition with the initial reaction probably being

$$H^+ + CH_2(OH)SO_2^- \rightarrow HSO_2^- + CH_2(OH) \quad (1)$$

In this case, the SFS becomes a source of HSO_2^-, and so its chemical behavior is similar to that of $S_2O_4^{-2}$ ions.

Decomposition studies performed by Kunim (*11*) were carried out in alkaline solution at elevated temperatures. For the temperatures between 70° and 120° C., he postulated the initial decomposition reaction to be

$$CH_2(OH)SO_2^- \rightarrow HSO_2^- + HCHO \quad (2)$$

Reactions subsequent to the initial decomposition were strongly temperature dependent so that the type and distribution of products varied significantly within the temperature range studied.

According to Furness (*4*), SFS was oxidized irreversibly at a stationary platinum electrode in a system buffered with citrate at a pH of 4. On the other hand, he found that under the same conditions of acidity, no anodic waves were obtained at the dropping mercury electrode.

The only quantitative study of the polarographic reactions of SFS was reported by Kolthoff and Tamberg (*10*). These authors obtained well-defined anodic waves in the pH range from 9 to 13 but no waves at or below pH 7. A plot of log $(i_d - i)/i$ *vs.* E yielded a straight line with a value of 0.9 for n, which indicated an irreversible process. The half-wave potential was dependent on pH but independent of SFS concentration. They also found that a direct linear relationship existed between the diffusion current and the concentration of SFS. Calculation of I, the average diffusion current constant, from the Ilkovic equation (*8*) yielded a value of 3.84 and likewise a value of 1.00×10^{-5} cm.^{2} sec.$^{-1}$ for the Fick diffusion coefficient of the SFS anion at 25° C.

The mechanism proposed by Kolthoff and Tamberg (*10*) for the electrode reaction at a pH greater than 9 included the direct oxidation of SFS anion to the formaldehyde sulfite anion, $CH_2(OH)SO_3^-$, followed by decomposition of the latter to formaldehyde and sulfite ion as shown in Equations 3 and 4:

$$CH_2(OH)SO_2^- + 2OH^- \rightarrow CH_2(OH)SO_3^- + H_2O + 2e \quad (3)$$

$$CH_2(OH)SO_3^- + OH^- \rightleftarrows HCHO + SO_3^{-2} + H_2O \quad (4)$$

The purpose of the present study was to extend the work of Kolthoff and Tamberg over a larger pH range, namely from 2 to 12, in order to gain new insights on the chemical nature of SFS.

EXPERIMENTAL

The electrolytic system consisted of an H-type cell mounted on a cushioned stand to minimize vibration. A saturated calomel electrode (SCE) was in the reference compartment. A cross member contained a glass frit and was filled with a 4% agar gel saturated with KCl. The other side was fitted with a dropping mercury electrode (DME) with drop times which could be varied from 2 to 6 seconds. That compartment was also fitted with a stopcock to facilitate drainage and with appropriate side arms to permit deaeration of the test solution by bubbling nitrogen through it. By means of a two-way valve, the gas was diverted over the solution during electrolysis. The current flowing in the cell and the voltage between the DME and the SCE were automatically recorded on a voltage scanning Sargent Model XV Recording Polarograph at a rate of 0.1 volt per minute. The cell was operated at 25° ± 1° C., and temperature changes were slow enough not to cause significant fluctuations in the experimental measurements.

Nitrogen used for purging oxygen from the cell was Linde HPD grade (99.95% purity) which was further purified by bubbling through chromous chloride solution and then humidified by scrubbing with oxygen-free distilled water. The SFS was a product of Matheson, Coleman, and Bell and was 99+% pure, with sodium sulfite and sodium thiosulfate being the major impurities. Mercury for the working electrode was doubly distilled. All other chemicals such as buffer agents, electrolytes, and formaldehyde were of reagent grade.

Buffer solutions with pH values from 2 to 12 were prepared by mixing measured proportions of a solution which was 0.2*m* in NaOH with a stock solution which was 0.04*F* in acetic acid, phosphoric acid, and boric acid and 0.1*m* in potassium chloride. Values of the pH were measured with a Beckman Model G pH meter.

Before each run, the solution compartment of the cell was thoroughly rinsed with distilled water and allowed to drain dry. A volume of 25.00 ml. of the buffered electrolyte was added to the compartment, and then the system was purged with nitrogen for at least 15 minutes. Changes in volume of the electrolyte as a result of the bubbling were negligible. Weighed amounts of the SFS were added and rapidly dissolved by brief, continued bubbling.

Drop times were computed from the measured time of at least 10 drops, with the DME polarized at the same potential at which the diffusion current was measured. The rate of mercury flow was determined by weighing the mercury collected from the DME over a measured time interval.

RESULTS

Basic Media. As shown in Figure 1, solutions of SFS which were 1×10^{-3} *F* gave single anodic waves in the pH range from 6.92 to 11.6. For the pH region from 8 to 12, the results of Kolthoff and Tamberg (*10*) were essentially confirmed. Contrary to the findings of Kolthoff, however, a reasonably well-defined irreversible wave was obtained at pH 6.92 with $E_{1/2} = +0.07$ volt *vs.* SCE. Also, at pH values > 10, two small but distinct cathodic waves were obtained with half-wave potentials of − 1.32 volts and −1.63 volts *vs.* SCE. Both waves were irreversible. The nature of the first cathodic wave is still under consideration, and the second cathodic wave resulted from reduction of formaldehyde in accord with the reaction

$$HCHO + 2H_2O + 2e \rightarrow CH_3OH + 2OH^- \quad (5)$$

For pH ≥ 6.92, values of the half-wave potentials were found to be independent of the SFS concentration between 0.3×10^{-3} and 2.0×10^{-3} *F*. The half-wave potentials were, however, dependent on the pH as may be noted in Figure 2, and became more cathodic with increasing hydroxyl concentration. This apparent decrease in free energy of oxidation with increasing basicity was indicative that OH^- ions were con-

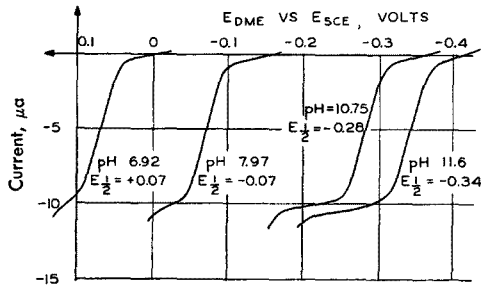


Figure 1. Polarograms for sodium formaldehyde sulfoxylate in the pH range of 6.92 to 11.6

SFS concn. = $1 \times 10^{-3}F$

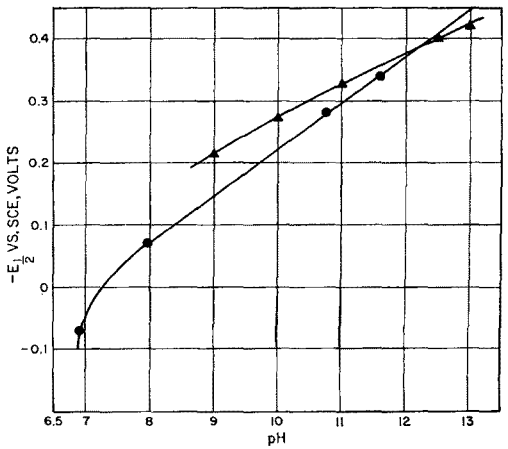


Figure 2. Half-wave potential for the anodic wave as a function of pH

Temp. = 25° C.
▲ Kolthoff and Tamberg (*10*)
● This work, SFS concn. = $1 \times 10^{-3}F$

sumed in the electrochemical step of oxidizing the SFS anion. On the other hand, as shown in Figure 2, the more rapid increase of $E_{1/2}$ with decreasing concentration of hydroxyl ions in the pH range 8 to 7 indicated a change in oxidation mechanism was occurring because of thermodynamic limitations.

The effect of added formaldehyde on the SFS electrode oxidation was studied. In agreement with Kolthoff and Tamberg (*10*) there was no detectable effect on the nature of the anodic waves. Thus, an initial reaction of the type

$$CH_2(OH)SO_2^- \rightleftarrows HSO_2^- + HCHO \quad (6)$$

in which the intermediate HSO_2^- is formed can be discarded since an excess of formaldehyde would certainly affect the characteristics of the waves.

A plot of log $[i/(i_d - i)]$ *vs.* E for pH 10.75 was essentially a straight line except at the beginning and end of the wave where the logarithmic term is sensitive and can easily be in error. A value of $n = 0.8$ was obtained from the reciprocal slope of the linear portion. This would indicate an irreversible electrode process. From similar plots for decreasing pH values, the value of n decreased and at pH 6.92 reached a value of 0.7. A plot of log $[i/(i_d - i)^2]$ *vs.* E was also obtained for the wave at pH 6.92. Such a plot should yield a straight line with a reciprocal slope of 0.030 if the wave resulted from reversible mercury dissolution (*8*) according to

$$Hg + 2SO_3^{-2} \rightleftarrows Hg(SO_3)_2^{-2} + 2e \quad (7)$$

The plot showed, however, a distinctly greater curvature than the one in which the log term contained $(i_d - i)$ to the first power.

A further test of irreversibility at pH 6.92 was the determination of β values at the toe and head of the wave. The β function (*7*) is defined as the ratio $(i/i_m)_E$. A value of $\beta = 0.68$ was obtained for the toe and $\beta = 0.86$ for the head of the wave. These values are reasonably close to the theoretical values of 0.64 and 0.85, respectively, for an irreversible wave of a single electrode reaction at the expanding spherical drop.

Because all the waves were irreversible, the value of n could not be determined directly from the Nernst equation. The final products of the oxidation of SFS were sulfite ion and formaldehyde, however, so that the increase in oxidation state of sulfur from +2 to +4 indicated that $n = 2$ for the total number of electrons transferred per molecule of SFS.

Variations in the limiting current with SFS concentration were measured at pH 11.6. The wave heights were found to be linearly proportional to the SFS concentration showing that the limiting current was diffusion controlled. No measurements were made of the variation in limiting wave heights with mercury pressure. Use of the Ilkovic equation gave a value of 3.73 for I, the average diffusion current constant. By assumption of a 2-electron reaction at the electrode, the Fick diffusion coefficient of the SFS anion was computed to be 0.95×10^{-5} cm.^{2} sec.$^{-1}$ at 25° C., which is within 5% of the value reported by Kolthoff and Tamberg (*10*).

Acidic Media. Acidification of SFS caused cleavage of the carbon–sulfur bond. The dominant cleavage fragment in acidic solution would be $HSO_2\cdot$, the protonated monomer (*13, 14*) of the $S_2O_4^{-2}$ ion. Pertinent previous studies of the $S_2O_4^{-2}$ ion were made by Čermák (*1, 2*), Gossman (*6*), and Kolthoff and Miller (*9*). In the present work for the pH range from 5 to 6, $HSO_2\cdot$ was detectable by its cathodic wave at $E_{1/2} = -1.20$ volts *vs.* SCE, according to the reaction

$$HSO_2\cdot + e \rightarrow HSO_2^- \quad (8)$$

The limiting current for this irreversible wave showed a slight time dependence at pH 5 for the lowest initial concentration of SFS. The wave disappeared below pH 5 because of rapid disproportionation according to the scheme

$$2HSO_2\cdot \rightarrow SO_2 + H_2SO_2 \quad (9)$$

A second cathodic wave which was kinetically controlled was observed in the pH range from 1 to 6 and was highly pH dependent. For that wave, $E_{1/2}$ varied linearly from −0.71 volt to −0.37 volt *vs.* SCE for a $10^{-3}F$ solution of SFS. Data for an equivalent concentration of $NaHSO_3$ coincide with the SFS data. The electrode reaction accounting for these interesting results was the reduction of SO_2 to H_2SO_2 given by the overall equation

$$SO_2 + 2H^+ + 2e \rightarrow H_2SO_2 \quad (10)$$

Quantitative measurements showed that the limiting current was not diffusion controlled and was not time dependent.

In a 0.1*m* HCl solution of SFS, the ion $S_2O_3^{-2}$ also appeared. This was not surprising in view of the above fact that H_2SO_2 became the dominant intermediate at pH < 4 in the decomposition of SFS. Presumably the thiosulfate was formed in a disproportionation reaction of the sulfoxylic acid according to the overall equation

$$2H_2SO_2 \rightarrow H_2S_2O_3 + H_2O \quad (11)$$

After 15 to 20 minutes in the cell, the highly acidified solutions of SFS became milky in appearance. This was due

primarily to the nucleophilic degradation of thiosulfate which yielded free sulfur according to the reaction

$$H_2S_2O_3 \rightarrow SO_2 + S + H_2O \quad (12)$$

Another contribution to the sulfur formation was the reaction

$$2H_2SO_2 \rightarrow SO_2 + S + 2H_2O \quad (13)$$

After an hour of standing, H_2S was detected in the 0.1*m* HCl solutions of SFS. According to Marshak (*12*), the H_2SO_2 can also disproportionate in the following overall manner:

$$3H_2SO_2 \rightarrow 2SO_2 + H_2S + 2H_2O \quad (14)$$

There were no major anodic waves in the acidic media. This observation was strong evidence that the concentration of $S_2O_4^{-2}$ or its protonated forms was negligible. Otherwise, the oxidation of $S_2O_4^{-2}$ to SO_2 would have been observed at $E_{1/2}$ = 0.45 volt *vs.* SCE.

At pH values <2, a small anodic wave did appear with half-wave potentials varying with time from −0.14 volt to −0.21 volt *vs.* SCE, respectively. Although no specific effort was made to identify the wave, it was most likely associated with the oxidation of mercury (*8*) by the reaction

$$2S_2O_3^{-2} + Hg \rightarrow Hg(S_2O_3)_2^{-2} + 2e \quad (15)$$

The shift of $E_{1/2}$ with time toward more cathodic potentials was then due to the increase in the concentration of $S_2O_3^{-2}$ with time.

LITERATURE CITED

(1) Čermák, V., *Chemicke Zvesti* **8,** 714 (1954).
(2) Čermák, V., *Collection Czech. Chem. Commun.* **23,** 1471 (1958).
(3) Delahay, P., "New Instrumental Methods in Electrochemistry," p. 64 Interscience, New York, 1954.
(4) Furness, W., *J. Soc. Dyers Colourists* **66,** 270 (1950).
(5) Goehring, M., *Z. Anorg. Chem.* **253,** 313 (1947).
(6) Gossman, B., *Collection Czech. Chem. Commun.* **23,** 1471 (1958).
(7) Grodzka, P. G., Elving, P. J., *J. Electrochem. Soc.* **110,** 225 (1963).
(8) Kolthoff, I. M., Miller, C. S., *J. Am. Chem. Soc.* **63,** 1405 (1941).
(9) *Ibid.*, p. 2818 (1941).
(10) Kolthoff, I. M., Tamberg, N., *J. Polarog. Soc.* **3,** 54 (1958).
(11) Kunim, T. I., *Zhur. Preklad Khim.* **21,** 685 (1948).
(12) Marshak, E. M., *Khim. Nauka i Prom.* **2,** 524 (1957).
(13) Rinker, R. G., Gordon, T. P., Corcoran, W. H., *Inorg. Chem.* **3,** 1467 (1964).
(14) Rinker, R. G., Lynn, S., Mason, D. M., Corcoran, W. H., *Ind. Eng. Chem. Fundamentals* **4,** 282 (1965).

REMIGIO FERNANDEZ-MARTIN
R. G. RINKER
W. H. CORCORAN

Chemical Engineering Laboratory
California Institute of Technology
Pasadena, Calif.

WORK supported by the Shell Companies Foundation and E. I. du Pont de Nemours and Co.

Chelometric Titration for Zinc in Municipal and Industrial Water Supplies

SIR: The determination of part-per-million concentrations of zinc in industrial and municipal water supplies is becoming increasingly important because of corrosion problems. Not only is zinc present as a product of corrosion, but there is also a growing use of zinc salts in corrosion inhibitors. A convenient analytical procedure for zinc in aqueous systems would be desirable for use as a control method. A number of photometric, turbidimetric, and titrimetric procedures for zinc are described in the chemical literature. All of these, however, lack either simplicity or specificity, or require the use of a toxic reagent, features which are undesirable in a control method for plant or field use.

A titrimetric procedure seemed the most promising and convenient. For this, chelating agents are eminently suitable. Such procedures have been described, but they are limited mostly to higher concentrations of zinc. Those that are sensitive enough for p.p.m. zinc levels cannot tolerate the high concentrations of hardness, primarily calcium, that are found in most municipal or industrial systems. The choice of indicators is also limited because of their reaction with hardness or because of the sensitivity required. In the report of a solvent extraction method devised by Medlin (*3*), the author states that there were no methods for determining p.p.m. of zinc in the presence of high concentrations of calcium.

Titrimetric procedures using EDTA and dithizone to determine zinc have been reported by many investigators (*1, 2, 4, 5, 11*). Although this approach provides the required sensitivity, over 20 p.p.m. of calcium as $CaCO_3$ causes dragging end points, and over 50 p.p.m causes serious error. Diethylenetriaminepentaacetic acid (DTPA), an analog of EDTA, is suitable for substitution as the titrant in this approach. DTPA is 200 times better than EDTA in its effective chelation of zinc over calcium, and thus the tolerance for calcium hardness is greatly increased. A method based on this approach has been applied successfully in analysis of industrial and municipal waters.

EXPERIMENTAL

Reagents. The buffer solution contained 270 grams of sodium acetate trihydrate and 225 ml. of glacial acetic acid per liter. The indicator solution was 0.04% dithizone in methanol and the titrating solution was exactly 0.6017 grams of DTPA (acid) plus 8.5 ml. of 1*N* NaOH diluted to 1000 ml.

Procedure. Measure 100 ml. of total sample in a 100-ml. graduated cylinder and pour it into a casserole or other suitable container. Rinse the graduate with no more than 10 ml. of deionized water. Then add 5.0 ml. of buffer solution and 0.5 ml. of 0.2*N* sodium thiosulfate solution and mix thoroughly. Add 100 ml. of isopropanol to provide for dissolution of the indicator. With stirring, add 0.5-ml. increments of indicator until the sample solution remains strongly pink.

Titrate with DTPA solution. The end point change is pink to blue-green. One milliliter of titrant is equivalent to 0.1 mg. of zinc as Zn.

RESULTS AND DISCUSSION

This procedure is convenient in plant and field operations over extended use in a variety of industrial applications. Concentrations as low as 0.2 p.p.m. can be titrated, and the method can tolerate up to 1000 p.p.m. of calcium as $CaCO_3$.

Besides dithizone as an indicator, Zincon (*o*-[[α-[(2-hydroxy-5-sulfophenyl) azo] benzylidene] hydrazino] benzoic acid) and Xylenol Orange (3′, 3″ - bis [[bis (carboxymethyl) amino] methyl]-5″, 5″ dimethylphenylsulfonephthalein) were also considered. Dithizone, however, is the best. The color change provides high sensitivity, indicating as little as 0.005 mg. of zinc. The addition of a water miscible organic solvent, however, is necessary to keep the dithizone in solution. Several solvents were investigated by Costa (*1*). Isopropanol (*2*) was chosen for our purposes. Zincon was rejected because, while sensitive to zinc, it gives a somewhat dragging end point. It is also very sensitive to copper which blocks the Zincon as an indicator. In the presence of as little as 0.05 p.p.m. of copper, no color change is observed. Xylenol Orange is not as sensitive to zinc as are dithizone and Zincon. Also, its color change

Table I. Effect of Common Anions

Anion	Allowable concn., p.p.m.	Remarks
CO_3^{-2}	1,000	Highest amt. tested
PO_4^{-3}	5,000	Highest amt. tested
$P_2O_7^{-4}$	500	Slightly dragging end point
SO_4^{-2}	10,000	Highest amt. tested
Cl^-	5,000	Highest amt. tested
NO_3^-	1,000	Highest amt. tested
NO_2^-	50	Oxidizes indicator. Can be overcome
$(NaPO_3)_6$	20	Above 20 p.p.m., low results and dragging end point
$C_2O_4^{-2}$	35	Dragging end point
S^{-2}	0	ZnS not titrated quantitatively in procedure, end point fades

from red-orange to yellow provides poor contrast and is especially difficult to see in colored waters.

pH was also a consideration in selecting the indicator. Zincon must be used at a basic pH. The use of an ammonia buffer reduces the effective chelating capacity of the DTPA for zinc due to the formation of the zinc–ammonia complex. Alternative buffers cause precipitation. Dithizone gives its best color change and contrast at a pH of 4.5. This pH also provides for the complete dissolution of zinc salts, which is desirable for the titration. Exceptions are for samples containing sulfide or oxalate. These can be overcome, however, with acid pretreatment.

Other chelating agents were also considered. Tetraethylenepentamine (Tetren) and triethylenetetramine (Trien) have been used in methods described by Reilley and others to determine heavy metals in the presence of large amounts of alkaline earths (*6–9*). These two chelating agents, however, are strongly protonated at acidic pH's and their chelating capacity for certain metals, including zinc, is weakened considerably. The use of these reagents at higher pH's limits the indicator choices to Zincon. There is also the question of these two chelating agents being contaminated even after recrystallization by less effective chelating amines resulting in sliding or dragging end points.

Effect of Interferences. The effect of various interferences has been studied as shown in Tables I and II. Table I summarizes the results of a study of various anions commonly found in industrial and municipal water samples. For each anion, the tolerable concentration is considerably higher than normally found. Nitrite is important since it is present in some cooling systems, but it can be eliminated by addition of sulfamic acid prior to testing. Oxalate was also tested because it is sometimes found in white water samples in paper manufacturing. Insoluble zinc oxalate is formed which slowly dissolves at the pH of the titration. In this case, acid pretreatment would be required to ensure dissolution prior to buffering and titrating. In the presence of sulfide, acid pretreatment is also necessary, the sulfide being evolved as hydrogen sulfide.

Chromate was also checked as a potential interference and was found to oxidize the dithizone indicator slowly. Three hundred parts per million of CrO_4^{-2} can be tolerated if the titration is carried out before the indicator is destroyed by oxidation. Fifty parts per million of CrO_4^{-2} causes no interference. The addition of the thiosulfate does not readily reduce the chromate to chromium(III) at the pH of the titration. This reduction could be accomplished by acidification, then buffering. Chromium(III) reacts only extremely slowly with DTPA and does not interfere.

Table II summarizes the results of a study of the cations commonly found in water supplies. Iron and copper are potentially the two most important interferences. Both are found in significant concentrations in a large number of industrial and municipal supplies, and both will react with the chelating agent used in the method. The pH used, 4.5, will keep dissolution of iron at a minimum rate and thereby increase the tolerance of the method for iron. The procedure has been further modified by the addition of thiosulfate prior to testing to increase the tolerance of the method for copper. The thiosulfate reduces any cupric ion present to

Table II. Effect of Common Cations

Cation	Allowable concn., p.p.m.	Remarks
Fe(III)	2.5	Reacts slowly with DTPA. Higher concn. causes fadeback and high results
Cu(II) or (I)	0.5	End point dark, but good
Pb(II)	0	High results; dragging end point
Ni(II)	0	Reacts slowly causing end point fadeback and high results
Co(II) and Cd^{+2}	0	Titrates quantitatively
Mn(II)	...	Similar to iron
NH_4^+	8000	Above 8000 p.p.m., slight drag in end point
Cr(III)	100	Reaction too slow to cause interference

cuprous ion which can then be masked with the dithizone indicator. The cuprous dithizonate is brownish yellow, providing an innocuous background and also a key to the amount of indicator required. An upper limit of 1.0 p.p.m. of copper is imposed by the strength of the color involved. Above this amount, the sample is too dark to obtain a good color change at the end point. When other heavy metals are present in quantities which are significant relative to the zinc concentration, a prior separation by ion exchange or solvent extraction must be effected. Such separation techniques have been described in many procedures using EDTA, and would be applicable in this procedure as well.

Table III shows a comparision of results by various operators to test the

Table III. Comparison of Results by Different Operators on Field Samples

Sample	Vol. (ml.) titration by various operators				
I	3.15	3.1	3.2	3.1	3.2
II	8.4	8.4	8.1	8.1	...
III	10.0	9.9	10.1	10.0	10.15
IV	4.6	...	4.5	...	4.5
V	2.1	...	2.1	...	2.1
Std.	4.35	4.4	4.4	4.3	4.4

Table IV. Analyses of Typical Industrial Water Samples

Iron concn., p.p.m.	Ca concn., p.p.m. ($CaCO_3$)	Mg concn., p.p.m. ($CaCO_3$)	Zinc by dithizone, p.p.m.	Zinc by titration, p.p.m.
1.9	270	130	2.7	2.8
5.0	320	170	3.7	4.2
1.1	...	...	4.0	3.8
2.4	400	180	3.8	4.0
5.2	310	220	3.4	3.9
1.4	405	175	4.0	4.1
8.2	530	430	9.3	9.0
0.8	84	10	14.9	14.5
2.5	920	230	8.2	8.3
0.7	48	48	2.7	2.8
1.2	300	105	4.5	4.4
1.0	430	180	4.5	3.8
0.7	430	185	2.4	2.4
1.4	...	...	2.8	2.6

precision of the method on five samples from operating industrial systems and one standard solution. As is true of any titration with an indicator end point, a certain amount of subjectivity can be expected, especially on colored or turbid samples frequently encountered in industrial water systems. These data show that the precision of the method is quite adequate.

Table IV shows a comparision of results between the dithizone extraction procedure (*10*) and the DTPA–dithizone titration. The samples selected were typical industrial water samples with varying concentrations of possible interferences. Even with iron concentrations as high as 8 p.p.m. and hardness levels in excess of 1000 p.p.m., the two methods show excellent agreement. This is even more significant when considering that the dithizone extraction procedure is very sensitive, requiring very small sample aliquots for analysis. The favorable agreement over 8 p.p.m. of iron was not anticipated. However, the particle size of suspended iron is a factor in the extent of interference. Very finely divided iron will be more readily dissolved, whereas coarser material will be dissolved more slowly and thus interfere to a lesser extent. Iron interference must be considered with samples that require acidification.

LITERATURE CITED

(1) Costa, A. C., *Chemist-Analyst* **47**, 39 (1958).
(2) Elo, A., Polky, J. R., ANAL. CHEM. **32**, 294 (1960).
(3) Medlin, W. L., *Ibid.*, **32**, 632 (1960).
(4) Mehlig, J. P., Guill, A. P., *Ibid.*, **23**, 1876 (1951).
(5) Negoiu, D., Vasilescu, C., *Analele Univ. "C. I. Parhon," Ser. Stiint. Natl.* **9**, 65 (1960).
(6) Reilley, C. N., Schmid, R. W., ANAL. CHEM. **31**, 887 (1959).
(7) Reilley, C. N., Sheldon, M. V., *Chemist-Analyst* **46**, 59 (1957).
(8) Reilley, C. N., Vavoulis, A., ANAL. CHEM. **31**, 243 (1959).
(9) Sadek, F. S., Schmid, R. W., Reilley, C. N., *Talanta* **2**, 38 (1959).
(10) "Standard Methods for the Examination of Water and Waste Water," 11th ed., p. 386, APHA, Inc., New York, 1960.
(11) Wanninen, E., Ringbom, A., *Anal. Chim. Acta* **12**, 308 (1955).

JAMES J. HICKEY
CHARLES J. OVERBECK

Analytical Laboratory
Nalco Chemical Co.
6216 W. 66th Pl.
Chicago, Ill. 60638

THIS laboratory has applied for a patent on this test procedure.

Quantitative Determination of Impurities in Salicylic Acid

SIR: A review of the literature indicates a lack of methods for the determination of impurities in salicylic acid in the p.p.m. concentration range. Various paper and column chromatographic methods (*2, 3, 6, 9*) are available for the separation of the hydroxybenzoic acids; however, none was sufficiently sensitive or broad enough to cover all possible impurities. Phenol (*5*) has been separated by steam distillation followed by a bromate–bromide determination. Recently, Bailey (*1*) determined salicylsalicylic acid by a thin layer chromatographic method to a stated lower limit of 0.05%. The procedure can probably be modified for greater sensitivity.

From an extension of earlier work on the separation of the isomers of hydroxybenzoic acid (*8*), neutral impurities and those of lesser acidity than salicylic acid were separated by nonaqueous ion exchange chromatography. The method developed did not require a special impurity-concentration step or the preparation of derivatives. Salicylsalicylic acid under specified conditions undergoes alcoholysis on the resin yielding equimolar amounts of salicylic acid and methyl salicylate, the latter moiety being used as a measure of the concentration of this impurity. When salicylsalicylic acid was introduced to the resin in the sample environment only partial alcoholysis took place. However, neutralization of the sample before introduction to the resin produced a 90–100% conversion at the 100- to 1000-p.p.m. level.

p-Hydroxyisophthalic acid has a pK value smaller than that of salicylic acid; therefore, it cannot be determined by the ion exchange–ultraviolet method. Consequently a thin layer chromatography (TLC) method was devised for its determination. This compound exhibits very intense fluorescence when activated by ultraviolet radiation. After the acid was separated on the TLC plate, this property was used for concentration determination.

EXPERIMENTAL

Apparatus and Reagents. Gradient elution equipment, the ultraviolet monitor, resin preparation, and the spectrophotometer are described in an earlier paper (*7*). However, 1-mm. capillary tubing was substituted for regular tubing in the gradient elution equipment.

Dow U.S.P. sublimed salicylic acid containing 20 p.p.m. of *p*-hydroxybenzoic acid was recrystallized four times from glacial acetic acid and dried in a vacuum oven at 60° C. for 2 hours. No impurities were detected within the limits of the method although a slight odor of acetic acid was present. This material was used for recovery studies. The following standards used had a minimum purity of 98%: phenol, phenyl salicylate, methyl salicylate, salicylsalicylic acid, benzoic acid, *m*-hydroxybenzoic acid, *p*-hydroxybenzoic acid, xanthone, and *p*-hydroxyisophthalic acid. ACS grade methanol and reagent grade glacial acetic acid were used without further purification.

Ion Exchange Procedure. A 1.000-gram sample of salicylic acid is dissolved in approximately 10 ml. of methanol and adsorbed on a 13- × 180-mm. bed of Dowex 2-X8 ion exchange resin (acetate form, 200–400 mesh). Column effluent together with washings are retained in a 100-ml. volumetric flask for phenol, xanthone, phenyl salicylate, and methyl salicylate (from alcoholysis of salicylsalicylic acid) analysis. To the mixing flask of the gradient elution equipment is added 200 ml. of methanol while the reservoir is filled with 15% acetic acid–methanol (v./v.). The ion exchange column is attached and, with the aid of approximately 2-p.s.i. nitrogen pressure, the gradient elution is carried out at 3 ml. per minute. Concentration determinations are made in 10-cm. absorption cells using methanol as the reference solvent. *p*-Hydroxybenzoic acid is measured at 270 mμ since acetic acid shows general absorption at 254 mμ, the wavelength of maximum absorption for this particular compound. All other components are measured at their respective ultraviolet maxima.

The salicylic acid can be removed from the resin with approximately 400 ml. of glacial acetic acid. Following removal of the acetic acid with methanol, the resin can be reused indefinitely.

TLC Procedure. TLC plates of 0.4-mm. thickness are prepared using silica gel G (E. Merck) and a Desaga spreader; they were dried at 105° C. for 1 hour before use. One-gram samples of specially purified salicylic acid are weighed into 10-ml. volumetric flasks. Sufficient *p*-hydroxyisophthalic acid is added to produce concentrations of 0.0, 0.01, 0.02, 0.04, 0.06, 0.08, and 0.1% relative to salicylic acid. The contents are diluted to volume with methanol and 10-μl. aliquots are spotted, together with an equivalent amount of the samples being examined, using a Hamilton 10-μl. syringe. The plate is developed with benzene/dioxane/acetic acid (90:25:4) (*4*). (*p*-Hydroxyisophthalic acid has an R_f value of 0.31 using this system.) Following air-drying of the plate, concentration determinations are made by a visual comparison of the fluorescence of the unknowns and standards under short wavelength ultraviolet radiation (254 mμ).

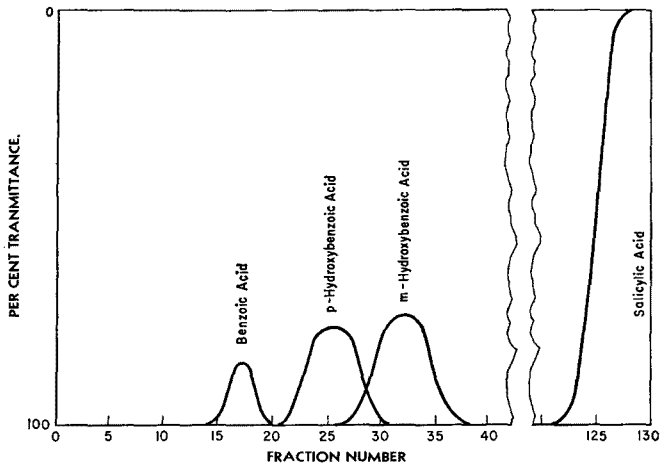


Figure 1. Separation of small amounts of the various acids in the pesence of a large amount of salicylic acid by ion exchange chromatography (10-ml. fractions) and monitered by an ultraviolet photometer

RESULTS AND DISCUSSION

The chromatogram for the separation of the lesser acidic impurities in salicylic acid is illustrated in Figure 1. Neutral and very weakly acidic impurities such as phenol, phenyl salicylate, and xanthone are found in the methanol eluate from sample introduction.

Sensitivities for the determination of the various impurities are calculated to be as follows: phenol: 20 p.p.m., xanthone: 10 p.p.m., phenyl salicylate: 20 p.p.m., salicylsalicylic acid: 40 p.p.m., *p*-hydroxybenzoic acid: 5 p.p.m., *m*-hydroxybenzoic acid: 20 p.p.m., benzoic acid: 50 p.p.m., *p*-hydroxyisophthalic acid by TLC: 200 p.p.m. The limits of detection were calculated on the basis of obtaining an absorbance of 0.04 for a 100-ml. solution using a 10-cm. absorption cell and a 1-gram sample of salicylic acid.

Table I illustrates representative recoveries of the various possible impurities added to 1-gram samples of specially purified salicylic acid and taken through the procedure. Recoveries were quantitative within an experimental error of about ±5% relative at the 100-p.p.m. level.

An exception to this was the determination of salicylsalicylic acid. When this compound is put through the resin in the sample environment, a moderately acidic medium, alcoholysis occurs to the extent of 30 to 40%. However, if the sample is first neutralized to form sodium salicylate, alcoholysis increases to greater than 90%. Because the sample is introduced to the resin in a nearly neutral or slightly basic medium, a portion of the methyl salicylate will be adsorbed on the resin. The remainder will be found in the methanol effluent. Gradient elution of the resin will remove that portion adsorbed with the first 40 to 50 ml. of effluent collected. In general it is best to examine the first fractions of the gradient elution for the presence of weakly acidic components.

If salicylsalicylic acid and phenyl salicylate are both present in a salicylic acid sample, it is generally difficult to distinguish between the two. However the presence of one or the other can be distinguished by the slight difference between their neutral and basic ultraviolet spectra. A possible method of determining whether a mixture of the two is present would be to pass the sample through separate ion exchange columns in neutralized and unneutralized form. The presence of salicylsalicylic acid causes the absorbance value to be lower for the unneutralized sample.

The alcoholysis of salicylsalicylic acid is definitely attributed to its contact with the resin. A stability study of salicylsalicylic acid in 0.1% sodium hydroxide–methanol solution, as measured by ultraviolet spectrometry, does not indicate the formation of either sodium or methyl salicylate. Further evidence to support the alcoholysis theory is an analogous reaction observed for salicylsalicylanilide. This compound alone or in the presence of salicylanilide undergoes alcoholysis with the formation of equimolar amounts of methyl salicylate and salicylanilide. Quantitative alcoholysis takes place without neutralizing the sample before it is introduced to the resin.

If the analysis of sodium salicylate is attempted, weakly acidic species such as phenol and phenyl salicylate are adsorbed by the resin. In the unneutralized sample analyses, these components are found in the methanol eluate together with any neutral components. This is explained by the fact that the acidity of salicylic acid is sufficient to prevent the adsorption of these components by acting either as an acidic eluent or as a contributor of a common ion suppressing dissociation of the weakly acidic compounds. Because these materials are weakly adsorbed, they appear in the first 50 ml. of effluent following the start of the gradient elution. The remainder of the weak acids are removed in the usual manner as illustrated in Figure 1.

The stability of salicylic acid in methanol solution was determined because of possible formation of methyl salicylate. One-gram samples of salicylic acid were weighed into respective 10-ml. volumetric flasks and diluted to volume with methanol. These were examined according to the method at 0, 1, 2, and 4-day intervals and showed the presence of <10, 107, 350, and 650 p.p.m. of methyl salicylate, respectively. Therefore the sample solution should be put through the resin immediately. However, it is not essential that the gradient elution be started at this same time.

A 1-gram sample of specially purified salicylic acid fortified with 10 μg. of *p*-hydroxybenzoic acid (10 p.p.m.) taken through the method gave an 80% recovery (8 p.p.m.). There appears to be no marked drop in recovery at the lower limit.

The only impurity consistently observed to be present in Dow U.S.P.

Table I. Analysis of Known Salicylic Acid–Impurity Mixtures

Component p.p.m.:	Mixture 1		Mixture 2		Mixture 3[a]	
	Added	Found	Added	Found	Added	Found
Phenol			100	104		
Xanthone	104	101			104	103
Salicylsalicylic acid	130	46			101	97
Phenyl salicylate			106	103		
Benzoic acid	102	101	105	102	102	109
p-Hydroxybenzoic acid	91	91			91	96
m-Hydroxybenzoic acid			102	99		

[a] Sample was neutralized before the ion exchange separation.

sublimed salicylic acid within the sensitivity of the method was, on the average, 100 p.p.m. of *p*-hydroxybenzoic acid. On rare occasions *p*-hydroxyisophthalic acid was observed at the limit of detection. The possibility does exist that an impurity may have been overlooked in this analysis. However, from examination of salicylic acid mother liquors, it was concluded that no other impurities of any significant concentration were present.

LITERATURE CITED

(1) Bailey, R. W., ANAL. CHEM. **36**, 2021 (1965).
(2) Lederer, M., *Australian J. Sci.* **11**, 208 (1949).
(3) Marvel, C. S., Rands, R. D. Jr., *J. Am. Chem. Soc.* **72**, 2642 (1950).
(4) Pastuska, G., *Z. Anal. Chem.* **179**, 355 (1961).
(5) Shcherbachev, K. D., *Khim. Form. Prom.* **1934** (5), 37.
(6) Sinton, F. C., *J. Assoc. Offic. Agr. Chemists* **13**, 344 (1930).
(7) Skelly, N. E., ANAL. CHEM. **33**, 271 (1961).
(8) Skelly, N. E., Crummett, W. B., *Ibid.*, **35**, 1680 (1963).
(9) Van Oame, H. C., *J. Assoc. Offic. Agr. Chemists* **43**, 593 (1960).

NORMAN E. SKELLY

Special Services Laboratory
The Dow Chemical Co.
Midland, Mich.

Division of Analytical Chemistry, Winter Meeting, ACS, Phoenix, January 1966.

Stability Constants of Some Dihydrazide Complexes of Cadmium

SIR: A recent polarographic investigation of the complexation of cadmium by alkyl and aryl carboxylic acid hydrazides (*6*) led to the conclusion that the complexing moiety was the neutral hydrazide rather than the anion, as had been found for other metal ions such as copper (*1*, *3*). At least three soluble cadmium complexes were found, and distinct differences in stability between the alkyl and aryl complexes were noted. Therefore, it appeared that, in the case of cadmium, the complexing hydrazide ligand was behaving like an amine.

In a manner analogous to the situation with organic mono- and diamine complexes, it was felt that the complexation of metal ions by dicarboxylic dihydrazides might be significantly different from that found with monohydrazides. Therefore, a study of the behavior of cadmium in the presence of some dihydrazides was undertaken.

The success obtained with the polarographic approach for the determination of complexity constants in the previous study (*6*) led to its use in the present case. The method of DeFord and Hume (*2*) was utilized to calculate stability constants from the polarographic data obtained.

EXPERIMENTAL

Chemicals. Carbohydrazide, succinic dihydrazide, and adipic dihydrazide (Olin Mathieson Chemical Corp.) were recrystallized twice from water, dried at 100° C., and stored under dry nitrogen.

All other chemicals were reagent grade and were used without further purification.

Apparatus and Procedure. Detailed descriptions of the apparatus and procedure have been given previously (*6*).

RESULTS AND DISCUSSION

Previous studies on the complexation of cupric ion by isonicotinic acid hydrazide established that the over-all reaction involves release of protons (*1*, *3*). Titration of the hydrazide with copper solution lowered the pH about 0.6 unit below that for the corresponding copper alone. The reaction of monohydrazides with cadmium, however, did not seem to be of the same type; no release of protons was found (*6*).

In the present instance, titration of the dihydrazides with Cd^{+2} produced the data shown in Figure 1. The pH of the solutions did not drop below that for Cd^{+2} itself. Therefore, any reaction of the dihydrazides with cadmium must occur without release of protons and, again, through a neutral hydrazide species.

Polarographic studies of complexation are well established (*5*). If single, strong complexes are involved, a simple plot of $E_{1/2}$ *vs.* log ligand concentration can give sufficient information for elucidation of the complex. With successive complexes, more elaborate calculations are required. DeFord and Hume (*2*) first derived the necessary equations for calculation of the stability constants of consecutive complexes. For a reversible reduction of a complexed metal ion to the amalgam, they have defined functions, $F_J(X)$, such that

$$F_0(X) = \text{antilog}\left\{0.435\,\frac{nF}{RT}\,[(E_{1/2})_s - (E_{1/2})_c] + \log\frac{I_s}{I_c}\right\} \quad (2)$$

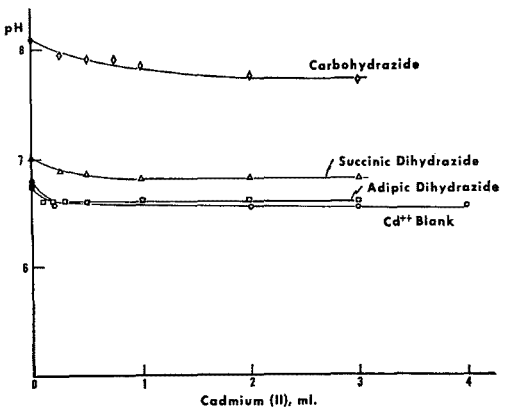


Figure 1. Titration of dihydrazides with cadmium ion

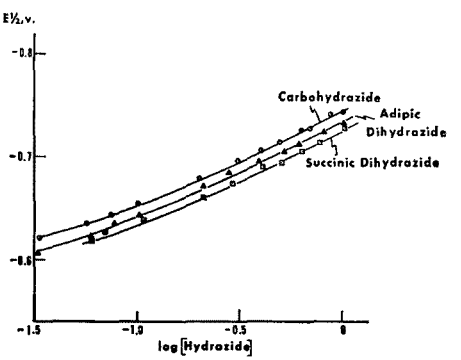


Figure 2. Half-wave potential of cadmium as a function of log hydrazide concentration

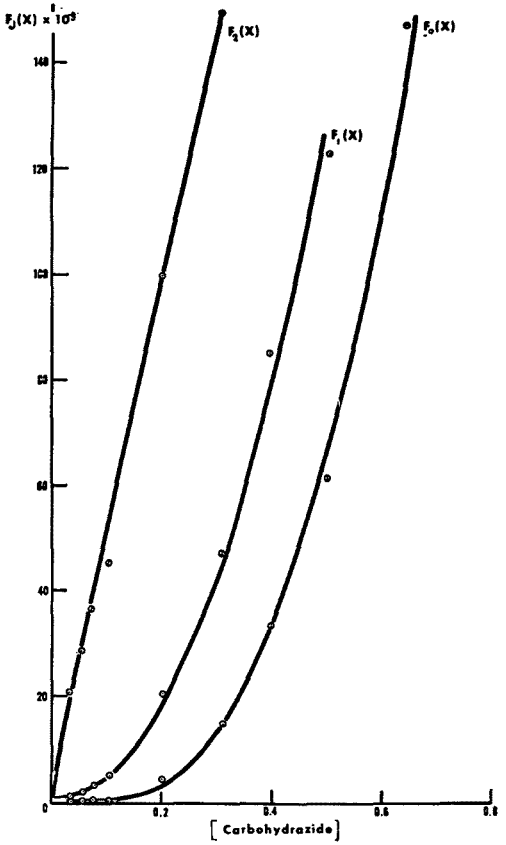


Figure 3. Values of $F_0(X)$, $F_1(X)$, and $F_2(X)$ for cadmium in carbohydrazide solutions

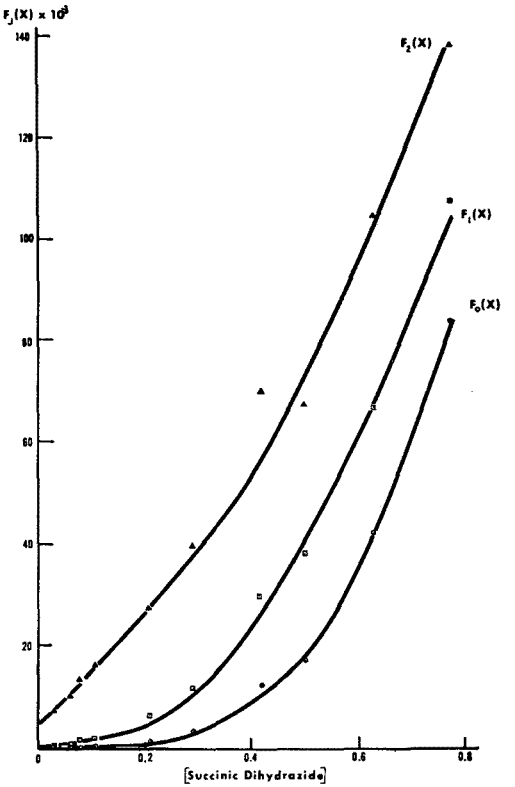


Figure 4. Values of $F_0(X)$, $F_1(X)$, and $F_2(X)$ for cadmium in succinic dihydrazide solutions

and

$$F_1(X) = \frac{F_0(X) - (K_0/f_s)}{C_x f_x} \qquad (3)$$

and

$$F_2(X) = F_1(X) - (K_1/f_{mx})C_x f_x; \text{ etc.} \qquad (4)$$

The values, $(E_{1/2})_s$ and $(E_{1/2})_c$, are the half-wave potentials for the uncomplexed and complexed metal ions, respectively; and I_s and I_c are the diffusion current constants for the same species. The formation constant of the zero complex, K_0, is defined as one. Terms, f_s and f_x, are the activity coefficients of the uncomplexed metal and the ligand; and C_x is the concentration of the latter. K_1 is the stability constant of the 1:1 complex, and f_{mx}, the activity coefficient of the complex.

The intercept of a plot of $F_J(X)$ *vs.* $C_x f_x$, when extrapolated to $C_x = 0$, is equal to K_J/f_{mx}. The activity coefficients may be equated to unity (*4*), and the stability constant thus obtained will include any activity coefficient factor.

Figure 2 shows the plot of $E_{1/2}$ *vs.* log hydrazide concentration for the systems studied. In all cases, a curved line, representative of the formation of successive complexes, was found.

Plots of $F_0(X)$, $F_1(X)$, and $F_2(X)$ for carbohydrazide are shown in Figure 3. When these curves were expanded in scale and extrapolated to $C_X f_X = 0$, formation constants for the first two consecutive complexes were found to be $K_1 = 500$ and $K_2 = 4{,}500$.

Curves also were prepared for $F_3(X)$ and $F_4(X)$, but these showed a large amount of scatter. Graphical extrapolation of these curves was difficult; but when expanded scales were used, formation constants of $K_3 = 420{,}000$ and $K_4 = 240{,}000$ were estimated. In order to obtain better values, a least squares method (*7*) was used to evaluate the $F_3(X)$ and $F_4(X)$ data; the data were assumed to fit a linear regression with the general form,

$$F_J(X) = K_J + m(C_X f_X) \qquad (5)$$

where m is the slope of the line. Calculations, using this technique, gave formation constants of $K_3 = 408{,}453$ and $K_4 = 182{,}002$. From the plots prepared, a definite slope was noticed with the $F_3(X)$ data, while the $F_4(X)$ plot was essentially horizontal, indicating that the 4:1 complex probably is the highest complex present under the conditions of the study (*2*).

In the case of carbohydrazide, the value for K_4 was found to be of the same order of magnitude as that for K_3, although the latter was approximately twice that of the former. In addition, the slopes of the two curves were different; the $F_3(X)$ plot had a definite slope, while $F_4(X)$ was horizontal. These data led credence to the presence of a 4:1 complex, which may not be as strong as the 3:1.

When the dihydrazide molecule is

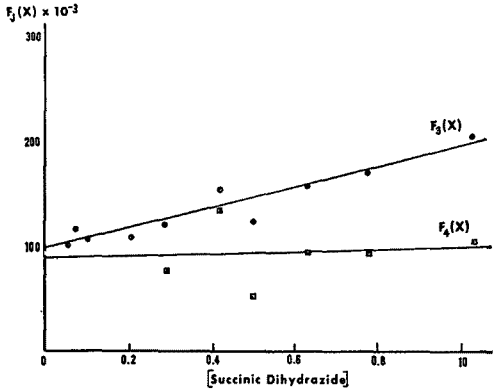


Figure 5. Values of $F_3(X)$ and $F_4(X)$ for cadmium in succinic dihydrazide solutions

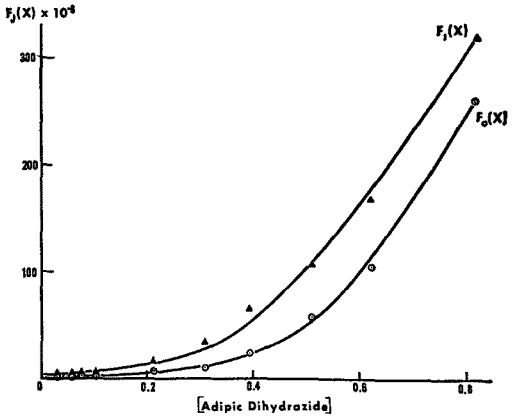


Figure 6. Values of $F_0(X)$ and $F_1(X)$ for cadmium in adipic dihydrazide solutions

expanded by inserting an alkyl chain between the hydrazide groups, the results are somewhat different. Plots of $F_0(X)$, $F_1(X)$, and $F_2(X)$ for succinic hydrazide are shown in Figure 4. Extrapolation of these curves on an expanded scale gave values of $K_1 = 80$ and $K_2 = 4{,}500$.

These are very similar to the corresponding acetic hydrazide values (*6*). Figure 5 shows the $F_3(X)$ and $F_4(X)$ plots for succinic dihydrazide. Closer examination of these plots gave stability constants of $K_3 = 98{,}000$ and $K_4 = 90{,}000$, with the $F_4(X)$ curve horizontal. Comparison of the K_3 value with the corresponding acetic hydrazide value disclosed a 4-fold increase in stability with the succinic dihydrazide. Furthermore, the K_4 value for succinic dihydrazide was the same as the K_3 value (within 10%), which again adds support for a 4:1 complex with this dihydrazide.

Further expansion of the chain of the dihydrazide to adipic dihydrazide gave enhanced stabilities. Figure 6 shows the $F_0(X)$ and $F_1(X)$, while Figure 7, the $F_2(X)$, $F_3(X)$, and $F_4(X)$ plots for adipic dihydrazide. Values for the stability constants were found to be $K_1 = 230$, $K_2 = 16{,}500$, $K_3 = 160{,}000$, and $K_4 = 395{,}000$.

From all these data, it appears that, as one increases the molecular weight of the alkyl dihydrazide, the stability of the complexes formed is increased and the likelihood of forming higher complexes also increases. The case of carbohydrazide is somewhat different in that it is possible to postulate formation of a six-membered ring with both hydrazide functional groups entering into the complexation reaction.

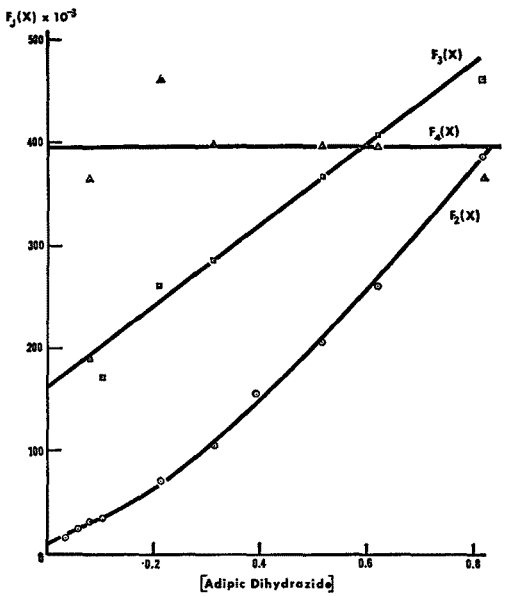


Figure 7. Values of $F_2(X)$, $F_3(X)$, and $F_4(X)$ for cadmium in adipic dihydrazide solutions

LITERATURE CITED

(1) Albert, A., *Experientia* **9**, 370 (1953).
(2) DeFord, D. D., Hume, D. N., *J. Am. Chem. Soc.* **73**, 5321 (1951).
(3) Fallab, S., Erlenmeyer, H., *Helv. Chim. Acta* **36**, 6 (1953).
(4) Hume, D. N., DeFord, D. D., Cave, G. C. B., *J. Am. Chem. Soc.* **73**, 5323 (1951).
(5) Kolthoff, I. M., Lingane, J. J., "Polarography," 2nd ed., Interscience, New York, 1952.
(6) Krivis, A. F., Supp, G. R., Doerr, R. L., ANAL. CHEM. **37**, 52 (1965).
(7) Snedecor, G. W., "Statistical Methods," 4th ed., Iowa State College Press, Ames, Iowa, 1946.

ALAN F. KRIVIS
GEORGE R. SUPP
RICHARD L. DOERR

Chemicals Division Research
Olin Mathieson Chemical Corp.
New Haven, Conn.

Trace Impurity Analysis of Plutonium–Uranium–Zirconium Alloys by Anion Exchange–Partition Chromatography

SIR: Anion exchange–partition chromatography has been applied previously (*3*) to the trace impurity analysis of binary thorium–uranium and ternary plutonium–thorium–uranium alloys. The present paper describes an extension of this technique to the determination of trace metal contaminants in ternary plutonium–uranium–zirconium alloys. These materials are presently under investigation (*1*) as possible fuels in fast breeder reactors; thus their characterization as to impurity content is of considerable interest. Since a large number of samples were not anticipated, analysis by direct excitation was not feasible because the variable matrix composition (plutonium 18.5 to 27.1%; uranium 67.4 to 71.6%; zirconium 2.4 to 1.4.1%) precluded the preparation of reliable standards.

A basic feature of the method was the adsorption of two matrix components by a mixed organic stationary phase. Optimum composition of the mixture for this application was determined by liquid–liquid extraction experiments with zirconium.

EXPERIMENTAL

Materials and Reagents. Anion exchange resin, chromatographic columns, and general laboratory ware were described previously (*3*).

Plaskon, Type CTFE 2300, a trifluorochloroethylene polymer, was obtained from Allied Chemical Corp. and used without further treatment.

Tri(2-ethylhexyl)phosphate[TEHP], a product of K and K Laboratories, Inc., was washed with 5% sodium carbonate, distilled deionized water, and 8*N* nitric acid. Di(2-ethylhexyl) hydrogen phosphate [HDEHP], obtained from Distillation Products Industries, was conditioned with 8*N* nitric acid and used without further purification. The TEHP–HDEHP mixtures were made by volume dilutions of these reagents.

A 20-mg./ml. zirconium standard was prepared by dissolution of high purity metal in 8*N* nitric acid and a minimum amount of 2*N* hydrofluoric acid.

Column Preparation and Separation. The previously described (*3*) column preparation technique was found to be satisfactory. However, because of the higher percentage of uranium in the alloy matrix, it was necessary to increase the organic support phase. This was prepared by stirring 3 to 5 grams of Plaskon polymer with 4 ml. of a 95% TEHP–5% HDEHP mixture until the resin was uniformly coated. The chromatographic column had the following approximate dimensions: A 1-cm.-high bed of settled anion resin lower phase, a 10-cm.-high TEHP–HDEHP-coated Plaskon middle phase, and a 3-cm.-high bed anion resin upper phase. Before use, the column was thoroughly washed with 1*N* nitric acid to ensure the removal of common blank impurities and finally conditioned with 8*N* nitric acid. A 0.20- to 0.30-gram alloy sample was dissolved in 8*N* nitric acid. Heating and the dropwise addition of 2*N* hydrofluoric acid hastened dissolution. The cooled sample solution was added to the chromatographic column and the nonabsorbed impurities were eluted with approximately 40 ml. of 8*N* nitric acid. The flow rate was kept between 0.5 to 1 ml. per minute, since a faster elution resulted in an excessive spreading of the yellow uranium(VI) band.

The columns were prepared for reuse by stripping of the ternary matrix with a mixture of 0.4*N* nitric–0.02*N* hydrofluoric acid (40–80 ml.) until the pink plutonium band completely disappeared from the organic phase. Elution was continued with a 0.5*N* nitric–3*N* hydrofluoric acid mixture to remove any remaining uranium and zirconium (40 ml.). Binary uranium–zirconium alloys were eluted with the latter stripping solution. Before reuse for other separations, the column was washed with 1*N* and conditioned with 8*N* nitric acid.

Concentrations of impurity elements were determined by the copper spark spectrographic method (*2*). Both visual and densitometric evaluation of line intensities were utilized.

Liquid–Liquid Extraction. The distribution ratio, *D*, of zirconium(IV) between 8*N* nitric acid and variable organic phase compositions was determined by standard liquid–liquid extraction techniques. The phase volumes were kept constant at 10 ml. and the equilibration time was 2 minutes. The concentration of zirconium in the aqueous phase after extraction was determined spectrographically by the copper spark method, using titanium (5 μg./ml.) as the internal standard in the construction of a working curve.

RESULTS

The precision and accuracy of the proposed separation procedure was determined by repeated analyses of a representative ternary plutonium–uranium–zirconium alloy. Quantitative recoveries of five common impurities were verified by the densitometric copper spark method, using cobalt (10 μg./ml.) as an internal standard. The results are shown in Table I. Table II contains data obtained by repeated analyses of a synthetic uranium–zirconium alloy. The latter results serve to show that the ternary alloys of higher purity than presently available could be analyzed with adequate precision by the discussed method. The behavior of additional elements on the chromatographic column was evaluated by visual spectrographic determination of added impurities. Duplicate 40-ml. elutions indicated quantitative recoveries of the following elements at concentrations of 1 to 100 μg.: Ag(I), As(V), Ba(II), Be(II), B(III), Ca(II), Cd(II), Co(III), Cu(II), Cs(I), Ga(III), In(III), K(I), Li(I), Mg(II), Mo(VI), Na(I), Pb(II), Rb(I), Rh(III), Ru(IV), Sc(III), Sr(II), Sn(IV), Te(IV), Ti(IV), V(V), Y(III), Zn(II), and the rare earths. Limits of detection were comparable to those reported previously (*3*).

The distribution ratios found for zirconium(IV) in TEHP and in TEHP mixtures containing variable amounts of HDEHP are shown in Table III. The

Table I. Recovery of Added Impurities from a 27.1% Plutonium–68% Uranium–4.9% Zirconium Alloy, p.p.m.

Element	Impurities Initial	Impurities Added	Total Theoretical	Total Found	Rel. std. dev.[a]
Al	94	100	194	208	±4
Cr	83	100	183	198	±2
Fe	402	100	502	538	±6
Mn	36	100	136	128	±10
Ni	52	100	152	152	±3

[a] Based on 6 determinations.

Table II. Recovery of Added Impurities from a 93.8% Uranium–6.2% Zirconium Alloy, p.p.m.

Element	Impurities Initial	Impurities Added	Total Theoretical	Total Found	Rel. std. dev.[a]
Al	4	13	17	20	±16
Cr	2	13	15	18	±4
Fe	14	13	27	30	±12
Mn	3	13	16	16	±3
Ni	<1	13	13	13	±4

[a] Based on 6 determinations.

Table III. Distribution Ratios of Zirconium as a Function of Organic Phase Composition

Phase compositions		
Organic	Aqueous	D^a
100% TEHP	8.0N HNO_3	7
97% TEHP–3% HDEHP	8.0N HNO_3	86
95% TEHP–5% HDEHP	8.0N HNO_3	260
90% TEHP–10% HDEHP	8.0N HNO_3	1170
80% TEHP–20% HDEHP	8.0N HNO_3	2580

[a] Average of 3 determinations.

results were calculated from the relationship $D = M_{org}/M_{aq}$, where $M_{org} = M_{tot} - M_{aq}$. Based on these data, an organic phase composition of 95% TEHP–5% HDEHP was used as the stationary extraction phase in column operations.

DISCUSSION

An experimental survey of reagents for application in partition chromatographic column separations indicated that the neutral organic phosphates and phosphonates, although efficient extractants for plutonium(IV) and uranium(VI), were not satisfactory for the quantitative retention of zirconium(IV) if present in macro concentrations. Therefore, contrary to earlier expectations (*3*), tri-*n*-butyl phosphate (TBP) did not extract zirconium(IV) effectively when present above the trace level. On the other hand, HDEHP was shown (*4*) to have a high affinity for zirconium over a wide nitric acid concentration range. The use of this reagent alone proved unsatisfactory in that the ternary alloy matrix, particularly plutonium(IV), could not be stripped from the column with simple mineral acids. Since a separation procedure was desired in which chromatographic columns could be reused for several elutions, mixtures of a neutral organic phosphate for the extraction of uranium(VI) and HDEHP for the retention of zirconium(IV) were found to be more acceptable. TEHP was chosen because this reagent showed exceptional stability in nitric acid, as evidenced by the absence of phosphorus during repeated elutions. The previously reported (*3*) line intensity suppression in the spectrographic analysis by column degradation products was not observed in these experiments. Generally, the zirconium content in the effluent was less than 1% of the original value, causing no significant interferences in the evaluation of impurity concentrations. A HDEHP concentration in excess of 5% resulted in incomplete stripping of plutonium with a mixture of 0.4N nitric–0.02N hydrofluoric acid. Because of the insolubility of plutonium tetrafluoride, a higher fluoride concentration could not be used.

The application of column separations to the analysis of high purity metals and alloys is particularly useful from the standpoint of the large number of elements that can be determined. Furthermore, blank contaminations are minimized by the use of highly purified reagents and inert plastic laboratory ware. This presents a distinct advantage over liquid–liquid extraction techniques, where several equilibrations have to be used to effect a preconcentration comparable to a one-pass column elution.

LITERATURE CITED

(1) Argonne National Laboratory Rept., ANL-7000, p. 11 (1964).
(2) Fred, M., Nachtrieb, N. H., Tomkins, F. S., *J. Opt. Soc. Am.* **37**, 279 (1947).
(3) Huff, E. A., ANAL. CHEM. **37**, 533 (1965).
(4) Japan Atomic Energy Research Institute Rept. JAERI-1047 (1963).

EDMUND A. HUFF
STANLEY J. KULPA

Argonne National Laboratory
Argonne, Ill.

BASED on work performed under the auspices of the U. S. Atomic Energy Commission.

AIDS FOR ANALYTICAL CHEMISTS

A Semiautomatic Device for Measuring and Drawing Mass Spectra

Richard N. Stillwell, Department of Biochemistry, Baylor University College of Medicine, Houston, Texas

THE BEST and most commonly used method of obtaining mass spectra from a low-resolution mass spectrometer equipped with a direct or gas chromatographic inlet system is by means of a three- or five-galvanometer oscillographic recorder. These records, however, are unsuitable for handling and study. They are cumbersome and light-sensitive (unless fixed), and they are difficult to study because the top of a large peak on the bottom trace is easily lost among the smaller peaks of the upper traces. Comparison of spectra in this form is difficult because, in general, they are of different intensities.

The primary records, then, should be converted into a more useful form, that is, either a table of mass numbers and relative intensities or a bar graph showing relative abundance *vs.* mass-to-charge ratio, preferably including a "per cent of total ionization" scale (*1*). Normally a spectrum is counted, then measured by means of a variable-scale comparator to make the table of intensities. The spectrum is then drawn from the table by conventional draftsman's techniques. Counting and measuring a spectrum over the mass range of, for example, 50 to 300 takes 15 or 20 minutes; drawing it takes 20 minutes or more, depending on the number of peaks present.

To deal with a large number of spectra which were to be studied and filed, but not necessarily reproduced for publication, it was desirable to have a rapid method of producing a mass and abundance table and, at the same time, of drawing a compact spectrum and of calculating the total ionization. Conventional commercial digitizers were not considered suitable for a number of reasons, but primarily because of the frequency response necessary for scanning during a gas chromatographic peak, and because of the uncertainty of mass determination at large values of m/e. Hence, a method was wanted for measuring and drawing spectra from selected oscillographic charts. For this purpose the device described below was constructed from components at hand in the author's laboratory. Once the peak count has been marked on the original spectrum and the instrument adjusted to the base lines and intensity of the chart, the spectrum is measured and drawn at the rate of one peak every 3 seconds. The mass range of 50 to 300 mentioned above, for example, is covered in 12.5 minutes.

A Leeds and Northrup Speedomax H recorder was used for reading the oscillo-

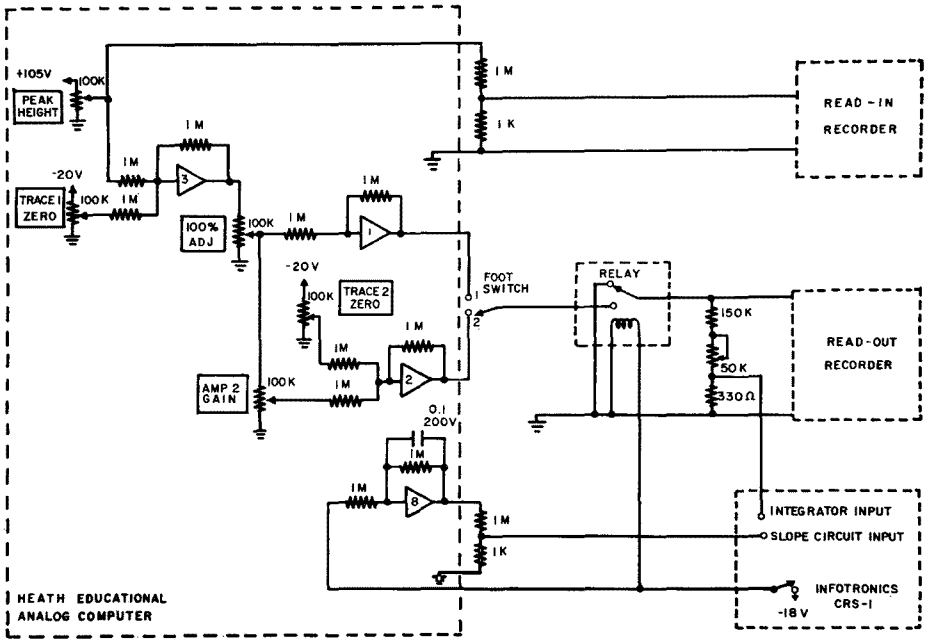


Figure 1. Schematic diagram of device for measuring and drawing mass spectra

graphic traces. The following minor modifications were made. The faceplate and pen were removed, the chart drive gears disengaged, a pair of guide collars placed on the chart roller, and an index marker was attached to the pen carrier. The oscillographic record could then be fed over the roller from front to back and pulled through by hand.

A Heath analog computer was used for most of the connecting circuitry (Figure 1). An initial-condition voltage source (marked Peak Height) was used to activate the read-in recorder through a 1000:1 voltage divider. The same voltage was fed through an amplifier (3) with unity gain to a potentiometer (100% Adj.) and thence to another amplifier (1), with unity gain. The output of this amplifier was used to record peaks on the lowest trace of the oscillographic chart. The input of a third unity-gain amplifier (2) was taken from the center tap of the 100% Adj. potentiometer through a potentiometer labeled Amp. 2 Gain. The resistance ratio of this potentiometer is nominally 10:1, the ratio of the sensitivities of the traces. Two more initial-condition voltages were fed (for easier adjustment) through potentiometers (Trace 1 Zero and Trace 2 Zero) to amplifiers 3 and 2 for zeroing on the base lines of the traces. The output of amplifier 1 or 2 was selected by a foot-operated switch (normally on position 2) and presented to the readout recorder, a Bausch and Lomb VOM-5 with its function switch set to 10 volts full scale and its pen slightly overdamped. A variable voltage divider was used to couple the amplifier output to the integrator input of an Infotronics Corp. Model CRS-1 digital chromatograph readout system. (A printing, digital voltmeter, suitably controlled by switches, could, of course, be substituted.)

The timer section of the Infotronics unit has a motor-driven toothed wheel which actuates a switch, producing a square wave alternating between 0 and −18 volts with respect to ground. A fiberboard disk was cut and mounted on the motor shaft so as to allow the switch to close for only two $^1/_2$-second periods during each revolution (6 seconds). A switch was wired into the timer motor circuit to allow interruption of the timer. A wire was connected to feed the square wave to the input of a unity-gain amplifier (8) which served to reduce the slope of the square wave to a finite value and to reverse its phase; the output of this amplifier was divided by 1000 and connected to the input of the slope detector circuit of the Infotronics unit. The instrument then automatically integrated the voltage presented to it during the $^1/_2$-second period. The 18-volt square wave was also used to actuate a sensitive relay (Phillips-Advance SV 1C10000D) which kept the input of the readout recorder grounded except during the $^1/_2$-second pulse, when it was connected to the appropriate amplifier through the foot switch.

To use the system, an oscillographic chart is placed in the read-in recorder and pulled through to the largest peak. The Peak Height potentiometer is adjusted to position the index of the recorder over the base line of the lowest trace (the second trace in the case of a weak spectrum). With the relay in the grounded position, the readout recorder and the integrator are zeroed. The foot switch is depressed to position 1, the timer started, and the Trace 1 Zero control turned to zero the output of amplifier 1. The read-in recorder is then set with the Peak Height control to the top of the base peak and the integrator set to Auto. The 100% Adj. potentiometer is set so that the peaks produced by the readout recorder are about four fifths of full scale. The 50K potentiometer is set so that the integrator reads 1000 counts in each cycle. (This adjustment need be made only once. For subsequent spectra, the integrator is set by means of the 100% Adj. potentiometer.) The read-in recorder is then adjusted to the base line of the second (or third) trace, the foot switch released to position 2, and amplifier 2 zeroed with the Trace 2 Zero control. The setting of Amp. 2 Gain is adjusted until a peak which is on scale on both traces gives the same count when read on the first trace with

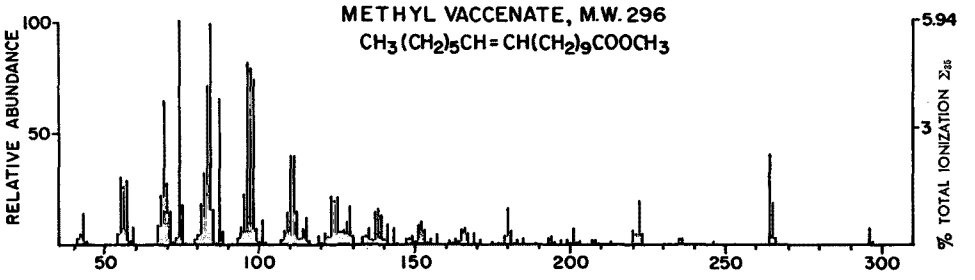


Figure 2. Mass spectrum drawn in 13 minutes using the device described

From a spectrum obtained at 20 e.v. on an Atlas-Werke CH-4 mass spectrometer equipped with a gas chromatographic inlet system. The sample was the major peak from a mixture of methyl esters of bacterial origin; the structure was assigned on the basis of this spectrum and that of the isopropylidene derivative of the corresponding diol (2). The tick marks for the mass numbers, relative abundance, and per cent of total ionization, and the lettering were added by hand.

the foot switch depressed as on the second trace with the switch released.

The timer is allowed to run until it reads the mass number at which reading of the spectrum is to begin. The readout chart paper drive is started at 1 inch per minute, and each peak of the spectrum is read by manipulating the Peak Height potentiometer and the foot switch during the intervals when the relay is grounded. The readout recorder produces a trace suitable for storage and study (Figure 2), while the integrator prints out a list of mass numbers and relative intensities (in tenths of a per cent) which are comparable in accuracy to those measured manually. When the spectrum is completed, the Total button on the printer is pressed to give the total ionization in tenths of a per cent of the base peak.

A number of possible modifications of this system suggest themselves. For example, if the chart drive of the readout recorder were arranged to advance in steps, a reproduction-quality spectrum might be obtained and, at the same time, speed and accuracy could be improved by providing switches to permit stopping the system between peaks (for example when there is a large change in intensity), or by scanning rapidly through a region of no peaks.

LITERATURE CITED

(1) Biemann, K., "Mass Spectrometry; Organic Chemical Applications," pp. 42–6, McGraw-Hill, New York, 1962.
(2) McCloskey, J. A., McClelland, M. J., *J. Am. Chem. Soc.* **87**, 5090 (1965).

WORK supported by National Institutes of Health Grant No. HE-05435.

Stainless Steel Capsule with Iron "Window" for Determining Hydrogen in Alkali Metal by Vacuum Extraction

Joseph W. Glass, Chris M. Larsen, and James M. Scarborough, Atomics International, A Division of North American Aviation, Inc., P. O. Box 309, Canoga Park, Calif.

HYDROGEN in alkali metals is normally determined by a technique wherein the alkali metal sample is sealed in an iron capsule (*1*) and hydrogen is extracted by heating in a vacuum at 700–750° C. The total quantity of gas produced is measured and the hydrogen is converted to water which is trapped. The residual quantity of gas is measured and the hydrogen is determined by difference.

Usually, the iron capsule which contains the alkali metal sample is sealed by welding. However, welding is very often inconvenient, expensive, and requires expert care to prevent contamination of the sample.

A simple, time-saving technique has been developed in which the welding operation for each sample is eliminated by substituting a reusable stainless-steel capsule having an iron "window" for the iron capsule. The stainless steel capsule can be made from a commercially available Swagelok reducer and plug as shown in the Figure 1. A thin iron window (nominally, 10 mils) is welded over the large end of the reducer.

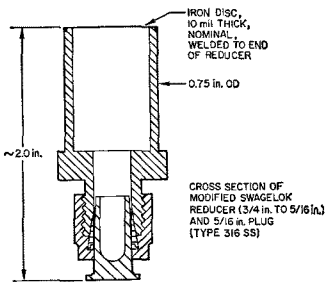


Figure 1. Hydrogen extraction capsule

The sample is transferred to the capsule in an inert atmosphere box and the plug fitting is sealed. The capsule is then placed in the hydrogen analyzer, with iron "window" at the top, and the analysis is performed in the conventional manner.

This technique has been used successfully for Na, K, and Na–K samples. No capsules have ruptured or leaked and it has been demonstrated that the capsules may be cleaned and reused.

LITERATURE CITED

(1) Pepkowitz, L. P., Proud, E. R., ANAL. CHEM. **21**, 1000 (1949).

WORK done under the auspices of the U. S. Atomic Energy Commission, Contract AT(11-1)-GEN-8.

Improvements in Carbon-14 Assay of Organic Compounds by Dry Combustion

Masayuki Hamada and Eiko Kawano, Radiation Center of Osaka Prefecture, Sakai, Osaka, Japan

MODIFICATIONS in the combustion procedures and counting system of carbon-14–labeled compounds used in this laboratory afford certain advantages over the apparatus which was originally designed by Anderson, Delabarre, and Bothner-By (*1*) and Christman *et al.* (*2*). Improvements are described chiefly with regard to a dry combustion system which allows reduction of nitrogen oxides in a stream of nitrogen and to a low background counting system.

One of the important problems during combustion of organic compounds is the removal of nitrogen oxides. This problem is magnified when the product of the combustion is desired for isotopic assay. In the procedure for isotopic compounds which has been developed by Anderson, Christman *et al.* (*1–5*), the nitrogen oxides produced during the dry combustion of nitrogen-containing organic compounds are successfully removed from the gas stream by manganese dioxide. However, in this procedure specially prepared manganese dioxide is necessary and, in general, the combustion of nitrogen-containing compounds is more troublesome than that of nonnitrogen-containing compounds.

Mitsui, Yoshikawa, and Furuki (*7*) have developed a new method in which a sample for microdetermination of carbon and hydrogen in organic compounds is burned in a stream of nitrogen gas by adding a suitable amount of oxygen generated electrolytically. Our combustion system for C^{14}-labeled organic compounds was set up based on the above principle. This system not only gives complete removal of nitrogen oxides without any extra component such as pure manganese dioxide, but makes the operation simpler than previous systems.

To reduce the background counting rate, metal (Kovar) cathode counting tubes were designed for use in a lead and iron shielded anticoincidence counting system. By this procedure, the background counting rate was reduced to about 4 c.p.m.

EXPERIMENTAL

Reagents and Filling of the Combustion Tube. To complete the combustion in a stream of nitrogen, the combustion catalyst must have not only good catalytic properties but also a high oxygen-releasing ability. The catalyst used by the present authors is a mixture of cupric oxide, manganese dioxide, and cobaltic oxide which was recommended by Mitsui, Yoshikawa, and Furuki (*7*). As the absorbent for halogen and sulfur, granules of metallic silver are used (*6*). As a reducing agent, commercial 40-mesh copper gauze is used after reduction with methanol.

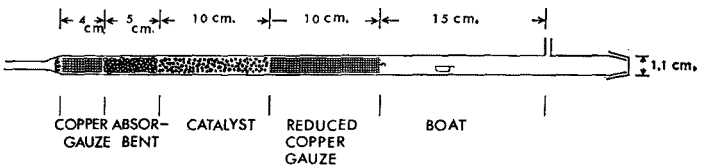


Figure 1. Fillings of the combustion tube

The combustion tube is packed from the end with absorbent, catalyst, and finally the reduced copper gauze roll. A diagram of a packed combustion tube is shown in Figure 1.

Apparatus. The assembled apparatus is shown in Figure 2.

Electrolytic Cell. An electrolytic cell was designed for the generation of oxygen gas. It has platinum wire (0.4 mm. in diameter) electrodes and the solution is a mixture of 30% hydrogen peroxide and a small amount of sulfuric acid. The cell is followed by tubes of heated copper oxide granules and Anhydrone to remove any trace of impurity.

Trap and Manometer System. Except for the elimination of the manganese dioxide trap, gas collection and measurement system is just the same as the system designed by Christman *et al.* (*2*).

Counting Tube. Metal counters of a design similar to the ordinary glass counter were used to reduce the background counting rate. The cathode metal is Kovar and the volume is about 100 ml.

Procedure. After the apparatus is assembled, the trap section is evacuated and then nitrogen gas is passed through the heated combustion tube at the rate of about 6 ml. per minute for 3 to 4 hours. During this period, the temperatures of the two furnaces are adjusted with the stationary furnace at 700° to 800° C. and the auxiliary furnace at 500° to 600° C., respectively. After cooling, the boat containing the weighed sample (2 to 8 mg.) is inserted into the combustion tube and pushed to the central part of the automatic combustion furnace; then the combustion is started.

In this procedure the combustion of the sample is carried out in two steps. In the initial stage, the time required is 10 minutes and the heating temperature of the sample is gradually raised to 300° C. In the second and final stage, another 10-minute period, the temperature is raised to 800° C. After the furnace has been switched off, nitrogen gas is allowed to flow for an additional 10 minutes to sweep the combustion products into the condensing trap. During the combustion period, nitrogen gas is passed through the combustion tube and trapping system at the rate of about 6 ml. per minute together with a certain amount of electrolytically generated oxygen as described below.

The electrolytic cell is connected parallel to the same terminals of the power supply as the automatic furnace. The amount of oxygen generated during the initial stage is very small. When the combustion reaches the final stage,

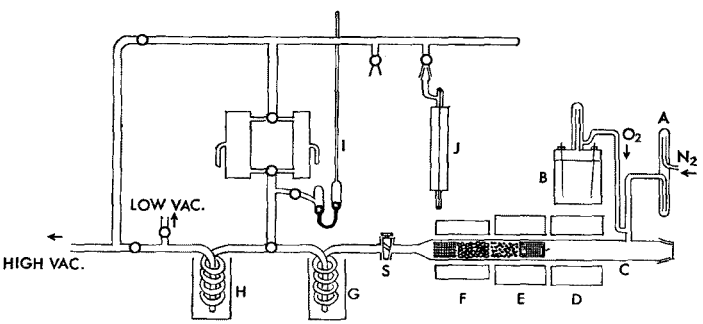


Figure 2. Assembled apparatus

A. Purification furnace
B. Oxygen gas generator
C. Combustion furnace
D. Automatic combustion furnace
E. Stationary furnace
F. Auxiliary furnace
G. Water trap
H. Carbon dioxide trap
I. Two-liquid manometer
J. Counting tube

Table I. Specimen Analyses

Compound	Sample, mg.	C, % Theor.	C, % Found	H, % Theor.	H, % Found
Benzoic acid		68.84		4.95	
	4.775		69.35		4.61
	5.188		68.35		4.78
	5.510		68.90		4.49
	4.036		69.28		4.90
	4.605		69.12		4.84
	5.315		68.92		4.42
	6.001		68.73		4.76
	5.482		68.85		4.91
Acetanilide		71.09		6.71	
	4.285		71.36		6.69
	4.235		71.38		6.97
	4.135		71.50		7.12
	3.985		71.04		6.50
	4.610		71.39		6.71
	4.235		70.75		6.38
	4.440		71.38		6.60

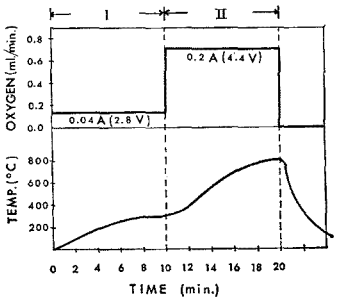


Figure 3. Temperature gradient of the automatic furnace and rate of generation of oxygen from electrolytic cell

I. Initial stage
II. Final stage

oxygen is generated at the rate of 0.7 ml. per minute and this amount is sufficient for the combustion (*7*). Figure 3 shows both the temperature gradient of the automatic furnace and the rate of generation of the oxygen.

During this operation, water produced is collected in the first trap (*G*), cooled with a dry ice–acetone mixture, and carbon dioxide is collected in the second trap (*H*), cooled with liquid nitrogen. At the end of the combustion, stopcock (*S*) is closed, and the trap and measurement system is evacuated to a high vacuum; then the amounts of carbon dioxide and water are measured by the two-liquid manometer described by Anderson *et al.* (*1, 2*).

Isotopic Assay. The total amount, or any desired portion, of carbon dioxide in the trap is introduced into a counting tube directly, and then P-10 gas (a proportional filling gas, 90% argon–10% methane) is added through the P-10 measuring bottle so as to make the inner pressure of the tube 1 atmosphere (*2*). Then the counting tube is set aside for a few hours to complete mixing of the gases. In our counting system, the counting tube is surrounded by 24 G.-M. tubes inside a 5-cm. thick lead and a 5-cm. thick iron shield, and anticoincidence counting circuits are employed.

RESULTS AND DISCUSSION

A list of analyses of carbon and hydrogen of specimens with this combustion method is shown in Table I.

The oxidized zone of the copper gauze extends gradually toward the exit end after repeated combustion, but a reduced copper gauze still remains

Table II. Assay of C^{14}-Labeled Compounds

Sample	Calcd., d.p.m./mg.	Sample, mg.	Found c.p.m.	Found d.p.m.	Found d.p.m./mg.	Average
Benzoic acid	7070[a]	4.629	26595	31642	6836	
		4.775	27169	32325	6780	6808
	1416[b]	5.768	6670	7936	1370	
		6.624	7766	9240	1395	
		7.146	8143	9690	1356	
		5.510	6413	7640	1387	1379
Benzamide		5.298	7209	8577	1619	
		6.354	8357	9958	1567	
		4.895	6486	7727	1579	
		5.254	7054	8404	1600	
		5.636	7584	9035	1603	
		5.430	7264	8654	1594	1590
Phenanthrene		6.220	2035	2421	389	
		6.972	2294	2727	391	390
5-Ethyl-2-propyl-acetanilide		2.914	44957	53488	18358	
		2.932	43813	52127	17785	
		3.302	48735	58059	17583	17909
2-Hexen-1-ol-1-C^{14}		2.432	69178	82306	33815	
		1.975	57035	67947	34404	
		2.804	78966	93951	33506	33908
2-Hexen-1-ol-5-C^{14}		3.902	7358	8765	2246	
		2.082	4026	4797	2303	2275
p-Aminobenzoic acid		4.170	364.3	433.4	103.9	
		5.197	456.6	544.0	104.7	104.3
p-Bromophenyl benzoate-1-C^{14}		6.064	14090	16786	2768	
		4.996	11817	14059	2814	2791

[a] The value of the standard benzoic acid purchased from New England Nuclear Assay Corp.
[b] The calculated value of benzoic acid which was obtained by the dilution of above standard.

usable after 20 combustions or more. When it is exhausted, it can be reactivated by reducing with methanol.

The results of the assay of various C^{14}-labeled compounds are shown in Table II.

By our counting system the background counting rate can be reduced to about 4 c.p.m. With a normal sample which contains no more than 5% carbon dioxide in the counting tube, the plateau runs from 2000 to 2300 volts and there is no appreciable slope to the plateau or shifting of the plateau to higher voltages.

Table II shows that nitrogen-containing compounds yield satisfactory results by the same operation as nonnitrogen-containing compounds. The results with halogenated or liquid compounds are also satisfactory.

After the measurement of relatively highly active compounds, the background rate of the counting tube is as low as 5 c.p.m. after evacuation for a few hours. But it is desirable to heat to 120° C. during evacuation after such measurements.

ACKNOWLEDGMENT

The authors thank David R. Christman, Brookhaven National Laboratory, and Tetsuo Mitsui, Kyoto University, for their kind help and valuable advice. The authors are indebted to Tadashi Kawano for constructing glassware.

LITERATURE CITED

(1) Anderson, R. C., Delabarre, Yvette, Bothner-By, A. A., ANAL. CHEM. **24**, 1298 (1952).
(2) Christman, D. R., Day, N. E., Hansell, P. R., Anderson, R. C., *Ibid.*, **27**, 1935 (1955).
(3) Christman, D. R., Paul, C. M., *Ibid.*, **32**, 131 (1960).
(4) Christman, D. R., Stuber, J. L., Bothner-By, A. A., *Ibid.*, **28**, 1345 (1956).
(5) Christman, D. R., Wolf, A. P., *Ibid.*, **27**, 1939 (1955).
(6) Mitsui, T., Yamamoto, O., Yoshikawa, K., *Mikrochim. Acta* 1962, p. 521.
(7) Mitsui, T., Yoshikawa, K., Furuki, C., *Ibid.*, p. 385.

Indium Capsules for Microdetermination of Carbon and Hydrogen

G. E. Secor and L. M. White, Western Utilization Research and Development Division, Agricultural Research Service, U. S. Department of Agriculture, Albany, Calif. 94710

INDIUM CAPSULES have been used to contain weighed samples of volatile liquids for analysis by mass spectrometry (*1*) and gas chromatography (*2*, *3*). Indium encapsulation should also have many advantages over existing techniques for handling volatile, unstable, and hygroscopic samples for carbon and hydrogen analysis. To test the suitability of indium capsules for use in this determination, a large variety of solid and liquid samples encapsulated in indium were analyzed for carbon and hydrogen by a conventional Pregl-type micro method. The results were as good as those with platinum boats or glass capillary tubes. In some determinations, a voluminous residue formed when solid samples containing sulfur or halogens were combusted in the capsules. This did not occur with volatile liquid samples.

EXPERIMENTAL

The capsules were made from 2-mm. i.d. × 3-mm. o.d. (0.080-inch i.d. × 0.120-inch o.d.), 99.99% pure indium tubing (The Indium Corp. of America, Utica, N. Y.), as received, cut into 15-mm. lengths. The ends of the tubes were sealed by cold-welding with a swaging tool (Wilkens Instrument and Research, Inc., Walnut Creek, Calif.) or with smooth, flat-tipped forceps. Because indium is a soft metal, care was taken to make sturdy welds without frangible ends; and the capsules were handled carefully between weighings to avoid loss of weighable amounts of indium through contact with other objects. When solid samples or additives were added to the capsules, precautions were taken to leave the weld area clean if it was essential to have an air-tight seal. When an additive was needed for the combustion, it was added to the sample inside the capsule, and the capsule was shaken vigorously after sealing. The capsule, containing 3 to 7 mg. of sample, was inserted into the combustion tube in a Coors No. 110, size 4/0 porcelain combustion boat.

The combustion train and general procedure for the microdetermination of carbon and hydrogen with indium capsules were the same as those used routinely in this laboratory with platinum boats or glass capillaries. After the combustion was completed, the indium was removed partially from the porcelain boat by "peeling" and final traces were removed by boiling in 1:1 nitric acid. Molten indium wets glass and adheres to it on cooling. If indium should contaminate the walls of the combustion tube, the metal can be oxidized by burning an organic sulfur compound in an open boat in the combustion tube and letting the vapor pass over the hot indium. The residue formed is removed with a moist cotton swab.

RESULTS AND DISCUSSION

Indium resists corrosion, has a low melting point (156.4° C.), and is available commercially in the form of highly pure (99.99%) tubing in a wide range of sizes. It self-welds at room temperature under moderate pressure. The capsules used in this study cost about 8 cents each and weigh ap-

Table I. Analytical Results for Indium Encapsulated Compounds

	Carbon, %		Hydrogen, %	
	Theoretical	Found[a]	Theoretical	Found[a]
Acetone	62.04	61.75	10.41	10.47
Methanol	37.49	37.63	12.58	12.54
2-Chloroethanol	29.84	29.99	6.26	6.35
Ethyl acetate	54.53	54.66	9.15	9.26
Di-*n*-propyl sulfite	43.35	43.47	8.49	8.40
Benzene	92.26	92.14	7.74	7.81
Bromobenzene	45.90	46.23	3.21	3.41
Iodobenzene	35.32	35.39	2.47	2.66
Toluene	91.25	91.37	8.75	8.79
Pyridine	75.92	75.87	6.37	6.50
Benzaldehyde	79.23	79.04	5.70	5.89
Vanillin	63.15	63.31	5.30	5.37
Urea	20.00	20.12	6.71	6.72
2,4-Dinitrophenylhydrazine	36.37	36.17	3.05	3.01
S-benzylthiuronium chloride	47.40	47.47	5.47	5.45
2-Iodophenol	32.76	33.02	2.29	2.46
4-Bromobenzoic acid	41.82	42.11	2.51	2.58
4-Fluorobenzoic acid	60.01	60.02	3.60	3.67
Potassium acid phthalate[b]	47.05	47.12	2.47	2.56
Sodium tartrate·$2H_2O$[b]	20.88	21.04	3.51	3.51
Triphenyl phosphate[b]	66.26	66.25	4.63	4.69

[a] Av. of two or three replicates.
[b] Combusted with WO_3 inside of capsule.

proximately 300 mg. They can be weighed as quickly and reproducibly as platinum boats and without error due to static charges.

The use of the capsules has many advantages in the carbon and hydrogen determination. A sample can be dried in a weighed capsule, sealed completely in a dry atmosphere, and weighed without the need of an additional container, such as a glass pig, to protect the dried sample from moist air. Because the capsules, unlike glass pigs are small and light-weight, they can be weighed on the 1-gram capacity electrobalances used for automated combustions. The capsules are air-tight if properly sealed and are not opened outside the combustion tube after the sample is added; therefore, a sample can be preweighed, easily stored, and analyzed when convenient. Unstable compounds can be encapsulated when freshly prepared; hygroscopic samples can be weighed under optimum conditions and transferred to the combustion tube without change in water composition; and liquid samples can be encapsulated without loss by heat decomposition or vaporization. Indium encapsulation is also faster and simpler for liquids than glass encapsulation. After the capsule is inside the combustion tube, the combustion system may be purged without loss of volatile sample if the temperature in the capsule area is not high enough to soften the indium and release the sample.

Indium capsules collapse in the combustion tube at approximately 200° C., a temperature below that required for complete combustion of most organic compounds. Though many compounds vaporize out of the capsule when the indium melts and the seal is broken, partially decomposed sample could be trapped in the melt. The results (Table I) and those obtained with National Bureau of Standards standard samples (anisic acid, benzoic acid, dextrose, sucrose, acetanilide, cystine, 2-chlorobenzoic acid) show that this did not occur. The average percentages were within ±0.3% of theory. The overall errors were positive, 0.09% above theory for carbon and 0.06% for hydrogen.

Indium usually did not spatter or leave a deposit on the wall of the combustion tube even at maximum burning temperature (750° C.) except when the encapsulated sample was a solid containing sulfur, iodine, bromine, or chlorine. When these samples were combusted in the capsules, the reaction at about 700° C. was sometimes sufficiently vigorous to ignite the melted indium to incandescence with a very large increase in the use of oxygen and the formation of a voluminous residue. However, the results were acceptable for the sulfur and halogen compounds analyzed, except for 2-iodobenzoic acid. Consistently good results were obtained for this compound only when it was combusted with cobalt oxide inside the capsule, or when the capsule ignited during the combustion. When the liquid samples containing sulfur or halogens, reported in Table I, were combusted in the capsules neither incandescent combustion nor troublesome residue occurred.

LITERATURE CITED

(1) Ehrhardt, C. H., Moeller, W. H., Grubb, H. M. (to Standard Oil Co. of Indiana), U. S. Patent **3,103,277**, September 10, 1963.
(2) Nerheim, A. G., ANAL. CHEM. **36**, 1686 (1964).
(3) Nerheim, A. G. (to Standard Oil Co. of Indiana), U. S. Patent **3,063,286**, November 13, 1962.

Reference to a company or product name does not imply approval or recommendation of the product by the U. S. Department of Agriculture to the exclusion of others that may be suitable.

Computerized Procedure for Editing Data from a Mass Spectrometer Digitizer

H. Evert Howard, Union Oil Company of California, Union Research Center, P. O. Box 76, Brea, Calif. 92621

A PRIMARY ADVANTAGE of mass spectrometry is the production of a wealth of fundamental data. However, many mass spectrometric (MS) methods do not require, nor can they use, all of the raw data produced by the MS. Hence a means is needed for identifying the mass numbers of those MS peaks required for any given analysis.

A mass spectrometer digitizer ("MSD" manufactured by Non Linear Systems of Del Mar, Calif.) is used in this laboratory to digitize the mass spectra from a Consolidated Electrodynamics Corporation 21-103 mass spectrometer. This MSD, described by Thomason (*1*), reads out the height of each MS peak along with mass identification in terms of ion accelerating voltage.

When accelerating voltage is known, mass number may be calculated using the following well known equation:

$$M/e = \frac{R^2B^2}{2E} \qquad (1)$$

where R = radius of curvature of the ion beam, B = magnetic induction, and E = ion accelerating voltage.
This equation may be simplified to

$$M/e = \frac{K}{E} \qquad (2)$$

where $K = \frac{R^2B^2}{2}$ and B is fixed.

Therefore, $K = E \cdot$ mass number (3)

Thomason (*1*) reported the derivation of average K factors from known sample runs for different magnet ranges. Using these average factors he obtained mass number reproducibilities of ±0.1 mass number up to mass 125 and ±0.25 mass number up to mass 250. Our experience indicates that very diligent control of instrumental conditions (magnet strength, etc.) must be maintained, along with appropriate correction factors, if mass identification is to be kept within these limits using average K factors. Theoretically a K-factor for a given magnet range will not change. However, due to temperature variations in the magnet environment, geometry of the MS ionization chamber and analyzer tube, magnet hysteresis problems, etc., K-factors do change, although not abruptly. Hence this change must be accounted for or mass number identification will be in error. Our approach to the solution of this problem is described as follows.

Preceding the analysis of any group of samples a calibration run on a suitable pure compound (*n*-butane for gas analysis and *n*-heptane for gasoline samples) is first obtained. An initial K-factor is calculated by application of Equation 3 to any readily identified peak in the spectrum. The mass spectrum of the first sample for analysis is next obtained, and the initial K-factor is used to identify the first mass number (K/E = mass number) required by the analysis. When more than one MS peak is found for this or subsequent mass numbers, the largest peak is assumed to be the one desired, on the premise that metastable ions, noise spikes, etc., are always of a lower magnitude than the whole mass ions.

After the first required mass number is identified as above, a *new* K-factor is computed by application of Equation 3 to this mass number. This new K-factor is then used to identify the next higher mass number required in the analysis, in the same way that the first required mass number was identified. This process is repeated, with intermediate calculation of K-factors for all mass numbers used in the analysis, until all of the mass numbers required for the sample in question have been identified. In this way all "normal" changes in K-factors which occur during the mass analysis of a given sample are sensed and maximum accuracy in the identification of each mass number is maintained. Any "abnormal" changes

in K are tested for by comparing adjacent K values. A change in K by more than 1 part in 300 between adjacent mass values is assumed to represent an abnormal change in K—e.g., discontinuous momentary shift in K—and the immediately preceding K value is used for the following mass value determination—i.e., the abnormal value of K is rejected. The first computed K-factor for each sample is used as a starting K-factor for analysis of the next sample, and the overall process is continued until all samples are analyzed.

All of the arithmetic operations are carried out by an IBM 1620 computer program in this laboratory.

At the time of this writing we have analyzed hundreds of samples, both gas and gasoline, by means of the described editing routine without a single failure. There are several innovations in the procedure, but the key to its success is the repetitive calculation of new K-factors each time a mass number is identified. The outstanding advantage of this procedure, as compared to that of Thomason (*1*), is the certainty of mass number identification (with this burden carried entirely by a computer) while requiring only normal MS operator effort.

The gasoline hydrocarbon type method used in this laboratory requires specific mass numbers starting at mass 43 and ending at mass 170. The K-factors computed during a typical day's production of these analyses vary between two extremes—e.g., 401,000 to 403,000. If either value had been used to determine a mass number where the other K-factor was correct, the mass unit would be incorrectly identified, with a resultant error in the final analysis of the sample. This illustrates the potential errors that can arise by the use of average K-factors.

LITERATURE CITED

(1) Thomason, E. M., ANAL. CHEM. **35**, 2165 (1965).

High Sensitivity Oxygen Analysis of Metallic Samples with Fast Neutrons

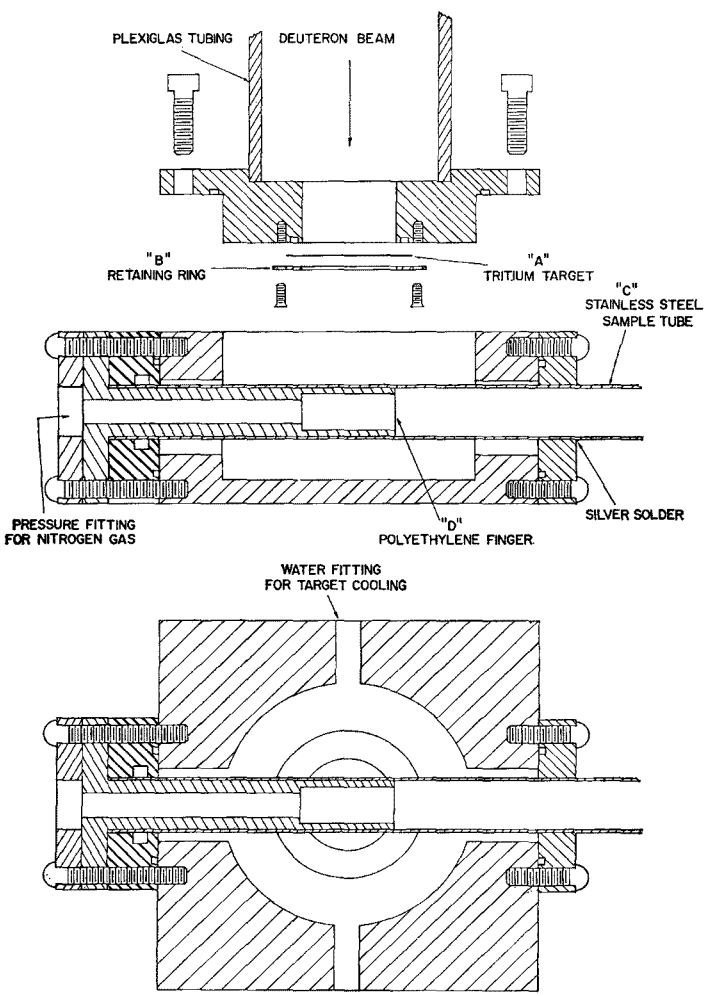
Richard W. Benjamin, Kenneth R. Blake, and Ira L. Morgan, Texas Nuclear Corp., Austin, Texas

TRACE ANALYSIS for oxygen in metallic samples has been performed for some time by using fast neutron activation analysis techniques in conjunction with a pneumatic rapid transfer system (*1*, *3*, *4*). A system has now been designed which is capable of measuring oxygen in concentrations below 10 p.p.m. in cylindrical metallic samples $^3/_{16}$ to 0.480 inch in diameter and $^1/_2$ to 1 inch long.

Oxygen activation analysis with fast neutrons may be done accurately and rapidly with the $O^{16}(n,p)N^{16}$ reaction. Because of the short half life of the N^{16} activity, it is advantageous to use some sort of rapid transfer system, such as has been described in some detail by Anders and Briden (*1*).

A 150-k.e.v. Texas Nuclear Corp. Cockcroft-Walton positive ion accelerator provides an abundant source of 14-m.e.v. neutrons through the $H^3(d,n)He^4$ reaction. The target used on the accelerator consists of 3 to 5 curies of tritium adsorbed onto a titanium layer which has been vacuum-deposited on a copper backing.

The target assembly appears in Figure 1. The deuteron beam impinges on the tritium target (*A*) which is held against an O-ring by the retaining ring (*B*), thus sealing the accelerator vacuum system. The target is cooled by water which flows directly over the copper backing. This allows higher beam currents and a longer target life. The thin stainless-steel sample tube (*C*) is fitted flush against the retaining ring, ensuring that the sample is exposed to the highest possible neutron flux. The sample is centrally and reproducibly constrained in the tube by a polyethylene finger (*D*), the inside diameter of



▶ Figure 1. Target assembly

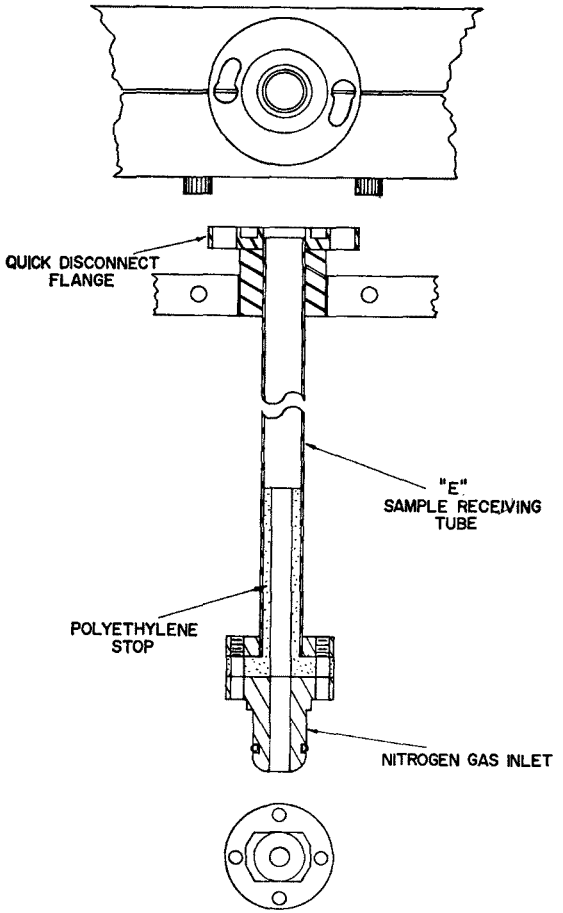


Figure 2. Sample receiving tube assembly

which is a maximum of 0.002 inch greater than the outside diameter of the sample. Although the sample is very close to the target and there is considerable difference in neutron flux from front to back, the sample was not rotated during irradiation as done by Anders and Briden (*1*) and Mott and Orange (*3*) because the counting geometry is nearly 4π. Reasonable values for the standard deviation (σ) of several measurements were obtained without sample rotation, although the lack of truly 4π counting geometry introduces some error. Provision is made at the bottom of the assembly for the pressure fittings required by the rapid transfer system, and at the top of the assembly for the flexible sample tube. Three removable sample tube assemblies have been built, along with several fingers for each assembly, so that all cylindrical samples from $^3/_{16}$ to 0.480 inch in diameter can be handled. Flexible sample transfer tubes are made from $^1/_8$-inch wall polyethylene tubing and from Nylobraid, a nylon reinforced polyvinylchloride plastic tubing. Polyethylene tubing is adequate, if available with requisite inside diameter and wall thickness.

The sample receiving tube assembly appears in Figure 2. The sample receiving tube (*E*), which is fitted with a quick disconnect for rapid sample removal and r placement, protrudes into a large paraffin and lead detector shield which houses two 3 × 3-inch NaI(Tl) scintillation detectors. Initially, polyethylene figures were built to position the sample in the detector assembly, but measurements indicated that several thousandths of an inch uncertainty in this positioning did not appreciably increase the uncertainty of the gamma ray measurements. The NaI(Tl) crystals are optically coupled to Dumont 6363 photomultiplier tubes whose outputs are amplified and gated so only the high energy gamma rays from N^{16} are accepted. This output is then fed into a decade scaler.

The entire system is automatically programmed to irradiate the sample for a predetermined time, transfer the sample to the detector (transfer time is 1 to 2 seconds), count the sample for a predetermined time, and then return the sample to the irradiation position where the cycle begins again. Ten runs per sample are made as a rule to provide good statistics. Unknown samples are compared with standards using the same geometry to determine the oxygen concentration. Neutron flux is monitored with a simplified recoil proton telescope as described by Bame *et al.* (*2*), and gamma ray counts for each run are normalized to a standard neutron monitor count. The recoil proton telescope has the advantages of being both very directional and neutron energy dependent.

To thoroughly test this high sensitivity oxygen analysis system, high purity beryllium samples covering a large range of sizes and purity were analyzed for oxygen. Each sample and standard was irradiated for 20 seconds and counted for 20 seconds after a constant delay of about 3 seconds which provided for transfer from the irradiation area. The standards used in these measurements were titanium rods which were machined to the same size as the unknown samples; the oxygen content of the

Table I. Precision of Measurements for Several Oxygen Concentrations

Sample	Rel. oxygen content, p.p.m.	Rel. std. dev., %	Total rel. std. dev., %	Sample size, inches	Wt. oxygen, mg.
Be 7, Run 1	11.0	10.6	10.7	0.249 × 1	0.016
Be 7, Run 2	11.8	14.0	14.1	0.249 × 1	0.017
Heat No. 3362	24700	1.22	1.90	0.2505 × 1	37.2
Heat No. 3363	14400	0.99	1.76	0.251 × 1	21.6
Be 6	5356	1.70	2.24	0.248 × 1	7.75
WA-58	1050	1.46	Std.	0.249 × 1	3.938
Ti-1	2850	1.57	Std.	0.360 × 1	21.95
Be 6	5080	2.88	3.28	0.358 × 1	15.1
WA-58	1050	1.74	Std.	0.479 × 1	14.550

standards was determined by several methods in several different laboratories.

The results of the measurements are presented in Table I; they give a good idea of the sensitivity of the system and the reproducibility of measurements at various levels of oxygen content. The column titled "Rel. std. dev." represents the relative standard deviation of the normalized gamma ray counts; this quantity was calculated from 10 measurements which were made on each sample. The column titled "Total rel. std. dev." represents the relative standard deviation of the measured relative oxygen content of each sample; this was calculated from the usual rules of error accumulation.

Some aspects of Table I merit special mention. Sample Be-7 weighed 1.44145 grams; thus, 11 p.p.m. of oxygen represents a weight of only 16 μg. of oxygen. Since beryllium is a low-density metal, 11 p.p.m. of oxygen in the same size sample of another metal could correspond to considerably more oxygen and a proportionally higher count rate. The standard deviation of 11 p.p.m. of oxygen would decrease then as the density of the sample increased. Conversely, considerably smaller relative oxygen contents could be measured with the same standard deviation with higher density metals.

ACKNOWLEDGMENT

The authors are grateful to Charles D. Houston, Wright-Patterson A.F.B., Ohio, for the beryllium samples and titanium standards which were used in this work.

LITERATURE CITED

(1) Anders, O. U., Briden, D. W., ANAL. CHEM. **36,** 287 (1964).
(2) Bame, S. J., Haddad, Eugene, Perry, J. E., Smith, K. R., *Rev. Sci. Instr.* **29,** 652 (1958).
(3) Mott, W. E., Orange, J. M., ANAL. CHEM. **37,** 1338 (1965).
(4) Steel, E. L., Meinke, W. W., *Ibid.*, **34,** 185 (1962).

Pulseless High-Pressure Pump for Liquid Chromatography

R. E. Jentoft and T. H. Gouw, Chevron Research Co., Richmond, Calif.

IN HIGH-PRESSURE liquid chromatography, the eluting solvent is generally pumped into the column by a reciprocating piston or bellows pump. Pulses generated by this pump can often be discerned by the detector. Besides introducing difficulties in the interpretation of the detector output, pulses also have a detrimental effect on the separating efficiency of the column. A major portion of these pulses can be eliminated by the use of surge tanks—e.g., spring-loaded bellows connected to tees in the line between the pump and the column inlet. But even careful design will not remove all pulses from the flow pattern and rather complicated and/or large surge tanks, with concurrent large holdup of material, are necessary to reduce the level of the flow variations to a negligible level. In addition, damage to this pump and surge system is feasible if the outlet line is accidentally blocked.

With the pump described here, high pressures up to 1000 p.s.i. can be generated at the outlet of the pump. In comparison, many of the commercially available pumps are incapable of operating above 100-p.s.i. pressure. Delivery into the chromatographic system can be carried out without any discernible pulses for any length of time and any amount of solvent. Accidental blocking of the outlet line does not damage the pump at all. Construction is simpler than reciprocating plunger pumps of equivalent rating.

DESCRIPTION AND OPERATION OF PUMP

A schematic drawing of the unit is given in Figure 1. Four 2-inch by 8-inch stainless steel reservoirs, constructed from pipe nipples, are half-filled with mercury, the displacing agent. High pressure air is used as the source of operating pressure. The use of mercury as the displacing agent prevents the dissolution of the air in the solvent.

The outlet of the pump is on the top of Vessel *A*. For operation up to 250 p.s.i., a dual back-reference flow controller with integral micrometering valves (Millaflow No. 9986 220) is mounted between this outlet and the inlet of the chromatographic column. Because these type flow controllers are currently not available for higher pressure ratings, a fine metering valve is used for work at higher pressures.

The pressure-reducing valve in the air line is adjusted to yield a pressure about one and one-half to two times the desired inlet pressure to the column, but not less than 100 p.s.i. to minimize the effect of the variations in the mercury levels. Prior to introduction into the pump, the solvent in the external reservoir is heated by an infrared lamp. This degases the liquid sufficiently to prevent air from coming out of solution in the column and creating artifacts in the chromatogram. At the normal mode of operation, neither of the three-way solenoid valves is energized. The air pressure, which is now connected to *B*, is transmitted through the mercury to the solvent in *A*. There is vacuum on *D*, and *C* is being refilled from the external solvent reservoir. Mercury rises in *A* as solvent is delivered to the chromatographic column. As soon as the mercury in Vessel *A* comes in contact with the upper electrode, the solenoids are energized. *B* is now connected to atmospheric pressure or to a regulated pressure somewhat lower than the operating air pressure in *D*. The latter is the desired mode of operation at high pressures. The air pressure, which is now on *D*, refills *A* from *C* and, at the same time, keeps up the uninterrupted delivery of the solvent at the

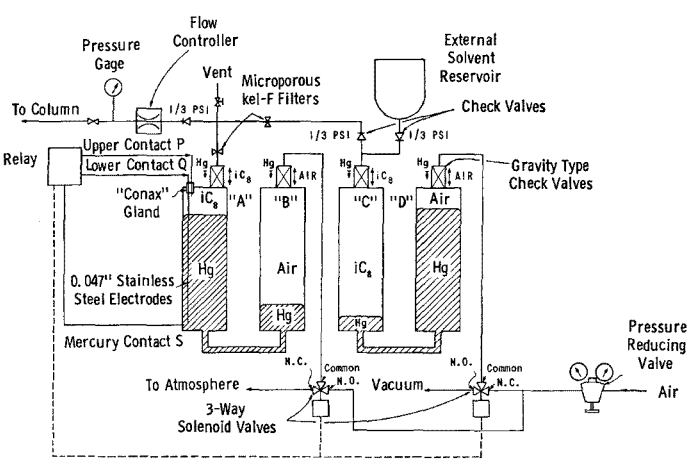


Figure 1. Pulseless high pressure pump

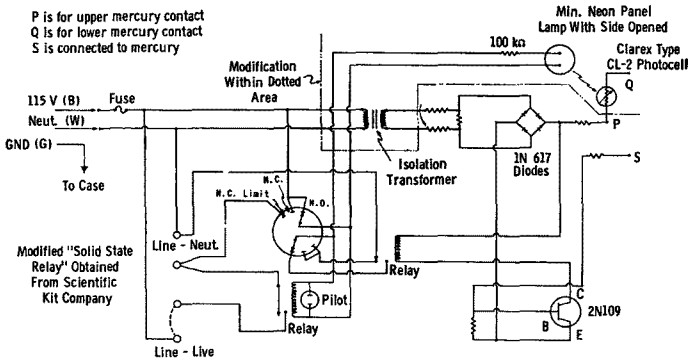


Figure 2. Wiring diagram of relay

adjusted pressure to the chromatographic system. As soon as the mercury in A drops below the lower electrode, the solenoids are de-energized, and the pump assumes operation at the normal mode.

Spring-loaded check valves in the solvent lines ensure the correct direction of flow. Gravity-type check valves above the cylinders prevent mercury from getting out but pass solvents in both directions. We have found it necessary to introduce an impedance to flow between the output lines and the solvent reservoirs, among others, to prevent these check valves from slamming shut during the change between the cycles. Microporous disks of Kel-F have been found satisfactory for this purpose. Figure 1 shows the locations of these disks.

The electrodes in A are 0.047-inch stainless steel rods which are mounted through a modified Conax packing gland assembly which is sealed at the base with epoxy cement. To provide for the cycling between the two mercury levels in A, we have modified a commercially available "Solid State Relay," obtained from Scientific Kit Co., so the relay can be locked up. This alteration is required because the initial electrical contact, which starts the refilling of A, is broken as soon as the refilling operation is initiated. The wiring diagram is given in Figure 2.

As the solvent in C should account for both the filling of A and the delivery to the chromatographic column during the time of filling, the displacement in this vessel should be larger than the amount displaced in A between the two electrodes. For the stated dimensions, flows up to 100 ml. per minute have been attained. For larger capacities, C and D should be larger than indicated. No major problems should be encountered during scaling up. The output pressure will vary with the heights of the mercury levels. To keep this variation negligible in relation to the output pressure, increase in size should preferably be found in increasing the reservoir diameter instead of the length. The limit is reached when the pressure rating of the vessel falls below the desired operating pressure.

The 2-inch stainless steel nipples are rated at 3000 p.s.i. All the Swagelok connections used throughout the pump and the thick-walled $\frac{1}{4}$-inch stainless steel tubing have ratings far in excess of this number. The maximum operating pressure is determined by the accessory equipment—i.e., the solenoids and the flow controller. Commercially available items are rated up to 250–500 p.s.i.; and to go to higher pressures, specially constructed equipment may be necessary. It is, however, not difficult to achieve operating pressures up to 1000 p.s.i. In comparison, a piston pump with the equivalent rating would have to be much heavier in construction.

Operation of the pump has been carried out at pressures up to 1000 p.s.i. and flow rates up to 100 ml. per minute with no discernible changes in output flow or output pressure during the different cycles of the pump.

ACKNOWLEDGMENT

The authors are indebted to J. F. Johnson for helpful discussions and to W. C. Eaton for assembling and testing this pump during initial development stages.

The Purity, Properties, and Analytical Determination of 4-sec-Butyl-2-(α-methylbenzyl)phenol

B. Z. Egan and W. D. Arnold, Oak Ridge National Laboratory, Oak Ridge, Tenn.

THE COMPOUND 4-*sec*-butyl-2-(α-methylbenzyl)phenol (BAMBP) has been used as a reagent in the analytical determination of cesium and rubidium (*18*), in process applications for the extraction of cesium from reactor waste solutions (*2*, *11*, *16*, *17*), and for the recovery of cesium and rubidium from ore leach liquors (*1*). These applications require that the purity and properties of the reagent be known, and that a reliable method be available for the determination of its concentration in solution.

This paper is concerned with the identification of impurities occurring in large-scale (10 to 50 lb.) preparations of BAMBP, the estimation by distillation and gas–liquid chromatography of the concentrations of the impurities, the determination of some of the chemical and physical properties of BAMBP, the development of a spectrophotometric method for accurately measuring the concentration of BAMBP in various diluents, and a comparison of this method with an existing potentiometric method.

DISTILLATION OF BAMBP AND IDENTIFICATION OF IMPURITIES

An Aerograph Autoprep Model A-700 gas chromatograph was used to obtain chromatograms of 1M solutions of BAMBP in benzene or in diisopropylbenzene. The $\frac{1}{4}$-inch × 20-foot copper column was packed with 60/80 mesh Chromosorb, treated with hexamethyldisilazane, and then with 20% silicone SE 30 rubber. Column temperature was programmed from 140° to 245° C. Helium flow rate was 65 ml./minute at 50 p.s.i.

The similarity of the chromatograms of different batches of BAMBP indicated that the same impurities occurred, but in different amounts, in the batches tested. A chromatogram of the most impure batch of BAMBP is shown in Figure 1*a*. The different batches contained 2–4% of impurities more volatile than BAMBP and 2–8% of impurities less volatile than BAMBP.

Samples of BAMBP were fractionated by distillation at reduced pressure in a Podbielniak distillation apparatus, equipped with a 1- × 36-inch column, packed with Heli-Grid packing. In two separate runs, a colorless BAMBP product was collected at 186° ± 1° C. (6 mm. of Hg) and 207° ± 2° C. (15 mm. of Hg). Distillation was discontinued during collection of the BAMBP product, leaving unrecovered BAMBP and any higher boiling impurities in the still pot residue. Comparison of the chromatograms of commercial BAMBP and the distilled product shows that distillation removed most of the impurities (Figure 1). The purity of the distilled product was estimated to be greater than 98% BAMBP.

During the synthesis of BAMBP,

it is possible to form isomers in which the 4-*sec*-butyl group is replaced by *n*-butyl, *iso*-butyl, or *tert*-butyl groups. The impurity which gives Peak II in Figure 1*a* is 4-*tert*-butyl-2-(α-methylbenzyl)phenol. This was established by comparing chromatograms of distilled BAMBP to chromatograms of BAMBP containing added amounts of the 4-*tert*-butyl isomer. The height of Peak II in distilled BAMBP changed in proportion to the amount of 4-*tert*-butyl-2-(α-methylbenzyl)phenol added. Chromatograms of mixtures of BAMBP and 4-*n*-butyl-2-(α-methylbenzyl)-phenol showed no coincident peaks, indicating that this isomer was not one of the impurities. The GLC emergence time for the 4-*n*-butyl-2-(α-methylbenzyl)phenol was greater than either of the peaks shown in Figure 1. Since pure 4-iso-butyl-2-(α-methylbenzyl)phenol was not available, neither its presence nor absence has been established, but it is considered a likely possibility as a higher-boiling impurity (Peak IV).

A small amount (less than 1% of the starting material) of 4-*sec*-butyl phenol, not evident in the chromatograms, was separated by the distillation, and was identified by its infrared spectrum, melting point (47–8° C.), and equivalent weight (130). This compound is a starting material in the synthesis of BAMBP.

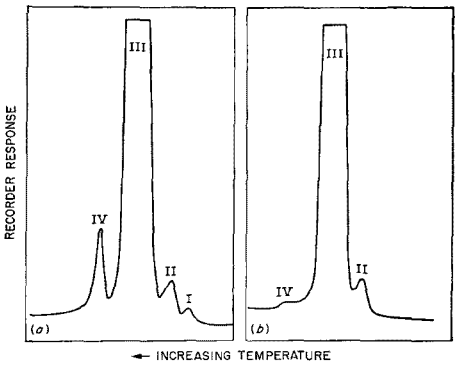


Figure 1. Gas chromatograms of BAMBP

a: Undistilled
b: Distilled

PHYSICAL PROPERTIES OF DISTILLED BAMBP

BAMBP is completely miscible with many organic solvents, including carbon tetrachloride, chloroform, toluene, benzene, diisopropylbenzene, *n*-octane, kerosene, and Amsco 125-82 (a highly refined naphtha). It is essentially insoluble in dilute acid solution but slightly soluble in alkaline solutions (*1*, *3*).

Physical properties of BAMBP which were determined on the distilled product are:

Density	= 1.004 gram/ml. (26° C.)
Refractive index, $n_D^{25.2}$	= 1.5570
Viscosity (relative to water)	= 390 centipoises (25° C.)
Boiling point	= 186° C. (6 mm. of Hg)
	= 207° C. (15 mm. of Hg)
	= 325° C. (calculated for 760 mm. of Hg)
ΔH_{vap}	= 20 kcal./mole/degree
Trouton's constant $= \frac{\Delta H_{vap}}{T}$	= 31.7 cal./mole/degree

The values for the normal boiling point, heat of vaporization, and Trouton's constant were calculated from the vapor pressure at 186° and 207° C., using the integrated form of the Clausius-Clapeyron relationship

$$\log p = -\Delta H_{vap}/2.303RT + \text{Constant}$$

and assuming ΔH_{vap} to be constant at higher temperatures and pressures. Because the vapor pressure was measured only at two different temperatures, the calculated quantities are considered to be estimates. The high Trouton's constant value, compared to the value of 21 for normal liquids, indicates association of the phenol in the liquid state. This is supported by the infrared spectrum of distilled BAMBP (Figure 2). Even though there is some steric hindrance in the BAMBP molecule, hydrogen bonding of the phenolic O—H readily occurs (*6*), as evidenced by the broad O—H absorption band around 3500 cm.$^{-1}$ Free O—H absorption, which generally appears as a sharp band at 3600 cm.$^{-1}$ or higher, is observed only as a weak shoulder.

DETERMINATION OF BAMBP CONCENTRATION IN SOLUTION

For process control and in analytical procedures, it is necessary in the solvent extraction steps to have a reliable method for measuring the extractant concentration in the diluent. Several general methods have been reported for the analytical determination of weak acids such as phenols. These include potentiometric titrations (*9*, *10*, *15*), spectrophotometric measurements (*8*, *12*, *14*), and bromination procedures (*19*).

The potentiometric and spectrophotometric methods were investigated for possible application to the determination of BAMBP in several diluents. The spectrophotometric method proved to be simpler, faster, and more accurate than the potentiometric method, though limited to diluents which do not absorb strongly at 278 and 284 mμ. Phenolic impurities were measured as BAMBP with both methods.

Spectrophotometric Determination. The ultraviolet spectra of BAMBP in carbon tetrachloride and in *n*-octane are shown in Figure 3. Two absorption peaks occur at 279.0 and 284.5 mμ in carbon tetrachloride, and 277.5 and 284.5 mμ in *n*-octane. The absorption spectrum of BAMBP in Amsco 125-82 was almost identical to that in *n*-octane with absorption peaks at 278.0 and 284.5 mμ. The spectra were obtained for $5.0 \times 10^{-4}M$ solutions, using a 10-mm. cell in a Cary Model XIVPM instrument. A Beckman DU spectrophotometer was used to ascertain that Beer's law holds in the concentration range 1×10^{-4} to $6 \times 10^{-4}M$ BAMBP in the three solvents when absorption is measured at either 278.0 or 284.0 mμ. The 278-mμ peak is considered more reliable for measurements due to its broadness and higher intensity (*13*). Also, the 284-mμ peak is not well resolved in carbon tetrachloride. Average molar absorptivities are given in Table I.

The accuracy of the spectrophotometric method of determining BAMBP concentration is shown in Table II. Solutions of BAMBP were prepared by adding weighed amounts of BAMBP to Amsco 125-82. A sample of the solvent Amsco 125-82 was used for the comparison cell and for diluting the samples

Table I. Molar Absorptivities for BAMBP

Solvent	ε λ_{278}	ε λ_{284}
Amsco 125–82	2545	2270
n-Octane	2550	2310
CCl_4	2618	2474

Table II. Accuracy of Spectrophotometric Determination of BAMBP Concentration

Phenol present (M)	Phenol concn. found (M) 278 mμ	284 mμ	Av.
0.504	0.501	0.505	0.503
0.614	0.615	0.618	0.617
0.736	0.737	0.727	0.732
0.858	0.856	0.861	0.858
1.014	0.998	1.017	1.008

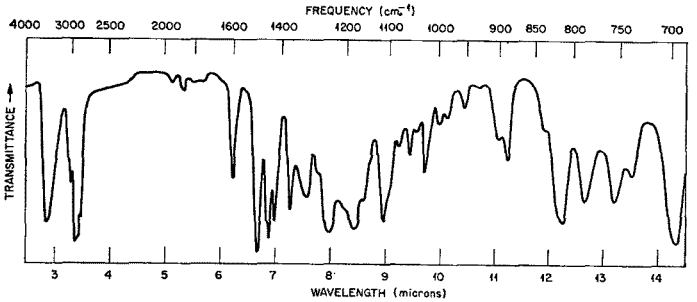


Figure 2. Infrared spectrum of BAMBP

Pure liquid, 0.025-mm. cell

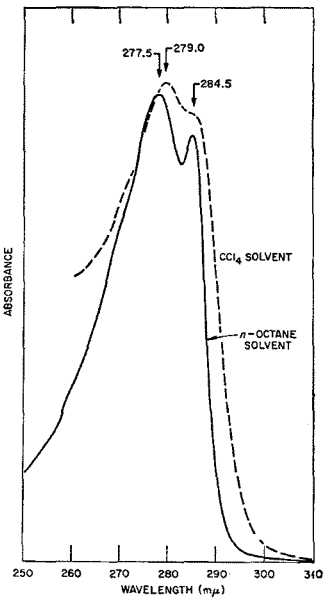


Figure 3. Ultraviolet spectrum of BAMBP

0.0005*M*, 10-mm. cell

2000-fold before absorbance measurements. Absorbance was measured at 278 and 284 mμ, and an average concentration was calculated.

The spectrophotometric method presumably could be used for other phenols after establishing appropriate absorptivities. Those given are specific for BAMBP. This method could not be used for determination of BAMBP in diluents having high ultraviolet absorbance at 278 and 284 mμ—e.g., kerosene.

Potentiometric Titration. Weak acids, including phenols, have been titrated with tetrabutylammonium hydroxide in solvents such as pyridine (*4*, *5*), *tert*-butyl alcohol (*7*), and ethylenediamine. Several other titrant–solvent systems have also been used (*4*, *9*, *15*). Some of these systems were evaluated for titrating BAMBP solutions. Best results were obtained with tetrabutylammonium hydroxide titrant and either pyridine or *tert*-butyl alcohol solvent (Table III). Sodium hydroxide and sodium ethoxide were unsatisfactory titrants because of extremely small potential changes at the end point. The potential change at the BAMBP end point was less than 75 mv. under the best conditions.

For comparison, the more acidic 4-chloro-2-benzylphenol gave a sharp end point, and the potential change was about 150 mv.

In a typical titration, 0.250 ml. of a 1*M* BAMBP solution was pipetted into 150 ml. of tertiary-butyl alcohol and stirred with a magnetic stirrer. Standard 0.078*M* tetrabutylammonium hydroxide (Eastman) solution in 80% benzene–20% isopropanol was added slowly, and the potential was measured with a pH meter, using calomel and glass electrodes. The titration end point was obtained from a plot of potential *vs.* volume of titrant. When titrated by this procedure, weighed 1.00*M* solutions of BAMBP and 4-chloro-2-benzyl-phenol in Amsco 125-82 and in diisopropylbenzene diluents gave values ranging from 1.01*M* to 1.06*M*.

The potentiometric titration has the advantage of being a more general method of determination, applicable to different phenols in various diluents. However, this method is more time-consuming and is not as accurate as the spectrophotometric method.

ACKNOWLEDGMENT

We thank R. A. Zingaro, W. E. Oxendine, and W. B. Howerton for assistance in obtaining data for this paper

Table III. Potentiometric Titration of BAMBP

Base	Titrating medium	BAMBP diluent	Remarks
NaOH	70% EtOH	DIPB[a]	Poor[b]
$NaOC_2H_5$	70% EtOH	DIPB	Poor[b]
$NaOC_2H_5$	95% EtOH	CCl_4	Poor[b]
$NaOC_2H_5$	ethylenediamine	CCl_4	Erratic[c]
Bu_4NOH	*tert*-butyl alcohol	DIPB, CCl_4, Amsco 125-82[d]	Good
Bu_4NOH	ethylenediamine	DIPB	Fair
Bu_4NOH	pyridine	DIPB, CCl_4, Amsco 125-82	Good

[a] DIPB: diisopropylbenzene.
[b] Insufficient potential change at end point.
[c] Unstable potential.
[d] Amsco 125-82: a highly refined naphtha.

LITERATURE CITED

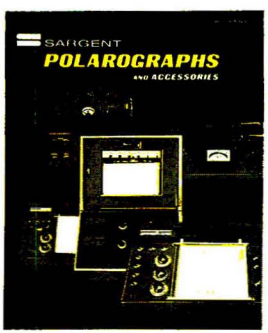
(1) Arnold, W. D., Crouse, D. J., Brown, K. B., *Ind. Eng. Chem., Process Design Develop.* **4**, 249 (1965).
(2) Bray, L. A., *Nucl. Sci. Eng.* **20**, 359 (1964).
(3) Brown, K. B., *U. S. At. Energy Comm. Rept.* **ORNL-TM-449** (1963).
(4) Bruss, D. B., Harlow, G. A., ANAL. CHEM. **30**, 1836 (1958).
(5) Cundiff, R. H., Markunas, R. C., *Ibid.*, **28**, 792 (1956).
(6) Egan, B. Z., Zingaro, R. A., Benjamin, B. M., *Inorg. Chem.* **4**, 1055 (1965).
(7) Fritz, J. S., Marple, L. W., ANAL. CHEM. **34**, 921 (1962).
(8) Harlow, G. A., Bruss, D. B., *Ibid.*, **30**, 1833 (1958).
(9) Harlow, G. A., Noble, C. M., Wyld, G. E. A., *Ibid.*, **28**, 784 (1956).
(10) Harlow, G. A., Noble, C. M., Wyld, G. E. A., *Ibid.*, **28**, 787 (1956).
(11) Horner, D. E., et al., *Nucl. Sci. Eng.* **17**, 234 (1963).
(12) Hummelstedt, L. E. I., Hume, D. N., ANAL. CHEM. **32**, 1792 (1960).
(13) Lothian, G. F., *Analyst* **88**, 678 (1963).
(14) McKinney, R. W., Reynolds, C. A., *Talanta* **1**, 792 (1956).
(15) Moss, M. L., Elliott, J. H., Hall, R. T., ANAL. CHEM. **20**, 784 (1948).
(16) Richardson, G. L., Hanford Laboratories *Rept.* **HW-80686** (1963).
(17) *Ibid.*, **HW-SA-3211** (1963).
(18) Ross, W. J., White, J. C., ANAL. CHEM. **36**, 1998 (1964).
(19) Stone, K. G., "Determination of Organic Compounds," p. 121, McGraw-Hill, New York, 1956.

RESEARCH sponsored by the U. S. Atomic Energy Commission under contract with the Union Carbide Corp.

Conventional, fast sweep— for all polarographic applications

ONLY SARGENT MAKES 5 POLAROGRAPHS®





read all about all 5 models in this booklet—complete with illustrations, specifications, and recommended selections...plus a full line of polarographic accessories.

E. H. Sargent & Co., Dept. AC-66
4647 W. Foster Ave., Chicago, Ill. 60630

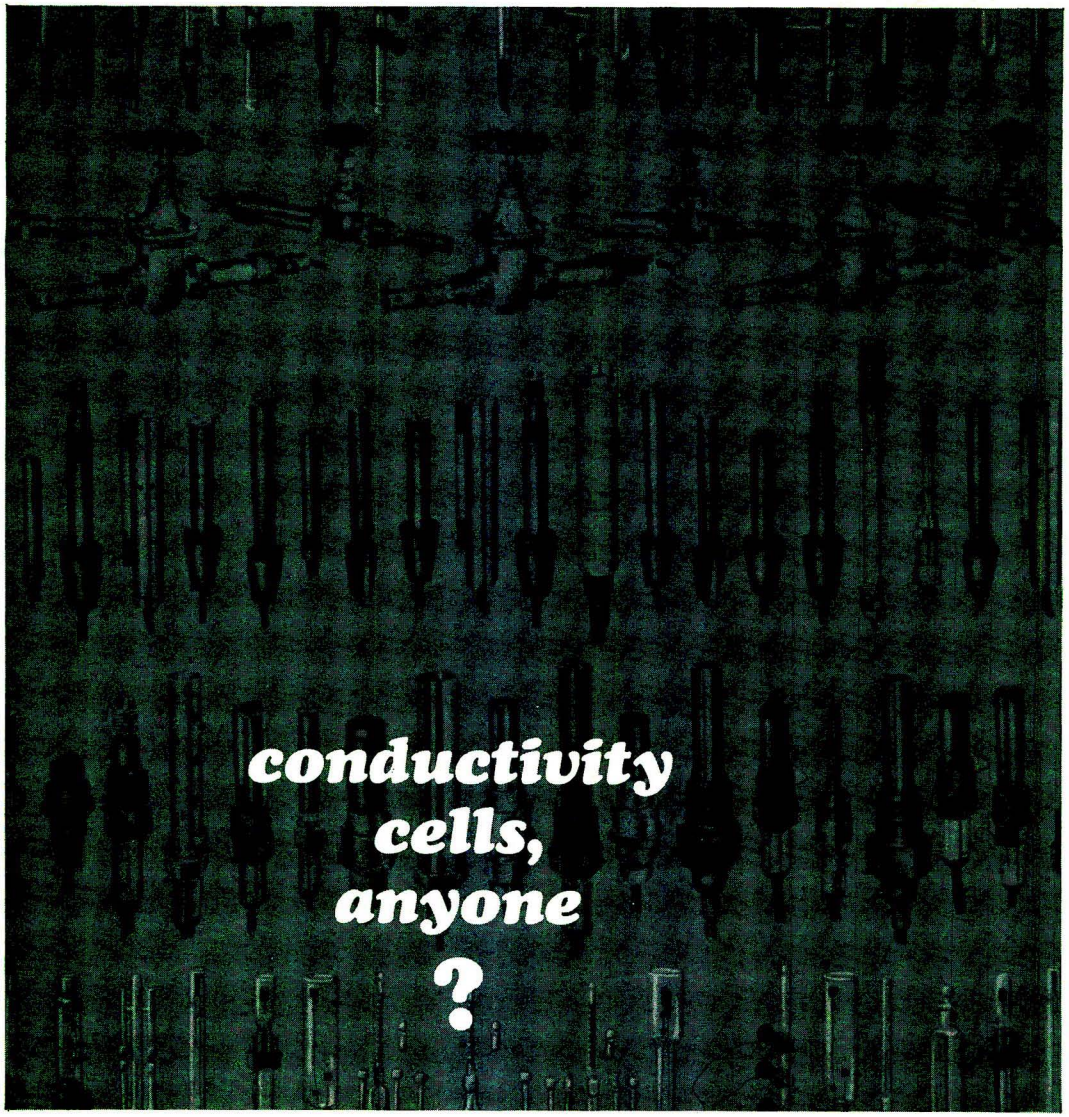
Yes, I would like a copy of your illustrated booklet (Bulletin P-5) about all five Sargent Polarographs.® Please send me my booklet.

Name_____
Title_____
Firm_____
Address_____
City_____ State_____ Zip_____

SARGENT® SCIENTIFIC LABORATORY INSTRUMENTS • APPARATUS • CHEMICALS

E. H. SARGENT & CO.
4647 West Foster Avenue
Chicago, Illinois 60630

Chicago • Anaheim, Calif. • Birmingham • Cincinnati • Dallas
Denver • Detroit • Springfield, N.J. • Toronto, Canada



Name the requirement—Dip cells for occasional testing?... Pipette cells for small volumes?... Flow cells for continuous monitoring?... Laboratory types for precise measurements?... Electrodeless cells for sulphuric acid or perhaps molten ammonium nitrate?... Why not turn to the one supplier who can offer over two decades of experience in the design and manufacture of conductivity cells covering a myriad of applications.

Choose among cell designs offering a wide range of body materials to cope with temperature, pressure and chemical resistance problems. Select electrodes matched to your needs. Decide upon the optimum range and cell constant whether your application is the measurement of ultrapure water or concentrated solutions of highly corrosive acids, alkalis and salts.

Put our years of experience to work for you. Send for our catalog today. It will prove to be a valuable reference each time conductivity is your special problem.

Beckman INSTRUMENTS, INC.

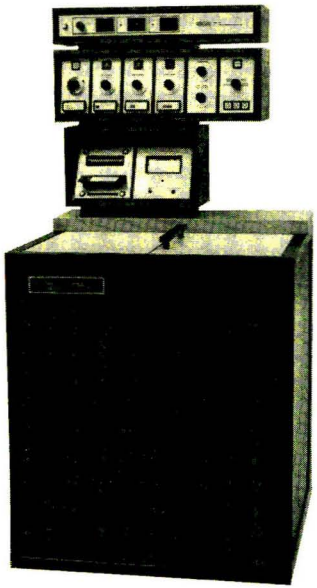
CEDAR GROVE OPERATIONS
89 Commerce Road
Cedar Grove, New Jersey 07009

Formerly Industrial Instruments; Inc.

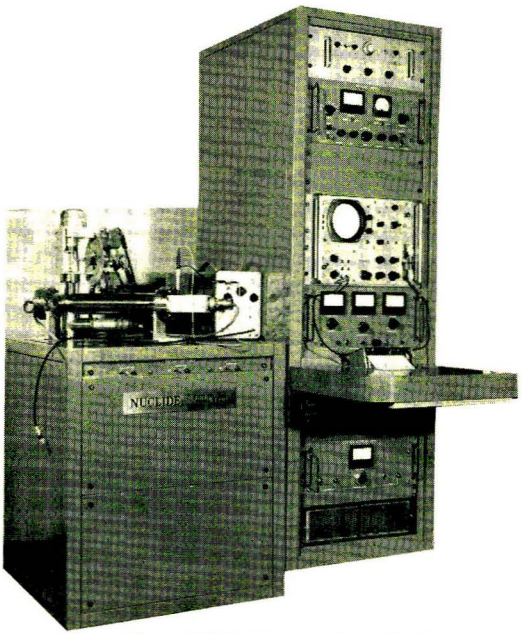
See Buyers' Guide for all products/sales offices.
Circle No. 29 on Readers' Service Card

←— Circle No. 84 on Readers' Service Card

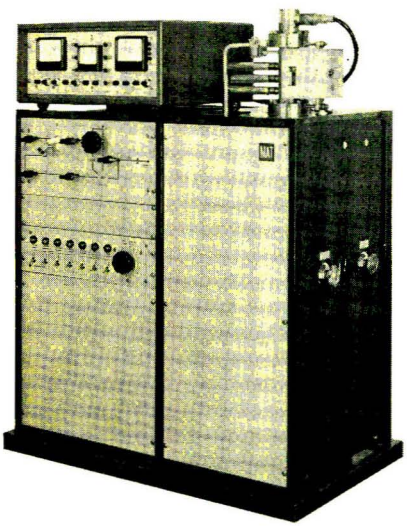
NEW PRODUCTS



Liquid scintillation spectrometers are designed primarily for counting soft-beta emitting isotopes. The CPM-100 provides readout in counts-per-minute and the DPM-100 offers disintegrations-per-minute and quench-corrected d.p.m., in addition to c.p.m. capability. Both 100-sample, ambient temperature systems are capable of automatic or manual counting in three separate channels, full electronic computation, and automatic external standardization. Beckman Scientific and Process Instruments Division, 2500 Harbor Blvd., Fullerton, Calif. **401**



Time-of-flight mass spectrometer is a general-purpose fast-scan gas analyzer capable of giving gas composition data at pressures down to 10^{-9} torr and up to 10^{-3} torr. There is no magnetic field, either in the ion source or the collector, or as a pump. Because of its noncritical alignment, the instrument can be mounted in any position. The TOF is bakeable to above 400° C., and can be furnished with a nude ion source for direct attachment to a vacuum system with the source inside; or the entire analyzer, source and collector can be furnished in a configuration suitable for mounting directly within a large vacuum chamber. Nuclide Corp., 642 E. College Ave., State College, Pa. 16801. **402**

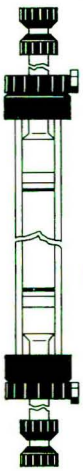


Mass spectrometer can analyze solids as well as any type of gas with sample sizes as small as 1×10^{-5} cc. The new low-cost spectrometer is Model GD 150 made by Atlas-MAT of West Germany. The four-collector analyzer permits simultaneous measurements of almost any four peaks because each collector can be moved mechanically during operation. The instrument's resolution is 120 (10% valley) over a mass range of 2 to 300. The GD 150 can measure total pressure and record mass spectra simultaneously. Applied Physics Corp., 2724 S. Peck Rd., Monrovia, Calif. **403**

NEW from PHARMACIA

SEPHADEX® LH-20

extends gel filtration to organic solvents



Pharmacia Fine Chemicals now introduces the *first* lipophilic derivative—Sephadex LH-20—to extend the use of Sephadex to organic solvents. Since it swells in water, polar organic solvents and in mixtures of these solvents, Sephadex LH-20 makes it possible to apply the conventional Sephadex gel filtration technique in fields such as lipid chemistry, polymer chemistry and other areas of organic chemistry and biochemistry where organic solvents must be used.

Sephadex Solvent-Resistant Column

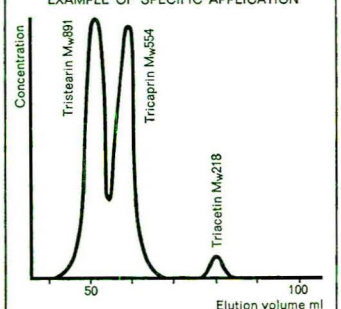
Having internal diameter 2.5 cm and 45 cm length, the new Sephadex Column SR 25/45 has been especially developed for chromatography in organic solvents. It is equipped with two specifically designed Upward-Flow Adaptors for conducting either ascending or descending chromatography as one of its many features.

RANGE OF APPLICATION

Solvent	Approx. solvent regain ml solvent/g dry gel	Approx. bed volume ml/g dry gel
Dimethylformamide	2.2	4
Water	2.1	4
Methanol	1.9	3.5-4.0
Ethanol	1.8	3.0-3.5
Chloroform*	1.8	3.0-3.5
n-butanol	1.6	3
Dioxane	1.4	2.5-3.0
Tetrahydrofuran	1.4	2.5-3.0
Acetone	0.8	1.5

*Containing 1% ethanol. Particle size: 25-100 μ

EXAMPLE OF SPECIFIC APPLICATION



Separation of glycerol esters in chloroform. Bed dimensions: 2.5x32 cm. Sample: 2 ml containing 4 mg of each substance. Flow rate: 0.6 ml/min.

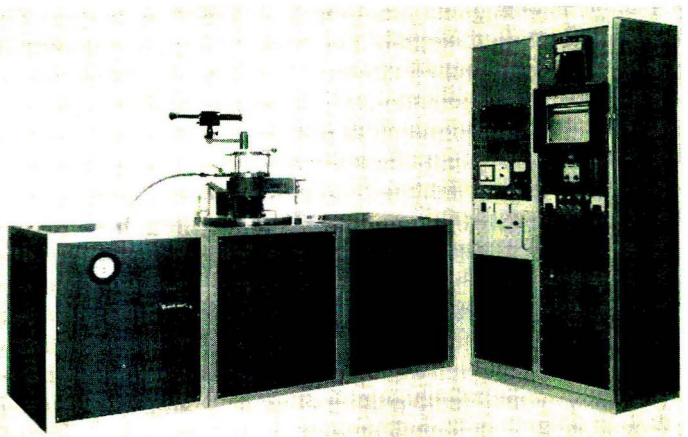
For additional technical information, including the booklets *Sephadex LH-20* and *The Sephadex Solvent-Resistant Column*, write to:

PHARMACIA FINE CHEMICALS INC.
800 Centennial Avenue
Piscataway, New Jersey 08854

Pharmacia (Canada) Ltd., 110 Place Crémazie, Suite 412, Montreal 11, P. Q.

(Inquiries outside U.S.A. and Canada should be directed to PHARMACIA FINE CHEMICALS, Uppsala, Sweden.)

Circle No. 180 on Readers' Service Card



Radial outward heat flow instrument measures the thermal conductivity of solid samples of a wide variety of high temperature materials. The TCRG-R 35(50)-E consists of a high temperature tantalum, cold-wall vacuum furnace into which a cylindrical thermal conductivity stack is inserted. Temperature range is from 1500° to 3500° F. with capability of expansion to 5000° F. by replacing tantalum elements with tungsten. Measurements are made by adjusting power to the furnace and core heater to provide the desired heat flux and temperatures. The conductivity value is calculated from the heat flux, temperature distribution, and geometry of the specimen. Dynatech Corp., 17 Tudor St., Cambridge, Mass. **404**



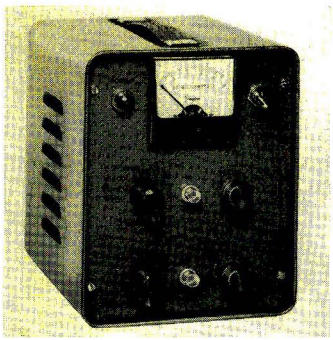
Gas chromatograph designed for routine clinical analyses is a self-contained bench-top unit. The minimum controls of the Model 400 provide all the functions for repetitive analysis of estrogens, 17 keto steroids, blood alcohols, pesticides, and other high molecular weight compounds. A combination oven houses both coiled glass column and plug-in detector. Argon ionization, hydrogen flame, and electron capture detectors can be easily interchanged. A reverse flow heat exchanger eliminates fans and blowers. A self-contained solid state temperature controller offers gradient-free isothermal operation. Fischer & Porter Co., 731 Jacksonville Rd., Warminster, Pa. **405**

Stainless-Steel TLC Plates

Chromaflex plates are a new series of support plates for thin layer chromatography. The plates are made of 0.005-inch-thick stainless steel and are available in several sizes. They are unaffected by most acids, bases, and solvents, permit the use of any detection agent, and can be easily cleaned in strong acid or caustic solutions. The Chromaflex plates are readily adaptable for direct quantitative reading of fluorescent spots and for cryogenic detection techniques. Penn-Chem Corp., 328 N. Marshall St., Lancaster, Pa. 17604. **406**

Mass Spectrometer

The 6-60 G3 has a resolution of 1 part in 1500 and can detect 10^{-7} gram with a mass range of approximately 2000 a.m.u. This modular mass spectrometer was designed for the study of gas chromatograph effluents and the analysis of complex compounds. It can also be converted to other uses such as ion-reaction studies, appearance potential, field ionization, and kinetic reaction studies. The modular design and open construction are for convenient expansion to meet special requirements. Nuclide Corp., 642 E. College Ave., State College, Pa. 16801. **407**



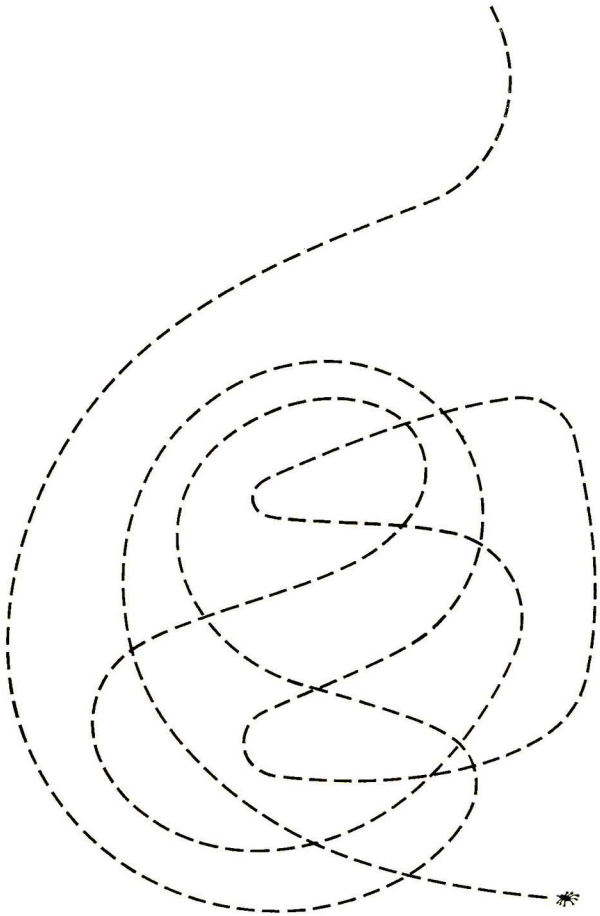
Portable electrometer detects and measures ion currents in the 10^{-5}- to 10^{-11}-ampere region. The output voltage rises to 90% of its final value 0.2 second after a step input current signal in the 10^{-10}-ampere range is applied. The unit has a built-in range changer that permits switching between six separate ranges. The electrometer's maximum overall error is 4%. Both battery operated and line operated versions of the Model EA-7 are available. The unit measures 6 × 8 × 8 inches and weighs less than 6 pounds. Nuclide Corp., 642 E. College Ave., State College, Pa. 16801. **408**

Liquid Scintillation Systems

Three new liquid scintillation counting system models are available. Two of these systems are controlled-temperature models with a new high-performance beta analyzer. Model 6766 includes a data lister and Model 6763 has a lister/calculator. The third system is a low-cost manual system, Model 4534, which includes a three channel beta analyzer and a single scaler/timer. Nuclear-Chicago Corp., 359 E. Howard Ave., Des Plaines, Ill. 60018. **409**

Electrolytic Cells

Electrolytic cells for electro-preparation of isotope samples in routine analysis and bio-assay are of two-piece construction. They can be used singly or connected in series or parallel. The cells are fabricated of transparent acrylic plastic, permitting visual positioning of the anode, and a stainless-steel planchet mount attached to an acrylic base. Electrical d.c. negative contact is made via any of the three stainless-steel binding posts which also fasten the cell chamber over the planchet to the base. Cells are available in any volume capacity and/or planchet diameter. General Nuclear Corp., 550 Fifth Ave., New York 36, N. Y. **410**



THERE'S NOTHING IN FISHER PESTICIDE SOLVENTS FOR PESTICIDE RESIDUES TO HIDE BEHIND Any of you Analytical Residue Chemists can rest assured that Fisher Pesticide Grade Solvents are so low in chlorine, phosphorus, sulfur, etc., that there is nothing in them to "bug" your pesticide residue analyses. Each lot of Fisher's Pesticide Solvents is tested by gas chromatography on *two* different columns. It passes only if there are *no* interfering GLC peaks greater than that given by 10 nanograms of heptachlor epoxide per liter of solvent. We take extra care to preserve this purity, too. During packaging, each bottle is purged with the pure solvent itself and nitrogen. And a special liner is used in the cap to prevent contamination from the cap material. There are now seven Fisher Pesticide Grade Solvents supplied in gallon bottles, all economically priced. Your Fisher branch can deliver 'em quick; or we'll send you our data sheet. **Just write** Fisher Scientific Company, 100 Fisher Building, Pittsburgh, Pa. 15219. J-527

FISHER SCIENTIFIC CO.

Instruments, Apparatus, Furniture and Chemicals for Laboratories

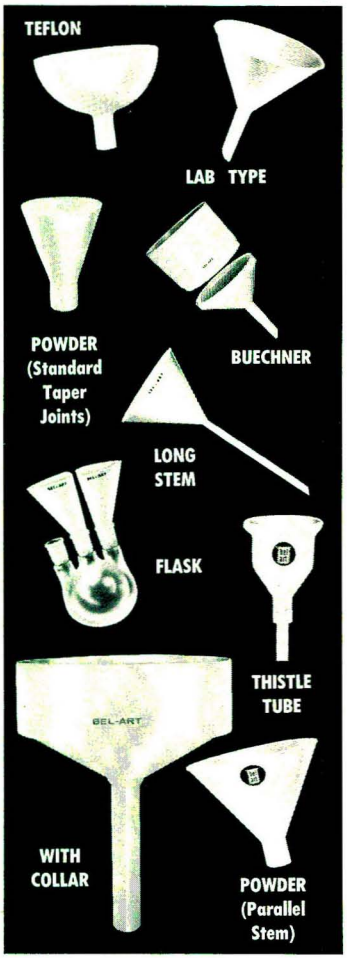
Complete stocks in all these locations: Atlanta • Boston • Chicago • Cleveland • Houston • New York Philadelphia • Pittsburgh • St. Louis • Union, N. J. • Washington • Edmonton • Montreal • Toronto • Vancouver

See Buyers' Guide for all products/sales offices.
Circle No. 41 on Readers' Service Card

BEL-ART

funnels

POLYETHYLENE
TEFLON*
POLYPROPYLENE
VINYL



*Teflon, ®Du Pont Co.

All types of plastic funnels.
A funnel for every purpose.

Available at your laboratory supply house.

Listed in NEW 1966 64-page catalog
For your FREE copy write Dept. A-6

BEL-ART PRODUCTS
PEQUANNOCK, N. J. 07440

Circle No. 32 on Readers' Service Card

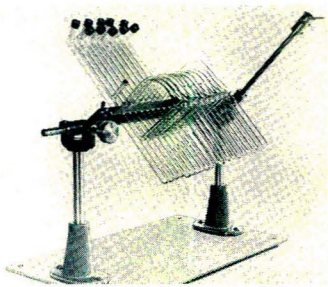
NEW PRODUCTS

Operational Amplifier

Model 300 is an electrometer operational amplifier offering: 10^{14}-ohms input resistance, 5×10^{-14}-amp. current offset, 10^{-15}-amp./24 hours current drift, and 11-volts, 11-ma. output. The new amplifier uses solid-state components except for electrometer input tubes. Input and feedback elements can be mounted within the amplifier case for complete shielding. Model 300 will operate from inexpensive power supplies or from batteries. Keithley Instruments, 12415 Euclid Ave., Cleveland 6, Ohio. **411**

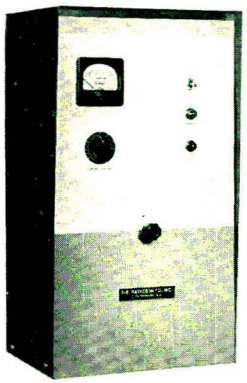
Analytical Data Processing

The CRS-50 is an analytical computation center adaptable to existing CRS systems—digital integrators, peak height digitizers, and magnetic tape systems. Data can be fed into the CRS-50 either from punched paper tapes or from M-100 electronic memory units. The computation center performs recognition of signal peaks, calculation of peak area or measurement of peak heights, measurement of peak retention times, baseline correction, function conversion, application of correction factors, and normalization to obtain percentage composition and presents a printed page tabulation of the results. Infotronics Corp., 7800 Westglen Dr., Houston, Texas 77042. **412**



Countercurrent distribution extractor, designed for separation of closely similar substances, has 10 cells mounted on an aluminum and steel rack. The cells are easily rotated and may be locked in position. Capacity of each cell is 10 ml. lower phase and 10–15 ml. upper phase. Similar units are available with 5, 10, 15, or 20 cells. Up to 40 cells can be accommodated in units of 5 cells. Pope Scientific, Inc., 13600 W. Reichert Ave., Menomonee Falls, Wis. 53052. **413**

Do-it Yourself Hydrogen



Matheson Ultra High Purity Hydrogen Generator

IMPURITIES: less than 10:1,000,000,000

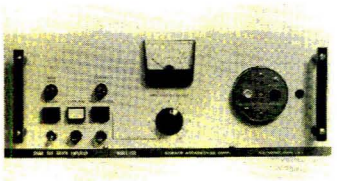
COST: 2¢ per 100 liters

Produce your own dry hydrogen, free of contamination, and of purity suitable for gas chromotography and semiconductor work. The Matheson UHP Hydrogen Generator is essentially self-regulating and operates on a new principle. Uses only water and electrical energy. Assures continuous hydrogen at pressures to 60 p.s.i.g. Rated capacity: 150 milliliters per minute (0.31 scfh.). Easy to install and operate. Needs no maintenance. Generator consists of electrolytic cell, rectifier, regulating valves and switches. Electrolytic cell anode is nickel; cathode is bundle of palladium-alloy tubes. Electrolyte is strong alkali. During electrolysis, oxygen collects at anode and is vented to atmosphere. Ionic hydrogen is deposited at cathode. Ions drawn by electrolytic solution pressure penetrate tubes and recombine to form molecular hydrogen under pressure. Price: $484.00 Write for complete data.

MATHESON

P.O. Box 85, East Rutherford, New Jersey
Plants in East Rutherford, N. J.; Joliet, Ill.; La Porte, Texas; Morrow, Ga.; Newark, Calif. Matheson of Canada, Whitby, Ont.

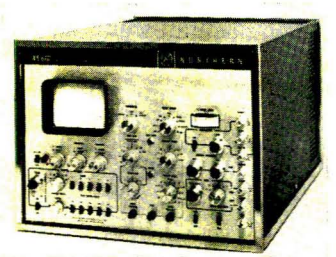
Circle No. 142 on Readers' Service Card



Spark chamber pulser system accepts ±250-mv. pulses from any commercial logic module and delivers up to five simultaneous pulses with amplitudes of 2 to 20 kv. and a delay of approximately 30 nsec. Model 022 is designed for driving spark chambers or several Model 011 fanouts. The spark gap is in an enclosure supplied with gas fittings to provide an inert atmosphere for safety purposes. The system may be pressurized to shorten both the delay and rise times. Science Accessories Corp., Southport, Conn. **414**

High Voltage Electrophoresis System

The Camag high voltage electrophoresis system gives rapid separations (20 minutes for most metabolic screening runs). The cooling system, using tap water, eliminates heat buildup without eluting specimens by buffer evaporation. The high resolution permits separations of inorganic ions and other low molecular weight substances. The high voltage eliminates specimen desalting. Gelman Instrument Co., P. O. Box 1448, Ann Arbor, Mich. 48106. **415**



Pulse height analyzer with digital stabilizer utilizes silicone semiconductors throughout plus integrated circuitry. The basic unit is a complete system primarily designed for signal amplitude distribution and also has the versatility of Mossbauer studies, multichannel scaling, with the flexibility of single channel analysis. The NS-610, 1024 channel pulse height analyzer offers a 16-Mc. analog digital conversion rate. Northern Scientific Inc., 303 Price Pl., Madison, Wis. 53711. **416**

Completely New Concept Offers:

ADDED SPEED • CONVENIENCE • ACCURACY



This combination drying unit and magnetically damped precision balance provides optimum functional ease. You'll enjoy full range, continuous read-out without manual rebalancing on the illuminated, centrally located, optical projection screen. The new "Swing-a-Way" infra-red heater swings completely clear of the sample bearing pan liner. Conveniently located heater and timer controls provide infinitely variable heat intensities. Case is of stainless steel.

MODEL 6010
Sample weight 10 gram.
Sensitivity .01 gram-0.1% **$375.00**

MOISTURE DETERMINATION BALANCE

110

The heart of this new Moisture Determination Balance is a magnetically damped box end beam with precision ground steel knives floating on self-aligning polished agate bearings designed to provide a simple, fast and fool-proof method for determination of moisture content of liquid or solid samples.

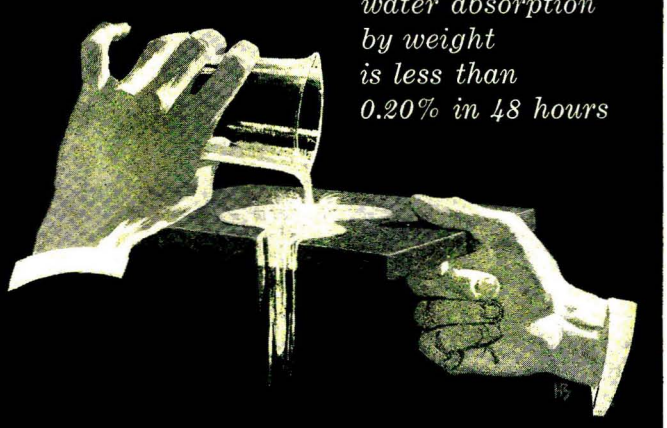
TO YOU *KNIFE EDGES MEAN: HIGHER ACCURACY, LOWER COST, LONGER BALANCE LIFE

OHAUS

OHAUS SCALE CORPORATION
1050 COMMERCE AVENUE • UNION, NEW JERSEY
dept. FA
Circle No. 12 on Readers' Service Card

Low absorbency protection

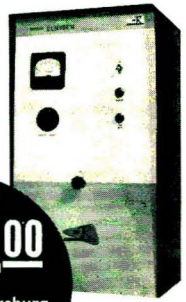
water absorption by weight is less than 0.20% in 48 hours



ALBERENE STONE for 75 years the only permanently satisfactory material for chemical laboratory table tops, shelving, sinks, splash backs, drain boards and fume hoods. Prompt delivery. ALBERENE STONE – A DIVISION OF THE GEORGIA MARBLE COMPANY. For FREE literature and technical assistance address: THE ALBERMAR COMPANY, 386 PARK AVE. SOUTH, NEW YORK 16, N. Y., DEPT. C.

Circle No. 1 on Readers' Service Card

INSTANT H_2 FROM H_2O in your lab, as you need it!



ONLY
$484.00
F.O.B. St. Petersburg
Lowest cost for highest purity H_2 you can buy!

- 99.999999% pure
- Bone dry
- No hazards of stored H_2
- 150 ml/min S.T.P.—Pressures to 60 psig
- Order direct with our guarantee

Just pour water into the Elhygen Electrolytic Hydrogen Generator and turn it on. Get a supply of ultra-pure H_2 at 60 psig, continuously and automatically. One liter of water produces nearly 1000 liters of H_2 . . . enough for 100 hours of continuous operation per liter. Ideal for chromatographs using hydrogen as a carrier gas, and other lab uses. Operating cost: less than 2¢/100 liters! Compare with cost of cylinders of standard purity! Model shown produces up to 150 ml/min. Compact. Only 12¼″ x 23″ x 13½″. Easily installed! Send check or purchase order. Backed by our national reputation in the field, you must be satisfied or money refunded.

HOW IT WORKS

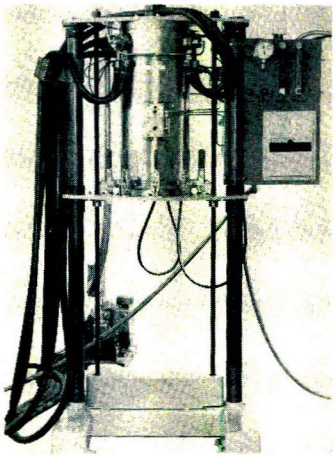
The Elhygen Hydrogen Generator produces H_2 by dissociating water and diffusing H_2 through a palladium membrane which acts as the cathode. Just add water periodically. Normally no other maintenance required. Extra safe! Made by leading manufacturer of industrial hydrogen separators.

Write for Bulletin No. 330

MILTON ROY COMPANY
TECHNOLOGY IN FLUIDS
P. O. BOX 12169
ST. PETERSBURG, FLORIDA

Circle No. 146 on Readers' Service Card

NEW PRODUCTS



Ultra-high temperature hydrogen-atmosphere furnace is a graphite furnace designed for processing at up to 2500° C. with inert gas, hydrogen, or moderate vacuum environments. An automatic safety purge system consisting of pressure relief, burst diaphragm, vacuum pump, pilot burner, and solenoid-operated valves is incorporated for hydrogen operation. Model 70-100 pilot process furnace has a cylindrical hot zone 7 inches in diameter and 12 inches long. Astro Industries, Inc., 606 N. Olive St., Santa Barbara, Calif. 93101. **417**

Residual Gas Analyzer

Type 21-615 is essentially a mass spectrometer without a vacuum system. The instrument is composed of a mass analyzer, magnet, and control unit. The analyzer can scan the full mass range from 2 to 100 in a single sweep with automatic repetitive scanning of any portion of the mass range. The 21-615 features a cycloidal resolving system. Consolidated Electrodynamics Corp., 360 Sierra Madre Villa, Pasadena, Calif. **418**

Atomic Absorption/Flame Emission Spectrometer

The S2-700 spectrometer is a single instrument capable of both atomic absorption and flame emission methods. Procedure includes dialing the element of choice, switching to the desired method, aspirating the sample, and adjusting the appropriate hollow cathode setting. As many as 120 analyses can be handled per hour. Required sample size is less than 1 ml. Jarrell-Ash Co., 590 Lincoln St., Waltham, Mass. 02154. **419**

If the heating system you want hasn't been built yet... build it!

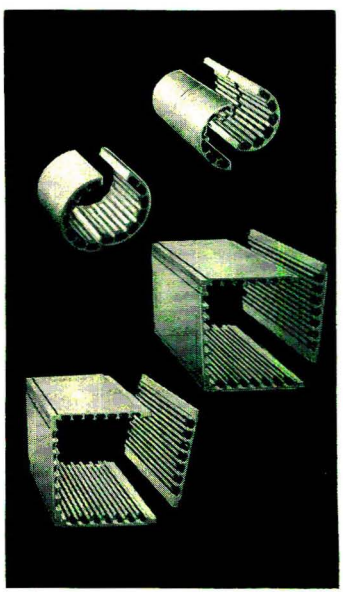
It's simple—with Lindberg Hevi-Duty building blocks of heat. These flexible, low-cost elements can be assembled in countless ways.

They're perfect to heat piping systems where liquids must be kept at constant temperature. Or for special lab requirements that don't justify a furnace. Or where there isn't a furnace to do the job.

They have excellent capacity. High watt density. 1000° or 1200° C. Control them manually, or automatically.

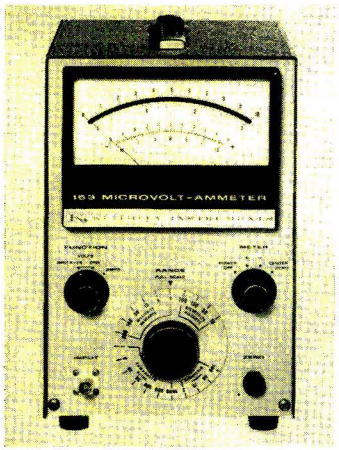
They're available from leading lab dealers in sizes, shapes, and lengths to fit your projects.

Write for bulletin 50910, Lindberg Hevi-Duty, Watertown, Wis. 53094.

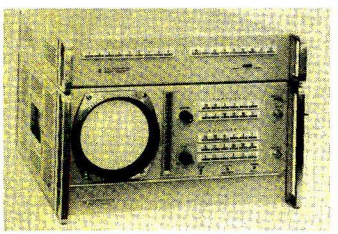


LINDBERG HEVI-DUTY SB
DIVISION OF SOLA BASIC INDUSTRIES

Circle No. 105 on Readers' Service Card



Low-cost, d.c. microvolt-ammeter measures from 5 μv. to 1000 volts and from 5 picoamp. to 0.1 amp. Model 153 offers 76 ranges for d.c. measurements: 17 zero-left ranges from 10 μv. full-scale to 100 volts, 17 zero-center ranges from 5 μv. to 500 volts, 21 zero-left ranges from 10^{-11} amp. to 10^{-1} amp., and 21 zero-center ranges from 5×10^{-12} amp. to 5×10^{-2} amp. The microvolt-ammeter is basically a photomodulator type microvoltmeter with a high input resistance. It is also a sensitive null detector with floating operation and high a.c. rejection. The instrument can be used as a voltmeter, amplifier, null detector, or ammeter. Keithley Instruments, 12415 Euclid Ave., Cleveland 6, Ohio.
420

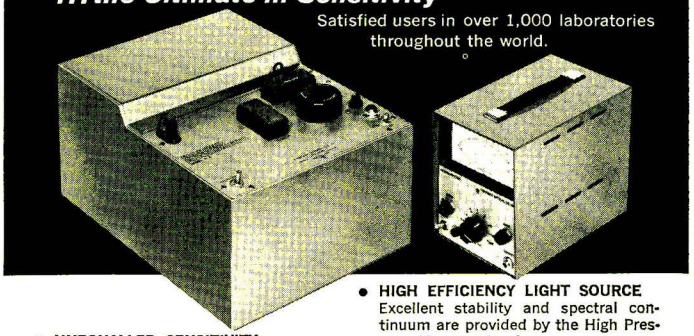


Model 155A oscilloscope is push-button controlled and free of d.c. drift. The new model is a 5-mv./cm., 25-MHz. instrument. Continual feedback corrections eliminate d.c. drift. With the optional companion programmer, Model 1550A, all major functions can be readily programmed. Programmers may be cascaded to extend the number of available programs. Hewlett-Packard, 1501 Page Mill Rd., Palo Alto, Calif. 94304.
421

Farrand PHOTOELECTRIC FLUOROMETERS

...the Ultimate in Sensitivity

Satisfied users in over 1,000 laboratories throughout the world.



- **UNEQUALLED SENSITIVITY** Routinely performs measurements of Riboflavin .0001 μg/ml, Quinine Sulfate .0001 μg/ml, Catecholamines .0002 μg/ml . . . with the sensitivity of the instrument not the limiting factor.
- **ALL QUARTZ OPTICAL SYSTEM** Features collimated light at both filter positions, essential for narrow band Interference Filters.
- **HIGH EFFICIENCY LIGHT SOURCE** Excellent stability and spectral continuum are provided by the High Pressure Mercury Arc Lamp.
- **SUPERIOR PERFORMANCE** Accurate, repeatable, linear measurements over a wide dynamic range. Recording capability.
- **ACCESSORIES** Tungsten Source, Continuous Flow Cell, Temperature Control Chamber, Surface Fluorescence Adapter for turbid solutions, Micro and Ultra Micro Cells.

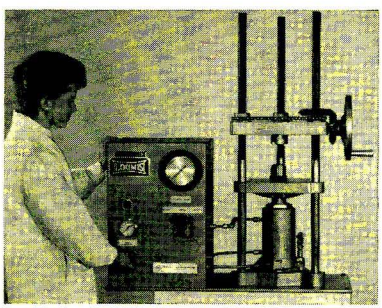
Write for descriptive literature

Farrand OPTICAL CO., INC. | 538-A So. 5th Avenue, Mount Vernon, New York 10550, 914-668-9393 / Cable Address: FOCIUS NY

The Pioneers in Fluorometry

Circle No. 40 on Readers' Service Card

the versatile LOOMIS laboratory press



Loomis 20 ton press with compact power unit. 30 and 50 ton models also available.

- Designed and engineered for multiple laboratory use.
- Forms KBr pellets and X-ray pellets.
- Plastic molding and forming operation.
- Adapts to extrusion and isostatic pressing.
- Quick changeover with handwheel for accurate change of opening.
- Sturdy design and construction protects expensive dies. Does all kinds of testing.

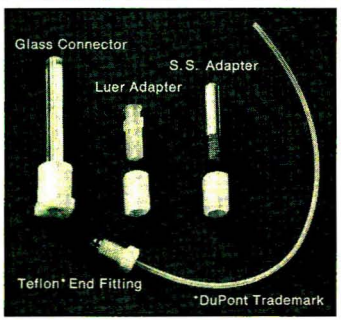
Call or write:

MIDVALE-HEPPENSTALL
PRESSURE EQUIPMENT DIVISION
Nicetown, Philadelphia, Pa. 19140 Area Code 215 225-5000
Subsidiary of HEPPENSTALL COMPANY, Pittsburgh, Pa.

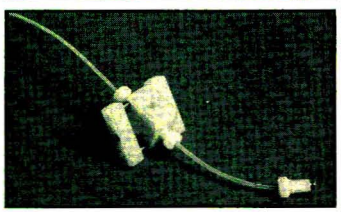
Circle No. 174 on Readers' Service Card

TIRED OF BEING A
PLUMBER?
GET INSTANT RELIEF WITH "CHEMINERT" FITTINGS AND VALVES

designed specifically for liquid chromatography and chemical analysis systems



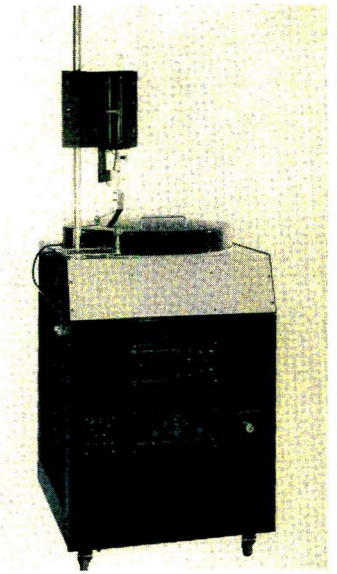
Chemically inert
Zero dead volume
500 psi pressure rating
For 1/16" Teflon* tubing



"Cheminert" valves eliminate the problem of dead volume or mixing cavities in flow shut-off and flow switching. Available in 2-way, 3-way and 4-way designs. Write for literature.

CHROMATRONIX
INCORPORATED
2743 8th St., Berkeley, Calif. 94710
Phone: (415) 841-7221

Circle No. 34 on Readers' Service Card



Refrigerated fraction collector uses an air, in place of a liquid, circulating system and a dual heat exchanger to maintain a temperature within ±2° C. The main fraction collection system of the Series 1000 is mounted on top of the refrigeration compartment and may be used independently from the refrigeration compartment. Both compartments are insulated with 1-inch-thick styrofoam. One heat exchanger cools the main chassis of the collector by blowing prechilled air through it. A second heat exchanger cools glycol solution which circulates through a chromatographic column by use of a separate pump. Chromatography Corp. of America, 60B E. Main St., Carpentersville, Ill. 60110.

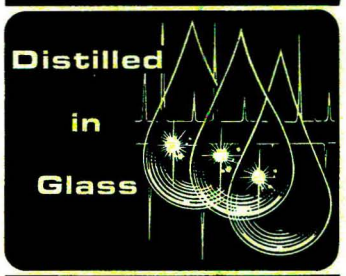
422

Calcium Activity Electrode

Model 92-20 electrode indicates directly the calcium ion activity in aqueous solutions by measuring the electrical potential across a thin membrane of liquid ion exchanger. This electrode can be used with any modern expanded scale pH meter or millivolt electrometer and a conventional saturated KCl reference electrode. It is 50 times more sensitive to calcium than to magnesium and about 1000 times more sensitive to calcium than to sodium or potassium. The electrode consists of a fluorocarbon plastic body with a replaceable membrane containing the ion exchanger. Temperature range is 1° to 50° C. Orion Research Inc., 11 Blackstone St., Cambridge, Mass.

423

THE SYMBOL OF EXCELLENCE SINCE 1959



SOLVENTS FROM BURDICK & JACKSON

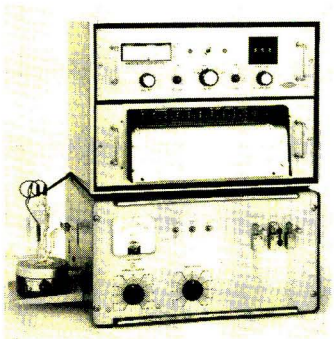
Purified to the exacting requirements of electron-capture gas chromatography. The list now numbers 30, and is still growing:

Acetone
Acetonitrile
Benzene
Butanol-1
Butanol-2
Butyl Ether
Carbon Tetrachloride
Chloroform
Cyclohexane
Dimethyl Formamide
Dimethyl Sulfoxide
Dioxane
Ethyl Acetate
Ethyl Ether
"Heptane", 95-99°
Hexane, 68-69°
Isobutyl Alcohol
Iso-hexanes, 59-63°
Methanol
2-Methoxyethanol
Methylene Chloride
Methyl Ethyl Ketone
N-Methylpyrrolidone
Neo-hexane, 49-50°
Pentane
Petroleum Ether, 30-60°
Propanol-2
Tetrahydrofuran
Toluene
2, 2, 4-Trimethylpentane (Iso-octane), 99-100°

Ask for Bulletin BJ-13j
U.S. Agencies use F.S.S.

BURDICK & JACKSON LABORATORIES, INC. 636 PA 2-2310
MUSKEGON, MICHIGAN 49442

Circle No. 28 on Readers' Service Card



Recording nitrogen analyzer is a system composed of the company's microcoulometric titrating system, a new T-400-H titration cell, and a new gas chromatography recorder. The analyzer has a lower detection limit of 1 ng. and is capable of p.p.m. nitrogen analysis. The instrument is a completely self-contained analyzer for total nitrogen assays, or can be used as a specific nitrogen detector with a gas chromatograph, or as a halogen–nitrogen screening device. Dohrmann Instruments Co., 990 Varian St., San Carlos, Calif. 94070. **424**

Air Monitoring Laboratory

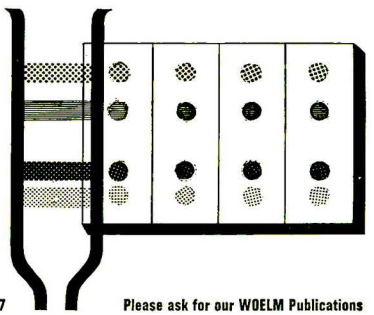
Mobile air monitoring laboratories are available either as completely equipped, motorized truck-type vans or as fully outfitted trailers which can be towed from one location to another. Both types of vehicles may be equipped with whatever type of air monitoring instrumentation is required. These laboratories may be modified to meet specific requirements. Beckman Scientific and Process Instruments Division, 2500 Harbor Blvd., Fullerton, Calif. 92634. **425**

Strip-Chart Recorder

A specially adapted 10-inch strip recorder for use with gas chromatographs is available from the modular design Series 7100B. This recorder is available as a single-pen (Model 7127A) or a dual-pen (Model 7128A) unit with several options. These models have a full-scale sensitivity of 1 mv., a 0.75-second pen response, noise and line frequency interference filter, full-scale zero suppression, instant selection of the four chart speeds, and a pressure-primed, cartridge inking system. Options include integrators, remote controlled event markers, high-low limit switches, electric pen lift, and 50-cycle operation. F & M Scientific Corp., Route 41 and Starr Rd., Avondale, Pa. 19311. **426**

WOELM

Adsorbents for Column and Thin-Layer Chromatography and for purification of organic solvents



M. Woelm, Eschwege

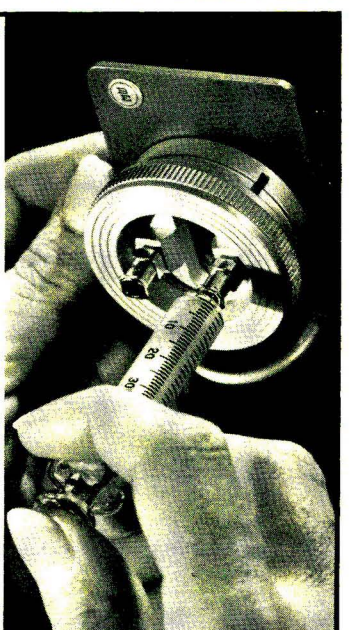
Sole Distributor:
Alupharm Chemicals
P. O. Box 30628
New Orleans, La.
Phone Jackson 5 - 3477

Please ask for our WOELM Publications

Circle No. 22 on Readers' Service Card

PRECISION

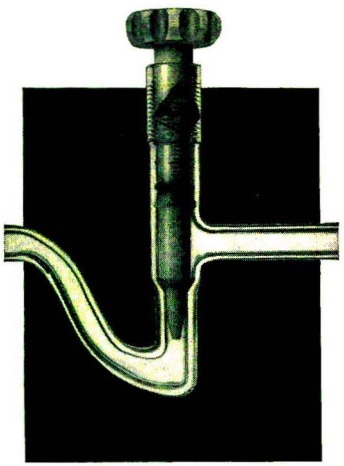
This series of infrared liquid cells gives you $50 worth of pathlength precision in a $30 cell (salt). From 0.015mm to 1.0mm. Volumes from 0.09cc to 3.0cc. Easy to fill. Easy to clean. Comes in all standard window materials. One holder fits any of the 49 cells comprising this series. Good for all Beckman and Perkin-Elmer spectrophotometers. Catalog BA-5 gives complete details.



BARNES ENGINEERING COMPANY
INSTRUMENT DIVISION/30 Commerce Rd./Stamford, Conn./Telephone 203 348-5381

Circle No. 141 on Readers' Service Card

Fine Control and Freedom from Leaks with Patented Lab-Crest Needle Valves



Precision Threaded Glass and Du Pont Teflon allow flow settings to be accurately reproduced.

Double-Sealed Stem won't leak at any pressure from 10^{-6} mm Hg to 500 psi. Machined Teflon stem is primary seal; O-ring adds back-up protection.

Inert Materials resist chemical attack. Body is glass; valve is Teflon. No metal is used.

The Lab-Crest Valve is also available in a one-turn model for rapid opening and closing. Same leak-proof features. Both models in straight-through or angle-valve designs. For full details and prices, write:

FISCHER & PORTER COMPANY

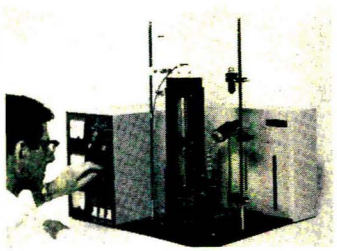
Lab-Crest® **SCIENTIFIC DIVISION**

1566 County Line Road
Warminster, Pa. Phone 215-675-6000

Laboratory and Scientific Glassware • Special Glass Fabrication • Glass Process Pipe and Drainline

Circle No. 126 on Readers' Service Card

NEW PRODUCTS



Continuous particle electrophoresis system, in less than 30 seconds, will separate particles in such diverse samples as plant and animal cells, mixed inorganic particles, intracellular particles, bacteria, soils, and blood. A fast-flowing electrolyte, descending in a "curtain" between two clear plastic plates in the electrophoresis cell, allows fractionation of mixtures containing relatively heavy, fast-settling particles. Capabilities of the instrument include fractionation, characterization, isolation, and retrieval of different particles within the sample mixture. Results can be studied visually, photographed, or recorded by adapting the unit for photoelectric scanning. Beckman Scientific and Process Instruments Division, 2500 Harbor Blvd., Fullerton, Calif. **427**

Heated Tubing

Heated tubing which may be bent or twisted into almost any configuration maintains temperatures as high as 250° C. Its primary use is for connecting the exhaust of a gas chromatograph to an infrared spectrophotometer. It may also be used with mass spectrophotometer–gas chromatograph systems and can be used to transfer liquids as well as gases. Wilks Scientific Corp., 140 Water St., South Norwalk, Conn. **428**

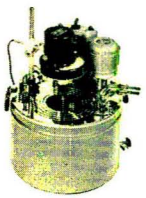
Infrared Source

Model 10 feedback-controlled infrared radiation source gives a constant infrared radiation output independent of line voltage changes, ambient temperature variations, and changes in the physical characteristics of the radiating element. The replaceable silicon carbide (Globar) radiating element is mounted in a water-cooled housing which may be remotely located from the control chassis. Warmup time is 15 minutes. Radiation will stay within 0.1% of the initial setting for a minimum of 200 hours. Controls can be set to obtain temperatures between 1000° and 1225° C. The Warner & Swasey Co., 32-16 Downing St., Flushing, N. Y. 11354. **429**

BROOKFIELD VISCOMETER ACCESSORIES

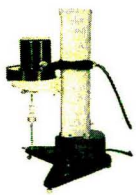
Sharpen Your Lab Capabilities, At Very Low Cost!

1. CONSTANT TEMPERATURE BATHS



Use with any Brookfield. Reservoir and circulating models. Temp. control to within ±.01°C.

2. HELIPATH STAND



Test, study, control highly-plastic materials. Automatic. Helical path through sample.

3. VISCOSITY STANDARDS



Permanently stable, Newtonian Silicone fluids. Blends from 10 to 100,000 cps. Guaranteed accurate ±1%.

PLUS . . . **4.** Ultra-Low Viscosity Adapter for measurements down to 1 cps; **5.** Lab Stands for all models; **6.** Extension Spindles to remove viscometer from high temperature or contaminated samples; **7.** Counter-Rotating Mixer, unique shear action, to 20,000 rpm; **8.** Custom design and testing in our labs.

ILLUSTRATED CATALOG TELLS ALL. WRITE FOR YOUR COPY NOW!

World's Standard For Viscosity Measurement and Control

Brookfield

ENGINEERING LABORATORIES

Stoughton 28, Massachusetts

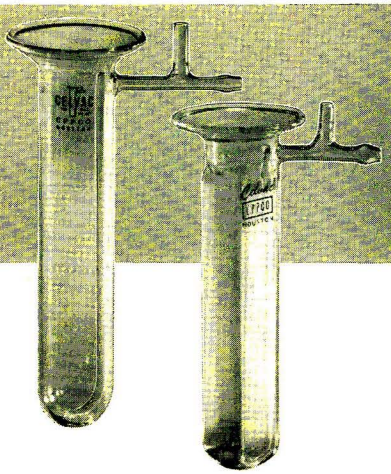
"See Us at the ASTM Materials Testing Exhibit, June 27, Booth 206, Atlantic City."

Circle No. 13 on Readers' Service Card

from CURTIN

The CELVAC CUVETTE with TVC

- evacuate completely and instantly
- increase the accuracy of readings
- minimize breakage
- save important time



The Celvac Cuvette is a unique device for eliminating cuvette problems normally encountered with spectrophotometers, photometers, colorimeters and related equipment. By connecting the Celvac Cuvette to a water filter pump (aspirator), electrically driven pump, or any practical vacuum source, you can instantly evacuate the cuvette by simply touching the vertical segment with your finger. You save time and the necessity to reposition the cuvette. You minimize handling and consequent breakage. You eliminate the need for expensive matched cuvettes required for optimum accuracy. And, you reduce the problems of smudge, smear, spilling and scratching associated with constant removal of the cuvette from the instrument.

The Celvac Cuvette is constructed of the highest quality optical borosilicate glass with a refractive index of 1.42. It is available in all standard sizes to fit most equipment models. It is furnished complete with Tygon tubing, connectors and check valve, ready to operate.

For more information, write W. H. Curtin and Company, P. O. Box 1546, Houston, Texas 77001.

W. H. CURTIN & CO.

CURTIN

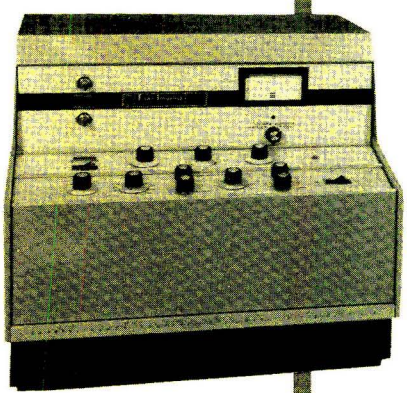
SCIENTIFIC APPARATUS AND CHEMICALS

HOUSTON • TULSA • BIRMINGHAM • NEW ORLEANS • MIAMI
DALLAS • JACKSONVILLE • ATLANTA • CORPUS CHRISTI
ALBUQUERQUE • MEMPHIS • SAN ANTONIO • MEXICO CITY

194

Circle No. 37 on Readers' Service Card

Flame Ionization Gas Chromatograph



MODEL 5320.....only $1250.00

This inexpensive chromatograph is excellent for routine analysis of chemicals, drugs, liquors, foods, paint, cosmetics or petroleum products.

FEATURES:

Simplified operation and maintenance without sacrifice of performance.

Step by step instructions reduce training time.

0.5% noise level on 3 x 10^{-12} ampere electrometer range.

Excellent limit of detection — 6 x 10^{-12} gram/second or better.

Dual Injection Ports

One or Two Flame Ionization Detectors

Manual Temperature Programming

Temperature range — Ambient to 400°C

12 Step Attenuator — 1 to 300,000

Integral Air Supply for detectors

BARBER COLMAN

BARBER-COLMAN COMPANY

Dept. F, 15104 Rock Street, Rockford, Illinois, U.S.A.

BARBER-COLMAN of CANADA, Ltd., Dept. F, Toronto & Montreal • Overseas Sales Mgrs.: Ad. Auriema, Inc., N.Y.

See Buyers' Guide for all products/sales offices.
Circle No. 64 on Readers' Service Card

Can Your Gas Suppliers Match Our Performance!

in High-Pressure Cylinders

● *calibration standards*

made to your specifications in cylinders containing from 10 to 200 cubic feet—1 to 20 trace or minor components—parts per billion to percent concentrations—"make" tolerance ±10% and analysis accuracies from ±5% to ±1% of the component value

● *carrier and zero gases*

standard to highest purity—many gases purified for special applications, including use as major components of calibration standards—pure air with total hydrocarbon content less than 0.1 ppm carbon

In Push-Button Cans

● *unique, handy, low-cost, analyzed gas mixtures*

for calibrating, evaluating or demonstrating chromatographs and many more applications—30 single and multiple trace component mixtures of hydrocarbons, CO and CO_2 in nitrogen, air and helium available from stock—nonstock mixtures available on special order—many technical advantages over high-pressure cylinders

● *c.p. grade gases*

seven individual gases available from stock

SCOTT RESEARCH LABORATORIES, Inc.

Perkasie, Penna. (215) 249-3526 — San Bernadino, California (714) 887-2571

In addition . . . testing of motor vehicle and industrial pollution control devices. Manufacturing of auto exhaust analysis and sampling systems, driver-aid for dynamometer test driving and controlled atmosphere test chambers.

Circle No. 168 on Readers' Service Card

NEW PRODUCTS

Atomic Absorption Spectrophotometer

Model EEL-140 is a self-contained atomic absorption spectrophotometer. The compact unit measures 14.5 inches in width × 11.25 inches in depth × 25 inches front to back. Concentrations are shown directly on an easily read meter. Accurate readings can be made with 0.1 ml. of sample. The burner can be rotated through a full 180°. The EEL-140 employs a Hilger-Watts quartz lens grating monochromator covering a range of 200 to 1000 mμ. Evans Electroselenium Ltd., Halstead, England. **430**

Surface Tension Measurement

Surface tension that varies dynamically with time or other factors may be continuously recorded using the new dynamic surface tension system. The system is a complete unit for surface tension measurement using the fundamental Wilhelmy technique. The #2670 dynamic surface tension accessory, an RG recording electrobalance, and any X-Y recorder comprise the unit. Readout on the recorder is in dynes/cm. with a sensitivity to 0.005 dynes/cm. *vs.* relative surface area. Cahn Instrument Co., 15505 Minnesota Ave., Paramount, Calif. **431**

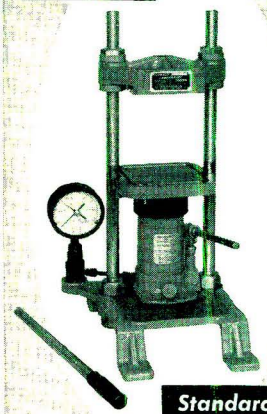
Scintillation Camera

The crystal configuration of the mosaic scintillation camera is designed to reduce the time required for typical scanning methods. The dimensions on the individual cells are held to ±0.001 inch. Features of the hermetically sealed housing for NaI (Tl) crystal are a low mass container and efficient light transfer. Various geometric arrangements can be made using multiples of the individual cell. The Harshaw Chemical Co., 1945 E. 97th St., Cleveland, Ohio. 44106. **432**

Photomultiplier Detector Accommodation

Small thermoelectric freezers for photomultiplier tubes permit their operation in sub-zero regions. Basic models for end on tubes 2.25 inches in diameter and up to 5 inches in length, and end on tubes up to 1.75 inches in diameter and 4 inches in length, and side on tubes such as the RCA 1P 21 Series have been developed. Dinode chain circuitry is provided for each individual tube either according to established specification or in accordance to customer requirements. Schoeffel Instrument Co., 15 Douglas St., Westwood, N. J. 07675. **433**

CARVER LABORATORY PRESS



Standard For Research

. . . solves the pressing problem of forming KBr Pellets

Many insoluble materials, mixed with Potassium Bromide, can be formed in a die **under pressure** into pellets or wafers for quantitative and qualitative analysis.

The CLP supplies the pressure — up to 40,000 lbs., if needed.

This specific use is only one of the ways this versatile laboratory assistant meets the challenge of research and development.

Some of the many uses are:

- Dehydrating
- Pressing out various oils, stearines and waxes
- Pressure filtering of thick fluids
- Compression tests
- Fatty acid determinations
- Plastic molding, forming and blocking
- Embossing and forcing
- Pressing mother liquors from crystals
- Extracting Vaccines and Viruses

The Standard (12-ton) CARVER LABORATORY PRESS complete with Gauge $345.00 (illustrated)

20 Ton Models also available — additional Standard Accessories for other applications can be supplied.

Send for latest bulletin.

FRED S. CARVER INC.
HYDRAULIC EQUIPMENT
54 RIVER ROAD, SUMMIT, N. J.

Circle No. 33 on Readers' Service Card

ANALYZE

AS EASILY AS 1-2-3

HERE ARE QUALITY ACCESSORIES FOR ATOMIC ABSORPTION AND FLAME-EMISSION SPECTROPHOTOMETRY . . .

1 LAMPS

- 60 elements from stock — hollow cathode
- Multi-element H. C. for faster analyses
- High-intensity lamps H. C.
- 'Osram' gas discharge lamps
- Power supplies for all above types
- Fully tested — immediate delivery

Write for Bulletin

2 BURNERS

- For AA and flame-emission
- Laminar-flow types — air-acetylene/air-hydrogen; nitrous oxide-acetylene; air-propane
- Complete burner-atomizer assemblies — readily adaptable — vertically and laterally adjustable for optical path positioning
- CK2-64 total consumption burner — for flame-emission — higher signal-to-noise ratio
- Kniseley total consumption burner — O_2 — C_2H_2 for refractory and rare earth elements
- PR-1 gas control unit for CK2-64 and Kniseley burners

Write for Bulletin

3 SYRINGE PUMPS

- A full line of constant-speed, variable-speed and uniform-flow syringe pumps. These pumps, manufactured by Sage Instruments, have a wide range of applications, including atomic absorption and flame-emission, gas chromatography, pilot plant studies, etc., wherever the analytical problem requires the delivery of fluids at a fixed and/or uniform flow rate.

Write for Bulletin

Specialists in Instruments and Accessories for Atomic Absorption and Flame-Emission Spectrophotometry

AZTEC INSTRUMENTS, INC.

2 Silverbrook Road • Westport, Connecticut 06882 • (203) — 227-1722

See Buyers' Guide for all products/sales offices.
Circle No. 181 on Readers' Service Card

THE FLOW SHEET

One of a series devoted to enriching the Art of conveying & controlling fluids

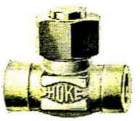
Working With GAS ANALYTICAL INSTRUMENTS?

Let Hoke Help You . . .



METER GAS SAMPLES.
This fine metering valve comes with a 1° stem, 1/16″ orifice, and a micrometer vernier handle for precise reproducibility of flow settings.

PROTECT SYSTEMS AGAINST IMPURITIES.
Sintered filtering element traps micron contaminants before they damage your costly equipment..





DELIVER A METERED AMOUNT OF GAS.
Constant flow regulator combines functions of a reducing valve, metering valve, and flowmeter in one unit. For use with any gas non-corrosive to brass and aluminum.

SELECT FLOW DIRECTION.
New Selecto-Mite, 3-way ball valve lets you select or divert 2 streams into a single line. "Dyna-Pak" Teflon packing and seats seal the valve against leakage.



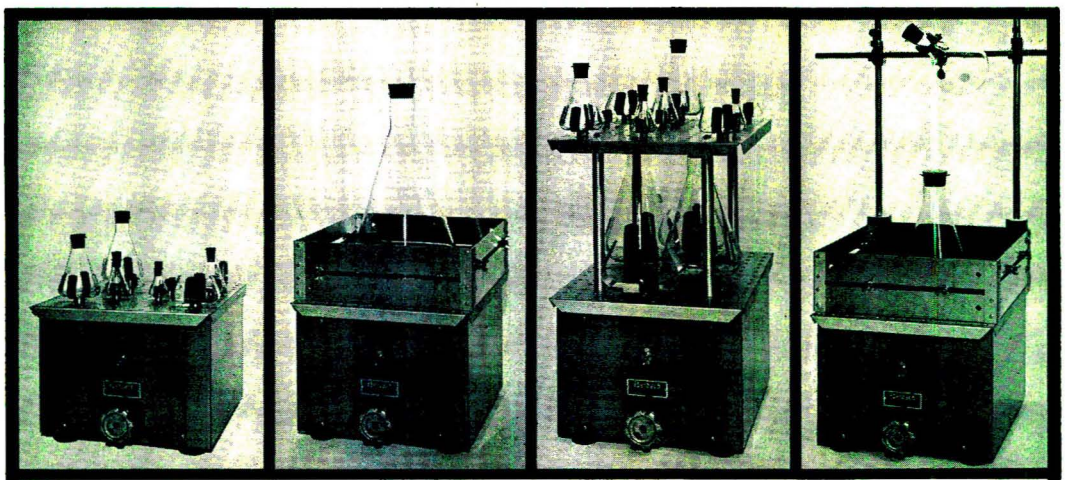
And don't forget to hook-up the entire system with New, Hoke **Gyrolok** Tube Fittings. A catalog is available.

For complete information on how these Hoke products can help you, contact your local Hoke distributor or write to us directly.

HOKE

Hoke Incorporated • 1 Tenakill Park • Cresskill, N. J.

See Buyers' Guide for all products/sales offices.
Circle No. 133 on Readers' Service Card



Power unit with platform | With utility box carrier | With platform & tiering posts | With utility box & vertical rods

- 20-240 excursions per minute
- Minimum space required—14″ x 12″ x 9⅜″ high

SMALL TABLE TOP RECIPROCATING SHAKER

This exceptionally wide speed range readily adapts this Shaker to low speed motion studies, as well as violent agitation. Stroke can be adjusted to ½″, 1″ or 1½″. 115 volt, 50/60 cycle. Shaker Power Unit with platform, Catalog No. 5850.....$195.00
Write for Bulletin No. 750

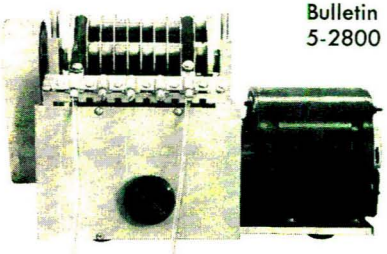
Eberbach CORPORATION P.O. Box 1024 Ann Arbor, Mich. 48106

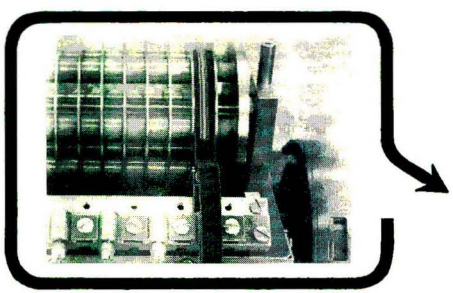
Circle No. 6 on Readers' Service Card

THE N.I.L. 10-CHANNEL FLOW PUMP

A NEW CONTINUOUS-FLOW PERISTALTIC PUMP FOR COLUMN CHROMATOGRAPHY—UNMATCHED FOR DURABILITY, USE IN COLD ROOMS, HEAD-PRESSURE CAPACITY, AND FREEDOM FROM TUBING WEAR.

Bulletin 5-2800





- Flow rate infinitely variable from less than 0.05 ml/min to 500 ml/min.
- Conformal geometry of tubing support eliminates local stresses, minimizes pulsing, and avoids tubing wear.
- Delivery volume controlled by varying tubing diameter and motor control.
- Accommodates tubing up to ⅜″ I.D.
- Can pump against 60-foot head pressure.

National Instrument Laboratories, Inc.

NIL

12300 Parklawn Drive, Rockville, Maryland 20852
In Metropolitan Washington, D. C.
PHONE: 933-1144 AREA CODE: 301

Circle No. 187 on Readers' Service Card

NEW CHEMICALS

Mossbauer Spectroscopy Standard

A standard reference material for Mössbauer spectroscopy, NBS Standard No. 725, sodium nitroprusside, is available from the National Bureau of Standards Office of Standard Reference Materials. The use of this material as a standard permits the reporting of data on chemical shifts as the difference between chemical shifts of a compound and that of the proposed standard. The standard is a single crystal of disodium pentacyanonitrosoferrate dihydrate, $Na_2[Fe(CN)_5NO]\cdot 2H_2O$. It was selected as a standard material because of its chemical stability, low temperature coefficient, narrow line width, and because of its doublet. Cost of the standard is $150.

For a list of available NBS standards, write for NBS Misc. Publ. 260 and enclose 45 cents to Superintendent of Documents, U. S. Government Printing Office, Washington, D. C. 20402.

Hydrocarbon Standards

Two new hydrocarbon standards have been purified by the American Petroleum Institute Research Project 58B. The standards are: Sample No. 1141-5S, C_7H_{14}, cis-3-heptene and Sample No. 1142-5S, $C_{14}H_{14}$, 1,1-diphenylethane. API standard samples of hydrocarbons are available only in units of 5 ml., each sealed in vacuum in a special glass ampoule with internal vacuum break-off tip. Price is $90 per unit. A list of the 326 compounds now available may be obtained by writing to Petroleum Research Laboratory, Carnegie Institute of Technology, Pittsburgh, Pa. 15213.

Glass Standards

Three new samples of standard glass are available from the Office of Standard Reference Materials, NBS Institute for Materials Research, Washington, D. C. 20234. The standards are available in 225-gram lots for $25 each. NBS No. 712 is a mixed alkali silicate glass; No. 713 is a dense barium crown 620/603 glass; and No. 714 is an alkaline earth alumina silicated glass. The glasses have been calibrated for softening, annealing, and strain points.

High-Chromium Wrought Alloy

A new alloy, Matreloy, is a wrought alloy of high chromium content. Advantages offered by the new material include room temperature workability, corrosion resistance, and high strength. Suggested applications are in springs, laboratory apparatus, and high temperature furnaces and instruments for corrosive environments. Materials Research Corp., Orangeburg, N. Y. 10962. **501**

Laboratory Gases

Highly purified laboratory gases are supplied in a newly designed disposable container called a Chemisphere. Advantages offered by this type of container over small-volume gas cylinders include integral diaphragm packless valve with stainless steel diaphragms, elimination of neck leakers, self-supporting tip-free low center of gravity, no deposit, no demurrage, and no rental charges. The following 14 gases can be supplied: oxygen, nitrogen, hydrogen, argon, helium, neon, krypton, zenon, carbon monoxide, carbon dioxide, air, cyclopropane, methane, and nitrous oxide. Lif-O-Gen, Inc., Triangle Industrial Center, P. O. Box 302, Lumberton, N. J. 08048. **502**

Viscosity Standards

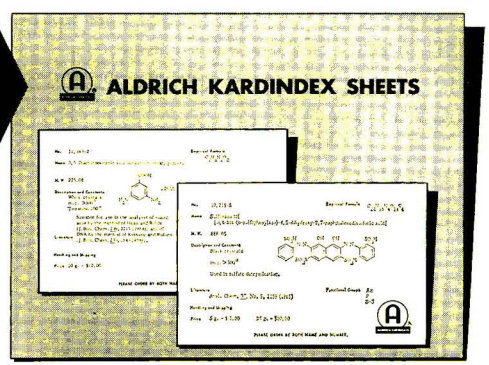
Viscosity standards are available for use in checking viscometer calibrations as well as procedures used in viscosity measurements. Viscosities of all the standards are based on the National Bureau of Standards value of 1.0038 cs. for water at 68° F. Included in the standards are viscosity oil standards, asphalt viscosity standards, low temperature standards, kinetic energy standards, and customized standards. Cannon Instrument Co., P. O. Box 812, State College, Pa. **503**

NMR Standard

Phosphorus oxide (P_4O_6) is available as a standard sample in ^{31}P nuclear magnetic resonance for finding a signal, setting up resolution, and as an external standard for referencing chemical shifts. This material is superior to phosphoric acid or trimethyl phosphite because the peak falls in a region which is convenient for chemical shift measurements for the great majority of phosphorus compounds. Gallard-Schlesinger Chemical Mfg. Corp., 584 Mineola Ave., Carle Place, L. I., N. Y. 11514. **504**

Are You Up On The Latest In Available ORGANIC ANALYTICAL REAGENTS?

Receive these free supplements to our 1966 catalog which already lists over 8000 chemicals!



Detailed descriptions of exciting new additions to our rapidly expanding product line are sent to you quarterly, keeping you up-to-date on the latest in organic, analytical and biochemical tools at your disposal.

For your FREE subscription to our Kardindex Service, simply fill in the coupon and mail to us at one of our offices shown below.

KARDINDEX
NAME_____ POSITION_____
COMPANY_____
ADDRESS_____
CITY_____ STATE_____ ZIP_____

ALDRICH CHEMICAL CO., INC.

Main Offices and Labs
2363 North 30th Street
Milwaukee, Wis. 53210

Eastern Office
78 Clinton Road
Fairfield, N. J. 07006

West Coast Distributor
Wilshire Chemical Co. Inc.
15324 So. Broadway
Gardena, Calif. 90247

Circle No. 104 on Readers' Service Card

THE FLOW SHEET

One of a series devoted to
enriching the Art of conveying & controlling fluids

Working With ULTRA-HIGH VACUUMS?

Let HOKE Help You . . .



Accelerate pumping time. Bake-out your system with this all metal diaphragm sealed valve. For vacuum as low as 10^{-10} TORR.

Maintain a vacuum tight seal. Here's a teflon sealed packless valve that'll handle vacuum down to 10^{-12} TORR with maximum reliability.





Automate your equipment. This lightweight air operator opens or closes valves when manual operation is undesirable.

Control system flow. The Kel-F stem tip in this bellows sealed valve provides vacuum tight closure at 10^{-3} TORR.



And don't forget to hook-up the entire system with New, Hoke Gyrolok Tube Fittings. A catalog is available.

For complete information on how these Hoke products can help you, contact your local Hoke distributor or write to us directly.

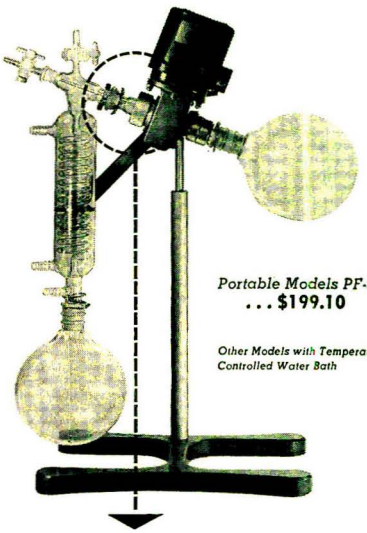
HOKE

Hoke Incorporated • 1 Tenakill Park • Cresskill, N.J.

See Buyers' Guide for all products/sales offices.
Circle No. 166 on Readers' Service Card

REVOLUTIONARY BECAUSE IT ISN'T!

THE IMPROVED
FLASH EVAPORATOR



Portable Models PF-9G
. . . $199.10

Other Models with Temperature Controlled Water Bath

NEW NON-ROTATING VACUUM JOINT MAKES BUCHLER FLASH EVAPORATORS BETTER THAN EVER!

Now all Buchler portable Flash Evaporators are equipped with a new, non-rotating vacuum connection affording a vacuum-tight seal without flaking! The vacuum connection remains stationary and only the evaporator flask rotates. This design gives the instrument an exceptionally long life while maintaining evaporation only within glass and Teflon to prevent contaminating back-drip. The new Flash Evaporator is easier to assemble and clean. Replacement parts are inexpensive. All features have been incorporated without losing the versatility of Buchler's original model. Made in U.S.A.

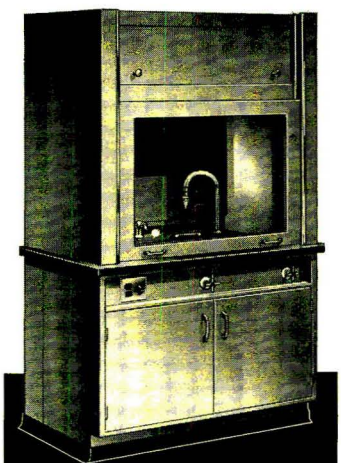
Find out more: Request
Buchler Bulletin AC-FE 1000

BUCHLER INSTRUMENTS

LABORATORY APPARATUS • PRECISION INSTRUMENTS
BUCHLER INSTRUMENTS, INC.
1327 16TH STREET, FORT LEE, NEW JERSEY 07024

See Buyers' Guide for all products/sales offices.
Circle No. 114 on Readers' Service Card

HEALTH preservers
IN STOCK



...Ready to go to work for you

Now, as an additional service, Kewaunee is STOCKING a wide range of Fume Hoods in both the AIRFLOW SUPREME and the IMPROVED CONVENTIONAL designs. These fume hoods are available for immediate delivery in 4′-0″, 5′-0″, 6′-0″ and 8′-0″ lengths. Send for the new 6 page brochure which details these Fume Hoods and also Blowers, Filters and Filter Housing.

KEMMETAL
KEWAUNEE MFG. CO. • ADRIAN, MICH.

5090 SOUTH CENTER STREET

Circle No. 167 on Readers' Service Card

MANUFACTURERS' LITERATURE

Laboratory Ware. Bulletin AC 566 features lab ware made of McDanel 997 high-purity alumina. Capacities, sizes, physical properties, and other data are given. McDanel Refractory Porcelain Co., 510 Ninth Ave., Beaver Falls, Pa. 15010. **601**

Null Detector. Data Sheet A12.1211, 2 pages, describes the improved version of the company's guarded d.c. electronic null detector. Leeds & Northrup, 4907 Stenton Ave., Philadelphia, Pa. 19144. **602**

Power Supplies. The 52-page Power Supply Handbook, P965, contains descriptions of the company's complete line of standard power supplies and modules. The handbook includes an application note section. Trygon Electronics Inc., 111 Pleasant Ave., Roosevelt, Long Island, N. Y. **603**

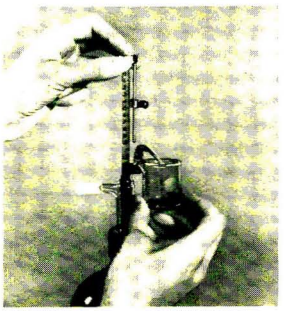
Level Indicator. The Model B-90 continuous level indicator and/or controller for application with liquids and granular solids is described in Catalog B-09-365, 4 pages. Instruments Inc., P. O. Box 556, Tulsa, Okla. **604**

Atomic Absorption. The Unicam SP 90 atomic absorption spectrophotometer and accessories are described in an 11-page bulletin. Micro Tek Instruments, Inc., P. O. Box 15409, Baton Rouge, La. **605**

Biochemicals and Analytical Reagents. Catalog B-6 is a listing of 2400 biochemicals and analytical reagents available from the company including rare sugars, intermediates, and derivatives; enzymes, coenzymes, and substrates; and phospholipids, nucleotides, venoms, and alkaloids. Pierce Chemical Co., Box 117, Rockford, Ill. **606**

Analytical Services. A 4-page brochure describes the company's analytical services, including thin layer chromatography, microanalysis (organic and inorganic), air and water pollution, chemical microscopy, x-ray diffraction and fluorescence, and forensic analyses. Analtech, Inc., 100 S. Justison St., Wilmington, Del. 19801. **607**





CUT YOUR LAB COSTS 50–95%

Our customers say L/I Automatic REPIPETS* and Dilutors save 50-95% of the time required for their determinations. It's logical, because these instruments dispense, transfer, mix, aspirate or dilute in seconds instead of minutes. Use them to automate any test with no change in procedures and complete freedom from contamination. Economical for 1 or 1,000 tests!

L/I REPIPETS and Dilutors handle any reagent, hot or cold, with a guaranteed accuracy of 1%, reproducibility ±0.1%. Volumes? From microliters to deciliters. L/I's new micropipets extend the range of Dilutors to such procedures as red and white cell dilutions. Clean-up? None.

Dilutors $89.50, including complete set of tips for highest precision in all ranges. REPIPETS $47.50. Immediate delivery in 1, 10, 20 and 50 ml sizes. Write for details on REPIPETS and new extended range Dilutors.

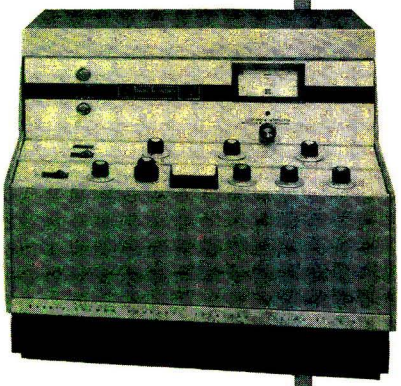
* Trademark (REpetitive PIPETS)

LABINDUSTRIES

1802 A Second Street
Berkeley, California 94710
TH3-0220 Cable LABIND

Circle No. 60 on Readers' Service Card

Thermal Conductivity Gas Chromatograph



MODEL 5340.....only $1150.00

This inexpensive chromatograph is excellent for quality control or teaching purposes.

FEATURES:

Simplified operation and maintenance without sacrifice of performance.

Step by step instructions reduce training time.

Dimbat-Porter-Strauss Index of 11,500 with noise level less than 1% of full scale.

Solid State Power Supply.

W2X Rhenium-Tungsten 4-filament Detector System.

Dual Injection Ports

Manual Temperature Programming

Temperature Range — Ambient to 400°C

Ten-Step Attenuation — 1 to 1000

BARBER COLMAN

BARBER-COLMAN COMPANY

Dept. F, 15104 Rock Street, Rockford, Illinois, U.S.A.

BARBER-COLMAN of CANADA, Ltd., Dept. F, Toronto & Montreal • Overseas Sales Mgrs.: Ad. Auriema, Inc., N.Y

See Buyers' Guide for all products/sales offices.

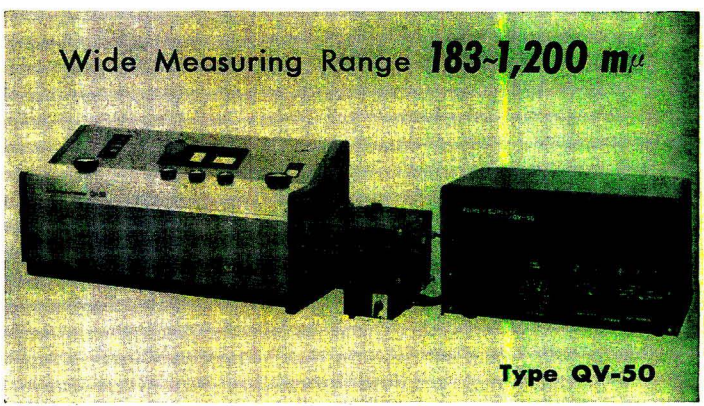
Circle No. 26 on Readers' Service Card

For more accurate Absorption Spectrophotometry

Shimadzu

SHIMADZU PHOTOELECTRIC SPECTROPHOTOMETER

Shimadzu QV-50 Photoelectric Spectrophotometer features a Littrow type Monochromator utilizing a fused silica 33 degree prism. Evacuated by a vacuum pump, it is capable of measurement in the extreme ultraviolet, down to 183 mμ. Constant temperature device is built in the cell compartment. More efficient for biological research. Especially flow dichroism measuring set and circular dichroism measuring set, both developed by Shimadzu, and other various accessory sets—Absorption Tube Accessory Set, Flame Photometry Accessory Set, Reflection Accessory Set, and Fluorometry, Nephelometry Accessory Set — are useful optional equipment to the QV-50.



SHIMADZU SEISAKUSHO LTD.

FOREIGN TRADE DEPT.

TOKYO OFFICE: 14-5, Uchikanda 1-chome, Chiyoda-ku, Tokyo (Cable Add.: SHIMADZU TOKYO

KYOTO OFFICE: Nishinokyo-Kuwabaracho, Nakagyo-ku, Kyoto (Cable Add.: SHIMADZU KYOTO)

Sole Agents in U.S.A.

ATAKA NEW YORK, INC.

633, Third Avenue, New York 17, N.Y.
Tel. No. OXford 7-7480

Distributors:

ACE SCIENTIFIC SUPPLY CO., INC.,

1420 E. LINDEN AVE., LINDEN, NEW JERSEY

PREISER SCIENTIFIC, INC.,

900 MACCORKLE AVE.,S.W., CHARLESTON 22, W. Va.

Circle No. 87 on Readers' Service Card

3RD CUMULATIVE ANALYTICAL CHEMISTRY INDEX

1959–1963

The third ANALYTICAL CHEMISTRY INDEX contains a complete author and subject index of every article and feature printed in ANALYTICAL CHEMISTRY during the period 1959-1963, volumes 31 through 35 inclusive. This useful reference volume costs only $7.

Use the space below to order your copy of this important index today.

Reprint Department
ACS PUBLICATIONS
1155 16th St., N.W./Washington, D. C. 20036

Gentlemen:

Please accept this as my order for ____ copies of the third CUMULATIVE ANALYTICAL CHEMISTRY INDEX (1959-1963) at $7 each.

☐ My payment is enclosed.
☐ Bill me.
☐ Bill company.

NAME

MAILING ADDRESS

CITY

STATE ZIP CODE

COMPANY NAME

Signature

MANUFACTURERS' LITERATURE

Benzoyl Cyanide. A 2-page bulletin gives specifications, properties, and reactions of benzoyl cyanide. Gallard-Schlesinger Chemical Mfg. Corp., 584 Mineola Ave., Carle Pl., L. I., N. Y. 11514. **608**

Atomic Absorption Standards. A 2-page sheet lists standardized solutions of 15 commonly determined metals available with compositions, catalog numbers, and prices. Fisher Scientific Co., 711 Forbes Ave., Pittsburgh, Pa. 15219. **609**

Centrifuges. An 8-page, illustrated brochure describes the complete Martin Christ line of laboratory, research, and refrigerated centrifuges. Special Products Sales, 72 Jericho Turnpike, Mineola, L. I., N. Y. 11501. **610**

Filter Manual. A revised, 80-page edition of Technical Manual ADM-70 contains updated information covering uses of the company's filters in microchemical analysis. Millipore Filter Corp., Bedford, Mass. 01730. **611**

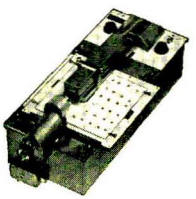
Data Process and Control. Brochure RC 495 describes the Norelco data processor and data control unit designed for use with analytical instrumentation. Philips Electronics Instruments, 750 S. Fulton Ave., Mount Vernon, N. Y. 10550. **612**

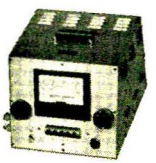
Nuclear Instrumentation. Catalog D, 24 pages, describes the nuclear equipment, labelled compounds, and laboratory accessories available from the company. Nuclear Equipment Chemical Corp., 145 Florida St., Farmingdale, N. Y. 11735. **613**

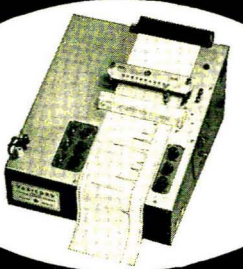
Moisture Analyzer. The Model 510 moisture analyzer, which senses moisture in the range of 0 to 25,000 p.p.m., is described in Bulletin MA, 4 pages. E. I. Du Pont De Nemours & Co., Wilmington, Del. 19898. **614**

Separational Products. A 9-page booklet describes the properties, applications, and quantities of the various separational products available from the company. It also illustrates the laboratory columns and upward flow adaptors designed for gel filtration and ion exchange chromatography with aqueous systems. Pharmacia Fine Chemicals, Inc., 800 Centennial Ave., Piscataway, N. J. 08854. **615**

thin Layer Chromatography DENSITOMETER





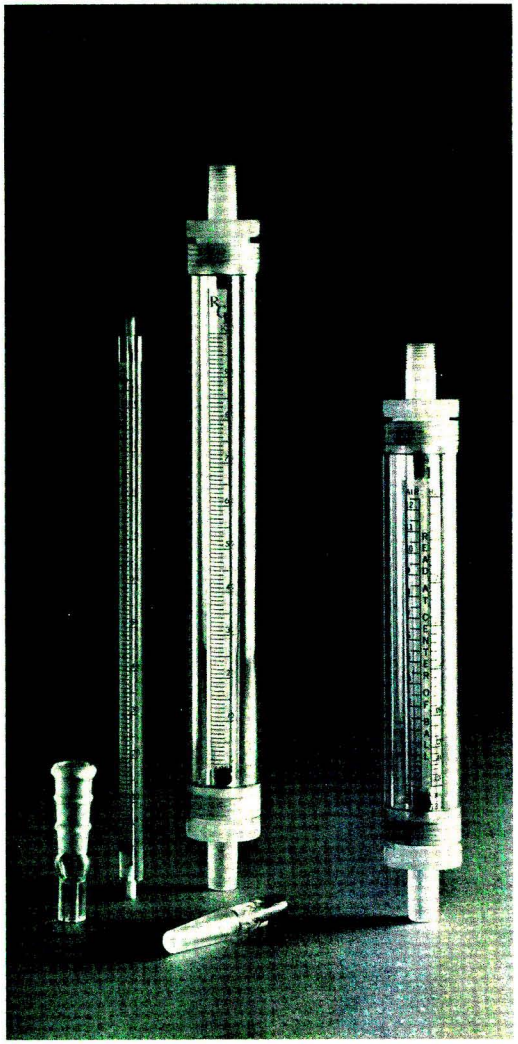


Write for Bulletin TLC-2

PHOTOVOLT

PHOTOVOLT CORPORATION
1115 Broadway
New York, N.Y. 10010

Circle No. 125 on Readers' Service Card



High accuracy flowmeters at low cost

RGI flowmeters* offer the highest accuracy of any spherical float meters in their price ranges.

High precision flowmeters, accurate to within 2% of reading, are individually calibrated and correlated. Priced as low as $27.00, they are available in five sizes—1 to 77,000 ml/min for air, .01 to 1900 ml/min for water. Where maximum precision is not required, our new "compact" flowmeters from $10.20 provide ±5% accuracy—still comparable to most higher priced meters. Range is 0.2 to 12,500 ml/min for air, .002 to 300 ml/min for water.

Air and water flow rates can be read directly off the calibration curve supplied with each instrument. A correlation chart lets you calculate a curve for other fluids.

Both types feature precision-bore plain ends with Teflon® stops for easy cleaning. Both accommodate optional standard taper joints or protective acrylic shields.

These flowmeters and other quality instruments are described in our 24 page catalog. Write for it today.

RGI INCORPORATED
BOX 732, VINELAND, NEW JERSEY

* U. S. Patent No. 3,183,713 ® Trademark of Dupont

Circle No. 55 on Readers' Service Card

Get Your Facts RIGHT —and Get Them RIGHT AWAY!

It's so easy! Just go to the right place — CHEMICAL MATERIALS CATALOG. All the facts you need are tucked away in its pages — and neatly ticketed in the 5-way index, ready to pop up for your **immediate** use. Facts about chemicals. Facts about raw materials. All up-dated, and carefully organized **for** process men **by** process men. Your copy of CMC is a one-volume **library** of basic information, ready to hand. Keep it on your desk. Let it work for you and **with** you. It's a tireless helper, a proven time-saver. And it's right as rain!

CHEMICAL MATERIALS CATALOG
cmc
REINHOLD PUBLISHING CORPORATION

430 PARK AVENUE, NEW YORK, N. Y. 10022

Circle No. 3 on Readers' Service Card

i/a PROPIPETTES®

® registered trade mark

SPEED

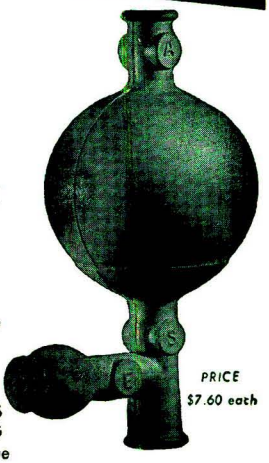
i/a propipettes used in one hand, technique easily mastered

SIMPLICITY

i/a propipettes have no moving parts, hold liquid until released, accurate to 0.01cc, fit all laboratory pipettes

SAFETY

i/a propipettes eliminate unpleasant, dangerous mouth pipetting



PRICE
$7.60 each

AVAILABLE IN FIVE COLORS FOR LABORATORY CODING
black, red, green, yellow, blue

IN STOCK AT YOUR LABORATORY DEALER

Write for additional information sent on approval

INSTRUMENTATION ASSOCIATES, INC.
17 West 60th Street, New York 23, N.Y. Circle 5-0840

Circle No. 16 on Readers' Service Card

MANUFACTURERS' LITERATURE

Tritium-Labelled Compounds. A revised, 16-page catalog, "Tritium Labelled Compounds," (April 1966) lists all tritium compounds offered by the company. Included are descriptions of the company's five different tritium labelling services and a selection of special tritium reference sources. Nuclear-Chicago Corp., 359 E. Howard Ave., Des Plaines, Ill. 60018. **616**

Elution Convection. A bulletin on elution convection describes its application to serum proteins. E-C Apparatus Corp., 222 S. 40th St., Philadelphia, Pa. 19104. **617**

Trace Gas Analyzer. Description, data, and specifications for Model 686 mass spectrometer–trace gas analyzer are given in a 7-page bulletin. Aero Vac Corp., P. O. Box 448, Troy, N. Y. **618**

Liquid Scintillation. Performance of the Ansitron II liquid scintillation counter is discussed in 4-page Bulletin N-6600. Picker Nuclear, White Plains, N. Y. **619**

Integrator/Calculator. A 4-page bulletin describes the operation of the company's integrator/calculator, which performs all of the integration and arithmetic needed to analyze any chromatogram. Technicon Chromatography Corp., Research Park, Chauncey, N. Y. **620**

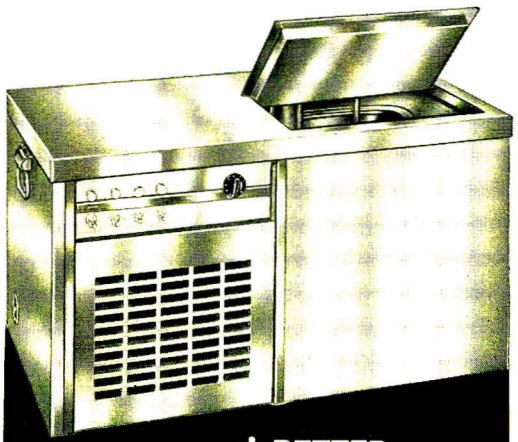
Separations. Additional analytical procedures for the Chromagram system include several pretreatments of the sheet. Descriptions of six new procedures are available. Distillation Products Industries, Rochester, N. Y. 14603. **621**

Gas Chromatographs. The Moduline Series Product Bulletin is a graphic presentation of the company's Moduline gas chromatographs. Types of operation and various detectors are discussed. Varian Aerograph, P. O. Box 313, Walnut Creek, Calif. 94597. **622**

Spectrophotometers. A 6-page bulletin contains description and specifications for the Model 11 Series of GC-IR spectrophotometers. Spectra indicating low level sensitivities and applications are included. Wilks Scientific Corp., 140 Water St., S. Norwalk, Conn. **623**

REVOLUTION IN BTU*

Savant's Recirculating Water Cooler



***BETTER TEMPERATURE UNIFORMITY**

A completely sef-contained, commercial type refrigeration system in a compact laboratory size package. Accurate and dependable for circulating liquids at controlled temperatures through:

- Cooling Jackets
- Distillation Columns
- Electrophoresis Apparatus
- Interferometers
- Polarimeters
- Refractometers
- Viscometers

. . . or any other instruments requiring circulation of controlled temperature liquids.

Savant's recirculator with ½ H.P. compressor will remove 3,500 BTU per hour, includes an all stainless steel insulated water bath, providing efficient cooling under exacting specifications.

A Savant Catalog RWC-50 will give you complete information on this versatile instrument.

HIGH VOLTAGE ELECTROPHORESIS LUCITE TANKS AND FLAT PLATE SYSTEMS

HIGH VOLTAGE POWER SUPPLIES 1 KV to 10 KV MODELS



Savant Instruments, Inc.

221 Park Avenue • Hicksville, New York 11801

(516) WE 5-8774

Circle No. 179 on Readers' Service Card

Pumps. A report on pumps used in analytical, medical, and biological fields includes product and application data. Sage Instruments, Inc., 2 Spring St., White Plains, N. Y. 10601. **624**

Spectrophotometer. Bulletin 14-380 features the Evans Electroselenium Ltd. Model 140 atomic absorption spectrophotometer and accessories. Fisher Scientific Co., 711 Forbes Ave., Pittsburgh, Pa. 15219. **625**

Resistance and Current Measurements. "A System for Accurate High Resistance and Low Current Measurements Traceable to the National Bureau of Standards" is a 42-page booklet which describes a method, using Model 515-10 high megohm measuring system, for measuring high resistances (10^5 to 10^{15} ohms) and for generating small currents (10^{-5} to 10^{-14} amp.). Keithley Instruments, Inc., 12415 Euclid Ave., Cleveland, Ohio 44106. **626**

Electrophoresis. A 34-page manual entitled "How to Do Rapid Electrophoresis" features the company's cellulose polyacetate strip medium Separphore III. Gelman Instrument Co., P. O. Box 1448, Ann Arbor, Mich. 48106. **627**

Research Microscope. A 10-page catalog highlights the Zetopan microscope which can be extended to cover special microscopic techniques. William J. Hacker & Co., Inc., P. O. Box 646, W. Caldwell, N. J. 07007. **628**

Filtration Membrane. Bulletin No. 2-66-1 describes the UM-3 Diaflo membrane and gives performance data and applications. Amicon Corp., 280 Binney St., Cambridge, Mass. 02142. **629**

Thin Layer Chromatography. Model 9/CR thin layer chromatography demonstration kit and Model 8/CR thin layer chromatography apparatus are detailed in two booklets. Quickfit Reeve Angel, Inc., 1 Bridewell Pl., Clifton, N. J. 07014. **630**

Mass Spectrum Data. A 4-page brochure describes the automatic mass spectrum data system for scanning photoplate records and transferring the data to a computer. Consolidated Electrodynamics, 1500 S. Shamrock Ave., Monrovia, Calif. 91016. **631**

Voltmeter. A 2-page technical data bulletin describes the Model 313-2031 multi-mode transistorized a.c./d.c. voltmeter. Trio Laboratories, Inc., Dupont St., Plainview, N. Y. **632**

Counter Current Distribution. A 20-page brochure describes the various applications of the steady state distribution machine. Quickfit Reeve Angel, 1 Bridewell Pl., Clifton, N. J. 07014. **633**

Flowmeters. Bulletin 1065 is a condensed 4-page listing of variable area, tapered tube flowmeters. Kontes Glass Co., 141 Spruce St., Vineland, N. J. 08360. **634**

Low-Foam Surfactant. Bulletin SAN 247-3 is a 6-page booklet describing the properties and uses of Triton DF-12, a biodegradable, 100% active, low-foam surfactant. Rohm and Haas Co., Independence Mall West, Philadelphia, Pa. 19105. **635**

New From Bio-Rad The Most Complete Catalog of Gel Filtration Materials

Bio-Rad's new Bulletin BG-4 includes data, applications and prices on:

Bio-Gel® P—Bio-Rad's gel filtration series for separation of water soluble materials from molecular weight 200 to molecular weights over 400,000.

Bio-Gel Exchangers—Bio-Gel P materials with ion exchange groups attached.

Bio-Glas—Bio-Rad's series of porous glasses for separation of high molecular weight materials from either aqueous or non-aqueous media.

Bio-Beads—Bio-Rad's series of porous polystyrene beads for separation of lipids, polymers and also water active compounds.

BIO-RAD Laboratories Dept. A-15

Bio-Rad Laboratories, 32 & Griffin Avenues, Richmond, California
Gentlemen: Please send my free copy of Technical Bulletin BG-4.

NAME TITLE

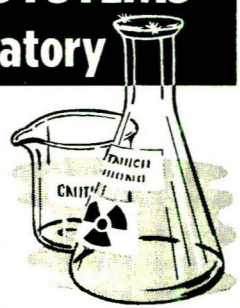
ORGANIZATION

ADDRESS

CITY STATE

Circle No. 110 on Readers' Service Card

LABELING SYSTEMS for the laboratory



Time pressure-sensitive Tapes and Labels provide a versatile system of identification for laboratory procedures. May be printed with quality control labels, diagrams, radiation warning symbols or consecutive numbers. Custom imprints for every labeling program. High quality vinyl coated tape can be marked with pen or pencil. Tapes and Labels have strong holding adhesive that leaves no sticky residue. Withstand temperatures from —70°F. to +250°F. (High temperature tapes with range to +550°F. also available.) Oil-proof, water-proof, and acid-resistant. Write for new 32-page catalog listing more than 100 laboratory labeling aids.



TIME® SELF STICKING LABELS VINYL COATED

AVAILABLE THROUGH LABORATORY DEALERS.

PROFESSIONAL TAPE CO., INC.
363 EAST BURLINGTON ROAD
RIVERSIDE, ILLINOIS 60546

Circle No. 81 on Readers' Service Card

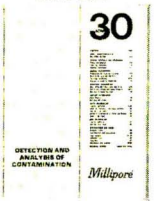
Technical Manual explains in detail how to use Millipore Filters for analyzing contamination in:

- Hydraulic Fluids
- Aviation Fuels
- Missile Propellants
- Solvents
- Photo Resists
- Plating Solutions
- D. I. Water
- Rinse Waters
- Lubricants
- Reactor Effluents
- Clean Room Air
- Clean Room Garments
- Surface Deposits
- Smoke and Fumes

40 pages of illustrated procedures in ADM-30 "Detection and Analysis of Contamination" available free of charge from

Millipore®
FILTER CORPORATION
115 Ashby Rd., Bedford, Mass. 01730

SEND FOR FREE COPY

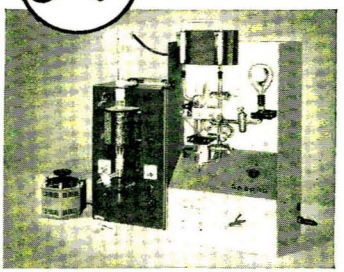


Circle No. 17 on Readers' Service Card

NEW HYDROGEN ANALYZER for metals

Leco®

3-10 Minute Analysis Time



Uses the hot extraction principle. Meets ASTM requirements (tentative procedure) of 1200°C or 2192°F operating temperature. Outgassing of a crucible is eliminated, due to a patented, inert, blank free susceptor. A unique device allows one sample to be loaded at a time, and removed from the system after extraction, without breaking the vacuum!

Write for literature today

LABORATORY EQUIPMENT CORP.
241 Hilltop Road, St. Joseph, Michigan

Circle No. 62 on Readers' Service Card

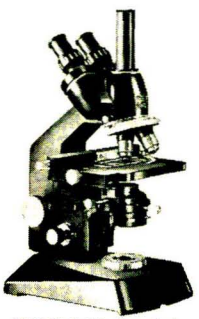
GALILEO SCIENTIFIC INSTRUMENTS

RESEARCH MICROSCOPE AT LABORATORY INSTRUMENT PRICE

The Model LN microscope has a pre-aligned 6V-15W illumination system built into the base. The inclined binocular head is an integral part of the arm assuring alignment at all times. A straight tube is provided for observation or photography and accepts cameras of different types.

Standard optics are: Achromatic objectives 3X, 10X, 40X and 100X corrected for flatness of field and high resolution. Paired Huyghenian compensated eyepieces 5X and 10X.

Optical accessories available for phase contact, dark field illumination, polarization, fluorescent microscopy and photomicroscopy.



$680.00 F.O.B. New York

Some territories available for sales representatives

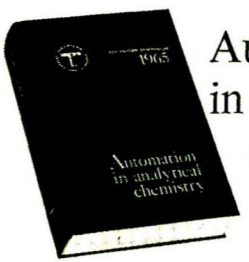
Write for A-6 illustrated catalog

Known world-wide since 1866 for precision scientific instruments

GALILEO CORPORATION OF AMERICA
18 East 53rd Street • New York, N.Y. 10022

Circle No. 45 on Readers' Service Card

The only reference volume devoted exclusively to...



Automation in analytical chemistry

More than 160 reports delivered at 1965 Technicon Symposia, covering the latest methods, techniques, flow diagrams, and instrumentation for: multiple clinical analysis; data processing; immunohematology; chromatography; health screening; enzyme, lipid, and in-vivo analysis; analysis and process control of foods, beverages, pharmaceuticals, fertilizers, pesticides, soils, metals, and power; air and water pollution; and many other topics.

TECHNICON INSTRUMENTS CORPORATION
Ardsley (Chauncey), New York 10502

Please send me _____ copies of "Automation in Analytical Chemistry," at $10.00 per copy.

☐ Payment enclosed ☐ Send C.O.D.

Name_____

Address_____

City_____ State_____ Zip Code_____

21 C-L

Circle No. 175 on Readers' Service Card

Research Chemicals. Organic and inorganic reagents, biochemicals, organo metallics, rare chemicals, and biological stains are included in a new 162-page catalog which lists over 14,000 research chemicals. Pfaltz & Bauer, Inc., 126-04 Northern Blvd., Flushing, N. Y. 11368. **636**

Company Periodicals

Requests for copies of the following publications, catalogs, etc., should be sent directly to the address shown. Business or professional letterheads are requested.

B.D.H. Laboratory News, Vol. 1, April 1966. This first issue of a new periodical reports on new compounds available from British Drug Houses Ltd. Gallard-Schlesinger Chemical Mfg. Corp., 584 Mineola Ave., Carle Pl., Long Island, N. Y. 11514.

LabLog, 1-66. The latest periodic supplement to the company's general sales catalog No. 9 is a 16-page listing which includes equipment specifications. Will Scientific, Inc., Box 1050, Rochester, N. Y. 14603.

Fluorescence News, Vol. 1, No. 1. This new bi-monthly, reporting the latest developments in fluorescence and phosphorescence techniques, is designed for users of the Aminco-Bowman spectrophotofluorometer and the Amino fluoro-microphotometer. This first issue discusses fluorometry in clinical chemistry and for pesticide residues. 1965 bibliographies of the larger American journals will be featured. American Instrument Co., Inc., 8030 Georgia Ave., Silver Spring, Md. 20910.

Facts & Methods, Vol. 7, No. 2. Sampling problems and their effect on analytical results are discussed. F & M Scientific Corp., Route 41 and Starr Rd., Avondale, Pa. 19311.

Aerograph Research Notes, Spring 1966. This issue reports on Porapak, a new polymer column packing which can serve both as liquid phase and solid support, and on Aeropak, a new solid support especially useful in steriod separation. Varian Aerograph, 2700 Mitchell Dr., Walnut Creek, Calif.

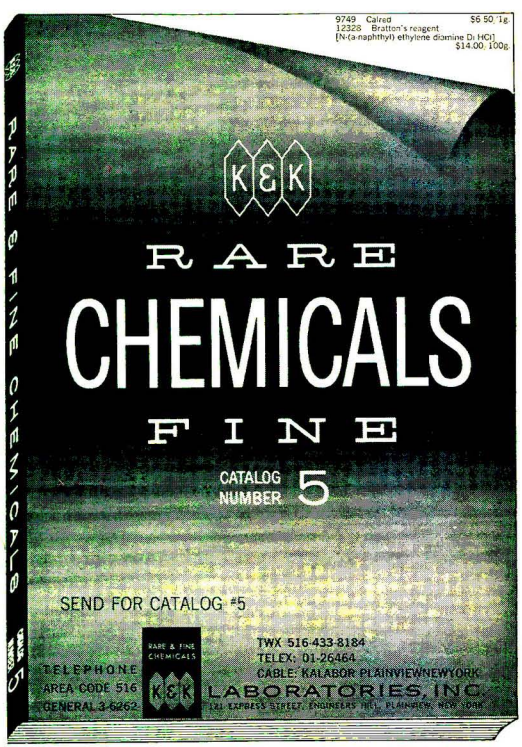
The Spex Speaker, Vol. XI, No. 1. This issue presents a background article on raman spectrometry. Spex Industries Inc., Box 798, Metuchen, N.J.

Dust Topics, Vol. 3, No. 2. "Impinger Techniques for Gas and Particle Sampling" is the featured article. The outdoor air test pack and other air sampling equipment are also described. Gelman Instrument Co., P.O. Box 1448, Ann Arbor, Mich. 48106.

What's New, No. 60. This 16-page supplement to Catalog 66 features a new blood pH system, precision vacuum pumps, student balances, and labware. Scientific Glass Apparatus Co., Inc., Bloomfield, N. J.

Solutions, March 1966. Featured in this issue is the Camag high voltage electrophoresis system. Other Camag thin layer chromatography systems are also described. Gelman Instrument Co., P.O. Box 1448, Ann Arbor, Mich. 48106.

Norelco Reporter, Vol. XIII, No. 1. The subject of the feature article is the company's new x-ray data handling system. The design of the system is discussed in detail. Another article discusses the x-ray spectrographic applications of the system. Philips Electronic Instruments, 750 S. Fulton Ave., Mount Vernon, N.Y.

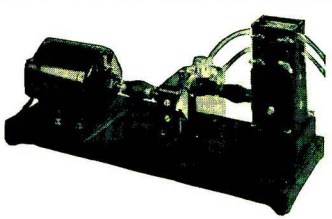


Circle No. 57 on Readers' Service Card

PUMP

YOUR SAMPLES

Liquids or solids in solution



There is no contamination of samples, no corrosion of the pump mechanism, since material is forced through tubing by wave-like action of fingers in the Sigmamotor pump. The tubing is easily removed from the pump or replaced. The pumping units are available separately, with motor drive or with motor and variable speed control as shown above. Capacity from 0.5 cc/min. to 4.5 gpm.

Write for complete information on sizes; capacities and tubing available.

SIGMAMOTOR, INC.

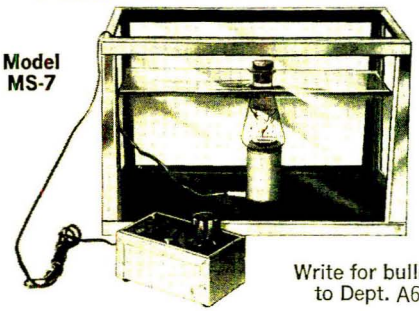
47 North Main Street • Middleport, New York

Circle No. 88 on Readers' Service Card

MICRO-SUBMERSIBLE MAGNETIC STIRRER

- ONLY 1½" DIAMETER BY 3" HIGH
- SEALED TO STIR UNDER WATER
- REMOTE SPEED CONTROL BOX
- LOW VOLTAGE MOTOR RUNS COOL
- OPERATES IN TIGHT SPACES

Model MS-7



Write for bulletin to Dept. A66

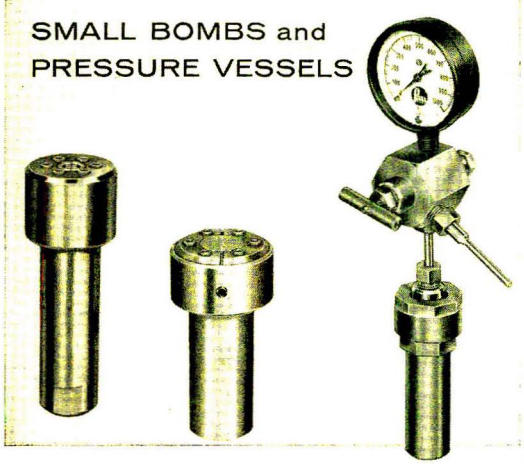
TRI-R INSTRUMENTS, Inc.

Developers of Electronic and Mechanical Instruments for Scientific Research

144-13 JAMAICA AVENUE, JAMAICA, N. Y. 11435

Circle No. 94 on Readers' Service Card

SMALL BOMBS and PRESSURE VESSELS



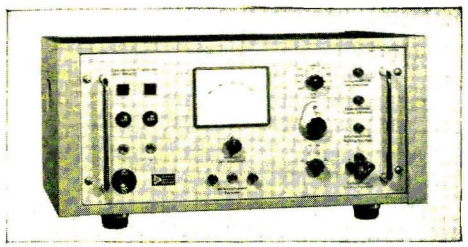
Sizes: 22, 45, 71, 128, 200, 310, 510 ml. and larger.
Materials: T316 stainless, Monel and other alloys.
Working pressures: up to 5000 psig. and higher.
Maximum temperatures: 350°, 500° C. and higher.
Valves, electrodes and other fittings can be provided. Let PARR help you select a combination suitable for your particular requirements.

PARR INSTRUMENT COMPANY

211 Fifty-Third St. Moline, Illinois

Circle No. 74 on Readers' Service Card

potentiostats



Because of their exceptional design and outstanding performance Wenking Potentiostats (galvanostats) are the most widely used instruments of this type for various electrochemical investigations. Ten basic models including "Fast Rise" versions (to ±100V) and "High Capacity" versions (to ±5A) are offered; also a multi-channel model, a precision voltmeter and a motor potentiometer.

BRINKMANN INSTRUMENTS

CANTIAGUE ROAD, WESTBURY, N.Y. 11590/ED 4-7500

Circle No. 4 on Readers' Service Card

LABORATORY SUPPLY CENTER

Be selective . . .
order EASTERN Organic Reagents!

Acids: 2-Acetamidoacrylic, Phenylthiohydantoic, Salicylhydroxamic
Benzalacetophenone • 2-Chloroquinoline • 3,5-Dimethoxyaniline
Citrulline • 2,6-Dichlorobenzaldehyde • Diethylchloromalonate
2,5-Diphenyl-3(4-Styrylphenyl)tetrazolium Chloride
Di-iso-propyl & Di-n-propyl Ketones • 3-Methyl-3-pentanol
3-Phenylpropylamine • Perfluoromethylcyclohexane • SPADNS

Write for list K-66 of other chemicals
Tel.: 201 696-1700 TWX: 510 234-5831 Zip Code 07440

EASTERN CHEMICAL CORPORATION BOX K PEQUANNOCK, N. J.

GARDNER/LOW COST AIDS FOR THE ANALYST



B-K Drying Recorder. For: Paints
Price: $200.
Write for fifty-page Testing Instrument Catalog.
PAUL N. GARDNER COMPANY
2000 South Ocean Drive (1507)
Fort Lauderdale, Florida 33316

MELTING POINTS in SECONDS with



THE KOFLER HOT BENCH
Range +50° to 260°C.
Accuracy ±1° C
Request literature
WILLIAM J. HACKER & CO., INC.
P. O. Box 646 West Caldwell, N. J.

TRACE ELEMENT PROBLEMS?

Contact General Atomic Division of General Dynamics.
FOR FREE BROCHURE, write to: Activation Analysis Service, Dept. AA-28 General Atomic Division, General Dynamics, P.O. Box 608, San Diego, California 92112. Or, phone: Area Code 714, 453-1000, Ext. 618.
Visit Booth 16, Chicago SAS Meeting

GENERAL DYNAMICS
General Atomic Division

1919—1966
LaMotte Chemical
Chestertown, Maryland U.S.A.
Specialists in
Colorimetric Techniques
Reagents—Standards—Comparator
Send for illustrated Controls Catalog
Dept. AC

YOUR ANNOUNCEMENT of Chemicals and Materials for Sale and/or Wanted can carry YOUR MESSAGE to the readers of the leading work magazine for instrumentation, control and analysis.

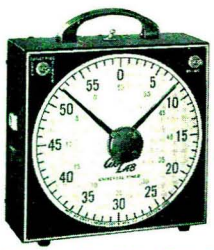
ANALYTICAL CHEMISTRY

Advertising Office:
430 Park Avenue New York, N. Y. 10022

SPECIAL
LIGHT
SOURCES

- Mercury Point Sources
- Raymaster Blacklight (long and short wave ultraviolet)
- Sodium Vapor
- Mercury Vapor
- Zirconium, Xenon, Deuterium and Hydrogen Arc Lamps
- Imported Spectral Lamps
- Photochemical or High Intensity "Uviarcs"
- Auxiliary Operating Equipment for above

WRITE FOR FREE CATALOG OR CONTACT YOUR LABORATORY SUPPLY DEALER
GATES
GEORGE W. GATES & CO.
LUCILLE AVE. FRANKLIN SQUARE, L.I., N.Y.



ELECTRIC LAB TIMER

GRA-LAB INTERVAL TIMERS Automatic signalling and switching. Various models each with 3600 possible settings.

GRA-LAB MICRO TIMERS 1/10 sec. or 1/1000 min. stop clocks. Remote start stop control. Write for catalog.

DIMCO-GRAY COMPANY
210 E. SIXTH ST. DAYTON 2, OHIO

Best for Fluoride

AMADAC-F™

Convenience-packaged mixture of lanthanum chelate of 3-aminomethylalizarin-NN-diacetic acid, buffers and stabilizers, affords accurate, sensitive and convenient quantitative colorimetric method for fluoride.

50 g. (for 100 detns.), with bibliography and complete instructions.....$15

BURDICK & JACKSON LABORATORIES
1953 S. HARVEY ST., MUSKEGON, MICHIGAN

CEC 21-103C MASS SPECTROMETER SERVICE

Accepted Industry standard. Resolution to mass 600. Suitable for most organic gases, liquids, solids (min. vapor press. 1 mm. Hg. at 300° C.). Complete petroleum laboratory • Continuous and batch distillations • Pilot plant facilities include high temp.-high pressure continuous feed reactor.

Since 1955—EXPERIENCE COUNTS!

Petroleum Analytical Research Corporation
P. O. Box 12334 Houston, Texas 77017
Tel. MI 9-2753

GAS ANALYSES
Mass Spectrometry • Gas Chromatography
• Leak Detection
• Vacuum and Inert Gas Fusion
GOLLOB ANALYTICAL SERVICE INC.
47 Industrial Road, Berkeley Heights, N. J. 07922
201-464-3331

INDEX TO ADVERTISERS IN THIS ISSUE

Ace Glass, Inc. 24
Heller Creative Advertising

Alberene Stone, Div. of Georgia Marble Co. 123
Basford, Inc.

Aldrich Chemical Co., Inc. 133
The Barry Agency

Alupharm Chemicals 127
M. Woelm

Anachemia Chemicals, Inc. 40
Brand Advertising, Ltd.

Applied Physics Corp. 98
Charles Bowes Advertising, Inc.

Applied Science Laboratories, Inc. 26
Barash Advertising

Aztec Instruments, Inc. 62:131
A. B. W. Toft & Co.

Baird-Atomic Inc. 57
Van Christo Associate

Barber-Colman Co. 129:136
E. R. Hollingsworth & Associates

Barnes Engineering Co. 42:127
Albert A. Kohler Co., Inc.

Bausch & Lomb, Inc. 60-61
Wolff Associates, Inc.

Beckman Instruments, Inc., Cedar Grove Operations 118
Lescarboura Advertising, Inc.

Beckman Instruments, Inc.
Scientific Instrument Div. 1:72:101
Spinco Div. 115
Hixson & Jorgensen, Inc.

Bel-Art Products 122
Gallard Advertising Agency, Inc.

James G. Biddle Co. 87
The Michener Co.

Bio-Rad Laboratories 140
Cappel, Pera & Reid, Inc.

S. Blickman, Inc. 46
J. M. Kesslinger & Associates

Brinkmann Instruments, Inc. 143
The Shaller-Rubin Co., Inc.

Bronwill Scientific, Div. of Will Scientific, Inc. 73
Hart-Conway Co., Inc.

Brookfield Engineering Laboratories, Inc. 128
Creamer, Trowbridge & Case, Inc.

Buchler Instruments, Inc. 134
Selvin & Jaffe

Burdick & Jackson Laboratories, Inc. 126
Studio 5 Advertising

Fred S. Carver, Inc. 130
J. C. Bull, Inc.

Chemical Materials Catalog 138
Persons Advertising, Inc.

Chromatronix, Inc. 126
Bonfield Associates, Inc.

Clay-Adams, Inc. 27
Cortez F. Enloe, Inc.

Coleman Instruments, Inc. 116C
Winfield Advertising Agency, Inc.

W. H. Curtin & Co. 129
Robinson-Gerrard, Inc.

Datex, Div. of Giannini Controls Corp. 71
Faust Day, Inc.

Delmar Scientific Laboratories, Inc. 34
Winfield Advertising Agency, Inc.

Harry W. Dietert Co. 54
Watkins-Rogers, Inc.

Distillation Products Industries 102
The Rumrill-Hoyt, Inc.

Durrum Instrument Corp. 18
Hal Lawrence, Inc.

Eastern Industries, Div. of Laboratory for Electronics 56
Hepler & Gibney, Inc.

Eberbach Corp. 132
Drury, Lacy, Inc.

Electronic Associates, Inc. 20
Gaynor & Ducas, Inc.

Esterline Angus Instrument Co., Inc. 16
Caldwell Larkin & Sidener Van Riper

Farrand Optical Co., Inc. 125
Snow & Depew, Inc.

Fischer & Porter Co. 128
The Harry P. Bridge Co.

Fisher Scientific Co. 33:70:121
Fuller & Smith & Ross, Inc.

Floridin Company 17
Muller, Jordan & Herrick, Inc.

Galileo Corp. 141
Faulkner Advertising, Inc.

Gallard Schlesinger Chemical Mfg. Corp. 69
Lewis Advertising Co., Inc.

General Electric Co. 108
George R. Nelson, Inc.

Gilford Instrument Laboratories, Inc. 89
Garber-Evans Advertising, Inc.

Greiner Scientific Corp. 42:110
Fairfax, Inc.

Hamilton Co., Inc. 113
Swain/Mealer, Inc.

The Harshaw Chemical Co. 87
The Griswold-Eshleman Co.

Hewlett-Packard, F & M Scientific Division 114
Richardson, Thomas, & Bushman, Inc.

Hewlett-Packard 5:99
Lennen & Newell, Inc.

Hitachi Ltd. 100
Dentsu Advertising Ltd.

Hoke Mfg. Co. 131:134
Tek-Mark, Inc.

Infotronics Corp. 85
Robinson-Gerrard, Inc.

Instrumentation Associates, Inc. 138
S. M. Sachs Associates, Inc.

Instrumentation Laboratory, Inc. 6
Pazolt & Co.

Instrumentation Specialties Co. 93
Graham Printing and Advertising Service

Instruments for Research & Industry ... 51
Allyn H. Jacobson

International Sales Associates 52
Edward J. Guilfoy

Jarrell Ash Co. 64
Culver Advertising, Inc.

JEOLCO, Inc. 38:39
Robert Hartwell Gabine

K & K Laboratories, Inc. 142
Newmark's Advertising Agency, Inc.

Keithley Instruments 106
The Bayless-Kerr Co.

Kewaunee Manufacturing Co. 135
Phillips Associates, Inc.

Klett Mfg. Co., Inc. 148

Labindustries 135
Bonfield Associates, Inc.

Laboratory Construction Co. ..... IFC
Valentine-Radford, Inc.

Laboratory Equipment Corp. 141
Creative Advertising, Inc.

Leeds & Northrup Co. 36:37
Gaynor & Ducas, Inc.

Lindberg/Hevi-Duty Marketing Services 67:124
Marstellar Inc.

The London Co. 88
James Lovick, Ltd.

McPherson Instrument Corp. 105
Briant Advertising

David W. Mann Co., Div. of GCA Corp. 19
Gaynor & Ducas, Inc.

Manufacturers Engineering & Equipment Corp. 147
Lesseraux & Tandler, Inc.

The Matheson Co., Inc. 122
Leonard M. Sive & Associates, Inc.

Matheson, Coleman & Bell 146
Leonard M. Sive & Associates, Inc.

Matheson Scientific, Inc. 83
Leonard M. Sive & Associates, Inc.

Melabs 91
Bonfield Associates, Inc.

Mettler Instrument Corp. 8:116B
Mort Barish Associates, Inc.

Microchemical Specialties, Co. 147

Micro-Tek Instruments, Inc. 25
Technical Advertising Associates

Midvale-Heppenstall 125
Sykes Advertising, Inc.

Millipore Filter Corp. 141
Culver Advertising, Inc.

Milton Roy Co. 124
The Harry P. Bridge Co.

INDEX TO ADVERTISERS IN THIS ISSUE

The Nalge Co., Inc. 53
Wolff Associates, Inc.

National Instrument Laboratories, Inc. 132
Leni Ellinger Agency

Nester/Faust Mfg. Corp. 45
Allyn H. Jacobson

Nuclear-Chicago Corp., Texas Nuclear Corp., Subsidiary 32:59
Sidney Clayton & Associates, Inc.

Nuclear Products Co. ..... IBC
Falls Advertising Co.

Ohaus Scale Corp. 123
Robert M. Baldwin Co.

Orion Research, Inc. 35
Mort Barish Associates, Inc.

Owens Illinois, Inc. 75
Meldrum & Fewsmith, Inc.

Packard Instrument Co., Inc. 10
Ross Llewellyn, Inc.

Parr Instrument Co. 143
F. Willard Hills

Perkin-Elmer Corp. 63:76:104:111
Gaynor & Ducas, Inc.

Pharmacia Fine Chemicals, Inc. 23:120
Paul Klemtner & Co., Inc.

Philips Electronic Instruments 92
Anders Advertising, Inc.

Photovolt Corp. 48:137
The M. B. Pearlman Co.

Picker Nuclear 28:94
Dean L. Burdick Associates, Inc.

Pope Scientific, Inc. 43
Max H. Mayer

Precision Scientific Co. 68
Tri-State Advertising Co., Inc.

Professional Tape Co., Inc. 140
Robert Peterson Advertising Agency

Puffer-Hubbard 18
Pippel-Patterson Co.

Radio Corp. of America 107
Al Paul Lefton Company, Inc.

RGI, Inc. 138
Garceau, Hargrave & McCullough, Inc.

Rosemount Engineering Co. 47
The Erle Savage Co.

Sadtler Research Laboratories, Inc. 12
Romer & Company, Inc.

Sage Instruments, Inc. 48
Lescarboura Advertising, Inc.

E. H. Sargent & Co. 41:117
Geyer, Morey, Ballard, Inc.

Savant Instruments, Inc. 139
Co-Art Associates, Inc.

Carl Schleicher & Schuell 31
Wildrick & Miller, Inc.

Scientific Products, Div. of American Hospital Supply 110
Alex T. Franz, Inc.

Scott Research Laboratories, Inc. 130
George H. McLaughlin Advertising

Sep-Ko Chemical, Inc. 49
Faber Advertising, Inc.

Shimadzu Seisakusho, Ltd. 136
New Asia Trading News Agency, Inc.

Siemens America 90
Mann-Wesley, Inc.

Sigmamotor, Inc. 142
Gelia and Wells, Inc.

Spectra-Physics, Inc. 73
Hal Lawrence, Inc.

Technicon Controls, Inc. 7:141
Mediad, Inc.

Texas Instruments, Inc. 112
Robinson Gerrard, Inc.

Texas Nuclear Corp. 32:59
Subsidiary of Nuclear-Chicago Corp.
Sidney Clayton & Associates

Thermal American Fused Quartz Co. 50
Kniep Associates

Thermolyne Corp. 72
E. R. Hollingsworth & Associates

Arthur H. Thomas Co. 116:116B

The Torsion Balance Co. 86
Michel-Cather, Inc.

Tracerlab, Div. of Laboratory for Electronics, Inc. 22
Hepler & Gibney, Inc.

Tracerlab, Div. of Laboratory for Electronics, Inc. 80
Bonfield Associates, Inc.

Tri-R Instruments, Inc. 143

Union Carbide Corp., Carbon Products Div. 74
J. M. Mathes, Inc.

Varian Associates 14:84
Hoefer, Dieterich & Brown, Inc.

Varian Aerograph 103
Bob Barriskill

The Victoreen Instrument Co. 21
Palm & Patterson, Inc.

Warner-Chilcott Laboratories 79
Lambert & Feasley, Inc.

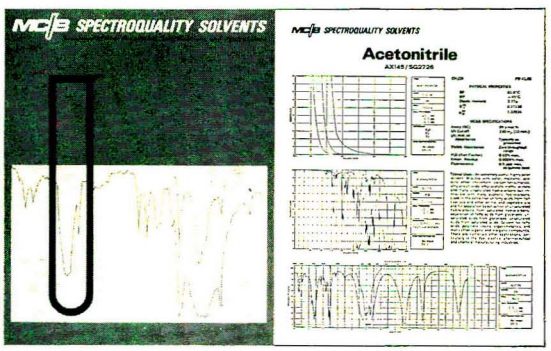
The Warner & Swasey Co. 66
Taube/Violante, Inc.

Waters Associates, Inc. ..... OBC
David B. Tibbetts

Wilkens-Anderson Co. 97
Mandabach & Simms, Inc.

Wilks Scientific Corp. 81
H. Edward Oliver Associates, Inc.

York Instrument Corp. 52
Kennis & Norris



Write for this 52-page book giving Spectra, Physical Properties, Specifications and Typical Uses of 46 MC&B Spectroquality Solvents

A time-saving book containing detailed information to aid the spectroscopist and researcher in selecting the best solvent for each application. For your free copy, write MC&B, P. O. Box 85, East Rutherford, N. J.

MC/B *Division of The Matheson Co. Inc., Norwood, Ohio, E. Rutherford, N. J., Los Angeles*

Circle No. 143 on Readers' Service Card

INDEX TO ADVERTISERS IN THIS ISSUE

Laboratory Supply Center..... 144

Burdick & Jackson Laboratories

Dimco-Gray Co.

Eastern Chemical Corp.

Paul N. Gardner Co.

George W. Gates & Co.

General Atomic Div., General Dynamics

Gollob Analytical Service, Inc.

William J. Hacker & Co., Inc.

LaMotte Chemical Products Co.

Petroleum Analytical Research Corp.

REINHOLD PUBLISHING CORPORATION

Advertising Management for the American Chemical Society Publications

430 Park Ave., New York, N.Y. 10022
Cable Address: REINPUB NYK

Thomas N. J. Koerwer
Advertising Sales Director, ACS Publications

Arthur P. Watts
Advertising Sales Manager, AC

J. Barry Stanford
Assistant Advertising Sales Manager, AC

SALES REPRESENTATIVES

New York 10022 . . . Arthur P. Watts, Clay S. Holden, Sam W. Percy, Robert N. Gillespie, William N. Wham, Reinhold Publishing Corp., 430 Park Ave., 212-688-8600

Chicago 60603 . . . Eugene P. Eldridge, Reinhold Publishing Corp., 10 So. La Salle St., 312-726-1282

Cleveland 44114 . . . Joseph C. Hoopes, Reinhold Publishing Corp., East Ohio Bldg., 1717 East 9th St., 216-771-4011

San Francisco 94105 . . . Morton McDonald, McDonald-Thompson, Inc., 625 Market St., 415-397-5377

Los Angeles 90005 . . . M. Jeffery Kaufman, McDonald-Thompson, Inc., 1313 West 8th Street, 213-483-1304

Portland 97221 . . . Francis M. Eaton, McDonald-Thompson, Inc., 2035 S.W. 58th Avenue, 503-292-8521

Denver 90203 . . . Robert H. Heidersbach, McDonald-Thompson, Inc., 846 Lincoln St., 303-825-3325

Houston 77006 . . . Frank I. Vikery, McDonald-Thompson, Inc., 3130 Southwest Freeway, 713-529-6711

Tulsa 74114 . . . Max C. Nelson, McDonald-Thompson, Inc., 570 South Harvard, 918-742-9961

Great Britain and Western Europe . . . Brayton Nichols, The American Magazine Group, 44 Conduit Street, London W, 1, England

Japan . . . Bancho Koheki Co., Ltd., 8 Shinanomachi, Shinjuku-ku Tokyo, Japan

PROMOTION DEPARTMENT

Robert Voepel
Promotion Manager

PRODUCTION DEPARTMENT

Alfred E. Gall
Advertising Production Director, ACS Publications

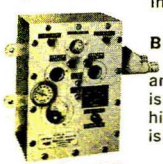
Anne Forrest
Advertising Production Manager, Analytical Chemistry

PRECISE MOISTURE MEASUREMENT



Type NEP-PL

The Type NEP-PL (Nonexplosion-proof) and Type MEP (Miniature Explosion-proof) Model W, Electrolytic Moisture Analyzers, are ideal for fast, accurate measurement of moisture content in continuous or batch gaseous samples, with standard metering in parts per million by volume (ppm/v).



Type MEP

Both instruments include adjustable sample and by-pass flow with metering, and signal for recording. The Type MEP is used in hazardous locations, or where a high degree of ruggedness in construction is required.

PRECISE SAMPLING

The Type 1-S stainless steel Vaporizing Valve permits stable controlled vaporization of liquids or expansion of gases having input pressures to 1000 psig. Cooling fins maintain intimate contact with ambient.



Type 1-S Vaporizing Valve

Write for more information

Manufacturers Engineering and Equipment Corp.

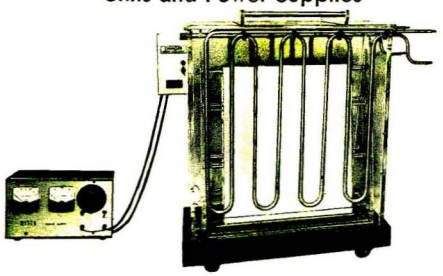
250 Titus Ave., Warrington, Pa.

Circle No. 9 on Readers' Service Card

Now Showing the . . . . .

MISCO

High-Voltage Electrophoresis Units and Power Supplies



For Superior Resolution • Fast Separations
***Low Cost *Versatile *Space Saving**

The MISCO Systems for HVE are ideal for Amino Acid and Peptide "Finger Printing," Nucleotide separation, Longer migration paths for steroids, Two-Dimensional work, etc.

We welcome your requests for our new brochure

MISCO *Scientific*

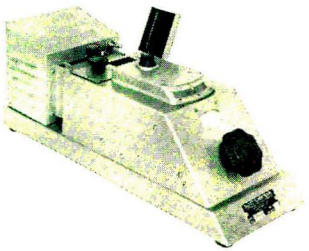
MICROCHEMICAL SPECIALTIES CO.
1825 EASTSHORE HIGHWAY • BERKELEY, CALIF. 94710

Circle No. 131 on Readers' Service Card

Klett . . .

Photometers

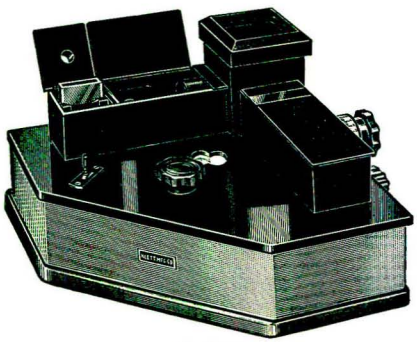
Klett-Summerson Photoelectric Glass Cell Colorimeter



No. 900-3

●

The Klett Fluorimeter



No. 2070

Designed for the rapid and accurate determination of thiamin, riboflavin, and other substances which fluoresce, in solution. The sensitivity and stability are such that it has been found particularly useful in determining very small amounts of these substances.

●

KLETT SCIENTIFIC PRODUCTS

PHOTOELECTRIC COLORIMETERS ● BIO-COLORIMETERS
COLORIMETER-NEPHELOMETERS ● COLONY MARKER
● KLETT REAGENTS ● GLASS CELLS

■

Klett Manufacturing Co., Inc.

179 EAST 87TH STREET, NEW YORK, N. Y.

Circle No. 59 on Readers' Service Card

FUTURE ARTICLES

Listed below are papers to appear in forthcoming issues of Analytical Chemistry

Determination of Micro Quantities of the C_1–C_4 Primary and Secondary Amines by Electron Affinity Detection

E. W. Day, Jr., Tomasz Golab, and J. R. Koons

Isotopic Analysis of Calcium-48 by Proton Activation

Max Peisach and Rene Pretorius

Use of a Multi-Channel Analyzer as a Data Acquisition System in Electrochemistry

George Lauer and R. A. Osteryoung

Voltammetric Applications of Rotating and Stationary Carbon-Epoxy Electrodes

H. S. Swofford, Jr., and R. L. Carman III

Determination of Radiostrontium by Solvent Extraction

W. C. Johnson, Jr.

A Study of the Feasibility of the Iron Hollow Cathode as a Multi-Element Atomic Absorption Unit

C. W. Frank, W. G. Schrenk, and C. E. Meloan

Apparatus for Reaction Gas Chromatography: Instantaneous Hydrogenation of Unsaturated Esters, Alcohols, Ethers, Ketones, and Other Compound Types, and Determination of Their Separation Factors

Morton Beroza and Rafael Sarmiento

Experimental and Theoretical Study of Specific Retention Volumes in Mixtures of Polar and Nonpolar Stationary Liquids

A. B. Littlewood and F. W. Willmott

The Acidity of Aromatic Sulfonic Acids and Their Use as Titrants in Nonaqueous Solvents

D. J. Pietrzyk and Jon Belisle

Fluorometric Determination of Indoxole [2,3-Bis(p-Methoxyphenyl)-Indole] in Biological Specimens

D. G. Kaiser, B J. Bowman, and A. A. Forist

Separation and Infrared Analysis of Products from the Nitration of Alpha-Olefins

Harry Morgan, R. M. Sherwood, and T. A. Washall

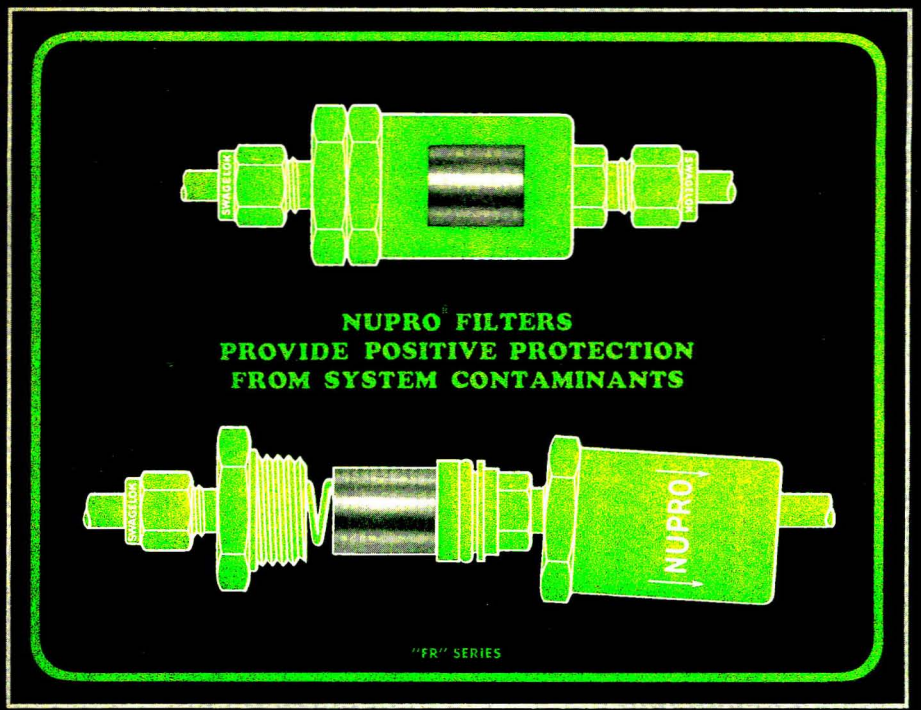
Theory of Gel Filtration (Permeation) Chromatography

J. C. Giddings and K. L. Mallik

Effects of Temperature upon the Barbital Buffers Used in Electrophoresis

R. D. Strickland and M. M. Anderson

Circle No. 14 on Readers' Service Card ⟶



NUPRO® FILTERS PROVIDE POSITIVE PROTECTION FROM SYSTEM CONTAMINANTS

All NUPRO filters contain sintered stainless steel filter elements which are available in various micron sizes for particle removal.

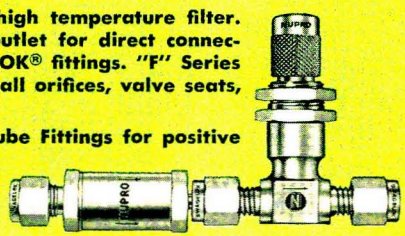
NUPRO offers two types of filters — The "F" and "FR" Series.

The "FR" Series Inline Removable Filter permits an element to be replaced without removing the entire filter unit from the system. This filter has been designed to absorb high pressures and provide a large filtering area to minimize pressure drop and increase element life.

The "F" Series is an extremely compact, reliable, high temperature filter. These filters can be supplied with a straight tube outlet for direct connection to metering valves, check valves, and SWAGELOK® fittings. "F" Series Inline Filters are recommended for protection of small orifices, valve seats, and sensitive instruments from contaminants.

All NUPRO Filters are available with SWAGELOK Tube Fittings for positive sealing and trouble-free service.

NUPRO Filters can be ordered directly from your local NUPRO Sales and Service Representative.



"F" SERIES

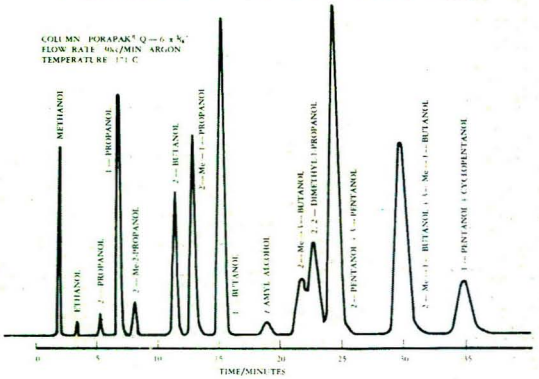
© 1960-1966 by NUCLEAR PRODUCTS COMPANY/all rights reserved

NUCLEAR PRODUCTS COMPANY / 15635 SARANAC ROAD / CLEVELAND, OHIO 44110

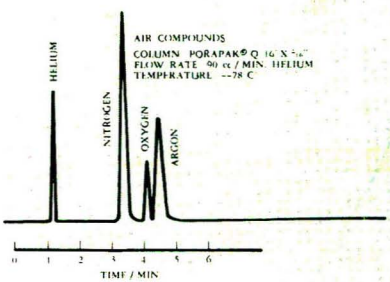
porapak®

PATENT PENDING

SEPARATIONS OF C_1-C_5 ALCOHOLS



SEPARATION OF INORGANIC COMPOUNDS



TYPICAL SEPARATIONS MADE WITH PORAPAK®

Porapak® is a porous polymer bead developed by O. L. Hollis of The Dow Chemical Company, Midland, Texas. Porapak® has a number of very significant advantages over commonly known packing materials for gas chromatography. Outstanding separations of volatile compounds have been achieved with columns packed with Porapak®. Notably, sharp, symmetical peaks and low retention volumes are found for water, alcohols, and glycols. Porapak® has the partition properties of a highly extended liquid surface without the problems of support polarity, liquid-phase volatility, or freezing point which hamper gas-liquid chromatography. Some of the advantages of Porapak® are as follows:

1. NO BLEEDING FROM THE PACKING MATERIAL
2. NO ADSORPTION OF POLAR COMPOUNDS
3. NO CHANGE IN RETENTION TIME
4. STABLE TO 250°C.
5. EASY COLUMN PACKING WITH HIGH EFFICIENCY
6. RAPID OVERLOAD RECOVERY
7. SEPARATION OF WATER FROM ORGANIC MATERIALS
8. COATING OF THE BEADS
9. LARGE SURFACE AREA.

6 MESH AVAILABLE: 200-250 / 120-150 / 150-200 50-80 80-100 / 100-120.

WE INVITE YOUR INQUIRY FOR COMPLETE INFORMATION

(Licensed under the patent rights of The Dow Chemical Company)

WATERS ASSOCIATES, INC.

executive offices, 61 FOUNTAIN ST., FRAMINGHAM, MASS., U.S.A. 617 • 872-6528

Overseas office: Waters Associates (Instruments) Ltd., 94 Offerton Lane, Cheshire, England

Circle No. 2 on Readers' Service Card